



HAL
open science

New Insights of Interactions between Cell Wall Polysaccharides and Procyanidins during Processing: Fate of Polysaccharides and Polyphenols during Processing

Xuwei Liu

► **To cite this version:**

Xuwei Liu. New Insights of Interactions between Cell Wall Polysaccharides and Procyanidins during Processing: Fate of Polysaccharides and Polyphenols during Processing. Agricultural sciences. Université d'Avignon, 2021. English. NNT : 2021AVIG0730 . tel-04042123

HAL Id: tel-04042123

<https://theses.hal.science/tel-04042123v1>

Submitted on 23 Mar 2023

HAL is a multi-disciplinary open access archive for the deposit and dissemination of scientific research documents, whether they are published or not. The documents may come from teaching and research institutions in France or abroad, or from public or private research centers.

L'archive ouverte pluridisciplinaire **HAL**, est destinée au dépôt et à la diffusion de documents scientifiques de niveau recherche, publiés ou non, émanant des établissements d'enseignement et de recherche français ou étrangers, des laboratoires publics ou privés.



THÈSE DE DOCTORAT D'AVIGNON UNIVERSITÉ

École Doctorale N° 536
Agrosciences & Sciences

Spécialité / Discipline de doctorat:
Food Science and Technology

INRAE UMR 408 « Sécurité et Qualité des Produits
d'Origine Végétale »

Présentée par
Xuwei LIU

New Insights of Interactions between Cell Wall Polysaccharides and Procyanidins during Processing

Fate of Polysaccharides and Polyphenols during Processing

Soutenue publiquement le 21/09/2021 devant le jury composé de:

M. Jean-Paul VINCKEN, Professor, Wageningen University & Research **Rapporteur**

M. Christian JAY-ALLEMAND, Professor, Université de Montpellier **Rapporteur**


M. Nuno MATEUS, Professor, University of Porto **Examineur**

Mme Catherine M.G.C. RENARD, Directrice de Recherche-HDR, INRAE **Directrice de thèse**

Mme Carine LE BOURVELLEC, Chargée de Recherche-HDR, INRAE **Co-directrice de thèse**

Mme Agnès Rolland-Sabaté, Ingénieure d'étude-Dr, INRAE **Encadrante de thèse**



- 
1. A fruit is not the fruit.
 2. Food determines your future.
 3. Good wine also needs bush.
 4. Some unopenable knots in the adult world find their answers in the world of fairy tales, e.g., Colmar.
 5. Designing various graphs is the most interesting in the thesis.
 6. Covid-19: to be or not to be; that is the question.

Propositions

Xuwei LIU, SQPOV
France, 21 September 2021

1000

Acknowledgements

This work is supported by **China Scholarship Council** (国家留学基金委) & **INRAE** (法国国家农业食品与环境研究院). I never thought that I can start the wonderful journey in France and obtained so much during my PhD, not only about knowledge in science, but also communication with so many adorable and respectful people.

First and foremost, I offer my gratitude to my supervisor, Ms. **Dr Catherine Renard**, who accommodated and supervised me throughout my thesis with her guidance and encouragement. Her detailed, wise and valuable comments on my every paper help me to improve my writing and logic thinking a lot. Without her effort, patience and availability during these four years, I would not have been able to complete this work. Once a teacher, always a teacher.

I would like to thank my co-supervisor Ms. **Dr Carine Le Bourvellec**, who always give me very good advices and encourage me in my work. I am very grateful to my daily supervisor Carine. Every time I proposed new idea for my topic, you always support me and encourage me to try. Your two sons are really cute and lovely.

I would like to thank Dr Agnès Rolland-Sabaté and Dr Sylvie Bureau. Agnès, thank you for introducing me into the world of polymer analysis; Sylvie, thank you for your ATR-FTIR technical help. They had always an open ear for all my questions. I appreciate the opportunity to work with them.

I would also like to thank my members of the annual PhD committee, Dr Marc Lahaye, Dr Claire Dufour and Dr Laetitia Mouls, for their prompt evaluation and comments to improve the quality of this dissertation, and also allowed me to see my work from another angle. Thank you for your invaluable suggestions and kind encouragement.

I would like to thank Prof. Jean-Paul Vincken from Wageningen University & Research and Prof. Christian Jay-Allemand from Université de Montpellier for having accepted being reviewers of this thesis and Prof. Nuno Mateus from University of Porto for evaluating my work within the PhD jury.

Acknowledgements

I also want to express my gratitude to Prof. Serge Perez from CNRS-Grenoble University and Prof. Sylvain Guyot from BIA-INRAE, thank you for all the help you have given me in the field of polysaccharides and polyphenols, respectively, and thank you for your countless effort to make article better.

Je tiens également à remercier Patrice, mon tuteur dans la vie et super collègue de bureau, pour son soutien psychologique, pour sa force d'esprit, pour sa bonne humeur, pour ses conseils et pour tout le reste. J'apprécie les quatre années pendant lesquelles vous avez pris soin de moi, et cette ligne française vous est dédiée. Merci de m'avoir invité chez vous, votre piscine et votre barbecue me manqueront.

Thanks to the whole unit of SQPOV, for their warm welcome and the friendly atmosphere. I especially thank the members of the team "Qualité et Procédés": Line, thank you for technical help on chemical analysis and your support throughout the thesis. You are like a kind grandmother. I really appreciated it. Romain, thank you for your GC-MS technical help. Caroline and Marielle, thank you for technical assistance. David, thank you for your scientific advices. Sylvaine, thank you for your safety reminder every time, and remember the little note you left me when I first came to SQPOV.

I would like to thank the team of MicroNut: Christian, Béatrice, Pascale and Marie-José, thank you for your help with the experiment. And I would also like to thanks to the secretaries and computer technicians of SQPOV, Barbara, Nelly, David and Eric, who were always there to fix any problem.

I also thank Alexandra, Carla, Weijie, Sarra, Armand, Miarka, Harish, Tanagra, Hanen, Fella, Cécile, Imed, and Thibault for some help in life and making the time in SQPOV unforgettable.

Thanks to my Chinese friends in Provence-Alpes-Côte d'Azur. Yu Jiahao (余佳浩), Liu Shouyang (刘守阳), Jin Xiuliang (金秀良), Diao Wanying (刁万英), Yang Tianchen (杨天成), Wu Haotao (吴海涛), Ju Min (巨敏), Jiang jingyi (蒋靖怡), Xue Danxia (薛丹夏), Wang Xueqiu (王雪秋), Xu Peng (徐鹏), Wang Kaiyue (王凯月), Zhao Jiantao

Acknowledgements

(赵建涛), Xu Yao (徐瑶), Wang Jingwen (王靖雯), Li Zeyu (李泽宇), Li Lingyuan (李林源), Zhang Xu (张旭), Chen Cao (陈操), thank you for your help in life and experiments, and organizing so many enjoyable activities.

I also want to thank my friends overseas, Xu Ruiyao (徐睿瑶), Feng Jilu (冯纪璐), Xu Huan (徐欢), Wang Wenzhi (王文志), Gao Chuan (高川), Wang Xiao (王晓), Zheng Yao (郑焱), Wen Zhonghang (文中行), Wu Dongmei (吴冬梅), Liu Xiaosong (刘小松), Li Jiayi (李甲乙), thank you for sharing your experience of living abroad and offering some help and welcome.

A big thanks to the Chinese Government and Ambassade de la République Populaire de Chine en République Française, thank you for the timely delivery of health packs and Chinese New Year packs for the students studying in France during COVID-19. A deep sense of the warmth of our country.

I would like to thank my master supervisor Wang Xuejin (王学进), and co-supervisor Prof. He Zhiwei (何志巍) from China Agricultural University (CAU), thank you for your help and encouragement during my master and the application of PhD position. I am so grateful for your valuable suggestion for my personal life and future career during my master and PhD. Special thanks to LC for your invaluable help and support in furthering my education.

I sincerely thank my family, especially my parents, for their encouragement and support throughout my life.

Thank you, merci & 感谢 !

THÈSE

**Nouvelles connaissances sur les interactions entre les
polysaccharides de la paroi cellulaire végétale et les
procyanidines au cours de la transformation**

THESIS

**New Insights of Interactions between Cell Wall
Polysaccharides and Procyanidins during Processing**

Xuwei LIU

SQPOV, INRAE, France, 2021

Thesis Committee

Promotor

Dr Catherine M.G.C. Renard

Directrice de Recherche-HDR, INRAE, Nantes, France

Co-Promotor

Dr Carine Le Bourvellec

Chargée de Recherche-HDR, INRAE, Avignon, France

Other Members

Dr Marc Lahaye, BIA, INRAE, France

Dr Agnès Rolland-Sabaté, SQPOV, INRAE, France

Dr Claire Dufour, SQPOV, INRAE, France

Dr Laetitia Mouls, Institut Agro | Montpellier SupAgro, France

Résumé

Les interactions entre les polysaccharides de la paroi cellulaire et les polyphénols revêtent une importance croissante au cours de la transformation et dans les systèmes alimentaires en général, et suscitent un regain d'intérêt depuis 2000. Les modifications de ces protagonistes au cours de la transformation et/ou leurs interactions sont essentielles à la nutrition globale et à la sécurité des produits alimentaires finaux. Au départ, lorsque ce sujet a été abordé dans l'équipe en 1999, la littérature était rare et dispersée, contrairement à la richesse des données sur les interactions protéines/polyphénols, concentrées notamment sur la perception des tanins et le phénomène d'astringence. Les conséquences des interactions entre les polysaccharides de la paroi cellulaire et les polyphénols ont une grande portée dans la transformation des aliments. Par exemple, elles contribuent à l'extraction sélective des polyphénols des fruits (e.g., la pomme et le raisin) lors de la fabrication des jus. La production de polyphénols non extractibles (antioxydants macromoléculaires) est également une découverte majeure. Les modifications physiques et chimiques engendrées lors de la transformation conduisent à l'émergence de nouvelles structures et de nouvelles fonctions biologiques, qui auront un impact sur les qualités organoleptiques et nutritionnelles de l'aliment. Il est donc nécessaire d'étudier les relations structure/affinité entre les polyphénols et les polysaccharides en utilisant différentes conditions externes et différentes structures intrinsèques. L'évolution des techniques de détection et d'analyse permet de créer des systèmes ou des plateformes simples qui peuvent être utilisés pour quantifier ces interactions.

Les modèles les plus étudiés d'interactions entre les polysaccharides de la paroi cellulaire et les polyphénols sont les pommes et les raisins, qui sont tous deux riches en polyphénols, notamment en tanins condensés, i.e., proanthocyanidines, qui en sont les principaux constituants phénoliques. Par ailleurs, les compositions des parois cellulaires des pommes et des raisins ont été bien étudiées et correspondent bien à ce modèle. Les interactions entre les polysaccharides pariétaux et les polyphénols sont influencées par des facteurs exogènes tels que le pH, la température, la force ionique et

la présence d'autres composants tels que les protéines, les lignines et les acides féruliques. Elles sont également façonnées par une multitude de facteurs internes aux molécules, dont les plus importants sont les propriétés physico-chimiques des partenaires: leur morphologie (surface et porosité/forme des pores), leur composition chimique (ratio des différents oses constitutifs, solubilité et composants non glucidiques) et leur architecture moléculaire (poids moléculaire, degré d'estérification, groupes fonctionnels et conformation).

Cependant, une étude systématique des effets de leur structure macromoléculaire et de leur composition fait encore défaut. Pour étudier les relations structure/propriété, et notamment pour moduler les structures des polysaccharides des parois cellulaires, des parois cellulaires de différentes sources ont été préparées et modifiées en simulant le traitement thermique des fruits et légumes (F&L). L'objectif était de disposer de parois cellulaires structurellement différentes et de pectines de différentes composition et conformation. Par conséquent, cette thèse a préalablement étudié les réponses communes et spécifiques des parois cellulaires de F&L de différentes sources après traitement thermique. Ensuite, les interactions entre les polysaccharides (i.e., les parois cellulaires, les pectines et les hémicelluloses) et les procyanidines ont été étudiée par spectroscopie UV-visible, calorimétrie de titration isotherme (ITC), chromatographie d'exclusion stérique à haute performance combinée à la diffusion de lumière laser multi-angle (HPSEC-MALLS) et modélisation moléculaire.

Les principales études sont les suivantes:

Dans la première partie (Chapitre 3), les interactions entre la structure de la paroi cellulaire, représentée par l'origine végétale, et le pH ont été explorées dans un système modèle mimant la transformation thermique des F&Ls. Les parois cellulaires isolées de pomme, de betterave et de kiwi ont été soumises à une ébullition (20 minutes) à des pH de 2.0, 3.5 et 6.0, permettant une variation indépendante de la structure de la paroi cellulaire et du pH. Dans tous les cas, les pectines ont été clairement les polysaccharides les plus impactés, mis en évidence soit par la perte d'oses neutres dans les parois cellulaires après traitement, soit par la composition des polysaccharides solubles

extraits après chauffage. Les modifications structurales ont été les moins prononcées à pH 3.5. Le squelette principal et les degrés de méthylation des pectines (notamment du kiwi) ont été dégradés de manière significative après traitement à pH 6.0 par réaction de β -élimination. Les pectines extraites à ce pH ont présenté des absorbances à 235 nm, indiquant la présence de doubles liaisons insaturées produites par β -élimination. A pH 2.0, les teneurs en arabinose ont fortement diminué (surtout dans le cas de la pomme et de la betterave), tandis que les teneurs en acide galacturonique ont été conservées, conformément à l'ordre de sensibilité à l'hydrolyse des liaisons glycosidiques. À ce pH, la teneur en acide férulique dans les parois cellulaires de la betterave a également diminué, ce qui a été attribué à la dégradation des chaînes latérales d'arabinanes contenant de l'acide férulique, qui participent à la réticulation intra et inter moléculaire des chaînes d'arabinanes. Par conséquent, le traitement à pH 2.0 a provoqué une augmentation de la linéarité des pectines (rapport molaire GalA/Rha) et diminué la ramification des zones de RG-I ((rapport molaire Ara+Gal)/Rha) dans toutes les parois cellulaires. L'hydrolyse acide et la β -élimination semblent être les mécanismes communs qui ont provoqué la perte des oses neutres constitutifs des chaînes latérales de pectines, et d'acide galacturonique, respectivement, mais leurs effets sont d'intensités différentes en fonction de l'origine des parois.

Au cours de l'étude susmentionnée, nous avons été surpris de constater que bien qu'ayant des structures et des compositions très différentes, les parois cellulaires de pomme et de betterave ont été très peu discriminées par l'analyse en composantes principales basée sur les spectres ATR-FTIR. Par conséquent, la contribution de la spectroscopie ATR-FTIR à l'étude des polysaccharides de la paroi cellulaire a également été étudiée avec soin. La composition de 58 polysaccharides de paroi cellulaire (CWP) extraits et commerciaux a été déterminée à la fois par des méthodes classiques et par la spectroscopie ATR-FTIR. Des nombres d'onde pertinents ont été mis en évidence pour chaque CWP: 1035 cm^{-1} a été attribué aux hémicelluloses contenant du xylose, 1065 et 807 cm^{-1} aux hémicelluloses contenant du mannose, 988 cm^{-1} à la cellulose, 1740 et 1600 cm^{-1} aux homogalacturonanes selon le degré de méthylation. Par

conséquent, les principaux composés de la paroi cellulaire: pectines, hémicelluloses et cellulose, ont pu être facilement déterminés par leurs bandes respectives. Cependant, certaines difficultés ont subsisté pour identifier les composants de la paroi cellulaire intacte et en particulier pour distinguer les parois cellulaires de pomme et de betterave en fonction de la présence de chaînes d'arabinanes et de galactanes. La chaîne principale d'arabinanes n'a pas donné de pics caractéristiques dans l'infrarouge moyen, tandis que la bande spécifique des galactanes à 1039 cm^{-1} a été superposée aux bandes caractéristiques des hémicelluloses. L'application de la spectroscopie ATR-FTIR pour la caractérisation des polysaccharides de la paroi cellulaire nécessite des recherches plus approfondies et devrait être utilisée en combinaison avec d'autres techniques analytiques.

Dans la deuxième partie (Chapitre 4), les parois cellulaires obtenues ci-dessus ont été utilisées pour comprendre le mécanisme d'interactions entre les polysaccharides pariétaux et les-procyanidines. Tout d'abord, les interactions ont été caractérisées entre deux procyanidines, une sous-classe de proanthocyanidines, de $\overline{DP}n$ intermédiaire et élevé (DP12 et DP39) et des parois cellulaires présentant des compositions chimiques et des structures physiques différentes. Ces parois cellulaires ont été préparées à partir de pomme, de betterave et de kiwi (deux maturités pour le kiwi, quatre modalités) et modifiées par des traitements thermiques à différents pH (douze modalités, traitement à pH 2.0, 3.5 et 6.0). L'ATR-FTIR a permis de distinguer les complexes des procyanidines et des parois cellulaires purifiées initiales. Les bandes à 1604 , 1519 et 1440 cm^{-1} pourraient être attribuées aux vibrations des liaisons C=C et C-C dans les cycles aromatiques typiques. Les bandes à 1284 et 1196 cm^{-1} pourraient être attribuées aux vibrations de déformation des groupes OH et C-O phénoliques et aux vibrations de flexion. Les isothermes de Langmuir et l'IITC ont montré que les parois cellulaires natives, de toutes origines botaniques, présentent une plus grande affinité pour les procyanidines que les parois modifiées, toutes plus pauvres en pectines. Les isothermes de liaison semblent être plus sensibles que l'IITC aux facteurs influençant les interactions, car ils peuvent prendre en compte les aspects physiques régissant les

interactions entre les procyanidines et les parois. Les parois cellulaires qui interagissent le plus avec les procyanidines se caractérisent par une forte teneur en pectines, une linéarité élevée de ces pectines et une porosité élevée. L'augmentation de la taille moléculaire des procyanidines a augmenté leur complexation avec les parois cellulaires. Pour les parois cellulaires (état insoluble), la porosité déterminée à sec semble être un facteur majeur, cependant leur porosité sous forme humide, c'est-à-dire, en suspension dans le milieu réactionnel devrait également être prise en compte.

Dans un deuxième temps le focus s'est porté sur les pectines, car il est connu que parmi les polysaccharides de la paroi cellulaire, les pectines ont la plus grande affinité pour les procyanidines. Par conséquent, une série de 12 pectines de compositions et de conformations spatiales différentes a été préparée par extraction à partir de parois cellulaires de pomme, de betterave et de kiwi (deux maturités pour le kiwi) après chauffage à pH 2.0, 3.5 et 6.0. Ces douze pectines différentes ont été caractérisées pour leurs compositions et leurs caractéristiques macromoléculaires, et ont été incubées avec des procyanidines de $\overline{DP}n$ intermédiaire et élevé (DP9 et DP79), respectivement. Les pectines ont interagit préférentiellement avec les procyanidines hautement polymérisées, à l'exception des pectines de betterave, en raison de la présence de résidus d'arabinane feruloylés qui limitent les interactions. De plus, les pectines de kiwi hautement linéaires, avec une teneur élevée en homogalacturonane et un taux de ramification plus faible, se sont liées préférentiellement aux procyanidines. La prédominance de régions homogalacturonanes et le degré de méthylation élevé sont donc apparus comme des caractéristiques structurelles clés des pectines pour une affinité élevée vis-à-vis des procyanidines, contrairement à un degré de ramification élevé.

Bien que les hémicelluloses soient en deuxième position après les pectines en termes d'affinité vis à vis des procyanidines dans les parois cellulaires, une étude détaillée de leurs interactions nous est apparue comme nécessaire du fait de leur prévalence dans les parois cellulaires. Par conséquent, dans une troisième étude, les interactions entre les hémicelluloses contenant du xylose (i.e., les xylanes, les

xyloglucanes et cinq arabinoxylyanes) et deux procyanidines (DP9 et DP39) ont également été étudiées. L'utilisation à la fois de méthodes expérimentales et computationnelles a donné des résultats convergents et complémentaires. Tout comme les pectines, les hémicelluloses ont interagit préférentiellement avec les procyanidines hautement polymérisées. Les xyloglucanes ont interagit le plus fortement avec les procyanidines contrairement aux xylanes. Les différents types d'arabinoxylyanes ont interagi quant à eux avec les procyanidines de manière similaire et avec une force intermédiaire. Ni la viscosité, ni la masse molaire, ni les chaînes latérales n'ont influencé fortement les interactions arabinoxylyanes-procyanidines.

Dans l'ensemble, ces résultats apportent des résultats précieux pour les chercheurs et l'industrie afin de mieux comprendre le lien entre la transformation des aliments et la bioaccessibilité/biodisponibilité des produits issus de la fermentation à la fois des polysaccharides pariétaux et des procyanidines par le microbiote intestinal humain. En outre, cela favorise la conception de produits issus de transformation plus rationnelles pour des aliments d'origine végétale plus sains et plus nutritifs.

Abstract

Cell wall polysaccharide-polyphenol interactions are of growing importance in the food system or during processing, and have attracted renewed interest since 2000. The modifications by processing and/or their interactions are essential to the overall nutrition and safety of the final food products. Initially, when this subject started in the team in 1999, the literature was sparse and scattered, in contrast to the wealth of data on protein/polyphenol interactions, concentrating on tannin and astringency perception. Consequences of cell wall polysaccharide-polyphenol interactions are far reaching in food processing. As an example, they contribute to the selective extraction of polyphenols from fruit (e.g., apple and grape) to juice. The production of non-extractable polyphenols (important macromolecular antioxidants) is also a major finding. Physical and chemical modifications lead to the emergence of new structures and new biological functions during processing, which would have an impact on the organoleptic and nutritional quality of the food. Therefore, it required to investigate the structure/affinity relationships between polyphenols and polysaccharides by using different external conditions and different intrinsic structures. Developments in detection and analysis techniques allow the creation of simple systems or platforms that can be used to quantify these interactions.

The most studied models of cell wall polysaccharide-polyphenol interactions are apples and grapes, both of which are rich polyphenols especially condensed tannins, i.e., proanthocyanidins that are the main phenolic constituents. Meanwhile the cell wall compositions of apples and grapes have been well studied and correspond well to this model. Various components and structures of cell wall polysaccharides and polyphenols have been observed to demonstrate common and characteristic behaviors during interactions. As previous studies highlighted, these interactions are influenced by the exogenous factors e.g., pH, temperature, ionic strength, and the presence of other components such as proteins, lignins and ferulic acids. They are also shaped by a multitude of molecular internal factors, the most important of which are the physicochemical properties of the partners: their morphology (surface area and

porosity/pore shape), chemical composition (sugar ratio, solubility, and non-sugar components), and molecular architecture (molecular weight, degree of esterification, functional groups, and conformation).

However, a systematic study of the effects of their macromolecular structure and composition is still missing. To study the structure / property relationships, we modulated the structures of cell wall polysaccharides, that is, cell walls from different sources were prepared and further modified under different conditions. By simulating F&Veg processing, the aim was to provide structurally broad and rich cell walls and different dissolved pectins. Therefore, this thesis first investigates the common and specific responses of cell walls of F&Veg from different sources under the same processing conditions. Furthermore, we describe the interactions between polysaccharides (i.e., cell walls, pectins and hemicelluloses) and procyanidins by UV-visible spectroscopy, isothermal titration calorimetry (ITC), high performance size-exclusion chromatography combined with multi-angle laser light scattering (HPSEC-MALLS) and computational simulation. The main studies are as follows:

In the first part (Chapter 3), the interactions between cell wall structure, proxied by plant origin, and pH are explored in a model system miming F&Veg processing. Cell walls isolated from apple, beet and kiwifruit are subjected to boiling (20 min) at pH 2.0, 3.5 and 6.0, allowing independent variation of cell wall structure and pH. In all cases, pectins were clearly the polysaccharides the most impacted, highlighted either from sugar loss in the modified cell walls or the composition of the extracted soluble polysaccharides after heating. The least disruptive condition is pH 3.5. The main skeleton and degrees of methylation of pectins (especially kiwifruit) are degraded significantly after treatments at pH 6.0 by β -elimination reaction. Pectins extracted at this pH had quite obvious absorbances at 235 nm, indicating the presence of unsaturated double bonds produced by β -elimination. At pH 2.0, the most marked difference concerned arabinose (especially apple and beet), while the galacturonic acid was mostly retained, in accordance to the order of sensitivity to hydrolysis of glycosidic linkages. At this pH, the content of ferulic acid in the beet cell walls was also relatively low,

which was attributed to the degradation of arabinan side-chains that contained ferulic acid, which participate in intra-/inter- molecular crosslink with arabinan chains. Therefore, pH 2.0 processing increased the pectin linearity (GalA/Rha molar ratio) and decreased the RG-I branching ((Ara+Gal)/Rha molar ratio) in all cell walls. Acid hydrolysis and β -elimination appeared to be common mechanisms that cause loss of neutral sugars, often from pectin side-chains, and galacturonic acid, respectively, but their effects are of different intensities as function of the plant origin.

During the above study, we were surprised to see that, in spite of very different structures and compositions, apple and beet cell walls were poorly discriminated by Principal Component Analysis based on ATR-FTIR spectra. Therefore, the contribution of ATR-FTIR spectroscopy to study cell wall polysaccharides was also carefully investigated. The compositions of 58 cell wall polysaccharides (CWPs) from extracted and commercial origin were determined by both classical methods and ATR-FTIR spectroscopy. Relevant wavenumbers were highlighted for each CWP: 1035 cm^{-1} was attributed to xylose-containing hemicelluloses, 1065 and 807 cm^{-1} to mannose-containing hemicelluloses, 988 cm^{-1} to cellulose, 1740 and 1600 cm^{-1} to homogalacturonans according to the degree of methylation. Therefore, the main cell wall compounds: pectins, hemicelluloses and cellulose, could be easily determined by their respective bands. However, some difficulties remain to identify intact cell wall components and in particular to discriminate cell walls of apple and beet in relation to the presence of arabinan and galactan. The main arabinan chain did not give characteristic mid-infrared peaks, while the specific band of galactan at 1039 cm^{-1} was overlapped with the bands of hemicelluloses. The application of ATR-FTIR spectroscopy for the characterization of cell wall polysaccharides requires more in-depth research and should be used in combination with other analytical techniques.

In the second part (Chapter 4), the abundant cell wall polysaccharides obtained above were used to understand cell wall polysaccharide-procyanidin interactions. First, interactions were characterized between two procyanidins, a proanthocyanidin subclass, of intermediate and high \overline{DP}_n (DP12 and DP39) and heterogeneous cell

walls (four native and twelve modified) from apple, beet and kiwifruit presenting various chemical compositions and physical structures. ATR-FTIR discriminated the complexes from the initial purified procyanidins and cell walls. Bands at 1604, 1519 and 1440 cm^{-1} could be attributed to C=C and C-C stretching bond vibrations in typical aromatic rings. Bands at 1284 and 1196 cm^{-1} could be assigned to phenolic OH and C-O group deformation vibrations and bending vibrations. Langmuir isotherms and ITC indicated that native cell walls, from all botanical origins, had a higher affinity for procyanidins than the modified ones, which were all poorer in pectins. Binding isotherms appear to be more sensitive than ITC to factors influencing interactions, as they could take into account the physical aspects of the binding. The cell walls that interact more with procyanidins were characterized by their high pectin content, high linearity of these pectins, and high porosity. Increasing the molecular size of procyanidins increased their complexation with cell walls. For cell walls (insoluble state), porosity appears to be a major factor, but their wet porosity (i.e., in suspension) should also be considered.

Second, among cell wall polysaccharides, pectins have the highest affinity for procyanidins. Therefore, a serie of 12 pectins with different compositions and spatial conformation was prepared by extraction from apple, beet and kiwifruit (two maturities for kiwifruit) cell walls after heating at pH 2.0, 3.5, and 6.0. These twelve different pectins were characterized for their composition and macromolecular characteristics, and incubated with procyanidins of intermediate and high \overline{DP}_n (DP9 and DP79), respectively. The interactions between procyanidins and twelve extracted pectins with different linearity and size are further investigated. Pectins interacted preferentially with highly polymerized procyanidins except beet pectins due to feruoylated arabinan. Moreover, highly linear kiwifruit pectins, with high homogalacturonan content and lower branching ratio bound preferentially to procyanidins. Predominance of homogalacturonan regions and high degree of methylation thus appeared key structural features of pectins for high affinity for procyanidins, while high degree of branching is detrimental.

Although hemicelluloses are second only to pectins in affinity for procyanidins in cell walls, a detailed study of their interactions missing was still. Therefore, in a third study, the interactions between xylose-containing hemicelluloses (i.e., xylan, xyloglucan and five arabinoxylans) and two procyanidins (DP9 and DP39) were also investigated. Experimental and computational methods gave congruent and complementary results on hemicellulose-procyanidin interactions. Stronger interactions with hemicelluloses were found for highly polymerized procyanidins. Xyloglucan and xylan exhibited respectively the strongest and weakest interactions with procyanidins. The different types of arabinoxylans interacted with procyanidins in a similar way and with intermediate strength. Neither viscosity, molar mass nor side-chains influenced strongly arabinoxylan-procyanidin interactions.

Overall, these findings provide valuable evidence for researchers and industry to better bridge the gap between food processing and the bioavailability of commensal microbiota fermentation products of cell wall polysaccharides and procyanidins. Further, this promotes the design of more rational processing conditions for healthier and more nutritious plant-based foods.

Acknowledgements	5
Résumé.....	11
Abstract.....	15
List of Figures.....	27
List of Tables	33
CHAPTER 1.....	39
1.1 Background	41
1.2 Motivation and Objectives	43
1.3 Contributions of the Thesis	44
1.4 Organization of the Thesis.....	47
1.5 Publications and communications	49
CHAPTER 2.....	53
2.1 Structure of cell walls and its evolution during processing.....	57
2.1.1 Cell wall polysaccharides	57
2.1.2 Processing methods	63
2.1.3 Cell wall modifications.....	66
2.1.4 Highlights and partial conclusion	71
2.2 Reactivity of flavanols: Their fate in physical food processing and recent advances in their analysis by depolymerization	76
2.2.1 Introduction	76
2.2.2 Structure and chemistry of flavanols	80
2.2.3 The effect of physical processing on flavanols	84
2.2.4 Reactivity of flavanols during processing	109
2.2.5 Recent developments in acidolysis of proanthocyanidins	117
2.2.6 Conclusions and future perspectives	126
2.3 Interactions between cell wall polysaccharides and polyphenols: Effect of molecular internal structure	132
2.3.1 Introduction	132
2.3.2 The participants in the interactions.....	135
2.3.3 Analytical methods.....	141
2.3.4 Structure-affinity relationships for cell walls and their polysaccharides.....	160
2.3.5 Polyphenol structure.....	176

Table of contents

2.3.6 The relative importance of different aspects of molecular structure	187
2.3.7 Adsorption mechanisms	187
2.3.8 Conclusions and future perspectives	193
CHAPTER 3.....	199
3.1 Modification of apple, beet and kiwifruit cell walls by boiling in acid conditions: Common and specific responses.....	205
3.1.1 Introduction	205
3.1.2 Materials and methods.....	208
3.1.3 Results and discussion.....	215
3.1.4 Conclusions	231
3.2 Revisiting the contribution of ATR-FTIR spectroscopy to characterize plant cell wall polysaccharides.....	239
3.2.1 Introduction	239
3.2.2 Materials and methods.....	241
3.2.3 Results and discussion.....	245
3.2.4 Conclusions	264
CHAPTER 4.....	269
4.1 Interactions between heterogeneous cell walls and two procyanidins: Insights from the effect of chemical composition and physical structure.....	276
4.1.1 Introduction	276
4.1.2 Material and methods	279
4.1.3 Results	283
4.1.4 Discussion	296
4.1.5 Conclusions	302
4.2 Exploring interactions between pectins and procyanidins: Structure-function relationships.....	309
4.2.1 Introduction	309
4.2.2 Materials and methods.....	312
4.2.3 Results	318
4.2.4 Discussion	330
4.2.5 Conclusions	336
4.3 Experimental and theoretical investigation on interactions between xylose-containing hemicelluloses and procyanidins	343

Table of contents

4.3.1. Introduction	343
4.3.2 Materials and methods.....	345
4.3.3 Results and discussion.....	348
4.3.4 Conclusions	364
Conclusions & Perspectives	367
Conclusions	369
Perspectives.....	372
References.....	375
Acronyms.....	429
Supplementary data.....	433

List of Figures

Figure 1.1 Outline of the experimental design of the different chapters of this thesis.....	47
Figure 2.1 The hierarchical structure, morphology and molecular structure of cellulose and its derivatives.	58
Figure 2.2 Schematic structures of hemicelluloses showing a. xyloglucan; b. xylan; c. arabinoxylan; and d. mannan.....	59
Figure 2.3 a. Schematic structure of pectin showing the homogalacturonan (HG), xylogalacturonan (XG), apiogalacturonan (AG), rhamnogalacturonan II (RG-II), and rhamnogalacturonan I (RG-I) regions; b. The types of degree of substitution groups and their distribution in HG; c. AFM imaging of pectic polysaccharides.	61
Figure 2.4 Schematic diagram of possible pectin conversion reactions in plant-based foods.	68
Figure 2.5 a. Schematic diagram illustrating the preparation methods of different types of cellulose; b. The numbering system for carbon atoms in anhydroglucose unit of cellulose; c. Chemical structures of unmodified and modified cellulose molecules.....	70
Figure 2.6 Structures of the flavanol units and oligomers: catechins, epicatechins, procyanidin B1, B2, A1, A2, A-type procyanidin trimer and procyanidin C1. (+)-Catechin and (-)-epicatechin are the two isomers often found in food plants.	81
Figure 2.7 Schematic representation of depolymerization of proanthocyanidins by nucleophiles. (A) Structures of proanthocyanidins containing procyanidin and prodelfinidin flavanol extension units and a terminal unit via C4 → C8 interflavan linkages. (B) Extension units and terminal unit are released as flavanol nucleophile adducts and free flavanols, respectively. (C) Calculation formula of mean DP of proanthocyanidins. (D) Three classic (thioglycolic acid, phloroglucinol and toluene- α -thiol/benzyl mercaptan) and one new (menthofuran: 3,6-dimethyl-4,5,6,7-tetrahydro-1- benzofuran) available nucleophilic trapping reagents.	83
Figure 2.8 Trend map of the preferential conditions for the main reactions of flavanols in aqueous solution as a function of temperatures, pH values and oxygen saturation solubility.	96
Figure 2.9 Transformation of tea catechins into major specific theaflavin by the action of polyphenol oxidase.	97
Figure 2.10 Overview of key enzymatic and chemical mechanisms of flavanols and their reactivity by food processing.	111
Figure 2.11 Coupled oxidation of the <i>o</i> -quinone of caffeoylquinic acid and flavanols.	112
Figure 2.12 Schematic model of type-I primary cell walls.....	136
Figure 2.13 Classes and chemical structures of some major polyphenols in plant foods.	139
Figure 2.14 Classification of the methods used for elucidation of cell wall polysaccharide-polyphenol interactions.	159
Figure 2.15 Schematic depiction of different aspects of internal structure that play a role in interactions between cell wall polysaccharides and polyphenols, with the relative importance of each.	161

Figure 2.16 Comparison of the adsorption of free and esterified phenolic acids on cell wall polysaccharides.	184
Figure 2.17 Different potential chemical mechanisms of interactions between cell wall polysaccharides and polyphenols.	190
Figure 2.18 Different potential physical mechanisms of interactions between cell wall polysaccharides and polyphenols. A. Effect of intrinsic solubility. B. Effects of porosity and pore shape.	191
Figure 3.1 Scheme of AISs preparation, cell walls modification and solubilized polysaccharides extraction at three pHs from apple, beet and kiwifruit.	210
Figure 3.2 Scanning Electron Microscopy showing the differences among native and three pH treatments (2.0, 3.5 and 6.0) after boiling for 20 min in apple, beet and kiwifruit cell walls.	216
Figure 3.3 Principal component analysis (PCA) of (A) Apple, beet and kiwifruit cell walls using mid-infrared spectral data between 2000 to 600 cm^{-1} and (B) score loadings of PC1 and PC2..	217
Figure 3.4 HPSEC-MALLS chromatograms (RID and DAD signals) and molar mass vs elution volume of the solubilized polysaccharides samples.	229
Figure 3.5 ATR-FTIR spectra (pre-processed with Standard Normal Variate) of commercial purified and extracted cell wall polysaccharides in solid form.	248
Figure 3.6 PCA scores scatter plots of 1) commercial and extracted pectins, 2) rhamnogalacturonan, 3) galactan, 4) arabinan, 5) mannose- containing hemicelluloses, 6) xylose- containing hemicelluloses and 7) cellulose (A), and all cell wall materials (excluding monosaccharides): 8) kiwifruit cell walls, 9) apple and beet cell walls (C). ATR-FTIR spectra in the range 1800 to 800 cm^{-1} with their PCA loading profile of components PC1 and PC2 (B) and (D).	258
Figure 3.7 Hierarchical cluster analysis dendrogram of 58 cell wall and cell wall polysaccharide and monosaccharide samples based on average ATR-FTIR spectra in the range 4000 to 600 cm^{-1} using Ward's clustering algorithm with Euclidian distance. From left to right, the groups are (i) commercial and extracted pectins; (ii) kiwifruit cell walls and RG; (iii) monosaccharides; (iv) cellulose and hemicelluloses and (v) apple and beet cell walls.	263
Figure 4.1 Principal component analysis of infrared spectra on cell walls, procyanidins and their complexes. A) Sample map; B) Loading profile of components PC1 and PC2 in the range of 4000 - 600 cm^{-1}	287
Figure 4.2 Binding isotherms for cell walls and procyanidins at pH 3.8, ionic strength 0.1 M, 25 °C.	289
Figure 4.3 Correlation matrix heatmap between carbohydrate compositions and structural characteristics of cell walls and binding properties after interaction with procyanidins.	297
Figure 4.4 HPSEC-MALLS chromatograms and molar mass vs elution volume of the pectin samples. A, B and C: AP2, AP3 and AP6, respectively; D, E and F: BP2, BP3 and BP6, respectively; G, H and I: KPR2, KPR3 and KPR6, respectively; J, K and L: KPO2, KPO3 and KPO6, respectively.	322
Figure 4.5 Heat map of the turbidity characteristics of pectin-procyanidin DP9 interactions. Absorbance	

at 650 nm after interactions in 0.1 M citrate/phosphate buffer pH 3.8 (in triplicates). (A) Variation of absorbance of pectins at different concentrations (galacturonic acid equivalent) with procyanidins DP9 (60 mM (-)-epicatechin equivalent). (B) Variation of absorbance of procyanidins DP9 ((-)-epicatechin equivalent) at different concentrations with pectins (30 mM galacturonic acid). 325

Figure 4.6 Heat map of the turbidity characteristics of pectin-procyanidin DP79 interactions. Absorbance at 650 nm after interactions in 0.1 M citrate/phosphate buffer pH 3.8 (in triplicates). (A) Variation of absorbance of pectins at different concentrations (galacturonic acid equivalent) with procyanidins DP79 (30 mM (-)-epicatechin equivalent). (B) Variation of absorbance of procyanidins DP79 ((-)-epicatechin equivalent) at different concentrations with pectins (15 mM galacturonic acid). 329

Figure 4.7 (A) High and low intrinsic viscosity pectin chains, (B) Conformations of pectin chain extended ($\text{pH} > \text{pKa}$) and compact ($\text{pH} < \text{pKa}$). 333

Figure 4.8 Schematic representation of four populations of pectins adsorption of procyanidins DP79 and the corresponding local details based on chemical composition and macromolecular characteristic data (molar mass and hydrodynamic radius). Representation of KPO2 a linear polymer chain and less branched polymer structures with KPR2 less long-chain branches, AP2 moderate RG content with long/short-chain mixture branches, and BP2 both much RG region with short-chain and long-chain branches, and some covalently bound ferulic acid. 336

Figure 4.9 HPSEC-MALLS chromatograms and molar mass vs elution volume for the hemicellulose samples..... 352

Figure 4.10 Heat map of the turbidity characteristics of interactions between hemicelluloses and procyanidins DP9/39. Absorbance at 650 nm, 25 °C, pH 3.8, 0.1 M, citrate/phosphate buffer. (A) and (C): Variation of absorbance of hemicelluloses at different concentrations (xylose equivalent, a similar concentration for xyloglucan) with procyanidins DP9/39 (60 mM epicatechin equivalent). (B) and (D) Variation of absorbance of procyanidins DP9/39 (epicatechin equivalent) at different concentrations with hemicelluloses (30 mM xylose equivalent, a similar concentration for xyloglucan: 7.5 g/L). 353

Figure 4.11 Thermogram of titration of xyloglucan with procyanidins DP39. The measurement of heat release at the top, while the molar enthalpy changes against (-)-epicatechin/xylose equivalent ratio after peak integration at the bottom..... 357

Figure 4.12 Molecular electrostatic potential maps. The optimized geometry of the five different hemicellulose compounds at the B3LYP-D3/6-31G(d,p)/SMD (water) level of theory and the molecular electrostatic potential (ESP) analysis results on 0.001 a.u. contours of the electronic density. (A): Xyloglucan, (B): AXLB (22% Ara), (C): AXMB (30% Ara), (D): AXHB (38% Ara), (E): Xylan, (F): Procyanidin B2, respectively. 361

Figure 4.13 Intermolecular interactions (isosurfaces: 0.05 a.u.) using Independent Gradient Model (IGM) analysis. The non-covalent interaction existed in procyanidin B2 and different hemicellulose compounds. Procyanidin B2-Xyloglucan (A), procyanidin B2-AXLB (B), procyanidin B2-AXMB (C), procyanidin B2-AXHB (D) and procyanidin B2-xylan (E). Blue color represented hydrogen bonding interaction, and green represented van der Waals interaction. All isosurfaces are colored according to a BGR (blue-green-red) scheme over the electron density range $-0.05 < \text{sign}(\lambda_2) \rho <$

0.05 a.u. Molecular structures were also colored based on atom g indices using IGM analysis for procyanidin B2-Xyloglucan (A'), procyanidin B2-AXLB (B'), procyanidin B2-AXMB (C'), procyanidin B2-AXHB (D') and procyanidin B2-xylan (E') colored according to their contributions to the binding. The relative importance of various atoms in inter-fragment interactions is demonstrated by color intensity. White indicates no contribution to the complexation, and atoms in brighter red contribute more strongly to the interactions. The green ovals indicate the presence of interactions. 362

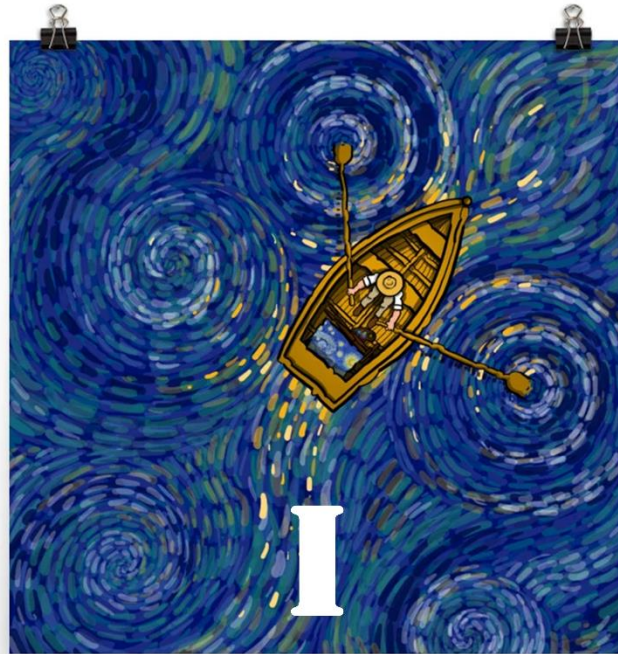
List of Tables

List of tables

Table 2.1 Impact of physical processing on the content and epimerization of flavanols.	85
Table 2.2 Comparison of the reagents and nucleophiles used to analyze proanthocyanidins.	121
Table 2.3 Comparison of the methods used to evaluate cell wall polysaccharide-polyphenol interactions.	142
Table 2.4 Binding between different polysaccharides and polyphenols: effects of structure on the interactions.	163
Table 2.5 Effects of hydroxylation, methylation, glycosylation, and esterification of phenolics on affinities for ARPP ^a /β-Glucan <i>in vitro</i>	180
Table 2.6 Evaluation of the relative importance of aspects of molecular internal structure in cell wall polysaccharide-polyphenol interactions.	188
Table 3.1 Yields (mg/g fresh weight), neutral sugars, galacturonic acid, lignin and ferulic acid compositions (mg/g cell walls) and ANOVA results of the different fruit flesh cell walls before and after modifications by boiling at different pH values.	220
Table 3.2 Yields (mg/g cell wall), neutral sugars, galacturonic acid and ferulic acid compositions (mg/g solubilized polysaccharide), macromolecular characteristics and ANOVA results of solubilized polysaccharides from the different cell walls before and after modifications by boiling at different pHs.	225
Table 3.3 The common names of cell wall components, their abbreviations and their ATR-FTIR frequencies (cm ⁻¹) determined with our spectrometer of the studied plant cell wall polysaccharides.	243
Table 3.4 Composition of extracted cell walls and pectins from fruits and vegetables and commercial purified cellulose, hemicelluloses and pectin components (mg/g dry weight, except for degree of methylation expressed in %).	246
Table 3.5 The main ATR-FTIR absorption bands, the polysaccharides in which they were detected and their tentative assignment. For polysaccharide identification (detailed in Table 3.3).	250
Table 4.1 Characteristic chemical content, sugar ratios, specific surface area and water binding capacity of the different cell wall components from apple, beet and kiwifruit.	285
Table 4.2 Binding isotherms between cell walls and procyanidins DP12 and 39: A) Apparent Langmuir parameters for binding isotherms of different cell walls with varying concentrations of procyanidin DP12 and DP39, and B) Procyanidin retention and free procyanidins characteristics at 1 g/L of procyanidins and 5 g/L of cell walls.	290
Table 4.3 Thermodynamic parameters of interactions between cell walls and procyanidins DP12 and DP39 (30 mM (-)-epicatechin equivalent) measured by Isothermal Titration Microcalorimetry.	295
Table 4.4 Chemical characteristics of the procyanidins and pectins. A) Composition (mg/g dry matter) of purified acetonetic fraction from ‘Marie Ménard’ and ‘Avrolles’ apple. B) Composition ratios and pectin region % based on the mol % quantifiable neutral sugars, galacturonic acid and pectin macromolecular characteristics.	320

List of tables

Table 4.5 Relationships between molar masses and intrinsic viscosity.....	323
Table 4.6 Thermodynamic parameters of interactions between pectins (7.5 mM galacturonic acid equivalent) and procyanidins DP9 (A) and DP79 (60 mM (-)-epicatechin equivalent) (B) measured by Isothermal Titration Microcalorimetry (ITC).....	324
Table 4.7 Changes in the molecular mass and concentrations of pectins and the degree of polymerization of procyanidins before and after interactions between pectic fractions and procyanidins DP9/79 (30/60 mM (-)-epicatechin equivalent).	328
Table 4.8 Neutral sugars composition (mg/g) and weight-average molar mass ($\times 10^3$ g/mol) of hemicelluloses.....	351
Table 4.9 Changes in molar mass of hemicelluloses and in the degree of polymerization of procyanidins before and after interactions between xylose-containing hemicelluloses and procyanidins DP9/39.	356
Table 4.10 Thermodynamic parameters of interactions measured by ITC: hemicelluloses (15 mM xylose equivalent, 7.5 mM for xyloglucan) and procyanidins DP39 (30 mM (-)-epicatechin equivalent).	358



I will build a boat
And cast it in starry lake
Sailing away from this land
The journey will be full of
thorns and whirlpools
I will keep going
I will keep sailing

CHAPTER 1.

General Introduction

1.1 Background

The first food items that come to mind for what constitutes a healthy diet are often fruit and vegetables (F&Vegs), which are colorful (De Mejia, Zhang, Penta, Eroglu, & Lila, 2020), rich in vitamins, minerals and dietary fiber (Gill, Rossi, Bajka, & Whelan, 2020), and beneficial in many aspects for health (Wallace et al., 2020). The United Nations has declared 2021 as the International Year of Fruit and Vegetables to raise awareness of the nutritional and health benefits of consuming more F&Vegs as part of a diversified, balanced and healthy diet and lifestyle (FAO, 2021). However, F&Vegs are highly perishable, therefore, their production industry faces the challenge of minimizing post-harvest losses and wastes (Esparza, Jiménez-Moreno, Bimbela, Ancín-Azpilicueta, & Gandía, 2020). Moderate processing can extend their shelf life and subsequently reduce their losses and wastes in the supply chain (Knorr & Augustin, 2021). Therefore, investing in the research of compound evolution during F&Veg processing could significantly help the industry to obtain a greater amount of F&Vegs with higher quality at a reasonable cost.

One of the important factors for health effects of F&Vegs is their richness in dietary fiber. Dietary fibers are defined as the edible parts of plants or analogous carbohydrates that are resistant to digestion and absorption in the human small intestine; this is a functional and not a chemical definition, and in fact it would be more correct to speak about a dietary fiber complex, which includes also non-carbohydrate components, of which polyphenols are a major part. Notably, cell walls and polyphenols form adducts which are important components of the dietary fiber complexes in plant-based foods.

Polyphenols are the major family, in terms of content and chemical diversity, among plant secondary metabolites, which are defined as molecules synthesized by plants and which are not directly involved in the normal growth, development, or reproduction of the organism (Manach, Scalbert, Morand, Rémésy, & Jiménez, 2004). A range of health related properties are reported for polyphenols, e.g., antioxidant (Diwani et al., 2020), cardioprotective, neuroprotective (Tu et al., 2019), immunomodulatory (Smeriglio, Barreca, Bellocco, & Trombetta, 2017), lipid lowering

and anti-obesity (Gao, Cunningham, Liu, Khoo, & Gu, 2018), antidiabetic (Campos, Jakobs, & Simon, 2020), anticancer and antimicrobial activity (X. Wu et al., 2020). Among polyphenols, proanthocyanidins are highly abundant in both raw and processed products and gained considerable attention (Gu et al., 2004). Polyphenols are located in the vacuoles of plant cells, and enzymes responsible for their degradation mostly in plastids. Many polyphenols have low to very low bioavailabilities in their native form, but there are strong evidences that they are antioxidant in the upper gut, and that their colonic fermentation metabolites play a major role in their health effects (Loo, Howell, Chan, Zhang, & Ng, 2020).

Cell walls are complex extracellular polysaccharide matrices with diverse structural and physiological roles determining the physical and nutritional properties of plant-based products (Mota, Oliveira, Marchiosi, Ferrarese-Filho, & Santos, 2018; Sila et al., 2009). However, their fate during processing is not fully understood. That is, plant origin and food processing are the two main factors influencing the presence and amount, and functional features of both cell walls and polyphenols in food products. Understanding their modification mechanisms and intrinsic changes during processing would provide effective guidance for the rational design of functionalized health foods.

During food processing, the plant cells de-compartmentalize under shearing and/or thermal treatment. Polyphenols are released from vacuoles, and can spontaneously and quickly bind to the cell walls through hydrogen bonds or hydrophobic interaction. Chemical compositions and structure of these components and their matrix interactions are some food-related factors that can hamper the bioaccessibility, bioavailability, and bioefficacy of bioactive compounds, e.g., proanthocyanidins, and that can be counteracted by food processing (Ribas-Agustí, Martín-Belloso, Soliva-Fortuny, & Elez-Martínez, 2018). Therefore, there is a growing appreciation of the importance of interactions between cell walls and proanthocyanidins in the food matrix. Moreover, their interactions are favorable rather than detrimental when considering the whole picture and the whole gut. However, at a fundamental level, the mechanisms that drive these interactions are still not fully understood. An improved understanding of the

molecular mechanisms that drive interactions between cell walls and proanthocyanidins may allow us to better establish a bridge between food processing and the bioavailability of colonic fermentation products from both cell walls and antioxidant polyphenols, which could lead to the development of new guidelines for the design of healthier and more nutritious foods.

1.2 Motivation and Objectives

In plant-based food systems (such as fruits, vegetables, and grains), secondary metabolites (e.g., polyphenols) and macromolecules (e.g., proteins and polysaccharides) coexist in distinct and strictly separated parts of the plant cells. How are these major components modified during processing, and how does this influence polyphenol / cell wall interactions?

Concerning polyphenols, proanthocyanidins, i.e., oligo- and polymeric flavan-3-ols, were used because they are the main class of polyphenols in foods, having been estimated to account for about half of polyphenol intake by Humans. They are also characterized by their strong affinity for plant cell walls, which is modulated by their size (degree of polymerization) and the nature of their structural units. Structure / affinity relationships have been studied notably for procyanidins, a subclass of proanthocyanidins composed of (+)-catechin and (-)-epicatechin constitutive units (see §2.2 and 2.3).

Major knowledge gaps were identified concerning the structure / affinity relationships for the polysaccharides. This concerned notably the lack of systematic information on the effect of native pectin's structural features (both composition and spatial conformation) on their interaction with procyanidins. There was also surprisingly little data on hemicelluloses. At the cell wall scale, it was not possible to ascertain whether chemical or physical factors are most important, and how they interact.

To understand the structure/property relationships of plant cell walls and their components, a better knowledge of the effects of processing on the whole cell walls is required. The first steps of cell wall modification during processing, which involve the

endogenous pectinases and their synergies, have been extensively studied as a function of temperature and pressure. Moreover, many studies also describe texture loss of plant tissues after enzyme inactivation or thermal processing, but each concerns a single plant material at its natural pH (from 3.0 to 6.5), while pH is known to have a major impact notably on pectin degradation. Different plant sources with their natural pH values may have specific responses to processing, and common responses may occur at distinct extents. However, it is difficult from the existing literature to ascertain whether these different responses are due to the structure of the cell walls or to the conditions during F&Veg processing (see §2.1). Notably, the natural internal pH is known to be a major driver for the degradation of polysaccharides, and primarily of pectins. Therefore, it is important to obtain a clear picture differentiating between the effects of the cell wall structure and the pH conditions during F&Veg processing.

Except for single components, such as the cell walls, which would be modified during overripening or processing, various phenomena occur such as adsorption, oxidation, solubilization, and migration, leading to the emergence of new structures and new biological functions. As an example, the interactions between cell walls and polyphenols may also occur during food processing, which modify their structure and composition, thereby affecting their bioefficacy or modulating susceptibility to gut microbiota. However, the knowledge of the influence of different types of cell walls (plant origin or processing modification) on the interactions is still lacking. Therefore, this thesis seeks to study the systematic variation of cell wall structural features thus allows to better understand polyphenol affinity and may pave the way to anticipate the variability of retention of polyphenols in different F&Vegs.

1.3 Contributions of the Thesis

This thesis investigates several related topics concerning cell wall modifications and their interaction with procyanidins. Cell wall-proanthocyanidin interactions can be mediated by their morphology, chemical composition and molecular architecture, that is, their porosity, the characteristics of their constitutive pectins, such as side-chains and branching ratios, degree of esterification, functional groups, molecular weight, and

conformation. What happens when these influencing factors are placed in the same cell wall-proanthocyanidin interaction system? Do they act as antagonists or synergists? This remains to be elucidated, by systematically investigating the impact of cell wall and pectin structure on the interactions, using botanical origins (i.e., apple, beet and kiwifruit), maturity modifications and processing (i.e., heating at pH 2.0, 3.5 and 6.0) and evolutions of cell walls to generate structural variation. These materials are then used in the establishment of cell wall-proanthocyanidin associations. The contributions of these topics are listed and explained in detail below.

1. Common and specific responses to cell wall modification: Plant-based foods are commonly processed, e.g., cooking and canning, before being consumed to improve palatability and for microbiological stability. In order to be able to investigate the structure / property relationships, the structure needs to be modulated. Therefore, cell walls from different sources were prepared and further modified under different conditions. This simulated F&Veg processing and provided different cell walls and different solubilized pectins for the next step. Therefore, we explored the interactions between cell wall structures, proxied by plant origin (i.e., apple, beet and kiwifruit), and pH (i.e., 2.0, 3.5 and 6.0) in a model system miming F&V processing, i.e., heating at 100 °C during 20 min. Our aim was to identify whether common chemical mechanisms (i.e., β -elimination and acid hydrolysis) or specific cell wall composition and structure had a higher impact on the cell wall susceptibility to degradation. The galacturonic acid, neutral sugar composition and degree of methylation of all cell walls and extracted pectins were determined by chemical analysis. Lignin, procyanidin, ferulic acid and acetic acid content were also measured. The surface topography of the cell walls was visualized using scanning electron microscopy (SEM). The extent of degradation of solubilized pectins was studied using HPSEC-MALLS. This part improved the understanding of structure/processing relationships and pointed out important differences concerning the behavior of individual species.

2. Cell wall-procyanidin interactions: Their interactions are an important guide to the encapsulation and controlled release of active compounds, their subsequent

respective digestive behavior, and as a consequence human health. In order to define the structure/property relationship of both cell walls and procyanidins, native and modified cell walls from apple, beet and kiwifruit with unique chemical composition, molecular architecture and physical structure were prepared and used as well as two procyanidins fraction of DP12 and DP39 from apple fruits. The cell wall sugar ratios based on their chemical compositions were calculated, and specific surface area and water binding capacity were determined. ATR-FTIR rapidly and sensitively detected the presence of procyanidins in cell wall-procyanidin complexes. Their interactions were quantified using Langmuir isotherms, as well as isothermal titration calorimetry to measure thermodynamic changes caused by non-covalent binding. All these factors interact with each other to influence the interactions. Systematic studies of interactions between biomacromolecules allows to better establish a bridge between food processing and the binding/retention of bioactive substances in food products.

3. Pectin-procyanidin interactions:

Of all cell wall polysaccharides, pectins have the highest affinity for proanthocyanidins. Interactions with proanthocyanidins has been studied using pectins of different commercial origins (apple or citrus) or with pectin structural units. Higher affinities were recorded for citrus pectins or for highly methylated homogalacturonans, while type I rhamnogalacturonans with different side-chains, or arabinans had lower affinities. However, there is little systematic information on the effect of native pectin's structural features, e.g., molar mass, size, proportion of branching, length and content of homogalacturonan (HG), HG / rhamnogalacturonan (RG) ratio and degrees of methylation and acetylation, on their interaction with proanthocyanidins. Therefore, interactions of twelve different pectins with procyanidins of DP9 and DP79 were studied. Their interactions were characterized by aggregates formation using UV-visible spectroscopy and by isothermal titration calorimetry. The pectin macromolecular characteristics before and after interactions were determined by size-exclusion chromatography coupled with multi-angle laser light scattering and viscometric detections to better understand the selectivity of their interactions with

procyanidins. This part can provide the structural foundation for selectivity of interactions at a molecular-level.

4. Hemicellulose-procyanidin interactions: The abundance of data on pectin-polyphenol interactions, but surprising little data on hemicelluloses, motivated a specific study on interactions between procyanidins and hemicelluloses. Moreover, the corresponding knowledge, i.e., the combined study of computational and experimental investigation (UV-visible, ITC and HPSEC-MALLS) of intra and intermolecular interactions, is limited. Therefore, this part evaluated the nature of the interactions between xylose-containing hemicelluloses, having either a xylan or a glucan backbone, and procyanidins.

1.4 Organization of the Thesis

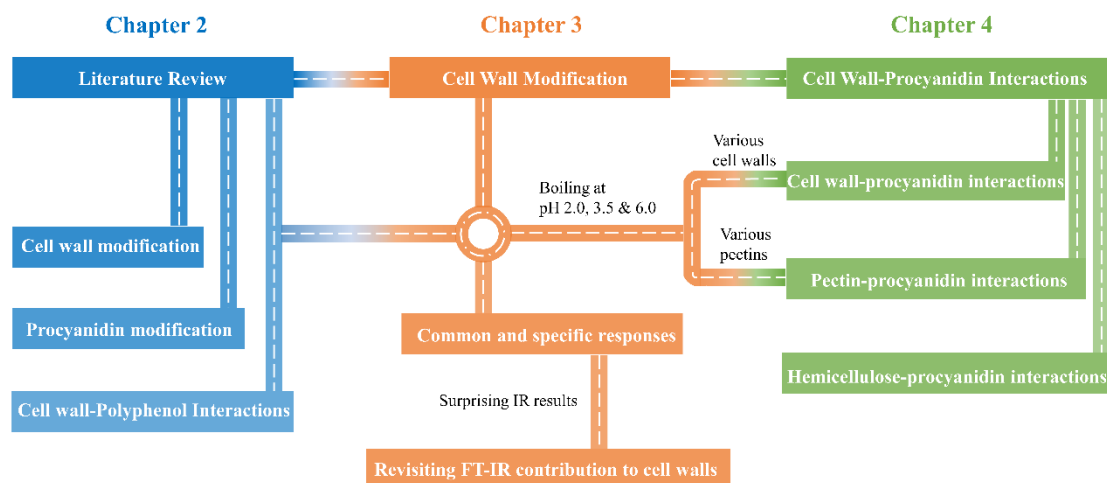


Figure 1.1 Outline of the experimental design of the different chapters of this thesis.

Chapter 1 introduces the main elements and innovations of the research work in this thesis, as well as the structural arrangement. The schematic structure and general experimental design of the different chapters of this thesis are shown in [Figure 1.1](#).

If we have seen further, it is by standing on the shoulders of giants. Therefore, we first need to understand the chemical and structural characteristics of the major components in plants, e.g., cell walls and polyphenols, and their modifications during F&Veg processing. Existing knowledge and gaps concerning the interactions between these components then need to be explored. In the **Chapter 2**, we will first describe the

different compounds of the plant cell wall: i) the description of its structure as well as its constituent elements (e.g., pectins, hemicelluloses and cellulose) with a focus on its evolution during maturity and/or overripening and processing (§ 2.1); ii) then the polyphenols by detailing the flavanols (§ 2.2), and their fate in physical food processing and recent advances in their analysis by depolymerization (X. Liu, Le Bourvellec, Guyot, & Renard, 2021); iii) we will end this discussing and reviewing of previous works by presenting the interactions between cell wall polysaccharides and polyphenols with a comprehensive overview of the effects of their macromolecular structure and composition (§ 2.3) (X. Liu, Le Bourvellec, & Renard, 2020).

Chapters 3 & 4 address the two core elements: modifications and interactions during F&Veg processing. **Chapter 3** discusses the modification of different fruit and vegetable cell walls (from apple, beet and kiwifruit) during thermal processing in acid conditions. It highlights their common and specific responses under the same mechanisms (acid hydrolysis and β -elimination reaction) (§ 3.1). The work of this section can be found in the publication (X. Liu, Renard, Rolland-Sabaté, Bureau, & Le Bourvellec, 2021b). However, the native and modified cell walls issued from different species and extraction conditions were not well separated by ATR-FTIR, especially for apple and beet cell walls. Therefore, based on § 3.1, we explored the limitations of ATR-FTIR spectroscopy in the characterization of plant cell wall polysaccharides, i.e., some polysaccharides can not be unambiguously identified (§ 3.2). The work of this section can be found in the publication (X. Liu, Renard, Bureau, & Le Bourvellec, 2021b).

Chapter 4 focuses on cell wall polysaccharide-procyanidin interactions. We will use the native and modified cell walls, and extracted pectins from § 3.1 to study their interactions with low and high polymerized procyanidins. It begins by focusing on the interactions between 16 natives and modified heterogeneous cell walls and 2 procyanidins. The effects of chemical composition and physical structure have been systematically studied (§ 4.1). The work of this section can be found in the publication (X. Liu, Renard, Bureau, & Le Bourvellec, 2021a). Among cell wall polysaccharides, pectins have the highest affinity for procyanidins. Therefore, § 4.2 presents the

interactions between 12 pectins and 2 procyanidins to explore the effect of native pectin's structural features (both composition and spatial conformation) on their interactions with procyanidins. The work of this section can be found in the publication (X. Liu, Renard, Rolland-Sabaté, & Le Bourvellec, 2021). However, even if pectins have the highest affinity for procyanidins, cell walls still have an affinity for procyanidins, after pectins removal meaning that hemicelluloses and cellulose may interact with procyanidins. However, little data are available on hemicellulose-procyanidin interactions. Therefore, § 4.3 discusses the interactions between xylose-containing hemicelluloses and procyanidins by experimental and computational methods.

Finally, the **Conclusion** brings together these results to highlight the insights gained and envisage future works.

1.5 Publications and communications

List of publications

Liu, X., Le Bourvellec, C., & Renard, M. G. C. C. (2020). Interactions between cell wall polysaccharides and polyphenols: Effect of molecular internal structure. *Comprehensive Reviews in Food Science and Food Safety*, 19(6), 3574-3617.

Liu, X., Renard, M. G. C. C., Rolland-Sabaté, A., Bureau, S., & Le Bourvellec, C. (2021). Modification of apple, beet and kiwifruit cell walls by boiling in acid conditions: Common and specific responses. *Food Hydrocolloids*, 112, 106266.

Liu, X., Renard, M. G. C. C., Rolland-Sabaté, A., & Le Bourvellec, C. (2021). Exploring interactions between pectins and procyanidins: Structure-function relationships. *Food Hydrocolloids*, 113, 106498.

Liu, X., Renard, M. G. C. C., Bureau, S., & Le Bourvellec, C. (2021). Revisiting the contribution of ATR-FTIR spectroscopy to characterize plant cell wall polysaccharides. *Carbohydrate Polymers*, 262, 117935.

Liu, X., Le Bourvellec, C., Guyot, S. & Renard, M. G. C. C. (2021). Reactivity of flavanols: Their fate in physical food processing and recent advances in their analysis by depolymerization. *Comprehensive Reviews in Food Science and Food Safety*, 20(5), 4841-4880.

Liu, X., Renard, M. G. C. C., Bureau, S., & Le Bourvellec, C. (2021). Interactions between heterogeneous cell walls and two procyanidins: Insights from the effects of chemical composition and physical structure, *Food Hydrocolloids*, 121, 107018.

Liu, X., Li, J., Renard, M. G. C. C., Rolland-Sabaté, A., Perez, S., & Le Bourvellec, C. (2021). Experimental and theoretical investigation on interactions between xylose-containing hemicelluloses and procyanidins. (In preparation for submission)

Participation in international congresses

Liu, X., Renard, M. G. C. C., Rolland-Sabaté, A., Bureau, S., & Le Bourvellec, C. Modification of apple, beet and kiwifruit cell walls by boiling in acid conditions: Common and specific responses. *3th Symposium on Fruit and Vegetable Processing*, November, 2020, Avignon, France. (Oral presentation)

Liu, X., Renard, M. G. C. C., Rolland-Sabaté, A., & Le Bourvellec, C. New Insights of Pectin-Procyanidin Interactions: Structure/Function Relationships, *30th Conference on phenols*, July 2021, Turku, Finland. (Oral presentation)

Liu, X., Renard, M. G. C. C., Rolland-Sabaté, A., Bureau, S., & Le Bourvellec, C. Modification of cell walls of apple, red beet and kiwifruit by heating in acid conditions: common and specific responses. *15th Cell wall meeting*, July 2019, Cambridge, United Kingdom. (Poster presentation)

Liu, X., Le Bourvellec, C., & Renard, M. G. C. C., Interactions between cell walls and polyphenols, *16th Summer Course Glycosciences*, June 2021, organized by the Graduate School VLAG, Wageningen University and Research, University of Groningen & Leiden University Medical Center, Wageningen, The Netherlands. (Poster presentation)

Other online courses, seminars or conferences attended

Large deformations, *GDR SLAMM Workshop*, June 18th, 2021, organized by the CNRS and INRAE, France.

7th Portuguese Young Chemists Meeting (7th PYChem), 19-21 May 2020, supported by Instituto Politécnico de Bragança, Universidade de Aveiro, Centro de Química da Universidade do Minho & Sociedade Portuguesa de Química, Bragança, Portugal.

Webinar, *Rheology and Food structuring & destructuring*, March 18th, 2021, organized by Marco Ramaioli (INRAE-SayFood) & Guy Della Valle (INRAE-BIA), France.

Bridging high-tech, food-tech and health: Consumer-oriented innovations, *34th EFFoST International Conference 2020*, 10-12 November 2020, hosted by Technion, Israel.



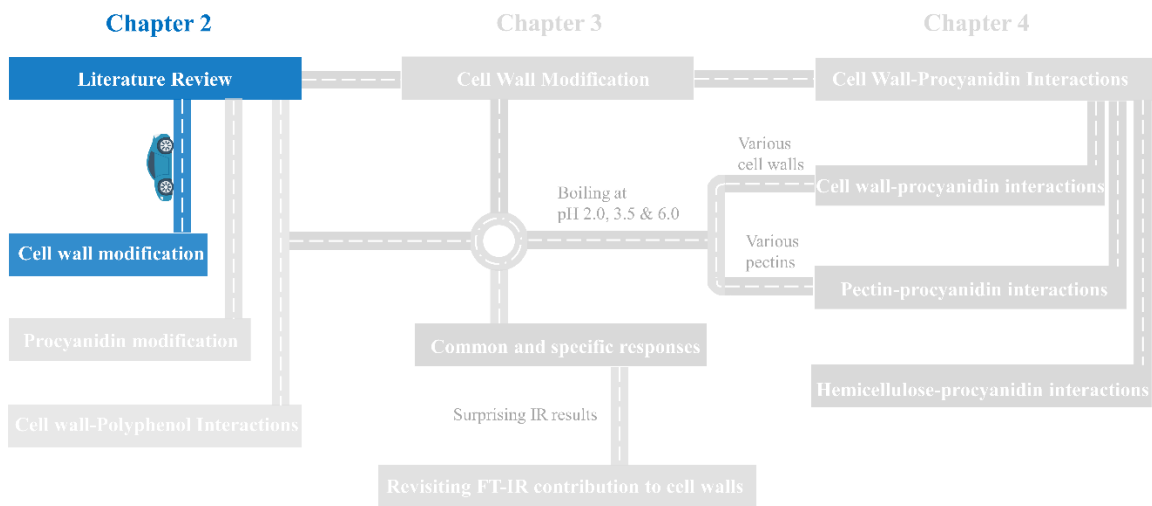
To do good research
Need enough accumulation
And always be on the way
Stand on the shoulders of giants
for the possibilities
to be ENDLESS

CHAPTER 2.

Literature Review

Section 2.1

Structure of cell walls and its evolution during processing



2.1 Structure of cell walls and its evolution during processing

2.1.1 Cell wall polysaccharides

Plant cell walls are complex polysaccharide matrices with diverse structural and physiological roles. The primary plant cell wall is essential for strength, growth and development of the plant. In edible tissue cell wall is also of major importance for texture. In higher plants, the plant cell wall predominantly consists of pectins, hemicelluloses and cellulose. Different plant taxa have differences in cell wall composition and structure. As an example, type I primary walls are widespread in dicotyledons and nongrass monocotyledons; they are rich in pectins and contain about equal amounts of cellulose and cross-linking xyloglucans, with various minor amounts of arabinoxylans, glucomannans, and galacto-glucomannans. Type II primary walls are found in cereals and grasses, they contain cellulose microfibrils of the same structure as those of the Type I wall, but glucuronoarabinoxylans are the principal polymers that interlock the microfibrils (Carpita & Gibeaut, 1993; Vogel, 2008). As this thesis focuses on cell walls in F&Vegs, the basic model discussed here will be the Type I primary cell wall.

2.1.1.1 Cellulose

Cellulose is an insoluble biopolymer, most involved in the primary and secondary wall network. It is used in many areas such as food, biomaterials, paper, and pharmaceutical industries due to its unique structure and properties (e.g., biocompatible, renewable, non-toxic and environmentally friendly) (Klemm, Heublein, Fink, & Bohn, 2005). The elucidation of the polymeric structure of cellulose can be traced back to the pioneering work of Hermann Staudinger in 1920. [Fig. 2.1](#) illustrates hierarchical structure, morphology, and molecular structure of cellulose and their derivatives (X. He et al., 2021). The molecular construction of cellulose is produced from repeating β -D-anhydroglucopyranose units that are covalently bound between the equatorial group of the C4 carbon atom and the C1 carbon atom via acetal functions (β -1,4-glycosidic bonds). In cellulose, the two consecutive glucose molecules orient themselves relative

to each other in a 180 ° rotation, forming the basic building block, cellobiose (Kroon-Batenburg & Kroon, 1997). Cellulose chains are linked to each other through hydrogen bonds or Van der Waals forces, forming crystalline microfibrils. The chemical stability of the cellulose molecule depends on the sensitivity to hydrolytic attack of the β -1,4-glycosidic bonds between the glucose repeating units.

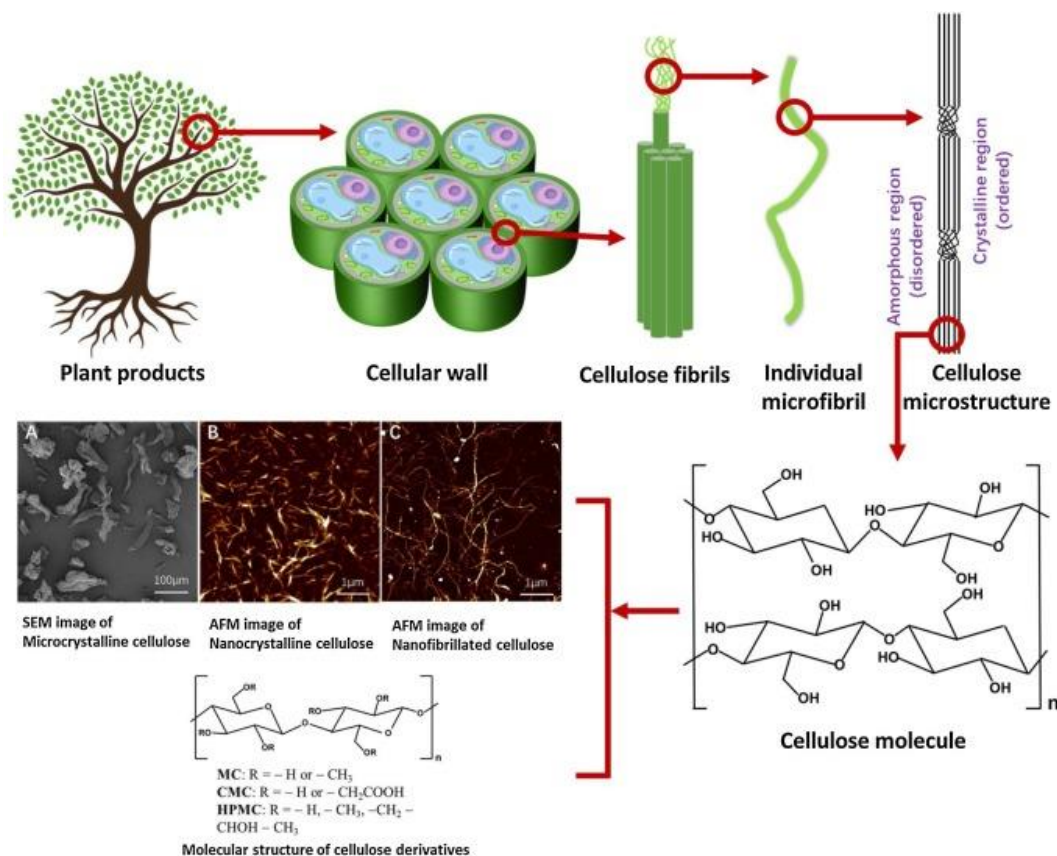


Figure 2.1 The hierarchical structure, morphology and molecular structure of cellulose and its derivatives (Adapted from He et al. (2021)).

2.1.1.2 Hemicelluloses

Hemicelluloses include non-cellulosic and non-pectic polysaccharides of the plant cell wall, of which they are the second major polysaccharide fraction. The main hemicelluloses in eudicots are xyloglucans, xylans and mannans. They are heterogeneous polymers with a linear structure and short side-chains. They are defined as polysaccharides whose backbone is composed of β -(1,4)-D-pyranose residues. Hemicellulose molecules bind tightly to the surface of cellulose microfibrils through hydrogen bonds. They represent around 20 to 40% of the dry weight of cell wall material of plants.

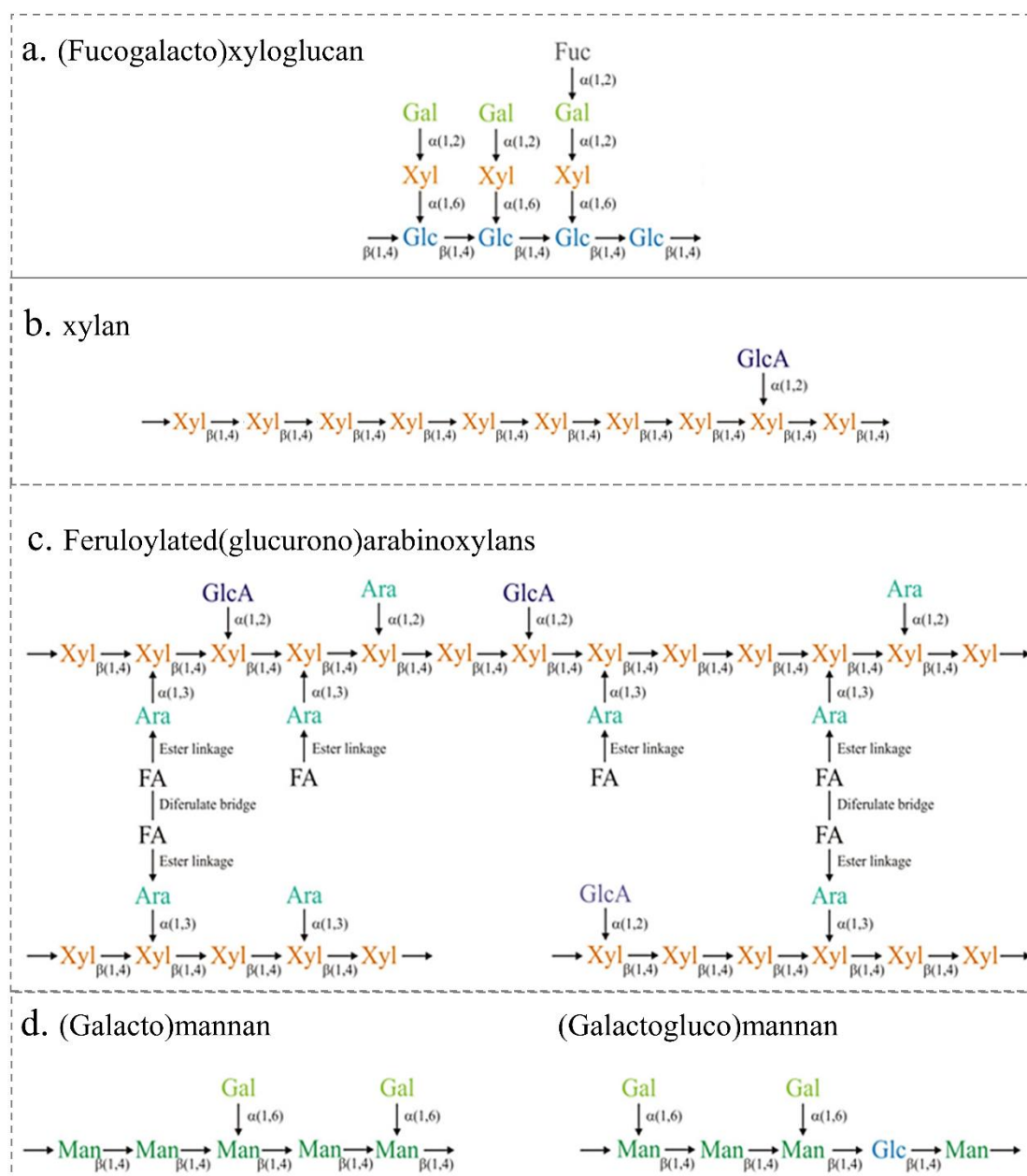


Figure 2.2 Schematic structures of hemicelluloses showing a. xyloglucan; b. xylan; c. arabinoxylan; and d. mannan (Adapted from Mota et al. (2018)).

Xyloglucan is the main hemicelluloses in eudicots and non-commelinid monocots, which consists of a cellulose-like backbone branched at O-6 by xylosyl residues (Pauly & Keegstra, 2016). They can further connect to galactosyl, arabinosyl and fucosyl residues, formally named fucogalactoxyloglucans (Fig. 2.2a).

Xylan is a primary hemicellulosic component in grasses, comprising of a β -1,4-linked D-xylose backbone (Fig. 2.2b) exhibiting different patterns of branching with arabinose and glucuronic acid, which are called arabinoxylans and

glucurono(arabino)xylans, respectively (Fig.2.2c). The more branched xylans are less bound to cellulose microfibrils and more soluble in water (Fry, 1988). Glucuronoarabinoxylan (GAX) may present hydroxycinnamic acids such as ferulic acid and *p*-coumaric acid, ester-linked to arabinosyl residues of the GAX structure (Oliveira et al., 2015). This association gives more rigidity to the cell walls (McNeil, Darvill, Fry, & Albersheim, 1984).

Mannans are the third most important kind of hemicelluloses. Mannans and glucomannans are the major hemicelluloses in charophytes, which comprise of β -1,4-linked mannose. When include both mannose and glucose in a non-repeating pattern, they called glucomannans and galactoglucomannans (Fig. 2.2d).

2.1.1.3 Pectins

Pectins are a family of heteropolysaccharides whose backbone consists mainly of α -(1,4)-linked D-galacturonic acid (GalA) residues with eighteen distinct monosaccharides connected to each other through twenty different linkages. Two major families of pectin structural members are normally considered: galacturonans and rhamnogalacturonan (RG) I. The galacturonan backbone may be unbranched (homogalacturonan) or branched with more or less complex side-chains. Four primary types of polymeric side-chains are generally identified, arabinans, galactans, type I arabinogalactans (AG-I) and type II arabinogalactans (AG-II) (Yapo, 2011). The linear and partially methylated and/or acetylated homogalacturonan (HG) backbone constituting the smooth pectin region is the dominating architecture accounting for ca. 60% of the total pectins (Mohnen, 2008); the hairy regions consist of highly branched RG I and RG II domains and, to a lesser extent, of xylogalacturonan (XG) and, in some aquatic plants (*Lemna*, *Zostera*), apiogalacturonan (AG) (Fig. 2.3a).

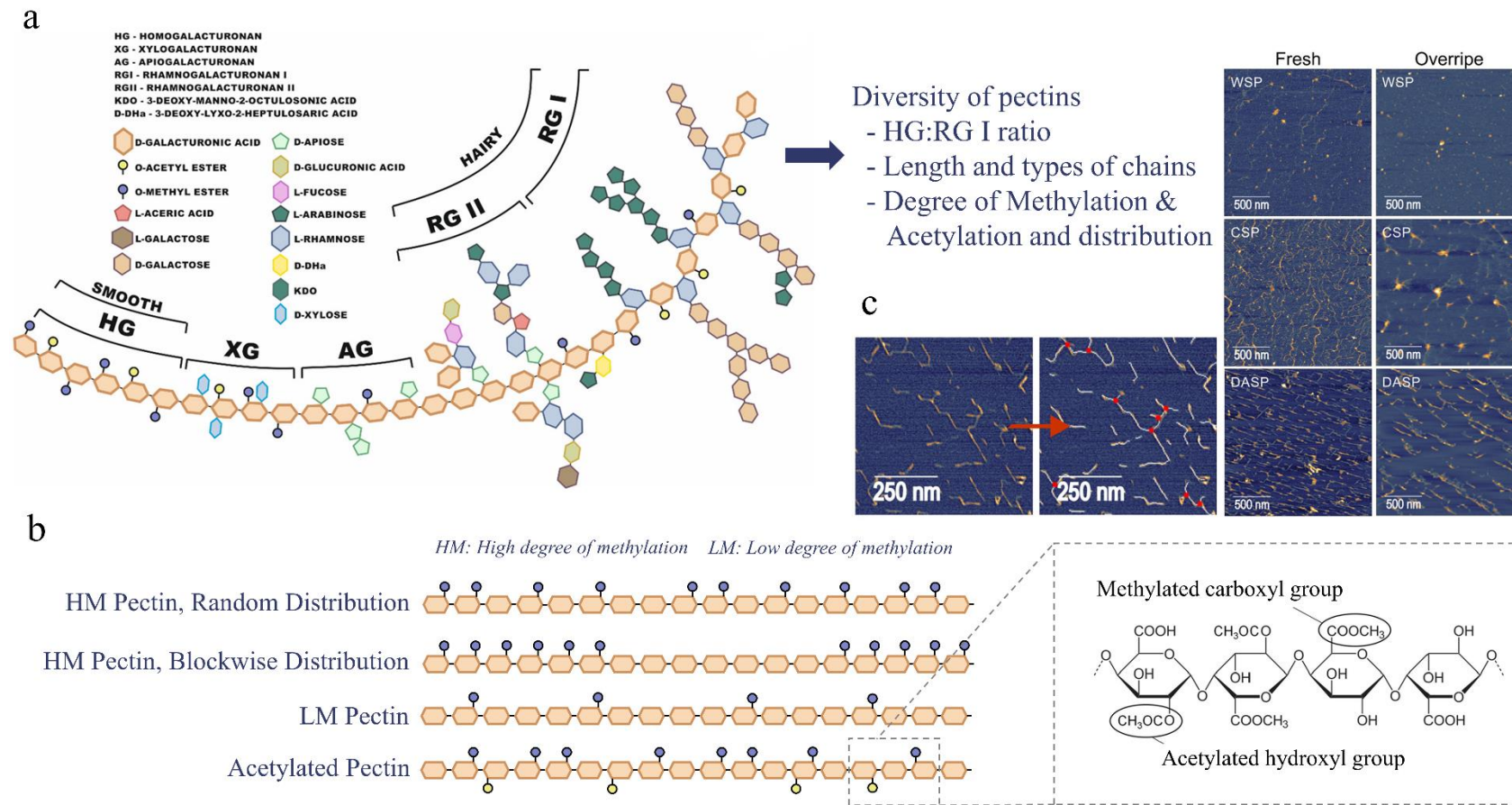


Figure 2.3 a. Schematic structure of pectin showing the homogalacturonan (HG), xylogalacturonan (XG), apiogalacturonan (AG), rhamnogalacturonan II (RG-II), and rhamnogalacturonan I (RG-I) regions; b. The types of substituting groups and their distribution in HG; c. AFM imaging of pectic polysaccharides (a. & c. adapted from Zdunek, Pieczywek, & Cybulska (2020)). Images of water soluble (WSP), calcium chelator soluble (CSP), and sodium carbonate soluble (DASP) pectins extracted from fresh apples compared with the pectin fractions obtained from overripe samples.

In HG, GalA units are normally partially methyl-esterified at C-6 and/or acetyl-esterified at O-2 and/or O-3 (Fig. 2.3b). The degree of substitution by these groups, e.g., degree of methylation (DM) and acetylation (DAc), and the distribution of esterification on homogalacturonans are critical factors for pectin functionality and property (Willats, Knox, & Mikkelsen, 2006). Degree of blockiness (DB) and the absolute degree of blockiness (DB_{abs}) can characterize the presence or absence of nonmethylesterified blocks (Daas, Meyer-Hansen, Schols, De Ruiter, & Voragen, 1999; Ralet et al., 2012). The higher DB of pectins with similar DM, the more blockwise the distribution of the methyl esters is in the pectins (Fig. 2.3b).

Pectins are highly complex macropolymers presenting a high degree of intra- and inter-molecular heterogeneity. The extractability of pectin is related to the stage of ripening and the physiological characteristics of the F&Vegs, therefore there are many parameters in the results that are difficult to control (J. Cui et al., 2021). Studying the fine structure of pectins means being able to control extraction conditions and implement adequate chemical and enzymatic tools to generate oligomers that can be separated and fully analyzed. To date, complete deconstruction of pectin into analyzable oligomers has not been achieved and non-degradable fractions whose structure is unclear always remain. These fractions, encompassing in particular side-chains, functional groups and complexes of pectin domains, should be targeted for getting a better understanding of the architecture of pectin macromolecules. The interaction between the molecular structure of the chain and the property of the solvent is not well understood in the results of the various studies. Exploring the issues raised above will lead to a better understanding of the function of pectins and help to tailor personalized pectins.

The most frequently used and/or effective methods for assessing the conformation of pectins and the persistence length are small angle X-ray diffractometry (SAXS) (Alba, Bingham, Gunning, Wilde, & Kontogiorgos, 2018), high performance size exclusion chromatography (HPSEC) combined with multi-angle laser light-scattering (MALLS) (Rolland-Sabaté, 2017), dynamic laser scattering (DLS), viscometry and

sedimentation (Morris et al., 2008). Moreover, atomic force microscopy (AFM) has been recently become a versatile tool for visualizing pectin macromolecules (Posé et al., 2019; J. Wang & Nie, 2019). As a complement to the methods above, the AFM imaging technique allows direct observation and quantitative analysis of the conformational characteristics of single molecules, e.g., their length, diameter, degree of branching, chain aggregation and supramolecular assembly (Zdunek et al., 2020). As an example, Fig. 2.3c, left show the AFM images of the "backbone" and branching points (red dots) of the sodium carbonate-extracted pectin molecule on magnified mica, and Fig. 2.3c, right show the images of water, calcium chelate and sodium carbonate soluble extracted pectin from fresh apples compared to pectin fractions obtained from overripe samples (Pieczywek, Kozioł, Płaziński, Cybulska, & Zdunek, 2020). The conformation of these molecules exhibits an extended and random coil character.

2.1.2 Processing methods

2.1.2.1 Thermal processing

Thermal processing (60 – 200 °C) is the most common method for manufacturing and preserving plant-based products. It involves a variety of methods, e.g., pasteurization, sterilization, steaming, boiling, roasting/baking and microwave heating, all of which can be applied to solid or liquid foods. This treatment is known to result in softening, which is mainly attributed to the solubilization and depolymerization of pectins involved in cell-cell adhesion. Pectinmethylesterases (PME) and polygalacturonase (PG) play a significant role here, as they allow enzymatic degradation by sequential demethoxylation and depolymerization, respectively. The control of temperature to facilitate enzyme activity enhancement and/or inactivation can be used to produce plant-based foods with specific functional properties, such as having desirable textural characteristics.

Moreover, pectin depolymerization during heating treatment can also be caused by purely chemical processes i.e., β -elimination and/or acid hydrolysis, depending on temperature, DM and pH. Heating normally accelerates the acid hydrolysis or β -elimination reaction and demethoxylation, which was assayed as a function of treatment

time, of cell wall polysaccharides (mainly for pectins) in plant-based products (Fraeye et al., 2007). With decreasing degree of methoxylation and pH, β -elimination rate constants decrease while acid hydrolysis rate constants increase. Demethoxylation rate constants are minimal at pH 3.0 and increase both at lower and higher pH. Reaction rate constants are not considerably influenced by the pattern of methoxylation. The pH of plant cell walls is generally between 3.5 and 6.0. At this pH value, β -elimination needs to be a key concern. Therefore, addition of PME into the tissue prior to processing may be beneficial, by reducing the DM of pectin and thus reducing the sensitivity to β -elimination. The optimum utilization of thermal processing will result in the production of a final plant-based product with desirable organoleptic, physico-chemical and nutritional properties.

2.1.2.2 Non-thermal processing

The potential of other emerging physical processing technology, e.g., high pressure processing, ultrasonic treatment and pulsed electric field (PEF), and their impact on food products have also been investigated (J. Liu et al., 2020; Sila et al., 2009; Van Buggenhout, Sila, Duvetter, Van Loey, & Hendrickx, 2009).

High-pressure processing is a group of techniques which can effectively destroy undesired microorganisms and reduce/inhibit enzymes activities while better maintaining the nutritional and organoleptic quality of the product. It includes high hydrostatic pressure (HHP), high pressure homogenization (HPH) and high pressure carbon dioxide (HPCD). HHP generally involves water as a medium to transfer pressure and apply pressure isostatically from all directions in a confined space (100-1000 MPa) (Bermúdez-Aguirre & Barbosa-Cánovas, 2011). HHP primarily influences non-covalent bonds (e.g., hydrogen, ionic and hydrophobic bonds) and causes changes in the structural properties of biomacromolecules such as pectins and proteins (pectin-related enzymes) (Gómez-Maqueo, Welti-Chanes, & Cano, 2020; San Martín, Barbosa-Cánovas, & Swanson, 2002). Different combinations of pressure and temperature can be modulated to achieve the desired effect on plant-based products (De Roeck et al., 2009; De Roeck, Sila, Duvetter, Van Loey, & Hendrickx, 2008). In addition, PME can

be considered a fairly pressure-resistant enzyme (>600 MPa at room temperature) (Jolie et al., 2012). When HP is combined with mild heating (up to approx. 70 °C), different effects are produced, depending on the temperature, precise pressure and PME source. HPH is a homogenization method relying on high shear during pressure release to destructure tissues and inactivate microorganisms. It is generally performed at pressures of 200-400 MPa. HPH is operated by using a piston to force the fluid through a small orifice. Rapid changes in velocity and pressure as the fluid passes through the valve create turbulence, shear and cavitation forces that can break down polymers, particles or cells in the system (Schultz, Wagner, Urban, & Ulrich, 2004). Homogenization can also impact weak bonds to change enzyme structure and catalytic activity.

Ultrasound treatment can be applied directly to liquid samples, whereas solid ones must be processed using fluids as the transmission medium (Bhargava, Mor, Kumar, & Sharanagat, 2021). The effect of ultrasound is mainly attributed to the phenomenon of acoustic cavitation, which is caused by the creation, growth and implosion of microbubbles during the propagation of high intensity ultrasound waves. Physical modifications of pectins by power ultrasound is achieved through multieffects of oriented modification and degradation of pectins, e.g., cavitation, disturbance, high shear, crushing, and stirring (Qiu, Cai, Wang, & Yan, 2019; W. Wang et al., 2018). Ultrasound may also impact the activity of pectin-degrading enzymes, by disruption of hydrogen bonds and van der Waals interactions in the polypeptide chain, leading to modification of the secondary and tertiary structure of the enzyme hence modifying its activity. The intensity, frequency, treatment time, solvent and temperature of the ultrasound combine to regulate the final result of the polysaccharide molecular modification (T. T. Chen et al., 2021; R. Cui & Zhu, 2021; M. N. Islam, Zhang, & Adhikari, 2014; Pieczywek, Koziół, Konopacka, Cybulska, & Zdunek, 2017; Pingret, Fabiano-Tixier, & Chemat, 2013). Generally, ultrasound treatment promotes solubilization of the pectins, leading to cleavage of pectin side-chains, a higher GalA content and also a reduction in the molar mass of the pectins.

PEF treatment involves the application of short pulses (μs - ms) of high voltage electric field to the samples placed between two electrodes (Arshad et al., 2021). This leads to the formation of pores in the cell membrane, causing membrane permeabilization and cell rupture, further allowing enzyme / substrate contact. Subsequently, PEF can also directly modify the microstructure and functional properties of biomacromolecules, e.g., proteins, polysaccharides and polyphenols (Giteru, Oey, & Ali, 2018). The energy released by PEF can cause ionisation of functional groups in biomacromolecules and disrupt electrostatic interactions in the macromolecular chains, leading to breakage or agglomeration of monomeric units. Therefore, the effect of PEF treatment on structural and functional properties of biomacromolecules depends upon the ability of the electric field to increase the fluctuation of a system internal energy. Electrical properties of the product, e.g., resistivity (R)/conductivity (σ), temperature, and pH are equally important. For example, PEF can induce modifications in the molecular weight, the degree of methylation, the conformation and the configuration of the pectin molecular chains (Moens, De Laet, Van Wambeke, Van Loey, & Hendrickx, 2020; Moens, Huang, Van Loey, & Hendrickx, 2021).

2.1.3 Cell wall modifications

In F&Vegs, and especially their preprocessed intermediates and processed final products, changes in functional properties (texture, rheological characteristics, juice extractability) are directly related to structural modifications of the cell wall during processing, in particular pectins (Sila et al., 2009). In addition, the primary cell wall modifications also involved in fruit ripening (Brummell, 2006) or softening (D. Wang, Yeats, Uluisik, Rose, & Seymour, 2018) are the hydrolysis of neutral sugars from pectin side-chains, depolymerization, and increased pectin and hemicellulose solubilization (Brahem, Renard, Gouble, Bureau, & Le Bourvellec, 2017). To a lesser extent changes in cellulose may occur during maturity and process (Houben, Jolie, Fraeye, Van Loey, & Hendrickx, 2011).

2.1.3.1 Pectins

The major changes in the cell walls during ripening/storage and processing are related to pectic macromolecules. Pectin constitutes a highly heterogeneous biopolymer whose functionality remains largely puzzling. Pectins can undergo transformations through endogenous and/or exogenous enzymes as well as post-harvest and/or post-processing dependent non-enzymatic conversion reactions (Sila et al., 2009). In most F&Vegs, pectin depolymerization and solubilization during processing and ripening, as well as the loss of pectin RG I side-chains decrease both cell adhesion and cell wall assembly, resulting in cell separation and thus tissue softening (Brahem, Renard, et al., 2017; Brummell & Harpster, 2001; Redgwell, Fischer, Kendal, & MacRae, 1997; Hui Wang et al., 2021). Processing causes effects on the structural and functional relationships of pectin in F&Vegs (Christiaens et al., 2016; Sila et al., 2009). In addition, structural modifications caused by processing can also lead to changes in the functionalities/properties of pectins (J. Liu et al., 2020).

Several important pectin metabolizing enzymes, e.g., HG-modifying enzymes (i.e., PG, PME and pectate lyase (PL)) and RG-I-modifying enzymes (i.e., β -galactosidase and α -arabinofuranosidase) can synergistically modify and degrade the smooth and hairy regions of pectins (Sila et al., 2009; D. Wang et al., 2018). Endogenous PG and PME in F&Vegs products are the major causes of pectin depolymerization during processing, but the intensity of enzyme activity varies as function of the botanical origin. PME catalyzes the specific demethoxylation of HG in the plant cell wall, releasing methanol and protons, and producing negatively charged carboxyl groups (Fig. 2.4). Hydrolase PG catalyzes the cleavage of α -1,4 glycosidic bonds between two nonesterified GalA residues by acid/base assisted catalysis (Fig. 2.4). The yield of enzymatic transformation depends on enzyme activity, substrate structure and accessibility, as well as on process-inducing factors (e.g., pH, salt concentration, temperature, pressure, etc.).

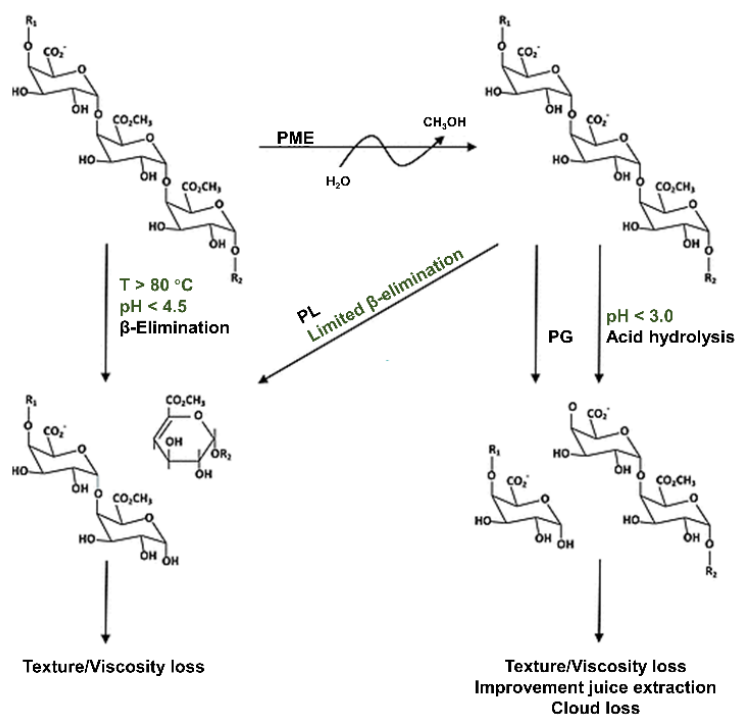


Figure 2.4 Schematic diagram of possible pectin conversion reactions in plant-based foods (Adapted from Sila et al. (2009)). PME = pectinmethyl esterase, PG = polygalacturonase, PL = pectate lyase, T = temperature.

The most common non-enzymatic transformations that occur during processing are β -elimination reaction and acid hydrolysis (Fig. 2.4). At neutral or weakly acidic pH under heating, the β -elimination reaction induced the alkali-catalyzed cleavage of the HG chain of pectins creating an unsaturated bond absorbing at 235 nm, this process occurs simultaneously with the de-esterification (Keijbets & Pilnik, 1974). This reaction is both strongly temperature and DM dependent. In addition, pectins with low DM hydrolyze more rapidly under acidic conditions ($\text{pH} < 3$) during thermal processing (Krall & McFeeters, 1998). Information on the kinetics of acid hydrolysis and β -elimination reactions is important for the elucidation and tuning of the properties of plant-based processed foods. The adverse effects of these two reactions on the product need to be mitigated further depending on the type of process type, conditions and exposure time (Fraeye et al., 2007).

2.1.3.2 Hemicelluloses

Little data can be found on the fate of hemicelluloses during F&V development or ripening and processing. A study has shown that there is no change in the molecular

weight distribution of total carbohydrate or xyloglucan content in the hemicellulose fraction during apple development (Percy, Melton, & Jameson, 1997). The molecular weight distribution of strawberry hemicellulose decreases at the onset of ripening, but no changes are seen during the swelling stage prior to ripening (Huber, 1984). Xyloglucan in kiwifruit decreases in molecular weight as it ripens (Redgwell, Melton, & Brasch, 1991). The important hemicelluloses modifications are solubility changes of the major xyloglucan, minor glucomannans and trace xylan components during fruit development and ripening (Galvez-Lopez, Laurens, Quéméner, & Lahaye, 2011). More work needs to in-depth investigate the hemicelluloses structural tailoring mechanisms and their relationships with cell development and/or processing.

2.1.3.3 Cellulose

Cellulose is least modified during maturation and food processing. Its fine variation may be observed by NMR spectroscopy or small-angle X-ray scattering (SAXS). For example, the cellulose microfibrils in the collenchyma wall become increasingly longitudinal and their walls increased greatly in thickness, and decreased in mobilities during development (D. Chen, Melton, McGillivray, Ryan, & Harris, 2019). For processing, the final morphology of the various extracted celluloses is directly influenced by their structure and properties, as well as the choice of extraction methods (chemical processes) (Fig. 2.5a). As an example, acid treatment parameters (e.g., feed to liquid ratio, concentration, temperature and reaction time) may affect the final yield and performance of cellulose nanocrystals (Mu et al., 2019). The source of cellulose should also be considered, i.e., cellulose nanocrystals with different sizes (diameter or length) can be obtained from different sources under the same acid hydrolysis conditions. However, natural extracted cellulose has some inherent drawbacks, e.g., poor solubility in common solvents, poor crease resistance, poor dimensional stability, lack of thermoplasticity and antimicrobial properties, high hydrophilicity (Roy, Semsarilar, Guthrie, & Perrier, 2009). Cellulose can be modified via chemical modification by functional groups to enhance its mechanical and interaction with other polymers, to enhance its mechanical properties, and physicochemical properties,

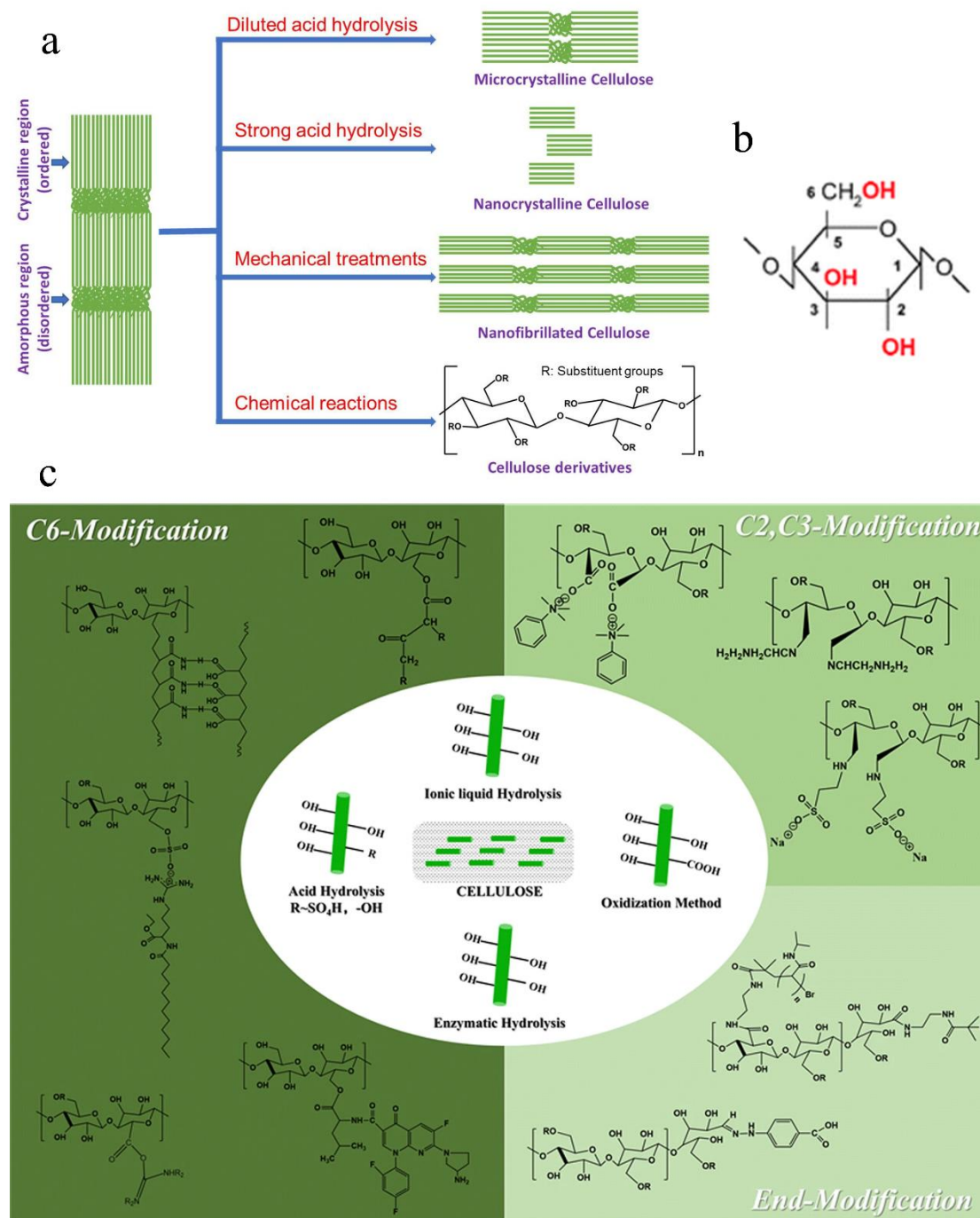


Figure 2.5 a. Schematic diagram illustrating the preparation methods of different types of cellulose (Adapted from He et al. (2021)); b. The numbering system for carbon atoms in anhydroglucose unit of cellulose; c. Chemical structures of unmodified and modified cellulose molecules (Adapted from Huang et al. (2020)).

therefore, expanding its applications (S. Huang et al., 2020). For example, the three hydroxyl groups present in each glucose residue are primarily responsible for cellulose reactivity, therefore, chemical modifications can occur at the C-6, C-2, C-3 positions and on the end of cellulose molecular chains (Fig. 2.5 b & c). The relative reactivity of

the hydroxyl groups can be expressed as OH-C6 >> OH-C2 > OH-C3 (Ali & Guthrie, 1981). Moreover, cellulose can be made more accessible by swelling, inclusion, solvent exchange, degradation or mechanical grinding treatments.

2.1.4 Highlights and partial conclusion

- The first steps of cell wall modification during processing, which involve the endogenous pectinases and their synergies, have been extensively studied as a function of temperature and pressure.

- The molecular structure of pectins is generally altered during food processing and is most sensitive to reactions in the plant cell walls. β -elimination reactions and acid hydrolysis are the major non-enzymatic reactions during thermal processing.

- β -elimination can occur at a slightly acidic pH (pH >4.5) and high temperature; it is in competition with saponification of methoxylated galacturonic acids. As temperature increases, the rate of β -elimination increases faster than that of demethylation.

- During thermal treatment in acidic conditions (pH < 3.0), acid hydrolysis occurs, leading to a loss of pectin side-chains, starting with arabinans, and a cleavage in the rhamnagalacturonan I regions of pectins.

Knowledge gaps

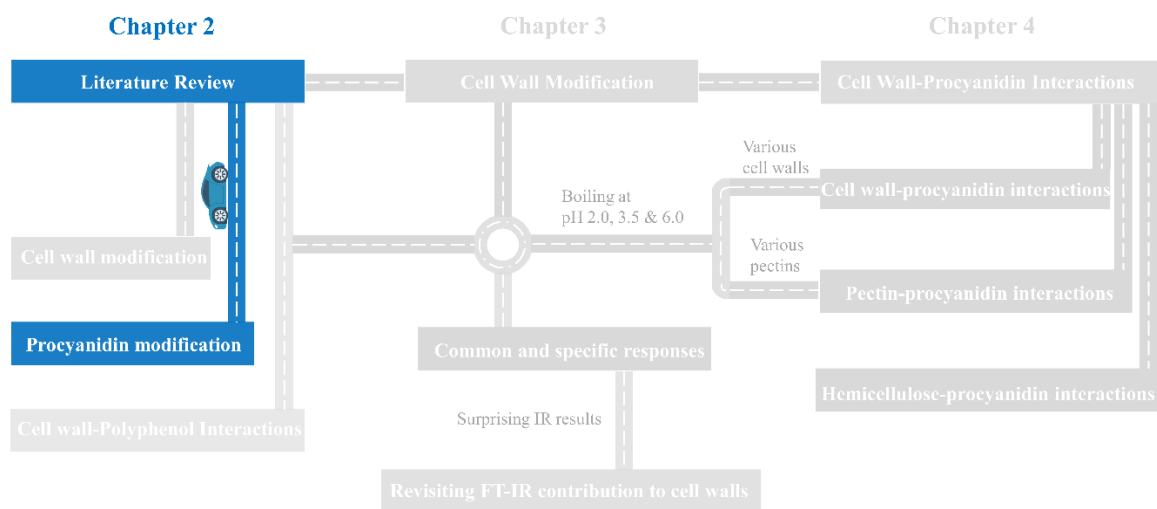
- On the one hand, it is difficult to control the action of endogenous enzymes during the first phase of heating. On the other hand, many studies describe texture loss of plant tissues after enzyme inactivation or thermal processing, but each concerns a single plant material at its natural pH.

- Effects of thermal processing on cell walls may depend on the botanical origins and their natural pH with specific and common responses to processing at distinct extents. However, it is difficult from the existing literature to ascertain whether these different responses are due to the structure of the cell walls or to the conditions during F&Veg processing.

- Many studies were done using purified pectins heated in model solutions, at different pHs, but we did not find any comparable model studies on complex cell wall matrices.

Section 2.2

Reactivity of flavanols: Their fate in physical food processing and recent advances in their analysis by depolymerization



A version of this section has been published as:

Liu, X., Le Bourvellec, C., Guyot, S. & Renard, M. G. C. C. (2021). Reactivity of flavanols: Their fate in physical food processing and recent advances in their analysis by depolymerization. *Comprehensive Reviews in Food Science and Food Safety*, 20(5), 4841-4880.

Flavanols, a subgroup of polyphenols, are secondary metabolites with antioxidant properties naturally produced in various plants (e.g., green tea, cocoa, grapes and apples); they are a major polyphenol class in human foods and beverages, and have recognized effect on maintaining human health. Therefore, it is necessary to evaluate their changes (i.e., oxidation, polymerization, degradation and epimerization) during various physical processing (i.e., heating, drying, mechanical shearing, high-pressure, ultrasound and radiation) to improve the nutritional value of food products. However, the roles of flavanols, in particular for their polymerized forms, are often underestimated, for a large part because of analytical challenges: they are difficult to extract quantitatively, and their quantification demands chemical reactions. This review examines the existing data on the effects of different physical processing techniques on the content of flavanols and highlights the changes in epimerization and degree of polymerization, as well as some of the latest acidolysis methods for proanthocyanidin characterization and quantification. More and more evidence show that physical processing can affect content but also modify the structure of flavanols by promoting a series of internal reactions. The most important reactivity of flavanols in processing includes oxidative coupling and rearrangements, chain cleavage, structural rearrangements (e.g., polymerization, degradation and epimerization), and addition to other macromolecules, i.e., proteins and polysaccharides. Some acidolysis methods for the analysis of polymeric proanthocyanidins have been updated, which has contributed to complete analysis of proanthocyanidin structures in particular regarding their proportion of A-type proanthocyanidins and their degree of polymerization in various plants. However, future research is also needed to better extract and characterize high-polymer proanthocyanidins, whether in their native or modified forms.

2.2 Reactivity of flavanols: Their fate in physical food processing and recent advances in their analysis by depolymerization

2.2.1 Introduction

Flavanols, or flavan-3-ols, are naturally found in wood, bark, cereals, seeds (cereal and oleaginous grains such as barley, sorghum and rapeseed, pulses such beans and pea, cocoa), fruits (e.g., apples, grapes, pears, apricots and blueberries), and beverages (e.g., chocolate, red wine, cider, tea and beer) (Gu et al., 2004). They are a major polyphenol class in typical human diets (Gu et al., 2004; Manach et al., 2004), with daily intakes that may reach 0.2 to 1 g, about half or more of the total polyphenol intake (Knaze et al., 2012; Zamora-Ros et al., 2016). They present several types of bioactivities (Rauf et al., 2019; Unusan, 2020), e.g., antioxidant (Diwani et al., 2020), cardioprotective, neuroprotective (Tu et al., 2019), immunomodulatory (Smeriglio et al., 2017), lipid lowering and anti-obesity (Gao et al., 2018), antidiabetic (Campos et al., 2020), anticancer and antimicrobial activity (X. Wu et al., 2020). Among polyphenols, flavanols present two distinctive features: one is that they exist not only as monomers (e.g., epicatechin and catechin), but also in the form of oligomers and polymers, e.g., proanthocyanidins; the second one is that they are usually present as aglycons, i.e., without glycosyl substituent. Their original content in food varies with several factors, e.g., variety, environment (e.g., climate, soil type, sun exposure and agricultural practices), harvest time, storage, processing technology and transportation conditions (Manach et al., 2004; Yang et al., 2019). Monomers of flavanols may be absorbed by the small intestine, and oligomers or polymers larger than the trimer are unlikely to cross the intestine epithelium in their natural form (Appeldoorn, Vincken, Gruppen, & Hollman, 2009; Serra et al., 2010; W. Tao et al., 2019). Therefore, the oligomeric and polymeric forms, i.e., proanthocyanidins, with complex structure are not absorbed in the small intestine (Donovan et al., 2002). They reach the colon, where they become fermentable substrates for the human gut microbiota, undergo biotransformation and produce low molecular weight metabolites which are readily absorbable (Déprez et al.,

2000; Loo, Howell, Chan, Zhang, & Ng, 2020). There is growing evidence that the biological effects of proanthocyanidins are mediated by these metabolites (Rodriguez-Mateos et al., 2014; Williamson, Kay, & Crozier, 2018). The absorption of these flavanols in the gut, or rather their metabolites, depends on the food source and food processing conditions which affect their structure, amount, and fermentescibility (Monfoulet et al., 2020). While bioaccessibility described as the part of flavanols soluble in the lumen, is a poor prediction of their actual absorption (Ribas-Agustí et al., 2018).

In addition to conventional physical heat treatment (baking/roasting, drying, canning, pasteurization and sterilization), novel physical methods (e.g., high-pressure processing, ultrasound treatments, pulsed electric field and radiation treatments) can be used in various stages of plant-based food processing. Processing of plant-based foods can have both positive and negative effects, e.g., enhance digestibility and palatability, improve the nutritional and functional properties, and extend the shelf life, but also lead to loss of vitamins and phenolic compounds and the formation of toxic compounds, e.g., acrylamide, furan or acrolein (van Boekel et al., 2010). The impact of food processing on flavanols has been extensively studied for wine and related alcoholic beverages such as cider or beer, due to the major impact of catechins and proanthocyanidins and their derivatives on color, taste and human health (Siyu Li & Duan, 2019; Matsui, 2015; Ottaviani, Heiss, Spencer, Kelm, & Schroeter, 2018; Soares et al., 2020). Beyond evolution during wine production and storage, there is also a growing body of knowledge on the fate of proanthocyanidins in other foods and beverages, e.g., chocolate, tea or fruits. Flavanols are also the major part of the so-called “macromolecular antioxidants”, the importance of which is more and more recognized (Aron & Kennedy, 2008; Pérez-Jiménez, Díaz-Rubio, & Saura-Calixto, 2013; Pérez-Jiménez & Saura-Calixto, 2015; Saura-Calixto & Pérez-Jiménez, 2018).

During the processing, flavanol monomers are sensitive to (bio)-chemical transformations, e.g., oxidation, polymerization, epimerization and cleavage (Ahmed & Eun, 2018; Debelo, Li, & Ferruzzi, 2020). Oxidation can actually occur through three mechanisms: direct oxidation by polyphenoloxidases (PPO), coupled oxidation by

transfer from other polyphenols, themselves substrates of PPO or peroxydases (POD), or autooxidation). The epimerization induced by food processing may have positive or negative impact on the functional properties and nutritional value of monomeric flavanols, of which (-)-epicatechin (EC) and (-)-catechin (C) are the most and least bioavailable isomers, respectively, while (+)-EC and (+)-C have a moderate bioavailability (Ellinger et al., 2020; Ottaviani et al., 2011). The main flavanol monomers in green tea are (-)-epigallocatechin gallate (EGCG), (-)-EC, (-)-epigallocatechin (EGC) and (-)-epicatechin gallate (ECG). Their corresponding *trans*-isomers produced during the tea production (gallocatechin gallate (GCG), catechin, gallocatechin (GC) and catechin gallate (CG)) are less bioavailable (Krupkova, Ferguson, & Wuertz-Kozak, 2016).

Moreover, proanthocyanidins (oligomer and polymers of flavanols) have risen as interesting biomolecules for their functional properties and bioactivities in both industrial and health-promoting applications (Neto, Santos, Oliveira, & Silvestre, 2020; W. Tao et al., 2019; Unusan, 2020). One of the principal aspects that are generally overlooked when discussing their processing and extraction is their fine structure, i.e., interflavanyl bond type (A-/B-type connectivity and proportion), hydroxylation pattern, percentage of galloylation and degree of polymerization (DP) (Aron & Kennedy, 2008; Hemingway & Karchesy, 1989). In terms of their applications, these diverse structures have a great impact on their properties. Procyanidins, i.e., proanthocyanidins composed of (-)-epicatechin and/or (+)-catechin units, with a higher DP also have a higher affinity for pectins (Watrelet, Le Bourvellec, Imbert, & Renard, 2013, 2014). Procyanidin oligomers (DP 2-6) in cocoa have higher antiobesity and antidiabetic biological activities than either flavanol monomers or procyanidin polymers (DP 7-10) (Dorenkott et al., 2014). Proanthocyanidins with higher molecular weight and A-type linkages proportions are more effective in inhibiting pancreatic lipase activity (Kimura, Ogawa, Akihiro, & Yokota, 2011). The binding affinity and precipitate capacity of proanthocyanidins for proteins (e.g., bovine serum albumin, lysozyme and alfalfa leaf protein) increase with increasing DP and percentage of galloylation and A-type linkages

(Zeller, Reinhardt, Robe, Sullivan, & Panke-Buisse, 2020). The DP of procyanidin is also positively correlated to the perception of astringency in beverages as a consequence of interactions with and precipitation of the salivary proteins (Symoneaux, Baron, Marnet, Bauduin, & Chollet, 2014; Vidal et al., 2003).

Methodological difficulties have limited studies on fine structure of proanthocyanidins. In the raw plant material, proanthocyanidins are a mixture of different molecules with a large distribution of molecular weight, bond type, galloylation and hydroxylation patterns (Mouls et al., 2014). Their quantification relies on depolymerization (acidolysis) strategies to obtain average features. To date, the most common acidolysis techniques however is thioacidolysis, which uses reagents that are unpleasant and may be toxic. Recent development of more accurate and environmentally friendly, equally effective depolymerization methods for proanthocyanidins may enable a better development of further analyzes of the structure of different proanthocyanidins, which will contribute to better understand their structure-function-activity relationships.

Some excellent reviews have summarized the fate of proanthocyanidins in production and aging of fruit-based alcoholic beverages, the mechanisms and consequences on taste and color (Fulcrand, Dueñas, Salas, & Cheynier, 2006; Siyu Li & Duan, 2019; Renard, Watrelot, & Le Bourvellec, 2017), therefore these will not be detailed here. Some reviews investigate effects of thermal and nonthermal processing on the flavonoid contents (Ahmed & Eun, 2018) and the bioaccessibility of bioactive compounds (Barba et al., 2017) in fruit and vegetables. Cheynier (2012), Khan et al. (2018) and Eran Nagar, Okun, & Shpigelman (2020) reported the changes in polyphenols during processing and digestion, respectively. However, most of the published reviews have focused on the effect of food processing on the content of various monomeric polyphenols or total polyphenols, without insight on the effects of processing on the structure and properties of flavanols, and end up diluting proanthocyanidins importance within phenolic compounds. Effects of physical processing methods on the content and structure (e.g., epimerization, DP and intra and

intermolecular bonds) of individual and polymeric flavanols (proanthocyanidins) have not been systematic discussed. Therefore, this work focusing on the changes and transformation/modification of flavanol structures and contents in processing, as well as how these changes can be evidenced by the latest depolymerization technologies (e.g., analysis after acidolysis) of proanthocyanidins. This information is essential to improve our understanding about their potential health-promoting properties and provides guidance for the precise control of flavanol structures in processing, which will be beneficial for further exploration of physical processing technologies in the precise extraction of proanthocyanidins.

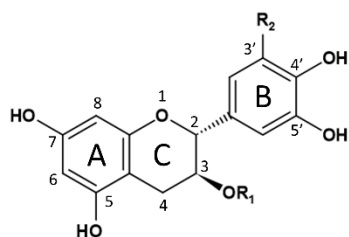
2.2.2 Structure and chemistry of flavanols

Flavanols are commonly divided in two subclasses: the monomers, also designated as “catechins” *sensu largo*, and the oligomers and polymers, which are proanthocyanidins, also known as condensed tannins. They are the second most abundant natural polyphenols after lignins. They are oligomers and polymers of flavanol units and their characteristics depend on their functional groups, hydroxyl position, galloylation, interflavanic linkages and stereochemistry (Hemingway & Karchesy, 1989; Quideau, Deffieux, Douat-Casassus, & Pouységu, 2011).

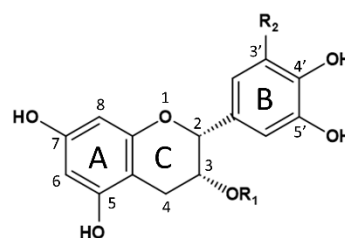
2.2.2.1 Flavanol subunit structures

Flavanols are a class of flavonoids, i.e., they have the characteristic C6-C3-C6 skeleton: two aromatic rings A and B, and one pyran ring (heterocycle C) (Aron & Kennedy, 2008). The monomers are differentiated by the stereochemistry of two asymmetric carbons C2 and C3, the presence of galloyl groups, as well as by the level of hydroxylation of ring B (Fig. 2.6). The dihydroxylated forms in C3' and C4' (catechol type of ring B) correspond to (+)-catechin and (–)-epicatechin; the trihydroxylated forms classify (+)-gallocatechin and (–)-epigallocatechin as a specific sub-group (Fig. 2.6). Catechins have *trans* orientation of the C-ring substituents, while epicatechins have *cis* orientation. The 2R configuration is the most common, while the 2S configuration is more rare (Haslam, 1989).

Flavanol monomers

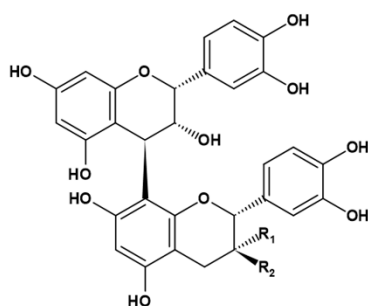


(+)-Catechins	R ₁	R ₂
(+)-Catechin	H	H
(+)-Catechin gallate	Gallyl	H
(+)-Gallocatechin	H	OH
(+)-Gallocatechin gallate	Gallyl	OH

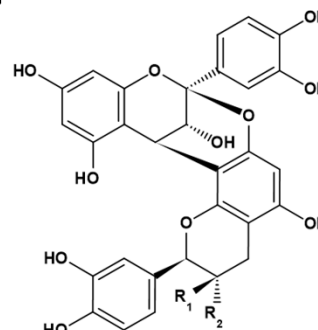


(-)-Epicatechins	R ₁	R ₂
(-)-Epicatechin	H	H
(-)-Epicatechin gallate	Gallyl	H
(-)-Epigallocatechin	H	OH
(-)-Epigallocatechin gallate	Gallyl	OH

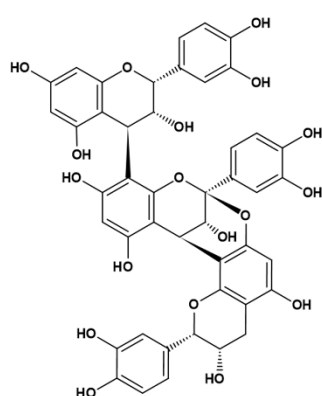
Flavanol oligomers



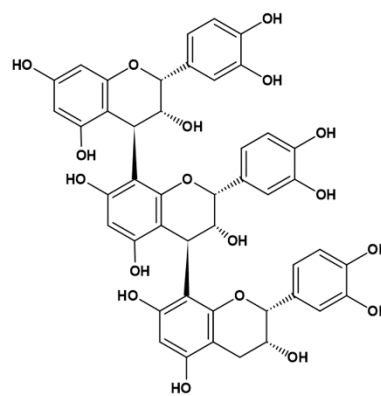
Procyanidins	R ₁	R ₂
B1	H	OH
B2	OH	H



Procyanidins	R ₁	R ₂
A1	H	OH
A2	OH	H



A-type procyanidin trimer



Procyanidin C1

Figure 2.6 Structures of the flavanol units and oligomers: catechins, epicatechins, procyanidin B1, B2, A1, A2, A-type procyanidin trimer and procyanidin C1. (+)-Catechin and (-)-epicatechin are the two isomers often found in food plants.

2.2.2.2 Interflavan linkages

The interflavan linkages between the flavanol monomers differentiate the proanthocyanidins of A-type and B-type (Hemingway & Karchesy, 1989). B-type proanthocyanidins are connected by only one C-C bonds, mainly located at C4 → C8 (Fig. 2.6) or less frequently at C4 → C6 (figure not shown). In contrast, A-type proanthocyanidins are characterized by an additional ether bond connecting carbons C2 and C7 (C2-O-C7) or C2 and C5 (C2-O-C5). Historically, the proanthocyanidin nomenclature for oligomers is based on the linkage types between these molecules. Therefore, proanthocyanidins A are dimers linked by A-type bonds, proanthocyanidins B are dimers linked by B-type bonds and proanthocyanidins C are trimers linked by B-type bonds (Fig. 2.6). For larger molecules, their size is designated by the degree of polymerization (Fig. 2.7). Proanthocyanidins composed entirely of catechin and epicatechin (procyanidins) are the most commonly reported in plants (Sieniawska, Ortan, Fierascu, & Fierascu, 2020).

2.2.2.3 Proportions of constitutive units

The constitutive units vary depending on the source, e.g., (+)-catechin and (–)-epicatechin are common in fruit and vegetables, while (+)-gallocatechin and (–)-epigallocatechin and their derivatives are commonly found in green tea, grape and wine (De Bruyne, Pieters, Deelstra, & Vlietinck, 1999; Pietta, 2000; Sakakibara, Honda, Nakagawa, Ashida, & Kanazawa, 2003). Based on hydroxylation of B-ring, proanthocyanidins with up di- and trihydroxylated units are called procyanidins (3',4' –OH) and prodelphinidins (3',4', 5' –OH), respectively (Fig. 2.7). A single polymer may contain both di- and trihydroxylated units in varying proportions, so that this division is not absolute. Procyanidins are generally considered to be the simplest, basic form of proanthocyanidins; therefore, proanthocyanidins including some trihydroxylated units are usually designed as prodelphinidins. In addition, the possible presence of gallic acid esterified structures with hydroxyl groups at C-3 in proanthocyanidins further contributes to the high structural diversity.

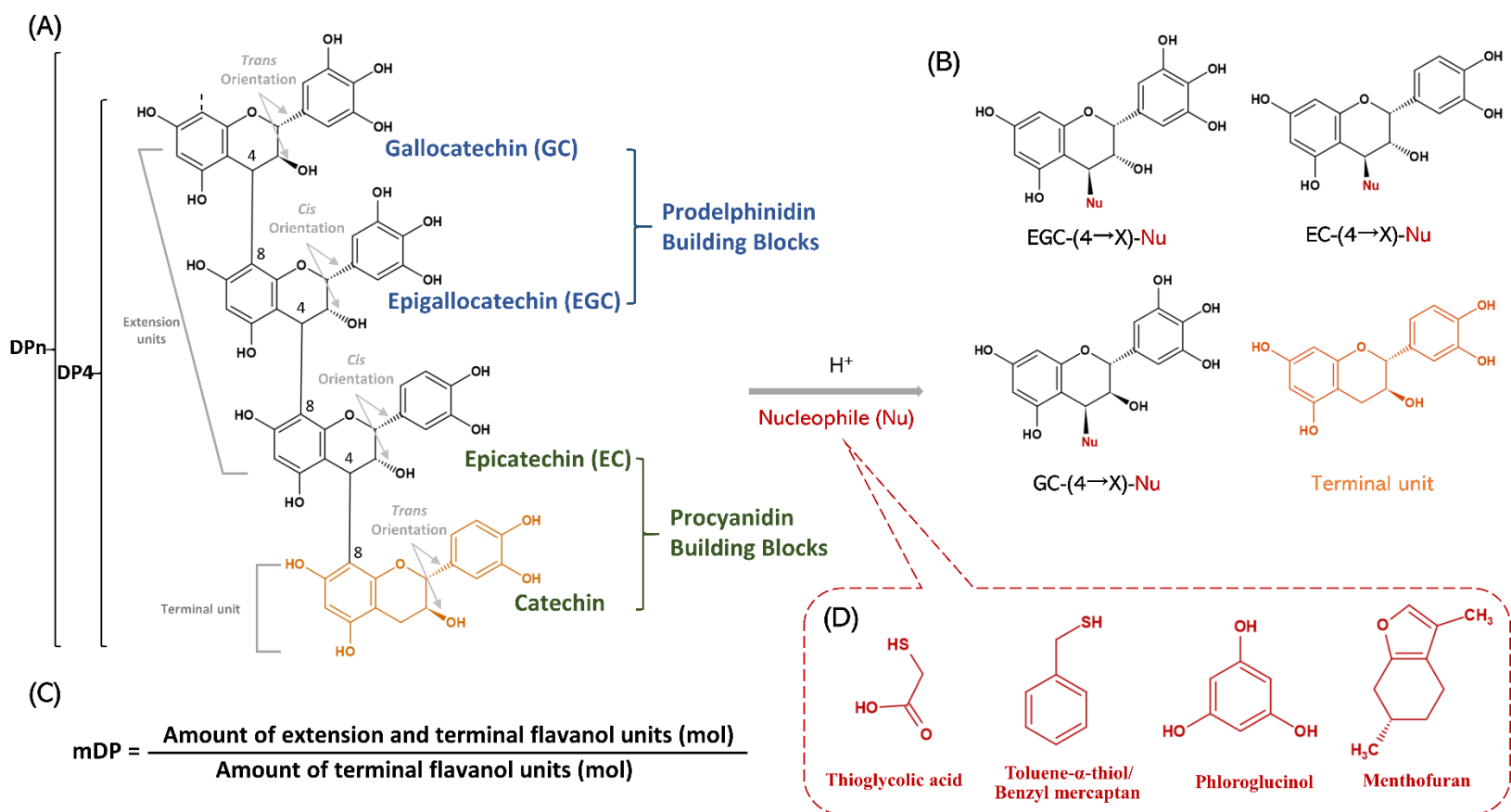


Figure 2.7 Schematic representation of depolymerization of proanthocyanidins by nucleophiles. (A) Structures of proanthocyanidins containing procyanidin and prodelphinidin flavanol extension units and a terminal unit via C4 → C8 interflavan linkages. (B) Extension units and terminal unit are released as flavanol nucleophile adducts and free flavanols, respectively. (C) Calculation formula of mean DP of proanthocyanidins. (D) Three classic (thioglycolic acid, phloroglucinol and toluene- α -thiol/benzyl mercaptan) and one new (menthofuran: 3,6-dimethyl-4,5,6,7-tetrahydro-1-benzofuran) available nucleophilic trapping reagents.

2.2.3 The effect of physical processing on flavanols

Many factors in food processing led to chemical changes in flavanols. Typically, some common and novel physical processes, e.g., drying, heating, roasting, high pressure treatment, ultrasound processing, irradiation and pulsed electric field, should be considered to evaluate their impact on the content, stability, degradation, polymerization and epimerization of flavanols. Crushing and pressing operations of raw material are also physical processing operations that highly impact flavanols, e.g., retention on the pomace and oxidation, but they have been already described in previous reviews (Aleixandre-Tudo & du Toit, 2018; Candrawinata, Golding, Roach, & Stathopoulos, 2013; Ioannou, Hafsa, Hamdi, Charbonnel, & Ghoul, 2012; Renard et al., 2011a, 2017), and will therefore not be described here. Reported effects of physical processing on the changes of flavanols are synthesized in [Table 2.1](#).

2.2.3.1 Drying

Fresh fruit and vegetables have high water activity and are easily affected by the environment. A suitable drying method can not only improve their storage stability, but also lead to higher retention of polyphenols in fruit and vegetables (McSweeney & Seetharaman, 2015). High temperature may also inactivate the enzymes, therefore preventing the oxidation and hydrolysis of polyphenols. Mild air drying (ca. 60 °C) can cause a significant reduction in catechins and procyanidin B2 of apricot fruit and puree (Madrau et al., 2009; Wani, Masoodi, Haq, Ahmad, & Ganai, 2020). As the oven temperature increases (from 60 to 100 °C), the catechin and epicatechin in dried grape skin are completely degraded and the amounts extractable in ethanol solutions also decrease (Pedroza, Carmona, Pardo, Salinas, & Zalacain, 2012). The contents of *Centella* leaf catechins are decreased by 78.1%, 65.2% and 34.9% with convective drying (45 °C), vacuum oven (45 °C) and freeze drying treatment, respectively (Zainol, Abdul-Hamid, Bakar, & Dek, 2009). The flavanols in the apple pomace decrease after drying irrespective of the variety or the presence of oxygen (Birtic, Régis, Le Bourvellec, & Renard, 2019). Oxidized flavanols may covalently links to cell wall

Literature Review

Table 2.1 Impact of physical processing on the content and epimerization of flavanols.

Samples	Product type	Processing conditions	Name of flavanols	Impact on flavanols content	Impact on flavanols epimerization/DP	References
DRYING						
Pear	Fruit	Sun-drying	(+)-Catechin, (-)-epicatechin and procyanidins	↓ (+)-Catechin, (-)-epicatechin and procyanidins.	Slight increase of procyanidins DP; pink discoloration.	(Dulcinea Ferreira et al., 2002)
Apricots (Pelese and Cafona)	Purees	Convective drying at 55 and 75 °C until dry matter to 80%	Catechin and epicatechin	↓ Epicatechin content (at higher temperature). Catechin decreases significantly at 55 °C.	Nd	(Madrau et al., 2009)
<i>Centella asiatica</i>	Leaf	Convective drying at 45°C for 48 h, vacuum oven at 45°C for 5 h, and freeze drying (-20°C/24 h; -45°C/3 days)	Catechin	↓ Catechin content.	Nd	(Zainol et al., 2009)
Apple	Fruit	Osmotic dehydration at 45°C or 60°C followed by convective drying	(+)-Catechin, (-)-epicatechin and procyanidins	↓ (+)-Catechin, (-)-epicatechin and procyanidins.	During osmotic dehydration increased loss at 60°C and increase of procyanidin DP (diffusion of small molecules to outer liquid); better retention for convective drying after osmotic step.	(Devic, Guyot, Daudin, & Bonazzi, 2010)
Grape	Skin	Convective drying at 60, 90 and 100 °C until constant moisture	Catechin and epicatechin	↓ Catechin and epicatechin contents (at higher temperature).	Nd	(Pedroza et al., 2012)
Sour Cherries	Whole fruit (pitted)	Convective drying at 50, 60 and 70 °C and vacuum-microwave drying (240, 360, 480 W)	(+)-Catechin, (-)-epicatechin and polymeric procyanidins	↓ Catechin for convective drying and vacuum-microwave drying; ↑ epicatechin for vacuum-microwave drying; ↓ epicatechin for convective drying; ↓ polymeric procyanidins.	Nd	(Wojdyło, Figiel, Lech, Nowicka, & Oszmiański, 2014)
Jujube fruit	Pulp	Convective drying at 50, 60 and 70 °C, vacuum-microwave drying (120, 480, 480-120 W), a combination of convective pre-drying (60 °C) and vacuum-microwave finish drying (480-120 W) and freeze drying	(+)-Catechin, (-)-epicatechin, dimers, trimers, tetramers and polymeric procyanidins	↑ Monomers, dimers, trimers and tetramers; ↓ polymeric procyanidins.	Nd	(Wojdyło et al., 2016)

(Continues)

Procyanidin modifications

Table 2.1 (Continued)

Samples	Product type	Processing conditions	Name of flavanols	Impact on flavanols content	Impact on flavanols epimerization/DP	References
Quince	Whole fruit (pitted)	Convective drying at 50, 60 and 70 °C, vacuum-microwave drying (120, 480, 480-120 W), a combination of convective pre-drying (50, 60 and 70 °C) and vacuum-microwave finish drying (480-120 W) and freeze drying	(+)-Catechin, (-)-epicatechin, dimers, trimers, tetramers and polymeric procyanidins	↑ Monomers, dimers, trimers and tetramers.	Nd	(Szychowski et al., 2018)
Cranberry	Juice	Freeze drying, vacuum drying at 40, 60, 80 and 100 °C and spray drying	A-type procyanidin-dimers	↓ A-type procyanidin-dimers for vacuum drying; ↑ for spray drying.	Nd	(Michalska, Wojdyło, Honke, Ciska, & Andlauer, 2018)
Saskatoon berry	Whole fruit	Freeze drying at -60°C, convective drying at 70°C, microwave-vacuum drying (480-120 W) and combined drying	(+)-Catechin, (-)-epicatechin, dimers, trimers, tetramers and polymeric procyanidins	↓ Monomers, dimers, trimers and tetramers; ↔ polymeric procyanidins	Nd	(Lachowicz et al., 2019)
Apricot	Whole fruit	Convective drying at 65 °C	Catechin and procyanidin B2	↓ Catechin and procyanidin B2	Nd	(Wani et al., 2020)
Strawberry	Whole fruit	Convective drying at 70 °C, vacuum-microwave at: 240, 360, and 480 W, freeze drying at -60°C and vacuum drying at 50°C	Catechin, procyanidin B3 and polymeric procyanidins	↑ Catechin content. ↓ Procyanidins B3 and polymers contents.	Different drying methods maintain or increase the procyanidins DP.	(Wojdyło, Figiel, & Oszmiański, 2009)
Apple	Pomace	Convective drying at 70 °C and freeze drying	(+)-Catechin, (-)-epicatechin and procyanidins	↓ (+)-Catechin, (-)-epicatechin and procyanidins.	Convective drying maintains or increases the procyanidins DP.	(Birtic et al., 2019)
Grape	Whole fruit	Convective drying at 60 °C	(+)-catechin, (-)-epicatechin, (-)-gallo catechin, (-)-epigallocatechin, (-)-epicatechin 3-gallate, procyanidin B1/B2/B4 and proanthocyanidin	↓ (+)-Catechin, (-)-epicatechin, (-)-gallo catechin, (-)-epigallocatechin, (-)-epicatechin 3-gallate, dimers and proanthocyanidin.	Convective drying increases the procyanidins DP.	(Olivati et al., 2019)
Jabuticaba	Peel and seed	Convective drying at 55, 65 and 75 °C for 14, 18 and 22 h, and freeze drying at -50 °C for 72 h	Catechin, gallo catechin, epicatechin gallate and epigallocatechin gallate	↓ Catechin, gallo catechin, epicatechin gallate and epigallocatechin gallate.	Convective drying (harsh) slightly increases the procyanidins DP.	(Pimenta Inada et al., 2020)

(Continues)

Table 2.1 (Continued)

Samples	Product type	Processing conditions	Name of flavanols	Impact on flavanols content	Impact on flavanols epimerization/DP	References
Green tea	Leaves and infusions	Convective drying at 80, 120 and 160 °C until moisture lower than 8% wet basis	(Non) Epi-structured catechins.	↓ (-)-EGC, (+)-EC and (-)-EGCG; ↑ (-)-GC and (-)-GCG; ↔ (+)-C and (-)-CG	The epimerization from the epistucture to the non-epistucture increases as the temperature increases.	(Donlao & Ogawa, 2019)
BAKING/ROASTING						
Cocoa	Beans	Roasting at 60, 70, 80, 90, 100, 110 and 120 °C	(-)-Epicatechin and (+)-catechin	↓ (-)-epicatechin; ↑ (+)-catechin	The epimerization from (-)-epicatechin to (+)-catechin occurs from 70 to 120 °C.	(Payne, Hurst, Miller, Rank, & Stuart, 2010)
Cocoa	Beans	Roasting at 140–150 °C for 20 min	(-)-Epicatechin, (+)-catechin, (-)-EGC, procyanidins B1 and B2	↓ (-)-epicatechin, (-)-EGC, procyanidins B1 and B2; ↑ (+)-catechin	The epimerization from (-)-epicatechin and procyanidin B1/B2 to (+)-catechin occurs from 140 to 150 °C.	(Mazor Jolić, Radojčić Redovnikovic, Marković, Ivanec Šipušić, & Delonga, 2011)
Cocoa	Beans	Roasting at 163°C for 12, 20 and 25 min	(-)-catechin, (+)-catechin and (-)-epicatechin	↓ (-)-epicatechin; ↑ (-)-catechin; ↔ (+)-catechin	The epimerization from (-)-epicatechin to (-)-catechin occurs at 163 °C.	(Hurst et al., 2011)
Cocoa	Beans	Roasting at 100, 120, 140, 150 and 160 °C for 30 min	(-)-Epicatechin, (+)-catechin, (-)-catechin, procyanidin B1/2/5 and procyanidin dimer1/2	↓ (-)-epicatechin, (+)-catechin and procyanidin B1/2/5; ↑ (-)-catechin and procyanidin dimer1/2	The epimerization from (-)-epicatechin, (+)-catechin and procyanidin B1/2/5 to (-)-catechin and procyanidin dimer1/2 occurs from 100 to 160 °C.	(Kothe, Zimmermann, & Galensa, 2013)
Coaoa	Beans	Roasting at 125, 135 and 145 °C from 0 to 74 min	Catechin, epicatechin, epigallocatechin, gallocatechin and total proanthocyanidin	↓ Catechin, epicatechin and total proanthocyanidin; ↑ epigallocatechin and gallocatechin	High temperature-short time (145 °C, 13 min) roasting processes minimised proanthocyanidins loss. Low temperature-long time (125°C, 74 min) roasting processes maximised chain-breaking.	(Ioannone et al., 2015)
Cocoa	Beans	Roasting at 110, 120, 135 and 150 °C until 2 % moisture content	(+)-Catechin, (-)-epicatechin, procyanidin B2 and procyanidin C1	↓ (-)-epicatechin and procyanidin B2/C1; ↑ (+)-catechin	The epimerization from (-)-epicatechin and procyanidin B2/C1 to (+)-catechin and procyanidin B1 occurs from 110 to 150 °C.	(Oracz, Nebesny, & Żyżelewicz, 2015)
Cocoa	Beans	Roasting at 90, 120 and 150 °C for 30, 60 and 90 min	(-)-Catechin, (-)-epicatechin, procyanidin B2/5 and C1	↑ (-)-catechin; ↓ epicatechin, procyanidin B2/5 and C1	Typical epimerization occurs at 150 °C.	(De Taeye, Bodart, Caullet, & Collin, 2017)
Cocoa	Beans	Roasting at 100, 130, 150, 170 and 190 °C for 40 min	Catechin, (-)-epicatechin and proanthocyanidin dimers –heptamers	↓ (-)-epicatechin and proanthocyanidin dimers – pentamers; ↑ catechin and proanthocyanidin hexamers and heptamers	Above 150 °C, lower molecular weight proanthocyanidins polymerize with each other or with monomers to form larger proanthocyanidins.	(Stanley et al., 2018)
Cocoa	Beans	Roasting at 130 and 150 °C until 2 % moisture content	(+)-Catechin, (-)-epicatechin, procyanidin B1 and procyanidin B2	↑ (+)-catechin and procyanidin B1; ↓ (-)-epicatechin and procyanidin B2	The epimerization from (-)-epicatechin and procyanidin B2 to (+)-catechin and procyanidin B1 occurs from 130 to 150 °C.	(Quiroz-Reyes & Fogliano, 2018)

(Continues)

Procyanidin modifications

Table 2.1 (Continued)

Samples	Product type	Processing conditions	Name of flavanols	Impact on flavanols content	Impact on flavanols epimerization/DP	References
Grape	Vine-shoots	Roasting at 180 °C for 45 min	Proanthocyanidins (dimer B1/2/4), (-)-EC, (-)-EGC, (-)-EGCG, (-)-ECG, (+)-C, (+)-GC, (+)-CG and (-)-GCG	↓ Proanthocyanidins (dimer B1/2/4), (-)-EC, (-)-EGC, (-)-EGCG, (-)-ECG, (+)-C, (+)-GC, (+)-CG and (-)-GCG	Slightly decreases the DP of proanthocyanidin.	(Cebrián-Tarancón et al., 2018)
Green tea	Leaves	Roasting at 180°C for 30 min	(-)-EC, (-)-EGC, (-)-EGCG, (-)-ECG, (-)-C, (-)-GC and (-)-GCG	Nd	Prduction of oligomeric products.	(Morikawa et al., 2019)
Large-leaf yellow tea	Leaves with stems	Roasting at 140-150 °C	(-)-EC, (-)-EGC, (-)-EGCG, (-)-ECG, (-)-C, (-)-GC and (-)-GCG	↓ (-)-EC, (-)-EGC, (-)-EGCG, (-)-ECG; ↑ (-)-GC and (-)-GCG	Roasting results in the epimerization and decomposition of catechins.	(Zhou et al., 2019)
Cocoa	Powder	Roasting at 90, 110, 130, 150, 170, 190, and 200 °C from 10 min to 50 min	Epicatechin and catechin	↓ Epicatechin (130 °C for 10 min, lowest degradation rate); ↑ catechin (130 - 200 °C for 10 min)	The maximum formation time and temperature of epimerization from epicatechin to catechin are at 170 °C for 30 min.	(Fernández-Romero, Chavez-Quintana, Siche, Castro-Alayo, & Cardenas-Toro, 2020)
THERMAL PROCESSING IN AQUEOUS SYSTEM						
Green tea	Green tea infusions	Heating at 20, 40, 80 and 100 °C for 20 min	(Non) Epi-structured catechins.	↓ Epi-structured catechins; ↑ nonepi-structured catechins	The epimerization from epicatechins to non-epicatechins occurs at 80 °C for 20 min. However, epimerization could also be observed after storing at 40 °C for several days.	(Huafu Wang & Helliwell, 2000)
Standard	(-)-EGCG solutions	Heating at 37 °C, pH 7.4 in the absence or presence of nitrogen for 24 h	(-)-EGCG and (-)-GCG	↓ (-)-EGCG; ↑ (-)-GCG	Epimerization rate constants increased with increasing oxygen levels.	(Sang, Lee, Hou, Ho, & Yang, 2005)
Pear	Fruit	Heating at 100°C up to 24h	Epicatechin and its procyanidin oligomers	Loss of monomers, decrease of procyanidins	Initial increase then decrease of DP; pink discolorations.	(Renard, 2005)
Green tea	Green tea liquors	Heating at 85, 95, 110 and 120 °C for 4 min	(-)-EC, (-)-EGC, (-)-EGCG, (-)-ECG, (-)-C, (-)-GC, (-)-CG and (-)-GCG	↓ (-)-EC, (-)-EGC, (-)-EGCG, (-)-ECG; ↑ (-)-C, (-)-GC, (-)-CG and (-)-GCG	The epimerization of catechins increases with increasing temperature (above 85 °C).	(E. S. Kim et al., 2007)
Green tea	(-)-EGCG solutions	Ambience (25 °C), incubation (40 °C), pasteurization (70–90 °C) and boiling (100 °C) in water bath	(-)-EGCG and (-)-GCG	↓ (-)-EGCG; ↑ (-)-GCG	Activation Energy from (-)-EGCG to (-)-GCG is 105 kJ/mol; from (-)-GCG to (-)-EGCG is 84 kJ/mol. The epimerization increases significantly above 98 °C.	(R. Wang, Zhou, & Jiang, 2008)

(Continues)

Literature Review

Table 2.1 (Continued)

Samples	Product type	Processing conditions	Name of flavanols	Impact on flavanols content	Impact on flavanols epimerization/DP	References
Standards	Procyanidins and catechins solutions	1 N methanolic HCl solution at 30 - 40 °C for 20 min in a water bath	Procyanidins, (+)-catechin and (-)-epicatechin	↑ Dimeric procyanidins	Depolymerization and recondensation leading to formation of dimers in presence of excess (+)-catechin or (-)-epicatechin.	(Esatbeyoglu & Winterhalter, 2010; Esatbeyoglu, Wray, & Winterhalter, 2010)
Apple	Puree	Cooking at 95 °C for 2 min	Flavanols	↓ Flavanols	The DP of procyanidins did not change from fresh fruits to puree.	(Le Bourvellec et al., 2011)
Pear and extracts	Fruit	Caning 98°C and heating at pH 2.7 to 4.0 from 234 to 662 min	Procyanidins	↓ Procyanidins	Pink reaction product was formed by procyanidin depolymerization and conversion into anthocyanin-type compounds	(Le Bourvellec et al., 2013)
Standard	(-)-Epicatechin and procyanidin B2 solutions	At 60 and 90 °C in aqueous or lipidic for 3 h	(-)-Epicatechin and procyanidin B2	↓ (-)-Epicatechin and procyanidin B2; ↑ (-)-catechin and procyanidin A2	(-)-Epicatechins and procyanidins B2 epimerization are enhanced at 90 °C and in aqueous medium.	(De Taeye, Kankolongo Cibaka, Jerkovic, & Collin, 2014)
Standard	Catechin solutions	Heating at 60 and 90 °C for 8 h	(-)-EC, (-)-EGC, (-)-EGCG, (-)-ECG, (-)-C, (-)-GC and (-)-GCG	↓ Epi-structured catechins and ↑ nonepi-structured catechins; ↓ nonepi-structured catechins and ↑ epi-structured catechins	The epimerization reaction of catechins occurs at high temperature (60 °C and 90 °C).	(Fan et al., 2016)
Standard	Procyanidin A2 solutions	Heating for 2 days at 40 °C or for 12 h at 90 °C	Procyanidin A2	↓ Procyanidin A2	Three other epimers and traces of the monomer (-)-epicatechin and of its epimer (-)-catechin are produced.	(De Taeye, Caullet, Eyamo Evina, & Collin, 2017)
Apricot	Fruit	Caning (95 °C) for 2 min and cooking (70 °C) for 20 min	(+)-Catechin and (-)-epicatechin (monomer) and procyanidins (polymers)	↓ All; partial diffusion to the syrup	The DP of procyanidins increases significantly from fresh fruits to canned products.	(Le Bourvellec et al., 2018)
Standard	(-)-GCG solutions	Heating at 40, 60, 80 and 100 °C for 6 h	(-)-EGCG and (-)-GCG	↓ (-)-GCG; ↑ (-)-EGCG	Three hours needed for the epimerization from (-)-GCG to (-)-EGCG occurs at 40 °C, and only 30 min need at high temperature (80 °C and 100 °C).	(Q. Wu, Liang, Ma, Li, & Gao, 2019)
Standard	(-)-EGCG solutions	Heating at 100 - 165 °C at high pH (7 - 8) from 0 to 1140 min	(-)-EGCG and (-)-GCG	↓ (-)-EGCG; ↑ (-)-GCG	Epimerization rate constants increased with temperature and the degree degradation rate constant is the highest at 135 °C. The rate of epimerization from EGCG to GCG is higher than that of GCG to EGCG.	(Xu, Yu, & Zhou, 2019)

(Continues)

Procyanidin modifications

Table 2.1 (Continued)

Samples	Product type	Processing conditions	Name of flavanols	Impact on flavanols content	Impact on flavanols epimerization/DP	References
IRRADIATION						
Cranberry	Syrup	γ -rays (5 kGy), stored for 6 months at 25 °C and 60% relative humidity	Proanthocyanidins	↑ Procyanidin A2 and procyanidin B isomer 1; ↔ Procyanidin B isomers 2 and 3, and prodelphinidin; ↓ Catechin	Nd	(Rodríguez-Pérez et al., 2015)
Red grape	Wine	Radiation(1.5kGy) at 25 °C	Catechin and epicatechin	↑ Catechin and epicatechin	Nd	(S. Gupta, Padole, Variyar, & Sharma, 2015)
Apple	Juice	UV-C irradiation, 0 – 240 mJ/cm ²	(-)-Catechin and (-)-epicatechin	↑ (-)-Catechin; ↓ (-)-epicatechin	Higher doses of UV-C irradiation may convert (-)-epicatechin to its corresponding epimer (-)-catechin.	(M. S. Islam et al., 2016)
Standard	Catechin solution	UV-B irradiation, 100 μ W/cm ² , 6h	(-)-EC, (-)-EGC, (-)-EGCG, (-)-ECG, (-)-C, (-)-GC, (-)-CG and (-)-GCG	↓ (-)-EC and (-)-C; ↔ (-)-EGC, (-)-EGCG, (-)-ECG, (-)-GC, (-)-CG and (-)-GCG	Epimers are only detected in the solutions of (-)-EC and (-)-C, but not of the other six catechins.	(M. Shi et al., 2016)
Green tea	Beverage	UV-C irradiation, 0 – 240 mJ/cm ²	(-)-EC, (-)-EGC, (-)-EGCG, (-)-ECG, (+)-C, (-)-GC and (-)-GCG	↑ (+)-C; ↔ (-)-EC and (-)-GCG;	UV-C irradiation may convert (-)-epicatechin to its corresponding epimers (-)-catechin and (+)-catechin.	(Vergne et al., 2018)
ULTRASOUND						
Apple	Cube	Ultrasonic at 40 °C fitted with ultrasound transducers (25 kHz, 0.1 W/cm ³ , 5- μ m wave amplitude) at 30 rpm for 45 min	(+)-Catechin, (-)-epicatechin, catechin dimers and procyanidins	↑ (+)-Catechin and (-)-epicatechin; ↓ catechin dimers and procyanidins	The mean degree of polymerization decreases	(Mieszcakowska-Fraç, Dyki, & Konopacka, 2016)
<i>C. longepaniculatum</i> leaf	Powder	Ultrasonic at 400 - 800 W	High polymeric procyanidins	Nd	The mean degree of polymerization is not changed.	(Z. Liu & Yang, 2018)
Standard	(-)-EGCG solution	42 kHz	(-)-EGCG	↔ Catechin (without oxygen); ↓ Catechin (exposure to oxygen)	In the absence of oxygen, the aqueous solution of EGCG is quite stable even when nebulised into a mist.	(Zeng et al., 2018)
Standard	Catechin solution	28 kHz, 40 Hz, 50 kHz, and 135 kHz at 0.35 W/cm ² , 50 °C for 60 min; 0.05, 0.15, 0.25, 0.35 and 0.45 W/cm ²	Catechin	↓ Catechin	The epimerization reaction of catechin occurs at 135 kHz, 50 °C for 60 min.	(Y. Zhu et al., 2018, 2020)
Grape	Wine with lees or oak chips	Ultrasonic at 400 W and 24 kHz below 30 °C	Proanthocyanidins	↑ Oligomeric proanthocyanidins; ↓ polymer	Nd	(Del Fresno et al., 2019)

(Continues)

Literature Review

Table 2.1 (Continued)

Samples	Product type	Processing conditions	Name of flavanols	Impact on flavanols content	Impact on flavanols epimerization/DP	References
HIGH PRESSURE						
Apple	Juice	400 MPa for 10 min	Catechin and procyanidin	↑ catechin and procyanidin	Nd	(Baron, Dénes, & Durier, 2006)
Standard	(-)-EGCG solutions	pH 7 and 25 °C at 200 MPa	(-)-EGCG	↓ (-)-EGCG	Nd	(Shkolnikov, Belochvostov, Okun, & Shpigelman, 2020)
Red bean	Powder	400, 500 and 600 MPa for 5 min at 25 °C	Proanthocyanidin	↓ Proanthocyanidin	Nd	(H. Lee et al., 2018)
Litchi	Juice	8 MPa for 2 min at 36°C by high-pressure carbon dioxide	(-)-Epicatechin	↓ (-)-Epicatechin	Nd	(L. Liu et al., 2015)
Grape	Red wine	600 MPa for 20 min and 500 MPa for 5 min at 20 °C	(+)-Catechin, (-)-epicatechin, procyanidin B1/2/4 and C1	↔ (+)-Catechin, (-)-epicatechin, procyanidin B1/2/4 and C1	The mean degree of polymerization increases	(Santos et al., 2016)
Grape	Red wine	500 MPa for 5 min at 20 °C and after 5 months of storage	(+)-Catechin, (-)-epicatechin, procyanidin B1/2/4 and C1	↓ (+)-Catechin, (-)-epicatechin, procyanidin B1/2/4 and C1	The mean degree of polymerization increases	(Santos et al., 2019)
Grape	Red wine	350 MPa for 10 min at 8 °C	Proanthocyanidin	Nd	The mean degree of polymerization is not changed	(Christofi, Malliaris, Katsaros, Panagou, & Kallithraka, 2020)
PULSED ELECTRIC FIELD						
Apple	Juice	450 V/cm, 10 ms, < 3 kJ/kg	(+)-Catechin, (-)-epicatechin, procyanidin B2 and procyanidins (polymer)	↓ (+)-Catechin, (-)-epicatechin, procyanidin B2 and procyanidins (polymer)	Enzymatic oxidation reduces the content of flavanols and increases their oxidised derivatives.	(Turk, Baron, & Vorobiev, 2010)
Apple	Juice	1000 V/cm, 200 Hz, 100 μs, 46 kJ/kg	(+)-Catechin, (-)-epicatechin, procyanidin B1 and B2, and procyanidins (polymer)	↓ (+)-Catechin, (-)-epicatechin, procyanidin B2 and procyanidins (polymer)	Enzymatic oxidation reduces the content of flavanols.	(Turk, Billaud, Vorobiev, & Baron, 2012)
Apple	Juice	650 V/cm, 200 Hz, 23.2 ms, 32 kJ/kg (with sodium fluoride)	(+)-Catechin, (-)-epicatechin, procyanidin B2 and procyanidins (polymer)	↑ (+)-Catechin, (-)-epicatechin and procyanidin B2; ↔ procyanidins (polymer)	Avoiding enzymatic oxidation can increase the content of flavanols oligomers. Procyanidins and their mean degree of polymerization were not sensitive to PEF.	(Turk, Vorobiev, & Baron, 2012)
Grape	Paste	400 Hz, 7.4 kV/cm, 20 μs	Catechin and epicatechin	↑ Catechin and epicatechin	Nd	(López-Giral et al., 2015)
Grape	Pomace	1.2 kV/cm, 18 kJ/kg energy input and extraction temperature (20 °C < T < 50 °C)	Catechin, epicatechin, procyanidin B1 and trimer C1	↓ Catechin; ↑ epicatechin, procyanidin B1 and trimer C1	Nd	(Brianceau, Turk, Vitrac, & Vorobiev, 2015)

(Continues)

Procyanidin modifications

Table 2.1 (Continued)

Samples	Product type	Processing conditions	Name of flavanols	Impact on flavanols content	Impact on flavanols epimerization/DP	References
Grape	Wine	5 kV/cm, 0.5 Hz, 1ms, 48 kJ/kg	Proanthocyanidins	↑ Proanthocyanidins	The mean degree of polymerization is not changed	(El Darra et al., 2016)
Apple	Whole fruit	0.4 kV/cm, 0.1 Hz, 4μs, 0.01 kJ/kg	Catechin, epicatechin, procyanidin B2 and trimer + dimer	↑ Catechin, epicatechin, procyanidin B2 and trimer + dimer	Nd	(Ribas-Agustí, Martín-Belloso, Soliva-Fortuny, & Elez-Martínez, 2019)
Grape	Wine	4 kV/cm, 100 μs	EGC	↑ EGC	The mean degree of polymerization is not changed	(Maza et al., 2019)
Grape	Wine	4 kV/cm, 100 μs	(+)-Catechin and (-)-epicatechin	↑ (+)-Catechin and (-)-epicatechin	Nd	(Maza et al., 2020)

Nd, not detected. ↓, decreased. ↑, increased. ↔, unchanged. →, transformed to. DP, Degree of polymerization.

Epi-structured catechins: (-)-EGCG, (-)-epigallocatechin gallate; (-)-ECG, (-)-epicatechin gallate; (-)-EGC, (-)-epigallocatechin; (±)-EC, (±)-epicatechin.

Nonepi-structured catechins: (-)-GCG, (-)-gallocatechin gallate; (-)-CG, (-)-catechin gallate; (-)-GC, (-)-gallocatechin; (±)-C, (±)-catechin.

materials, which may result in newly formed colored compounds and compromise their accurate quantification (P. A. R. Fernandes et al., 2019). Because the oxidized samples did not contain any carbohydrates or polyphenols as determined after thiolysis, the occurrence of oxidized structures with bonds resistant to thiolysis can be inferred from this work. Generally, two phenomena occur during the drying process: enzymatic degradation under low temperature conditions and chemical modification (epimerization and cleavage) under high temperature conditions.

A-type procyanidin-dimers decrease significantly as the temperature of the vacuum oven increases (Michalska et al., 2018). Wojdyło et al. (2009) reported a marked decrease in procyanidin B3 and oligomers in strawberry fruits by convection and vacuum drying. It may be attributed to the fact that oligomeric procyanidins are preferentially decomposed. In jujube (Wojdyło et al., 2016), most of the flavanols are polymeric procyanidins, a small amount of oligomers are found while catechins and epicatechins are not detectable. Compared to freeze drying, some drying methods (convective drying at 50 °C and vacuum-microwave drying 480-120 W) induced higher content of monomers, trimers and tetramers in dried jujube fruits, but this increase is associated with the reduction of polymeric procyanidins meaning that interflavanic bonds are cleaved during drying (Wojdyło et al., 2016). Similar effects are observed in other dried fruit and vegetables: quince (Szychowski et al., 2018) and sour cherry (Wojdyło et al., 2014). Lachowicz et al. (2019) reported that microwave vacuum drying (480/120 W) has the same ability to retain saskatoon berry polymeric procyanidins as freeze drying. Moreover, the percentage of galloylation in grape does not change after drying (60 °C) (Olivati et al., 2019). Harsh drying (high temperature or power) may destroy flavanols, while mild drying or combined methods may maintain or depolymerize the polymeric procyanidins into oligomeric procyanidins or monomers, leading to variable outcomes depending on fruit source. Notably, the effect of drying is not only function of the temperature and time, but also of the DP of flavanols, the matrix and the protective effect of the matrix for the flavanols.

Pimenta Inada et al. (2020) reported that the DP of procyanidins in jaboticaba peel

and seed increases during convective drying (75 °C). Similar effects are observed in other convective dried fruits: apple pomace (70 °C) (Birtic et al., 2019), grape (60 °C) (Olivati et al., 2019) and strawberry (70 °C) (Wojdyło et al., 2009). This may be a marker that the procyanidin terminal units form a (non-) covalent bond with the cell walls. This phenomenon may occur due to the cell ruptures during heating and drying, and could also be due to a better extractability of procyanidins with high DP caused by cell wall degradation via heating (Brownmiller, Howard, & Prior, 2009; Le Bourvellec & Renard, 2012; Le Bourvellec, Watrelot, Ginies, Imberty, & Renard, 2012a). Adding an osmotic dehydration step before convective drying is beneficial to the retention of procyanidins and leads to higher DP in the final product (Devic et al., 2010). This is because smaller molecules (oligomers) diffuse into the external fluid, which the larger ones (polymers) may bind more strongly with cell wall polysaccharides through weak interactions (Renard, Baron, Guyot, & Drilleau, 2001a). Using lower temperatures, as may occur in traditional sun-drying, leads to different outcomes. Sun-drying of pears (D. Ferreira et al., 2002) led to a limited increase in DP of procyanidins. Simultaneously, temperatures during sun-drying are mild enough to allow enzymatic oxidation of caffeoylquinic acid and catechins by PPO, which causes browning of the dried pear (D. Ferreira et al., 2002). In green tea, the contents of (–)-EGCG, (–)-EGC and (–)-EC decrease with increasing of the convective drying temperature, while (–)-GCG and (–)-GC are opposite (Donlao & Ogawa, 2019). This suggests that tea catechins have undergone partial epimerization at high drying temperatures. The thermally induced epimerization occurs at position 2 of the ring-C in flavanols through ring opening reactions and cyclization in favor of *trans*-form (Mehta & Whalley, 1963). Their conversion percentages are usually below 100% due to other reactions, e.g., oxidation and degradation (Seto, Nakamura, Nanjo, & Hara, 1997). The final effect of drying on procyanidins depends on many factors: (i) whether the heating history (temperature/time) may allow enzymatic oxidation; (ii) the acidity or pH, which may favor the acidic depolymerization of procyanidins and also strongly affect the PPO activity; (iii) the procyanidins may bind strongly to the cell wall material during the

drying process as the cell membranes melt and the cell wall is destructured due to heating.

2.2.3.2 Thermal processing in aqueous system

Beverages (e.g., juices and green tea) and wines are rich in flavanols, i.e., epicatechins and non-epicatechins, which are beneficial to health. The flavanols can undergo oxidation, epimerization and chain cleavage during pasteurization, brewing or processing into canned beverages (Ahmed & Eun, 2018; Z. Chen, Zhu, Tsang, & Huang, 2001; Fan et al., 2016; Fuleki & Ricardo-Da-Silva, 2003; Kiatgrajai, Wellons, Gollob, & White, 1982; E. S. Kim et al., 2007; H. Wang & Helliwell, 2000; R. Wang et al., 2008; Q. Wu et al., 2019; Xu et al., 2019). An illustration of the range and trend of the main reactions of flavanol in aqueous solution with successive temperatures, pH and oxygen saturation solubility is provided in [Fig. 2.8](#). The stability of flavanol monomers in aqueous systems depends on the temperature and pH, and the specific temperature and pH at which the epimerization of catechins take place appears to be somewhat different in various studies. Moreover, proanthocyanidins also undergo various reactions such as thermal degradation, depolymerization and polymerization.

2.2.3.2.1 Oxidation

Many processing operations include more or less prolonged phases at low temperatures (up to about 40°C) after tissue destructure, which allow extensive enzymatic oxidation. This mechanism is thus highly relevant to understand the final effect of thermal processing. During the fermentation, production and storage of black tea, the polyphenol oxidase in tea catalyzes the oxidation of most catechins into benzotropolone compounds (e.g., theaflavins, theaflavin-3-gallate, theaflavin-3'-gallate and theaflavin-3,3'-digallate) ([Fig. 2.9](#)), thereby reducing the content of catechins (Ananingsih, Sharma, & Zhou, 2013; Engelhardt, 2020). Catechins and theaflavins can be further oxidized into thearubigins, which accounts for 20% w/w of the total solids of black tea (L. Zhang et al., 2019). For example, (-)-EGCG aqueous solution (37 °C

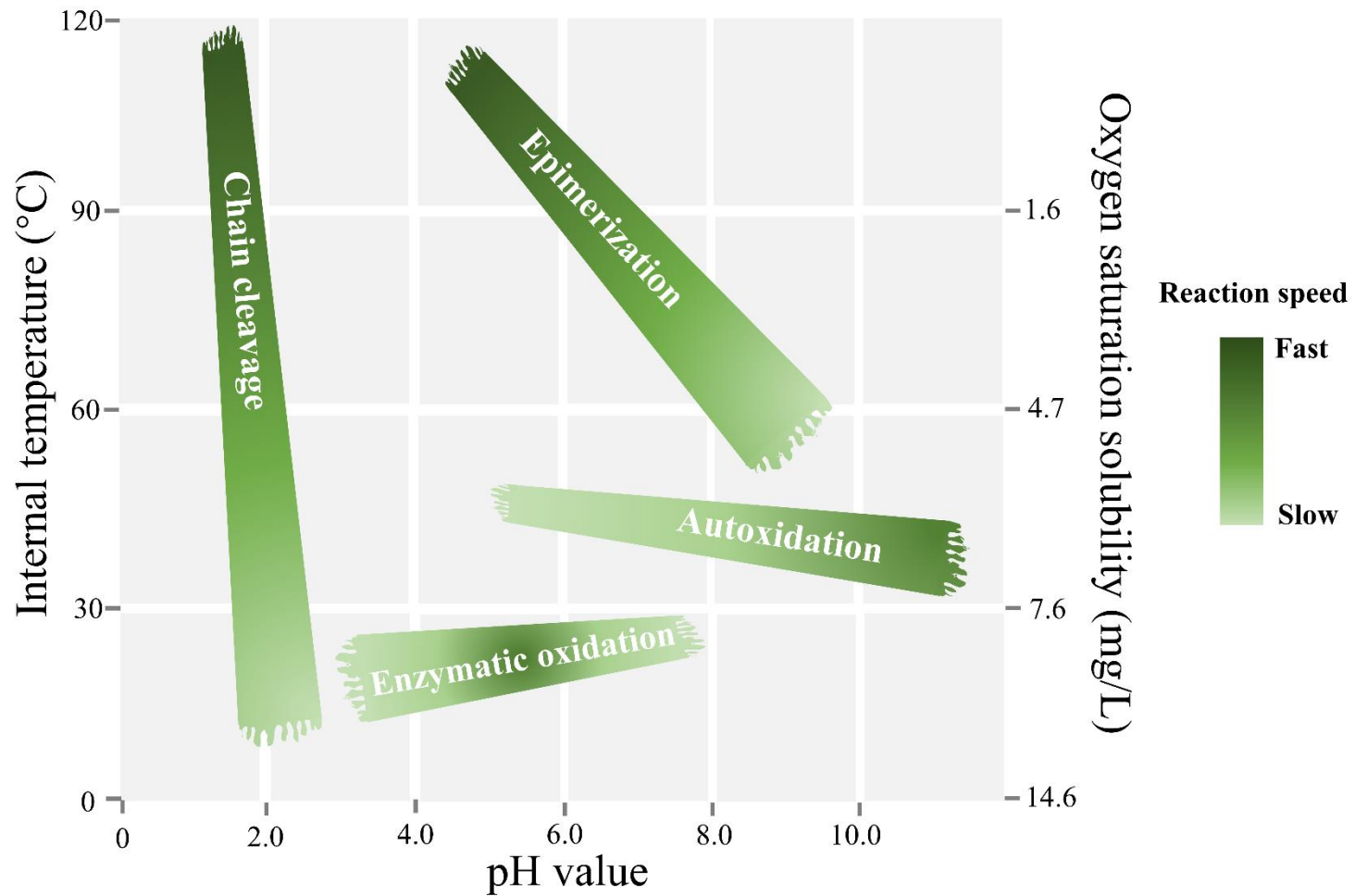


Figure 2.8 Trend map of the preferential conditions for the main reactions of flavanols in aqueous solution as a function of temperatures, pH values and oxygen saturation solubility.

and pH 7.4) degrades rapidly by 90% at higher oxygen levels, and no (-)-EGCG remains after 6 h (Sang et al., 2005). The main oxidation product of (-)-EGCG is an EGCG dimer (theasinensin A), which is produced by dehydrotheasinensin A (Y. Wang & Ho, 2009). In addition, nitrogen-purging leading to oxygen-free conditions or the addition of antioxidants prevent the auto-oxidation of (-)-EGCG and cause its epimerization to (-)-GCG (Sang et al., 2005). Oxidation may also occur in green tea liquid, as when the temperature increased (from 85 °C to 120 °C), the color of liquid became darker due to the oxidation of catechins and the degradation of chlorophyll (E. S. Kim et al., 2007).

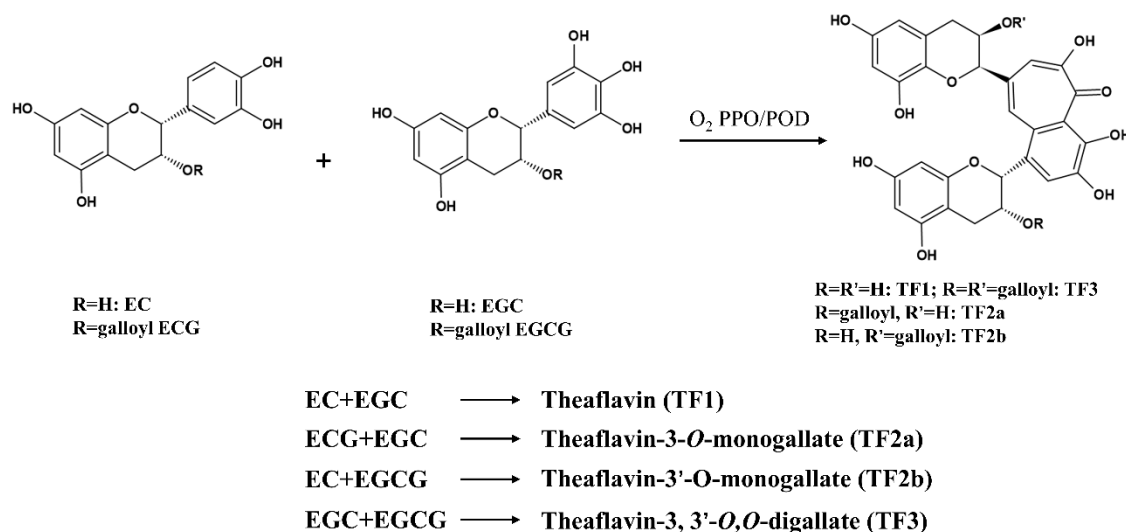


Figure 2.9 Transformation of tea catechins into major specific theaflavin by the action of polyphenol oxidase.

2.2.3.2.2 Epimerization

The epimers of tea catechins can be detected after heating at 60 °C and 90 °C during 8 h (Fan et al., 2016). The conversion level from (-)-epicatechin to (-)-catechin accounts for 25% in 60 °C aqueous solution and reaches 70% at 90 °C (De Taeye et al., 2014). Similarly, H. Wang & Helliwell (2000) reported that tea catechins can undergo epimerization from epicatechins to non-epicatechins at high temperature (80 °C) in a short time (20 min). R. Wang et al. (2008) determined two specific temperature points, 44 °C and 98 °C: (-)-EGCG degrades by oxidation below 44 °C, while epimerization reaction increases at 98 °C and above. Between 44 °C and 98 °C, the epimerization from (-)-GCG to (-)-EGCG may occur faster, and then epimerization from (-)-EGCG

to (-)-GCG, followed by the degradation (R. Wang et al., 2008). However, in another study, the rate constant for epimerization from (-)-GCG to (-)-EGCG is always lower than that of (-)-EGCG to (-)-GCG (Xu et al., 2019). After (-)-GCG was heated at 100 °C for 6 hours, the content of (-)-EGCG did not rise and only remained at c.a. 8.5% (Q. Wu et al., 2019). This indicated that the auto-oxidation proceeds simultaneously with epimerization. In addition, the concentration of gallic acid also increases after heat treatment, probably related to the release of the gallate group linked to the C-ring of procyanidins or the hydrolysis of gallotannins in the grape pomace (Chamorro, Goñi, Hervert-Hernández, Viveros, & Brenes, 2012; Davidov-Pardo, Arozarena, & Marín-Arroyo, 2011; Del Pino-García, González-SanJosé, Rivero-Pérez, García-Lomillo, & Muñiz, 2017).

Many foods (e.g., tea beverages) contain catechins processed at different pH conditions, which also have a significant effect on the epimerization of catechins. The degradation of EGCG is much slower when the pH is below 4.0 (Z. Chen et al., 2001; N. Li, Taylor, Ferruzzi, & Mauer, 2012; H. Wang & Helliwell, 2000). EGCG is a weak acid with a pK_{a1} value of 7.5, and its ionization state strongly affects its chemical stability (N. Li, Taylor, Ferruzzi, & Mauer, 2013). The increase in pH from 6.0 to 8.0 increased the degradation of EGCG from 38% to 88% (Xu et al., 2019). The production of GCG and gallic acid increased with increasing pH. At higher pH values, epimerization and degradation were more obvious. For pyrogallol-type catechins, under acidic conditions (pH 6.0), both the epimerization and hydrolysis reactions were enhanced, while for non-pyrogallol-type catechins, under neutral/alkaline (pH 7.0 and 8.0) conditions, the epimerization was also enhanced, but the hydrolysis reaction was inhibited (Y. Zhu et al., 2020).

The conversion level of epi-structured catechins at 90 °C (EC for 56.1% and EGC for 28%) were higher than that of non epi-structured catechins (C for 23% and GC for 12.0%) (Fan et al., 2016). Moreover, the conversion levels of *o*-diphenolic catechins (EC for 56% and C for 23%) were higher than their pyrogallol-type (EGC for 28% and GC for 12%) (Fan et al., 2016). These results suggest that epi-configuration may

contribute to the epimerization of non-galocatechin, while the extra -OH at the 5' position of the B ring seems to prevent epimerization (M. Zhang et al., 2018). High temperature is beneficial to promote the epimerization of tea catechins, whether from epi-structured catechins to non epi-structured catechins, or vice versa. Simultaneously, -OH substituents and spatial configuration also influence the epimerization of catechins. Compared to the aqueous medium, the epimerization in a lipid medium proved to be slow and degraded faster (De Taeye et al., 2014). This may be due to the relatively higher stability of epimerized intermediates in an aqueous environment.

2.2.3.2.3. Chain cleavage, rearrangement and adsorption

Meanwhile, as more and more fruits are consumed after processing, it is necessary to understand the effect of traditional hydrothermal processes (e.g., canning, cooking and pasteurization) on flavanols in fruit productions. Hence, during the canning and the cooking process, two phenomena are observed, i.e., the losses of procyanidins, and the diffusion of the smallest ones into the syrup (Le Bourvellec et al., 2011, 2018). Under certain temperature (30 - 40 °C) and acidity conditions (1 M hydrochloric acid), the interflavanic bonds of polymeric procyanidins can be cleaved, and the released flavanyl carbocations can react with free catechins to form procyanidin dimers and other oligomers. Interestingly, this reaction can be used to produce several procyanidin dimers by a semisynthetic approach (Esatbeyoglu & Winterhalter, 2010; Esatbeyoglu et al., 2010). When cooked for a long time, pears can lose the bulk of their procyanidins, due to their leaching in the juice for the small molecules, and to their heat degradation, while a light pink color appears in pear sections indicating their conversion into an anthocyanin-type structure (Le Bourvellec et al., 2013; Renard, 2005). This may be due to the cleavage of B-type bonds (chemical depolymerization) between epicatechin units in hot acidic conditions leading to the formation of carbocations that further react (intermolecular or intramolecular addition) with plant substrates, e.g., themselves and cell walls to form covalent bonds. Moreover, short time (20 min) can increase the DP of pear procyanidins, while prolonged cooking (> 7h) decreases their DP (Renard, 2005). This DP increase, at a certain pH range, has already been observed extensively (Le

Bourvellec et al., 2013). This could be due to the leaching of the small molecules into the syrup (Devic et al., 2010) and to the reaction of the intermediate cleavage product, i.e., positive charged carbocation, with the nucleophilic group of flavanols.

Moreover, the production of commercial fresh fruit juices (e.g., apple and grape) and industrial non-craft beer includes pasteurization, therefore it is also interesting to consider the effect of this process on the catechins and procyanidins. Generally, the effect of pasteurization on flavanols was related to the cold/hot-extraction/pressure treatment used in the processing of the juice (Genova, Tosetti, & Tonutti, 2016). Pasteurization had a negative effect on the proanthocyanidins/flavanols content of juices extracted by hot-pressing (Fuleki & Ricardo-Da-Silva, 2003). However, pasteurization applied to cold-pressed juices did not affect or may even increase their flavanol contents. The increase in flavanols observed in cold-pressed pasteurized juices may be due to a transient increase in temperature, which may have facilitated the release of proanthocyanidins bound to cell wall materials in the juice. Notably, flavanols were poorly extracted in cold-pressed juices without maceration; the use of hot press/break or extraction with steam (at artisanal scale) led to higher flavanol concentrations (Silva et al., 2019). In beer, the phenolic compounds can be derived from grains or hops (70-80 %), and the process of wort boiling (also hop addition) may change their content and composition (Wannenmacher, Gastl, & Becker, 2018). During wort boiling, highly polymerised proanthocyanidin oligomers were removed by forming complexes with proteins, either by precipitating or later by being adsorbed to yeast cells during fermentation (Asano, Ohtsu, Shinagawa, & Hashimoto, 1984; Fumi, Galli, Lambri, Donadini, & De Faveri, 2011; Siebert, Troukhanova, & Lynn, 1996). Knowledge of the fate of flavanols throughout the brewing process is still incomplete, therefore more work is needed on this.

2.2.3.3 Roasting

Roasting and baking are basically the same unit operation, i.e., heating with limited water, and are important methods for food processing, because they add unique aroma and flavor (Ruosi et al., 2012; L. Zhang et al., 2019). Among foods rich in flavanols, tea and cocoa powder are generally roasted before consumption.

2.2.3.3.1 Tea

Tea has a mild taste after roasting, which may be due to the modification of flavanols. Some researchers believe this is due to the reduced level of astringent catechins. Morikawa et al. (2019) reported that the reduction in astringency is due to the oligomerization of catechins after roasting. After the green tea leaves are heated at 180 °C for 30 minutes, oligomerized products appear; the reaction occurs on the methine carbon of catechin A ring, as identified by ¹³C NMR spectroscopy (Morikawa et al., 2019). When large-leaf yellow tea was roasted at 140 - 150 °C, the levels of (-)-EC, (-)-EGC, (-)-EGCG, (-)-ECG decreased significantly (Zhou et al., 2019). In addition, gallic acid and (-)-GCG appeared in the epimerization product, and the content of (-)-GC more than doubled. The bitterness intensity of flavanols is related to their degree of polymerization (Lea & Arnold, 1978), and the linking bonds are also critical to the intensity of astringency (Gacon, Peleg, & C.Noble, 1999; L. Zhang, Cao, Granato, Xu, & Ho, 2020). Moreover, the configuration of flavanols also affects tea taste, for instance, both bitterness and astringency of (-)-(2R, 3R)-epicatechin are stronger than for (+)-(2R, 3S)-catechin (Thorngate & Noble, 1995). Therefore, the bitterness and astringency of the tea may be adjusted by appropriate roasting treatment.

2.2.3.3.2 Cocoa

In cocoa, the formation of the catechin epimers starts slowly from 130 °C until it reaches a maximum temperature of 190 °C. After roasting at 170 °C for 30 minutes, more epimerization from epicatechin to catechin can occur, and is followed by degradation when the temperature rises to 200 °C (Fernández-Romero et al., 2020). The original epicatechin content decreases at 150 °C, while the catechins content increases

by a factor 6 (Quiroz-Reyes & Fogliano, 2018). Similar results were reported by De Taeye, Bodart, Caullet, & Collin (2017), Hurst et al. (2011), Oracz, Nebesny, & Żyżelewicz (2015) and Payne, Hurst, Miller, Rank, & Stuart (2010). At roasting temperatures above 70 °C, (-)-epicatechin epimerization begins (Payne, Hurst, Miller, et al., 2010). Typical epimerization occurs at 150 °C and the content of (-)-catechin increases significantly (De Taeye, Bodart, et al., 2017). These studies did not reach a unified conclusion about the epimerization temperature of flavanols at maximum conversion level. This may be affected by the variety, maturity, and processing time of the cocoa beans. It is considered that the roasting at high temperatures (ca. 145 °C) for a short time better minimized proanthocyanidin losses (Ioannone et al., 2015).

Compared with unprocessed cocoa beans, roasting results in significantly lower levels of procyanidins B2 and C1 (Cebrián-Tarancón et al., 2018; Oracz et al., 2015; Quiroz-Reyes & Fogliano, 2018). The content of procyanidins dimers B1, B2, B5 and procyanidin trimers C1, and proanthocyanidins dimer B1, B2, and B4 decreased during the roasting of cocoa beans (Kothe et al., 2013; Mazor Jolić et al., 2011). However, in other studies, roasting resulted in an increase in two other procyanidin B-type dimers and another procyanidin trimer (Kothe et al., 2013; Oracz et al., 2015). During the roasting process, procyanidins combine with other biomacromolecules e.g., polysaccharides, proteins and Maillard reaction products, resulting in the formation of complex molecules. Therefore, procyanidin levels are decreased by high-temperature roasting.

Stanley et al. (2018) reported that cocoa bean roasting at 150-190 °C for 40 min can cause monomers or DP2-6 of proanthocyanidins to polymerize. Various types of reactions (e.g., thermal degradation, depolymerization, and polymerization reactions) are the main reasons for the change in the degree of polymerization of proanthocyanidins during the roasting process. The epimerization of cocoa proanthocyanidins during processing is more complicated, because there are more types of epimers. There are also certain challenges for the detection of such compounds, therefore more work in this area is needed to deepen the understanding of this gap.

The roasting process can impart great variability in cocoa flavor and quality. Flavanols participates in complex biochemical reactions during roasting process, which are important for cocoa texture, taste, flavor and color formation (Aprotosoai, Luca, & Miron, 2016). The total proanthocyanidin contents and epicatechin/catechin ratio can be considered as useful and sensitive indicator in cocoa bean processing (Ioannone et al., 2015). Therefore, processing remains a challenge to the balance between the biological activity and flavor/taste of cocoa.

Interestingly, similar phenomena with the same decrease of procyanidin levels were observed where roasting grape vine-shoots (Cebrián-Tarancón et al., 2018). However, in opposition to cocoa, vine-shoot roasting decreases the DP of proanthocyanidins, on average by one monomer unit (Cebrián-Tarancón et al., 2018).

2.2.3.4 High pressure treatment

High-pressure treatment or high hydrostatic pressure processing can be applied for food preservation and processing to inhibit microorganisms and inactivate enzymes, i.e., in wine (Santos et al., 2016, 2019) and juice (Baron et al., 2006), and adjust their organoleptic properties. High pressure processing has three characteristic parameters: final pressure level, pressure duration time and temperature. The principle of high pressure is based on the reduction of molecular volume changes, which may cause physicochemical reactions, especially in changing the integrity of cell walls and cell membranes. They can be applied to different types of food liquid, solid or matrices.

High pressure treatment can reduce the content of flavanols, but also increase their extraction rate. For example, the degradation rate of (-)-EGCG increases by high pressure processing (pH 7, 25 °C at 200 MPa) and has a linear relationship with pressure (Shkolnikov et al., 2020). Meanwhile, the degradation of EGCG was accompanied by a significant production of gallic acid (Christofi et al., 2020; Shkolnikov et al., 2020). Similarly, the proanthocyanidin contents decrease during high pressure treatment (400-600 MPa), although remaining higher than those of the heat treatment group (H. Lee et al., 2018). One of the dominants of the effects of high pressure processing is the

increased dissolved oxygen concentration. However, some systems saturate the medium with other gases instead, such as high pressure CO₂. High-pressure CO₂ treatment has no significant effect on the polyphenols of litchi juice, while high-temperature treatment results in a significant decrease in (-)-epicatechin content due to non-enzymatic oxidation (L. Liu et al., 2015). However, high pressure processing may improve the extractability of flavanols and suppress polyphenoloxidase activity. This method increases the mass transfer rate during the extraction process, thereby increasing the permeability of the cells and enhancing the diffusion of secondary metabolites (Dörnenburg & Knorr, 1993).

High pressure processing accelerates the polymerization and oxidation of flavanols in wine, which leads to the formation of proanthocyanidins with a higher degree of polymerization. For example, in comparison to 500 MPa pressurized and untreated red wines, the polymerization rate of larger proanthocyanidins increases slightly during processing at 600 MPa for 20 min resulting in higher DP without modifying the content of flavanols monomers and oligomers (Santos et al., 2016). The authors believed that this polymerization reaction could be due to a higher solubilization rate of the O₂. However, if the increase in polymerization was the result of an oxidation reaction, it could not be observed by phloroglucinolysis used to calculate mean DP. The number average molar mass of proanthocyanidin can be calculated from the molar mass of flavanols units and DP. Therefore, an increase in the polymerization state associated with high pressure treatment could not be convincingly demonstrated. The mechanism of polymerization may be related to the intra and intermolecular auto-oxidation of proanthocyanidins (Mouls et al., 2014; Vernhet, Carrillo, & Poncet-Legrand, 2014). Moreover, Christofi et al. (2020) reported that the DP values are not significantly different between pressurized and non-pressurized wines. This result may be due to the simultaneous occurrence of polymerization of proanthocyanidins as well as their precipitation with other macromolecules i.e., proteins and polysaccharides (Christofi et al., 2020).

2.2.3.5 Ultrasound processing

Ultrasonic treatment can accelerate the extraction of flavanols. Therefore, it is of great significance to evaluate their degradation and epimerization process under different ultrasonic conditions. This method has the advantages of reducing processing time and energy consumption, and increasing throughput. Ultrasound causes cavitation bubbles, with locally high temperatures, and induces the formation of free radicals. This can result in the degradation of catechins (Pingret et al., 2013). At four different ultrasound frequencies (28, 40, 50 and 135 kHz, 50 °C for 40 min), the degradation levels of (+)-catechin in model solutions are 21, 23, 32 and 37%, respectively (Y. Zhu et al., 2018). The degradation also gradually increased with the increase of ultrasonic power (from 0.05 to 0.35 W/cm²). Moreover, longer processing time and higher pressure environment lead to the reduction of flavanol contents. Previous studies have shown that catechin may undergo epimerization at high temperature. Ultrasonic treatment (135 kHz, 50 °C for 60 min) can also induce the epimerization reaction from catechin to epicatechin (Y. Zhu et al., 2018). This may be caused by local temperature and pressure increases. In addition, for all catechin monomers, epimerization occurred between the epi- and nonepi-structures, and no conversion reaction was observed between the pyrogallol-type catechins and the non-pyrogallol-type catechins (Y. Zhu et al., 2020). Meanwhile, the content of gallic acid increased due to it being a by-product of the hydrolysis reaction in standard solutions of EGCG, GCG, ECG and CG (N. Li et al., 2013; Y. Zhu et al., 2020).

Moreover, oxygen exposure may significantly reduce the stability of EGCG (Zeng et al., 2018). Ultrasound itself did not cause the degradation of EGCG, while EGCG in the aqueous solution may be in extreme contact with oxygen, thereby accelerating its degradation. Compared with untreated samples, ultrasonic processing increases the (+)-catechin and (-)-epicatechin content in apple cubes soaked in water, while the procyanidin dimers and procyanidin polymers are degraded (Mieszczakowska-Frać et al., 2016). Cell wall disruption caused by cavitation and polymer decomposition might be responsible for the increased flavanol monomer contents. In addition, Del Fresno et

al. (2019) reported that ultrasound promoted a significant increase in the content of oligomeric proanthocyanidins in wine with lees and oak chips. This may be due to the migration of some oligomers in the oak chips from the wood to the wine. Moreover, ultrasound processing (25 kHz for 45 and 90 min at 40 °C) can reduce the degree of polymerization of procyanidins, which may be related to the mechanical or chemical degradation of polymer molecules caused by cavitation. However, ultrasonic method did not induce a decrease in the polymerization degree of procyanidins in *C. longepaniculatum* leaf powder (Z. Liu & Yang, 2018). This might be related to the ultrasonic frequency intensity, duration time and temperature. The formation of cavitation, structural changes and the destruction of microstructures may all affect the flavanols content and degree of polymerization during ultrasonic treatment.

2.2.3.6 Irradiation

Radiation is a recognized non-thermal physical process that extends the shelf life of food, which is also known as cold pasteurization (Allothman, Bhat, & Karim, 2009). Irradiation may be divided in two forms: ionizing radiation (high-energy electron beam, gamma- and X-rays) and non-ionizing radiation (ultraviolet (UV)-A, UV-B, UV-C, visible light and infrared radiation) (Lagunas-Solar, 1995; F. Li, Chen, Zhang, & Fu, 2017).

2.2.3.6.1 Ionizing radiations

After γ -rays irradiation of cranberry syrup, procyanidin B isomer 1 and procyanidin A2 contents were significantly increased (Rodríguez-Pérez et al., 2015). The increase in procyanidin A2 may be due to the degradation of more polymerized molecules presenting a A2 dimeric structure at the terminal position, which could only be observed in unirradiated syrup. Procyanidin B isomers B2 and B3, and prodelphinidins are relatively stable after γ -irradiation and during storage (Rodríguez-Pérez et al., 2015). These authors observed a variety of proanthocyanidin isomers, but could not quantify them because of lack of standards for higher polymers. Moreover, the degradation of proanthocyanidin polymers may be related to their oxidation, hydrolysis or

isomerization. Catechins are less stable than other simple flavonoids (e.g. myricetin hexose, quercitrin and quercetin-3-O-glucoside) and their contents are significantly decreased after irradiation processing (Rodríguez-Pérez et al., 2015). However, Gupta et al. (2015) reported that catechin and epicatechin contents increased in irradiated wine (1500 Gray).

2.2.3.6.2 Non-ionizing radiations

Islam et al. (2016) reported that the content of (-)-epicatechin decreased significantly (35%) with the increase of UV-C dose (from 0 to 240 mJ/cm), while the absolute content of catechin increased (17%) remarkably in apple juice. This may be due to the epimerization of (-)-epicatechin to its corresponding epimer (-)-catechin under high-dose UV-C irradiation. Vergne et al. (2018) reported that (-)-epicatechin can also isomerized (conversion level 9%) into (-)-catechin and (+)-catechin by UV-C irradiation in green tea beverage. Epimers can occur in the aqueous and ethanol solution of (-)-catechin and (-)-epicatechin after UV-B irradiation, but are not detected for (-)-EGC, (-)-EGCG, (-)-ECG, (-)-GC, (-)-CG and (-)-GCG (M. Shi et al., 2016). This insensitivity of the other six catechins to UV-B irradiation indicates that the presence of gallic acid and pyrogallol partially hindered their chemical conversion (Suzuki et al., 2003). The percentage of conversion from (-)-epicatechin to its epimer (-)-catechin is much higher than that from (-)-catechin to (-)-epicatechin, which implies that epi-type catechins are conducive to photoisomerization. Moreover, the conversion rate of (-)-epicatechin to (-)-catechin in water is higher than that in ethanol, which seems to be related to solvation effect (M. Shi et al., 2016). The epimerization from (-)-epicatechin to (-)-catechin induced by UV-B is generated by ionization of intermediate quinone methide (Huvaere, Sinnaeve, Van Bocxlaer, & Skibsted, 2012). Higher polarity water promotes the ionization process and increases the formation of intermediate quinone methide. Light radiation exposure also accelerates flavanols degradation and epimerization. The specific wavelengths of light affect their metabolism in various plants. Visible light favors to proanthocyanidins biosynthesis in young berry skins, while UV-B radiation has no effect (Koyama, Ikeda, Poudel, & Goto-Yamamoto, 2012).

2.2.3.7 Pulsed electric field

Pulsed electric field (PEF) is a promising tool that has been extensively studied in food processing, where it can be applied to enhance extraction, or for sterilization and drying. The use of PEF leads to permeabilization of the biological membranes allowing small molecules to penetrate into the cytoplasmic membrane, which might cause swelling and eventually rupture of the cell membranes (Bevilacqua et al., 2018). High-intensity fields (1.1 to 100 Hz, 40 to 700 μ s, 15–40 kV/cm) have been applied for microbial inactivation, while medium-low intensity fields (1 Hz, 0.6-2.6 V/cm, treatment time less than 10^{-2} s) can enhance mass transfer in food matrices (Rawson et al., 2011). Through PEF treatment prior to pressing, the juice yield and the content of natural polyphenols (inhibitor of the enzymatic oxidation was added) are significantly improved, the turbidity of the juice is lower, and the overall taste and odor intensity are significantly stronger than for the untreated sample (Turk, Billaud, et al., 2012; Turk, Vorobiev, et al., 2012).

Catechin and epicatechin contents are significantly higher after treatment with pulsed electric field in grape paste than untreated samples (López-Giral et al., 2015). Similarly, (+)-catechin, (-)-epicatechin, (-)-epigallocatechin and total proanthocyanidin contents also increase in wines obtained from PEF-treated grapes (El Darra et al., 2016; Maza et al., 2020, 2019). Therefore, PEF process is an efficient method in increasing extraction of flavanols during the brewing of different grape varieties. This may be related to improved extraction linked to cell membrane degradation. However, Brianceau et al. (2015) reported that catechin content decreases in extracts of grape pomace after PEF treatment, whereas epicatechin, procyanidin B1 and trimer C1 contents increase, whatever the extraction temperature. This might be due to the epimerization of catechin to epicatechin and the condensation reaction of catechin to form proanthocyanidin oligomers. In addition, PPO can oxidize 5-caffeoylquinic acid (5CQA), and CQA quinone in turn further oxidize flavanols, causing their loss (Turk et al., 2010; Turk, Billaud, et al., 2012). The combination of PEF process (to increase juice yield) and the addition of an inhibitor (e.g., sodium

fluoride) (to avoid enzymatic oxidation) could increase the content of flavanols in apple juice, while it decreased in absence of the PPO inhibitor (Turk, Vorobiev, et al., 2012). Moreover, Ribas-Agustí et al. (2019) observed that different pulse energy input has different effects on flavanol contents in fresh apple. The contents of epicatechin, procyanidin B2 and procyanidins (trimer + dimer) are significantly decreased after PEF processing at 1.8 and 7.3 kJ/kg. For 0.01 kJ/kg PEF treatment, the contents of epicatechin, procyanidin B2 and procyanidin trimers/dimers increased by 32%, 46% and 38%, respectively (Ribas-Agustí et al., 2019). Apple tissues under mild PEF processing can activate the corresponding regulatory metabolism, which includes, at least, the activation of phenylalanine ammonia lyase (PAL), an enzyme that prompts the accumulation of flavanols (Treutter, 2001). For high PEF energy input, even though stress-induced biosynthesis may be present, it cannot offset the degradation of flavanols. The color change (strong browning) indicates cell damage and the irreversible permeability of the cell membrane, namely, reactive oxygen participates in the redox reactions that occur in the PEF-damaged apple tissue (Ribas-Agustí et al., 2019). In addition, the percentage of galloylation in the wines obtained from the PEF-treated grapes was a little higher than in the untreated samples, but such differences did not have practical implications (Maza et al., 2019).

There are three main reasons for the changes in flavanols content by PEF: the formation of new compounds through biochemical reactions; the rupture of the cell membrane releases free flavanols; the inactivation of PPO prevents the loss of flavanols and PAL activity improve their concentrations. In addition, the average DP of proanthocyanidins is not affected by PEF treatment (El Darra et al., 2016; Maza et al., 2019; Turk, Vorobiev, et al., 2012).

2.2.4 Reactivity of flavanols during processing

During the initial (e.g., peeling, chopping and crushing) or deep processing (e.g., puree, juice and beverage) of plant tissues, the integrity of the cells is destroyed. Therefore, in addition to the effects of different physical processes themselves on

flavanols, these physical treatments increase the exposure of proanthocyanidins to various environmental conditions, i.e., light, oxygen, enzymes, and interaction with other biomacromolecules in the food matrix (Fig. 2.10).

2.2.4.1. Autoxidation

The flavan-3-ol monomers or dimers have been evidenced to undergo oxidation reactions resulting in the formation of intramolecular and intermolecular new covalent bonds (Tanaka, Matsuo, & Kouno, 2005; Vernhet et al., 2011). The oxidation of flavanol polymers exposed to higher O₂ concentrations in the atmosphere also leads to the formation of intermolecular and intramolecular bonds (Poncet-Legrand et al., 2010). For proanthocyanidins with a short oxidation time, terminal-to-terminal unit intermolecular reactions may occur to form linear polymers (Poncet-Legrand et al., 2010). Under oxidizing conditions for a long time, most of them are terminal-to-intermediate unit reactions, resulting in a substantial increase in the DP of the branched polymers, but the overall size stays relatively small (Poncet-Legrand et al., 2010). Intramolecular oxidation may also lead to additional cyclization, such as the formation of A-type proanthocyanidins, the newly formed structures being resistant to acidolysis (Mouls & Fulcrand, 2012). This result was also confirmed by MALDI/UPLC-MS analysis (Mouls & Fulcrand, 2015; Mouls et al., 2014). Moreover, proanthocyanidins with low DP have a higher proportion of intramolecular reactions in dilute solutions, while proanthocyanidins with high DP have more favorable intermolecular reactions in concentrated solutions (Vernhet et al., 2014).

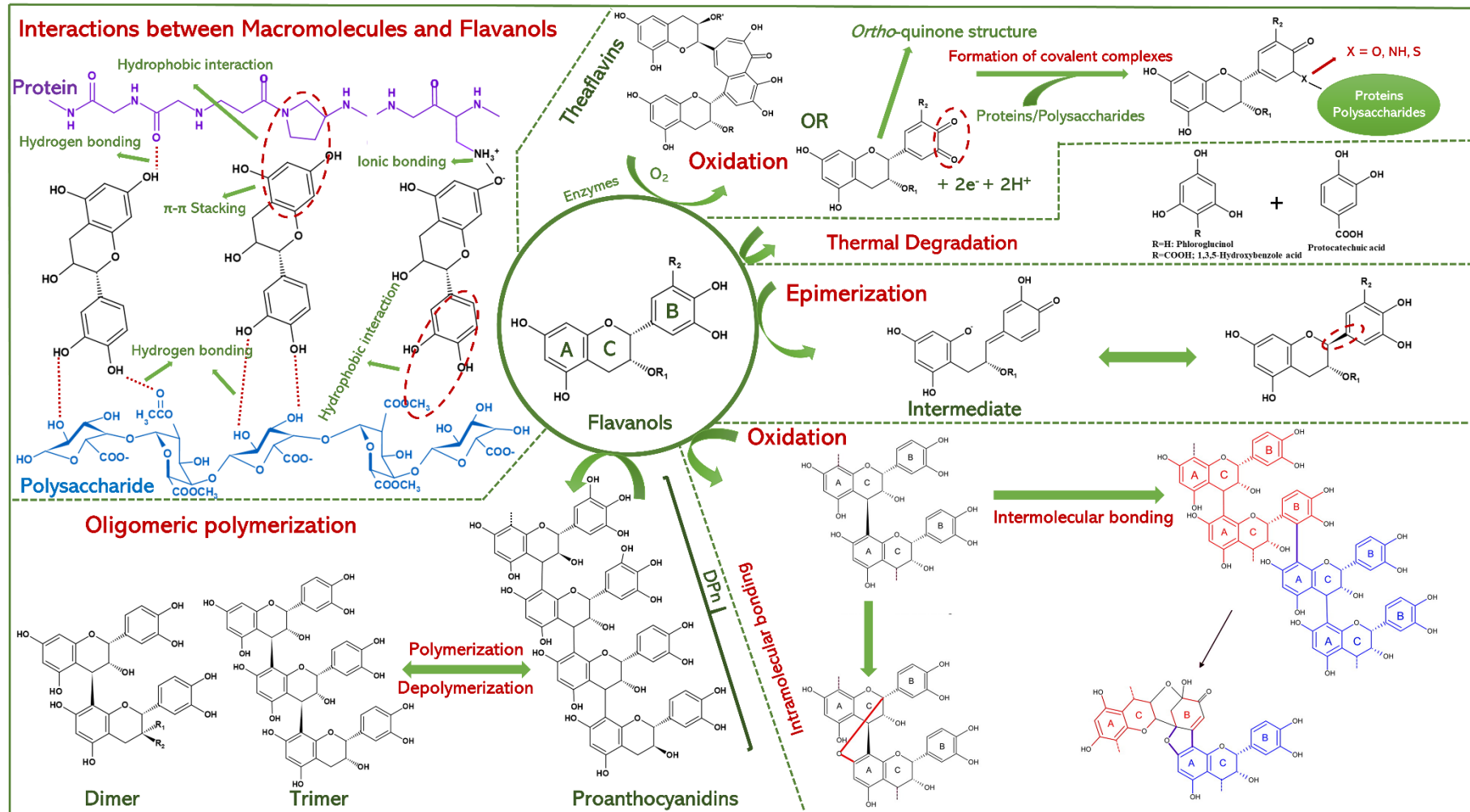


Figure 2.10 Overview of key enzymatic and chemical mechanisms of flavanols and their reactivity by food processing.

2.2.4.2. Indirect enzymatic reactions

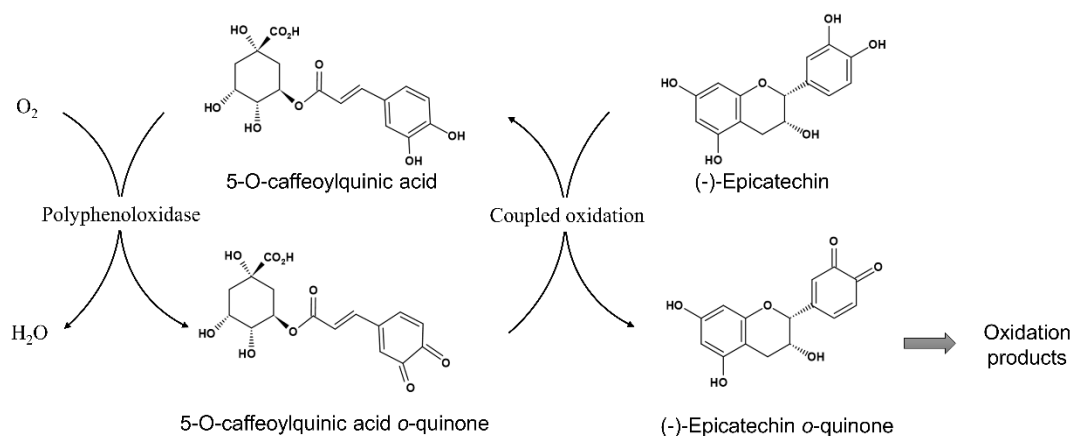


Figure 2.11 Coupled oxidation of the *o*-quinone of caffeoylquinic acid and flavanols.

In the presence of oxygen and endogenous enzymes (e.g., endogenous polyphenol oxidase (PPO) and peroxidase (POD)), the *o*-diphenols and *p*-diphenols of flavanol monomers may react with molecular oxygen to generate the corresponding semiquinone and quinone (Debelo et al., 2020; Janeiro & Oliveira Brett, 2004). Generally, proanthocyanidins are not substrates of these enzymes, but they can be converted into their corresponding *o*-quinones by coupled oxidation (Fig. 2.11), in which a quinone, e.g., from chlorogenic acid or another PPO substrate, reacts with a flavanol (Cheynier & da Silva, 1991; Le Bourvellec, Le Quéré, Sanoner, Drilleau, & Guyot, 2004). Moreover, oxidation leads to the formation of quinone intermediates (Fig. 2.10), which can further react to produce browning resulting from complex reactions (Singh et al., 2018). Enzymatic browning is a major problem in fruit and vegetables processing, leading to unsuitable color changes. The color deterioration is just as unacceptable to consumers as the smell of food and the decline in nutritional value. However, in some cases, such as the production of certain beverages (e.g., wine, beer, black tea, apple juice or cider), this coloring effect (oxidation) may be required.

Moreover, the enzymatically generated *o*-quinones are highly electrophilic, allowing the nucleophilic addition of other polyphenols or proteins (Le Bourvellec & Renard, 2012), or forming covalent bonds with other biomacromolecules (Fig. 2.10), e.g., polysaccharides (Le Bourvellec, Guyot, & Renard, 2009; Renard et al., 2017).

High temperature (70 - 90 °C) and freezing can play the role of destroying and inhibiting enzyme activity, respectively (Tinello & Lante, 2018). In addition, high-pressure treatment may also inactivate the enzyme without affecting the freshness, nutrition and flavor of fruit and vegetables (Iqbal et al., 2019). Therefore, the enzymatic browning can be prevented by refrigeration, freezing, bleaching and controlling the atmosphere and temperature during processing. Moreover, combining some physical processing techniques, e.g., hydrostatic pressure, ultrasound and pulsed electric fields treatments, can also effectively inhibit enzyme activity thereby preventing enzymatic browning (Iqbal et al., 2019; Tinello & Lante, 2018).

The oxidation of catechins in fresh tea leaves may catalyzed by endogenous PPO and POD during fermentation, resulting in oxidation and polymerization into higher molecular weight polyphenols, e.g., theaflavins and thearubigins (K. Zhu, Ouyang, Huang, & Liu, 2020). Theaflavins contribute to the lightness and brightness of the tea, while the thearubigins are responsible for the color and luster of the tea (Engelhardt, 2020). The reaction between flavanol quinones and non-quinone flavanols can form theaflavins, that is, the quinone arising from oxidation of B-ring dihydroxycatechin can condense with quinones produced by the oxidation of trihydroxycatechin to form different theaflavins (H. He, 2017). As the substrate catechins are oxidized during the fermentation process, theaflavins are continuously formed or degraded. Increasing the temperature and prolonging the fermentation time can increase the enzymatic oxidation, resulting in faster consumption of tea catechins and theaflavins, and the percentage of thearubicin are increased accordingly (Ngure, Wanyoko, Mahungu, & Shitandi, 2009).

Two different proanthocyanidin oligomeric chains can form new polyflavanolic molecules by intermolecular reactions through biaryl interflavanic bonds, while intramolecular reactions can lead to the formation of A-type proanthocyanidins (Bernillon, Guyot, & Renard, 2004; Poupard, Sanoner, Baron, Renard, & Guyot, 2011; Wong-Paz et al., 2021). Procyanidin B2 may undergo a coupled oxidation–reduction reaction with caffeoylquinic acid *o*-quinone. The *o*-quinone formed on the E-ring of the B2 dimer is converted into quinone methide by reciprocal isomeric rearrangement. This

is followed by nucleophilic addition of the 7-hydroxyl group of the A-ring to the carbon 2 on the F-ring forming an C2-O-C7 A-type ether-linkage. Finally, procyanidin B2 was thus converted into procyanidin A2 via intramolecular coupling (Poupard et al., 2011). In addition, the intermolecular coupling between two procyanidins B2 can produce homo-dimers, and the intermolecular coupling between a procyanidin B2 molecule and a caffeoylquinic acid molecule can produce hetero-dimers, with for example formation in apple juices of flavanol derivatives resulting from an oxidative coupling between (–)-epicatechin and caffeoylquinic acid. Notably, oxidation of (+)-catechin in the presence of PPO results in the formation of several dimers, e.g., dehydrodicatichin A (yellow) and dehydrodicatichins of type B (colorless) in apple, grape and wine models (Guyot, Vercauteren, & Cheynier, 1996; Poupard, Guyot, Bernillon, & Renard, 2008). These reactions may contribute to stabilize and rigidify the structure of the oxidation product, and affect their properties (e.g., solubility, polarity and tanning), and thus affect the sensory and nutritional quality of the fruit-derived foods and beverages.

2.2.4.3. Thermally induced chemical and enzymatic reactions

At intermediate processing temperatures, the oxidation process is favored, while epimerization may occur at higher processing temperatures, especially for flavanols in tea and cocoa (M. Zhang et al., 2018). Epimerization usually transforms flavanols from the epi structure to the non-epi structure. Thermally induced epimerization occurs at the 2-position of the C ring in flavanols via ring-opening reactions and cyclization in favor of trans-form (Mehta & Whalley, 1963). There is no fixed dihedral angle (the angle between the A/C ring plane and the B ring plane) between the ring systems of the intermediates, which makes the isomerized quinone intermediates flexible (Fig. 2.10).

There are two main types of proanthocyanidin oligomers, i.e., A-type and B-type, in plants. However, the knowledge about the transformation of A-type proanthocyanidins is still underdeveloped during processing, but there is evidence that B-type proanthocyanidin dimers can oxidize to A-type dimers under mild conditions (Alejo-Armijo, Salido, & Altarejos, 2020; Burger et al., 1990; L. Chen, Yuan, Chen, Jia,

& Li, 2014; Kondo et al., 2000; Osman & Wong, 2007). Some early authors proposed that B-type proanthocyanidin form A-type proanthocyanidin (oxidized procyanidins) through the C-2 oxidation of the upper monomer (Fig. 2.10), but the conversion rate is low (3-12%) (Burger et al., 1990; Kondo et al., 2000). The conversion of B-type proanthocyanidin to A-type proanthocyanidin may also involve enzyme-catalyzed oxidation reactions in plants, e.g., laccase (EC 1.10.3.2), rather than just a free radical-driven process (Osman & Wong, 2007; Poupard et al., 2011). For this intramolecular reaction, the dissociation enthalpy of C–H bond at the C-2 of the upper flavanol unit is relatively low (68.7 Kcal/mol). Therefore, the C-7 hydroxyl group of the lower unit can do a nucleophilic attack to form A-type proanthocyanidin (Kondo et al., 2000). To further verify this conversion mechanism, L. Chen et al. (2014) demonstrated that the conversion rate of B- to A-proanthocyanidin is greatly affected by temperature and pH, but is not affected by type of oxidant used to catalyze the reaction (DPPH, O²⁻, polyphenol oxidase, and xanthine oxidase). However, the result remains unclear on which mechanism (free radical-driven processes or enzymatically catalyzed free radicals) is induced in the plant kingdom or subsequent food processing.

2.2.4.4. Formation of adducts with macromolecules

Flavanols can also react with other food constituents and neo-formed compounds, such as Maillard reaction products, which have sensory and safety risks. To understand the related chemical reactivity and transformations that occur in complex food systems, these indirect effects of flavanols have to be considered. For example, flavanols may interact with other macromolecules either with non-covalent or covalent bonds (Le Bourvellec & Renard, 2012; X. Liu et al., 2020; Renard et al., 2017), e.g., proteins (De Freitas & Mateus, 2001; Gibis, Thellmann, Thongkaew, & Weiss, 2014; Guerreiro et al., 2020), polysaccharides (Brahem, Renard, Bureau, Watrelot, & Le Bourvellec, 2019; Le Bourvellec et al., 2012a; X. Liu, Renard, Rolland-Sabaté, & Le Bourvellec, 2021; Renard et al., 2017) and other polyphenols (Çelik & Gökmen, 2021; Gordillo et al., 2015) (Fig. 2.10) in the same processing system (Ribas-Agustí et al., 2018). Moreover, the interactions between flavanols and polysaccharides and proteins can also be

influenced by each other, for example, polysaccharides compete with proteins for proanthocyanidins binding (Brandão et al., 2020; Soares, Gonçalves, Fernandes, Mateus, & De Freitas, 2009; Thongkaew, Gibis, Hinrichs, & Weiss, 2014), or cross-linking to enhance their functional properties (Girard & Awika, 2021). The non-covalent interactions are still the most commonly described in the literature. They affect directly the stability of flavanols and change the physiochemical properties of other compounds (Le Bourvellec & Renard, 2012; Renard et al., 2017; Watrelot & Norton, 2020). Non-covalent interactions between flavanols and other macromolecules generally involve hydrogen bonding, hydrophobic interactions, or π - π stacking (Fig. 2.10). There are multiple binding sites between them, and these types of interactions may occur at these sites. Theoretically, the interaction between flavanols and proteins or polysaccharides may occur in three stages: first, a small amount of flavanol molecules can bind to proteins (or polysaccharides) to form soluble complexes, then if the concentration of polyphenols is high enough, aggregates are formed, and finally higher concentrations of flavanols lead to precipitates. Nature of the flavanols, polysaccharides and proteins and as well as various processing conditions all have compounding effects upon these interactions.

Interactions with polysaccharides, e.g., cell wall polysaccharides and starch, are considered regulators of flavanols stability and bioaccessibility/bioavailability (Amoako & Awika, 2019; Le Bourvellec et al., 2019; X. Liu et al., 2020; X. Liu, Renard, Rolland-Sabaté, & Le Bourvellec, 2021; Monfoulet et al., 2020). For instance, polymeric proanthocyanidins and amylose can form resistant starch. These complexes may withstand digestion in the upper digestive tract and reach the colon intact, where they can play a healthy role as a substrate for human gut microbiota (Amoako & Awika, 2019). The interaction between procyanidins (or flavanol monomers) and cell wall polysaccharides can regulate their bioavailability and their response to anti-inflammatory biological activity (Le Bourvellec et al., 2019; Monfoulet et al., 2020). The presence of flavanols, e.g. (-)-ECG/EC/EGCG, can cause the aggregation with polysaccharides and reduce the viscosity of the solution (Tudorache & Bordenave,

2019). These phenomena may have a broad impact on food formulation and processing.

The interaction with proteins has been an issue of concern during the food processing, because it affects the sensory attributes and functional characteristics, and the nutritional quality of food. For example, astringency, the drying or puckering feeling in the mouth, plays a key role in the taste of wine, and it is also considered an important quality parameter of wine (Ramos-Pineda, Carpenter, García-Estévez, & Escribano-Bailón, 2020; Soares et al., 2020; Vidal et al., 2003). The ternary mixture of polysaccharides/proteins/flavanols is considered to be the main reason for regulating the astringency of red wine (Lei et al., 2019; Watrelot, Heymann, & Waterhouse, 2020). EGCG can improve the physicochemical properties and bio-accessibility of zein-based curcumin nanoparticles (Yan et al., 2019). The presence of rice glutelin can enhance the antioxidant capacity of procyanidin dimer (Dai et al., 2019). The colloidal complex of bayberry proanthocyanidins and gelatin formed by hydrogen bonding shows higher emulsifying ability and oxidation resistance than gelatin or proanthocyanidins alone (S. Chen et al., 2020). These interactions have a significant impact on food quality and potential health benefits, and have an important guiding role in the application and delivery of flavanols in food systems.

2.2.5 Recent developments in acidolysis of proanthocyanidins

Several analytical methods are commonly used to determine the composition of proanthocyanidins, their DP and their galloylation percentage: colorimetry, chromatography and mass spectrometry (Hümmer & Schreier, 2008; Rue, Rush, & van Breemen, 2018; Schofield, Mbugua, & Pell, 2001). However, more complex structural information needs to be obtained by acidolysis, which is probably the most convenient and appropriate analytical method for confronting the complexity of flavanol oligomers and polymers, as well as various food matrices. For example, the analysis of proanthocyanidins generally depends on the development of high-performance liquid chromatography (HPLC) technology. The composition and structure information can be obtained online by combining UV-visible light, mass and nuclear magnetic

resonance spectroscopy. However, sample extraction, separation and purification are essential steps in the development of analytical procedures. Normal-phase HPLC has been widely used to resolve oligomeric proanthocyanidins. The retention time is directly proportional to the DP of proanthocyanidins and inversely proportional to the isomer resolution, but when DP is higher than DP 10, proanthocyanidins present broader peaks (Gu et al., 2002; Le Bourvellec, Picot, & Renard, 2006). Although there is a lack of commercial standards for establishing calibration curves, NP-HPLC combined with a mass spectrometer (MS) can determine the DP of chromatographic peaks (Neilson, O'Keefe, & Bolling, 2016). Rue et al. (2018) have conducted a comprehensive review on the quantitative analysis of proanthocyanidins by mass spectrometry, e.g., LC-MS and matrix-assisted laser desorption ionization (MALDI)-MS. Detailed structural information of each molecule can be obtained by analyzing the fragmentation pattern. However, to date, these existing analysis methods have somewhat limitations (e.g., limitation for diverse structures and lack of standards), and the research of high polymeric proanthocyanidins has been hindered to a certain extent. Although the analysis and quantification of high-molecular-weight proanthocyanidins are analytical challenges, their monomeric forms are easy to analyze. A good option is to depolymerize proanthocyanidins to determine their composition and structure, of which acidolysis is the most used method, e.g., phloroglucinolysis, thiolysis and thioglycolysis. Advances in acidolysis methods can promote the determination of proanthocyanidins in foods, and have a guiding role in further understanding the fate of flavanols. Therefore, we will focus on the latest developments in acidolysis methods. The earliest acidolysis methods will be described as followed, together with a brief description of the colorimetry.

2.2.5.1. Colorimetry

The colorimetric methods were the first methods to be used: (i) butanol-HCl (acidolysis); (ii) 4-dimethylaminocinnamaldehyde (DMAC) and vanillin assays (electrophilic addition of aromatic aldehydes) (Haslam, 1989; Payne, Hurst, Stuart, et al., 2010; Sun, Ricardo-da-Silva, & Spranger, 1998). In the butanol-HCl method,

proanthocyanidins are first cleaved and converted into anthocyanins, and then the absorbance (550 nm) is measured. In the vanillin-H₂SO₄ assay, the vanillin aldehyde group can react with proanthocyanidins to form a colored compound with an absorbance at 510 nm. However, in many cases, the presence of anthocyanins with similar absorption spectra (520 nm) may interfere with the proanthocyanidins' absorbance. DMAC assay has higher sensitivity than vanillin and butanol-HCl analysis. In most cases, DMAC and the A-ring carbon C8 of the terminal unit of proanthocyanidins preferentially undergo condensation reaction (acidic conditions) to form a colored compound that can be detected at 640 nm, thereby reducing the possibility of anthocyanin interference. Moreover, the DMAC staining does not distinguish between flavanol monomers (catechins) and polymers (procyanidins), and the proanthocyanidin–DMAC molar absorption coefficients are affected by both the DMAC reagent environment and proanthocyanidin structural variations (Yifei Wang et al., 2016). However, the reaction of acid butanol and vanillin assay are not limited to the terminal unit. These methods have the advantages of being cheap, fast and easy to implement, and are often used for preliminary analysis of proanthocyanidin. It should be noted that however their results are structurally different, due to reaction either with the terminal (DMAC) or with extension (butanol-HCl) units of the proanthocyanidins (see § 5.3 for in-depth discussion). Moreover, these assays are not specific and have a series of interfering compounds; they also lack of appropriate standards, which makes them difficult to reproduce between different types of samples and purity (Neto et al., 2020; Yifei Wang et al., 2016) and therefore to compare between articles.

2.2.5.2. Principle of acidolysis

The C-C bond between proanthocyanidin units is relatively labile in mild acid conditions. In the presence of strong or weak acids at variable concentrations and depending on temperature, these interflavanic bonds can be cleaved due to acid-catalyzed depolymerization. Following the rupture of the bonds, the terminal unit is released in the reaction medium in the form of free flavanols, while a carbocation is formed in position 4 of the extension units. This allows consecutive condensation with

a nucleophile, most often in the case of proanthocyanisins a thiol-carrying moiety. Therefore, the acidolysis methods are very flexible in the choice of solvents and reagents. For these reasons, much attention has been focused on the acidolysis of proanthocyanidins. Numerous works have been published, in which the reaction has been carried out in a wide range of temperature, time and nucleophile / proanthocyanidin ratio. Researchers have been committed to develop more effective acidolysis studies and analyze the products of acidolysis in more depth, which will be discussed in detail later in this work.

2.2.5.3. Choice of nucleophile for liquid chromatography

[Table 2.2](#) summarizes both the advantages and drawbacks of various nucleophilic reagents. Butanolysis (acid butanol assay) is considered the earliest acidolysis assay, that is, to depolymerize proanthocyanidins into their terminal (flavanols) and extension (anthocyanins) units at 100°C in acid- and iron-catalyzed conditions (Porter, Hrstich, & Chana, 1985). The red colored compounds (anthocyanidins) can be measured at 550 nm. However, this method is not perfect. The presence of anthocyanins in the sample may overestimate the content of proanthocyanidins and must be deducted from the final result before depolymerization (Neilson et al., 2016). Generally, a more accurate determination of extractable and non-extractable proanthocyanidins can be performed when thioacidolysis is applied directly to fruit powder rather than prior solvent extraction followed by HPLC-DAD analysis of the reaction medium, because some highly polymeric proanthocyanidins are not effectively extracted from plant tissues (Saura-Calixto & Pérez-Jiménez, 2018). In butanolysis, the higher the polymerization of proanthocyanidins is, the more realistic their content in terms of color intensity.

Table 2.2 Comparison of the reagents and nucleophiles used to analyze proanthocyanidins.

Reagent	Advantages	Drawbacks	Optimal conditions	References
Colorimetric methods				
Butanol/HCl (550 nm) and Vanillin/H ₂ SO ₄ (510 nm)	Less expensive, time-saving and easier to implement. Rapid estimate of the total content of proanthocyanidins.	The stereochemistry at positions C2-C3 of the polymer unit is destroyed. Presence of side reactions, which can decrease recovery yields of the products. The content of recalcitrant and bound proanthocyanidins may be underestimated. Lack of specificity and sensitivity. Some non- proanthocyanidins (e.g., anthocyanin, chlorophyll and ascorbic acid) interfere with quantitation of proanthocyanidins.	HCl-butanol (5%, v/ v), 95 °C for 40-60 min; Vanillin/H ₂ SO ₄ : 30-60 °C min for 15-30 min.	(Makkar, Gamble, & Becker, 1999; Neilson et al., 2016; Zeller, 2019)
Dimethylaminocinnamaldehyde (DMAC) (640 nm)	Highly specific reagent, which only reacts with terminal unit of proanthocyanidins. Higher sensitivity than Butanol/HCl and Vanillin.	The reaction is proportional to molar and not ponderal content; the degree of polymerization of proanthocyanidins modulates colorimetric response.	DMAC reagent (0.1%), 25% v/v HCl (37%).	(Feliciano et al., 2012; Prior et al., 2010; Yifei Wang et al., 2016)
Phloroglucinolysis				
Phloroglucinol	Odorless	In nonoptimized conditions, the yields of phloroglucinol (flavanol equivalent) is lower than that of benzyl mercaptan.	Methanolic solution of 50 mg/mL phloroglucinol and 10 mg/mL ascorbic acid, 0.1 M HCl, 50 °C for 20 min.	(R. K. Gupta & Haslam, 1978; Kennedy & Jones, 2001; Matthews et al., 1997; Wong-Paz et al., 2021)

(Continues)

Table 2.2 (Continued)

Reagent	Advantages	Drawbacks	Optimal conditions	References
Thioglycolysis				
Thioglycolic acid/2-mercaptoethanol	This method does facilitate differentiation of A- and B-type proanthocyanidins.	Thioglycolic acid may polymerize into thioester at room temperature.	Thioglycolic acid solution: 40 μ L of thioglycolic acid in 4960 μ L of methanol / concentrated HCl 95/5 v/v, 90 $^{\circ}$ C for 6 min.	(Mouls & Fulcrand, 2012; Wong-Paz et al., 2021)
Thiolysis				
Benzyl mercaptan/toluene- α -thiol	Specific and more sensitive than the classically colorimetric methods. It is suitable for either low amounts of proanthocyanidins or insoluble proanthocyanidins.	Solvent toxicity. Undesirable and nauseating smell. Thiolysis is influenced by the solvent. Acid/thermal conditions may cause residue epimerization after release. The thiolysis rate of C4 \rightarrow C8 is higher than that of C4 \rightarrow C6, and the thiolysis rate of 2,3,-cis residues is higher than that of 2,3-trans residues. The double bond between A-type proanthocyanidin units and biaryl or biaryl ether linkages have an anti-thiolysis effect.	Toluene- α -thiol solution (5%, v/v in dried methanol) with dried acidified methanol, 40 $^{\circ}$ C for 30 min.	(Birtic et al., 2019; Guyot, Marnet, & Drilleau, 2001; Guyot, Marnet, Laraba, Sanoner, & Drilleau, 1998; Matthews et al., 1997; Thompson, Jacques, Haslam, & Tanner, 1972; Wong-Paz et al., 2021)
Furanolysis				
Menthofuran	High efficiency, fast conversion and low concentration used. Easily available.	For some structures (e.g., 5-deoxy tannins or A-type proanthocyanidins), more stringent conditions must be used for testing (e.g., higher temperature and/or acid concentration).	Methanolic solution of menthofuran at equimolar or equal weight as proanthocyanidins, 0.1 M HCl, 30 $^{\circ}$ C for 2 h.	(Billerach, Roumeás, Dubreucq, & Fulcrand, 2020)

To improve the quantification of proanthocyanidins, Grabber, Zeller, & Mueller-Harvey (2013) found that butanol-HCl with co-solvent acetone increased the anthocyanins production from forage *Lotus*. Acidified acetone (50%, 70 °C) can effectively extract proanthocyanidins that are firmly bound to fibers. Furthermore, this research group optimized the sequential analysis of the acetone water extract and insoluble residues extracted from various plants, compared the direct analysis of whole tissue, and found that a sequential method provided a good recovery rate and accurate estimation value for proanthocyanidins (Grabber & Zeller, 2020). This was confirmed by Zuleta-Correa et al. (2020) who found that the solvent mixture (acetone-butanol-ethanol) may be a sustainable alternative for anthocyanin and polyphenol extraction.

Generally, conventional acidolysis, including phloroglucinolysis, thiolysis and thioglycolysis, performs one of the most effective methods for the depolymerization of proanthocyanidins. The carbocation reacts with a nucleophilic compound (e.g., benzylthioether for thiolysis reactions) to form stable C-4 thioethers (e.g., benzylthioether derivatives) derived from the extension units (Fig. 2.7). There are several classical types of nucleophiles: mercaptans (e.g., thioglycolic acid and toluene- α -thiol/benzyl mercaptan) (Betts, Brown, Brown, & Pike, 1967; Guyot, Marnet, & Drilleau, 2001; Guyot et al., 1998; Prieur, Rigaud, Cheynier, & Moutounet, 1994; Sanoner, Guyot, Marnet, Molle, & Drilleau, 1999; Thompson et al., 1972) and catechin A-ring analogs, such as phloroglucinol (Kennedy & Jones, 2001; Matsuo, Tamaru, & Ito, 1984; Matthews et al., 1997), 2,4,6-trihydroxytoluene and resorcinol (Fletcher, Porter, & Haslam, 1976). The different adducts obtained with the different proanthocyanidin units can be quantified by HPLC-DAD to identify the structural characteristics of the initial proanthocyanidins, e.g., the constituent units and the degree of polymerization and galloylation. The DP corresponds to the average number of monomeric units which constitute proanthocyanidins (Fig. 2.7). To distinguish between the native monomers naturally present in the samples and the monomers resulting from the release of the proanthocyanidin terminal units after acidolysis, a direct analysis without acidolysis is necessary. The benzyl mercaptan derivatives result in less polar

compounds eluting at the end of a reverse phase (typically C18) chromatogram and are generally easily separated for other phenolic compounds. In contrast, phloroglucinol adducts are polar compounds and sometimes co-elute with phenolic acids and other phenols (Matthews et al., 1997).

The application of the classical nucleophiles is particularly mature and has been significantly optimized in the reaction conditions and solvents (Wen et al., 2019), but the nauseating odor of mercaptans it is a great obstacle in proanthocyanidin analysis. Moreover, the toxicity of the trapping nucleophiles has also been questioned due to the extensive use of nucleophilic reagents. Recently, an improved nucleophilic trapping reagent, namely menthofuran, has been shown to be possible in the depolymerization of proanthocyanidins (Billerach et al., 2020). Billerach et al. (2020) report that menthofuran (3,6-dimethyl-4,5,6,7-tetrahydro-1-benzofuran) exhibits excellent acidolysis capability in the same conditions (30 °C and 0.1 M HCl) and lower weight ratio (1:1) compared to classical used nucleophiles, phloroglucinol and 2-mercaptoethanol. The yield of proanthocyanidin constituent units by menthofuran was the same as 10-times molecular equivalent phloroglucinol and 100-times 2-mercaptoethanol (Billerach et al., 2020). It is recommended to use 1 g/L menthofuran for 1 g/L soluble proanthocyanidins in methanol and to use 2 g/L menthofuran for 10 g/L dry raw biomass at 30 °C over 2 h. Compared with the large molar excess and relatively high temperature required by routinely used nucleophiles, its high efficiency leads proanthocyanidins to be quickly converted at low temperature into monomer units without reversible reactions. In addition, the condensed compounds of menthofuran and the extension units are more stable than the benzylthioether compounds, allowing more reactions to be performed in a day.

Suo et al. (2019) introduces a novel nucleophile: based on thiopronin containing thiol, which can capture the flavanol monomers depolymerized from proanthocyanidins and generate (+)-catechin / (-)-epicatechin / (-)-epicatechin gallate-4 β -S-thiopronin methyl ester. The optimal conditions for proanthocyanidin thiolysis are 55 °C and 60 min in the presence of 0.4 M methanolic HCl (Suo et al., 2019).

2.2.5.4. Specific methods for A-type procyanidins

One of the main limitations of acidolysis is that only the B-type interflavanic linkage can be broken during the depolymerization reaction. The A-type ether bond remains stable during thiolysis, therefore the ratio of A-type linkages cannot be directly obtained. However, thiolysis results in production of A-type dimers, either simple type A procyanidins or substituted (A-thio). Consequently, the percentage of A-type proanthocyanidins can be calculated by thiolysis and using a calibration curve of commercially available A-type proanthocyanidin dimers standards (Bujor, Ginies, Popa, & Dufour, 2018; Tarascou et al., 2011). The ratio of A-type linkage was calculated using the following equation: % A-type bond = $(A_2 + A_2\text{-thio}) / (\text{thio-epicatechin} / \text{catechin} / \text{epigallocatechin} + 2 \times A_2\text{-thio} + A_2)$. Gao et al. (2018) also developed a method to quantify the A-type bond ratios of cranberry proanthocyanidins and the equivalent of A-type proanthocyanidins. They determined the proportion of A-type bonds in proanthocyanidins using commercially available standards after thiolysis using cysteamine as the nucleophile. Five products were obtained by thiolysis of three proanthocyanidin trimers using cysteamine: catechin (P₁), epicatechin (P₂), epicatechin cysteamine thioether (P₃), procyanidin A₂ (P₄) and procyanidin A₂ cysteamine thioether (P₅), and then separated and quantified by the reverse-phase HPLC. The average degree of polymerization and A-type linkage ratio can be calculated by molar number of $(P_1 + P_2 + P_3 + 2P_4 + 2P_5) / (P_1 + P_2 + P_4)$ and the peak area of $(P_4/2 + P_5/2) / (P_1 + P_2 + P_3 + P_4/2 + P_5/2)$, respectively. The optimal acidolysis conditions are at 70 °C, 20 min and in the presence of 0.3 M HCl with low-odor nucleophilic cysteamine (Gao et al., 2018). Y. Wang et al. (2016) report that a method superior to the vanillin-acid assay, but using 4-dimethylaminocinnamaldehyde (DMAC) to quantify proanthocyanidins and assess the effects of DP, linkage type and its position on the reactivity of proanthocyanidins with DMAC reagents. DMAC can selectively react with C8 of the A-ring in flavanols, thereby producing structurally distinct flavanol oligomers that have distinct spectra. B-type proanthocyanidin dimers (including procyanidin B₁, B₂ and mixed cocoa dimers) give a green tone by reaction with DMAC, while A-type dimers

(including procyanidin A1, A2 and mixed cranberry dimers) give a blue tone. In addition, the B-type dimers with DMAC show a major 640 nm peak and a secondary 440 nm peak in the absorbance spectrum, while the A-type dimer conjugates show only a 640 nm absorption peak (Y. Wang et al., 2016). Similar to B-type dimers, A-type peanut trimer A and cranberry DP3, and B-type trimers show two absorption peaks. The difference between these two trimers and other trimers is absence of double interflavan linkage between the first and second flavanol units in proanthocyanidin molecule.

2.2.6 Conclusions and future perspectives

In this review, we emphasize the changes (content, chemical structure, epimerization, and degree of polymerization) and reactivity of flavanols during physical processing. The bioactivity of flavanols depends to a great extent on their content and chemical structure, while the effect of various processing and interaction with the food matrix during the process determines their structural changes. Food processing can be used to stabilize and produce long-lasting foods, but also to adjust the structural changes of flavanols. Therefore, food scientists need to find the operating conditions to balance the target structure of flavanols. These precise processing will provide guidance information for the precise regulation of flavanols during processing. Therefore, a focus for future research will be how to process foods more wisely, so that they can retain, release (bioavailable) or at least convert flavanols into a bioavailable form through structural modification or decomposition of parent compounds.

In addition, the impact of processes on the final structure of proanthocyanidins (especially for DP) is a poorly explored issue, and more attention should be paid to this matter. Proanthocyanidins, the major polyphenol in human foods/drinks, remain a challenge: long neglected (except for wine color/astringency), complex, difficult to analyze and highly reactive. Emerging data indicate that polymerized proanthocyanidins also have potential health benefits after fermentation in the colon, therefore this is an untapped opportunity, but it is also a big challenge. Although new methods, to a certain extent, have opened up the study of this class of molecules beyond

wine, they are relatively complex and limited. Because of wider availability of commercial standards, easy analysis, and relatively high bioavailability, most of the work has focused on monomers, few data can be found on oligomers, and even fewer on polymers. Therefore, the development of efficient and flexible methods for proanthocyanidins based on various structures has not been developed to a large extent, at present, which seems to be the main obstacle to be overcome. Innovative, green and user-friendly analytical methods need to be further developed.

Highlights

- The most important reactivity of flavanols during processing includes oxidative coupling and rearrangements, chain cleavage, structural rearrangements (e.g., polymerization, degradation and epimerization), and addition to other macromolecules, i.e., proteins and polysaccharides.

- Acidolysis is an indispensable step for the analysis of high-polymeric proanthocyanidins.

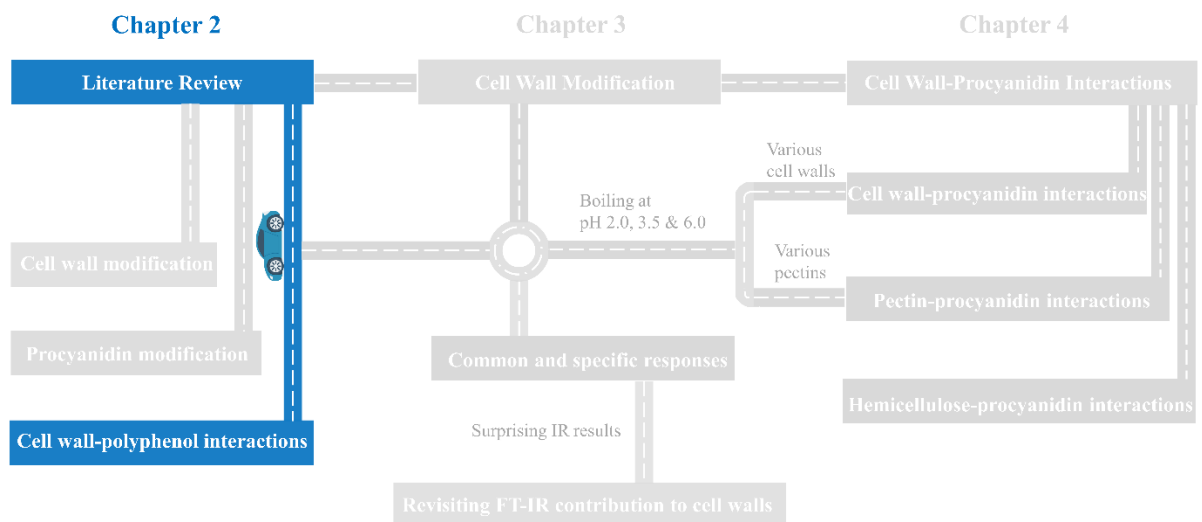
Knowledge gaps

- The impact of processes on the final structure of polymerized proanthocyanidins is a poorly explored issue, and more attention should be paid to this matter.

- The development of efficient and flexible methods for proanthocyanidins based on various structures has not been developed to a large extent, at present, which seems to be the main obstacle to be overcome.

Section 2.3

Interactions between cell wall polysaccharides and polyphenols: Effect of molecular internal structure



A version of this section has been published as:

Liu, X., Le Bourvellec, C., & Renard, M. G. C. C. (2020). Interactions between cell wall polysaccharides and polyphenols: Effect of molecular internal structure. *Comprehensive Reviews in Food Science and Food Safety*. 19(6), 3574-3617.

Cell wall polysaccharides (CPSs) and polyphenols are major constituents of the dietary fiber complex in plant-based foods. Their digestion (by gut microbiota) and bioefficacy depend not only on their structure and quantity, but also on their intermolecular interactions. The composition and structure of these compounds vary with their dietary source (i.e., fruit or vegetable of origin) and can be further modified by food processing. Various components and structures of CPSs and polyphenols have been observed to demonstrate common and characteristic behaviors during interactions. However, at a fundamental level, the mechanisms that ultimately drive these interactions are still not fully understood. This review summarizes the current state of knowledge on the internal factors that influence CPS-polyphenol interactions, describes the different ways in which these interactions can be mediated by molecular composition or structure, and introduces the main methods for the analysis of these interactions, as well as the mechanisms involved. Furthermore, a comprehensive overview is provided of recent key findings in the area of CPS-polyphenol interactions. It is becoming clear that these interactions are shaped by a multitude of factors, the most important of which are the physicochemical properties of the partners: their morphology (surface area and porosity/pore shape), chemical composition (sugar ratio, solubility, and non-sugar components), and molecular architecture (molecular weight, degree of esterification, functional groups, and conformation). An improved understanding of the molecular mechanisms that drive interactions between CPSs and polyphenols may allow us to better establish a bridge between food processing and the bioavailability of colonic fermentation products from CPSs and antioxidant polyphenols, which could ultimately lead to the development of new guidelines for the design of healthier and more nutritious foods.

2.3 Interactions between cell wall polysaccharides and polyphenols:

Effect of molecular internal structure

2.3.1 Introduction

From the perspectives of both manufacturers and consumers of food products, there is a growing appreciation of the importance of interactions between polyphenols and macromolecules in food. Polyphenols have potential health benefits that, particularly for non-extractable or complex dietary polyphenols, are largely mediated by the products of their colonic fermentation (Loo et al., 2020; Tuohy & Del Rio, 2014). Therefore, their health properties can be strongly affected by the food matrix in which they are processed and consumed (Kardum & Glibetic, 2018). This matrix contains cell wall polysaccharides (CPSs), a common component of plant-based foods that is found in a variety of natural sources. CPSs are known to interact with various polyphenols, modifying their bioaccessibility, bioavailability, and bioefficacy (Holland, Ryden, Edwards, & Grundy, 2020; Ribas-Agustí et al., 2018). In addition, CPSs can affect host health through a variety of mechanisms depending on their dietary source, specific physicochemical structure, fermentability, and physiological properties in the gut (J. Cui et al., 2019). While the interaction of CPSs with polyphenols during processing has been widely reported in the past decade, the specific structural determinants behind these macromolecular interactions have not been systematically established; likewise, little is known about their consequences on host health. Might a better understanding of such interactions yield new ideas for improvements in food processing and human nutrition? To answer this question, it is necessary to integrate analyses of traditional processing phenomena, internal mechanisms, and new insights from different systems of CPS-polyphenol interactions. The time has come for a thorough discussion of this area of study, from large-scale patterns down to the roles of individual atoms. From our perspective, a major issue that remains to be explored is the effect of internal structure at the molecular level. In the context of food processing, this is of particular relevance for the bioavailability of polyphenols, especially complex polyphenols (e.g.,

proanthocyanidins) which are metabolized by the human gut microbiota (Saura-Calixto et al., 2010) into low-molecular-weight metabolites.

Most polyphenols are localized in plant vacuoles, which are separated from the cell walls by cell membranes. For this reason, interactions between CPSs and polyphenols are impossible in the living cells of healthy plants. A remarkable exception is found in a few botanical families in which polyphenols form part of the primary cell wall structure. Hydroxycinnamic acids (for example ferulic acid) are linked to arabinogalactans in members of the Chenopodiaceae such as sugar beet (Rombouts & Thibault, 1986) or spinach (Fry, 1983), and to arabinoxylans in species of Poaceae such as bamboo (Ishii, 1991), wheat (Tuyet Lam, Iiyama, & Stone, 1992), or maize (Grabber, Hatfield, Ralph, Zon, & Amrhein, 1995). With the exception of these specific cases, CPS-polyphenol interactions are likely to occur during and after the physical damage and senescence of plants. CPSs and polyphenols are present together in many plant-based food systems, in which their interactions play an important role in determining the ultimate bioavailability of polyphenols as well as their extractability in food processing. As an example, the quantities of phenolic acids and proanthocyanidins found in wine, apple juice, and pear juice are generally lower than what would be expected from the composition of the fruit, and differ widely among plant varieties (Bindon & Kennedy, 2011; Bindon & Smith, 2013; Bindon, Smith, Holt, & Kennedy, 2010; Bindon, Smith, & Kennedy, 2010; Brahem, Eder, Renard, Loonis, & Le Bourvellec, 2017; Guyot, Marnet, Sanoner, & Drilleau, 2003; Le Bourvellec, Le Quere, & Renard, 2007; Renard et al., 2011). This has been linked to the formation of CPS-polyphenol complexes during food processing, which can also be accompanied by the oxidation of polyphenols by polyphenol oxidase in damaged plant tissues (Guyot et al., 2003; Le Bourvellec et al., 2009).

In addition, fruit processing leads to the production of non-extractable polyphenol (NEPP), which cannot be directly absorbed by the small intestine (Saura-Calixto et al., 2010). NEPPs are polymeric polyphenols that are linked to the food matrix (e.g., cell walls) during food processing and consumption (Eran Nagar et al., 2020; Saura-Calixto,

2012). As an example, heat treatment and acidic conditions during the production of applesauce may cause apple procyanidins to depolymerize and form carbocations, which then form covalent bonds with the nucleophilic groups of CPSs (Le Bourvellec et al., 2013). Compared with extractable polyphenols, NEPPs remain poorly known, and very little is known about the effects of processing on CPS-NEPP interactions and their digestive fates. Although many NEPPs and complex polyphenols, e.g., proanthocyanidins, have very low bioavailability in the upper gut, their resulting metabolites (mostly phenolic acids), produced by the colonic microbiota, are highly available (Aura et al., 2013; Palafox-Carlos, Ayala-Zavala, & González-Aguilar, 2011; Saura-Calixto et al., 2010). This process can also be modulated by interactions with CPSs, both noncovalent and covalent (Le Bourvellec et al., 2019; Saura-Calixto, 2011). Compared to unbound polyphenols, interactions with CPSs reduce the degradation of procyanidins during digestion and the production of anti-inflammatory bioactive metabolites, but favor butyrate production, which is known for its beneficial effects on health. Consequently, processing prior to ingestion may modify the nutritional quality of foods, with particular effects on their metabolism via the gut microbiota. There is already abundant evidence that CPS-polyphenol interactions modulate the fermentation of polyphenols in the gut (Le Bourvellec et al., 2019; Monfoulet et al., 2020; Phan et al., 2020; Tarko & Duda-Chodak, 2020). It is likely that these effects translate into changes in the bioactive metabolites present and their potential beneficial effects, which might have far-reaching implications for food processing and human health.

Previous reviews have summarized what is known about interactions between polyphenols and major macromolecules, e.g., carbohydrates, lipids, and proteins (Bordenave, Hamaker, & Ferruzzi, 2014; González-Aguilar, Blancas-Benítez, & Sáyago-Ayerdi, 2017; Jakobek, 2015; Le Bourvellec & Renard, 2012; Renard et al., 2017; F. Zhu, 2015, 2017). Recently, Jakobek & Matic (2019) published a review of the associations between polyphenols and dietary fiber. However, extensive new evidence suggests that CPS-polyphenol interactions can be dramatically affected by physicochemical characteristics of both partners (e.g., the chemical composition,

molecular weight, degree of esterification, side chains and branching ratios, and porosity of CPSs and the solubility, molecular weight, functional groups, and conformation of polyphenols). To date, there has not been a systematic review of the effects of molecular structure and composition on CPS-polyphenol complexes. A basic understanding of how changes in CPS structure and composition can affect interactions with polyphenols is essential from the perspective of human health, as well as for potential commercial and industrial applications.

The purpose of this review was to collate and summarize the current state of knowledge regarding CPS-polyphenol interactions. We describe the most common technologies and methods that can be used to study these interactions, along with recent developments, and highlight the effects of internal steric structure and molecular composition. We then conclude with an outline of the remaining gaps in our knowledge and directions for future research.

2.3.2 The participants in the interactions

2.3.2.1 Plant cell walls

The plant cell wall is the extracellular matrix that surrounds plant cells, and can be divided into three main types: primary walls, secondary walls, and, in certain species, gelatinous layer walls (Carpita & Gibeaut, 1993). Its main roles are to provide physical protection as well as a porous medium for exchanges with the external environment. Cell walls determine the texture of plant-based foods, and are the main source of dietary fiber in human food (Waldron, Smith, Parr, Ng, & Parker, 1997). Among different species, cell types, and developmental stages, though, the physicochemical structure and function of cell walls can vary widely (Anderson & Kieber, 2020; Burton, Gidley, & Fincher, 2010). Similarly, among different plant taxa, there can also be notable differences in cell wall composition and structure, e.g., type I primary walls are widespread in dicotyledons and non-grass monocotyledons, while type II primary walls are found in cereals and grasses (Carpita & Gibeaut, 1993; Vogel, 2008). There have been excellent reviews of cell wall heterogeneity, complexity, imaging, and health

effects (Burton et al., 2010; Padayachee, Day, Howell, & Gidley, 2017; Y. Zhao, Man, Wen, Guo, & Lin, 2019); therefore, these topics will not be extensively discussed here. Because most research on CPS-polyphenol interactions concerns fruit species (dicotyledons), the basic model under discussion here will be the type I primary cell wall. An illustration of the current model of primary cell walls is provided in Fig. 2.12, which takes into account the proportions of homogalacturonan, rhamnogalacturonan, and xyloglucan.

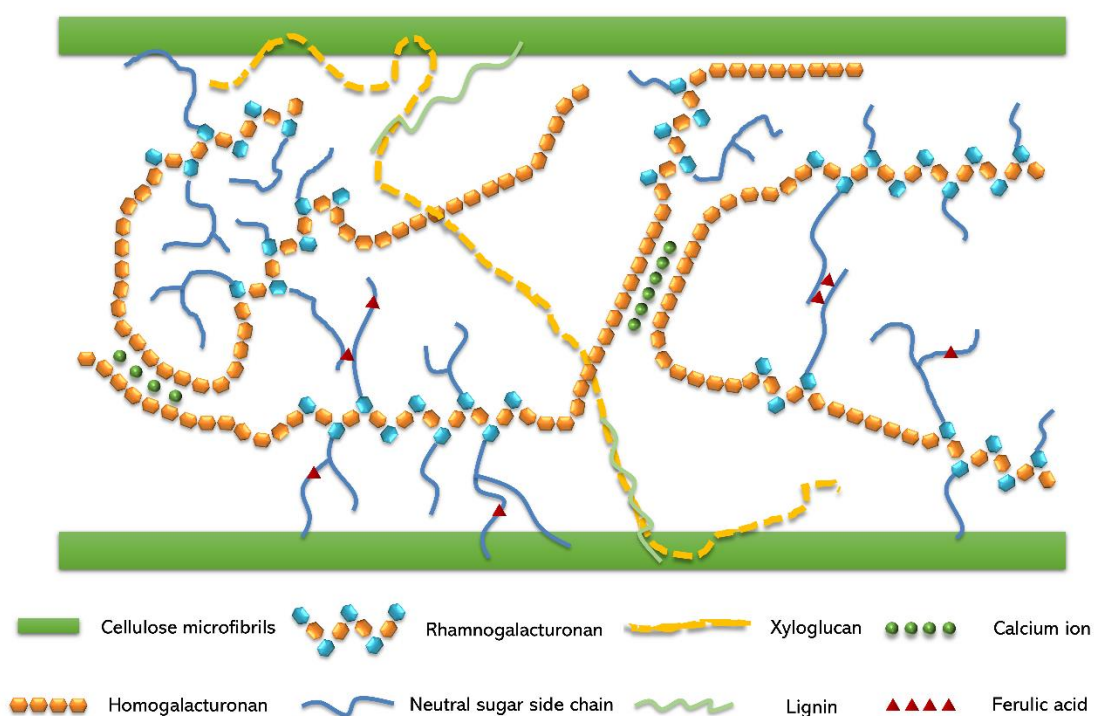


Figure 2.12 Schematic model of type-I primary cell walls (modified and redrawn from a figure of Zykwincka et al. (2005)).

The most abundant component in cell walls is cellulose, a linear homopolymer of β -1,4-linked glucose residues that are arranged in parallel in natural structures to form crystalline microfibrils a few nanometers in diameter. Their growth is directional and the main microfibrils are usually oriented transversely to the direction of cell growth. Microfibrils consist of crystalline and amorphous domains, in proportions that vary depending on both the botanical source and the degree/type of processing.

Hemicelluloses, which include xyloglucans, xylans (arabinoxylans, glucuronoxylan, and glucuronoarabinoxylan), glucomannans, and mixed-linkage glucans, attach to cellulose microfibrils through H-bonds. Xyloglucan is the main hemicellulose in most fruits and vegetables, while in grasses and cereals (Poaceae), the cell wall contains a large amount of xylans and variable proportions of mixed linkage β -glucan.

Pectins are the most complex and heterogeneous group of biopolymers, and are mainly composed of homogalacturonan (HG) and rhamnogalacturonan (RG) I and II (Ridley, O'Neill, & Mohnen, 2001b; Vorwerk, Somerville, & Somerville, 2004). The main sugar constituent of pectins is galacturonic acid, and they can contain different neutral sugar side chains.

Cell walls may contain polyphenols as part of their structure. For example, lignin is a complex hydrophobic polymer characteristic of secondary cell walls, and is linked to non-cellulosic CPSs through ester and ether bonds. Furthermore, ferulic acid and its dehydrodimers, which are mainly ester-linked to arabinoxylans or pectins, enhance the rigidity and strength of some cell walls (Ishii, 1997).

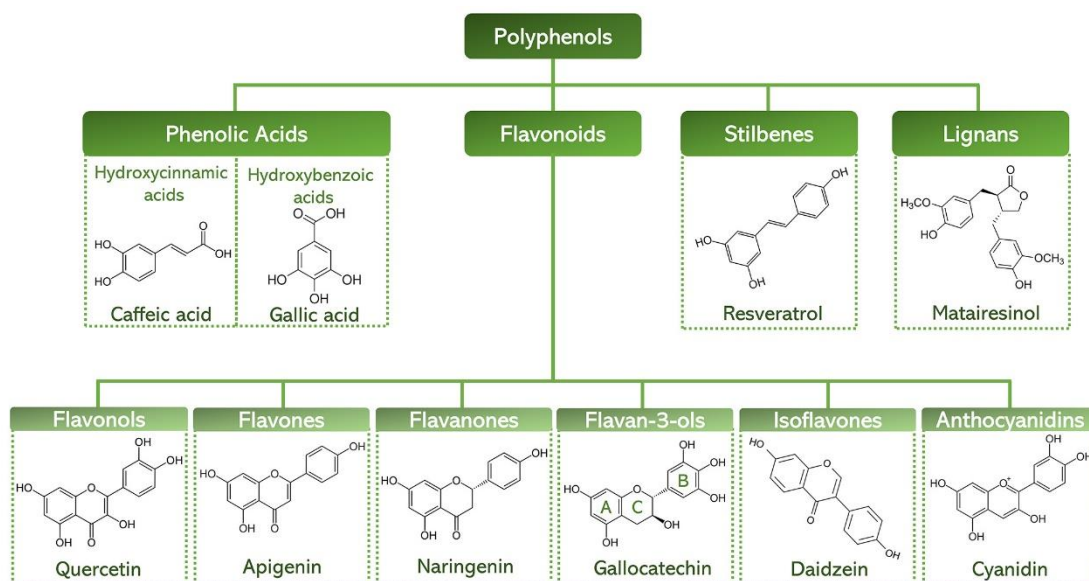
There is a rich diversity of CPSs, shaped by differences in sugar composition, size distribution, shape, charge, extractability, and combinations with other polymers. All CPSs, but especially pectins, are susceptible to physical and chemical conversion reactions during food processing, which alter their structure and result in changes in their functional properties. Under certain processing conditions of pH, temperature, and pressure, pectins can undergo acid hydrolysis and β -elimination reactions, which result in the demethoxylation and depolymerization of HG (Christiaens et al., 2016; Fraeye et al., 2007). Furthermore, food processing can also result in different types of textural changes, which are often related to alterations in the porosity and specific surface area of the cell wall. A wide variety of physical treatments, such as thermal, high-pressure, and drying conditions, can all cause extensive changes in the physicochemical structure of CPSs, which then translate into modifications in their functional characteristics.

Furthermore, the functional properties of polysaccharides can also be altered by the presence of polyphenols, with effects reported on the texture, rheological properties, and stability of food systems (Dobson et al., 2019; Jin et al., 2020; X. Li, Liu, Tu, Li, & Yan, 2019; Tudorache & Bordenave, 2019; Tudorache, McDonald, & Bordenave, 2020). As an example, by crosslinking with arabinan, ferulic acid inhibits the softening of radish during boiling (X. Li et al., 2019). Polyphenols can lead to a decrease in the viscosity and pseudoplasticity of polysaccharides through the formation of polysaccharide-polyphenol aggregations (Tudorache & Bordenave, 2019; Tudorache et al., 2020). CPS-polyphenol interactions play an important role in the modification of polysaccharide properties, and a deeper understanding of these interactions may help to develop and improve upon polysaccharides that serve specific functions in the food industry.

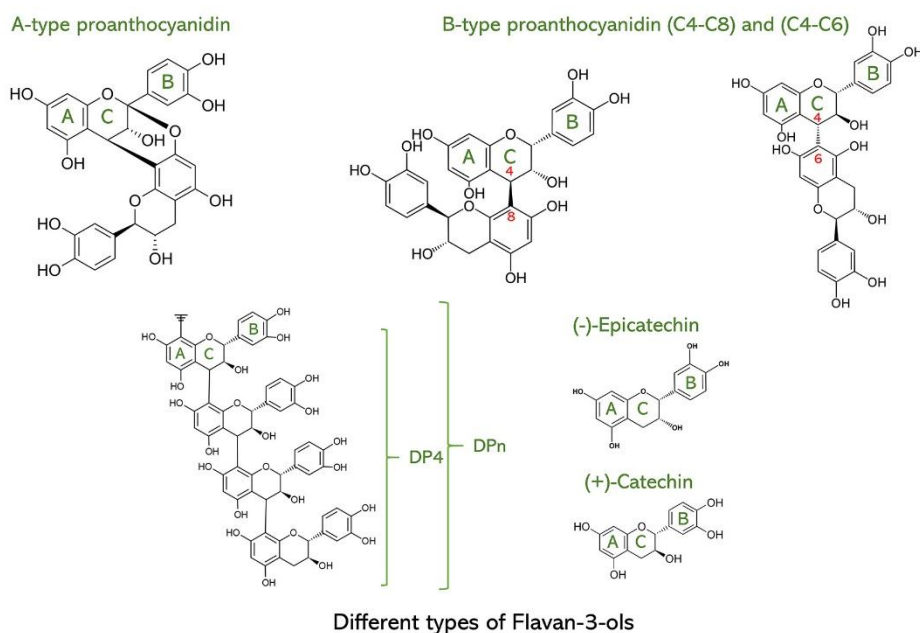
2.3.2.2 Phenolic compounds

Phenolic compounds include multiple sub-classes, such as phenolic acids, flavonoids, stilbenes, and lignans, and vary in molecular weight, type of linkage, mean degree of polymerization, and functional groups. One of the main groups of phenolic compounds is flavonoids; their general structure has a 15-carbon (C₆-C₃-C₆) skeleton, which consists of two phenyl rings (A and B) and a heterocyclic ring (C) (Fig. 2.13) (Pietta, 2000). Depending on the degree of oxidation of the C-ring, they can be further characterized as flavonols, flavones, flavanones, flavan-3-ols, isoflavones, and anthocyanins (Fig. 2.13).

The majority of research on CPS-polyphenol interactions has focused on condensed tannins (proanthocyanidins), which are polymers and oligomers of flavan-3-ol units that are mainly connected by B-type bonds (C₄-C₈ or C₄-C₆ interflavanic linkages). However, degradation-resistant NEPPs account for a large portion of the total polyphenol content in foods and have also been a focus of study. In addition to non-extractable proanthocyanidins, NEPPs also include hydrolyzable or oligomeric polyphenols, which are attached to the cell walls or retained in the food matrix.



Classification and typical structures of major food polyphenols



Different types of Flavan-3-ols

Figure 2.13 Classes and chemical structures of some major polyphenols in plant foods (modified and redrawn from figures of Quideau et al. (2011) and Ribas-Agustí et al. (2018)).

Polyphenols are widely distributed in plants and can have a positive impact on human health (X. Wu et al., 2020). Some monomeric polyphenols are readily absorbed in the upper gastrointestinal tract, notably non esterified phenolic acids (El-Seedi et al., 2012; Santhakumar, Battino, & Alvarez-Suarez, 2018) and the glucosylated ones (Marka, Mullen, Borges, & Crozier, 2009), but they are the exception rather than the rule. In general, polyphenol activity depends on the structure of the food matrix and interactions with other food ingredients, e.g., carbohydrates, lipids, and proteins. One

of their beneficial health effects is the prevention of oxidation of lipids and proteins in the stomach (Gobert et al., 2014; Boléa, Ginies, Vallier, & Dufour, 2019; Lee et al., 2020). Furthermore, many recent studies have shown that CPS-polyphenol complexes have a positive effect in the colon (Kardum & Glibetic, 2018; Le Bourvellec et al., 2019; Grant et al., 2020; Monfoulet et al., 2020; Phan et al., 2020; Tarko & Duda-Chodak, 2020). Polyphenols can be released from their complexes through the action of enzymes or microorganisms in the intestinal tract and biotransformed by the colonic microbial metabolism (i.e., from the non-absorbable to the absorbed form). It has also been reported that these complexes can promote the growth of beneficial microflora and inhibit the growth of pathogenic microbes (Dobson et al., 2019). To more fully exploit these beneficial effects, a more in-depth understanding is needed of the molecular-level mechanisms of CPS-polyphenol interactions.

Food processing may cause the degradation or oxidation of some polyphenols, thereby reducing the amount that can be detected in processed foods (Ribas-Agustí et al., 2018). However, as mentioned above, foods can also be chemically or physically modified during processing in such a way as to enhance the stability or bioavailability of phenolic compounds. For example, heat-induced gelation of xanthan gum/glucomannan can inhibit the thermal degradation of anthocyanins (Jin et al., 2020). Although the interactions between CPSs and polyphenols have been the focus of extensive research, it is not yet clear how, and the extent to which, these interactions are influenced by common or specific factors. The most logical approach toward studying CPS-polyphenol interactions is to first consider the different chemical structures, functional groups, and conformations of the participants (Fig. 2.15) as described in detail below (Section 5).

2.3.3 Analytical methods

Interactions between CPSs and polyphenols generally involve non-covalent bindings that are low-energy and largely reversible. To analyze these, numerous methods have been used, with different working principles and modalities of measurement. By itself, each method provides piecemeal evidence that complements the information obtained from other strategies. To fully determine the affinity and/or binding capacity of these molecules, it is necessary to combine the information from multiple techniques to obtain a global perspective. [Table 2.3](#) summarizes the methods and techniques that can be used, and the advantages and drawbacks of each. Here we present a comprehensive description of various methods that have been applied to the study of CPS-polyphenol interactions, with examples that highlight differences in the information that can be obtained.

2.3.3.1 Thermodynamic measurements

2.3.3.1.1 Isothermal titration calorimetry (ITC)

ITC is a potent tool that has been widely used to identify the thermodynamic changes (endothermic and exothermic) associated with the formation of complexes via the interactions of natural products (e.g., proteins, polysaccharides, and polyphenols). It can even provide complete kinetic profiling in a single experiment (Callies & Hernández Daranas, 2016). ITC can be used to probe binding affinities in the range of 100 mM^{-1} to 1 nM^{-1} ; it yields direct measurements of the binding constant (K_{av}), the stoichiometry (n), and the enthalpy of binding (ΔH), and indirect access to other thermodynamic parameters such as the free energy (ΔG) and entropy (ΔS) of binding (Brahem et al., 2019; Callies & Hernández Daranas, 2016; A. Fernandes et al., 2020; Y. He et al., 2019; Ladbury & Doyle, 2004; Le Bourvellec et al., 2012a; Mamet et al., 2018; Patel et al., 2013, 2011; Watrelot et al., 2013, 2014; Wei et al., 2019). However, ITC has some limitations. Analysis of a single sample usually takes several hours, which means that the potential for automated or high-throughput screening is limited, and that some sensitive polyphenols (e.g., anthocyanins) may be unstable during titration.

Polysaccharide-polyphenol interactions

Table 2.3 Comparison of the methods used to evaluate cell wall polysaccharide-polyphenol interactions.

Technique	Advantages	Limitations and additional information	References
Isothermal Titration Calorimetry (ITC)	ITC provides direct thermodynamic information about the enthalpy, association constant, and stoichiometry of the interaction. It does not require samples to be optically transparent and has high sensitivity. Therefore, ITC is carried out to characterize the energetics of complex formations.	It is important to choose a suitable model to fit the data. In general, the ΔH values reported in the literature are more reliable than the ΔS and K values (ΔS and K values are model-dependent). In addition, polydisperse polyelectrolytes and different experimental conditions have a large effect on ΔS and K values.	Brahem et al., 2019; A. Fernandes et al., 2020; He et al., 2019; Le Bourvellec et al., 2012; Mamet et al., 2018; Patel et al., 2013, 2011; Watrelot et al., 2013, 2014; Wei et al., 2019
Differential Scanning Calorimetry (DSC)	Rapid, simple, versatile, and highly sensitive.	Destructive, only provides data on temperature and enthalpy. It is usually combined with other technologies. An increase in particle size indicates aggregation, while increased turbidity implies the formation of insoluble complexes. Accurate for monodisperse samples, but not for polydisperse samples. Peak resolution is low. When the sample size is too small, dust particles may hinder size determination.	Bermúdez-Oria et al., 2020; Guo et al., 2018; R. Liu et al., 2017
Dynamic Light Scattering (DLS)	DLS provides information about particle size. Very fast and generally straightforward, requires only a small amount of sample.		Carn et al., 2012; He et al., 2019; S. Li et al., 2019; Mamet et al., 2018; Wei et al., 2019
Nanoparticle Tracking Analysis (NTA)	NTA is able to provide a visualization of the sample and give a more complete overview of the aggregation process. It yields an approximate particle concentration and dimensional information based on the Brownian motion of the individual particles. Size analysis for monodisperse and polydisperse samples is very accurate and has significantly better peak resolution than dynamic light scattering.	NTA can be very time-consuming and requires some operational skill to set all software parameters. Reproducibility is poor.	S. Li et al., 2019
Turbidimetry (determined by UV-vis spectrophotometry)	Efficient, simple, cheap, and fast. It can be used to characterize relationships between structure and properties, and gives qualitative information on the size of the aggregates and the rate of aggregation in solution.	Only produces qualitative data, and no information on the binding sites.	De Freitas & Mateus, 2001; A. Fernandes et al., 2020; Haslam & Lilley, 1988; He et al., 2019; S. Li et al., 2019; Mamet et al., 2018; Watrelot et al., 2013, 2014; Wei et al., 2019
X-ray Photoelectron Spectroscopy (XPS)	Provides quantitative information about chemical bonds and elemental mapping in a non-destructive and surface-sensitive manner.	High vacuum and large area are required. Processing is slow, and H cannot be recognized.	Wei et al., 2019
Small-Angle X-ray Scattering (SAXS)	The size, density, and shapes of particles in the solution can be conveniently studied. Sample preparation is simple. It can be applied to dynamic processes.	Requires high sample concentrations and an ordered structure.	Carn et al., 2012
Nuclear Magnetic Resonance (NMR) – solution state	Not destructive and requires a moderate amount of sample (a few mg). It enables determination of affinity constants, K_d , and identification of H or C atoms involved in the interaction. It can be coupled with accurate structure determination; chemical shifts can be related to interaction types. Nuclear Overhauser effect (NOE) and rotating-frame Overhauser effect (ROE) spectroscopy may yield additional structural information for macromolecules.	Requires a highly homogeneous sample, works best with small molecules.	Cai et al., 1990; Connors, 1997; A. Fernandes et al., 2014, 2020; Ishizu et al., 1999; R. Liu et al., 2017
Nuclear Magnetic Resonance (NMR) – solid state	Provides precise information on distances, spatial proximities between specific nuclei, intramolecular hydrogen bonding, and π - π stacked arrangements. There is no size limit.	Longer experimental time, lower sensitivity and resolution. Larger amounts of sample required.	Bermúdez-Oria et al., 2020; Kang et al., 2019; Phan et al., 2017

(Continued)

Table 2.3 (Continues)

Technique	Advantages	Limitations and additional information	References
Fourier Transform Infrared Spectroscopy (FTIR)	Simple, non-destructive, fast, and highly sensitive.	Sheds light on the presence of molecules but not the mechanisms of interaction.	Bermúdez-Oria et al., 2020; Brahem et al., 2019; Guo et al., 2018; Liang et al., 2019; R. Liu et al., 2017; Y. Liu et al., 2018; M. Shi et al., 2019
Fluorescence Microscopy	Adsorption can be directly observed, and the obtained images are very reliable in terms of visualization and internal quantification. It is non-invasive; limited additional sample preparation is required and the sample can be re-used for further characterization. Polyphenols have strong fluorescence, polysaccharides none unless marked with specific probes.	Relatively slow, different images can only be compared qualitatively, many flavonoids require an excitation wavelength that is too low for the usual instrumentation.	Y. Liu et al., 2019, 2018
Confocal Laser Scanning Microscopy (CLSM)	Non-invasive, can be used to see the distribution of polyphenols within living tissue. Fluorescence intensity can be quantified and different dyes can be recorded simultaneously in different channels. Limited image blur caused by light scattering.	The coherence of laser light and laser fluctuations can cause artifacts. A large amount of photobleaching occurs. Scanning is slow and limited in dynamic tracking studies. Lasers can destroy living cells. The resolution is lower than the camera detection. Many flavonoids require an excitation wavelength that is too low for the usual instrumentation.	Gómez-Mascaraque, Dhital, López-Rubio, & Gidley, 2017; D. Liu, Lopez-Sanchez, & Gidley, 2019; Padayachee et al., 2013, 2012a; Phan et al., 2017, 2015
Scanning Electron Microscopy (SEM)	Produces detailed 3D and topographical images of the surface morphology of complexes. The sample preparation is simple, and non-conductive samples can be sprayed with gold.	The preparation of samples can result in artifacts; the method is limited to solid samples.	Guo et al., 2018; Wei et al., 2019
Transmission Electron Microscopy (TEM)	Enables the study of internal structures and offers very powerful magnification and resolution. Images can provide chemical information.	The instrument is large and very expensive. Cumbersome sample preparation; the sample needs to be very thin, less than 150 nm, and as flat as possible. Limited to materials that are electron-transparent.	He et al., 2019; Mamet et al., 2018; Patel et al., 2013, 2011
Molecular Dynamics (MD) Simulation	Removes the limitations of experimental conditions and equipment. It can verify the results of real experiments.	Models of complex systems require more computer power, memory, and time.	A. Fernandes et al., 2014, 2016; Y. Liu et al., 2018

The required concentration of the injection sample can be relatively high, so that it is not possible to study polyphenols with very low solubility (e.g., quercetin). The sample must be as pure as possible and dust-free. Therefore, this technique may be more suitable for samples of higher purity and stability.

Using data generated by ITC, values of Gibbs' binding energy can be calculated using the equation $\Delta G = -RT \cdot \ln K_{av}$, where R is the ideal gas constant and T is the absolute temperature. The change in entropy can be determined according to the relationship $\Delta G = \Delta H - T\Delta S$. From a thermodynamic point of view, ΔG consists of two different contributions (ΔS and ΔH), which together represent the binding affinity (K_{av}). ΔS (the entropy contribution) is generally associated with hydrophobic interactions, loss of water molecules and ions, and conformational changes, whereas ΔH (enthalpy contribution) is attributed mainly to hydrogen bonding, van der Waals forces, electrostatic interactions, and protonation (Callies & Hernández Daranas, 2016; Ladbury & Doyle, 2004). The hydrophobic interactions are long-range phenomena, depend on the corresponding solubilities of both CPSs and polyphenol in the solvent, derived from the elimination of stable water molecules from the binding pocket upon complexation. Instead, hydrogen bonds are considered to be short-range phenomena and tend to enhance the stability of the complex (Israelachvili, 2011). Generally speaking, different combinations of ΔH and ΔS can lead to the same binding affinity, i.e., the same ΔG , and hence the same K_{av} . This means that, even if the binding affinity is the same, the behavior and response of polyphenols to changes in the environment or CPS adsorption could be different, as well as the enthalpy or entropy components (Leavitt & Freire, 2001).

The application of ITC to CPS-polyphenol interactions has revealed that such interactions generally involve both hydrophobic interactions and hydrogen bonds (Le Bourvellec, Bouchet, & Renard, 2005; Le Bourvellec, Guyot, & Renard, 2004; Le Bourvellec & Renard, 2005; Renard, Baron, Guyot, & Drilleau, 2001b). Furthermore, most of these interactions seem to be exothermic, and accompanied by coexisting enthalpy- and entropy-driven phenomena (WatreLOT et al., 2013, 2014). Research on

pear cells determined that the affinity constant (K_{av}) of the interactions between pear cell walls and procyanidins (degree of polymerization (DP): 26) was on the order of $10^2 M^{-1}$ (Brahem et al., 2019), while interactions between pectins (including commercial pectins and the hairy regions of pectins) and procyanidins presented association constants ranging between $10^2 M^{-1}$ and $10^4 M^{-1}$ (Le Bourvellec et al., 2012a; Watrelot et al., 2013, 2014). The affinity constants of interactions between procyanidins and sugar beet arabinan and debranched arabinan were calculated as $391 M^{-1}$ and $540 M^{-1}$, respectively (P. A. R. Fernandes et al., 2020). In general, an association constant larger than $10^4 M^{-1}$ suggests a high degree of affinity (Turnbull & Daranas, 2003). One point that must be considered, though, is that comparison between studies is hindered by the use of different bases for calculation. ITC was designed for monodisperse ligands and proteins with definite molecular structure. However, procyanidins and polysaccharides are polydisperse and can vary in molecular weight, composition, and structure even in highly purified samples. Therefore, the adaptation of ITC to these types of applications is not conceptually obvious. Two options have been presented in the literature: 1) using an average molecular weight to calculate molarities, or 2) using the concentrations of individual subunits of the polyphenols and polysaccharides. Neither is completely satisfactory and the two approaches will yield different constants for the same strength of interaction.

2.3.3.1.2 Differential scanning calorimetry (DSC)

DSC can be used to characterize the thermal properties of complexes, such as the denaturation temperature (T_d)—including the onset (T_o), peak (T_p), and conclusion (T_c)—and enthalpy change (ΔH). Values of T_d and ΔH reflect, respectively, the thermal stability and the ordered conformation of samples (Höhne, Hemminger, & Flammersheim, 2013). This method has been applied to the melting of various biopolymers and the interactions between ligands and proteins (Bruylants, Wouters, & Michaux, 2005), but its use on CPS-polyphenol interactions has been very limited. Although DSC has not been used as much as ITC for this purpose, it requires fewer materials and provides rapid detection for different samples due to its high sensitivity,

reliability, and relative scanning speed (Bermúdez-Oria et al., 2020; Guo et al., 2018; R. Liu et al., 2017). However, since DSC is a dynamic technique, changes in experimental parameters such as particle size, sample weight, and heating rate can have a large effect on the results. Another potential drawback is that this method can only describe the macroscopic properties of a research system, and cannot obtain information at the molecular level. Therefore, it needs to be used in combination with other technologies such as spectroscopy or chromatographic techniques.

Using DSC, Guo et al. (2018) determined that the T_d and ΔH values of corn silk polysaccharide-flavonoid complexes (CSP-CSF complexes) were significantly higher than values from unbound corn silk polysaccharides (CSP), indicating that the CSP-CSF complexes may be more stable and have a more ordered structure than the polysaccharides alone. In an analysis of different maize starches, R. Liu et al. (2017) reported that the addition of low concentrations of oligomeric procyanidins (OPCs) inhibited the retrogradation of amylose maize (HAM), normal maize (NM), and amylopectin maize (APM) starches, and further analysis of the DSC curves revealed different trends in ΔH value among HAM-OPC, NM-OPC, and APM-OPC complexes. In this case, the ΔH value reflects the orientation and stacking energy of the double helix in the crystalline and amorphous regions of starch granules. The hydroxyl groups of OPCs can interact with the OH groups of starch to form hydrogen bonds and modify the order of starch polymer chains. OPCs thus appear to inhibit the retrogradation of starches in a concentration-dependent manner (R. Liu et al., 2017). Another application of DSC is to generate thermograms that can provide the melting temperature for complexes. The heat flow intensity observed for a complex of olive phenolic compounds and apple cell walls was several times that of the apple cell walls alone, providing evidence of significant changes at high temperatures in the internal structure of complexes due to the presence of olive phenolic compounds (Bermúdez-Oria et al., 2020).

2.3.3.2 Spectral measurements

2.3.3.2.1 Turbidimetry determined by UV-vis spectrophotometry

Turbidimetry is the measurement of the loss of light intensity upon its transmission through a suspension of particles. This method was first used to study the binding of polyphenols to proteins (De Freitas & Mateus, 2001; Haslam & Lilley, 1988), and is now widely used to characterize the interaction between polyphenols and polysaccharides (A. Fernandes et al., 2020; Y. He et al., 2019; Sijing Li et al., 2019; Mamet et al., 2018; Watrelot et al., 2013, 2014; Wei et al., 2019). Turbidity or cloudiness at 650 or 600 nm is generally chosen as neither polyphenols nor CPSs absorb at this wavelength; instead, absorbance can be used to detect the formation of cloud and precipitate and provide indications on the formation of insoluble complexes. However, it cannot give information on the mechanism, binding sites, or the morphology/structure of the complexes, nor the quantity of aggregates. This method is suitable for soluble polysaccharides (e.g., pectins) and polyphenols.

2.3.3.2.2 Fourier transform infrared spectroscopy (FTIR)

FTIR spectroscopy can provide useful information on the structure and dynamics of CPS-polyphenol interactions (Bermúdez-Oria et al., 2020; Brahem et al., 2019; Guo et al., 2018; Liang et al., 2019; R. Liu et al., 2017; Y. Liu et al., 2018; M. Shi et al., 2019). It is fast and sensitive, and may be used to detect the presence of polyphenols in CPS matrices. However, it is unable to provide information on binding capacity and sites. Among studies that have made use of FTIR spectroscopy, two recent publications illustrate the different potential applications of this method. Brahem et al. (2019) used principal component analysis to identify specific wavelengths that may be assigned to polyphenols or CPSs. Then, M. Shi et al. (2019) used this method to distinguish samples of puree and pomace with and without epigallocatechin gallate (EGCG). The infrared spectra reflect, in a quantitative manner, the presence of polyphenols or polysaccharides in a complex, with no modification of the signals (i.e., no specific peak or shift of a peak either of the polysaccharide or of the polyphenol). Thus, the difference spectra can

be used to monitor the variations in intensity of polysaccharide/polyphenol-specific vibrations. This type of analysis also demonstrates that CPS-polyphenol interactions have very limited impact on molecular structure at the scale that is investigated by infrared (i.e., covalent bonds).

2.3.3.2.3 Nuclear magnetic resonance spectroscopy (NMR)

From the initial low-resolution NMR analyses, which were limited to moisture, to high-resolution studies involving multiple uses of liquid and solid matrices, NMR has played an important role in interaction studies (Koshani, Jafari, & van de Ven, 2020).

Solution-NMR spectroscopy provides accurate information about the basic structure of a sample. It can also be used to investigate the mechanism behind an interaction. As the result of an interaction between a CPS and a polyphenol, there may be variations in the chemical shifts of hydrogen or carbon atoms; these can be either the direct results of interactions, or indirectly derived from a conformational change that occurs due to binding (Cai et al., 1990). Since the chemical shift is specific to a given carbon or hydrogen on a CPS or polyphenol, the binding site can be precisely identified to determine the mechanism of interaction (Bermúdez-Oria et al., 2020; Cai et al., 1990; A. Fernandes et al., 2020; Ishii, 1997; Ishizu et al., 1999; Phan et al., 2017). For example, this method has enabled the direct inference of information about the ways in which polyphenols form inclusion complexes with cyclodextrins (CD), starch-derived cyclic oligosaccharides composed of glucose units, from 6 to more residues. Specifically, the chemical shifts of the H-3 and H-5 protons in the molecule reflect the fit of the polyphenol inside the cyclodextrin cavity (Cai et al., 1990; Connors, 1997; Ishizu et al., 1999). This technique can then be used to determine the structure of the complexes: if only H-3 of CD is displaced during the interactions, the penetration of the polyphenol into the CD cavity is shallow, while if H-5 is also shifted, the molecule is completely included within the hole (Connors, 1997).

Saturation transfer difference NMR (STD NMR) is a method in which only the protons involved in interactions produce a signal. This method was used by A.

Fernandes, Brás, Mateus, & De Freitas (2014) and A. Fernandes et al. (2020) to establish the affinity scale of the interactions between pectins and anthocyanin.

There are two other variations of NMR with useful applications for the improved understanding of inter- and intra- molecular interactions: nuclear Overhauser effect spectroscopy (NOESY) and rotating-frame Overhauser effect spectroscopy (ROESY) (Sedaghat Doost, Akbari, Stevens, Setiowati, & Van der Meeren, 2019). These can provide direct proof of the spatial proximity between two molecules. For example, Jahed, Zarrabi, Bordbar, & Hafezi (2014) reported that complexes of CD and curcumin produce nuclear Overhauser effect (NOE) cross peaks and changes in the chemical shifts of internal protons, indicating that curcumin forms a complex with CD through its hydrophobic aromatic ring and thereby increases its solubility. Similarly, Gong et al. (2016) confirmed the interaction site of the eugenol-CD complex using its 2D NOESY spectrum, and concluded that eugenol interacts through the methyl group of its aromatic ring with the hydrophobic site in the cavity of CD.

One potential drawback for solution-NMR is that relatively high concentrations are required. This has caused problems of insolubility for some polyphenols and polysaccharides, especially in aqueous or buffered media. Therefore, it can be necessary to use solvent systems such as acetone or dimethyl sulfoxide to maintain the solubility of the complexes. However, the use of organic solvents and ionic liquid solutions for solution-NMR disrupts the physical state and interactions of the molecules under investigation, which introduces some uncertainty to the interpretation of the results.

The application of solid-state NMR (ssNMR) alleviates this limitation to some extent, as it can provide the atomic details of assembled complexes without restrictions on size or solubility. For example, Phan et al. (2017) compared the ^{13}C CP/MAS NMR spectra detected for freeze-dried cell wall fiber-polyphenol complexes to those of cell wall alone. They reported additional peaks from 110 ppm to 160 ppm, indicating the rigidification of polyphenol molecules bound to the polysaccharide matrix. However, they did not find any significant chemical shift changes in the polysaccharide-

polyphenol complexes, providing evidence that neither component undergoes extensive conformational change upon binding. Similarly, Bermúdez-Oria et al. (2020) also found that the ^{13}C CP/MAS NMR spectrum of complexes between olive phenolic compounds and apple dietary fibers was not significantly different from that of the control apple dietary fiber alone.

Another advantage of ssNMR is that it can provide fine-scale details about the spatial proximity of complexes. ssNMR analysis of intact maize stems, enhanced by dynamic nuclear polarization, revealed that the interactions between xylans and lignins are mainly extensive sub-nanometer surface contacts rather than covalent bonds, and that lignin preferentially binds to xylan with a twofold or threefold helical screw conformation (Kang et al., 2019).

2.3.3.2.4 X-ray photoelectron spectroscopy (XPS)

XPS is a quantitative energy spectroscopy technique used to determine the elemental composition, experimental formula, and chemical and electronic states of elements contained in samples (Hollander & Jolly, 1970). Polysaccharide and polyphenol molecules all consist of carbon, hydrogen, and oxygen, with the former containing higher ratios of oxygen to carbon. After the interaction, the O/C ratio decreases as a result of the increased adsorption of polyphenols to polysaccharides. As an example, Wei et al. (2019) reported that the O/C ratio decreased with an increase in the mass ratio of tannic acid (TA) to wheat starch (WS). Further investigation with Scanning Electron Microscopy (SEM) revealed a three-step interaction process. Namely, TA gradually adsorbs to the surface of WS, aggregates, and reabsorbs (forming a thicker TA molecular layer), then eventually reaggregates (producing larger aggregates and even precipitate). This is similar to the interactions between proline-rich proteins and flavan-3-ols (Pascal et al., 2007). To our knowledge, there have not yet been any published studies that use this method to determine changes in O/C ratio after CPS-polyphenol interactions; therefore, this technology may be able to provide new insight in future studies of element ratio changes before and after CPS-polyphenol

interactions. One drawback of XPS is that, while it can identify which elements are in the complexes and their ratio, it cannot pinpoint the binding site. Furthermore, this technique is slow to process, requires high vacuum and a large area, and cannot recognize the element H.

2.3.3.2.5 Small-angle X-ray scattering (SAXS)

SAXS can characterize geometric parameters and structural information such as size distribution, shape, and domain organization of particles, as well as the interaction of macromolecules in solution (Muroga, Yamada, Noda, & Nagasawa, 1987). This method has been used to study the structure of bovine serum albumin (BSA) and trypsin complexes with tea polyphenols and the interactions between β -casein and epigallocatechin gallate (EGCG) (Jöbstl, O'Connell, Fairclough, & Williamson, 2004; C. Shi et al., 2017). Specifically, it was reported that EGCG has a stronger ability to bind to trypsin and BSA than catechin, and its complexes have a denser core and a relatively smooth surface (C. Shi et al., 2017). However, little is known about the interactions between CPSs and polyphenols. By applying SAXS based on synchrotron radiation, Carn et al. (2012) reported that procyanidins longer than DP10 (globular) may assemble with the polysaccharide hyaluronan (HA) into a wide range of 3D aggregates. In contrast, procyanidins shorter than DP10 preferentially form low-density oligomers with HA. This suggests that the structure and molecular weight of procyanidin-HA complexes are primarily dependent on the length of the procyanidin: short procyanidins form coil-like aggregates while long procyanidins form aggregations of large bushy objects or microgels with HA, regardless of the procyanidin concentration. To date, this method has only been infrequently used as it requires access to a synchrotron radiation source, but future use may provide detailed information about the conformation and shape of the complexes.

It should be noted that this technology has strict requirements regarding the light source. The X-ray wavelength in SAXS is generally 0.1–0.2 nm (e.g., Cu target: 0.154 nm), but most of the energy is absorbed by the target in the form of thermal energy. The

density of X-rays is lower and the time required for testing is long. Synchrotron radiation is an ideal light source, but the conditions for obtaining it can be arduous. The advantage of synchrotron radiation scattering technology is that it provides an extremely high incident optical density, which can effectively reduce the size of the light spot, improve the signal-to-noise ratio, achieve rapid exposure of the sample, track the dynamic processes of structural changes at the nanoscale, and reliably analyze the nanostructure of the samples. However, the results obtained using this technology require complex data analysis, which can, to a certain extent, limit its use for the study of macromolecular complexes.

2.3.3.3 Polymer particle tracking and analysis

Dynamic light scattering (DLS) and nanoparticle tracking analysis (NTA) have been used to monitor shifts in the size distribution of particles due to polysaccharide-polyphenol aggregation (Carn et al., 2012; Y. He et al., 2019; Sijing Li et al., 2019; Mamet et al., 2018; Wei et al., 2019).

2.3.3.3.1 Dynamic light scattering (DLS)

Like turbidimetry, DLS is a precipitation-based method. As the size of aggregates increases, they may form insoluble complexes that scatter light and then precipitate. Depending on their diameter/size (usually in the sub-micron realm), differences among particles can be observed by DLS. However, DLS requires filtration of the solution to remove dust particles as this can have a large impact on the results. In one application of this technique, Carn et al. (2012) found that hyaluronan-tannin complexes form a population of small particles, with a diameter of about 25 nm, as well as a population of large particles (about 10 times larger), and the intensity of both populations increased with the quantity of tannins added to the mixture. Another study using DLS determined that Konjac glucomannan (KGM) polysaccharides have a high polydispersity index (PDI), and this PDI decreases when the weight ratio of tannic acid to KGM increases. These authors also detected an increase in the average diameter, possibly indicating that the TA/KGM complexes were forming larger particles (Y. He et al., 2019). Similarly,

the presence of citrus pectin was reported to decrease the PDI of a persimmon tannin solution (PDI decrease from 0.8 to 0.5), indicating that a more homogeneous aggregate group was formed (Mamet et al., 2018). DLS is thus able to generate different types of results depending on the polyphenol and polysaccharide present.

2.3.3.3.2 Nanoparticle tracking analysis (NTA)

NTA can track the Brownian motion of individually identified particles and analyze them separately to infer their hydrodynamic diameters, thus generating highly accurate results. NTA is a powerful tool for the characterization of aggregation, particularly as a complement to DLS. DLS allows faster evaluation of average size and polydispersity, while NTA usually provides higher resolution. Furthermore, even if there is no significant change in particle size, NTA can still be used to monitor the light-scattering intensity of each particle, and thus demonstrate the presence of aggregates. NTA has been applied to assess shifts in the size distribution of colloids formed by aggregation between commercial polysaccharide supplements (mannoprotein (MP) or gum arabic (AG)) and grape seed tannins in wine (Sijing Li et al., 2019). When combined with tannins, MP formed large, highly light-scattering aggregates, while AG showed relatively weak interactions.

2.3.3.4 Microstructure observation

2.3.3.4.1 Scanning electron microscopy (SEM)

In SEM, the surface of a sample is scanned by an electron beam to obtain its surface topography, with a resolution that can be less than 1 nanometer (Goldstein et al., 2017). The sample can be of any thickness or (non)electrical, but should be solid. Using this method, it is possible to describe the surface morphology of biomacromolecules, such as proteins and polysaccharides, and their complexes. For example, Martin et al. (2006) observed both casein micelle-carrageenan complexes and strands of carrageenan: the aggregates become larger as the concentration of carrageenan increased. In another study, a structural difference was observed when crude polyphenols (grape extract, green tea extract, and dehydrated cranberry powder) were added to cheese, resulting in

a rough structure and granular shape (Han et al., 2011). Unfortunately, the majority of studies on interactions involving polysaccharides have only reported on their surface topography (Le Bourvellec et al., 2005, 2012a; Le Bourvellec & Renard, 2005; D. Liu, Martinez-Sanz, Lopez-Sanchez, Gilbert, & Gidley, 2017; Phan et al., 2017, 2015; L. Y. Wu et al., 2016). Information about polysaccharide-polyphenol complexes is very limited, probably because polyphenol molecules are not easy to observe. We are aware of two recent studies that used SEM to describe such complexes. From SEM images obtained at a 1:20 ratio of polyphenols to polysaccharides by weight, Guo et al. (2018) observed that some particles of flavonoids congregated on the surface of corn silk polysaccharides (CSP) after adsorption, and the polysaccharide crystallized. Wei et al. (2019) observed that complexes of tannic acid (TA) and wheat starch (WS) formed roughly spherical particles. As the mass ratio of TA to WS increased to 1.6, 2.0, and 2.4, the complexes grew from smaller to larger aggregates, eventually forming micelles. The TA molecules were first adsorbed onto the WS surface by hydrogen bonds to form a single layer, and then the TA monolayer further absorbed the TA around the complexes, to finally form a thicker TA molecular layer (Wei et al., 2019).

2.3.3.4.2 Transmission electron microscopy (TEM)

TEM is a method of microscopic analysis with higher resolution and magnification than SEM. It is an effective tool to observe and analyze the morphology, organization, and structure of materials (Reimer, 2013). Because the electron beam needs to pass through the sample, though, TEM is only possible with specially prepared thin samples (less than 100 nm). The resulting image shows a two-dimensional projection of the sample. TEM images can also confirm the results obtained by DLS, as demonstrated by He et al. (2019). Using three weight ratios of tannic acid (TA) and konjac glucomannan (KGM), the authors used DLS to distinguish among particles by their size distributions and shapes, then obtained a TEM image that revealed how the TA/KGM complexes assemble and aggregate to form a sediment. Similarly, a published TEM image of the colloidal complex of epigallocatechin gallate and methyl cellulose clearly shows what appear to be spherical particles gathered together (Patel et al., 2011).

2.3.3.4.3 Confocal laser scanning microscopy (CLSM)

CLSM uses a laser beam to acquire a focused image at a selected depth, with a resolution at the sub-micron level. The image can be of a two-dimensional structure, or a reconstruction of a three-dimensional structure (Hutzler et al., 1998). However, scanning speed is slow and has lower resolution than camera detection, which limits its use in dynamic tracking studies. To determine the position and morphology of the sample (e.g., polyphenols) at the interface, the polyphenols must be either fluorescent themselves or treated with fluorescent dye; the cell wall of certain polysaccharides can also be labeled with a fluorescent dye to simplify phase identification. For the visualization of flavonoids, 2-aminoethyl-diphenylborinate can be used to amplify the fluorescence signal (excitation: 488 nm, emission: 430 nm). The pontamine Fast Scarlet P4B enables cell wall visualization (excitation: 555 nm, emission: 615 nm) (D. Liu, Lopez-Sanchez, & Gidley, 2019) and Congo red labels bacterial cellulose (excitation: 488 nm, emission between 554 and 663 nm) (Padayachee et al., 2012a). In these conditions, CLSM can provide direct evidence of the adsorption of polyphenols (e.g., anthocyanin) around the interface of the cell wall and its polysaccharides (e.g., cellulose) (D. Liu, Lopez-Sanchez, & Gidley, 2019; Padayachee et al., 2013, 2012a; Phan et al., 2017, 2015).

While powerful, none of these microscopic methods give information on the intrinsic binding sites at the molecular level, and must therefore be combined with other methods to obtain a more complete understanding of the molecular-level interactions (refer to [Table 2.3](#)).

2.3.3.5 Molecular dynamics (MD) simulation

Experimental methods have a limited ability to provide detail at the atomic level, and they rarely yield information about the orientation and conformation of biomolecules on a particular surface. MD simulation is a computational technique that enables predictions of the dynamic evolution of a system of interacting molecules using Newton's laws. This simulation method is able to identify cryptic or allosteric binding

sites and can directly predict small-molecule binding energies (A. Fernandes et al., 2014, 2016; Y. Liu et al., 2018; Mohanta, Madras, & Patil, 2014). For example, to better understand the different steps controlling particle recognition and molecular interaction at the atomic level, A. Fernandes et al. (2016) used MD simulation to analyze the mechanisms of copigmentation using models of oenin, catechin, and pectin in aqueous solution. A 16-monosaccharide pectin fragment with limited methylation and acetylation was used as a simplified model of a pectic polysaccharide. In oenin-pectin model simulations, the sugar molecules interacted strongly and covered the anthocyanins on both sides. For the more complex model simulation of oenin, catechin, and pectin, the distance between the catechin atom and the pectin molecule to the C₂ atom of oenin was about 3.0 Å, which prevented the entrance of solvent molecules and interaction with oenin; this explained the more stable state of the ternary complex (A. Fernandes et al., 2016). The combination of MD simulation with other simulation methods (e.g., molecular docking, Brownian motion, and Monte Carlo simulation) may expand its applications to the elucidation of interactions between biological macromolecules (G. Chen, Huang, Miao, Feng, & Campanella, 2019).

Before MD simulation can be carried out on CPS-polyphenol interactions, it is necessary to first obtain the 3D structures of the system of interest. However, CPSs are complex, and there is only a limited amount of information on their 3D structures available in public databases. Three-dimensional structures are available for some carbohydrates from Glyco3D (Pérez, Sarkar, Rivet, Breton, & Imberty, 2015), which is a portal for the study of structural glycoscience. In addition, 3D structures of polyphenols can be obtained from PubChem (S. Kim et al., 2019), ZINC (Sterling & Irwin, 2015), ChEMBL (Gaulton et al., 2017), or food-related molecular libraries, e.g. FooDB (<http://foodb.ca/>). However, these databases are far from complete, and are not always able to provide complex 3D structures of polysaccharides and polyphenols. Moreover, the MD method is computationally intensive; if it is performed on a medium-sized computer or a microcomputer, simulations are limited to small systems of 500-1000 atoms due to the memory and computing speed required. In practice, then, this

method tends to be limited to the study of small polyphenols and polysaccharides made up of a small number of sugars. Furthermore, although this method is able to shed light on the distance between molecules and their orientation, it is only valid for verification. Therefore, it also needs to be used in conjunction with other approaches.

2.3.3.6 Indirect “wet chemistry” methods

This section discusses methods that quantitatively analyze unbound polyphenols or polysaccharides, and can be labeled ‘indirect’ because they do not characterize the complexes themselves. They can produce information on bound/unbound polyphenols or polysaccharides, which can contribute to our understanding of the impact of structure. However, these methods do not provide information about the internal mechanisms of interactions, and they therefore have significant limitations when used alone. Generally speaking, these methods work by allowing CPSs and polyphenols to interact, then separating the remaining unbound polyphenols by filtration, equilibrium dialysis, or centrifugation. The unbound polyphenols are then quantified using HPLC-DAD (High Performance Liquid Chromatography Diode Array Detector), Ultra-HPLC-DAD-Mass Spectrometry and/or Spectrophotometry, Gel Permeation Chromatography for polyphenols, and High Pressure Size Exclusion Chromatography (HPSEC) for polysaccharides in order to obtain information on the structure. Spectrometry has the advantages of being rapid and requiring only small amounts of solution, but its specificity is limited. To investigate the effects of interactions on polyphenol degradation, the unbound polyphenols may also be detected quantitatively using *in vitro* enzymatic digestion (Barros, Awika, & Rooney, 2012; Grant et al., 2020; R. Liu et al., 2017; Padayachee et al., 2013; M. Shi et al., 2019).

Using indirect methods, it is possible to determine the relationships between the structure/properties of both polyphenols and polysaccharides and to calculate the number of polyphenols bound to each polysaccharide molecule. Adsorption can be characterized using the Langmuir isotherm to determine binding parameters, including the apparent affinity constant (K_L) and total amount of available binding sites or

apparent saturation level (N_{\max}) (expressed in g/g adsorbent) (Bindon, Bacic, & Kennedy, 2012; Le Bourvellec, Guyot, et al., 2004; Renard et al., 2001b). Recently, Y. Liu, Ying, Sanguansri, & Augustin (2019) and Y. Liu et al. (2018) went further by investigating the adsorption behavior and binding mechanism of catechins on cellulose/pectins using a time function; specifically, they evaluated the kinetics of the adsorption process using pseudo-first-order, pseudo-second-order, and Weber-Morris interparticle diffusion models. The initial adsorption of catechins on pectin (outer surface diffusion) was faster than on cellulose, and the adsorption rate of both cellulose and pectin slowed down in the later stages of adsorption (inner particle diffusion and equilibrium) (Y. Liu et al., 2019). A great advantage of these methods is their flexibility, i.e., the environmental conditions can be modified in order to investigate the mechanism(s) more deeply, and the structure of polysaccharides and polyphenols can be modulated to better understand the structure/function relationship.

Notably, some recent studies have provided clear evidence that polyphenols may actually change the supramolecular structure and physical properties (e.g., rheology, encapsulation efficiency, and structural stability) of polysaccharides through their interactions (Dobson et al., 2019; Jin et al., 2020). For instance, polyphenols can decrease the viscosity and the pseudoplastic (Newtonian) behavior of polysaccharide solutions (e.g., β -glucan, galactomannan, guar and xanthan gum) (Tudorache & Bordenave, 2019; Tudorache et al., 2020). However, to date only very limited data have been collected on this type of phenomenon.

2.3.3.7 General overview of the different methods and their complementarity

Broadly speaking, the above-mentioned techniques and methods for studying CPS-polyphenol interactions can be divided into four categories (Fig. 2.14): 1) Methods for studying the aggregation and precipitation of complexes, e.g. turbidimetry, DLS, and NTA; 2) Methods for characterizing the morphology of complexes, e.g. SEM, TEM, and CLSM; 3) Techniques for analyzing the mechanisms underlying the interactions, including information on binding capacity/affinity, thermodynamics, stoichiometry,

kinetics, and conformational changes; 4) Flexible “wet chemistry” methods, which indirectly characterize interactions by describing changes in the functional properties of CPSs or the nutritional properties of polyphenols.

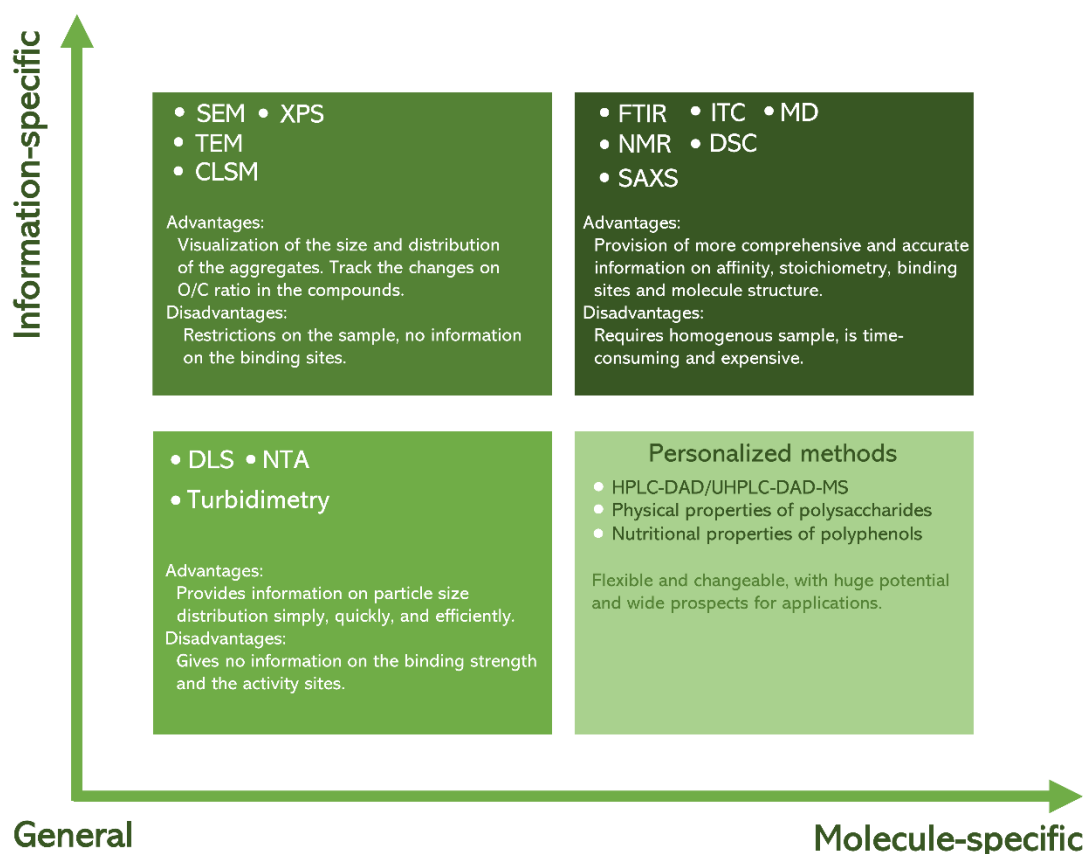


Figure 2.14 Classification of the methods used for elucidation of cell wall polysaccharide-polyphenol interactions.

The first group of methods (detection of aggregates) can simply, quickly, and efficiently provide qualitative information about aggregates in solution, such as their hydrodynamic radius and particle size distribution. However, these methods cannot provide information on binding strength and activity sites. The advantage of the second group of methods (morphology of complexes) is that they can provide visual evidence of the size and distribution of aggregates. In this group, XPS has the added benefit of being able to track changes in the O/C ratio in the compounds. The third group, thermodynamics-related methods, provides a more comprehensive and accurate overview of CPS-polyphenol interactions. For example, to obtain complementary information on the thermodynamics of interactions between CPSs and polyphenols,

ITC and DSC techniques can be used. Data on the kinetics of the adsorption process can be obtained from indirect “wet chemistry” and/or aggregation and precipitation methods. Advanced physical methods (e.g., NMR and SAXS) can also be used to study the conformational changes (intra- and inter-molecular) of CPS-polyphenol complexes. Finally, the MD simulation method can predict possible binding and active sites of CPSs, which can help to explain conformational changes. Particularly with respect to the last group of methods (“wet chemistry” methods), there are large gaps in our knowledge which can be easily overlooked by researchers. However, future research in this area should be particularly promising for efforts to understand how knowledge of these interactions may be applied to the food industry. The deciding factors that influence the choice of method also include the availability of techniques and their associated costs. Turbidimetry, colorimetry, or “wet chemistry” approaches are typically much more accessible in a food chemistry environment, and are still widely used as a first step in spite of their limitations. The availability of expertise in various technologies will also contribute to the decision of which method to use.

2.3.4 Structure-affinity relationships for cell walls and their polysaccharides

CPSs are structurally diverse and complex biomacromolecules that have been obtained from various botanical sources (e.g., apple, citrus, blueberry, sugar beet, grape, pear, and strawberry) and have been investigated in different systems (Table 2.4). Fig. 2.15 summarizes the relationships between the intrinsic structure of the molecules and their potential for interactions, and a more detailed discussion is provided below. To date, the majority of research has been carried out on pectin, likely because it is the CPS with the most structural variations. Extensive research has identified multiple characteristics that affect the interaction capacity of different CPSs, including:

- Botanical origin of cell wall and pomace (cellulose, hemicellulose, and pectin) (Brahem et al., 2019; Costa, Rogez, & Pena, 2015; Le Bourvellec et al., 2005, 2012a; Y. Liu et al., 2019; Padayachee et al., 2012a; Phan et al., 2017, 2015; Ruiz-Garcia, Smith, & Bindon, 2014; M. Shi et al., 2019; L. Y. Wu et al., 2016; L. Y. Wu, Sanguansri,

- Side chains and branching ratios (Brahem et al., 2019; Koh, Xu, & Wicker, 2020; Watrelot et al., 2014);

- Other molecules in the cell walls (P. A. R. Fernandes et al., 2020; Le Bourvellec et al., 2012a; D. Liu et al., 2017; Ye et al., 2009).

2.3.4.1 Effects of supramolecular organization

Cell wall polysaccharides are complex and heterogeneous polymers that can be insoluble (e.g., celluloses, mannans), soluble (e.g., pectins, hemicelluloses), or form complex insoluble structures (e.g., cellulose-pectin complexes within cell walls). In addition to differences in solubilities, they also demonstrate a diversity of flow behaviors, chemical structures, and conformations in solution, all of which cause them to exhibit significant differences in adsorption capacity (Gidley & Yakubov, 2019).

2.3.4.1.1 Bacterial cellulose-based frameworks

To overcome the limitations inherent in studying complex and heterogeneous plant cell wall structures, some researchers have used pure cellulose produced via fermentation by the bacterium *Gluconoacetobacter xylinus* as a model for cell walls. Bacterial cellulose (BC), with its simple and uniform structure, has been extensively used to study the interactions between cellulose and polyphenols (Padayachee et al., 2013, 2012b, 2012a; Phan et al., 2017, 2015). While it has the same crystalline arrangement of cellulose molecules, BC has many more cellulose chains, and forms microfibrils that have much larger diameters than cellulose microfibrils in primary cell walls, meaning that BC has a much lower surface-to-volume ratio. The affinities of ferulic acid, gallic acid, catechin, and cyanidin-3-glucoside are similar for BC, while that of chlorogenic acid is lower (Phan et al., 2015). Furthermore, these affinities are relatively unaffected by alkali treatment of bacterial cellulose (Phan et al., 2015), which

Literature Review

Table 2.4 Binding between different polysaccharides and polyphenols: effects of structure on the interactions.

Polysaccharides	The comparison	Polyphenol	Binding mode*	Effect on adsorption capacity	References
PECTINS					
Apple and citrus pectins	HG with 30% degree of methylation (DM) and 70% DM.	Apple procyanidins: degree of polymerization (DP) 9 and DP30	Hydrogen bonds and hydrophobic interactions	Pectins with a high DM for homogalacturonans have the strongest hydrophobic interactions with procyanidins.	Watrelet et al., 2013
Citrus pectins	Different types and degrees of esterification (DE): amidated (AHG 30%), low (HG 30%) and high methyl esterified fractions (HG 70%); (blockwise (HG-B 70%) vs random (HG-R 70%).	Cyanidin-3-O-glucoside	π - π stacking, hydrogen bonds, hydrophobic and electrostatic interactions	The affinity scale for cyanidin-3-O-glucoside is in the order HG 30% > AHG 30% > HG-B 70% \approx HG-R 70%.	A. Fernandes et al., 2020
Citrus peel pectins	High/low methoxyl (DE74 and DE30)	Tannins (DP26 and DP5)	Hydrogen bonds and hydrophobic interactions	DE74 ($K_a = (8.50 \pm 3.0) \times 10^3 M^{-1}$) > DE30 ($K_a = (3.62 \pm 1.92) \times 10^3 M^{-1}$)	Mamet et al., 2018
Apple, citrus, and sugar beet pectins	Low esterified amidated pectin (AM); low methoxylated pectin (LM); high methoxylated pectin (HM)	Purified black currant extract comprising anthocyanins and non-anthocyanin phenolics (PP-E), and purified anthocyanin (ACN-E)	Hydrogen bonds, hydrophobic interaction, and electrostatic interactions	AM pectins provide the best anthocyanin stabilization followed by LM and HM pectins; the stabilization depends on the source of pectin: citrus > apple > sugar beet. Pectin-derived stabilizing effects are stronger on delphinidin than on cyanidin glycosides.	Buchweitz et al., 2013a
Apple, citrus, and sugar beet pectins	AM, LM, and HM	Strawberry extracts (E-1, E-2) (83.6% and 81.7% total anthocyanins, respectively)	Hydrogen bonds	Compared to a solution without pectin, apple and sugar beet pectins moderately enhance the stability of anthocyanins, while citrus pectin does not. The degree of amidation (DA) and DE of pectins do not affect pigment stability.	Buchweitz et al., 2013b
Different pectins with different neutral sugar side chains	Different hairy fractions of pectins	Apple procyanidins of DP9 and DP30	Hydrogen bonds and hydrophobic interactions	Complex neutral sugar side chain components limit interactions between pectins and procyanidins.	Watrelet et al., 2014
Arabinan-rich pectic polysaccharides (ARPPs)	Sugar beet arabinans (branched and debranched) and apple arabinan	Chlorogenic acid, phloridzin, and procyanidins	Hydrogen bonds and hydrophobic interactions.	The higher degree of branching of arabinan limits its interaction with polyphenols.	P. A. R. Fernandes et al., 2020
ARPPs	Different molecular weights	27 phenolic acid monomers	Non-covalent interactions	Native ARPP affinity increases in the following order: P4 (153 kDa) < P3 (24 kDa) < P1 (114 kDa) < P2 (76 kDa)	J. Zhu et al., 2018
Blueberry pectins	Water-soluble pectin fraction (WSF) and chelator-soluble pectin fraction (CSF)	Anthocyanins	π - π stacking, hydrogen bonds, hydrophobic interaction, and electrostatic interactions	A stronger association occurs with the highly linear and more negatively charged pectin structure (CSF) than with the more-branched, neutral-sugar-rich WSF.	Koh et al., 2020

(Continued)

Polysaccharide-polyphenol interactions

Table 2.4 (Continues)

Polysaccharides	The comparison	Polyphenol	Binding mode*	Effect on adsorption capacity	References
Blueberry pectin-rich fractions	Pectin was extracted from water-soluble (WSF), chelator-soluble (CSF) and sodium carbonate-soluble (NSF) fractions	Anthocyanins	Electrostatic interactions and anthocyanin intermolecular stacking	Binding is pH dependent. WSF has endogenous anthocyanins and relatively poor anthocyanin binding ability. CSF has relatively strong anthocyanin binding ability at pH 2.0–3.6, while NSF has relatively strong anthocyanin binding ability at pH 3.6–4.5.	Lin et al., 2016
Iron-enriched pectin (IRP)	HM pectin with a mixture of Fe ²⁺ and Fe ³⁺	Quercetin and rutin	Via iron ions as a mediator	Iron-rich pectin has a stronger affinity for flavonols.	Chirug et al., 2018
Sugar beet pectin (SBP)	Modified by an enzyme or ultrasound treatment	Anthocyanins	Van der Waals forces, hydrophobic interactions, and hydrogen bonds	Pectins with higher molecular weight form insoluble anthocyanin-pectin complexes. Ultrasound and enzyme treatment to create lower-weight SBP (HG-like and RG-like oligosaccharides) results in a soluble complex.	Larsen et al., 2019
CELL WALLS					
Apple cell wall	Native cell wall and cell wall modified by mild or harsh drying	Apple, grape seed, and pear procyanidins	Hydrogen bonds and hydrophobic interactions.	Harsh drying decreases the affinity of the cell walls for procyanidins but increases the saturation level.	Le Bourvellec & Renard, 2005
Apple cell wall	Modified by boiling and drying	Procyanidin	Hydrogen bonds and hydrophobic interactions	The presence of proteins in the cell walls does not affect the interactions between procyanidins and cell walls. Boiling and drying decrease the apparent affinity and simultaneously increase the apparent saturation levels of cell walls.	Le Bourvellec et al., 2012
Apple cell wall	Three apple varieties: ‘Pink Lady’, ‘Red Delicious’, and ‘Granny Smith’; three treatments: boiling, oven-drying, and freeze-drying	Chlorogenic acid, epicatechin, and phloridzin	Hydrogen bonds and hydrophobic interactions	‘Pink Lady’ cell walls with a high proportion of uronic acid levels in pectin have a higher binding capacity. Fresh ≈ boiled > oven dried > freeze-dried.	D. Liu, Lopez-Sanchez, Martinez-Sanz, et al., 2019
Apple cell wall	Pectin, xyloglucan, starch, and cellulose.	Procyanidins of apple, pear, and grape seed	Non-covalent interactions	The binding capacity of different cell wall polysaccharides for procyanidins are: pectin>>xyloglucan>starch>cellulose.	Le Bourvellec et al., 2005
Grape cell wall	Different tissues: skin and flesh from grape	Grape skin and seed proanthocyanidin obtained by different types of solvent extraction	Non-covalent interactions	Flesh cell wall has a higher binding capacity for proanthocyanidin than skin cell wall does.	Bindon, Smith, & Kennedy, 2010
Grape and pomace cell walls	Skin and flesh from grape and pomace cell walls	Ripe grape and wine proanthocyanidin	Non-covalent interactions	Flesh cell wall has high selectivity for higher molecular mass PAs; however, ripe skin cell wall has poor affinity for very high molecular mass proanthocyanidins.	Bindon, Smith, Holt, et al., 2010
Grape cell wall	Different tissues: skin and flesh from grape	Skin proanthocyanidins of different ripeness	Non-covalent interactions	The affinity of flesh cell wall material for proanthocyanidin is higher than that of skin cell wall material.	Bindon & Kennedy, 2011

(Continued)

Table 2.4 (Continues)

Polysaccharides	The comparison	Polyphenol	Binding mode*	Effect on adsorption capacity	References
Cell walls from grape skin and flesh	Different stages of grape maturity	Skin proanthocyanidins	Non-covalent interactions	Flesh cell walls consistently bind more proanthocyanidin than those from skin. Proanthocyanidin adsorption properties of the flesh cell wall do not change much after the onset of maturation, while the adsorption capacity of skin cell walls decreases markedly.	Bindon et al., 2012
Grape skin cell wall	Cell walls fractionated (F1-F4) by the extraction solvents CDTA, 50 mM KOH, 1 M KOH, and 4 M KOH, respectively, and CWM residue.	Proanthocyanidins from fresh grape skins	Non-covalent interactions	Most of the cell wall-bound proanthocyanidins are in the pectin-rich fraction (CDTA). The lignocellulosic fraction (cell wall residue) has the lowest adsorption capacity for proanthocyanidin.	Ruiz-Garcia et al., 2014
Grape cell wall	Soluble and insoluble fractions of cell walls	Proanthocyanidins from grape skins (DP21)	Non-covalent interactions	Removal of the pectic fraction from skin cell walls reduces the adsorption of PA relative to the native cell walls. Polygalacturonase treatment reduces PA adsorption by mesocarp cell walls.	Bindon, Li, Kassara, & Smith, 2016
Grape cell wall from skins	Ripe skin cell walls (rCWs) (higher protein and non-cellulosic glucose contents) and veraison skin cell walls (vCWs) (higher lignin content)	Proanthocyanidins (DP3)	Non-covalent interactions	Maceration enzymes favor the desorption of proanthocyanidin in must and wine. The rCWs retain more proanthocyanidins than vCWs.	Castro-López, Gómez-Plaza, Ortega-Regules, Lozada, & Bautista-Ortín, 2016
Strawberry cell wall	Oven drying at 60°C and 80°C or freeze-drying	Hydroxytyrosol (HT) and 3,4-dihydroxyphenylglycol (DHPG) in olive fruit	Probable ester bond, hydrogen bonds, and electrostatic interactions	Drying enhances the binding of strawberry dietary fiber with HT/DHPG.	Bermúdez-Oria et al., 2019
Pear cell wall	Ripe and overripe; whole flesh (FL), parenchyma cells (PC), stone cells (ST), and skin (SK)	Pear procyanidin	Hydrogen bonds and hydrophobic interactions	The proportion of bound procyanidins increases at the overripe stage; PC > FL > ST > SK. Overripening promotes the adsorption of procyanidins on the pear cell walls, which may be due to the loss of pectic side chains.	Brahem et al., 2019
POMACES AND FIBERS					
Lignocelluloses	Prepared from woody tea stalk, pine sawdust, and sugarcane bagasse	Tea catechins	Hydrogen bonds and interaction of π -orbits	The binding capacities for lignocellulose increase by the order of tea stalk > pine sawdust > bagasse.	Ye et al., 2009
Apple pomace	The major components are pectin (10.4%), cellulose (25.3%), and lignin (4.8%).	Epigallocatechin-3-gallate (EGCG)	Non-covalent interactions	Binding to apple pomace increases with increased EGCG concentration but decreases with increasing temperature.	L. Y. Wu, Melton, et al., 2014
Apple pomace	Wet pomace, high-pressure processing, and heat treatment	EGCG	Non-covalent interactions	Both high-pressure and heat treatments reduce the adsorption capacity of apple pomace.	L. Y. Wu, Sanguansri, et al., 2014

(Continued)

Table 2.4 (Continues)

Polysaccharides	The comparison	Polyphenol	Binding mode*	Effect on adsorption capacity	References
Apple pomace	Wet pomace, freeze-dried pomace, and extruded apple pomace.	EGCG	Non-covalent interactions	Freeze-drying or extrusion of apple pomace enhances the adsorption of EGCG. At low temperature (25 °C), freeze-dried pomace has a stronger adsorption capacity for EGCG than extruded pomace, but the opposite is true at higher temperatures (40–55 °C).	L. Y. Wu et al., 2015
Apple pomace	NaOH-HCl-modified	EGCG	Non-covalent interactions	Modification by NaOH-HCl contributes to the adsorption of EGCG on apple pomace by increasing the exposure of active binding sites.	L. Y. Wu et al., 2016
Puree, pomace, and juice from broccoli by-products	Different carbohydrate and total fiber contents: the carbohydrate contents were 56% (37% total fiber) for puree, 65% (50% total fiber) for pomace, and 49% (6% total fiber) for juice.	EGCG	Hydrogen bonds and hydrophobic interactions	Fiber content, including cellulose and pectins, contributes to the adsorption of EGCG; adsorption by broccoli by-products decreases in the following order: pomace (43.20 mg/g, dry weight) > puree (39.47 mg/g) > juice (25.22 mg/g).	M. Shi et al., 2019
Potato cells and cellular components	Intact potato cells, broken cells, cooked cells, isolated cell walls, and starch granules	(+)-catechin, phloridzin, and vanillic acid	Hydrogen bonds and hydrophobic interactions	Broken cells and cell walls have a relatively higher binding affinity for polyphenols. Adsorption capacity can be enhanced by cooking (boiling).	Gómez-Mascaraque et al., 2017
ARTIFICIAL COMPOSITES					
Bacterial cellulose (BC) and cellulose-pectin composites	BC: bacteria cellulose; L-BCP: 39% pectin/61% cellulose; and H-BCP: 17% pectin/83% cellulose.	Anthocyanins derived from purple carrots (a dietary source of both acylated and non-acylated anthocyanins)	Ionic interactions (with pectins) and hydrophobic interactions (with cellulose)	The composite with the highest pectin content binds more anthocyanin: L-BCP composite > H-BCP composite and BC.	Padayachee et al., 2012a
Bacterial cellulose and cellulose-pectin composites	Cellulose-pectin composites: a low DE pectin (DE 30) (L-BCP) and high DE pectin (DE 60) (H-BCP)	Phenolic acids (sum of chlorogenic acid, neo-chlorogenic acid, ferulic acid derivatives, and caffeic acid)	Non-covalent interactions	The trend in the amount of adsorption was BC > H-BCP > L-BCP.	Padayachee et al., 2012b
BC	Native BC or alkali-treated BC (0.5 M/0.1M NaOH)	(+/-)-catechin, ferulic acid, chlorogenic acid, gallic acid, and cyanidin-3-glucoside	Non-covalent and non-ionic interactions	BC composites adsorb a larger amount of polyphenols. The total amount of adsorbed polyphenols on BC composites increases after treatment with boiling alkali solution. BC treated with different concentrations of NaOH has similar binding capacities.	Phan et al., 2015
BC, cellulose-arabinoxylan (BC-AX), cellulose-xyloglucan (BC-XG), cellulose-pectin (BC-pectin), and apple cell wall (ACW)	Different formulations of cellulose-based composites	(+/-)-catechin, ferulic acid, and cyanidin-3-glucoside	Electrostatic interactions	At low temperature (25 °C), freeze-drying produces a better adsorbent for EGCG than extrusion but the opposite is true at higher temperatures (40–55 °C).	Phan et al., 2017

(Continued)

Table 2.4 (Continues)

Polysaccharides	The comparison	Polyphenol	Binding mode*	Effect on adsorption capacity	References
BC	Treatment by boiling, autoclaving, freeze-drying, and rehydrating	Epicatechin, phloridzin, and procyanidin B2	Non-covalent interactions	Boiling or autoclaving cellulose has little effect on subsequent polyphenol binding. In contrast, freeze-drying greatly reduces polyphenol binding. Rehydration of the freeze-dried cellulose enhances its adsorption of polyphenols.	D. Liu et al., 2017
MISCELLANEOUS POLYSACCHARIDES					
Cellulose and xylan	Two dietary fibers	Catechin, caffeic acid, and ferulic acid	Non-covalent interactions	Cellulose and xylan have low adsorption to catechins, caffeic acid, and ferulic acid.	Costa et al., 2015
Cellulose and pectins	Polysaccharide structures and compositions	Catechin	“Physisorption” mechanism (non-covalent interactions)	Cellulose (2 mg/g) < pectin (21 mg/g)	Y. Liu et al., 2019
Methylcellulose (MCE)	Different molar ratios	EGCG/tannic acid	Hydrophobic interactions and hydrogen bonds	The interaction is strongest when the stoichiometry is 21 mol of EGCG or 33 mol of TA molecules combined with 1 mol of MCE.	Patel et al., 2013, 2011
Corn silk polysaccharides (CSPs)	Different molecular weights	Luteolin	Van der Waals forces and hydrogen bonds	Affinities decrease in the following order: CSP3 (106.6 kDa) > CSP2 (61.3 kDa) > CSP1 (43.3 kDa)	Guo et al., 2018
Konjac glucomannan (KGM)	Molecular weight changed by sonication	Tannic acid (TA)	Hydrogen bonds	The average size of the TA/KGM complexes decreases with the molecular weight of KGM.	He et al., 2019
Chitosan/Fe3O4 composite microparticles (MCTS)	Magnetic treatment	Polyphenols in sugarcane juice	Electrostatic interactions	MCTS adsorbent has considerable reusability.	Liang et al., 2019
Starch	Pure amylose; pure amylopectin; waxy, normal, and high amylose starches	Tannins and other phenolic compounds of sorghum	Hydrogen bonds, hydrophobic interactions, and chemical interaction	Pure amylose interacts more strongly than amylopectin with oligomeric and polymeric PA.	Barros et al., 2012
Maize starch	Different amylose/amylopectin ratios	Oligomeric procyanidins (OPCs)	Hydrogen bonds	OPCs have stronger interactions and form more-resistant structures with high amylose maize starch than with normal maize starch or amylopectin.	R. Liu et al., 2017
Wheat starch (WS)	Different concentrations and mass ratios of TA to WS	TA	Non-covalent interactions	The formation of TA/WS complexes increases with an increase in the TA/WS mass ratio.	Wei et al., 2019

*: as described by the authors.

has little impact on its crystallization and amorphous area. BC can also be combined with other cell wall polysaccharides to create model systems of increasing complexity. For example, a BC-pectin composite was found to initially (in the first hour of the experiment) demonstrate a lower affinity for polyphenols than BC, but after a few days their absorption levels were similar (ca. 30%) (Padayachee et al., 2012b). This suggests that BC and pectins may have the same ability to bind polyphenols, and that the BC-pectin composite could form hydrophobic pockets (as pectins do) that enhance the binding affinity with polyphenols. Going further, Phan et al. (2017) compared the adsorption of polyphenols on BC and different BC-based composites (cellulose-arabinoxylan (BC-AX), cellulose-xyloglucan (BC-XG), cellulose-pectin (BC-pectin), and apple cell wall (ACW)). They found that BC binds more catechins than BC-AX, BC-XG, BC-pectin, and ACW. With its rigid and hydrophobic structure, highly condensed BC is able to bind more polyphenols (cyanidin-3-glucoside) through hydrophobic interactions than hydrophilic arabinoxylan can (Phan et al., 2017); the same pattern was also noted for the interaction of phenolic acids with BC and hydrophilic xyloglucan (Padayachee et al., 2012b). The interactions of charged anthocyanins with BC-pectin complexes can also be enhanced by ionic bonds: Padayachee et al. (2012a) found that the complexes with the highest pectin content had the most anthocyanin binding, probably because they had a higher number of charged (non-esterified) galacturonic acid groups.

2.3.4.1.2 Cell walls and modified cell walls

Pectins have a relatively higher affinity for polyphenols than most other polysaccharides in solution or suspension (Brahem et al., 2019; Le Bourvellec et al., 2005, 2012a; Y. Liu et al., 2019; Ruiz-Garcia et al., 2014). In particular, Le Bourvellec et al. (2005) demonstrated that reticulated pectins have a higher ability to associate with procyanidins than reticulated xyloglucan, starch, and cellulose do. Within the structure of reticulated pectins, hydrophobic pockets can form that capture procyanidins, but these molecules still have low levels of apparent saturation as a result of steric hindrance. Cellulose and reticulated xyloglucan have a higher degree of apparent

saturation due to their conformations, which favor stacking and cooperativity (Le Bourvellec et al., 2005). When cell wall materials are stripped of pectins by boiling (Le Bourvellec & Renard, 2012), by enzymatic treatment (Renard et al., 2001b), or by extraction with a chelating agent (Ruiz-Garcia et al., 2014), their binding capacity for procyanidins is correspondingly reduced. Similarly, Y. Liu et al. (2019) reported that pectins have a much higher affinity for catechins than cellulose does, and that the mechanisms of adsorption differ between the two types of polysaccharides. Compared with insoluble, highly crystalline cellulose, which has few amorphous domains (Ilharco, Garcia, Lopes da Silva, & Vieira Ferreira, 1997), soluble pectins have an open, long-molecular-chain conformation in solution, so that they have more exposed catechin binding sites than cellulose (Y. Liu et al., 2019). Ruiz-Garcia et al. (2014) used CDTA (cyclohexanediaminetetraacetic acid, a complexant) and NaOH to extract pectin-rich and hemicellulose fractions, respectively, from grape cell walls. They reported that the majority of the initially cell-wall bound proanthocyanidins were co-extracted with the pectin-rich fraction (CDTA extract), followed by the hemicellulose fractions (NaOH extracts), while the cellulose-enriched cell wall residue retained the smallest proportion of proanthocyanidins. With sequential extraction, the ability of residues to bind proanthocyanidins gradually decreased. A recent study of the difference in adsorption of procyanidins by the cell walls of different tissues (parenchyma cells > flesh > stone cells > skin) in pears confirmed this result (Brahem et al., 2019). Specifically, the cell walls of skin and stone cells demonstrated the lowest affinities, which was likely the result of the presence of lignin, cellulose, and hemicelluloses, and a lower pectin content.

2.3.4.1.3 Pomaces

Pomaces are solid residues from juice production that consist largely of dietary fibers, including lignins and pectins, with a substantial amount of bound polyphenols, including oxidized moieties, and a smaller amount of proteins. In food, these solid residues can be a useful vehicle for the protection of polyphenols from degradation in gastrointestinal fluids (M. Shi et al., 2019; L. Y. Wu et al., 2016, 2015; L. Y. Wu, Melton,

et al., 2014; L. Y. Wu, Sanguansri, et al., 2014). For example, L. Y. Wu, Melton, et al. (2014) found that apple pomace (oven-dried) has good adsorption characteristics for epigallocatechin gallate (EGCG). Moreover, both high-pressure and heat treatment were found to alter the molecular and microstructural conformation of apple pomace, and thus reduce its adsorption capacity; however these treatments can also reduce enzymatic browning of the apple pomace during storage and protect EGCG from degradation (L. Y. Wu, Sanguansri, et al., 2014). In contrast, extrusion and freeze-drying increase the ability of apple pomace to adsorb EGCG (L. Y. Wu et al., 2015). Acid-alkaline and ethanol pretreatment of pomace also increase the adsorption of EGCG, to a greater degree than the above-mentioned physical treatments (L. Y. Wu et al., 2016). These chemical treatments remove free soluble compounds such as monosaccharides, proteins, and phytochemicals, and can thus expose an abundance of binding sites for EGCG on the cellulose, hemicelluloses, and pectin that are retained in the pomace surface (L. Y. Wu et al., 2016). Similarly, M. Shi et al. (2019) studied the adsorption of EGCG on different broccoli by-products, i.e. puree, concentrated particles, and serum from the puree juice. Of the materials (“pomace” and “puree”) that contained cell wall particles, those with higher concentrations of carbohydrates, especially total fiber, had the higher binding capacity for EGCG (39 mg·g⁻¹ dry weight (DW) and 43.20 mg·g⁻¹ DW for puree and pomace, respectively); both of these materials bound more EGCG than juice did (25 mg·g⁻¹ DW). This suggests that the fiber components, including cellulose and pectins, promote the adsorption of EGCG in broccoli by-products (M. Shi et al., 2019).

2.3.4.2 Effects of structure and morphology of isolated polysaccharides

2.3.4.2.1 Surface area/porosity

During CPS-polyphenol interactions, one important method of mass transport is diffusion, including film diffusion on a surface, pore diffusion inside the cell walls, and the resulting equilibrium (H. Zhang, Chen, Lu, Li, & Han, 2016). In general, the limiting pore size of the cell wall is around 5 nm (Carpita, Sabularse, Montezinos, &

Delmer, 1979), which may limit the adsorption of polyphenols with molecular weights larger than 10 kDa (equivalent to 34 catechin units). Modifications of cell walls by physical methods greatly affect their adsorption characteristics for polyphenols through the change of their specific surface area and porosity (Bermúdez-Oria et al., 2019; Bindon et al., 2012; Le Bourvellec et al., 2005, 2012a; Le Bourvellec & Renard, 2005; D. Liu, Lopez-Sanchez, Martinez-Sanz, et al., 2019; D. Liu et al., 2017). These two parameters are positively correlated: the more porous the cell wall is, the larger the surface area. As an example, different drying regimes (harsh and mild) caused notable differences to arise in the adsorption characteristics of two cell-wall materials with otherwise similar chemical compositions (Le Bourvellec & Renard, 2005). The severe drying conditions reduced the binding capacity for procyanidins by reducing the surface area of the cell wall, specifically, its macroporosity, which was impaired by the drying-induced compaction and collapse of the cell wall network. The reduction in or loss of porosity limits the pore diffusion of the largest procyanidins, as fewer or no potential binding sites are available on the cell walls (Le Bourvellec et al., 2005; Le Bourvellec & Renard, 2005). Similarly, freeze-drying markedly decreases polyphenol adsorption onto cellulose (D. Liu et al., 2017). This may be due to a decrease in cellulosic surface area resulting from a collapse in the cellulose network as water is removed during the freeze-drying process. This would be in accordance with the findings of Le Bourvellec et al. (2012), who reported that a reduction in the porosity of cell walls as a result of freeze-drying reduced the potential for polyphenols to enter their binding sites. Boiling and autoclaving can also lead to irreversibly smaller pores and a denser cellulose network (D. Liu et al., 2017), but these treatments have only a minor effect on the adsorption characteristics of cellulose (D. Liu, Lopez-Sanchez, Martinez-Sanz, et al., 2019; D. Liu et al., 2017). A recent evaluation of various boiling/drying treatments found clear differences in the resulting saturation levels of three polyphenols (epicatechin, phloridzin, and chlorogenic acid) on cell walls: fresh \approx boiled > oven-dried (OD) > freeze-dried (FD) (D. Liu, Lopez-Sanchez, Martinez-Sanz, et al., 2019). Compared with oven-drying, cell wall materials dried by solvent exchange have notably higher

porosity because of the expansion of the tissues (Le Bourvellec et al., 2012a), which can have a positive effect on the encapsulation of polyphenols within a more open conformation. However, Bermúdez-Oria et al. (2019) found the opposite pattern: oven drying (60 °C, 72 h) slightly enhanced the saturation levels of strawberry dietary fiber to hydroxytyrosol / 3,4-dihydroxyphenylglycol. To make sense of this, we must take into account the size of different polyphenols, as well as differences in the initial porosity of cell walls among species, among different tissues within a species, or among tissues of differing maturity. For example, the stone cells of pear cell walls are secondary cell walls that have a more compact structure, less flexibility and porosity, and a lower affinity for procyanidins (Brahem et al., 2019) compared to flesh (primary) cell walls. In grapes, ripening leads to cell wall remodeling, which may increase the porosity of the cell wall matrix and result in greater adsorption of proanthocyanidins (Bindon et al., 2012). It is possible that this effect arises as a function of available surface area, and is not a direct effect of chemical composition. For insoluble cell wall materials, the greater the porosity, and the better the match between pore size and the adsorbed polyphenol, the higher the resulting adsorption.

2.3.4.2.2 Molecular weight

Recent studies have noted the impact of a polysaccharide's molecular weight on its interactions with polyphenols (Guo et al., 2018; Y. He et al., 2019; Larsen et al., 2019; J. Zhu et al., 2018). For example, the adsorption of flavonoids on corn silk polysaccharides (CSP) increases with the latter's molecular weight (Guo et al., 2018); this was further supported by the work of He et al. (2019). Higher-molecular-weight polysaccharides possess more glycosidic linkages and have a relatively higher number of branched chains. Therefore, a high-molecular-weight polysaccharide may have several binding sites that can interact with polyphenols, thus facilitating the interaction. Interestingly, though, J. Zhu et al. (2018) found contrasting results. Using hydrolysis of different durations, these authors obtained rapeseed meal polysaccharides whose molecular weights varied between 153 kDa and 24 kDa; however, they found no relationship between higher molecular weights and binding with polyphenols. However,

the compositions of the different polysaccharides were not analyzed in the article, which limits the conclusions that can be drawn. It does seem, though, that the correlation between adsorption and high molecular weight has its limits: each polysaccharide has its own ideal structure or conformation at which it can adsorb the maximum amount of polyphenols. Moreover, the presence of neutral sugar side chains can hinder adsorption through the steric hindrance effect, as has been reported for procyanidins on complex pectins (P. A. R. Fernandes et al., 2020; Watrelot et al., 2014). Larsen et al. (2019) reported a similar pattern: using ultrasound, they modified sugar beet pectins to eliminate RG I side chains, which resulted in a limited decrease in hydrodynamic volume. However, this reduction in molecular weight was accompanied by an increase in the number of accessible homogalacturonans that could interact with anthocyanins to form insoluble complexes. This pared-down structure was more conducive to the accumulation of anthocyanins (self-copigmentation) than the original pectins because it had fewer branched RGs, thus reducing the hindering influence of side chains or entanglements on anthocyanin binding.

2.3.4.2.3 Degree of esterification

The degree of esterification of pectins may greatly influence their interactions with polyphenols (Buchweitz et al., 2013b, 2013a; A. Fernandes et al., 2020; Larsen et al., 2019; Mamet et al., 2018; Padayachee et al., 2012b; Watrelot et al., 2013). Compared to pectins with low or no methylation, highly methylated pectins (degree of methylation (DM): 70) interact strongly with procyanidins via hydrophobic interactions (Watrelot et al., 2013). A possible explanation for this might be that the dihydropyran heterocycles (C-rings) of procyanidins are able to form stronger hydrophobic interactions with the methyl groups of pectins. Similarly, pectins with a high degree of esterification (DE 60) adsorb more phenolic acids than low-DE pectin (DE 30) after 24 h exposure (Padayachee et al., 2012b). Pectins with a high methoxyl content (DE74) also have a stronger affinity for highly polymerized tannins (DP26) than low-methylated pectin does (DE30) (Mamet et al., 2018). However, the interaction mechanisms are different for anthocyanin-pectin complexes because they rely on the positive charge of the

individual anthocyanin. For example, in the case of black currant anthocyanins, low methylated (LM) and amidated (AM) pectins have a stronger stabilization effect than highly methylated pectins (Buchweitz et al., 2013a). This may be due to the specific electrostatic interactions that arise between anthocyanins and negatively charged pectin carboxylate groups in LM pectins or with the more freely available electrons of the amide groups in AM pectins. Both functional groups can have strong interactions with the positively charged flavylium ion, being protected from nucleophilic water and subsequent degradation. Likewise, A. Fernandes et al. (2020) showed that anthocyanin-3-O-glucoside binds more to low-esterified citrus pectins than to highly-esterified citrus pectins mainly due to the electrostatic interactions involved, but also as a result of the hydrogen bonds and hydrophobic interactions present. Similarly, ultrasound-modified sugar beet pectins with lower DE have more potential binding sites for anthocyanins (Larsen et al., 2019). However, Buchweitz et al. (2013b) reported that reactions between anthocyanins and pectins from different sources (e.g., apple, citrus, and sugar beet) differed depending on their DE and degree of amidation (DA). The DE and DA of apple and citrus pectins did not affect the stability of strawberry anthocyanins. Instead, the authors found that the stabilization of strawberry anthocyanins can be attributed to the hydrogen bonds between the carboxyl/carboxylate and hydroxyl groups of pectin and the B-ring of the anthocyanins, and depends on the number of hydroxyl groups in the anthocyanin B ring (Buchweitz et al., 2013b). Generally speaking, a reduction in DE increases the amount of dissociated galacturonic acid residues (COO⁻) and hydroxyl groups accessible on the surface. In addition, the removal of esters reduces steric hindrances by acetyl groups at adjacent positions on potential binding sites, therefore favoring the accumulation of anthocyanins on the surface of pectins (Larsen et al., 2019).

2.3.4.2.4 Side chains and branching ratios

Various studies have investigated the effects of neutral sugar side chains of pectin on the adsorption of polyphenols (Brahem et al., 2019; Koh et al., 2020; Watrelot et al., 2014). Rhamnogalacturonan I (RG I) and rhamnogalacturonan II (RG II) have, to

varying extents, branched structures with complex neutral sugar side chains, which affect their ability to adsorb polyphenols. Watrelot et al. (2014) reported that the presence of ramifications in pectins (e.g., pectic hairy regions) strongly limited their association with procyanidins. However, this association appeared to be modulated by the degree of polymerization (DP) of the procyanidin. For a procyanidin with a DP of 9, no differences were observed in its interaction between different pectin hairy regions, possibly because a low DP is unfavorable for adsorption. Instead, for procyanidins of a high DP (DP30), binding capacities were clearly different among pectic polysaccharides, following the order of rhamnogalacturonan > arabinans + galactan I + xylogalacturonans > galactan I > arabinans + galactans II > arabinans (Watrelot et al., 2014). This suggests that pectins with a linear structure and fewer neutral sugar side chains are better able to associate with procyanidins, and that pectins with more branched regions interact less. Similarly, a stronger association with anthocyanins was observed for more-linear pectin (“linearity”: $\text{Gal A}/(\text{Rha}+\text{Fuc}+\text{Ara}+\text{Xyl}+\text{Gal}) = 11.5$, “degree of branching”: $(\text{Ara}+\text{Gal})/\text{Gal A} = 0.09$) than with more-branched pectin (linearity: 1.5, degree of branching: 0.64) (Koh et al., 2020). For pectins in pear cell walls, the loss of the arabinan (and galactan) side chains as a result of overripening also increased the adsorption of procyanidins (Brahem et al., 2019). Finally, a recent study noted that pectin-polyphenol interactions were strongly affected by the degree of branching of arabinan side chains in the pectins (P. A. R. Fernandes et al., 2020). Highly branched arabinans have more globular structures, which limit their interaction with polyphenols. Non-branched arabinans have a more linear and helical structure, which may facilitate the formation of hydrophobic domains via polymer entanglement, and thus promote the encapsulation of polyphenols.

2.3.4.2.5 Other molecules in cell walls

Several studies have investigated how interactions with polyphenols may be affected by non-polysaccharide components of cell walls or cellulose complexes, such as residual water, lignin, ferulic acid, and protein.

Water content appears to play an important role in CPS-polyphenol interactions. Specifically, a strong correlation was reported between the degree of rehydration of freeze-dried cellulose samples (20%–63%) and their adsorption capacity for polyphenols (D. Liu et al., 2017). This result might be attributed to the establishment of strong hydrogen bonds between the cellulose microfibers/ribbons after water elimination, which reduce the number of free hydroxyl sites for polyphenol binding.

In lignocellulose, high lignin content was found to increase the adsorption of catechins (Ye et al., 2009). The lignin might interact with catechins via the interaction of π -orbits and the formation of hydrogen bonds between the nucleophilic groups on lignin and the hydroxyl groups of the catechins. However, ferulic acid seems to have the opposite effect: its presence in the side chains of sugar beet arabinans appeared to limit interaction with procyanidins, compared to the results obtained from apple arabinans without ferulic acid (P. A. R. Fernandes et al., 2020). This may be due to a structural effect, in which the presence of ferulic acid reduces the number of binding sites, thus limiting procyanidin adsorption.

Finally, an investigation of protein in cell walls did not find any effect on polyphenol adsorption under the study conditions: protein-enriched cell walls (99 mg/g dry matter) had the same degree of interaction with procyanidins as cell walls with a lower protein content (26 mg/g dry matter) (Le Bourvellec & Renard, 2012).

2.3.5 Polyphenol structure

Similarly, the ability of polyphenols to bind to CPSs can also be shaped by the structure of the polyphenol, specifically its size (Bindon, Smith, & Kennedy, 2010; Le Bourvellec, Guyot, et al., 2004; Le Bourvellec & Renard, 2005; D. Liu et al., 2017; McManus et al., 1985; Renard et al., 2001b; Tang, Covington, & Hancock, 2003), functional groups (Buchweitz et al., 2013b; Chirug et al., 2018; Le Bourvellec, Guyot, et al., 2004; Mamet et al., 2018; Tang et al., 2003; Yuxue Wang, Liu, Chen, & Zhao, 2013; J. Zhu et al., 2018) and conformation (Cai et al., 1990; De Freitas & Mateus, 2001; Ishizu et al., 1999; Le Bourvellec, Guyot, et al., 2004; McManus et al., 1985).

2.3.5.1 Effect of molecular weight

A polysaccharide's binding capacity for polyphenols is positively correlated with the molecular weight of the polyphenols (Bindon, Smith, Holt, et al., 2010; Le Bourvellec, Guyot, et al., 2004; Le Bourvellec & Renard, 2005; R. Liu et al., 2017; McManus et al., 1985; Renard et al., 2017; Tang et al., 2003). For example, the affinity of epicatechin monomers for apple cell walls is much weaker than that of procyanidins composed of (–)-epicatechin units (Renard et al., 2001b). Likewise, interaction between cell wall material and procyanidins increases markedly with the degree of polymerization of the latter (Le Bourvellec, Guyot, et al., 2004; Le Bourvellec & Renard, 2005). D. Liu et al. (2017) investigated the equilibrium adsorption amounts for three polyphenols on cellulose, and reported that they followed the order of procyanidin B2 > phloridzin > epicatechin. These results probably reflect the number of ortho phenolic groups (which contribute to hydrogen bonds) and aryl rings (which contribute to hydrophobic interactions) in these three molecules. In addition, the improved binding ability of higher-DP procyanidins stems from the fact that procyanidins are multidentate ligands capable of simultaneously binding more than one point on the surface of a polysaccharide, which enables procyanidins to form more bonds with the cell walls.

2.3.5.2 Functional groups of polyphenols

Another structural factor that can strongly influence the reactivity of polyphenols with polysaccharides is the presence of functional groups, such as galloyl groups, hydroxyl groups, glycoside groups, and methyl and methoxy groups, as well as the number, projection, and position of these groups in the aryl rings (Buchweitz et al., 2013b; Le Bourvellec, Guyot, et al., 2004; Mamet et al., 2018; Tang et al., 2003; Yuxue Wang et al., 2013; Watrelot et al., 2013).

2.3.5.2.1 Galloylation

Polyphenol/polysaccharide interactions increase noticeably with the percentage of galloylation (Le Bourvellec, Guyot, et al., 2004; Mamet et al., 2018; Tang et al., 2003; Y. Wang et al., 2013). For example, by examining a group of 24 polyphenols, Tang et

al. (2003) reported a positive correlation between a polyphenol's number of galloyl groups and its adsorption on cellulose. Likewise, Le Bourvellec et al. (2004) showed that increasing the galloylation of procyanidin increased the strength of binding. Wang et al. (2013) characterized the binding of three (-)-epicatechin derivatives to oat β -glucan as being in the following order: epigallocatechin-3-gallate > epicatechin-3-gallate > epicatechin. This was presumably the result of the increase in both the number of aromatic groups and hydroxyl groups with the addition of the galloyl group, which thereby enhanced the hydrophobic interactions and hydrogen bonding. However, it has also been reported that intergalloyl C-C linkages may severely restrict the conformational flexibility of galloyl groups and therefore hinder the hydrophobic interactions (Tang et al., 2003).

2.3.5.2.2 Hydroxylation

Similarly, the presence of more hydroxyl groups on polyphenols seems to promote adsorption to polysaccharides (Buchweitz et al., 2013b; Le Bourvellec, Guyot, et al., 2004). Buchweitz et al. (2013b) reported that the number of hydroxyl groups in the anthocyanin B-ring influenced anthocyanin-pectin interactions and their stabilization. Likewise, among flavonoids of generally similar structure (similar average molecular sizes and numbers of aromatic and phenolic hydroxyl groups), binding to polysaccharides was significantly affected by the degree of hydroxylation on the A, B, and C rings (Y. Wang et al., 2013; J. Zhu et al., 2018). A summary of the effects of phenolic hydroxylation of various flavonoids and phenolic acids on their affinities for arabinan-rich pectic polysaccharides (ARPP) and β -glucan is presented in [Table 2.5](#). In general, flavonoids are retained on oat β -glucan following the order flavonol > flavone > flavanone > isoflavone (Y. Wang et al., 2013). However, within these classes, the degree and location of hydroxylation can have dramatic effects on binding affinity. For example, in flavones, the introduction of hydroxyl groups on the B (apigenin \rightarrow luteolin) and C (apigenin \rightarrow kaempferol) rings increases their adsorption into oat β -glucan. Furthermore, the effect of hydroxylation at the 3-position on the C ring is markedly higher than that of the 3'-position on the B ring. However, the introduction of hydroxyl

groups on the C ring (luteolin → quercetin) also has the ability to decrease the adsorption capacity, due to the lower solubility of quercetin (Y. Wang et al., 2013). In flavonols and flavanols, the same numbers of hydroxyl groups at different positions on the B ring can have significant consequences for the adsorption capacity, e.g., quercetin (204 mol/mol) > (-)-epicatechin (96 mol/mol) > morin (65 mol/mol) (Y. Wang et al., 2013). Moreover, the introduction of hydroxyl groups on the A ring of isoflavone or the B ring of flavanone leads to the same increase in adsorption. One interesting finding is that, for flavonoids, the presence of three or fewer hydroxyl groups increases adsorption, but the presence of four or more hydroxyl groups inhibits it, as was found with, for example, luteolin (5, 7, 3', 4'-OH, 395 mol/mol), quercetin (3, 5, 7, 3', 4'-OH, 204 mol/mol), and myricetin (3, 5, 7, 3', 4', 5'-OH, 171 mol/mol) (Y. Wang et al., 2013). For different isomers of coumaric acid, the binding capacities for oat β -glucan increase by the order of *o*-coumaric acid (2-OH) > *m*-coumaric acid (3-OH) \approx *p*-coumaric acid (4-OH) (Y. Wang et al., 2013), possibly as a result of differences in the forces that drive interactions between oat β -glucan and individual coumaric acids (Y. Wang et al., 2013). More recently, J. Zhu et al. (2018) investigated the interactions between ARPP and 27 different phenolic acids. These authors determined that the introduction of hydroxyl groups enhanced polyphenol adsorption on ARPP, and hydrogen bonds were the main driving force behind this result. Moreover, the precise location of the hydroxyl group had a significant impact on adsorption: for hydroxycinnamic acids, a hydroxyl group added at the 4-position ($(\Delta Q = (Q_{\text{after}} - Q_{\text{before}}) / Q_{\text{before}} \times 100\%)$, 271%) increased adsorption on ARPP more than an addition at the 3-position did (34%), and for hydroxylation on hydroxybenzoic acids, the binding capacities increased in the order of 4-position (46%) > 5-position (44%) > 3-position

Polysaccharide-polyphenol interactions

Table 2.5 Effects of hydroxylation, methylation, glycosylation, and esterification of phenolics on affinities for ARPP^a/β-Glucan *in vitro*.

Main class	Sub-class	Ring	Position	Example	Polysaccharides	Effect	References
Phenolic acids	Hydroxycinnamic acids	-	4-H → OH	<i>m</i> -coumaric acid → caffeic acid	ARPP	↑	J. Zhu et al., 2018
		-	3-H → OH	<i>p</i> -coumaric acid → caffeic acid	ARPP	↑	J. Zhu et al., 2018
		-	3-OH → OCH ₃	caffeic acid → ferulic acid	Oat β-Glucan	↑	Wang et al., 2013
		-	3-OH → OCH ₃	caffeic acid → ferulic acid	ARPP	↓	J. Zhu et al., 2018
		-	5-H → OCH ₃	ferulic acid → sinapic acid	Oat β-Glucan	↓	Wang et al., 2013
		-	5-H → OCH ₃	ferulic acid → sinapic acid	ARPP	↑	J. Zhu et al., 2018
		-	3-H → OCH ₃	<i>p</i> -coumaric acid → ferulic acid	ARPP	↓	J. Zhu et al., 2018
Hydroxybenzoic acids		-	4-H → OH	3-Hydroxybenzoic acid → protocatechuic acid	ARPP	↑	J. Zhu et al., 2018
		-	3-H → OH	4-Hydroxybenzoic acid → protocatechuic acid	ARPP	↑	J. Zhu et al., 2018
		-	5-H → OH	protocatechuic acid → gallic acid	ARPP	↑	J. Zhu et al., 2018
		-	3-H → CH ₃	salicylic acid → 3-methyl salicylic acid	ARPP	↓	J. Zhu et al., 2018

(Continued)

Table 2.5 (Continues)

Main class	Sub-class	Ring	Position	Example	Polysaccharides	Effect	References
		-	4-H → CH ₃	salicylic acid → 4-methyl salicylic acid	ARPP	↓	J. Zhu et al., 2018
		-	3-H → OCH ₃	4-Hydroxy benzoic acid → vanillic acid	ARPP	↓	J. Zhu et al., 2018
		-	5-H → OCH ₃	vanillic acid → syringic acid	ARPP	↑	J. Zhu et al., 2018
		-	3-OH → OCH ₃	protocatechuic acid → vanillic acid	ARPP/ Oat β-Glucan	↓	Wang et al., 2013; J. Zhu et al., 2018
		-	3,4-OH → OCH ₃	protocatechuic acid → veratric acid	ARPP/Oat β-Glucan	↓	Wang et al., 2013; J. Zhu et al., 2018
		-	4-OH → OCH ₃	vanillic acid → veratric acid	Oat β-Glucan	↓	Wang et al., 2013
		-	3,5-OH → OCH ₃	gallic acid → syringic acid	ARPP/Oat β-Glucan	↓	Wang et al., 2013; J. Zhu et al., 2018
Flavonoids	Flavones	B	3'H → OH	apigenin → luteolin	Oat β-Glucan	↑	Wang et al., 2013
		C	3H → OH	apigenin → kaempferol	Oat β-Glucan	↑	Wang et al., 2013
		C	3H → OH	luteolin → quercetin	Oat β-Glucan	↓	Wang et al., 2013
	Flavonols	B	4-OH → OCH ₃	luteolin → diosmetin	Oat β-Glucan	↓	Wang et al., 2013
		A	7OH → 7-neohesperidose	naringenin → naringin	Oat β-Glucan	↓	Wang et al., 2013
		B	3'H → OH	kaempferol → quercetin	Oat β-Glucan	↓	Wang et al., 2013
		B	4'H → OH	galangin → kaempferol	Oat β-Glucan	↑	Wang et al., 2013

(Continued)

Polysaccharide-polyphenol interactions

Table 2.5 (Continues)

Main class	Sub-class	Ring	Position	Example	Polysaccharides	Effect	References
		B	5'H → OH	kaempferol → morin	Oat β-Glucan	↓	Wang et al., 2013
		B	2'H → OH	quercetin → myricetin	Oat β-Glucan	↓	Wang et al., 2013
		B	3-OH → OCH ₃	quercetin → isorhamnetin	Oat β-Glucan	↑	Wang et al., 2013
		B	3OH → 3-O-α-L- rhamnoside	myricetin → myricetrin	Oat β-Glucan	↑	Wang et al., 2013
		B	3OH → 3-α-L-Rham- 1,6-D-Glc	quercetin → rutin	Oat β-Glucan	↓	Wang et al., 2013
	Isoflavones	A	5H → OH	daidzein → genistein	Oat β-Glucan	↑	Wang et al., 2013
		A	7OH → 7-glucoside	genistein → genistin	Oat β-Glucan	↓	Wang et al., 2013
		A	7OH → 7-glucoside	daidzein → daidzin	Oat β-Glucan	↑	Wang et al., 2013
		A	8H → 8-C-glucose	daidzein → puerarin	Oat β-Glucan	↓	Wang et al., 2013
	Flavanone	B	4'H → OH	naringenin → eriodictyol	Oat β-Glucan	↑	Wang et al., 2013
		A	7OH → 7- neohesperidose	naringenin → naringin	Oat β-Glucan	↓	Wang et al., 2013

a: arabinan-rich pectic polysaccharides from rapeseed meal (ARPP).

(36%) (J. Zhu et al., 2018). In contrast to the results of Wang et al. (2013), J. Zhu et al. (2018) argued that *p*-coumaric acid had the highest adsorption to ARPP; this was followed by *o*-coumaric acid, and *m*-coumaric acid with the least. As the three coumaric acid isomers are ranked differently in binding to oat β -glucan and ARPP, these findings suggest that the effect of the location of hydroxyl groups is more complicated than the effect of the number of hydroxyl groups. What seems to be undisputable, though, is that both the number of hydroxyl groups and their positions on the aromatic ring play important roles in the interactions. The effect of differences in solubility of polyphenols should also be considered. In the end, it seems likely that the fates of interactions are determined by a balance among these different factors.

2.3.5.2.3 Methylation and methoxylation

Increasing the degree of methylation ($-H/OH \rightarrow -CH_3$) and methoxylation ($-H/OH \rightarrow -OCH_3$) of a polyphenol can either decrease or increase its ability to interact with polysaccharides depending on the specific spatial structure in question (Table 2.5) (Yuxue Wang et al., 2013; J. Zhu et al., 2018). For flavones and hydroxybenzoic acids, methylation and methoxylation do not increase their binding to oat β -glucan (Yuxue Wang et al., 2013). However, for flavonols, the addition of a methoxy group to the B ring of quercetin (3'-OH), leading to the creation of isorhamnetin (3'-OCH₃), dramatically increases binding capacities to oat β -glucan (by a factor of four). This could be attributed to a significant increase in the solubility of isorhamnetin compared to quercetin as a result of methylation (Y. Wang et al., 2013). With respect to hydroxycinnamic acid derivatives, ferulic acid, a methylated derivative of caffeic acid, has a higher binding capacity than the unmethylated form of caffeic acid, but further methylation of ferulic acid to sinapic acid results in a decrease in adsorption capacity with oat β -glucan by a third (Y. Wang et al., 2013). Methylation greatly decreases the binding capacity of hydroxycinnamic acid and hydroxybenzoic acid for ARPP (J. Zhu et al., 2018). Finally, the addition of a methoxyl group at the 3-position seems to be detrimental to the adsorption capacities of phenolic acids to ARPP, while addition at the 5-position promotes adsorption by ARPP (J. Zhu et al., 2018).

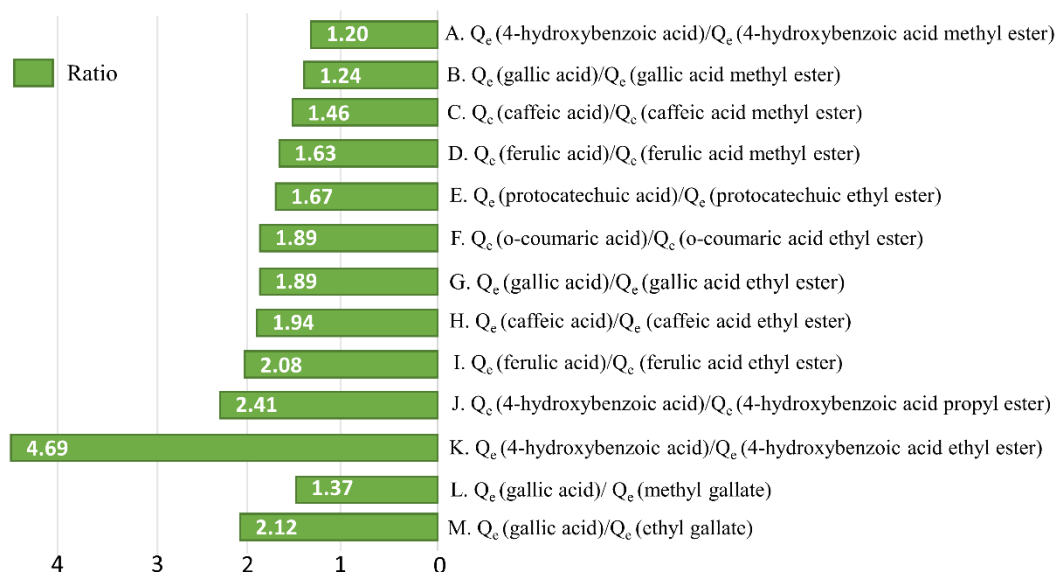


Figure 2,16 Comparison of the adsorption of free and esterified phenolic acids on cell wall polysaccharides: esterification lowers the affinities of phenolic acids for arabinan-rich pectic polysaccharide from rapeseed meal (ARPP) (A - K) by a factor of 1–5 (J. Zhu et al., 2018) and decreases the affinities of hydroxybenzoic acids for oat β -glucan (L and M) by a factor of 1–2 (Yuxue Wang et al., 2013). Q_e represents the adsorbed amounts of phenolic acids in $\mu\text{g}/\text{mg}$ of ARPP/oat β -glucan.

Esterification (polyphenol \rightarrow polyphenol-methyl/ethyl ester) markedly reduces the adsorption capacity of phenolic acids to ARPP (Fig. 2.16). Specifically, J. Zhu et al. (2018) found that the adsorption ($\Delta Q=(Q_{\text{ester}} - Q_{\text{original}})/Q_{\text{original}} \times 100\%$) of ferulic acid, caffeic acid, 4-hydroxybenzoic acid, and gallic acid decreased by 39%, 32%, 16%, and 21%, respectively, after methyl esterification. Ethyl esterification of these phenolic acids also reduced adsorption on ARPP by 52%, 48%, 79%, and 47%, respectively (J. Zhu et al., 2018). The effect of ethyl esterification appears to be greater than that of methyl esterification, because $-\text{CH}_2-\text{CH}_3$ results in more hydrophobicity than CH_3 . However, after the hydroxyl group in the carboxyl group is substituted with an alkoxy group, the carboxyl group of phenolic acids is blocked. This means that the esterified forms of phenolic acids have lower hydrophilicity than their unesterified analogues, leading to a decrease in adsorption capacity (J. Zhu et al., 2018).

2.3.5.2.4 Glycosylation

Most flavonoids are naturally present in the form of β -glycosides, and the presence of a glycoside group can affect their ability to interact with polysaccharides (Table 2.5)

(Chirug et al., 2018; Y. Wang et al., 2013). Wang et al. (2013) found no definitive correlation between glycosylation and adsorption. In their study, glycosylation did not affect the adsorption capacity of genistein, but 7-glucosylation of daidzein and 3-O- α -L-rhamnosylation of myricetin improved their binding capacities to oat β -glucan. Instead, rutin, naringin, and puerarin demonstrated lower adsorption capacities with oat β -glucan than unglycosylated forms (Y. Wang et al., 2013). Despite the lack of a clear pattern, it is clear that different degrees of glycosylation among flavonoids may lead to differences in both solubility and glycosyl steric hindrance, which then translate into differences in adsorption. Chirug et al. (2018) also reported that interactions between pectins and quercetin were significantly stronger than those between pectins and rutin. This could be due to the presence of the disaccharide, which reduces the number of binding sites on the flavonol and/or creates steric hindrance, thereby limiting the interaction.

2.3.5.3 Effect of conformational changes

A good example of the effect of conformational changes on binding is provided by proanthocyanidins, which can be classified into either A-type or B-type depending on the interflavanic bond. A-type proanthocyanidins (such as those from cranberry) bind more effectively to α -amylase, and thus have a stronger inhibitory effect, than B-type proanthocyanidins (from grape) (Barrett et al., 2013). However, the former has a higher degree of polymerization than the latter, it is also possible that the additional ether bonding may cause increased tannin hydrophobicity, and thus explain the higher affinity (McRae, Falconer, & Kennedy, 2010).

The subunits of B-type proanthocyanidin are connected by two main interflavanic bonds: C(-4)-C(-6) or C(-4)-C(-8) (Fig. 2.13). Procyanidin dimers with a C(-4)-C(-8) interflavanic linkage interact more readily than those with a C(-4)-C(-6) interflavanic bond (De Freitas & Mateus, 2001). To date, we lack similar information about the effects of the structure of A-type proanthocyanidins and their interflavanic linkages on the interaction with cell walls. In part, this can be attributed to the constraints of existing

analytical methods, which have limited research on the interaction of A-type proanthocyanidins.

The importance of stereochemistry has also been noted in other studies of the interactions between polysaccharides and flavan-3-ols, particularly with respect to the pyran rings of the latter: multiple studies have confirmed that (+)-catechin binds more readily to polysaccharides than (–)-epicatechin does (Cai et al., 1990; Ishizu et al., 1999; Le Bourvellec, Guyot, et al., 2004; McManus et al., 1985). Specifically, (+)-catechin has much higher affinity for β -cyclodextrin (β -CD) than (–)-epicatechin, and β -CD/(+)-catechin complexes fit more tightly together (Cai et al., 1990; Ishizu et al., 1999). The arrangement of the hydroxyl groups at C-3 of (+)-catechin enables hydrogen bonds with possible hydroxyl groups around C-2 and C-3 at the top edge of the β -CD cavity (Cai et al., 1990). Furthermore, Ishizu et al. (1999) hypothesized that the steric hindrance of the C3-OH group in the equator of (+)-catechin is lower than that of the axial C3-OH group of (–)-epicatechin, and the four hydroxyl groups of the (+)-catechin A and B rings are excluded from the hydrophobic cavity of β -CD due to their hydrophilicity. Likewise, a grape procyanidin of DP8, with 13% (+)-catechin and a degree of galloylation of 22%, had a higher binding capacity for apple cell walls than an apple procyanidin of DP10 with very few (+)-catechin subunits (1.8%) and no galloylation (Le Bourvellec, Guyot, et al., 2004). The difference in interaction intensity may arise from the different helical forms in the polymer's structure: (+)-catechin gives a right-handed helix, while (–)-epicatechin gives a left-handed helix (Fletcher, Porter, & Haslam, 1976). Polymers derived from right-handed (+)-catechin may have a more open and flexible conformation that is conducive to the formation of hydrogen bonds and hydrophobic interactions (Le Bourvellec, Guyot, et al., 2004). Conformationally open and random coiled polyphenols have much higher affinities for polysaccharides than tightly coiled globular polyphenols, probably because of the increased accessibility of the backbone of the former in addition to a higher degree of exposure to the hydrophobic aromatic rings.

2.3.6 The relative importance of different aspects of molecular structure

Because CPS-polyphenol interactions depend on the structures of both partners, they can be altered by many factors, including morphology (surface area and porosity), chemical composition (sugar ratio, solubility, and non-sugar components), and molecular architecture (molecular weight, degree of esterification, functional groups, and conformation). Here, we conduct a comparative evaluation of all of the structural factors discussed in this review, and attempt to estimate the importance of each factor as high, medium, or low (Fig. 2.15, Table 2.6).

In general, characteristics of CPSs such as their solubility, and degree of branching and esterification, and cell wall attributes such as porosity, are of high importance. For polyphenols, factors such as molecular weight, galloylation, and hydroxylation are clearly important in determining interactions. Although this work provides molecular-level new insights into the current state of research in the interaction field, it is still a challenge to explicitly rank the various important factors that drive the CPS-polyphenol interactions, because they may be antagonists or synergists in the same interaction system.

2.3.7 Adsorption mechanisms

Non-covalent interactions between polyphenols and polysaccharides mainly involve the following three interaction forces: van der Waals forces, hydrogen bonds, and hydrophobic interactions. Moreover, some physical characteristics play a crucial and often-overlooked role, as the intrinsic solubility and porosity/pore shape of molecules also determine the strength or weakness of the interactions. The mechanisms of CPS-polyphenol interactions at the molecular level are summarized in Figs. 2.17 and 2.18.

Hydrophobic interactions take place between the hydrophobic sites of polysaccharides, such as the methoxy group of galacturonic acid, and the aromatic rings of polyphenols (Fig. 2.17). Evidence for the importance of hydrophobic interactions in adsorption has come from multiple sources: for example, polyphenol adsorption on

Polysaccharide-polyphenol interactions

Table 2.6 Evaluation of the relative importance of aspects of molecular internal structure in cell wall polysaccharide-polyphenol interactions.

Structure	Factors	Main mechanisms	Additional information	Levels of importance	References
Cell wall polysaccharide	Solubility/composition	Hydrophobic interactions, hydrogen bonds, and ionic bond	Extracted pectins have the highest affinity.	High	Brahem et al., 2019; Le Bourvellec et al., 2005, 2012; Y. Liu et al., 2019; Ruiz-Garcia et al., 2014
	Surface area/porosity	Hydrophobic interactions, hydrogen bonds, surface adsorption, surface diffusion, and pore diffusion	This factor applies only to insoluble polysaccharides. The greater the porosity, and the better the match is between pore size and the polyphenol, the higher adsorption is.	High	Bermúdez-Oria et al., 2019; Bindon et al., 2012; Le Bourvellec et al., 2005, 2012; D. Liu, Lopez-Sanchez, Martinez-Sanz, et al., 2019; D. Liu et al., 2017
	Molecular weight	Hydrophobic interactions and hydrogen bonds	High-molecular-weight polysaccharides may not have a high affinity for polyphenols.	Medium	Guo et al., 2018; He et al., 2019; Larsen et al., 2019; J. Zhu et al., 2018
	Degree of esterification	Hydrophobic interactions and hydrogen bonds	High affinities are observed between highly methylated pectin and polyphenols.	High	Buchweitz et al., 2013b, 2013a; A. Fernandes et al., 2020; Larsen et al., 2019; Mamet et al., 2018; Padayachee et al., 2012b; Watrelot et al., 2013
	Side chains and branching ratios	Hydrophobic interactions and hydrogen bonds	Polyphenols bind more to linear pectins.	High	Brahem et al., 2019; Koh et al., 2020; Watrelot et al., 2014
	Non-sugar components	π -orbits and hydrogen bonds	Protein enrichment of cell walls does not change interactions; water and lignin in cellulose contribute to interactions; ferulic acid limits interactions.	Low	Le Bourvellec et al., 2012; D. Liu et al., 2017; Ye et al., 2009

(Continued)

Table 2.6 (Continues)

Structure	Factors	Main mechanisms	Additional information	Levels of importance	References
Polyphenols	Molecular weight	Hydrophobic interactions and hydrogen bonds	The molecular weight of polyphenols is positively correlated with their binding capacity for polysaccharides.	High	Bindon, Smith, Holt, et al., 2010; Le Bourvellec et al., 2004; Le Bourvellec & Renard, 2005; R. Liu et al., 2017; Renard et al., 2017
	Glycosylation	Hydrophobic interactions, hydrogen bonds, surface adsorption, surface diffusion, and pore diffusion	Different glycosylated flavonoids may have different solubilities and degrees of glycosyl steric hindrance, which can affect adsorption capacity.	Medium	Chirug et al., 2018; Wang et al., 2013
	Galloylation and hydroxylation	Hydrophobic interactions and hydrogen bonds	Polyphenol/polysaccharide interactions increase noticeably with the percentage of galloyl and hydroxyl groups. The position of hydroxyl groups has a significant impact on monomeric polyphenols.	High	Buchweitz et al., 2013a; Le Bourvellec et al., 2004; Mamet et al., 2018; Wang et al., 2013; J. Zhu et al., 2018
	Methylation and acetylation	Hydrophobic interactions and hydrogen bonds	Increasing the degree of esterification of polyphenols may decrease or increase their ability to interact with polysaccharides depending on the specific spatial structure.	Medium	Wang et al., 2013; J. Zhu et al., 2018
	Conformational changes	Hydrophobic interactions, hydrogen bonds, and physical adsorption.	Conformationally open and random coiled polyphenols are more likely to interact.	Medium	Cai et al., 1990; Ishizu et al., 1999; Le Bourvellec et al., 2004; McManus et al., 1985

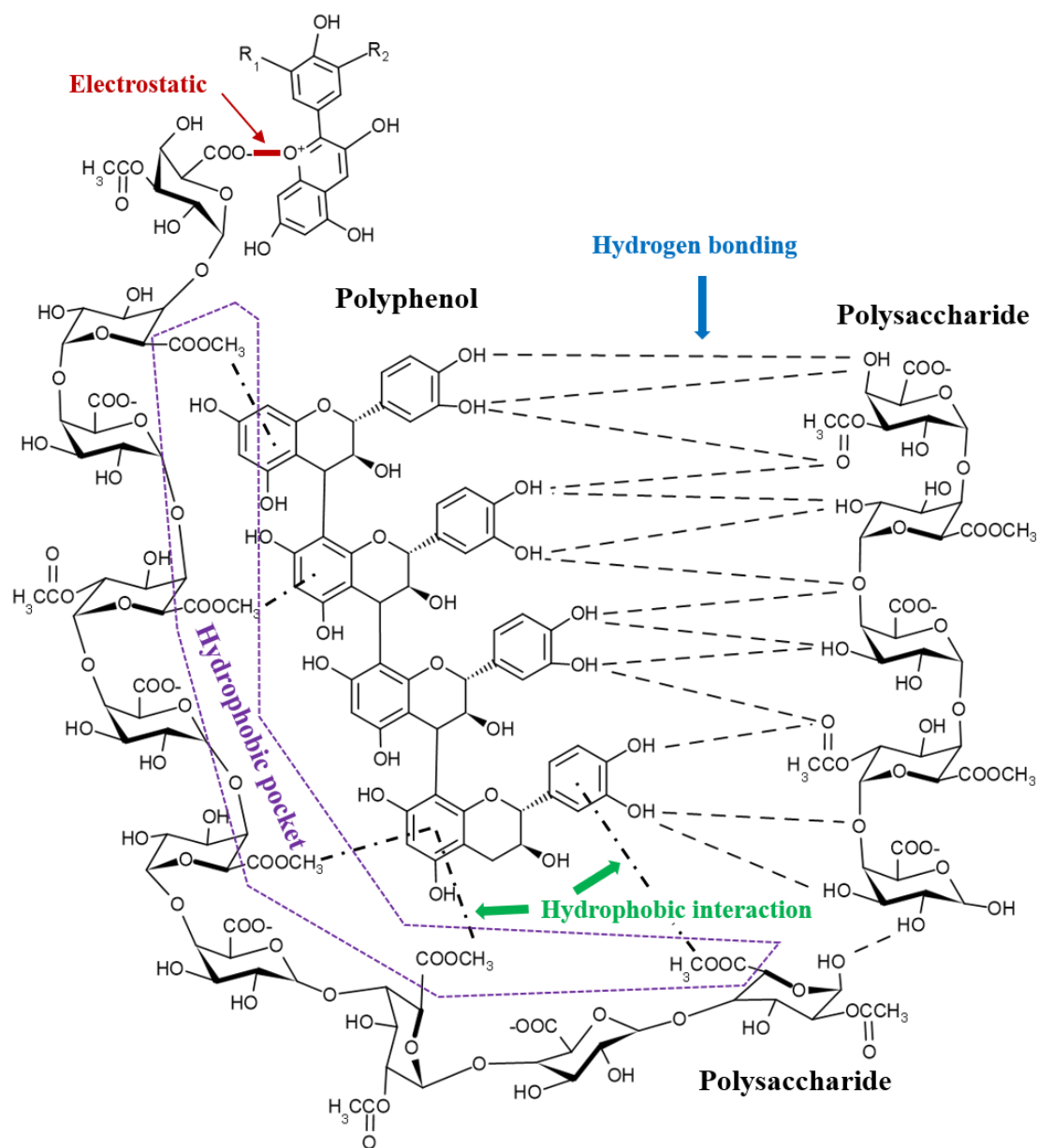


Figure 2.17 Different potential chemical mechanisms of interactions between cell wall polysaccharides and polyphenols.

pectins increases with the degree of methoxylation (Mamet et al., 2018; Padayachee et al., 2012b; Watrelot et al., 2013), and the addition of the polar solvents ethanol or dioxane has been shown to disrupt the binding (Le Bourvellec, Guyot, et al., 2004). Instead, hydrogen bonds often form between the hydroxyl group of polyphenols and the oxygen atom of the glycosidic bonds or the hydroxyl groups of homogalacturonan (Fig. 2.17). An increase in temperature can disrupt these bonds and reduce the adsorption of polyphenols on polysaccharides. This has been noted in multiple interaction systems, such as procyanidins/apple cell walls (Le Bourvellec, Guyot, et al.,

2004), tea polyphenols/ β -glucans (Z. Wu, Li, Ming, & Zhao, 2011) and cellulose/cyanidin-3-glucoside and ferulic acid (Phan, D'Arcy, & Gidley, 2016). Likewise, the use of urea, which destroys hydrogen bonds, also inhibits interactions (Renard et al., 2001b). As the use of Isothermal Titration Calorimetry has become widespread in the study of interactions between polysaccharides and polyphenols, it has become possible to characterize not only the binding affinity but also changes in enthalpy (ΔH) and entropy (ΔS). Different types of interactions make different contributions to changes in enthalpy and entropy: Van der Waals interactions and hydrogen bonds are conducive to binding enthalpy, while hydrophobicity mainly contributes to favorable binding entropy. Moreover, reactions involving exotherms are driven by van der Waals forces and hydrogen bonds, while endotherms are driven by hydrophobic interactions (Callies & Hernández Daranas, 2016; Ladbury & Doyle, 2004). Most interactions between CPSs and polyphenols are exothermic, accompanied by coexisting enthalpy- and entropy-driven phenomena.

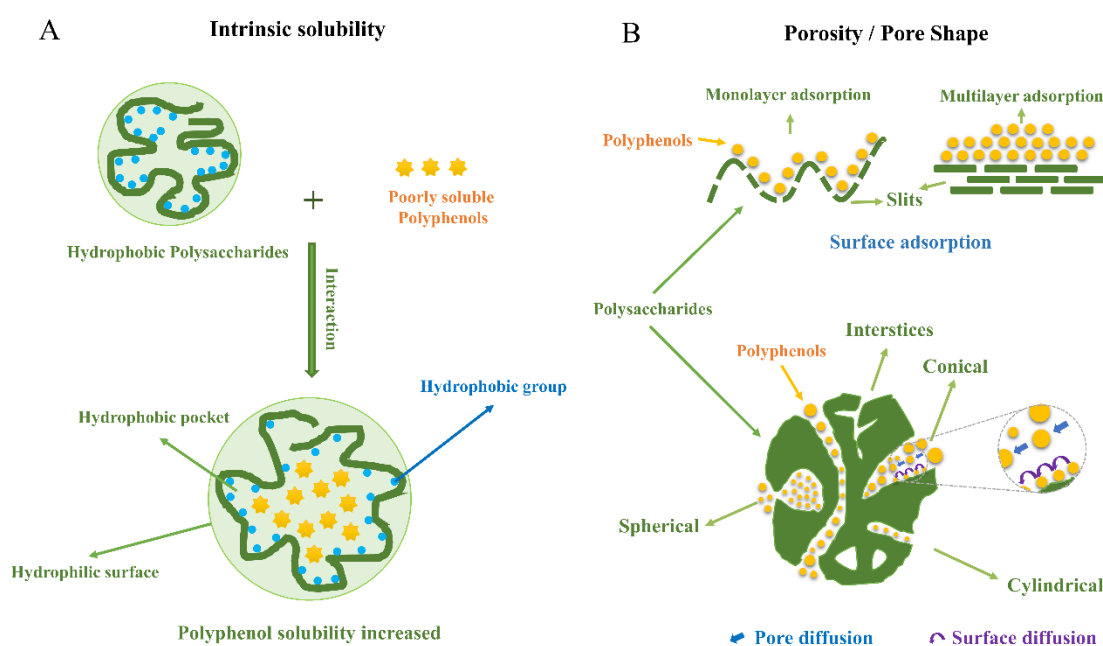


Figure 2.18 Different potential physical mechanisms of interactions between cell wall polysaccharides and polyphenols. A. Effect of intrinsic solubility. B. Effects of porosity and pore shape.

Other associations, such as ionic bonds between charged groups of pectins and charged hydroxyl groups of polyphenols (primarily anthocyanins), could play a

secondary role (Fig. 2.17). For example, the ionic interactions between flavylum cations of anthocyanin and free carboxyl groups of blueberry pectins might be the driver of this particular interaction (A. Fernandes et al., 2020; Koh et al., 2020; Lin, Fischer, & Wicker, 2016). In addition, D. Liu, Lopez-Sanchez, Martinez-Sanz, et al. (2019) described how the association between charged chlorogenic acid and pectins can be affected by pH. The pKa of pectin and chlorogenic acid are 3.5 and 3.3, respectively. When the pH is less than 3.5, their repulsive force decreases, which therefore increases the adsorption of chlorogenic acid to pectic polysaccharides. In studying CPS-polyphenol interactions, however, it should be noted that polyphenols can also self-associate (i.e. accumulate aromatic rings and form micelles) in aqueous solutions, which can affect their interactions (Pianet et al., 2008). For example, any π - π stacking that occurs between polyphenols (e.g., anthocyanins) will have a large impact on adsorption capacities (A. Fernandes et al., 2020; Koh et al., 2020).

CPS-polyphenol interactions can also be shaped by the intrinsic solubility of both partners. In general, polyphenols with lower solubility are more likely to coagulate with hydrophobic polysaccharides. This interaction may occur in one of two ways: 1) Polysaccharides form hydrophobic pockets that encapsulate polyphenols (Fig. 2.18A); 2) The hydrophobic groups of the polysaccharide are exposed to the exterior environment, and are then bound by the less-soluble polyphenols to form a hydrophobic layer. In this way, the solubility of polyphenols can be improved by interacting with hydrophobic polysaccharides.

Finally, the effect of porosity/pore shape may be one of the least understood phenomena driving CPS-polyphenol interactions (Fig. 2.18B). CPSs are heterogeneous in terms of molecular structure, shape, size, and surface characteristics (Burton et al., 2010). Even within the same botanical species, cell wall structure and morphology (e.g., parenchyma, stone, and skin cells in pears) are not uniform (Brahem et al., 2019). Generally speaking, pores can be divided into three size categories: large pores, with pore radius (r) > 50 nm; mesopores, with 2 nm $< r < 50$ nm; and micropores, with $r < 2$ nm (Thommes et al., 2015). In cell walls, micropores and mesopores are most common,

with typical pore diameters of 3.5 - 5 nm (Carpita et al., 1979; Chesson, Gardner, & Wood, 1997). In addition to size, pores can also be described by their shapes, which can be roughly described as slits, spherical, interstices, conical, and cylindrical (Fig. 2.18B). Even within a single insoluble CPS or cell wall, pores of different shapes can have distinctly different methods of adsorbing polyphenols, with sometimes dramatic effects on the final adsorption capacity. For example, in slit pores, polyphenol molecules can only be adsorbed in a single layer or stacked. When the size of a polyphenol is smaller than the pore size, it can diffuse into the cavity of the polysaccharide via either surface diffusion or pore diffusion (Medved' & Černý, 2011). However, these processes can also occur simultaneously, as reported by Tao et al. (2020), who observed the mass transfer of blueberry anthocyanins at the same time as adsorption by macroporous resins (average pore diameter, 8 nm). In that study, ultrasonic treatment increased the contribution of surface diffusion to the overall diffusion, and the higher the porosity, the easier the diffusion. In addition, Dhital, Brennan, & Gidley (2019) showed that the microstructural characteristics of surface pores and channels in starch granules affect their reactivity with non-starch components (e.g., polyphenols, proteins, and lipids).

2.3.8 Conclusions and future perspectives

The application of knowledge on CPS-polyphenol interactions to food processing is a relatively new and emerging research area. Much has been learned from the study of interactions between CPSs and polyphenols, especially using relatively simple biomolecules such as pectin backbones and polyphenol monomers. It is our hope that this review may ultimately facilitate and provide guidance for the study of more complex systems of CPS-polyphenol interactions in the food industry. More research is needed to better understand the mechanisms involved, because we believe this will pay dividends in terms of fostering the development of new plant-based foods, formulations, and supplements.

Major challenges remain in this area; in order to move forward, there are several significant questions that still need to be addressed. Future research should focus on the following points:

- Understanding the conformational changes of polyphenols, e.g., interflavanic bonds and chirality, and how these affect interactions with CPSs in food processing; investigating how greater structural flexibility of polyphenols facilitates binding to CPSs.
- Studying their digestion, absorption efficiency, and bioavailability in the human body. In addition, more attention should be paid to the nutritional consequences of CPS-polyphenol complexes in the colon, i.e., the different fermentation modes of the complexes, as well as the enzymes and bacteria involved. Their dietary significance and potential health benefits for humans should also be assessed.
- Combining studies of different animal and cell models to compare and confirm the results of *in vitro* digestion models, in order to help us understand the bioavailability of polyphenol-polysaccharide complexes *in vivo*. For the non-extractable polyphenols in fruits, such as ellagitannins, flavanones, and procyanidins, it is the intestinal microbial metabolites, rather than the natural macromolecules, that have anti-inflammatory and anti-oxidative effects. Therefore, there is still a need to describe the biological effects of intestinal microbial metabolites produced from the most common polyphenols, such as procyanidins, with human intervention studies as the “Gold-Standard”.
- Comparing the proportions and concentrations of various polyphenols among different foodstuffs, and investigating the implications of these differences on interactions in actual food systems to reinforce the implications of this study.
- Exploring the effects of non-thermal processing on polyphenols, the majority of which are sensitive to high temperature. For example, ultra-high-pressure processing, pulsed electric fields, nonthermal plasma, and UV and infrared light should all be assessed for their effects on the interactions between polyphenols and polysaccharides.

Highlights

- Of all cell wall polysaccharides, pectins have the highest affinities for polyphenols, and these affinities are the highest for high molecular weight, highly methylated pectins.

- Proanthocyanidins are the polyphenols which have the most propensity to bind to cell walls, and this is increased by high degree of polymerization and galloyl substitution.

Knowledge gaps

- Interactions of procyanidins has been studied with pectins of different commercial origins (apple or citrus) or with pectin structural units, but there is little systematic information on the effect of native pectin's structural features (both composition and spatial conformation) on their interaction with procyanidins.

- Also, there is surprising little data on hemicelluloses, which motivates a specific study on interactions of procyanidins with hemicelluloses.

- Drying of cell walls as well as pectin extraction impact the affinity for polyphenols, but whether chemical or physical factors are most important, and how they interact. This question will be approached by generating a series of cell walls with a diversity of chemical compositions and physical characteristics.



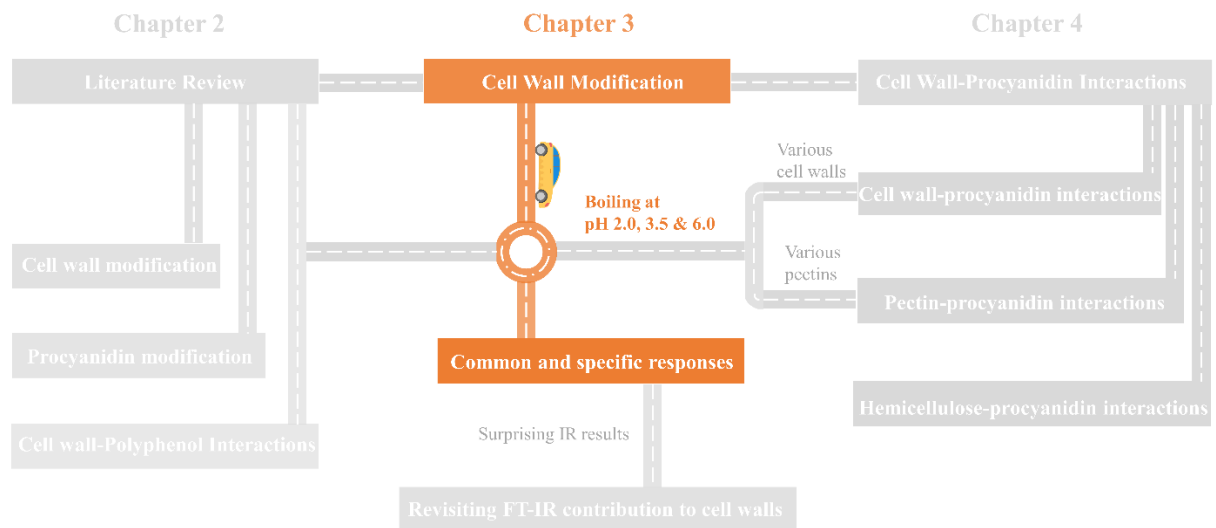
When Moon goes to sleep
Silent is Cambridge tonight
That has XV Cell Wall Meeting
At West Road Concert Hall

CHAPTER 3.

Cell wall characterization

Section 3.1

Modification of apple, beet and kiwifruit cell walls by boiling in acid conditions: Common and specific responses



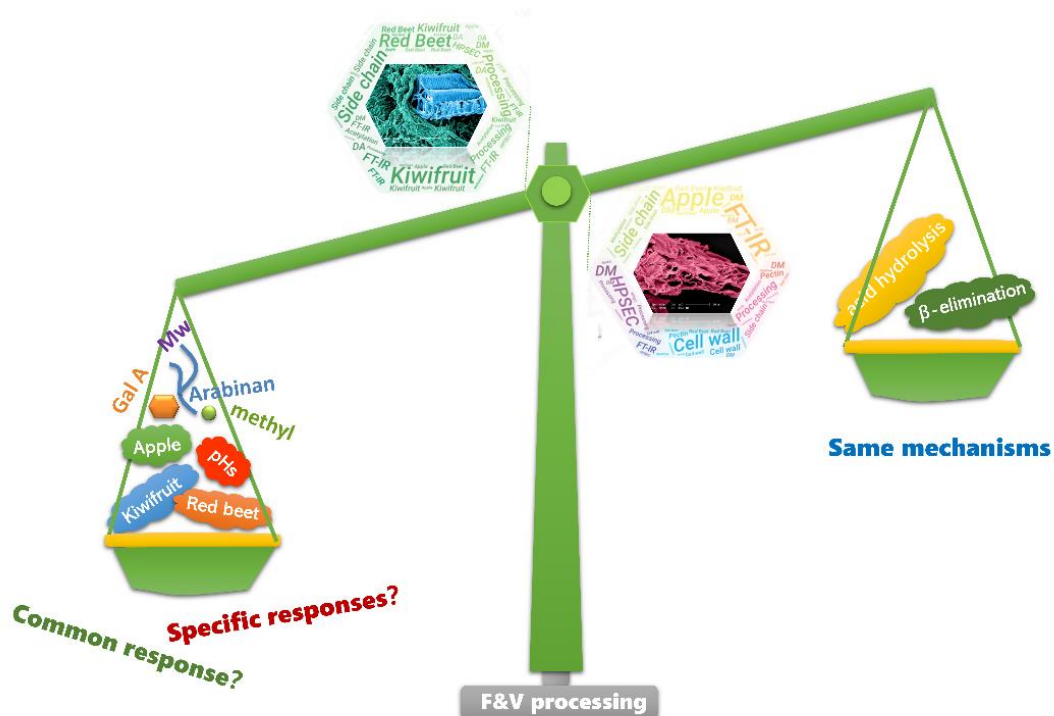
A version of this section has been published as:

Liu, X., Renard, M. G. C. C., Rolland-Sabaté, A., Bureau, S., & Le Bourvellec, C. (2021). Modification of apple, beet and kiwifruit cell walls by boiling in acid conditions: Common and specific responses. *Food Hydrocolloids*, 112, 106266.

This chapter deals with the question of whether common thermal processing or specific cell walls had a higher impact on the cell wall susceptibility to degradation. In this study, the composition of the cell wall polysaccharides from apple, beet and kiwifruit were compared before and after modification by boiling (20 minutes) at different pH values (2.0, 3.5 and 6.0). The common chemical mechanisms (e.g., β -elimination and acid hydrolysis) were also evaluated.

This allowed to answer the following questions:

- ※ How are cell wall's composition and structure modified during processing?
- ※ What are the common and specific responses of the different cell walls?
- ※ Which processing conditions have the least degrading effect on pectins?



Cell wall (CW) degradation causes texture loss of plant-based products after processing. However, these losses differ in intensity, which could be due to cell wall structure or plant tissue internal pH conditions. To distinguish these two factors, CWs isolated from apple, beet and kiwifruit were subjected to boiling at pH 2.0, 3.5 and 6.0. Pectin depolymerization was the least pronounced at pH 3.5, while galacturonic acid contents of all CWs decreased at pH 6.0 due to the β -elimination. Pectins were solubilized, and their size decreased with increased pH during CW treatment. At pH 6.0, degrees of methylation decreased mostly in apple and beet CWs while galactose decreased more in kiwifruit CW. At pH 2.0, arabinan was lost in apple and beet CW due to acid hydrolysis. Apple CW was the most susceptible to degradation either at pH 2.0 or 6.0, while beet CW was more degraded at pH 2.0. In contrast, kiwifruit CW was the least susceptible to degradation whichever the pH. Acid hydrolysis and β -elimination appeared to be common mechanisms that cause loss of neutral sugars, often from pectin side chains, and galacturonic acid, respectively, but their effects were of different intensities. This work has a guiding significance for improving texture in the thermally canning process.

3.1 Modification of apple, beet and kiwifruit cell walls by boiling in acid conditions: Common and specific responses

3.1.1 Introduction

Cell walls and their constituent polysaccharides play an important role in plant-based foods, where they control the texture and its evolution during maturation and processing (Ranganathan, Subramanian, & Shanmugam, 2016). Plant cell walls are a complex, porous, polysaccharidic material composed of cellulose, hemicelluloses and pectins. The relative amounts of these constituents are dependent upon the species and maturity of plant tissue. Plant-based foods are commonly processed, e.g. cooking and canning, before being consumed to improve palatability and for a microbiological stability (M. Li, Ho, Hayes, & Ferruzzi, 2019). The first steps of cell wall modification during processing, which involve the endogenous pectinases and their synergies, have been extensively studied as a function of temperature and pressure (Sila et al., 2009). However, it is difficult to control the action of endogenous enzymes during the first phase of heating. Many articles also describe texture loss of plant tissues after enzyme inactivation or thermal processing, but each concerns a single plant material at its natural pH (from 3.0 – 6.5), such as apple (Le Bourvellec, Watrelot, Ginies, Imberty, & Renard, 2012b), apricot (Ella Missang, Maingonnat, Renard, & Audergon, 2012), pear (Renard, 2005), radish (Ando, Hagiwara, & Nabetani, 2017; X. Li et al., 2019), potato (W. Zhao, Shehzad, Yan, Li, & Wang, 2017) or asparagus (Peng, Song, Zhang, Pan, & Tu, 2019). Different plant sources with their natural pH values may have specific responses to processing, and common responses may occur at distinct extents. However, it is difficult from the existing literature to ascertain whether these different responses are due to the structure of the cell walls or to the conditions during fruit and vegetable (F&V) processing. Notably, the natural internal pH is known to be a major driver for the degradation of polysaccharides, and primarily of pectins. It is therefore important to obtain a clear picture differentiating between the effects of the cell wall structure and the pH conditions during F&V processing.

Non-enzymatic cell wall modifications during processing involve an increased solubilization accompanied by a depolymerization of pectins (Fraeye et al., 2007). Cellulose and hemicelluloses show minimal structural changes compared to pectins, which therefore appear to be a key to texture loss (Houben et al., 2011). Many studies were done using purified pectins heated in model solutions, at different pHs (J. Chen et al., 2015; Diaz, Anthon, & Barrett, 2007; Fraeye et al., 2007), but we did not find any comparable model studies on complex cell wall matrices. Moreover, work on the impact of thermal processing on the cell wall is mainly focused on the entire plant tissue, but confounding parameters such as the cell wall structure and degradation in pH conditions were not controlled (at natural pH) (Renard, 2005; Ella Missang et al., 2012; Zhao et al., 2017; X. Li et al., 2019). The chemical mechanisms vary with pH conditions. β -elimination, which is specific for methoxylated pectins, cleaves the methoxylated homogalacturonan chains creating an unsaturated bond (between C4 and C5 of a methoxylated uronic acid) with absorption at 235 nm (Albersheim, Neukom, & Deuel, 1960). Pectins with a higher degree of methylation (DM) are more sensitive to β -elimination (Fraeye et al., 2007). β -elimination is in competition with saponification of methoxylated galacturonic acids, which is favoured by high pH. As temperature increases, the rate of β -elimination increases faster than that of demethylation, so that heating at a neutral to slightly acidic pH (> 4.5) may lead to an extensive pectin depolymerization. During thermal treatment in acidic conditions (pH < 3.0), acid hydrolysis occurs, leading to a loss of pectin side-chains, starting with arabinans, and a cleavage in the rhamnogalacturonan I regions of pectins, in the order of sensitivity of the glycosidic bonds in a following order: Ara - Ara $>$ Gal - Gal $>$ Rha - GalA $>$ GalA - Rha $>$ GalA - GalA (C.M.G.C. Renard, Crépeau, & Thibault, 1995). In this condition, the rate of hydrolysis of pectins with low DM is faster (Fraeye et al., 2007). The β -elimination reaction and acid hydrolysis may occur simultaneously when the heating is performed at a weakly acidic pH, with the maximal stability of pectins being observed at circa pH 3.5. As the pH increases, the reaction rates of β -elimination increase whereas they decrease for the acid hydrolysis (Fraeye et al., 2007; Smidsrød et al., 1966).

Therefore, in order to avoid confounding factors like action of endogenous enzymes at the beginning of heating, tissue structure and natural pH without control, three pH values (2.0, 3.5 and 6.0) were chosen to explore how the balance between β -elimination and hydrolysis affects pectins within the multi-scale structure of purified cell walls.

Two fruits (apple and kiwifruit) and one vegetable (beet) were chosen because the structure and composition of their cell walls are different (Latorre, de Escalada Plá, Rojas, & Gerschenson, 2013; Le Bourvellec et al., 2011; Redgwell, Melton, & Brasch, 1988), as well as their responses to processing and their internal pH values. Since there is little information about the modification of the kiwifruit cell wall, we separately compared the phenomenon at two maturity stages. To schematize, apple cell walls are rich in highly methylated pectins, beet cell walls are rich in arabinans and pectins of intermediate DM, while kiwifruit cell walls have few pectins with very few side-chains. Apple rapidly loses its texture upon heating (less than 30 min, (Kebe, Renard, El Maâtaoui, Amani, & Maingonnat, 2015)), while beet fails to soften completely after several hours, which may be due to the ferulic acid cross-linking of pectins (Waldron, Ng, Parker, & Parr, 1997). The texture loss of kiwifruit is also limited but with different responses to processing according to ripe and overripe stages, and show extensive swelling after ripening (Redgwell, MacRae, et al., 1997).

Therefore, our aim was to identify whether common chemical mechanisms (β -elimination and acid hydrolysis) or specific cell wall composition and structure had a higher impact on the cell wall susceptibility to degradation. The originality of this study is that purified cell walls from apple, beet and kiwifruit, were first isolated then subjected to boiling (20 min) at pH 2.0, 3.5 and 6.0, allowing an independent variation of cell wall structure and pH. The surface topography of the cell walls was visualized using scanning electron microscopy (SEM). Native and modified cell walls as well as extracted solubilized polysaccharide compositions were analyzed. The extent of degradation of solubilized polysaccharides was studied using HPSEC-MALLS. This work provides some implications for the F&Veg processing, such as fine-tuning of pH conditions that may improve the quality of thermally processed plant-based products.

3.1.2 Materials and methods

3.1.2.1 Standards and Chemicals

Ethanol and acetone were from Fisher Scientific (Strasbourg, France). Acetonitrile of HPLC grade was obtained from VWR International (Radnor, USA). Hexane, methanol, hydrochloric acid and acetic acid were from Merck (Darmstadt, Germany). Sugar standards (arabinose, fucose, galactose, xylose, mannose and rhamnose) and polygalacturonic acid were from Fluka (Buchs, Switzerland). Formic acid, benzyl mercaptan, sodium carbonate, sodium hydroxide, NaBH₄, N-methylimidazole, acetic anhydride, lignin alkali, toluene- α -thiol, (+)-catechin, (-)-epicatechin, inositol and galacturonic acid were provided from Sigma-Aldrich (Saint Quentin Fallavier, France). Methanol-d₃ was from Acros Organics (Geel, Belgium).

3.1.2.2 Plant Material

Apple fruits (*Malus × domestica* Borkh.) from the ‘Golden Delicious’ cultivar, beets (*Beta vulgaris* L.) from the round red beetroot type, and kiwifruits (*Actinidia deliciosa*) from the ‘Hayward Green’ cultivar were purchased at commercial maturity in September 2017 at the supermarket (Auchan, Avignon, France). For kiwifruits, two maturity stages were studied: “Ripe” corresponding to kiwifruits at the date of purchase and “Overripe” (described as “soft under the fingers”) obtained after three weeks at 10 °C followed by one week at room temperature (26 °C). To quantify this evolution, the kiwifruit flesh firmness was measured using a multi-purpose TApplus Texture Analyser (Ametek, Lloyd Instruments Ltd., Fareham, UK). Kiwifruits were peeled in a 10 × 10 mm area on the upside and downside, placed on a stationary steel plate and penetrated to depth of 50 mm with a 12.57 mm² probe at a speed of 5 mm/s. A batch of five fruits was constituted for each maturity stage. Two determinations were conducted on the two opposite sides of each fruit. Clear texture differences were obtained with respectively 1.4 ± 0.41 N (eating-ripe, soft) and 0.6 ± 0.31 N (overripe, very soft). All plant materials were peeled, apples were cored, kiwifruits were cored and deseeded, and cortex tissues were used for the preparation of cell wall materials.

3.1.2.3 Preparation of cell wall

Alcohol-insoluble solids (AIS) were prepared from apple (pH 3.8), beet (pH 5.0) and kiwifruit (pH 3.4 for ripe and 3.3 for overripe) according to the method of Renard (2005). More than 10 batches of 0.5 to 1.0 kg were processed for each plant material, then mixed to obtain an uniform sample. The samples were named as apple native cell wall (ACN), beet native cell wall (BCN), ripe kiwifruit native cell wall (KCRN) and overripe kiwifruit native cell wall (KCON), respectively.

3.1.2.4 Modification of cell walls by boiling at different pH values

The cell walls (25 g/L) were separately incubated in a citrate/phosphate buffer (pH 2.0, 3.5, and 6.0; 0.1 M) in sealed glass bottles in a boiling water bath for 20 min. After treatments, the cell walls and the buffer solution were separated by hot filtration under vacuum in a G0 sintered glass filter. The cell walls were dried by solvent exchange using 96% ethanol (three times) and acetone (three times), then overnight in an oven at 40 °C.

The cell wall samples after boiling at pH 2.0, 3.5, and 6.0 are designated (AC, BC, KCR or KCO) - 2, (AC, BC, KCR or KCO) -3, and (AC, BC, KCR or KCO) - 6, respectively.

The buffer solutions containing solubilized polysaccharides (SP) were dialyzed (a dialysis tube of theoretical porosity of 12 kDa, Sigma Chemical Co., St. Louis, MO, USA) against 0.1 M NaCl during 48 h, and then against water before freeze-dring. SP at pH 2.0, 3.5, and 6.0 are designated (AP, BP, KPR or KPO) - 2, (AP, BP, KPR or KPO) -3, and (AP, BP, KPR or KPO) - 6, respectively (Fig. 3.1).

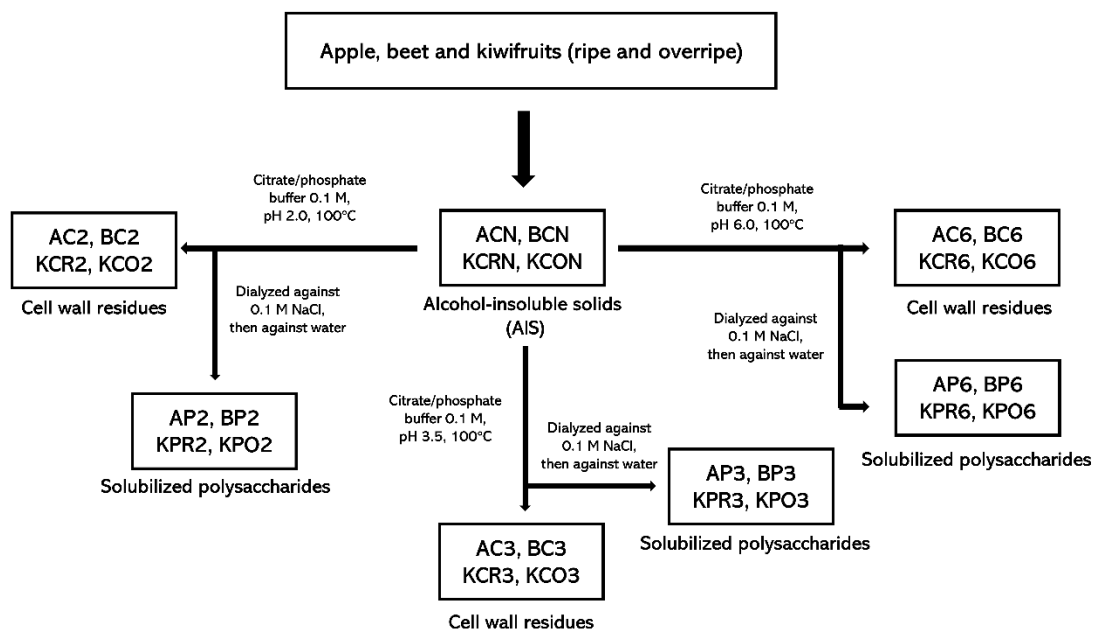


Figure 3.1 Scheme of AISs preparation, cell walls modification and solubilized polysaccharides extraction at three pHs from apple, beet and kiwifruit. Abbreviations: A, Apple; B, Beet; K, Kiwifruit; C, cell walls; P, solubilized polysaccharides; 2, pH 2.0; 3, pH 3.5; 6, pH 6.0; R, Ripe; O, Overripe.

3.1.2.5 Surface morphology analysis by scanning electron microscopy (SEM)

Samples were mounted on SEM specimen stubs with a carbon double-sided, carbon-conductive, adhesive tape prior to coating. Samples were then coated with 20 nm gold layers by ion sputtering using Balzers SCD 004 sputter coater (Balzers, Bal Tec.AG, Furstentum, Lichtenstein) and subsequently photographed using a PhilipsXL30 (FEI/Philips, Eindhoven, The Netherlands) scanning electron microscope operated at an accelerating voltage of 10 kV.

3.1.2.6 ATR-FTIR spectra

The spectral data of cell walls and solubilized polysaccharides were both acquired with a Tensor 27 FTIR spectrometer (Bruker Optics®, Wissembourg, France). Native cell walls and modified cell walls were stored in P₂O₅ atmosphere before analysis to remove residual water. ATR-FTIR spectra were acquired at room temperature on sample powder using a single-reflectance horizontal ATR cell (Golden Gate equipped with a diamond crystal, Bruker Optics) as described by Bureau et al. (2012), by scanning from 4000 to 600 cm⁻¹ and correcting against the background spectrum of air. Each sample was analyzed three times, and each spectrum was an average of 16 scans.

Spectral pre-processing and data treatment using multivariate analyses were performed with Matlab 7.5 (Mathworks Inc. Natick, MA) software using SAISIR package (Cordella & Bertrand, 2014). The spectral data were transformed with baseline correction and standard normal variate (SNV) to correct multiplicative interferences and variations in the baseline shift before any multivariate analysis. A Principal Component Analysis (PCA) was applied using FT-IR spectra in the range between 2000 and 600 cm^{-1} to evaluate the distribution of the different samples (species and pH treatments).

3.1.2.7 High-Performance Size-Exclusion Chromatography Coupled with Multi-Angle Laser Light Scattering (HPSEC-MALLS)

The molar mass distribution of SP was determined using a HPSEC system involving a Ultra Fast Liquid Chromatography Prominence system (Shimadzu, Kyoto, Japan) including a LC-20AD pump, a DGU-20A5 degasser, a SIL-20AHT autosampler, a CTO-20 AC column oven, a SPD-M20A diode array detector and a RID-10A refractive index detector. In addition, a multi-angle laser light scattering (MALLS) detector DAWN HELEOS 8+ (fitted with a K5 flow cell and a GaAs laser at $\lambda = 660$ nm) from Wyatt Technology Corporation (Santa Barbara, CA) was coupled with the HPSEC system. Separations were achieved at 40 °C using three HPSEC columns in series (PolySep-GFC-P3000, P5000 and P6000 300 \times 7.8 mm) and a guard column from Phenomenex (Torrence, CA, USA). 100 μL of SP (2.5 mg/mL) solutions were injected and eluted at 0.6 mL/min using a 0.1 M citrate/phosphate buffer at pH 3.8, previously filtered through a 0.1 μm , OmniporeTM membrane (Millipore, Milford, USA) and degassed. Before injection, SP were solubilized under magnetic stirring in the filtered eluant at 4°C overnight. The solutions were centrifuged 10 min at 8000 g and the supernatant was filtered through a 0.45 μm hydrophilic PTFE syringe filter (Macherey-Nagel, Düren, Germany) before injection. M_i , the molar mass at each slice of the chromatogram, was determined using the concentration and the light scattering signal from 5 angles (from 20.4° to 90°) and data extrapolation to zero angle using the Zimm formalism with a one order polynomial fit (A. Rolland-Sabaté, Colonna, Potocki-

Véronèse, Monsan, & Planchot, 2004). Then, the weight-average (\bar{M}_w) was calculated using the summations taken over the whole peaks using ASTRA® software from Wyatt Technology Corporation (version 7.1.4 for PC) as previously described (A. Rolland-Sabaté et al., 2004). A value of 0.146 mL/g was used as the refractive index increment (dn/dc) for glucans and the normalization of photodiodes was achieved using a low molar mass pullulan standard (P20) from Showa Denko K.K. (Tokyo, Japan).

3.1.2.8 Chemical composition analysis

3.1.2.8.1 Hydrolysis

For cell walls, approximately 10 mg of AIS were prehydrolyzed with 72% sulfuric acid (250 μ L) for 1 h at 26 °C (Saeman, Moore, Mitchell, & Millett, 1954), before dilution to 1 M sulfuric acid by the addition of water and an internal standard (inositol); simple hydrolysis was also carried out to estimate cellulose content by difference. For SP, the sample was directly dissolved in 1 M sulfuric acid with internal standard without prehydrolysis. All samples were hydrolysed at 100 °C for 3 hours.

3.1.2.8.2 Neutral sugar composition

Neutral sugars were analyzed as alditol acetates (Canteri, Renard, Le Bourvellec, & Bureau, 2019; Englyst, Wiggins, & Cummings, 1982). The samples were injected in a GC-FID HP 5890 Series II (Agilent, Inc., Palo Alto, USA) equipped with a capillary column (30 m \times 0.25 mm i.d. coated with DB225 MS, 0.25 μ m film thickness) using: split mode (1:25 ratio); injector temperature 250 °C; hydrogen as carrier gas at 45 cm/s (215 °C); column flow 1.3 mL/min and oven temperature 215 °C (isothermal).

3.1.2.8.3 Galacturonic acid content

Uronic acids were measured by the meta-hydroxyl-diphenyl assay as described by (Blumenkrantz & Asboe-Hansen, 1973; Canteri et al., 2019) after Saeman hydrolysis (§ 2.8.1). The absorbance was read at 520 nm using a spectrophotometer (V-530 Jasco, Tokyo, Japan), and concentrations were calculated against a calibration curve with galacturonic acid as external standard.

3.1.2.8.4 Methanol and degree of methylation

The methanol content was measured by stable isotope dilution assay using headspace-GC-MS (QP2010 Shimadzu, Kyoto, Japan) as described by Renard & Ginies (2009) after saponification. The degree of methylation (DM) was calculated as molar ratio of methanol to galacturonic acid.

3.1.2.8.5 Lignin content

Lignin was measured spectrophotometrically (V-530Jasco, Tokyo, Japan) as described by Metaxas, Syros, Yupsanis, & Economou (2004) with alkali lignin as external standard. Cell wall samples (15 mg) were digested in 1 mL 25 % acetyl bromide in acetic acid containing 2.7% (v/v) perchloric acid and incubated for 30 minutes at 70 °C. The samples were cooled and 10 µL were transferred into a test tube, then 570 µl of 17 % 2N NaOH and 83 % acetic acid were added, followed by 20 µL of 7.5 M hydroxylamine hydrochloride to stop the reaction. The volume was corrected to 2 mL with acetic acid and the absorbance was read at 280 nm using a spectrophotometer V-530 (Jasco, Tokyo, Japan). The amount of lignin was calculated from a linear calibration curve with commercial alkali lignin as standard.

3.1.2.8.6 Procyanidin content

Procyanidins were measured by HPLC-DAD after thioacidolysis as described by Guyot, Marnet, & Drilleau (2001). Their characterization and quantification were performed using an Ultra Fast Liquid Chromatography Prominence system (Shimadzu, Kyoto, Japan) controlled by the LabSolutions software (Version 5.57, Shimadzu, Kyoto, Japan). Separation conditions, identification and quantification were performed as described (Guyot, Marnet, & Drilleau, 2001; Le Bourvellec et al., 2011).

3.1.2.8.7 Acetic acid content

Acetic acid was released by saponification and quantified according to the acetic acid assay kit (K-ACET, ACS Manual Format, Megazyme International, Ireland). Samples (10 mg) were incubated in 5 ml NaOH 0.2 M for 3 h. 2 ml deionized water, 0.1 ml sample, 0.5 ml buffer (30mL, pH 8.4) plus L-malic acid and sodium azide (0.02 % w/v), and 0.2 ml NAD⁺/ATP/PVP/CoA solution were added into cuvettes and mixed.

The absorption was read at 340 nm (A0) after approx. 3 min using a spectrophotometer V-530 (Jasco, Tokyo, Japan). Then the reaction was started by addition of 20 µl L-malate dehydrogenase plus citrate synthase suspension. The absorption was read at 340 nm (A1) after approx. 4 min and the reaction was started again by addition of 20 µl acetyl-coenzyme a synthetase suspension. The reaction mixture was mixed and the absorbance of the solutions (A2) at the end of the reaction (approx. 12 min) was read at 340 nm. The acetic acid content was calculated based on an acetic acid standard curve using *Mega-Calc*TM software tool (Megazyme International, Ireland).

3.1.2.8.8 Ferulic acid content

Ferulic acid was released by saponification according to the method of Micard, Renard, & Thibault (1994). Samples (25 mg) were incubated in 25 mL of 2 M NaOH at room temperature for 1 h under a stream of argon followed by two hours at 35 °C. The extracts were filtered on G1 sintered glass filters, adjusted to pH 2.0 by fuming hydrochloric acid and extracted by ethyl acetate (3 times). The upper organic phases were recovered, dried over anhydrous Na₂SO₄, filtered and evaporated. The dry extracts were taken up in 1 mL of methanol and 20 µL were injected into the HPLC-DAD system (§2.8.5) with detection at 320 nm.

3.1.2.9 Statistical Analysis

Results are presented as mean values of analytical triplicates and the reproducibility of the results is expressed as pooled standard deviations (Pooled SD). Pooled SD were calculated for each series of replicates using the sum of individual variances weighted by the individual degrees of freedom (Box, Hunter, & Hunter, 1978). Analysis of variance (ANOVA) was performed using Excelstat package of Microsoft Excel. Spectral pre-processing and Principal Component Analysis (PCA) were performed using MATLAB 7.5 (Mathworks Inc. Natick, MA) software using the SAISIR package (Cordella & Bertrand, 2014).

3.1.3 Results and discussion

3.1.3.1 Surface morphology of cell walls

Apple, beet and kiwifruit cell wall preparations had thin cell walls and showed a network of empty cells of irregular shape and size (Fig. 3.2). The kiwifruit cell wall preparations exhibited the smallest cavities, non-porous and compact, with a wrinkled appearance comparable to tree cuticles or the surface of mountain heavily eroded by wind and sand. These preparations contained sieve tubes in xylem and phloem tissues and thin rods, probably raphide crystals of calcium oxalate, as described previously in kiwifruit (Redgwell et al., 1988). The surface of the apple cell walls was the flattest and had large empty spaces, followed by beet cell walls. The tissular structure of beets was similar to a honeycomb, with thin interconnected walls, matching earlier studies (Dongowski, 2001).

All treatments, whichever the pH and cell wall, seemed to have similar effects on the surface morphology of cell walls, i.e., all cell walls became more wrinkled and crumpled. The appearance of cell walls treated at pH 3.5 was the most similar to those of the initial cell walls. In apple and beet cell walls treated at pH 6.0, the cell walls became less smooth and some regular patterns were faintly visible, so that a substructure seemed to emerge, probably linked to the organization of the cellulose microfibrils (McCann, Wells, & Roberts, 1990), but the treatment was not sufficient to clearly reveal it. Rougher surfaces were obtained for kiwifruit cell walls, notably after overripening. Another remarkable point was the persistence of calcium oxalate crystals in the kiwifruit cell wall preparations after treatment at pH 3.5. Heating and drying can modify the physical properties of the cell wall material by inducing collapse of β -glucans and pectins (Le Bourvellec & Renard, 2005). However, in the present case, all cell walls were subjected to hydrothermal treatment and gentle drying. Therefore, less modifications were observed, compared with apple cell walls dried in harsh conditions (Le Bourvellec & Renard, 2005).

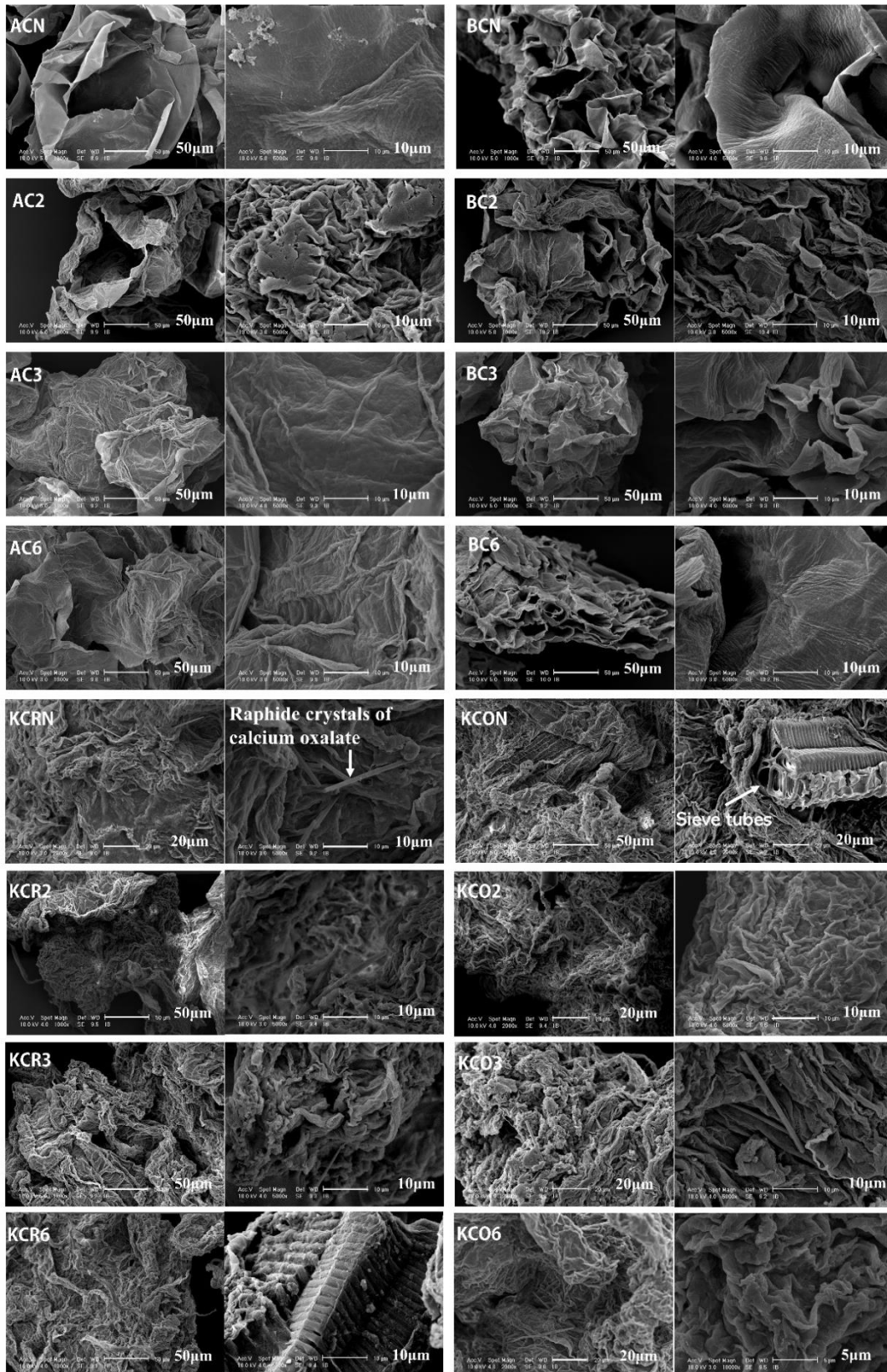


Figure 3.2 Scanning Electron Microscopy showing the differences among native and three pH treatments (2.0, 3.5 and 6.0) after boiling for 20 min in apple, beet and kiwifruit cell walls. Abbreviations: A, Apple; B, Beet; K, Kiwifruit; C, cell walls; P, solubilized polysaccharides; 2, pH 2.0; 3, pH 3.5; 6, pH 6.0; R, Ripe; O, Overripe.

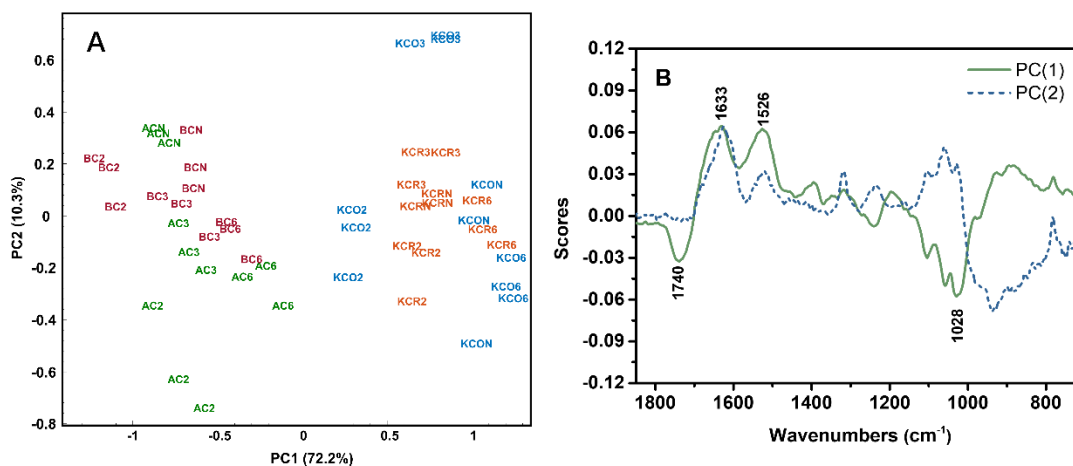


Figure 3.3 Principal component analysis (PCA) of (A) Apple, beet and kiwifruit cell walls using mid-infrared spectral data between 2000 to 600 cm^{-1} and (B) score loadings of PC1 and PC2. Abbreviations: A, Apple; B, Beet; K, Kiwifruit; C, cell walls; 2, pH 2.0; 3, pH 3.5; 6, pH 6.0; R, Ripe; O, Overripe.

3.1.3.2 Characterization of native and modified cell walls after boiling at three different pHs

3.1.3.2.1 Global characterization by FTIR spectra

A principal component analysis (PCA) was carried out using the spectral data (Fig. 3.3) to highlight the distribution of all AIS samples. The first two axes (PC1 and PC2) explained more than 82% of the total variance and allowed the discrimination of the three species, apple, beet and kiwifruit (Fig. 3.3A). Since the composition of apple and beet cell walls are very different (Latorre et al., 2013; Le Bourvellec et al., 2011), one would have expected the samples according to their spectra to be separated on the PC1 x PC2 plane. However, this was not the case, indicating that the complex internal cross-linking type in cell walls may also influence the spectral data and not only chemical composition *per se*. Concerning the treatments (at pH 2.0, 3.5 and 6.0), the samples were also separated in four groups (one for each treatment plus the non treated cell walls) for each species (Fig. 3.3A). PC1 discriminated cell walls at pH 2.0 on the left and pH 6.0 on the right in each species group, highlighting a common impact. Samples treated at pH 3.5 were close to the native cell walls, at least along PC1. The study of eigenvectors (Fig 3.3B) and especially of PC1 showed two negative peaks at 1740 and 1028 cm^{-1} which could be due to galacturonic acid and its ester carbonyl group

absorptions whereas the positive peak at 1633 cm^{-1} could be due to its free carbonyl group (Gnanasambandam, Proctor, 2000; Kohn, 1975; Szymanska-Chargot & Zdunek, 2013). The positive peak at 1526 cm^{-1} , characteristic of kiwifruit cell walls, might be due to lignin (Huck, 2015). PC1 thus differentiated apple and beet cell walls (pectin-rich) from kiwifruit cell walls (pectin-poor), and within each species group common mechanisms, probably also linked to the pectic backbone.

PC2 only expressed 10% of the variability and presented bands linked to galacturonic acid and neutral sugars, but sample discrimination was more variable per species. Two kinds of samples stood out along PC2, namely apple cell walls treated at pH 2.0 (lower) and kiwifruit cell walls treated at pH 3.5 (higher than the initial cell walls). For apple and beet cell walls, all the treatments resulted in a shift in the same direction along PC2, but not for the kiwifruit cell walls. This PC could thus be more related to specific effects.

3.1.3.2.2 Native cell wall yields

The cell walls of the apples, beets and kiwifruits were pure white, reddish gray and light grayish white, respectively. The beet cell wall yields (Table 3.1) were twice those of apple and kiwifruit. The cell wall yields were comparable to, though generally slightly lower than, those reported earlier: for apple 17.2 to 27 mg/g (FW, fresh weight) (Le Bourvellec et al. (2011), 12 cultivars); for beet 30.4 mg/g (Dongowski (2001) and 36 mg/g (FW) (Latorre et al. (2013), after 10 min boiling); for kiwifruit 32.1 mg/g FW with whole, unpeeled kiwifruits (Sauvageau, Hinkley, Carnachan, & Sims, 2010), and 16 mg/g FW with outer parenchyma (Fischer, Wegryzn, Hallett, & Redgwell, 1996).

3.1.3.2.3 Compositions of native and modified cell walls

Native cell wall compositions were in agreement with literature data (Le Bourvellec et al., 2011; Redgwell et al., 1988; Renard & Thibault, 1993). Concerning polysaccharides, the cell walls of all three species were rich in glucose and galacturonic acid (Table 3.1). Glucose was mainly derived from cellulose. Contents of mannose and

galactose were very similar in all cell walls, though differences were still statistically significant. Rhamnose and fucose were minor components (5-16 mg/g CW).

One marked difference between the cell walls was the arabinose content, particularly high in the cell walls from beet, while it was very low in the cell walls of kiwifruit (10 mg/g CW). The pectic substances of apple were more highly methylated (DM 82) than those of beet or kiwifruit, while acetyl groups were higher in beet, giving apparent degrees of acetylation (for pectins) > 100, and higher than reported in beet varieties used for sugar productions (DAc from 66 to 69 %) (Renard & Jarvis, 1999; Renard & Thibault, 1993). It should be mentioned that most cell wall polymers can be acetylated, especially hemicelluloses and pectins (Gille & Pauly, 2012), and that reporting acetylation relative only to galacturonic acid might lead to overestimated degree of acetylation.

Cell walls can contain polyphenols or be contaminated by intracellular polyphenols, and these patterns were different per species. All three native cell walls contained some low amounts of lignin, with higher concentrations in the kiwifruit cell wall. These were the only phenolic compounds detected in the kiwifruit cell wall. Beet cell walls contained ester-bound phenolic acids, primarily ferulic acid (7.0 mg/g CW) lower than reported earlier (13-20 mg/g CW) (Renard & Jarvis, 1999; Renard & Thibault, 1993). Ferulic acid is an intrinsic component of beet cell walls, where it is bound to arabinans and galactan side chains of pectins (Fry, 1986). The native apple cell wall was slightly contaminated by vacuolar procyanidins (0.26 mg/g CW) of high \overline{DP}_n (15). These procyanidins became non detectable in the modified apple cell walls perhaps due to their removal with soluble polysaccharides as procyanidins have a high affinity, among polysaccharides, for pectins (Le Bourvellec et al., 2005). The AIS preparation used here includes a specific step for elimination of this artefact, the efficiency of which was validated.

Cell wall modifications

Table 3.1 Yields (mg/g fresh weight), neutral sugars, galacturonic acid, lignin and ferulic acid compositions (mg/g cell walls) and ANOVA results of the different fruit flesh cell walls before and after modifications by boiling at different pH values.

Sample	pH	Maturity	Yields ^b	Rha	Fuc	Ara	Xyl	Man	Gal	CGlc	NCGlc	Gal A	Ac. A	MeOH	DM (%)	Lig	FA
ACN	Native ^a	Ripe	14.3	14	16	66	65	16	65	286	13	206	21	31	82	26	-
AC2	2.0	Ripe	-	12	14	27	75	19	65	347	5	191	19	30	86	26	-
AC3	3.5	Ripe	-	13	15	57	67	16	63	302	15	140	19	24	89	20	-
AC6	6.0	Ripe	-	12	16	66	74	18	67	332	16	120	18	13	60	18	-
BCN	Native	Ripe	31.4	15	7	178	10	17	52	220	2	225	45	27	65	46	7.0
BC2	2.0	Ripe	-	14	5	111	13	20	57	292	9	205	41	21	58	44	7.7
BC3	3.5	Ripe	-	15	4	174	11	17	54	255	6	153	39	20	72	47	9.6
BC6	6.0	Ripe	-	13	4	189	11	18	54	262	6	141	32	11	42	45	8.8
KCRN	Native	Ripe	13.3	6	5	10	47	23	51	241	21	210	11	26	67	49	-
KCR2	2.0	Ripe	-	4	5	7	63	30	41	334	18	133	12	15	62	55	-
KCR3	3.5	Ripe	-	4	5	9	60	25	43	279	26	98	11	12	70	72	-
KCR6	6.0	Ripe	-	3	4	7	62	29	38	329	24	58	11	7	69	56	-
KCON	Native	Overripe	13.6	4	7	8	52	22	25	223	16	173	11	22	72	26	-
KCO2	2.0	Overripe	-	2	4	5	66	31	24	335	11	73	13	9	58	46	-
KCO3	3.5	Overripe	-	2	4	6	62	30	22	316	17	74	11	9	65	49	-
KCO6	6.0	Overripe	-	2	4	5	60	30	21	332	14	53	11	5	55	37	-
		Pooled SD		0.7	0.8	2.1	2.0	0.9	1.0	13.2	1.0	8.7	0.8	0.4	4.1	3.8	0.2

(Continued)

Table 3.1 (Continues)

Sample	pH	Maturity	Yields ^b	Rha	Fuc	Ara	Xyl	Man	Gal	CGlc	NCGlc	Gal A	Ac. A	MeOH	DM (%)	Lig	FA
ANOVA																	
CW	Species			170***	159***	4401***	898***	674***	401***	79***	241***	38***	1319***	628***	21***	91***	99***
	pH			5**	2	173***	13***	65***	6**	73***	9***	79***	26***	1072***	10***	19***	2
	Species*pH			0.1	1	52***	3**	8***	14***	3*	8***	3*	14***	43***	4*	4**	3*
CW-K	pH			40***	6**	14***	28***	16***	38***	14***	11***	148***	3	603***	2	56***	10**
	Maturity			158***	1	34***	2	3	1284***	0.2	91***	37***	0.3	136***	2	17***	37***
	pH*Maturity			6**	4*	1	1	1	16***	1	2	4*	0.1	7**	2	2	1

Fisher's Value F value, $P \leq 0.05$: *, $P \leq 0.01$: **, $P \leq 0.001$: ***. Pooled SD: pooled standard deviation (degree of freedom: 32 except for ferulic acid, DF = 8). a: Natural pH values, Apple (pH 3.8); beet (pH 5.0); kiwifruit (pH 3.4 for ripe and 3.3 for overripe). b: Yields (mg/g fresh weight). Rha: rhamnose, Fuc: fucose, Ara: arabinose, Xyl: xylose, Man: mannose, Gal: galactose, Glc: glucose, Gal A: galacturonic acid, CGlc: glucose from cellulose, NCGlc: glucose from non-cellulose, Ac.A: acetic acid, MeOH: methanol, DM: degree of methylation, FA: ferulic Acid, Lig: lignin. CW: Apple, beet, kiwifruit cell walls at ripe stage. CW-K: Kiwifruit cell walls at ripe and overripe stages. Abbreviations: A, Apple; B, Beet; K, Kiwifruit; C, cell walls; 2, pH 2.0; 3, pH 3.5; 6, pH 6.0; R, Ripe; O, Overripe.

What about their common and specific responses after modification? For all cell walls, all the treatments led to a marked loss of arabinose and galacturonic acid, and by balance a relative increase in xylose, mannose and cellulose (Table 3.1). Whichever the treatment and the species, xylose and mannose from hemicelluloses and glucose from cellulose were not affected by acid hydrolysis nor β -elimination reactions, so that their contents increased. The rhamnose and galactose contents were stable, so that their losses appeared to be close to the average cell wall loss. Intensity of loss of the different sugars appeared to depend primarily on pH, then on species. The least pronounced pectin depolymerization was observed at pH 3.5, that is, the neutral sugar, galacturonic acid, lignin contents were intermediate between values obtained in pH 2.0 and 6.0. This is a common response for all cell walls. It suggested that the β -elimination reaction and acid hydrolysis occur simultaneously at pH 3.5, but both had a low intensity. This is consistent with Ella Missang et al. (2012) who reported the composition of the cell wall material from cooked apricot at natural pH (c.a. 4.0) for 10 min did not change significantly, compared with the cell wall isolated from fresh apricot fruit. The same result was also observed in the pear cell walls (cooked at 85 °C for 20 min) (Renard, 2005). Therefore, thermal processing at this pH can protect fruits and vegetables by reducing the pectin degradation reaction rates by both β -elimination and hydrolysis.

At pH 2.0, the most marked difference concerned arabinose, while the galacturonic acid was mostly retained, in accordance to the order of sensitivity to hydrolysis of glycosidic linkages. Arabinose is in the furanose form in the cell walls, and bonds involving furanose sugars are particularly susceptible to acid hydrolysis (Fry, 1988). Moreover, significant specific responses were observed in the degree of arabinose loss in different cell walls at this pH. The percentages of arabinose loss for AC2, BC2 and KCR2 were 59 %, 38 % and 30 %, respectively. Therefore, the arabinose in the apple cell walls was the most sensitive to acid hydrolysis. At this pH, the content of ferulic acid in the beet cell walls was also relatively low, which is attributed to the degradation of arabinan side chains. Ferulic acid can participate in intra-/inter- molecular crosslinking with arabinan chains (Morris & Ralet, 2012; Wefers, Gmeiner, Tyl, &

Bunzel, 2015) and limit beet texture loss (Waldron, Ng, et al., 1997). Therefore a more acidic pH, by enhancing arabinan degradation and loss of ferulic cross-links, might favour softening of beets. Li, Liu, Tu, Li, & Yan (2019) also confirmed that the addition of ferulic acid led to better preservation of the cell wall structure of cooked radish. This may be due to ferulic acid reaction with neutral sugar side chains, preventing the leaching of pectins from the cell wall matrix. Compared with the other two pH treatments and untreated cell walls, pH 2.0 processing increased the pectin linearity (GalA/Rha molar ratio) and decreased the RG-I branching ((Ara+Gal)/Rha molar ratio) in all cell walls.

With regard to treatment at pH 6.0, the galacturonic acid content decreased significantly after treatment in all cell walls, especially the kiwifruit cell walls, due to β -elimination. The percentage of galacturonic acid loss for KCR6, AC6 and BC6 was 72 %, 42 % and 37 % in order. The galactose in AC6 and BC6 was not significantly different from the untreated cell walls, while KCR6 lost 25 %. The common response under this condition is that the modified cell walls had the lowest pectin linearity and the highest RG-I content. The cell walls also had significantly lower methanol and slightly lower lignin contents. The acetyl groups of the cell walls were more stable in apple and kiwifruit cell walls than beet cell walls, and also more stable than methyl-esters during the processing (Broxterman, Picouet, & Schols, 2017), probably because some O-acetyl-substituents were carried by other cell wall constituents (Gille & Pauly, 2012). Lower acetic acid content of beet cell walls after treatment at pH 6.0 may be due to the initial presence of acetylated pectins and loss during treatment. Acid hydrolysis and β -elimination appeared to be common mechanisms that cause loss of neutral sugars, often from pectin side chains, and galacturonic acid, respectively, but their effects were of different intensities.

This was confirmed by the ANOVA (Table 3.1): while the species was the most significant factor, pH values and ripeness (for kiwifruit) had also significant effects. Only fucose was not significantly modified by treatment at different pHs, while the effect on galactose and rhamnose was less marked than for all other parameters. The interaction ‘species \times pH’ influenced significantly acetic acid, methanol and neutral

sugars such as arabinose, mannose, galactose and non-cellulosic glucose. This confirmed the existence of common effects on galacturonic acid (and absence of effect on cellulose) and more specific effects on pectic substituents and some neutral sugars.

3.1.3.2.4 Comparison of kiwifruit cell walls at two maturity stage

After harvest, the kiwifruit underwent a marked softening. As is shown in [Table 3.1](#), the neutral sugars, galacturonic acid, acetic acid, methanol and lignin contents were reduced from KCRs to KCOs, and the most relevant differences with maturity concerned rhamnose, arabinose, galactose, glucose and galacturonic acid in accordance with literature data on fruit softening: ripening involves hydrolysis of neutral sugars from pectin side chains, depolymerization and increased solubilization of pectins and hemicelluloses (Brummell, 2006). The degrees of methylation and acetylation of pectins increased, signaling potential preferential degradation of the less methylated and acetylated pectins during overripening. The cell walls of ripe kiwifruit were more sensitive to the treatment at different pHs than that of overripe as the main modifications had occurred during ripening. The interaction ‘pH × maturity’ influenced significantly galactose.

3.1.3.3 Characterization of solubilized polysaccharides

Solubilized polysaccharides represented a minor part of the original cell walls, with recoveries between 9.6 and 22% of the original cell walls, however, they were of interest as indicators of involved mechanisms.

3.1.3.3.1 Composition of the solubilized polysaccharides

Similar to cell walls, solubilized polysaccharides (SP) from different cell walls or after treatment at different pHs also showed both common and specific features. Galacturonic acid was the main component in all SP, which were thus clearly mainly of pectic nature, but significant differences were observed between the various pH treatments and species ([Table 3.2](#)). Beet solubilized polysaccharides (BPs) had the

Table 3.2 Yields (mg/g cell wall), neutral sugars, galacturonic acid and ferulic acid compositions (mg/g solubilized polysaccharide), macromolecular characteristics and ANOVA results of solubilized polysaccharides from the different cell walls before and after modifications by boiling at different pHs.

Sample	pH	Maturity	Yields	Rha	Fuc	Ara	Xyl	Man	Gal	NCGlc	GalA	Ac. A	MeOH	DM (%)	DAc (%)	FA	\bar{M}_w ($\times 10^3$ g·mol ⁻¹)	M_p ($\times 10^3$ g·mol ⁻¹)
AP2	2.0	Ripe	9.6	13	4	89	26	3	55	18	456	17	71	86	17	-	431	541
AP3	3.5	Ripe	16.1	10	6	63	27	3	40	13	419	14	59	77	15	-	149	82
AP6	6.0	Ripe	16.5	14	4	56	16	2	35	10	452	15	78	95	16	-	217	32
BP2	2.0	Ripe	17.3	6	1	187	2	3	27	3	325	47	49	83	67	8.1	147	120
BP3	3.5	Ripe	9.9	6	2	96	1	4	19	4	402	64	66	90	73	4.3	117	112
BP6	6.0	Ripe	15.4	9	3	54	1	4	19	3	491	71	73	81	67	2.2	65	38
KPR2	2.0	Ripe	13.9	7	2	13	10	3	73	51	473	5	65	73	5	-	287	88
KPR3	3.5	Ripe	11.2	8	3	16	6	3	67	19	616	4	89	75	3	-	285	74
KPR6	6.0	Ripe	22.1	11	2	16	6	3	75	20	449	6	67	79	6	-	161	37
KPO2	2.0	Overripe	14.4	4	3	10	12	4	23	34	465	2	72	82	2	-	80	28
KPO3	3.5	Overripe	16.4	7	4	13	12	4	28	28	567	8	89	82	7	-	137	31
KPO6	6.0	Overripe	18.3	9	3	11	9	4	26	15	465	4	72	81	4	-	79	15
		Pooled SD	-	0.6	0.3	2.7	1.5	0.2	1.8	2.1	16.1	1.1	2.2	3.3	1.3	0.1	11.3	6.4

(Continued)

Cell wall modifications

Table 3.2 (Continues)

Sample	pH	Maturity	Yields	Rha	Fuc	Ara	Xyl	Man	Gal	NCGlc	GalA	Ac. A	MeOH	DM (%)	DAc (%)	FA	\bar{M}_w ($\times 10^3$ g·mol ⁻¹)	M_p ($\times 10^3$ g·mol ⁻¹)
ANOVA																		
PC	Species			55***	45***	724***	127***	9**	441***	1229***	43***	3046***	22***	9**	1940***	4128***	394***	1076***
	pH			21***	7**	235***	7**	5*	20***	345***	15***	53***	25***	2	0.4	507***	279***	1994***
	Species*pH			2	6**	132***	4*	5**	7***	215***	30***	62***	36***	4*	4*	507***	123***	1183***
PC-K	pH			56***	56***	47***	87***	15***	4*	39***	28***	0.04	67***	0.312	0.4	-	602***	305***
	Maturity			26***	134***	239***	183***	97***	3447***	3	1	3	7*	5	2	-	90***	65***
	pH*Maturity			3	5*	3	23***	6*	21***	10**	1	6	1	1	8*	-	35***	18***

Fisher's Value F value, $P \leq 0.05$: *, $P \leq 0.01$: **, $P \leq 0.001$: ***. Pooled SD: pooled standard deviation (degree of freedom: 24). PC: Apple, beet, kiwifruit solubilized polysaccharides at ripe stage. PC-K: Kiwifruit solubilized polysaccharides at ripe and overripe stages. Species: Apple, beet and kiwifruit; pH treatments: 2.0, 3.5 and 6.0; Maturity: Ripe and overripe stages. Rha: rhamnose, Fuc: fucose, Ara: arabinose, Xyl: xylose, Man: mannose, Gal: galactose, Glc: glucose, Gal A: galacturonic acid, NCGlc: glucose from non-cellulose, Ac. A: acetic acid, DAc: degree of acetylation, MeOH: methanol, DM: degree of methylation, FA: ferulic Acid. \bar{M}_w : weight average molar mass; M_p : molar mass at the apex of the major peak. Abbreviations: A, Apple; B, Beet; K, Kiwifruit; P, solubilized polysaccharides; 2, pH 2.0; 3, pH 3.5; 6, pH 6.0; R, Ripe; O, Overripe.

highest arabinose content with less xylose, galactose and galacturonic acid than apple and kiwifruit. They were also the richest in glucose and acetic acid. Kiwifruit solubilized polysaccharides (KPs) had the highest galactose and glucose contents, and apple solubilized polysaccharides (APs) the highest rhamnose and xylose contents. For all species, rhamnose content rose with increasing pH of the treatment. For apple and beet cell walls treated at pH 6.0 SP were relatively enriched in galacturonic acid. This could be linked to a larger amount of galacturonic acid solubilized from the cell wall at pH 6.0. In addition, for APs and BPs, more acidic pH led to more extraction of arabinose (Ara) and, for BPs, ferulic acid (FA), with a constant ratio of Ara/FA indicating that there was no specific extraction nor degradation of feruloylated moieties during extraction. In the case of kiwifruit, the highest content of galacturonic acid was at pH 3.5, and there were less differences as a function of pH. The Gal A/(Rha+Ara+Gal) ratio of KPs (from 3.9 to 10.9) was larger than APs (from 2.4 to 3.5) and BPs (from 1.1 to 4.7) indicating KPs were less ramified. The DM showed differences between the various species and pH in [Table 3.2](#). For the ANOVA result of apple, beet, kiwifruit solubilized polysaccharides, arabinose, galactose, glucose, acetic acid and ferulic acids were the most relevant compounds for differentiating pH values ([Table 3.2](#)). The interaction ‘species × pH’ influenced significantly arabinose, acetic acid and methanol.

Less arabinose, galactose and galacturonic acid were solubilized in SP from overripe kiwifruit cell walls, probably due to preliminary degradation of pectins by endogenous enzymes during overripening ([Table 3.2](#)). The most statistically significant differences that distinguished maturity were rhamnose, fucose, arabinose, xylose, mannose and galactose contents. The interaction ‘pH × maturity’ influenced significantly xylose and galactose ([Table 3.2](#)).

3.1.3.3.2 Molar mass distribution of the solubilized polysaccharides

HPSEC-MALLS chromatograms showed generally one main peak at 20-26 mL with shoulders, representing high molar mass polymers, and a peak around 29-30 mL which could be attributed to oligomers ([Fig. 3.4 a, b, e and f](#)). With increasing pH value,

the main peaks of APs, BPs, KPRs and KPOs shifted to higher elution volumes indicating a decrease in hydrodynamic volume, which was generally accompanied by a decrease of the molar mass of the main fraction, M_p (Table 3.2).

APs had higher \bar{M}_w than BPs, KPRs and KPOs especially at pH 2.0 (AP2) (Table 3.2). The difference of molar mass and size between AP2 and AP3 (Table 3.2, Fig. 3.4 a, b, e and f) was much more marked than that of the three series of three pHs for beet and kiwifruit, while all pectins extracted at pH 6.0 were clearly differentiated. Apple cell walls thus appeared to react differently from beet and kiwifruit upon acidic treatment, which was also coherent with the analysis of their infrared spectra (Fig. 3.3).

For AP2 and BP2, there were two distinct populations of SP, one major peaking at 20-22 mL with high molar masses, and a minor population peaking at 27-28 mL corresponding to lower molar masses probably arising acid hydrolysis (Fig. 3.4 a and b). In BP2, these two fractions were also marked by relatively intense UV signals at 235 and 320 nm, which can be attributed to the presence of ferulic acid covalently bounded to SP molecules (Fig. 3.4d). Moreover, the highest UV signals at 235 and 320 nm were found for low molar mass fractions of BP extracted at pH 2.0 (Fig. 3.4d), mainly produced by acid hydrolysis. As ferulic acid is known to link preferentially to arabinose side chains of pectins, this may indicate that this low molar mass fraction is richer in arabinans. The higher extraction of Ara observed at pH 2.0 for BP and AP might then be due to higher hydrolysis of arabinan during acid extraction in line with the higher sensitivity of Ara-Ara linkages to acid hydrolysis (Renard et al., 1995).

KPs chromatograms exhibited one main peak with a shoulder at a lower elution volume (24 mL) than APs and BPs, i.e., lower sized SP, but no peak at 27-28 mL, even for KPR2. Moreover, even if the shoulder in the main peak diminished when pH increased, the molar mass observed for KPR2 and KPR3 were not significantly different (Table 3.2), this indicates that very low acid hydrolysis occurred during extraction at pH 2.0, probably because KPs contain fewer neutral sugars (Table 3.2). AP2, BP2 and KPR2 exhibited a higher \bar{M}_w than their homologs extracted at higher pHs (Table 3.2),

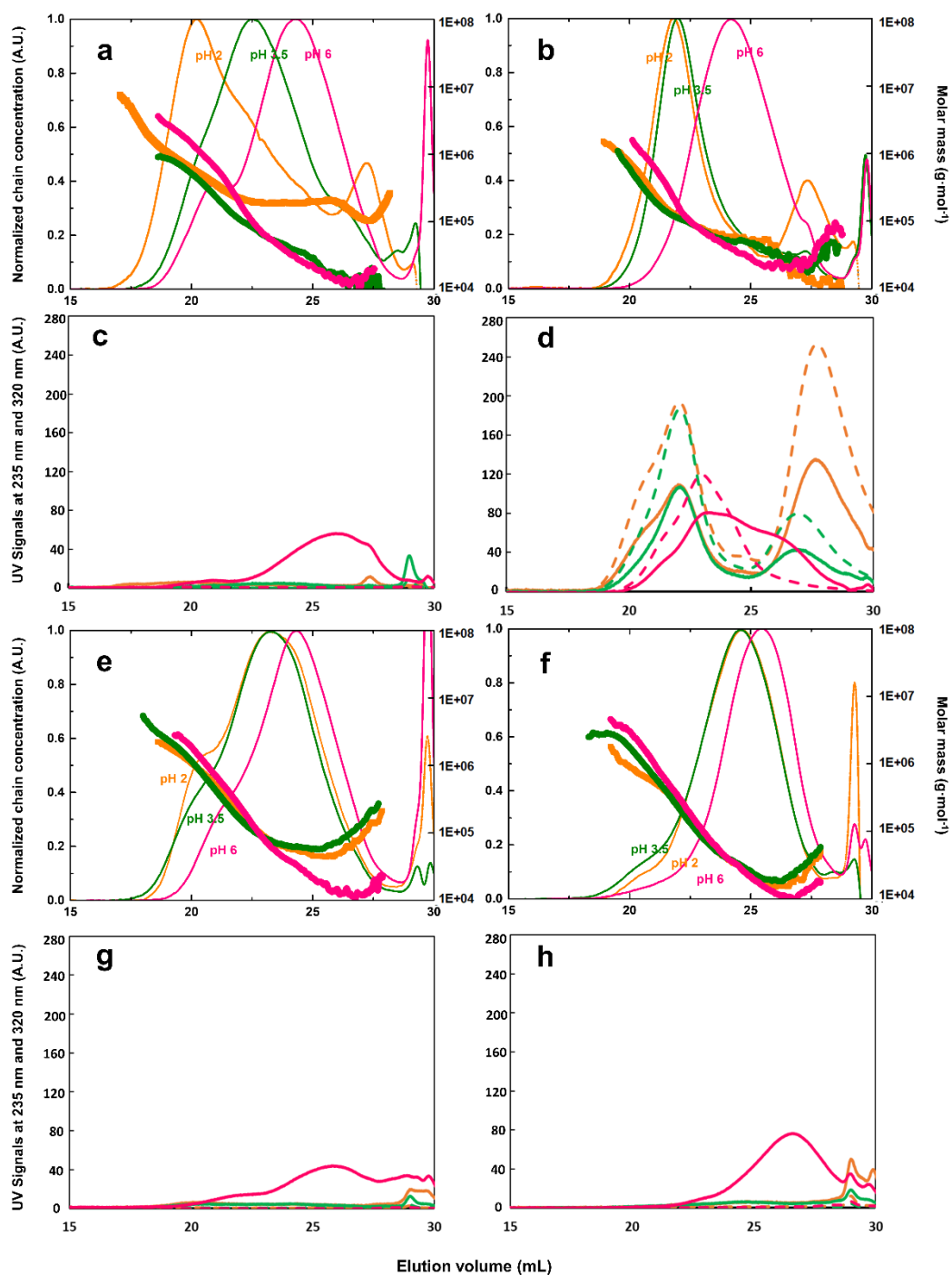


Figure 3.4 HPSEC-MALLS chromatograms (RID and DAD signals) and molar mass vs elution volume of the solubilized polysaccharides samples. a, c: Apple; b, d: Beet; e, g: Kiwifruit at ripe stage; f, h: Kiwifruit at overripe stage. a, b, e and f: — pH 2.0; — pH 3.5; — pH 6.0 represent normalized chain concentration and — pH 2.0; — pH 3.5; — pH 6.0 represent molar mass. c, d, g and h: — pH 2.0; — pH 3.5; — pH 6.0 represent UV signal at 235 nm and - - - pH 2.0; - - - pH 3.5; - - - pH 6.0 represent the UV signal at 320 nm.

which suggested that larger SP were extracted at pH 2.0 even if a small amount of hydrolysis was observed as well. Interestingly, the specific extraction of high molar mass pectins from apple cell walls might explain the preferential industrial use of apples for pectin extraction, and imply the existence of specific, acid-labile bonds retaining pectins in apple cell walls.

After extraction at pH 6.0, all SP absorbed at 235 nm indicating β -elimination. APs size and molar mass distributions were broader and tighter for the others (Fig. 3.4 a, b, e and f). This suggests that apple SP were the most sensitive to pH treatment. This may be attributed to the origin of the cell walls, i.e., to the intrinsic 3D cell wall network and especially to the intermolecular interactions of the wall polysaccharides. In particular, the pectin populations in the cell walls can interact with cellulose or hemicelluloses, with variation between different species (Broxterman & Schols, 2018). These more or less strong interactions between the polysaccharides of the cell wall drive the response to the different pH extraction conditions. For KPs in particular, when treatment pH increased the shoulder observed at 20 mL generally decreased. These results are in agreement with previous observations on SP extraction by heating at pH 6.0 which showed that the extraction led to one pectic fraction for beet and two pectic fractions for apple: one of high hydrodynamic volume, rich in neutral sugars, and one of low hydrodynamic volume rich in galacturonic acid (Renard & Thibault, 1993). The main fraction of AP6 peaking at 3.2×10^4 g/mol might then be enriched in galacturonic acid. In addition to the molar mass decrease, a signal at 235 nm was obvious in the middle molecular size part of the chromatograms (elution volume around 24-27 mL) for all the SP extracted at pH 6.0 (Fig. 3.4 c, d, g and h), indicating the presence of unsaturated double bonds such as produced by β -elimination. As for APs, KPRs and KPOs extracted at pH 2.0 and pH 3.5 absorbances at 235 nm were quite minors, this confirmed that the degradation of pectic fractions mainly occurred through β -elimination at pH 6.0 for APs, KPRs and KPOs. Nevertheless, for BPs UV signals at 235 nm were present for all pHs: at pH 2.0 and 3.5 they closely followed those at 320 nm, suggesting minor absorption from ferulic acid. At pH 6.0 however, the two bands were not superimposable, with a

shoulder at higher elution volumes for the signal at 235 nm, closely following the RI signal and again suggesting extraction of homogalacturonan-rich pectins after β -elimination.

All SP from overripe kiwifruit were markedly smaller than their analogs from ripe kiwifruit (\bar{M}_w of 6.4×10^4 g/mol and 1.53×10^5 g/mol for KPO6 and KPR6 respectively, [Table 3.2](#)) confirming SP degradation during maturation as a result of endogenous enzymic process (Matsumoto, Obara, & Luh, 1983). Nevertheless, the variation of molar mass observed between the extraction at different pHs occurred in the same proportions for KPs ([Table 3.2](#)) whatever their maturity.

3.1.4 Conclusions

We explored the interactions between cell wall structures, proxied by plant origin, and pH in a model system miming F&V processing. Cell wall modifications and polysaccharide solubilization occurring in commonly used fruits (apple and kiwifruit) and vegetable (beet) revealed some common features but also some striking differences for the same pH. In all cases, pectins were clearly the polysaccharides the most impacted, highlighted either from sugar loss in the modified cell walls or the composition of the solubilized polysaccharides. The acid treatment at pH 2.0 removed the arabinan side chains but the solubilized polysaccharides had a higher hydrodynamic volume, especially in apple. Galactose in kiwifruit cell walls was the most sensitive to boiling treatment, especially at pH 6.0. The main skeleton of pectins was significantly degraded after treatments at pH 6.0 by β -elimination reaction, leading to a higher extraction of smaller molecules, especially from kiwifruit cell walls. Under this condition, the molar mass of solubilized polysaccharides with more unsaturated double bonds was the smallest. The effectiveness of the pH treatments on different fruits and vegetables was different, and this was particularly marked for apple.

This study improved the understanding of structure/processing relationships and pointed out important differences concerning the behavior of individual species. This aspect means that each fruit or vegetable species should be regarded to have putatively

some specificities in relation to their modified cell walls. The knowledge of such specificities in different natural sources can improve the quality of canned fruit and vegetable processing and open up prospects for their fine-tuning of functional characteristics.

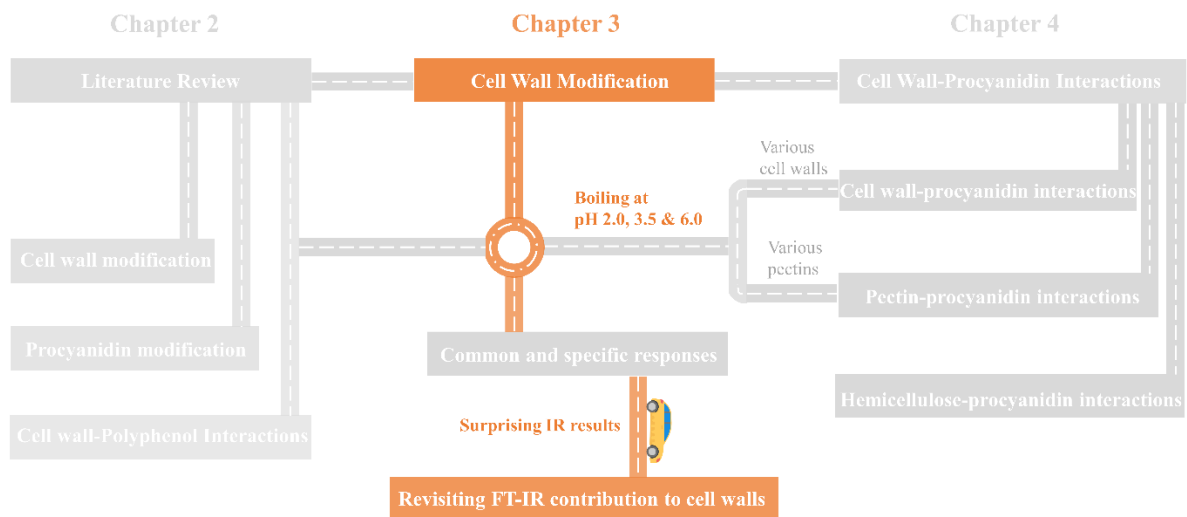
Highlights

- All tested cell walls were susceptible to β -elimination.
- The arabinans of apple and beet cell walls were susceptible to acid hydrolysis.
- Treatment at pH 6.0 led to a decrease in galactose in kiwifruit cell wall.
- Boiling at pH 3.5 involved less pectin depolymerization in cell walls.
- Apple pectins were the most sensitive to pH treatment.

However, the FTIR results were puzzling: apple and beet cell walls were not separated very well by ATR-FTIR, hence we added a methodology study (§ 3.2), not initially planned.

Section 3.2

Revisiting the contribution of ATR-FTIR spectroscopy to characterize plant cell wall polysaccharides



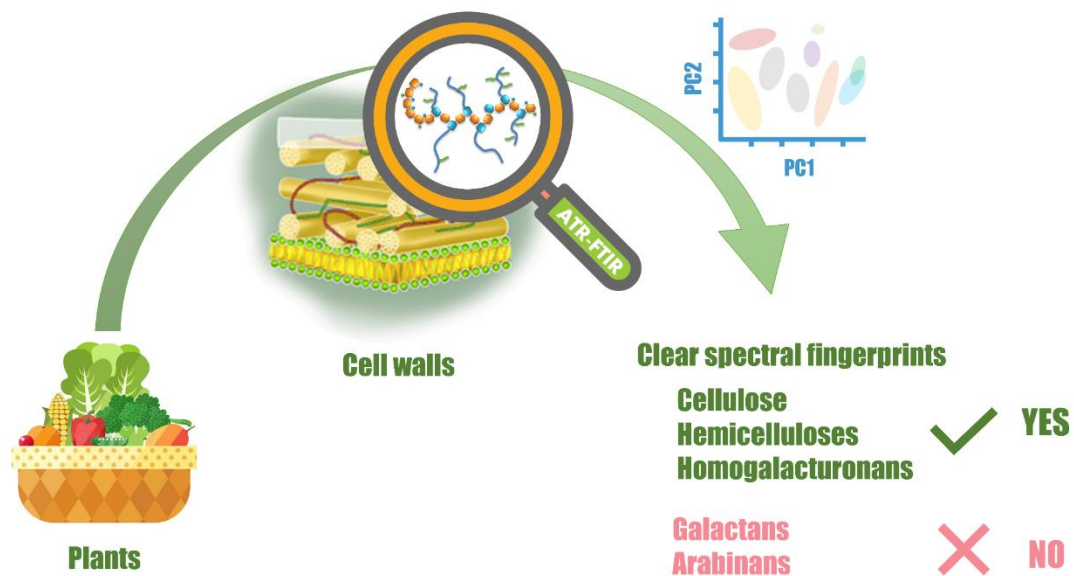
A version of this section has been published as:

Liu, X., Renard, M. G. C. C., Bureau, S., & Le Bourvellec, C. (2021). Revisiting the contribution of ATR-FTIR spectroscopy to characterize plant cell wall polysaccharides. *Carbohydrate Polymers*, 262, 117935.

This section deals with the question of the ATR-FTIR response for the different cell wall polysaccharides. The compositions of 58 cell walls and cell wall polysaccharides from extracted and commercial origin were determined in this study by both, the classical methods and ATR-FTIR spectroscopy. To identify the typology of the cell walls spectral data, both Principal Component Analysis (PCA) and Hierarchical Cluster Analysis (HCA) were performed.

This allowed to answer the following questions:

- ※ Which cell wall polysaccharides can be distinguished by ATR-FTIR?
- ※ What are the limitations of the application of ATR-FTIR on cell wall polysaccharides?



The contribution of ATR-FTIR spectroscopy to study cell wall polysaccharides (CWPs) was carefully investigated. The region 1800-800 cm^{-1} was exploited using principal component analysis and hierarchical clustering on a large range of different powders of CWPs based on their precise chemical characterization. Relevant wavenumbers were highlighted for each CWP: 1035 cm^{-1} was attributed to xylose-containing hemicelluloses, 1065 and 807 cm^{-1} to mannose-containing hemicelluloses, 988 cm^{-1} to cellulose, 1740 and 1600 cm^{-1} to homogalacturonans according to the degree of methylation. Some band positions were affected by macromolecular arrangements (especially hemicellulose-cellulose interactions). However, as arabinan and galactan did not reveal distinctive absorption bands, ATR-FTIR spectroscopy did not allow the discrimination of cell walls differing by the abundance of these polysaccharides, e.g., those extracted from apple and beet. Therefore, the application of ATR-FTIR could remain sometimes limited due to the complexity of overlapping spectra bands and vibrational coupling from the large diversity of CWP chemical bonds.

3.2 Revisiting the contribution of ATR-FTIR spectroscopy to characterize plant cell wall polysaccharides

3.2.1 Introduction

Plant cell walls of the primary walls of dicots and non-grass monocots are dynamic and ordered networks of natural carbohydrate polymers, constituted by an amorphous matrix mainly composed of pectins embedded in a network of cellulose and hemicelluloses, as well as minor amounts of structural glycoproteins, phenolic compounds and enzymes (Carpita et al., 1979). Cell walls are highly variable according to species, developmental and maturity stages, plant organs and environmental conditions (Anderson & Kieber, 2020; Burton et al., 2010). Therefore, this makes it difficult to easily identify and quantify cell wall components.

In general, the structure and composition of plant cell walls are characterized after sample extraction, pretreatment (e.g., acid hydrolysis) and diverse specific biochemical analyses (e.g., chromatography, mass spectrometry, spectrophotometry), which are expensive and time-consuming. An advanced tool based on mid-infrared spectroscopy would provide the advantages of rapid and easy analysis of the prepared samples. Attenuated Total Reflectance Fourier Transform Infrared Spectroscopy (ATR-FTIR) has been increasingly used for the rapid characterization of cell walls of fruits and vegetables (Chylinska, Szymanska-Chargot, & Zdunek, 2016; Coimbra, Barros, Barros, Rutledge, & Delgadillo, 1998; Coimbra, Barros, Rutledge, & Delgadillo, 1999; D. Ferreira, Barros, Coimbra, & Delgadillo, 2001; Kacurakova, Capek, Sasinkova, Wellner, & Ebringerova, 2000; Szymanska-Chargot, Chylinska, Kruk, & Zdunek, 2015). Especially in recent years, it has become a powerful research technology to clarify the composition of dry carbohydrate samples (Canteri et al., 2019). This method appears really convenient insofar as it avoids undesirable structural changes that may occur during sample analysis, e.g., extraction and preparation. Moreover, ATR-FTIR can detect changes in the fruit and vegetables during processing at the cell wall level (Lan, Renard, Jaillais, Leca, & Bureau, 2020).

The identification of cell wall polysaccharides by infrared spectroscopy is generally carried out on the different polysaccharide fractions obtained by sequential extractions (the extraction of pure polysaccharides is imperfect), followed by ethanol precipitation and anion exchange chromatography. These extracted polysaccharides are then characterized using chemical and biochemical methods (Brahem, Renard, et al., 2017; Coimbra et al., 1999; Renard, 2005b; Szymanska-Chargot et al., 2015; Szymanska-Chargot & Zdunek, 2013). However, these studies do not use purified polysaccharides to confirm the absorption bands identified by comparison with the literature. Moreover, some studies have also performed polysaccharide analysis using spectral data but obtained from KBr pellets or aqueous solutions, the classical way before the development of the ATR method (Kacurakova et al., 2000). Fruits and vegetables are highly hydrated and susceptible to environmental conditions. Drying, not only prevents samples from oxidation and hydrolysis under the action of endogenous enzymes, but also concentrates samples by water elimination, so it significantly improves the reflectance spectra of some specific components present in lower content than water (Lan et al., 2020). Therefore, the systematic analysis of purified solid materials from cell wall polysaccharides by ATR-FTIR may improve their identification.

Moreover, some challenges exist due to the ATR-FTIR response of the different cell wall polysaccharides. For example, according to our previous research, in spite of very different structures and compositions, apple and beet cell walls were poorly discriminated by Principal Component Analysis (PCA) based on ATR-FTIR spectra (X. Liu, Renard, Rolland-Sabaté, Bureau, & Le Bourvellec, 2021). Therefore, we need to reconsider these results, knowing that the interactions between the internal components of the cell walls (Le Bourvellec & Renard, 2012a; X. Liu et al., 2020) may affect the absorption of these very complex mixtures. This study combined ATR-FTIR and stoichiometry to characterize the abundance and composition of cell wall polysaccharides, taking into account the heterogeneity and interactions between different cell wall components. To track the characteristic peaks of each cell wall

component, spectral data and conventional chemical methods are used to study the composition of cell walls and internal structures. In order to evaluate the available information based on extracted samples, powders of cellulose, hemicelluloses, and pectins were also scanned in ATR-FTIR. To identify the typology of the cell walls, both PCA and Hierarchical Cluster Analysis (HCA) were performed. This study provided new explanations and experimental ideas for studying complex natural polymer systems, and guidance for using ATR-FTIR data to clarify carbohydrate structures, physical properties and interactions.

3.2.2 Materials and methods

3.2.2.1 Monosaccharide and polysaccharide samples

Monosaccharides (D-(+)-Arabinose, D-(–)-Fucose, D-(+)-Xylose, D-(+)-Mannose, L-Rhamnose, D-(+)-Glucose, and D-(+)-galactose) and D-(+)-Galacturonic acid monohydrate were obtained from Fluka (Buchs, Switzerland). Arabinan (sugar beet), linear 1,5- α -L-arabinan (sugar beet), debranched arabinan, galactan (potato), rhamnogalacturonan I (from potato pectic fibre), and rhamnogalacturonan (from soybean pectic fibre), xylan, arabinoxylan, glucomannan, and xyloglucan were provided from Megazyme (Bray, Ireland). Commercial apple and citrus peel pectins (degrees of methylation ~75%), microcrystalline cellulose and poly-galacturonic acid were provided by Sigma-Aldrich (Deisenhofen, Germany). Homogalacturonan DM 70 was supplied by Watrelot et al. (2013). The common names of cell wall components and their abbreviations used in this study are presented in [Table 3.3](#).

Native and modified cell walls and pectins from apple, beet and kiwifruit were supplied and characterized by Liu et al. (2021). The native cell wall samples were named as apple cell wall (ACN), beet cell wall (BCN), ripe kiwifruit cell wall (KCRN) and overripe kiwifruit cell wall (KCON), and samples after boiling at pH 2.0, 3.5, and 6.0 are designated (AC, BC, KCR or KCO) - 2, (AC, BC, KCR or KCO) - 3, and (AC, BC, KCR or KCO) - 6, respectively. Extracted pectins at pH 2.0, 3.5 and 6.0 from apple, beet and two kiwifruit cell walls at pH 2.0, 3.5, and 6.0 are designated (AP, BP, KPR or

KPO) - 2, (AP, BP, KPR or KPO) - 3, and (AP, BP, KPR or KPO) - 6, respectively.

3.2.2.2. Characterization of carbohydrate composition

Sugar analysis was performed as previously described by Liu et al. (2021). For neutral sugars analysis, 10 mg of cell walls or cellulose were submitted to a Saeman acid hydrolysis (Saeman et al., 1954) and then to simple hydrolysis (dissolved in 1 M sulfuric acid) whereas soluble polysaccharides (10 mg) were only submitted to simple hydrolysis. The derivatization to alditol acetates (Englyst et al., 1982) allows the detection of sugars by gas chromatography with a flame ionization detector (Agilent, Inc., Palo Alto, USA). Galacturonic acid was measured by a meta-hydroxyl-diphenyl assay (Blumenkrantz & Asboe-Hansen, 1973). The methanol was measured by a stable isotope dilution assay using headspace-GC-MS (QP2010 Shimadzu Kyoto, Japan) as described by Renard & Ginies (2009). The degree of methylation (DM) was then calculated as the molar ratio of methanol to galacturonic acid.

3.2.2.3 ATR-FTIR spectra

All cell wall polysaccharide samples, in the form of dry powder, were stored in P₂O₅ atmosphere before analysis to remove residual water. ATR-FTIR spectra data (4000 to 600 cm⁻¹) were acquired at room temperature in a Tensor 27 FTIR spectrometer (Bruker Optics®, Wissembourg, France), using a single-reflectance horizontal ATR cell (Golden Gate with a diamond crystal, Bruker Optics®) equipped with a system to press the dried homogenized samples on the crystal surface (Bureau et al. 2012). Each sample was analyzed three times (using after homogenization three different aliquots of the powders) to consider its heterogeneity, and each spectrum was the average of 16 scans. Spectral pre-processing and data treatment using multivariate analyses were performed with MATLAB 7.5 (Mathworks Inc. Natick, MA) software using the SAISIR package (Cordella & Bertrand, 2014). The spectral data were pretreated with baseline correction and standard normal variate (SNV) to correct multiplicative interferences and variations in baseline shift before any multivariate analysis.

Table 3.3 The common names of cell wall components, their abbreviations and their ATR-FTIR frequencies (cm^{-1}) determined with our spectrometer of the studied plant cell wall polysaccharides.

	Sample names	Abbreviations	Linkable peaks or regions (cm^{-1})
Monosaccharides	D(-)-Arabinose	Ara	1312, 1128s, 1088s, <u>1050vs</u> , <u>991vs</u> , 940, 890s, 841s
	D(+)-Xylose	Xyl	1146, 1123s, <u>1034vs</u> , 1016s, 930s, 902s
	D(+)-Mannose	Man	1110s, 1064s, <u>1034vs</u> , <u>1016vs</u> , 966s, 949s, 912, 879
	D(+)-Galactose	Gal	1154s, 1142, 1100s, <u>1056vs</u> , <u>1039vs</u> , 990, 971, 953s, 827s
	L-Rhamnose	Rha	1375, 1290, 1226, 1145, 1116s, 1074s, <u>1026vs</u> , 976s, 907, 874, 827s
	D(+)-Glucose	Glc	1228, 1206, 1150s, 1100s, 1052s, <u>1016vs</u> , <u>991vs</u> , 912s, 840s
	D(-)-Fucose	Fuc	1334s, 1140s, 1095s, <u>1083vs</u> , <u>1050vs</u> , <u>976vs</u> , 921, 868, 814
	D(+)-Galacturonic acid monohydrate	Gal A	1756s, 1708s, 1275, 1218, 1155, <u>1095vs</u> , <u>1062vs</u> , <u>1025vs</u> , 823s
β-glucans	Microcrystalline cellulose	MCCE	1640, 1428, 1367, 1320, 1308, 1200, 1160, 1052s, <u>1030vs</u> , 988s, 893
	Yeast β -glucan	YGLU	1640, 1428, 1367, 1308, 1200, 1160, 1068s, <u>1030vs</u> , 988s, 886
	Curdlan (1,3- β -o-glucan)	CGLU	1640, 1428, 1367, 1308, 1200, 1160, 1068s, <u>1030vs</u> , 988s, 886
Hemicelluloses	Rye Arabinoxylan (59% xylose)	ARHV	1164, <u>1035vs</u> , 983s, 890
	Wheat Arabinoxylan (64% xylose)	AXMB	1164, <u>1035vs</u> , 983s, 890
	Wheat Arabinoxylan (77% xylose)	AXLB	1164, <u>1035vs</u> , 983s, 890
	Xylan (Beechwood)	XYBW	1164, <u>1035vs</u> , 983s, 890
	1,4- β -D-Mannan	MANB	1367, <u>1065vs</u> , 1035s, <u>1013vs</u> , 938s, 890, 870s, 807s
	Galactomannan (Carob)	GAMA	<u>1065vs</u> , <u>1027vs</u> , 870s, 807s
	Xyloglucan (from tamarind seed)	XYGT	<u>(1040-1010)vs</u> , 939, 890
	Xyloglucan Oligosaccharides	XYGO	<u>(1040-1010)vs</u> , 939, 890
	Xyloglucan (Hepta-, +Octa-, +Nona-saccharides)	XYGH	<u>(1040-1010)vs</u> , 939, 890
Pectins	Citrus peel pectin	CPPC	1740s, 1600, 1440, 1230, 1141, 1097s, <u>1014vs</u> , 954, 914, 831

(Continued)

Application of ATR-FTIR to cell wall polysaccharides

Table 3.3 (Continues)

Sample names	Abbreviations	Linkable peaks or regions (cm ⁻¹)
Commercial apple pectin	APPC	1740 _s , 1600, 1440, 1230, 1141, 1097 _s , <u>1014_{vs}</u> , 954, 914, 831
Arabinan (sugar beet)	ARSB	1600, the region of (1100 - 950)
Linear 1,5- α -L-arabinan (sugar beet)	LNAR	1208, 1115, 1086 _s , 1071 _s , <u>1043_{vs}</u> , <u>1022_{vs}</u> , <u>1004_{vs}</u> , <u>982_{vs}</u> , 948 _s
Debranched arabinan (sugar beet)	DBAR	1600, 1208, 1115, 1086 _s , 1071 _s , <u>1043_{vs}</u> , <u>1022_{vs}</u> , <u>1004_{vs}</u> , 982 _{vs} , 948 _s
Galactan (Potato)	GTAN	1600, 1405, <u>1039_{vs}</u> , 884 _s
Rhamnogalacturonan I (from potato pectic fibre)	RGPP	1740, 1600 _s , 1410, 1238, 1141 _s , 1097 _s , 1074 _s , <u>1014_{vs}</u> , 954
Rhamnogalacturonan (from soybean pectic fibre)	RGSP	1600 _s , 1410, 1141 _s , 1097 _s , 1074 _s , <u>1014_{vs}</u> , 954
Homogalacturonan DM 70	HGTN	<u>1740_{vs}</u> , 1440, 1230, 1140, 1097 _s , <u>1014_{vs}</u> , 970 _s , 914
Poly-galacturonic acid	GALN	1590 _s , 1410 _s , 1330, 1141 _s , 1097 _s , <u>1014_{vs}</u> , 954 _s

* IR band intensity: *vs*, very strong; *s*, strong.

3.2.2.4 Statistical analysis

All biochemical analyses were presented as mean values of analytical triplicates and the reproducibility of the results was expressed as pooled standard deviations (Pooled SD). Pooled SD was calculated per series of replicates using the sum of individual variances weighted by the individual degrees of freedom (Box, Hunter, & Hunter, 1978). A PCA was applied on the ATR-FTIR spectra in the range between 1800 and 800 cm^{-1} in order to study the repartition of the cellulose, hemicelluloses and pectins in a space according to their composition and absorption bands. Spectral data pre-processing and PCA were performed using MATLAB 7.5 (Mathworks Inc. Natick, MA) software using the SAISIR package (Cordella & Bertrand, 2014). HCA was performed using R software using FactoMineR (for computing) and factoextra (for visualizing the results) (R Core Team., 2014).

3.2.3 Results and discussion

3.2.3.1 Characteristic bands of cell wall polysaccharides in the ATR-FTIR spectra

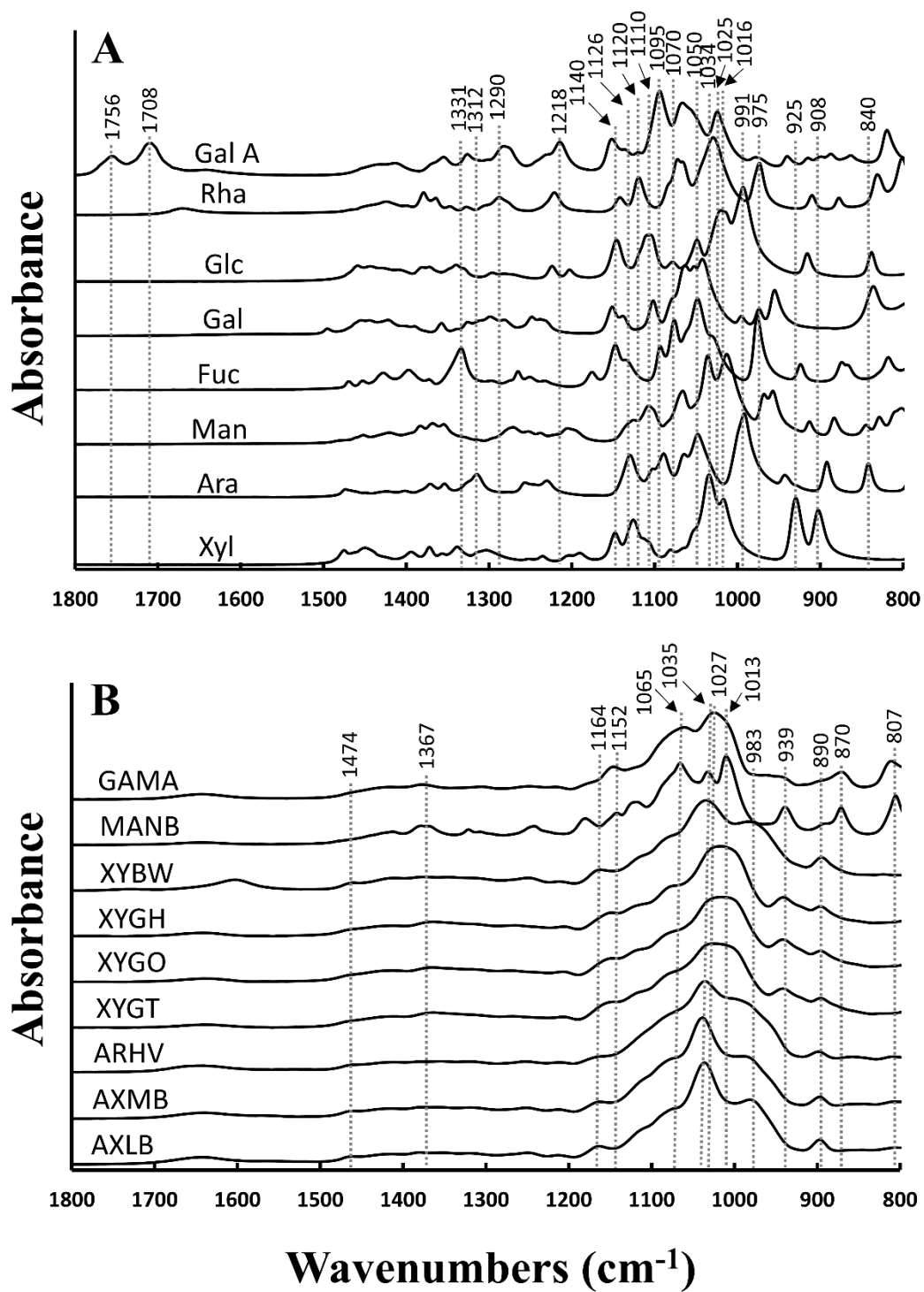
The compositions of the 58 cell wall polysaccharides from extracted and commercial origin were determined in this study by both, the classical methods (Table 3.4, see Liu et al., 2021 for cell walls and extracted pectins) and ATR-FTIR spectroscopy (Table 3.3, Fig. 3.5). Detailed peak positions and assignments of each pure cell wall polysaccharide were limited to the specific bands in the range of 1800-800 cm^{-1} (detected in solid or liquid form) in agreement with the previous works (Canteri et al., 2019; Coimbra et al., 1998, 1999; Ferreira et al., 2001; Filippov & Kohn, 1975; Gnanasambandam, Proctor, 2000; Kacurakova et al., 2000; Kyomugasho, Christiaens, Shpigelman, Van Loey, & Hendrickx, 2015; McCann, Hammouri, Wilson, Belton, & Roberts, 1992; Monsoor, Kalapathy, & Proctor, 2001; Szymanska-Chargot et al., 2015; Szymanska-Chargot & Zdunek, 2013) and summarized in Table 3.4 Strong absorption bands in this region corresponding to the specific wavenumbers assigned to pectins (e.g., rhamnogalacturonan and homogalacturonan), hemicelluloses (e.g., xyloglucan, mannan, galactomannan, arabinoxylan and xylan) and cellulose (Fig. 3.5), are detailed below.

Application of ATR-FTIR to cell wall polysaccharides

Table 3.4 Composition of extracted cell walls and pectins from fruits and vegetables and commercial purified cellulose, hemicelluloses and pectin components (mg/g dry weight, except for degree of methylation expressed in %).

Codes	Rha	Fuc	Ara	Xyl	Man	Gal	Glc	Gal A	MeOH	DM
β-glucans										
MCCE	3	0	0	17	13	0	861	-	-	-
CGLU	0	0	0	0	0	0	705	-	-	-
YGLU	0	0	0	10	6	0	650	-	-	-
Hemicelluloses										
GAMA	0	0	5	0	776	190	7	-	-	-
ARHV	0	0	321	486	0	17	0	-	-	-
AXMB	1	0	288	693	0	7	5	-	-	-
AXLB	1	0	209	733	0	6	5	-	-	-
XYBW	12	0	6	716	0	10	8	-	-	-
MANB	0	0	0	0	960	18	8	-	-	-
XYGT	1	0	12	282	0	140	399	-	-	-
XYGO	3	0	37	287	0	123	515	-	-	-
XYGH	1	0	3	281	0	106	506	-	-	-
Commercial										
pectins										
CPPC	20	1	21	4	0	138	33	535	74	73
APPC	12	0	20	8	1	88	63	564	77	79
ARSB	52	0	584	0	0	114	0	83	-	-
LNAR	25	0	841	0	0	78	0	51	-	-
DBAR	68	0	504	0	0	193	48	98	-	-
GTAN	51	0	23	4	0	628	9	79		
RGPP	54	0	10	3	0	105	0	473	-	-
RGSP	81	64	21	120	0	96	0	403	-	-
HGTN	-	-	-	-	-	-	-	814	100	68
GALN	-	-	-	-	-	-	-	850	0	0
<i>Pooled SD</i>	<i>1.0</i>	<i>0.3</i>	<i>8.3</i>	<i>7.0</i>	<i>5.8</i>	<i>2.3</i>	<i>8.6</i>	<i>4.0</i>	<i>2.5</i>	<i>3.2</i>

Pooled SD: pooled standard deviation. Rha: rhamnose, Fuc: fucose, Ara: arabinose, Xyl: xylose, Man: mannose, Gal: galactose, Glc: glucose, Gal A: galacturonic acid, MeOH: methanol, DM: degree of methylation. Hemicelluloses (ARHV: Rye Arabinoxylan (59% Xylose), AXMB: Wheat Arabinoxylan (64% Xylose), AXLB: Wheat Arabinoxylan (77% Xylose), XYBW: Xylan (Beechwood), MANB: 1,4-β-D-Mannan, XYGT: Xyloglucan (from tamarind seed), XYGO: Xyloglucan Oligosaccharides, XYGH: Xyloglucan Oligosaccharides (Hepta-, +Octa, +Nona-saccharides), GAMA: Galactomannan (Carob)); Pectins (APPC: Apple pectin, CPPC: Citrus peel pectin, HGTN: Homogalacturonan DM 70, GALN: Polygalacturonic acid, DBAR: Debranched arabinan, ARSB: Arabinan, LNAR: Linear arabinan, RGPP: Rhamnogalacturonan I, RGSP: Rhamnogalacturonan, GTAN: Galactan (Potato)); β-glucans (MCCE: Microcrystalline cellulose, CGLU: 1,3-beta-o-glucan and YGLU: Yeast beta-g-lucan).



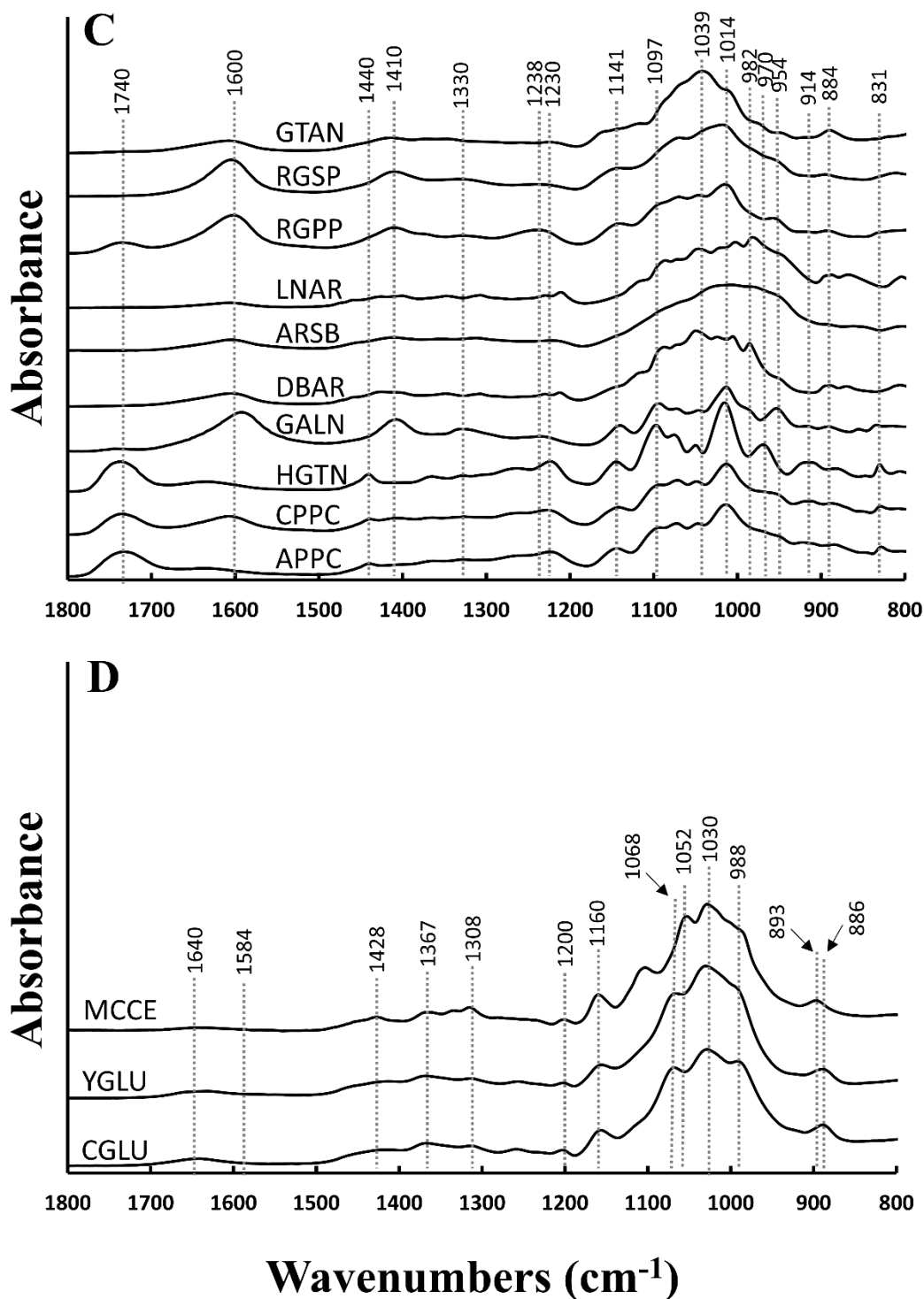


Figure 3.5 ATR-FTIR spectra (pre-processed with Standard Normal Variate) of commercial purified and extracted cell wall polysaccharides in solid form: A. Monosaccharides (Rha: rhamnose, Fuc: fucose, Ara: arabinose, Xyl: xylose, Man: mannose, Gal: galactose, Glc: glucose, Gal A: galacturonic acid); B. Hemicelluloses (ARHV: Rye Arabinoxylan (59% Xylose), AXMB: Wheat Arabinoxylan (64% Xylose), AXLB: Wheat Arabinoxylan (77% Xylose), XYBW: Xylan (Beechwood), MANB: 1,4- β -D-Mannan, XYGT: Xyloglucan (from tamarind seed), XYGO: Xyloglucan Oligosaccharides (Hepta-, +Octa, +Nona-saccharides), GAMA: Galactomannan (Carob)); C. Pectins (APPC: Apple pectin, CPPC: Citrus peel pectin, HGTN: Homogalacturonan DM 70, GALN: Polygalacturonic acid, DBAR: Debranched arabinan, ARSB: Arabinan, LNAR: Linear arabinan,

RGPP: Rhamnogalacturonan I, RGSP: Rhamnogalacturonan, GTAN: Galactan (Potato)); D. β -glucans (MCCE: Microcrystalline cellulose; CGLU: curdlan 1,3-beta-o-glucan; YGLU: Yeast beta-glucan).

3.2.3.1.1 Monosaccharides

Monosaccharides, without any glycosidic linkage to other units, are the simplest component units of the cell wall polysaccharides, and have been shown to be important in polymer analysis and structure elucidation (Wiercigroch et al., 2017). It was necessary to consider here hexopyranoses (glucose, mannose and galactose), dehydrohexopyranoses (rhamnose and fucose), pentopyranose (xylose), and pentofuranose (arabinose), standards with different positions of hydroxyl groups on C-2, C-3, and C-4 (Fig. 3.5A). The spectra of pentoses (arabinose and xylose) were dominated by a band at 991 and 1034 cm^{-1} , respectively, mainly due to the $\nu(\text{C-C})$, $\nu(\text{C-O})$ and $\beta(\text{C-CH})$ vibrations (Edwards, 1976). For hexoses, D-(+)-glucose was observed by the main band at 991 cm^{-1} . D-(+)-galactose is almost identical in structure to D-(+)-glucose, with a different orientation in the C-4 OH group, but with a distinct spectral difference due to their free crystalline structure (Fig. 3.5A). Similarly, the spectrum of other hexopyranoses with different hydroxyl group orientations on C-2, C-3, and C-4 was also significantly different. Therefore, the relative positions of (C-OH) essentially affected the spectrum through variations in their spatial arrangement and interactions. The detailed ATR-FTIR bands of monosaccharides with modes assignments are listed in Table 3.3.

3.2.3.1.2 Pectic components

Pectins are acidic hetero-polysaccharides mainly composed of homogalacturonan, rhamnogalacturonan I and II, and different neutral sugar side chains (e.g., arabinan and galactan). The spectra of apple pectins (APPC) and citrus peel pectins (CPPC) had very similar characteristic bands (Fig. 3.5C) centering at 1740, 1600, 1440, 1230, 1141, 1097, 1014, 954, 914 and 831 cm^{-1} . They have also similar levels of neutral sugars, galacturonic acid and degree of methylation (Table 3.5). The band at 1740 cm^{-1} is assigned to the esterified galacturonic acids. This band is characteristic of pectins with a high degree of methylation (DM) such as high methylated homogalacturonan

Application of ATR-FTIR to cell wall polysaccharides

Table 3.5 The main ATR-FTIR absorption bands, the polysaccharides in which they were detected and their tentative assignment. For polysaccharide identification (detailed in Table 3.3).

Wavenumber range (cm ⁻¹) (detected)	Mono- or polysaccharide in which it was detected	Band assignments	Corresponding Wavenumber range (cm ⁻¹)*	References
1756 & 1708	Gal A	Galacturonic acid (absence of glycosidic bond)	-	-
1740	APPC, CPPC and HGTN	C=O stretching vibration of alkyl ester (pectin)	1745-1730	(Filippov & Kohn, 1975; Gnanasambandam, R., Proctor, 2000b; Maureen C. McCann et al., 1992; Monsoor et al., 2001; Szymanska-Chargot & Zdunek, 2013)
1640	MCCE, CGLU and YGLU	H–O–H bending vibration absorbed water	1640	(Szymanska-Chargot et al., 2015)
1605 - 1595	GALN, CPPC, ARSB, DBAR, RGPP and RGSP	COO ⁻ antisymmetric stretching polygalacturonic acid, free carboxyl group	1630-1600	(Filippov & Kohn, 1975; Gnanasambandam, R., Proctor, 2000b; Maureen C. McCann et al., 1992; Monsoor et al., 2001; Szymanska-Chargot & Zdunek, 2013)
1525	KCR/Os	Amid II N–H deformation (proteins); lignin and phenolic back bone	1550	(Maureen C. McCann et al., 1992)
1474	ARHV, XYBW and XYGT	Xylose-containing hemicellulose	-	-
1440	APPC, CPPC and HGTN	Asymmetric stretching modes vibration of methyl esters (pectin)	1440	(Canteri et al., 2019; Szymanska-Chargot et al., 2015)
1428	MCCE, CGLU and YGLU	CH ₂ symmetric bending (cellulose)	1428	(Szymanska-Chargot & Zdunek, 2013)
1410	GALN, RGPP and RGSP	COO ⁻ symmetric stretching, free carboxyl group (rhamnogalacturonan and homogalacturonan)	1410	(Szymanska-Chargot & Zdunek, 2013)
1367	MCCE, CGLU and YGLU, XYGT, GAMA and MANB	C–H vibrations and CH ₂ bending (cellulose, hemicelluloses)	1370, 1362	(Szymanska-Chargot et al., 2015; Szymanska-Chargot & Zdunek, 2013)

(Continued)

Table 3.5 (Continues)

Wavenumber range (cm ⁻¹) (detected)	Mono- or polysaccharide in which it was detected	Band assignments	Corresponding Wavenumber range (cm ⁻¹)*	References
1331	Fuc	Fucose (absence of glycosidic bond)	-	
1330	HGTN, GALN, RGPP and RGSP	Bending of O–H groups in pyranose ring of pectins	1331-1320	(Szymanska-Chargot et al., 2015; Szymanska-Chargot & Zdunek, 2013)
1312	Ara	Arabinose (absence of glycosidic bond)	-	
1308	MCCE, CGLU and YGLU	CH ₂ symmetric bending or CH ₂ rocking vibration (cellulose)	1317-1313	(Szymanska-Chargot et al., 2015; Szymanska-Chargot & Zdunek, 2013)
1290	Rha	Rhamnose (absence of glycosidic bond)	-	
1238	RGPP	Rhamnogalacturonan	-	
1230	APPC, CPPC and HGTN	C–O stretching (pectins)	1240, 1230	(Szymanska-Chargot et al., 2015; Szymanska-Chargot & Zdunek, 2013)
1218	Gal A	Galacturonic acid (absence of glycosidic bond)	-	-
1164	ARHV, XYBW and XYGT	Glycosidic bond vibrations (O–C–O) (xylose- containing hemicellulose)	1173, 1153, 1147	(Coimbra et al., 1999; Kacurakova et al., 2000)
1160	KCR/Os	Glycosidic bond vibrations (O–C–O) (cellulose in cell walls)	1160	(Canteri et al., 2019; Szymanska-Chargot & Zdunek, 2013)
1152	MANB and GAMA	Glycosidic bond vibrations (O–C–O) (mannose- containing hemicellulose)	1150	(Szymanska-Chargot et al., 2015)
1141	APPC, CPPC, GALN, HGTN, RGPP and RGSP	Glycosidic bond vibrations (O–C–O) (pectin)	1150-1143	(Coimbra et al., 1998, 1999)
1126	Ara	Arabinose (absence of glycosidic bond)	-	

(Continued)

Table 3.5 (Continues)

Wavenumber range (cm ⁻¹) (detected)	Mono- or polysaccharide in which it was detected	Band assignments	Corresponding Wavenumber range (cm ⁻¹)*	References
1097	APPC, CPPC, HGTN, GALN, RGPP and RGSP	C–O stretching, C–C stretching ring pectin	1100-1090	(Coimbra et al., 1998; Szymanska-Chargot et al., 2015; Szymanska-Chargot & Zdunek, 2013)
1074	GTAN, RGPP and RGSP	C–C stretching ring (galactan and rhamnogalacturonan)	1072, 1070	(Kacurakova et al., 2000)
1068	MCCE, CGLU and YGLU	C–O stretching, C–C stretching, C6–H2–O6 (cellulose)	1059, 1047	(Szymanska-Chargot et al., 2015)
1065	MANB and GAMA	C–O stretching, C–C stretching (mannose-containing hemicellulose)	1064	(Kacurakova et al., 2000)
1039	GTAN	C–C stretching ring (galactan)	1038	(Kacurakova et al., 2000)
1035	ARHV, XYBW and XYGT	C–O stretching, C–C stretching (xylose-containing hemicellulose)	1042, 1041, 1038	(Canteri et al., 2019; Coimbra et al., 1999; Kacurakova et al., 2000)
1030	MCCE, CGLU and YGLU	C–O stretching, C–C stretching, C6–H2–O6 (cellulose)	1034, 1030	(Kacurakova et al., 2000; Szymanska-Chargot & Zdunek, 2013)
1027	GAMA	C–O stretching, C–C stretching, C6–H2–O6 (galactomannan)	1034	(Kacurakova et al., 2000)
1014	APPC, CPPC, GALN, HGTN, DBAR, ARSB, GTAN, RGPP and RGSP	C–O stretching, C–C stretching pectin (C2–C3, C2–O2, C1–O1) backbone vibrations (pectin)	1020, 1015, 1014	(Coimbra et al., 1998, 1999; Szymanska-Chargot et al., 2015; Szymanska-Chargot & Zdunek, 2013)
1013	MANB	C–O stretching, C–C stretching (mannan)	-	
991	Glc and Ara	Glucose and arabinose (absence of glycosidic bond)	-	
988	MCCE, CGLU and YGLU	C–O stretching, C–C stretching cellulose (C6–H2–O6)	1000, 985	(Canteri et al., 2019; Szymanska-Chargot & Zdunek, 2013)

(Continued)

Table 3.5 (Continues)

Wavenumber range (cm ⁻¹) (detected)	Mono or polysaccharide in which it was detected	Band assignments	Corresponding Wavenumber range (cm ⁻¹)*	References
983	ARHV and XYBW	Xylan and arabinoxylan	-	
982	DBAR, ARSB and LNAR	Arabinan	-	
970	APPC, CPPC and HGTN	Pectins	972	(Kacurakova et al., 2000)
954	RGSP	CO bending (pectins)	952	(Coimbra et al., 1999; Szymanska-Chargot & Zdunek, 2013)
939	XYGT, GAMA and MANB	Ring vibration (hemicellulose and arabinan)	941	(Szymanska-Chargot et al., 2015; Szymanska-Chargot & Zdunek, 2013)
925 and 908	Xyl	Xylose (absence of glycosidic bond)	-	
914	APPC, CPPC, HGTN and GALN	Ring vibration (pectin)	-	
890	XYGT, ARHV and XYBW	C1-H bending (xylose-containing hemicellulose)	893	(Szymanska-Chargot & Zdunek, 2013)
886	KCR/Os	C1-H bending (cellulose)	899, 895	(Canteri et al., 2019; Szymanska-Chargot & Zdunek, 2013)
884	GTAN	C1-H bending (galactan)	883	
870	GAMA and MANB	C1-H bending (mannose-containing polysaccharide)	-	
840	Ara	Arabinose (absence of glycosidic bond)	-	
831	APPC, CPPC, GALN and HGTN	Ring vibration (pectin)	833-830	(Szymanska-Chargot et al., 2015; Szymanska-Chargot & Zdunek, 2013)
807	GAMA and MANB	Ring vibration (mannose-containing hemicellulose)	-	

* Reference from the literatures. Monosaccharides (Rha: rhamnose, Fuc: fucose, Ara: arabinose, Xyl: xylose, Man: mannose, Gal: galactose, Glc: glucose, Gal A: galacturonic acid); Hemicelluloses (ARHV: Rye Arabinoxylan (59% Xylose), AXMB: Wheat Arabinoxylan (64% Xylose), AXLB: Wheat Arabinoxylan (77% Xylose), XYBW: Xylan (Beechwood), MANB: 1,4-β-D-Mannan, XYGT: Xyloglucan (from tamarind seed), XYGO: Xyloglucan Oligosaccharides, XYGH: Xyloglucan Oligosaccharides (Hepta-, +Octa, +Nona-saccharides), GAMA: Galactomannan (Carob)); Pectins (APPC: Apple pectin, CPPC: Citrus peel pectin, HGTN: Homogalacturonan DM 70, GALN: Polygalacturonic acid, DBAR: Debranched arabinan, ARSB: Arabinan, LNAR: Linear arabinan, RGPP: Rhamnogalacturonan I, RGSP: Rhamnogalacturonan, GTAN: Galactan (Potato)); β-glucans (MCCE: Microcrystalline cellulose; CGLU: curdlan, 1,3-beta-glucan; YGLU: Yeast beta-glucan). Bands of monosaccharides such as mannose and galactose were not shown due to their overlapping with bands of polysaccharide polymers.

(DM=70) (HGTV). Inversely, the band of poly-galacturonic acid (GALN), which is non-esterified, was at 1600 cm^{-1} due to the COO^- carboxylate ion stretching. These two main characteristic bands of pectins are fixed and similar to those previously reported (Coimbra et al., 1999; Filippov & Kohn, 1975; Gnanasambandam, Proctor, 2000b; Kacurakova et al., 2000; Reintjes, Musco, & Joseph, 1962; Szymanska-Chargot et al., 2015; Wojdyło et al., 2014).

For a further interpretation of these spectra, pure pectic components were characterized in the same conditions. Notably, although these parts of the polysaccharide components were not a complete pectin structure found in the plant, they are representative of different subunits of the pectins. For rhamnogalacturonan (RGPP and RGSP), the band at 1014 cm^{-1} was the strongest (Fig. 3.5C). However, this peak overlapped with the main peak of commercial pectins (APPC and CPPC). Some other specific bands, assigned to rhamnogalacturonan (RGPP and RGSP) can be used such as 1410 , 1238 and 1074 cm^{-1} . In fact, RGSP contained more xylose than RGPP (120 mg/g vs 3 mg/g respectively) (Table 3.4). Based on the maximum peak of xylose at 1035 cm^{-1} for RGSP, but not for RGPP (Fig. 3.5C), 1035 cm^{-1} may be used to differentiate the abundance of xylose in cell wall polysaccharides.

In the case of the main neutral sugar side chains of pectins (Fig. 3.5C): (i) galactan (GTAN) was characterized by bands at 1039 cm^{-1} , 1014 and 884 cm^{-1} ; and (ii) arabinan, such as present in sugar beet arabinan (ARSB), linear arabinan (LNAR) and debranched arabinan (DBAR), were more visible in the region between 1100 and 950 cm^{-1} . The arabinans with different linearity and branching degrees had some minor peak intensity differences in this region. For example, the main band of LNAR (with the highest arabinose content, Table 3.4) was close to 980 cm^{-1} , which may be used to assess arabinan. However, the characteristic peaks of arabinan (sugar beet) were in the region and also within the range of the main peaks of other pectins (e.g., commercial pectins, rhamnogalacturonan and galactan) not allowing a clear assignment of bands between 1100 and 950 cm^{-1} . In aqueous solutions, Kacurakova et al. (2000) observed bands at 1070 and 1043 cm^{-1} for rhamnogalacturonan, 1072 cm^{-1} for galactan and 1039 cm^{-1}

arabinan, which were too close for reliable discrimination. These differences may be due to the different states (solid or solution) of the cell wall compounds and probably also to the specificity of the used spectrometers.

For pectic homogalacturonans with more or less methylation, the main characteristic peaks (especially 1740, 1600, 1097 and 1014 cm^{-1}) were stable regardless of whether they are in a solid state or in an aqueous solution. However, the identification of spectral characteristic peaks of arabinan, galactan, and rhamnogalacturonan required caution as their peaks were dependent on the sample state, which could lead to their overlapping with those of hemicelluloses and pectins.

3.2.3.1.3 Hemicelluloses and cellulose

Bands at 1474, 1367, 1164, 1152, 1065, 1035, 1027, 1013, 983, 939, 890, 870 and 807 cm^{-1} were identified for hemicelluloses (Fig. 3.5B). Xylan (XYBW) had characteristic absorption bands at 1035 cm^{-1} and 983 cm^{-1} . The arabinoxylans with different xylose contents (Table 3.4), e.g., ARHV (59%), AXMB (64%) and AXLB (77%), showed a main band at 1035 cm^{-1} for which the intensity varied with the xylose content. Xyloglucan (XYGT, XYGO and XYGH) absorbed in the region of 1040-1010 cm^{-1} , like hemicelluloses and cellulose making it difficult to be identified. Galactomannan (GAMA) and mannan (MANB) had bands at 1027 and 1013 cm^{-1} , respectively. In addition, they had a common secondary band at 1065 cm^{-1} , and two specific peaks at 870 and 807 cm^{-1} (also found in softwood sample, Simonović, Stevanic, Djikanović, Salmén, & Radotić, 2011), which allowed them to be distinguished from others (Fig. 3.5B). Therefore, the bands which could be assigned to xylose- and mannose- containing hemicelluloses were 1474, 1164, 1035, 983 and 890 cm^{-1} for xylose-, and 1152, 1065, 1027, 1013, 939, 870 and 807 cm^{-1} for mannose-, respectively (Table 3.5). This was confirmed for xylose- containing hemicelluloses including XYBW, ARHV, AXMB, AXLB, XYGT, XYGO and XYGH, and mannose-containing hemicelluloses including MANB and GAMA.

The bands characteristic of cellulose, β -(1 \rightarrow 4)-linked glucan, for MCCE, were at 1640, 1428, 1367, 1320, 1308, 1200, 1160, 1052, 1030, 988 and 893 cm^{-1} (Fig. 3.5D), whereas bands at 1068 and 886 cm^{-1} (instead of 1052 and 893 cm^{-1}) were identified for β -(1 \rightarrow 3)-glucans (YGLU and CGLU). These slight differences for two peaks may contribute to distinguish 1,3- β - and 1,4- β - bonds.

3.2.3.1.4 Glycosidic linkage

The glycosidic linkages are an important characteristic structure in polysaccharides and influence the spectral changes in aqueous solutions (Jockusch et al., 2004; Kačuráková & Mathlouthi, 1996; Kanou, Nakanishi, Hashimoto, & Kameokaj, 2005; Nikonenko, Buslov, Sushko, & Zhabankov, 2000; Wiercigroch et al., 2017). For example, the spectra of the glycosidic bonds with different positions and configurations of oligo- and poly- saccharides in aqueous solution differ markedly from monosaccharides, with stretching vibrations [$\nu(\text{CO})$] of the C-O-C glycosidic linkage being the marker of the polysaccharide configuration. These vibrations appear in the two spectral ranges 1160-1130 and 1000-960 cm^{-1} (Kacurakova et al., 2000; Kačuráková & Mathlouthi, 1996; Wiercigroch et al., 2017). Similarly, these bands appear in cell wall polysaccharides in the solid states when compared with monosaccharides (Fig. 3.5). For xylose units with β -(1 \rightarrow 4) glycosidic linkage (XYBW) bands were found at about 1164 cm^{-1} , for glucose units with β -(1 \rightarrow 4) glycosidic linkage (YGLU, CGLU and MCCE) bands were found at 1160 cm^{-1} and for mannose units with β -(1 \rightarrow 4) glycosidic linkage (MANB) bands were found at 1152 cm^{-1} . Bands at 1141 cm^{-1} for pectins originate from the stretching motion of the CO bond within the glycosidic linkage (Coimbra et al., 1999). Therefore, the involvement of glycosidic bonds influenced the spectrum through changes in their spatial arrangement, type and position.

However, some monosaccharides also showed spectral bands in the region between 1100 to 1000 cm^{-1} presenting overlapping with those of polysaccharides (Fig. 3.5, Table 3.3).

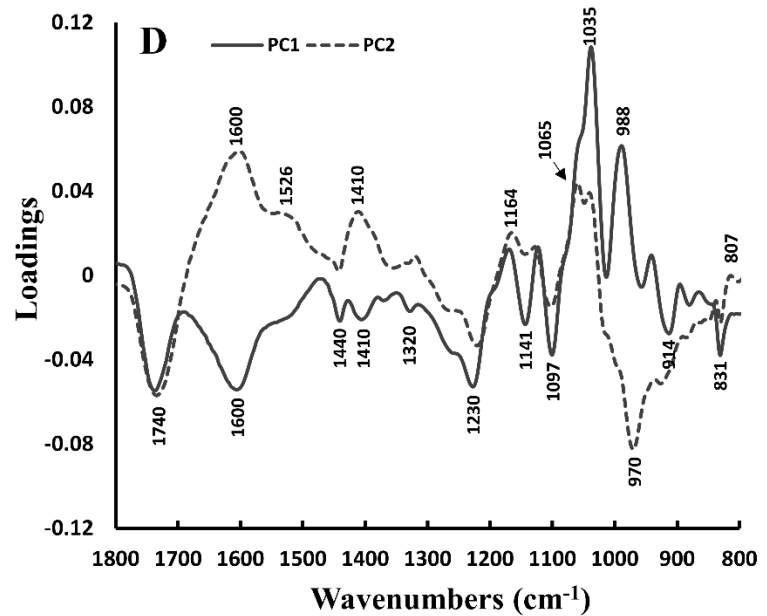
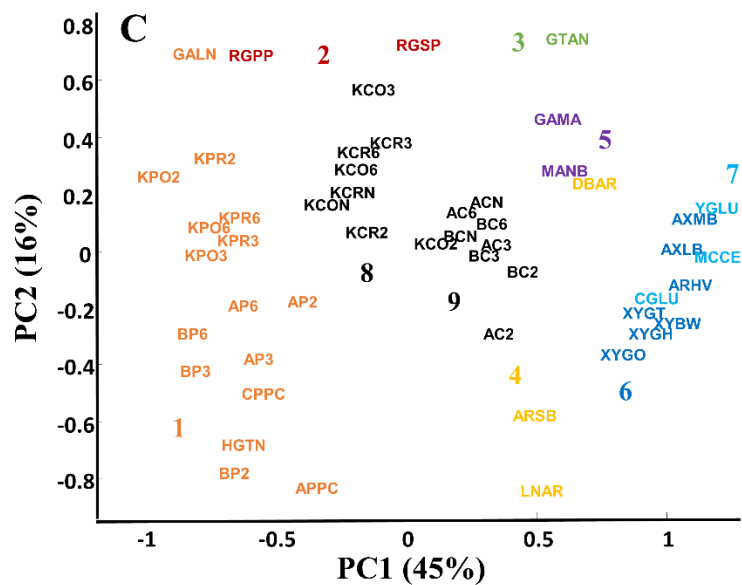
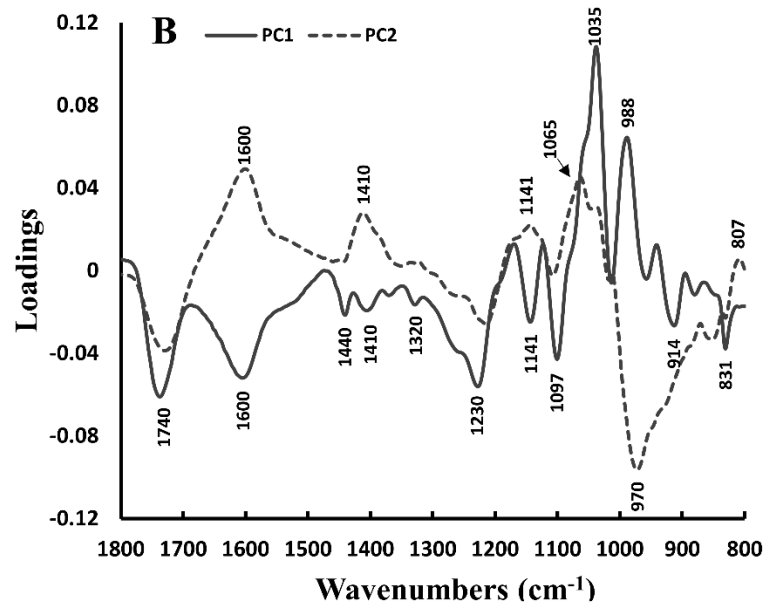
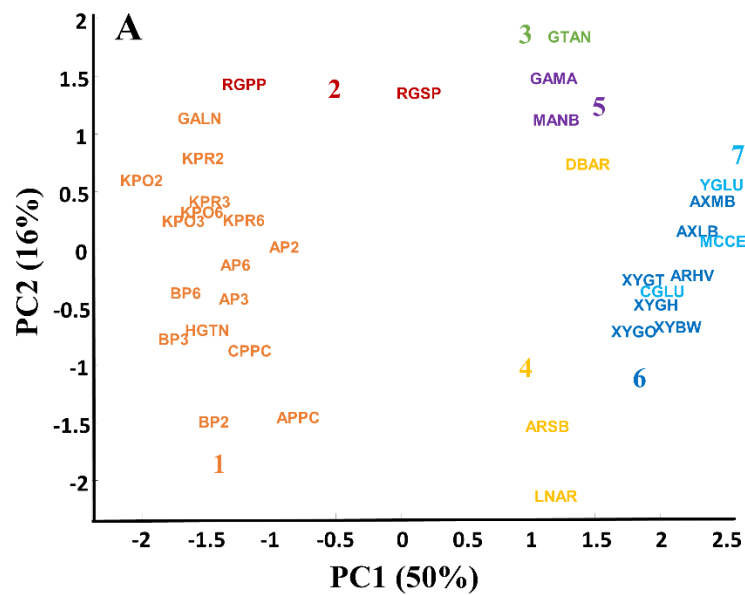


Figure 3.6 PCA scores scatter plots of 1) commercial and extracted pectins, 2) rhamnogalacturonan, 3) galactan, 4) arabinan, 5) mannose- containing hemicelluloses, 6) xylose-containing hemicelluloses and 7) cellulose (A), and all cell wall materials (excluding monosaccharides): 8) kiwifruit cell walls, 9) apple and beet cell walls (C). ATR-FTIR spectra in the range 1800 to 800 cm^{-1} with their PCA loading profile of components PC1 and PC2 (B) and (D). Monosaccharides (Rha: rhamnose, Fuc: fucose, Ara: arabinose, Xyl: xylose, Man: mannose, Gal: galactose, Glc: glucose, Gal A: galacturonic acid); Hemicelluloses (ARHV: Rye Arabinoxylan (59% Xylose), AXMB: Wheat Arabinoxylan (64% Xylose), AXLB: Wheat Arabinoxylan (77% Xylose), XYBW: Xylan (Beechwood), MANB: 1,4- β -D-Mannan, XYGT: Xyloglucan (from tamarind seed), XYGO: Xyloglucan Oligosaccharides, XYGH: Xyloglucan Oligosaccharides (Hepta-, +Octa, +Nona-saccharides), GAMA: Galactomannan (Carob)); Pectins (APPC: Apple pectin, CPPC: Citrus peel pectin, HGTM: Homogalacturonan DM 70, GALN: Polygalacturonic acid, DBAR: Debranched arabinan, ARSB: Arabinan, LNAR: Linear arabinan, RGPP: Rhamnogalacturonan I, RGSP: Rhamnogalacturonan, GTAN: Galactan (Potato)); β -glucans: (MCCE: Microcrystalline cellulose; CGLU: curdlan, 1,3-beta-o-glucan; YGLU: Yeast beta-glucan).

3.2.3.2 Discrimination of cell walls

Two multivariate analyses were used to study the discrimination of complex fruit cell walls in comparison with that obtained on standard compounds. A Principal component analysis (PCA) was carried out using the spectral data (Fig. 3.6A) to identify the mapping of cell wall polysaccharides (excluding extracted cell walls and monosaccharides). PC1 and PC2 explained respectively 50% and 16% of the total variance. Along the PC1, the samples were well discriminated due to the different types of cell wall polysaccharides. Positive loadings of PC1 covered wavenumbers characteristic of xylose-containing (1035 cm^{-1}) hemicellulose and cellulose (988 cm^{-1}) (Fig. 3.6B). The negative high values of PC1 were obtained for wavenumbers at 1740 and 1600 cm^{-1} characteristic of esterified and non-esterified carboxyl groups in pectins (Fig. 3.6B), respectively and of 1440 , 1320 , 1230 , 1141 , 1097 , 914 and 831 cm^{-1} bands characteristic of pectins (Fig. 3.6B). In addition, negative PC1 loading appeared for wavenumbers at 1410 cm^{-1} characteristic for rhamnogalacturonan. The PC2 separated the esterified pectins and arabinan on the negative side (at the bottom) from the less esterified pectins, galactan and mannose-containing hemicelluloses (at the top). The bands at (1600 and 1141 cm^{-1}), 1410 cm^{-1} , and (1065 and 807 cm^{-1}) were attributed to respectively free carbonyl group of pectins, rhamnogalacturonan and mannose-containing hemicelluloses with a positive correlation to PC2. The region closes to 1740 and 970 cm^{-1} corresponded to the esterified pectins with a negative correlation to PC2.

The same approach was used on the extracted cell walls from apple, beet and kiwifruit (Fig. 3.6C). The cell wall polysaccharides were divided into nine groups: 1) commercial and extracted pectins; 2) rhamnogalacturonans; 3) galactans; 4) arabinans; 5) mannose- containing hemicelluloses; 6) xylose- containing hemicelluloses; 7) cellulose; 8) kiwifruit cell walls; 9) apple and beet cell walls. The first seven groups are similar to Fig. 3.6A, with the later addition of the extracted cell walls in the center of the Fig. 3.6C. This is consistent with the expected results as they contain intact cell wall polysaccharide components. However, the extracted cell walls issued from different species and extraction conditions were not well separated, especially for apple and beet

cell walls. How can we explain the lack of discrimination of cell walls between apple and beet, whereas their composition differ significantly (X. Liu, Renard, Rolland-Sabaté, Bureau, et al., 2021)? As shown on the PCA, the kiwifruit cell walls were at the upper left in the middle of the Fig. 3.6C, while the apple and beet cell walls were at the bottom right in the middle of the Fig. 3.6C. This was probably linked to the high cellulose and relatively low galacturonic acid for kiwifruit, and the high galacturonic acid for both apple and beet (140 to 206 mg/g for apple, 141 to 225 mg/g for beet) (X. Liu, Renard, Rolland-Sabaté, Bureau, et al., 2021). However, the cell walls of apple and beet were not distinguished, in spite of marked chemical and structural differences (X. Liu, Renard, Rolland-Sabaté, Bureau, et al., 2021). Even a PCA performed on the ATR-FTIR spectra of the cell walls of apple and beet alone did not separate them well (data not shown). Beet cell walls are rich in arabinan (111 to 189 mg/g), contain ferulic acid, and have only minor amounts of rhamnose, fucose, xylose and mannose. Apple cell walls contain as much or more xylose (65 to 75 mg/g) and galactose (63 -67 mg/g) than arabinose (27 to 66 mg/g). However, the expected separation of apple and beet cell walls spectra by the characteristic peaks of arabinan (982 cm^{-1}) or galactan (1039 cm^{-1}) was not observed. Probably the characteristic peaks were not detected or were overlapped with those of other cell wall components, e.g., hemicelluloses or cellulose (Fig. 3.5). This may be a limitation of ATR-FTIR in cell wall characterization, because arabinan and galactan are well known to change during ripening or processing.

PC loadings (Fig. 3.6D) were very close to those obtained on the standard compounds (Fig. 3.6B), probably reflecting the fact that the cell walls are by themselves combinations of pectins, hemicelluloses and cellulose. PC2 loadings had an extra shoulder peak at 1526 cm^{-1} , which may be attributed to lignin and ferulic acid, but occurring in combination with hemicelluloses (e.g., xylans and xyloglucans). The non-polysaccharide compounds in the cell wall, such as proteins (e.g., C = O of amides at 1655 cm^{-1} and N-H of amides at 1540 , and 1234 cm^{-1}), lignins (e.g., 1520 , 1410 and 921 cm^{-1}) and other phenolic compounds (e.g., 1520 , 1440 , 1284 , 1196 and 1075 cm^{-1}) have absorption bands which may interfere with those of polysaccharides. This needs

to be taken into account when characterizing cell walls using ATR-FTIR. Moreover, the structure of xylans varies with the source of the plant, such as wheat or beechwood. As an example, some phenolic compounds can couple beechwood xylan chains via ferulate dimerization (dehydrodiferulate cross-links) and/or incorporation into lignin, thus affecting their spectral bands (Kačuráková et al., 1999).

Hierarchical cluster analysis (HCA) is widely applied as an unsupervised classification method to calculate distances between samples and cluster them according to this distance, based here on their spectra (Granato, Santos, Escher, Ferreira, & Maggio, 2018). HCA highlighted five groups (Fig. 3.7). Group 1 clustered samples with high galacturonic acid contents from apple, beet, citrus and kiwifruit pectins. Group 2 contained samples with linear pectins and less side chains from kiwifruit cell walls, polygalacturonic acid and rhamnogalacturonan. Group 3 associated monosaccharide samples with absence of glycosidic bonds. Group 4 clustered samples including hemicelluloses and cellulose. Group 5 clustered samples with high methylated pectins and rich in arabinose and galactose, extracted from apple, beet cell walls, galactan and arabinan. Therefore, ATR-FTIR spectroscopy coupled with chemometrics allowed a good discrimination of cell walls related to their compositions and structures, giving some classes according to the different kinds of pectins, hemicelluloses and cellulose.

The cell walls represented a polymer system in a complex mixture with a diversity of both compositions and structures. PCA and HCA performed on the spectral data allowed to discriminate samples according to their cell wall polysaccharides. ATR-FTIR could be considered as a fast/easy way to distinguish different types of cell walls. Due to their complexity and the numerous spectral bands for each component, with the addition of overlapping, it was difficult to assign each band to a compound chemical structure. However, the observed changes in intensity or presence/absence of some bands reflected the differences in composition between cell walls. Slight changes in the strength and position of individual bands could also be due to the different conformations of cell wall polymers and interactions between individual components.

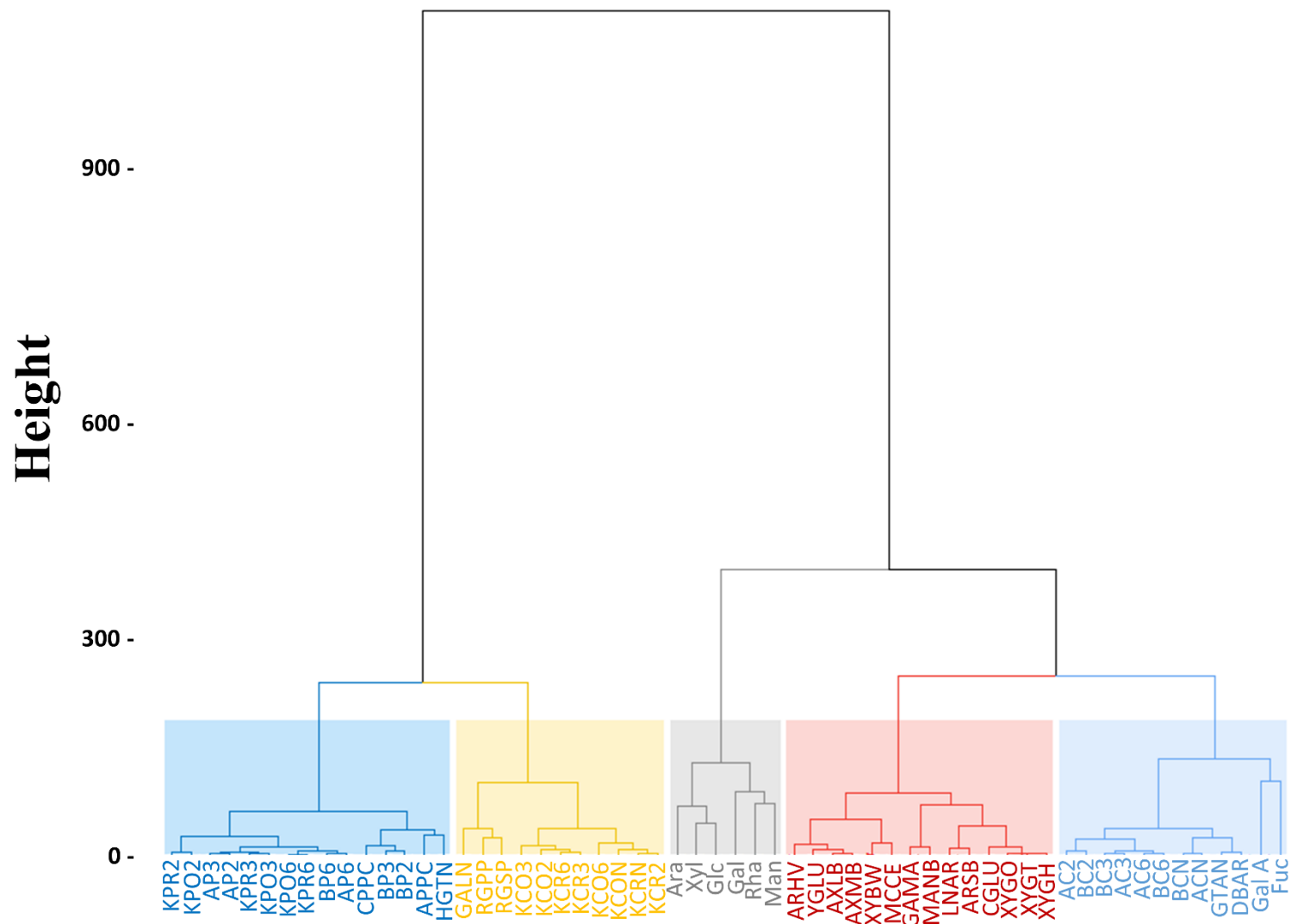


Figure 3.7 Hierarchical cluster analysis dendrogram of 58 cell wall and cell wall polysaccharide and monosaccharide samples based on average ATR-FTIR spectra in the range 4000 to 600 cm^{-1} using Ward's clustering algorithm with Euclidian distance. From left to right, the groups are (i) commercial and extracted pectins; (ii) kiwifruit cell walls and RG; (iii) monosaccharides; (iv) cellulose and hemicelluloses and (v) apple and beet cell walls. Monosaccharides (Rha: rhamnose, Fuc: fucose, Ara: arabinose, Xyl: xylose, Man: mannose, Gal: galactose, Glc: glucose, Gal A: galacturonic acid); Hemicelluloses (ARHV: Rye Arabinoxylan (59% Xylose), AXMB: Wheat Arabinoxylan (64% Xylose), AXLB: Wheat Arabinoxylan (77% Xylose), XYBW: Xylan (Beechwood), MANB: 1,4- β -D-Mannan, XYGT: Xyloglucan (from tamarind seed), XYGO: Xyloglucan Oligosaccharides, XYGH: Xyloglucan Oligosaccharides (Hepta-, +Octa-, +Nona-saccharides), GAMA: Galactomannan (Carob)); Pectins (APPC: Apple pectin, CPPC: Citrus peel pectin, HGTN: Homogalacturonan DM 70, GALN: Polygalacturonic acid, DBAR: Debranched arabinan, ARSB: Arabinan, LNAR: Linear arabinan, RGPP: Rhamnogalacturonan I, RGSP: Rhamnogalacturonan, GTAN: Galactan (Potato)); β -glucans: (MCCE: Microcrystalline cellulose; CGLU: curdlan, 1,3-beta-o-glucan; YGLU: Yeast beta-glucan).

3.2.4 Conclusions

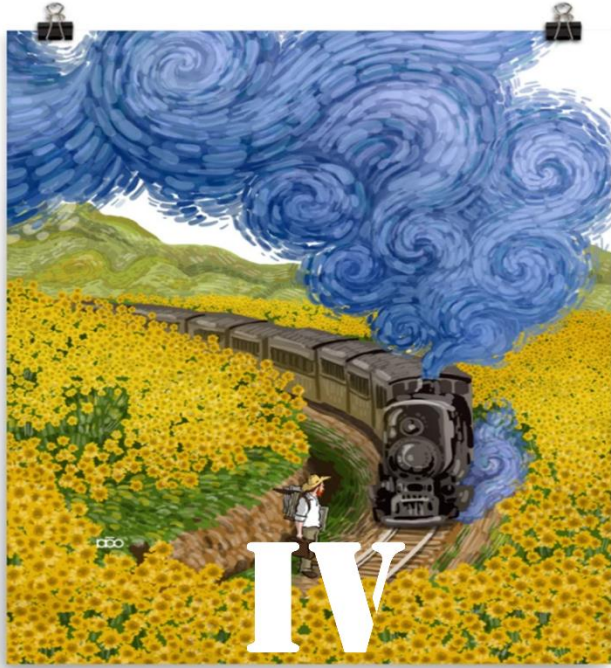
ATR-FTIR spectra in the region between 1800 and 800 cm^{-1} combined with PCA has been widely applied to study the main polysaccharides present in the complex cell walls. However, it is not always possible to analyze the structural changes in cell wall polysaccharides at the molecular level and not all absorption bands allow differentiation. Their complex structures, compositions, glycosidic linkage patterns and the interactions between polysaccharides (or even with polyphenols and proteins) make the application of ATR-FTIR to plant cell walls still challenging.

What can be determined is that: 1) xylan, arabinoxylan and xyloglucan all had the same characteristic band at 1035 cm^{-1} ; 2) cellulose showed a characteristic band at 988 cm^{-1} ; 3) the mannan and galactomannan were identified by the bands at 1065 and 807 cm^{-1} ; 4) the degree of methylation of pectin homogalacturonans was easily determined by the relative height of the two bands at 1740 and 1600 cm^{-1} . According to these results, the analysis of purified cell wall polysaccharides could be easily and successfully performed directly with these bands giving information on the main cell wall compounds: pectins, hemicelluloses and cellulose.

However, some difficulties remain to identify intact cell wall components and in particular to discriminate cell walls of apple and beet in relation to the bands of arabinan and galactan. The main chain made of arabinan did not give available characteristic peaks. The specific band of galactan at 1039 cm^{-1} was overlapped with the bands of hemicelluloses. Therefore, the application of ATR-FTIR spectroscopy for the characterization of cell wall polysaccharides requires more in-depth research and should be used in combination with other analytical techniques.

Highlights

- 58 cell wall polysaccharides were analyzed by reference analysis and ATR-FTIR spectroscopy.
- The cellulose, hemicelluloses and pectin homogalacturonans can be distinguished by ATR-FTIR.
- ATR-FTIR has limitations in the identification of complex systems, e.g., whole cell walls in relation to the signals of arabinan and galactan.



Sun for Procyanidin
Flower for Polysaccharide
Sunflower for Interaction
The train of life never stops
Sometimes we need to pause
And take breath

CHAPTER 4.

Cell wall-procyanidin interactions

This chapter deals with the question of cell wall polysaccharide-procyanidin interactions: section 4.1, 4.2 and 4.3 are the study for cell wall-procyanidin interactions, pectin-procyanidin interactions and hemicellulose-procyanidin interactions, respectively.

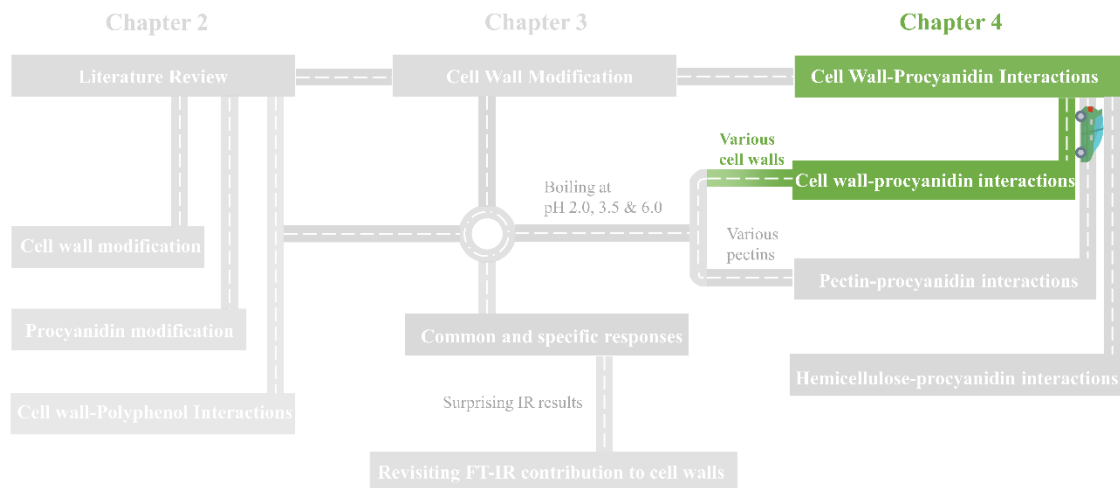
In the first part, the interaction capacity of sixteen native and modified cell walls, from apple, beet and kiwifruit at two maturity stages (ripe and overripe) differing in both their physical and chemical characteristics with procyanidins is examined.

This allowed to answer the following questions:

- ※ How the chemical composition and physical structure of the cell wall affect their interactions with procyanidins?
- ※ Which factors favor interactions and which do not?

Section 4.1

Interactions between heterogeneous cell walls and two procyanidins:
Insights from the effect of chemical composition and physical structure



A version of this section has been published as:

Liu, X., Renard, M. G. C. C., Bureau, S., & Le Bourvellec, C. (2021). Interactions between heterogeneous cell walls and two procyanidins: Insights from the effects of chemical composition and physical structure. *Food Hydrocolloids*, 121, 107018.

Cell wall polysaccharides (CWPs) and phenolic substances, e.g., procyanidins, widely co-exist in fruit and vegetables and interact in complex patterns during chewing, food processing and in *vivo* digestion, impacting the food physicochemical and nutritional qualities. Interactions were characterized between two procyanidins and heterogeneous CWPs (four native and twelve modified) from apple, beet and kiwifruit presenting various chemical compositions and physical structures. ATR-FTIR discriminated the complexes from the initial purified procyanidins and CWPs. Langmuir isotherms and ITC indicated that native CWPs, from all botanical origins, had a higher affinity for procyanidins than the modified ones, which were all poorer in pectins. The CWPs that interact more with procyanidins were characterized by their high pectin content and linearity, and high porosity. Increasing the molecular size of procyanidins increased their complexation with CWPs. This work is an important guide to the encapsulation and controlled release of active compounds and the subsequent respective digestive behavior and human health.

4.1 Interactions between heterogeneous cell walls and two procyanidins: Insights from the effect of chemical composition and physical structure

4.1.1 Introduction

Cell walls and polyphenols are important components of the dietary fiber complexes in plant-based foods. They coexist in plants in a separated cell compartment (Renard et al., 2017). The interactions between cell walls and polyphenols may occur during chewing, pre-consumption food processing and subsequent digestion, which modify their structure and composition, thereby affecting their bioefficacy or modulating gut microbiota (Loo et al., 2020). There seems to be a lack of understanding of the interactions between the different components in the food matrix. This may limit the possibility of linking the specific components to the potential effects of diet, particularly the role of macromolecular polyphenols such as procyanidins. These procyanidins can spontaneously and quickly bind to the cell walls through hydrogen bonding or hydrophobic interaction (X. Liu et al., 2020; Renard, Baron, Guyot, & Drilleau, 2001c; Renard et al., 2017). However, the knowledge of the influence of different types of cell walls (plant origin or processing modification) on the interactions is still lacking.

Plant cell walls are the extracellular matrices surrounding plant cells, which determine the texture of plant-based food (Carpita & Gibeau, 1993). The dominant thin, hydrophilic and highly hydrated type I cell wall of fruit and vegetables (Waldron, Smith, et al., 1997) is one of the major source of dietary fiber in human food. It consists of a network of cellulose microfibrils, tethered by hemicelluloses such as xyloglucans, xylans and mannans, embedded in an amorphous matrix constituted mostly of pectins. These cell walls are very diverse, depending on the composition, size distribution, shape, charge, extractability and combination of their constituent components. They are susceptible to physiochemical transformation reactions during food processing, thereby

changing their structure and leading to changes in their functional characteristics. For example, textural alterations related to changes in cell wall porosity impact affinity for procyanidins (Le Bourvellec et al., 2005). In addition, the presence of polyphenols can also change the functional properties of cell wall polysaccharides. For example, feruloylated arabinans can inhibit the softening of radishes during thermal processing (X. Li et al., 2019). The polysaccharide-polyphenol aggregation may decrease the viscosity of a polysaccharide solution (Tudorache & Bordenave, 2019). Therefore, the application of these interactions could improve the development of functional polysaccharides in the food industry.

Polyphenols are broadly distributed in fruit and vegetables, and have a positive effect on human health. Some unesterified phenolic acids and glucosylated monomeric polyphenols are easily absorbed in the upper digestive tract, while macromolecular polyphenols, e.g., procyanidins, are poorly absorbable (Santhakumar et al., 2018; Saura-Calixto & Pérez-Jiménez, 2018) and reach the colon. However, many studies have shown that the cell wall-polyphenol complexes can improve the metabolization of polyphenols in the colon (Le Bourvellec et al., 2019; Loo et al., 2020; Phan et al., 2020; Tarko & Duda-Chodak, 2020). Microbiological enzymes in the colon can promote the metabolism of the polyphenols from the complexes, and further bioprocess them from a non-absorbable form to a bioavailable one. Simultaneously, the interactions between polyphenols and cell walls and commensal microorganisms during the digestion process can adjust the balance between the growth of beneficial bacteria and pathogenic microorganisms (Dobson et al., 2019). A comprehensive understanding of the cell wall-macromolecular polyphenol interactions may enable food manufacturers to take full advantage of these beneficial effects.

Cell wall-procyanidin interactions can be mediated by their morphology, chemical composition and molecular architecture, that is, their porosity, the characteristics of their constitutive pectins, such as side-chains and branching ratios, molar mass, degree of esterification, functional groups, and conformation (X. Liu et al., 2020; X. Liu, Renard, Rolland-Sabaté, & Le Bourvellec, 2021). Cell walls with high pectin contents

have higher affinities for procyanidins, as in the case of pear tissues where the affinity decreases in the order: parenchyma cells > mesocarp (i.e., flesh) hypanthium > stone cells > epidermis (Brahem et al., 2019). Cell walls are complex and composed of heterogeneous polymers, of which, pectins have the highest affinity for procyanidins (Le Bourvellec & Renard, 2005; Le Bourvellec et al., 2012a). Moreover, high affinities are typically observed between highly methylated pectins and highly polymerized procyanidins (WatreLOT et al., 2013). Concerning branching of pectins, the general rule can be summarized as follows: the more linear the structure and the less branching areas of pectins in the cell walls, the better their association with procyanidins (P. A. R. Fernandes et al., 2020; X. Liu, Renard, Rolland-Sabaté, & Le Bourvellec, 2021; WatreLOT et al., 2014). This result also applies to the interaction with anthocyanins (Koh et al., 2020). For polyphenols, highly polymeric procyanidins with more hydroxyl and aryl rings bind more tightly to cell walls (Renard et al., 2017; Tang et al., 2003). However, what happens when these influencing factors are placed in the same cell wall-procyanidin interaction system? Do they act as antagonists or synergists? This still remains to be elucidated.

Although the interactions between the cell walls and procyanidins have been the focus of previous research (Brahem et al., 2019; Le Bourvellec et al., 2005; Le Bourvellec, Guyot, et al., 2004; Le Bourvellec & Renard, 2005; Renard et al., 2001c), to date, there does not appear to be systematic interaction studies which investigate the impact of botanical origins, processing and maturity modifications and evolutions of cell walls in the establishment of cell wall-procyanidin associations. We are now interested in identifying the cell wall factors, that is, their spread and diversity of structures and composition, that may influence their interactions with procyanidins. In the current work, we examined the capacity of sixteen cell walls, from apple, beet and kiwifruit at two maturity stages (ripe and overripe) differing in both their physical and chemical characteristics to adsorb procyanidins. Interactions were quantified via Langmuir isotherms, as well as isothermal titration calorimetry to measure thermodynamic changes caused by non-covalent binding. A better understanding of the

interactions between plant cell wall polysaccharides and polyphenols (especially procyanidins, important macromolecular antioxidants) is crucial for the development of plant-based food industry.

4.1.2 Material and methods

4.1.2.1 Standard

Sugar standards (arabinose, mannose, fucose, xylose, rhamnose, and galactose) and phloridzin were purchased from Fluka (Buchs, Switzerland). Methanol-d₃ was from Acros Organics (Geel, Belgium). 4-Coumaric acid was provided from Extra synthèse (Lyon, France). All other reagents and solvents were of analytical grade.

4.1.2.2 Procyanidins extraction, purification and analysis

Procyanidins of DP12 and DP39 were prepared from apple fruits (*Malus × domestica* Borkh.) of the ‘Marie Menard’ and ‘Avrolles’ cider cultivars, respectively, as described in X. Liu, Renard, Rolland-Sabaté, Bureau, & Le Bourvellec (2021). Briefly, this included extraction by aqueous acetone from the freeze-dried apple powders after washing by hexane and methanol, purification on a LiChrospher 100 RP-18 (12 µm, Merck, Darmstadt, Germany) column, concentration and storage under vacuum at -80 °C.

Purified procyanidins were characterized by high-performance liquid chromatography with diode array detection (with/without thioacidolysis) on a Shimadzu Prominence system (Kyoto, Japan) as described in principle by Guyot, Marnet, Sanoner, & Drilleau (2001). The separation condition were as described by Le Bourvellec et al. (2011).

4.1.2.3 Preparation and characterization of cell wall polysaccharides

Sixteen cell walls were prepared as described by X. Liu, Renard, Rolland-Sabaté, Bureau, et al. (2021). In brief, Alcohol-Insoluble Solids (AIS) were first prepared from apple, beet and kiwifruit (ripe and overripe) parenchyma, and named native apple cell wall (ACN), native beet cell wall (BCN), native kiwifruit cell wall ripe (KCRN), native

kiwifruit cell wall overripe (KCON). Then the four native cell walls modified by heating in a citrate-phosphate solution (0.1 M) at pH 2.0, 3.5 or 6.0, and the insoluble cell wall residues were retained; the extracted pectins have been used in another study (X. Liu, Renard, Rolland-Sabaté, & Le Bourvellec, 2021). The modified insoluble cell wall residues were used for the following experiments, i.e., apple cell walls modified at pH 2.0/3.5/6.0 (named AC2/3/6, respectively), beet cell walls modified at pH 2.0/3.5/6.0 (named BC2/3/6, respectively), kiwifruit cell walls ripe modified at pH 2.0/3.5/6.0 (named KCR2/3/6, respectively) and kiwifruit cell walls overripe modified at pH 2.0/3.5/6.0 (named KCO2/3/6, respectively).

Cell wall compositions were analyzed as described by X. Liu, Renard, Rolland-Sabaté, Bureau, et al. (2021). Approximately 10 mg of cell walls were prehydrolyzed with 72% sulfuric acid (250 μ L) for 1 h at room temperature (Saeman et al., 1954). Neutral sugars were analyzed as alditol acetates (Englyst et al., 1982) by GC-FID HP 5890 Series II (Agilent, Inc., Palo Alto, USA). Galacturonic acid was measured by the meta-hydroxyl-diphenyl assay using a spectrophotometer (V-530 Jasco, Tokyo, Japan). The methanol content was measured by stable isotope dilution assay using headspace-GC-MS (QP2010 Shimadzu, Kyoto, Japan) after saponification. The acetic acid content was measured by the acetic acid assay kit (K-ACET, ACS Manual Format, Megazyme International, Ireland). Ferulic acid was released by saponification according to the method of Micard, Renard, & Thibault (1994) by spectrophotometry (V-530Jasco, Tokyo, Japan).

Brunauer-Emmett-Teller (BET) isotherms (Brunauer, Emmett, & Teller, 1938) were used to determine the surface area of the cell walls by nitrogen adsorption isotherms at -196 °C using the Micromeritics AZAP 2010 system and monitored by AZAP 2010 version 5.01 (Micromeritics, Norcross, GA, USA).

The water-binding capacity was measured by filtration method using approximately 250 mg (dry weight) of cell walls left to soak with 10 mL of water containing NaN₃ (1 g/l) for 1 h at room temperature, then filtered and dried (103°C,

overnight). The water binding capacity (WBC) was calculated as follows:

$$\text{WBC (g/g)} = (M2 - M3) / (M3 - M1) \times 100 \% \quad (\text{Eq. 1})$$

With M1: weight of filter, M2 total weight after filtration and M3 after drying. Each sample was analyzed in triplicate.

4.1.2.4 Procyanidin-cell wall interactions

4.1.2.4.1 Binding isotherm methodology

The experiments were performed (duplicate) at 25 °C using buffer (citrate/phosphate system, pH 3.8, ionic strength 0.1 M) according to Renard et al. (2001). The procyanidin solution (from 0.25 to 12 g/L) and the cell wall suspension (5 mg/mL) were incubated under agitation in 8 mL empty Sep-pack preparation columns. After incubation, the free procyanidins solution and the cell wall-procyanidin complexes were isolated by filtering (20 µm porosity). The free procyanidins content was measured by spectroscopy at 280 nm (JASCO V-730 UV-visible spectrophotometer, Tokyo, Japan). Adsorbed procyanidins were measured by deducting the amount in the supernatant from that in the initial procyanidin solution. The average degree of polymerization of procyanidins (\overline{DP}_n) was calculated as the molar ratio of all flavan-3-ol units (thioether adduct plus terminal units minus (+)-catechin and (-)-epicatechin naturally present in the samples and determined by analysis of the samples by HPLC-DAD with and without thiolysis) to (+)-catechin and (-)-epicatechin corresponding to the terminal units minus (+)-catechin and (-)-epicatechin naturally present in the samples and determined by analysis of the samples by HPLC-DAD with and without thiolysis.

The binding isotherms were interpreted according to the type-I Langmuir approach (Renard et al., 2001c), which expresses bound solute (procyanidins) PP_b (in g/g of adsorbent) as a function of the free solute (procyanidins) concentration $[PP_f]$ at equilibrium.

$$PP_b = \frac{N_{\max}K_L[PP_f]}{1+K_L[PP_f]} \quad (\text{Eq. 2})$$

where N_{\max} is the total amount of available binding sites (expressed in g/g adsorbent) and K_L is an apparent affinity constant (in L/g).

4.1.2.4.2 Isothermal Titration Calorimetry (ITC)

The thermodynamic parameters changes caused by the cell wall-procyanidin interactions were measured by ITC using TAM III microcalorimeter (TA instruments, USA) as describe by Liu, Renard, Rolland-Sabaté, & Le Bourvellec (2021). In brief, purified procyanidins (30 mM in (-)-epicatechin equivalent) and cell walls (ca. 8 mg) were dissolved and suspended, respectively, in the same citrate/phosphate buffer pH 3.8, ionic strength 0.1 M. The procyanidin was titrated into the sample cell by 50 injections of 5 μ L; each injection lasted 5 s, with separating delay of 900 s for return to horizontal baseline. The content of the sample cell was stirred throughout the experiment at 90 rev/min. Blanks (titration of procyanidin fractions into citrate/phosphate buffer) are deducted from sample titration experiments. Experiments were performed in duplicates. All errors shown in the paper are based on the accuracy of the data fitting.

4.1.2.4.3 ATR-FTIR spectra

The cell wall samples retained by filtration after the binding isotherm experiment were further analyzed by ATR-FTIR. Cell wall-procyanidin complexes were selected at four concentrations in binding isotherm experiment, i.e., the initial procyanidin concentrations added were 0.25, 1, 6 and 12 g/l. The ATR-FTIR spectra of cell walls, procyanidins and freeze-dried complexes were recorded in triplicate (16 scans per spectrum, 4000 to 600 cm^{-1}) using a Tensor 27 FT-IR spectrometer (Bruker Optics, Wissembourg, France) equipped with a single-reflectance horizontal ATR cell (Golden Gate equipped with diamond crystal, Bruker Optics). Spectra were analyzed and controlled by OPUS software Version 5.0 as described by Liu, Renard, Rolland-Sabaté, Bureau, et al. (2021).

4.1.2.5 Statistical analysis

Results were expressed as mean values, and their reproducibility presented as the pooled standard deviation (Pooled SD) (Box, Hunter, & Hunter, 1978b). MATLAB 7.5 software (Mathworks Inc., Natick, MA, USA) with SAISIR package (Cordella & Bertrand, 2014) was used for pre-processing (baseline correction and standard normal variate) and Principal Component Analysis (PCA). Calculated and observed Langmuir curves were fitted by minimizing the sum of the square of the difference between observed and calculated values to obtain the Langmuir parameters (K_L and N_{max}) using the solver package of Microsoft Excel. Moreover, the confidence intervals ($P > 0.95$) of the Langmuir formula's constants were calculated using the Marquardt estimation method of the non-linear regression package of XLSTAT (version 2020.1.1, Addtionsoft SARL, Paris, France). Heatmap was performed with Python 3.5 software using the Seaborn package (Waskom, 2014).

4.1.3 Results

4.1.3.1 Composition and structure of the macromolecules and cell wall complexes

4.1.3.1.1 Procyanidin fractions

The two apple varieties, i.e., 'Marie Ménéard' and 'Avrolles', were selected to obtain two procyanidins with different degree of polymerization (Le Bourvellec et al., 2009). The purified extracts contained about 850 mg/g of phenolic compounds, mainly procyanidins plus traces of other phenolic compounds ([Supplementary Table 4.1](#)). 'Marie Ménéard' and 'Avrolles' procyanidins were composed of more than 99 % (-)-epicatechin units and differed by their degree of polymerization ($\overline{DP}_n = 12$ and 39, respectively). All the results were in accordance with (Le Bourvellec et al., 2012a; X. Liu, Renard, Rolland-Sabaté, & Le Bourvellec, 2021).

4.1.3.1.2 Cell wall polysaccharides

Detailed chemical compositions of the cell walls are available in our previous paper (X. Liu, Renard, Rolland-Sabaté, Bureau, et al., 2021) and the sugar ratios based on the

sugar content, specific surface area and water binding capacity for cell walls were calculated (Table 4.1). A large diversity was obtained on two major parameters, namely (i) the nature and levels of cell wall polymers and (ii) physical characteristics, which further varied independently in this series of cell walls. Concerning the chemical composition and physical structure, apple cell walls were characterized by high xylose content, signaling presence of xylogalacturonans and fucogalactoxyloglucans (Le Bourvellec, Guyot, et al., 2004; Renard, Voragen, Thibault, & Pilnik, 1990, 1991), with intermediate specific surface area and relatively high water-binding capacity. Only beet cell walls contained detectable ferulic acids. They also had the highest content of pectic neutral sugar side-chains, notably arabinans, and the highest acetyl contents, with a high specific surface area. Kiwifruit cell walls appeared to be the richest in homogalacturonans (conservely, contained pectins with the highest linearity), with the lowest side-chain, arabinose/galactose ratio and acetyl content, with a relatively low specific surface area.

All these characteristics were further modulated after processing at different pH values. For example, at pH 2.0, arabinan or galactan side-chains in the cell walls were lost due to acid hydrolysis, while galacturonic acid and DM were retained to the greatest extent possible. β -elimination reduced the content of galacturonic acid and esterification (DM and Ac.A) in the cell walls after modification at pH 6.0. Pectin depolymerization was least significant and structural modification modest (both acid hydrolysis and β -elimination) at pH 3.5. Different pH modifications enhanced or reduced, to varying degrees, the porosity/specific surface area and water-binding capacity of the cell walls. The ferulic acid cross-linked to the cell wall was present only in the beet cell wall.

Therefore, a large diversity of structural features was obtained in the cell wall set for structure linearity, branching degree and length of side-chains, arabinose/galactose ratio, degree of methylation and acetylation, specific surface area and water-binding capacity. In addition, these factors, which were assigned to the cell wall to influence their interactions, showed varying degrees of importance.

Cell wall-procyanidin interactions

Table 4.1 Characteristic chemical content, sugar ratios, specific surface area and water binding capacity of the different cell wall components from apple, beet and kiwifruit.

Samples	Gal A/ (Rha+Ara+Gal)	Gal A/Rha	(Ara+Gal)/Rha	Ara/Gal	Xyl/Man	FA* (mg/g)	DM* (%)	Ac.A* (mg/g)	BET (m ² /g)	WBC (g/g)
ACN	1.2	12.4	9.5	1.2	4.9		82	21	5.4	7.8
AC2	1.6	13.0	7.3	0.5	4.9		86	19	1.1	8.5
AC3	0.9	9.1	9.3	1.1	5.1		89	19	1.5	5.9
AC6	0.7	8.9	11.7	1.2	5.0		60	18	2.6	3.9
BCN	0.7	12.3	16.0	4.2	0.7	7.0	65	45	4.5	3.7
BC2	0.9	12.1	12.5	2.4	0.8	7.7	58	41	6.3	7.7
BC3	0.5	8.5	16.3	4.0	0.8	9.6	72	39	2.4	4.2
BC6	0.4	8.9	19.7	4.3	0.8	8.8	42	32	16.7	6.0
KCRN	2.7	28.7	9.5	0.2	2.5		67	11	1.3	5.6
KCR2	2.3	26.5	10.7	0.2	2.6		62	12	0.5	8.0
KCR3	1.5	18.2	11.0	0.3	2.9		70	11	5.9	6.0
KCR6	1.1	15.6	13.4	0.2	2.6		69	11	7.0	6.6
KCON	4.1	38.4	8.4	0.4	2.9		72	11	0.3	4.6
KCO2	2.4	33.4	12.9	0.2	2.6		58	13	1.3	6.9
KCO3	2.2	30.4	13.0	0.3	2.6		65	11	11.4	5.9
KCO6	1.6	18.2	10.4	0.3	2.4		55	11	0.6	4.0
<i>Pooled SD</i>	<i>0.1</i>	<i>1.9</i>	<i>0.9</i>	<i>0.03</i>	<i>0.1</i>	<i>0.2</i>	<i>4.1</i>	<i>0.8</i>	<i>-</i>	<i>1.2</i>

Ratios are calculated using the yields of neutral sugar expressed in mol%. Ratios Gal A/(Rha+Ara+Gal) is characteristic for linearity of pectin. Gal A/Rha for contribution of homogalacturonans to pectin. (Ara+Gal)/Rha for branching of RG-I. Ara/Gal for the proportion of arabinans/galactans. Xyl/Man for contribution of mannans to hemicelluloses. Gal A: galacturonic acid, Rha: rhamnose, Ara: arabinose, Gal: galactose, Man: mannose, Xyl: xylose. DM: degree of methylation. FA and Ac.A: ferulic acid and acetic acid content, respectively. BET and WBC are characteristic for specific surface area and water-binding capacity, respectively. AC: apple cell wall, BC: beet cell wall, KC: kiwifruit cell wall, pH values-: 2: pH 2.0, 3: pH 3.5, 6: pH 6.0. Maturity-: R: –Ripe, O: –Overripe. Pooled SD: pooled standard deviation. * data adapted from (X. Liu, Renard, Rolland-Sabaté, Bureau, et al., 2021b).

4.1.3.2 Global characterization by ATR-FTIR spectroscopy

ATR-FTIR can be used to detect changes in the main components of cell wall polysaccharides as well as their modification by other components (X. Liu, Renard, Bureau, & Le Bourvellec, 2021b). On the principal component analysis, the first two principal components (PC1 48.5 % and PC2 22.7 %) explained 71.2% of the total variance (Fig. 4.1A). Cell walls, cell wall-procyanidin DP12/39 complexes and procyanidins were separated into three distinct groups. Within the cell wall-procyanidin group, complexes constituted two distinct subgroups: cell wall associated with a low procyanidin concentration (0.25 g/l and 1 g/l) and a high procyanidin concentration (6 g/l and 12 g/l). A gradation of the groups was observed along the PC1 from the left to the right with the increasing of procyanidin concentration.

No clear discrimination according to botanical origins, processing conditions or procyanidin sizes was obtained. The loadings on PC1 and PC2 revealed similar patterns and some relevant wavenumbers (Fig. 4.1B). Along the PC1 axis, the samples were distributed owing to the presence or absence of procyanidins (Fig. 4.1A). PC1 separated cell walls on the left bottom, cell wall-procyanidin complexes in the middle and purified procyanidins on the right bottom according to the presence of linked procyanidins or/and purified cell wall/procyanidin complexes. The negative loadings of PC1 were characterized by the peaks at 1740 and 1015 cm^{-1} which could be due to pectic compounds. Positive loadings for PC1 concerned wavenumbers mostly characteristic of procyanidins (1604, 1519, 1440, 1284 and 1196 cm^{-1}), which progressively increased from 0.25 g/l to 12 g/l. PC2 allowed discrimination between apple/beet cell wall-procyanidin complexes and kiwifruit cell wall-procyanidin complexes in the middle of plot (Fig. 4.1A).

4.1.3.3 Binding isotherms

The binding isotherms of all cell wall-procyanidin complexes (DP12 and DP39) were obtained by placing the suspended cell walls in contact with procyanidin solutions. The isotherms are illustrated by the Langmuir formulations (Eq. (2)) in Fig. 4.2 and the

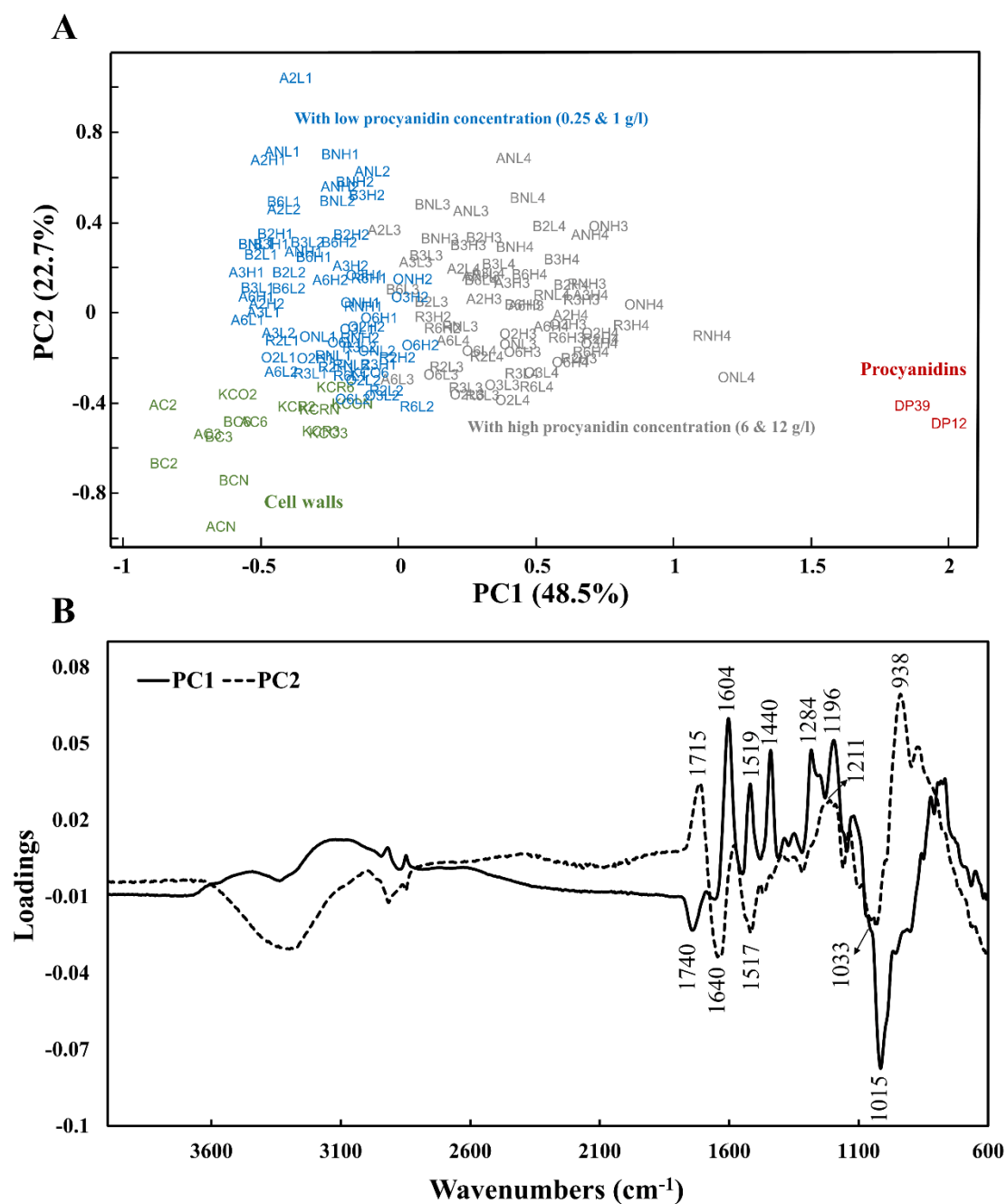


Figure 4.1 Principal component analysis of infrared spectra on cell walls, procyanidins and their complexes. A) Sample map; B) Loading profile of components PC1 and PC2 in the range of 4000 - 600 cm^{-1} . A(C): apple cell wall, B(C): beet cell wall, (KC)R: kiwifruit cell wall (ripe), (KC)O: kiwifruit cell wall (overripe), L/H1: 0.25 g/l DP12/39, L/H2: 1 g/l DP12/39, L/H3: 6 g/l DP12/39, L/H4: 12 g/l DP12/39, N: native, pH values-: 2: pH 2.0, 3: pH 3.5, 6: pH 6.0. Maturity-: R: -Ripe, O: -Overripe.

Langmuir parameters (K_L and N_{max}) were calculated (Table 4.2), both in the form of per g or per m^2 of adsorbent. The data were fitted satisfactorily ($r^2 > 0.85$) using the Langmuir isotherm formula. The amount of adsorbed procyanidins increased with their concentration and finally reached a plateau at high concentrations indicating cell wall saturation (Fig. 4.2).

4.1.3.3.1 Interactions with Procyanidins of DP 12

Isotherm curves varied depending on the composition and the structure of the cell walls (Fig. 4.2). For the isothermal adsorption curve of procyanidin DP12, beet cell walls had the highest saturation level (plateau of the curve) of bound procyanidins and the highest affinity (slope of the curve) together with apple cell walls. Moreover, after processing, two distinct changes could be noted between chemical compositions and physical surface morphology for different cell walls: ACs, BC2/3 and KCOs cell walls were characterized by a decrease of bound procyanidin after modification. This may be attributed to the loss of pectins from the native cell walls. By contrast, affinity increased for KCOs and BC6, which may be due to an increase of their specific surface area after processing, thus increasing their adsorption capacity for the procyanidin DP12. The Langmuir constants (K_L and N_{max}) obtained after fitting confirmed these results (Table 4.2A).

The different chemical compositions and physical surface morphologies observed between botanical origins and after processing had an impact on both apparent affinity (K_L) and apparent saturation level (N_{max}). ACN, BC3, KCRN, KCR6 and KCON/2/3 had close K_L values between 0.21 L/g and 0.29 L/g, while their apparent saturation level (N_{max}) ranged from 0.39 to 0.75 g/g. These could be due to two contrasting observations: (i) either all their features were at an intermediate level, e.g., ACN with moderate pectin linearity (homogalacturonan chains), neutral sugar side-chains and specific surface area; or (ii) they combined features at the two extremes, e.g., KCON had the highest pectin linearity and the lowest specific surface area. BC6 with the highest specific surface area (16.7 m^2/g) had the highest affinity ($K_L=0.54$ L/g). This may be due to the fact that the

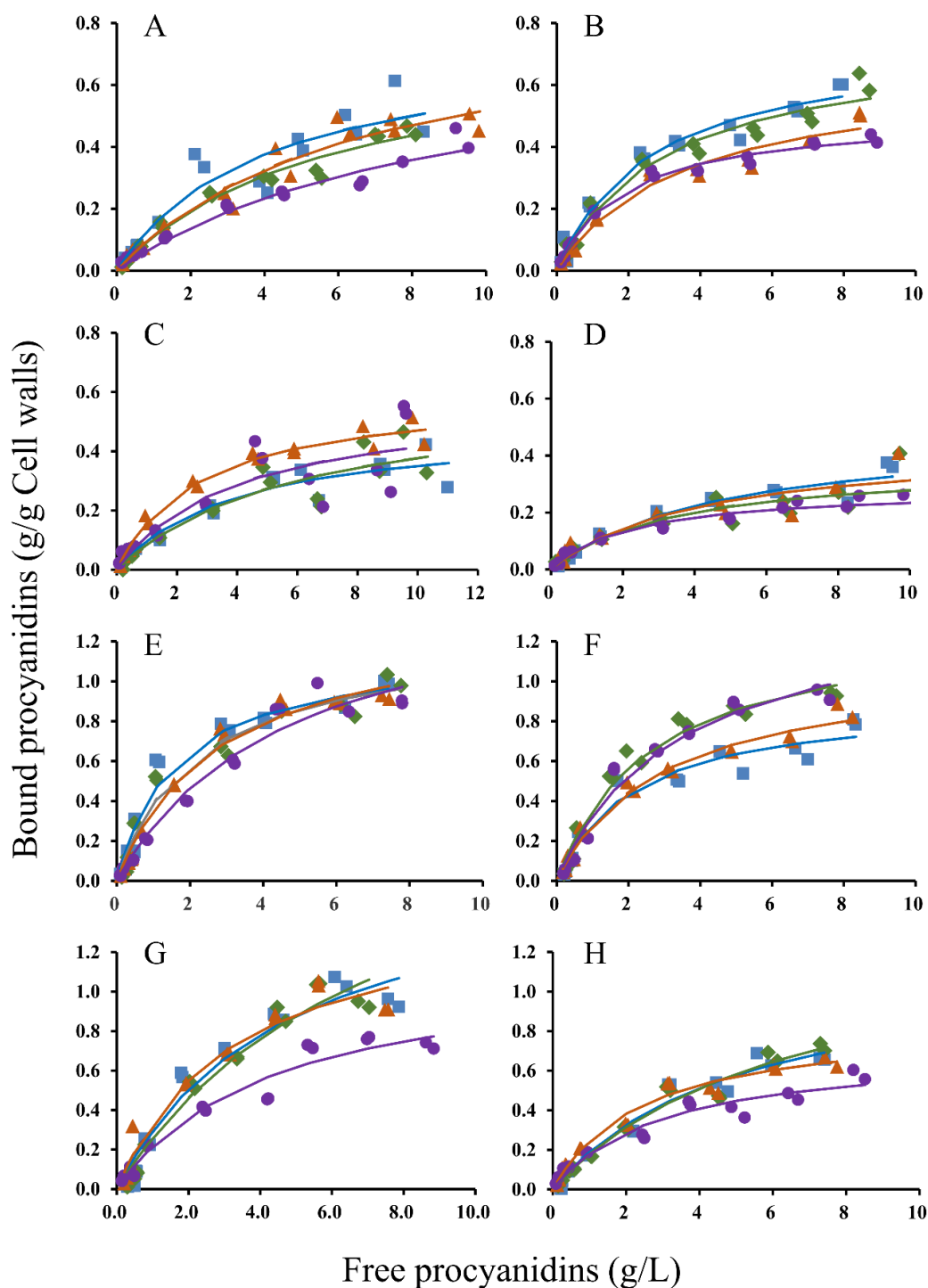


Figure 4.2 Binding isotherms for cell walls and procyanidins at pH 3.8, ionic strength 0.1 M, 25 °C. A: experimental curve for ACs-DP12 complexes, B: experimental curve for BCs-DP12 complexes, C: experimental curve for KCRs-DP12 complexes, D: experimental curve for KCOs-DP12 complexes, E: experimental curve for ACs-DP39 complexes, F: experimental curve for BCs-DP39 complexes, G: experimental curve for KCRs-DP39 complexes, H: experimental curve for KCOs-DP39 complexes. The points and lines are the corresponding Langmuir adsorption isotherms for which the calculated parameters are given in Table 2 for different cell walls: ■ and — Native cell walls, ◆ and — Cell walls modified at pH 2.0, ▲ and — Cell walls modified at pH 3.5, ● and — Cell walls modified at pH 6.0.

Table 4.2 Binding isotherms between cell walls and procyanidins DP12 and 39: A) Apparent Langmuir parameters for binding isotherms of different cell walls with varying concentrations of procyanidin DP12 and DP39, and B) Procyanidin retention and free procyanidins characteristics at 1 g/L of procyanidins and 5 g/L of cell walls.

A										
	Procyanidin DP12					Procyanidin DP39				
	K_L (L/g)	N_{max} (g/g)	K_L (L/m ²)	N_{max} (g/m ²)	R^2	K_L (L/g)	N_{max} (g/g)	K_L (L/m ²)	N_{max} (g/m ²)	R^2
ACN	0.25±0.09	0.75±0.13	0.05±0.02	0.14±0.02	0.91	0.6±0.10	1.18±0.07	0.11±0.02	0.22±0.01	0.96
AC2	0.17±0.03	0.75±0.08	0.15±0.03	0.68±0.07	0.98	0.46±0.09	1.23±0.09	0.42±0.08	1.12±0.08	0.96
AC3	0.16±0.04	0.85±0.12	0.11±0.03	0.57±0.08	0.96	0.36±0.05	1.34±0.07	0.24±0.03	0.89±0.05	0.99
AC6	0.11±0.03	0.76±0.12	0.04±0.01	0.29±0.06	0.97	0.21±0.05	1.56±0.17	0.08±0.02	0.60±0.07	0.97
BCN	0.38±0.06	0.75±0.05	0.08±0.01	0.17±0.01	0.97	0.46±0.10	0.91±0.07	0.10±0.03	0.20±0.02	0.95
BC2	0.33±0.06	0.75±0.05	0.06±0.01	0.12±0.01	0.97	0.37±0.06	1.32±0.09	0.06±0.01	0.21±0.02	0.97
BC3	0.28±0.05	0.65±0.05	0.12±0.02	0.27±0.02	0.97	0.34±0.05	1.09±0.06	0.14±0.03	0.45±0.04	0.98
BC6	0.54±0.05	0.51±0.01	0.03±0.01	0.03±0.01	0.99	0.29±0.05	1.43±0.12	0.02±0.01	0.09±0.01	0.98
KCRN	0.25±0.07	0.49±0.06	0.19±0.05	0.38±0.05	0.93	0.21±0.06	1.73±0.25	0.16±0.05	1.33±0.19	0.95
KCR2	0.17±0.07	0.6±0.13	0.34±0.14	1.20±0.26	0.89	0.13±0.04	2.18±0.42	0.26±0.08	4.36±0.84	0.97
KCR3	0.35±0.05	0.6±0.03	0.06±0.01	0.10±0.01	0.98	0.3±0.08	1.47±0.17	0.05±0.02	0.25±0.03	0.95
KCR6	0.25±0.14	0.58±0.13	0.04±0.02	0.08±0.02	0.89	0.23±0.06	1.15±0.12	0.03±0.01	0.16±0.02	0.96
KCON	0.21±0.05	0.49±0.05	0.70±0.17	1.63±0.17	0.96	0.19±0.05	1.17±0.14	0.63±0.17	3.90±0.47	0.97
KCO2	0.29±0.12	0.37±0.06	0.22±0.09	0.28±0.04	0.85	0.15±0.03	1.36±0.17	0.12±0.02	1.05±0.13	0.98
KCO3	0.24±0.09	0.44±0.07	0.02±0.01	0.04±0.01	0.89	0.41±0.06	0.85±0.05	0.04±0.01	0.07±0.01	0.98
KCO6	0.45±0.09	0.29±0.02	0.75±0.15	0.48±0.03	0.95	0.34±0.08	1.11±0.07	0.57±0.12	1.88±0.2	0.95

(Continued)

Cell wall-procyanidin interactions

Table 4.2 (Continues)

B	Procyanidin DP12			Procyanidin DP39		
	Bound procyanidins (g/g CW)	% of initial PCA	\overline{DPn} of Free PCA	Bound procyanidins (g/g CW)	% of initial PCA	\overline{DPn} of Free PCA
ACN	0.083	44%	3.7	0.148	61%	15.7
AC2	0.078	40%	4.5	0.120	70%	20.8
AC3	0.075	36%	4.4	0.113	59%	15.1
AC6	0.061	32%	4.5	0.104	55%	16.4
BCN	0.085	51%	3.8	0.116	59%	20.7
BC2	0.086	45%	3.8	0.110	55%	16.4
BC3	0.067	42%	4.2	0.111	55%	12.4
BC6	0.091	53%	4.2	0.108	54%	15.7
KCRN	0.071	38%	4.4	0.091	47%	19.7
KCR2	0.069	37%	4.1	0.084	46%	16.7
KCR3	0.083	41%	4.3	0.100	57%	21.9
KCR6	0.077	41%	4.4	0.112	64%	21.5
KCON	0.063	35%	4.5	0.104	57%	20.8
KCO2	0.077	42%	4.3	0.104	48%	14.1
KCO3	0.090	47%	4.2	0.126	69%	14.4
KCO6	0.071	40%	4.3	0.114	61%	18.5
<i>Pooled SD</i>	<i>0.002</i>	<i>0.01</i>	<i>0.2</i>	<i>0.003</i>	<i>0.02</i>	<i>1.0</i>

Average of duplicates for each; uncertainty on the parameters of the Langmuir isotherms in Table 4.2A was calculated using the Marquardt estimation approach, precision on the analytical results in Table 4.2B using pooled standard deviation. \overline{DPn} : number-average degree of polymerization of procyanidins, K_L : apparent affinity constant, N_{max} : apparent saturation level. AC: apple cell wall, BC: beet cell wall, KC: kiwifruit cell wall, pH values-: 2: pH 2.0, 3: pH 3.5, 6: pH 6.0. Maturity-: R: –Ripe, O: –Overripe. Pooled SD: pooled standard deviation.

morphology of large specific surface area favors the stacking of intermediate-size procyanidins. Conversely, AC2/3/6 and KCR2 had relatively low affinity (≤ 0.17 L/g) and high saturation level (≥ 0.70 g/g), which may be explained by the fact that they had at least two of the following features, namely relatively low pectin linearity, low specific surface area, low degree of methylation or high xylose contents.

The apparent Langmuir parameters were also converted as a function of the amount of procyanidins bound per cell wall surface area (Table 4.2B). This expression had most impact on the relative ranking of cell walls which had a larger specific surface area. An increase of cell wall surface area was accompanied by a decrease of K_L and N_{\max} related to cell walls with lower surface areas so to their physical characteristics.

Table 4.2B also provides cell wall-procyanidin interaction characteristics (the amount of bound procyanidins and $\overline{DP}n$ of free procyanidins). The average amount of bound procyanidins varied between 0.061 g/g cell wall (AC6) and 0.091 g/g (BC6), corresponding to 32 % and 53 % of the initial added procyanidins. Different levels of bound procyanidins were found for each cell wall. The binding levels of native cell walls could be ranked: $ACN \approx BCN > KCRN > KCON$. For AC2/3/6 and BC2/3, the amount of bound procyanidins decreased after pH modifications, while conversely for BC6, KCR3/6 and KCO2/3/6 it increased. Cell walls with higher specific surface area had a higher affinity for procyanidin DP12. The initial procyanidin fractions were more polymerized ($\overline{DP}n = 12$) than the free procyanidins remaining in the supernatant ($3.7 < \overline{DP}n < 4.5$) after interaction. Therefore, all cell walls were selective for highly polymerized procyanidins.

4.1.3.3.2 Interactions with Procyanidins of DP 39

The binding isotherms for cell walls and procyanidin DP 39 are presented in Fig. 4.2 Compared to procyanidin DP 12, the amount of bound procyanidins were higher for the highly polymerized fractions (DP 39). Binding isotherms demonstrated the key role of the $\overline{DP}n$ in modulating the interactions between cell walls and procyanidins. The calculated apparent constants are given in Table 4.2 For ACs, BCN/2/3, and KCO3,

higher apparent affinities (K_L) were obtained when \overline{DPn} increased. However, for BC6, KCRs and KCON/2/6, lower apparent affinities (K_L) were obtained when \overline{DPn} increased. In these cell walls, high content of neutral sugar side-chains, both low degree of methylation and specific surface area may limit their affinity. Their apparent saturation levels (N_{max}) were higher than those of procyanidins of low \overline{DPn} (Table 4.2). These binding isotherms did not reach a stable plateau (Fig. 4.2), probably due to a lack of data in the high concentration range, i.e., above the limit of procyanidin solubility.

The average amount of bound procyanidins varied between 0.084 g/g cell wall (KCR2) and 0.148 g/g (ACN), corresponding to 46 % and 61 % of the initial used procyanidins (Table 4.2B). The binding levels of native cell walls decreased in the following order: ACN > BCN > KCON > KCRN. For AC2/3/6, BC2/3/6 and KCR2, the amount of bound procyanidins decreased after pH modifications, while it increased for KCR3/6 and KCO2/3/6. The initial procyanidin fractions were more polymerized ($\overline{DPn} = 39$) than the free procyanidins remaining in the supernatant ($12.4 < \overline{DPn} < 21.9$). This again indicated that all cell walls were selective for highly polymerized procyanidins.

4.1.3.4 Isothermal titration calorimetry

4.1.3.4.1 Interactions with Procyanidins of DP12

Thermodynamic parameters from ITC titration of cell walls by procyanidins DP12 are shown in Table 4.3. Typical thermograms were obtained for all cell walls (ca. 8 mg) titrated by procyanidin DP12 (30 M epicatechin equivalent) with strong exothermic peaks (data not shown). Stoichiometry (defined as ratio of epicatechin/galacturonic acid) was fixed at 0.1 for all cell walls (1 molecule of epicatechin bound 10 units of galacturonic acid) using a one-site model. This value was determined from previous studies (Brahem et al., 2019).

The association constant ranged between $1.0 \times 10^2 \text{ M}^{-1}$ and $3.2 \times 10^3 \text{ M}^{-1}$ and the top three highest affinities decreased in the following order: ACN > KCRN > KCON (Table

4.3). ACN with a low (Ara+Gal)/Rha ratio (9.5), both medium Gal A/(Rha+Ara+Gal) ratio (1.2) and specific surface area (5.4 m²/g), and a high DM (82 %) (Table 4.1) had the highest affinity for procyanidin DP12, showing that a combination of positive factors contributed to its high interactions. Similarly, KCRN and KCON had a high pectin linearity (homogalacturonan chains) and a low degree of branching, and they also contained a high affinity component, i.e., kiwifruit pectins as shown by Liu, Renard, Rolland-Sabaté, Bureau, et al. (2021). For ACN/2/6, BC6, KCRN and KCON/6, analysis of the thermodynamic contributions ($\Delta G = \Delta H - T\Delta S$) related to the exothermic reactions indicated a strong entropy contribution ($-T\Delta S$ from -18 to -9 kJ/mol) showing that the interactions were mostly driven by entropy. This indicated that the binding system was mostly driven by hydrophobic interactions. By contrast, the enthalpy contributions were high for AC3, BCN/2/3, KCR2/3/6 and KCO2/3 (ΔH from -46 to -12 kJ/mol) indicating that the interactions were mostly driven by hydrogen bonds.

4.1.3.4.2 Interactions with procyanidins of DP 39

Titration of all cell walls by procyanidins DP39 showed complex curves characterized by strong exothermic peaks. Thermodynamic parameters are shown in Table 4.3. To avoid over-fitting, the stoichiometry (n) was also fixed at 0.1 for all cell walls to allow fit and determination of association parameters.

The association constant K_a between cell walls and procyanidins DP39 ranged from $1.0 \times 10^2 \text{ M}^{-1}$ to $1.6 \times 10^3 \text{ M}^{-1}$ in the decreasing order: KCO2/6 > KCR6 > ACN > AC3 > KCR2 \approx AC2 > KCRN/3 \approx KCON/3 > AC6 \approx BCN/2/3/6. The affinity of the beet cell walls was generally low. Regarding the interactions between all cell walls and procyanidins DP39, contribution of enthalpy (ΔH from -4 to -26 kJ/mol) related to the exothermic reactions indicated that the interactions were mostly driven by hydrogen bonds due to the high number of hydroxyl groups in procyanidins DP39.

Cell wall-procyanidin interactions

Table 4.3 Thermodynamic parameters of interactions between cell walls and procyanidins DP12 and DP39 (30 mM (-)-epicatechin equivalent) measured by Isothermal Titration Microcalorimetry.

	Procyanidin DP12						Procyanidin DP39				
	n	K _a (M ⁻¹)	ΔH (kJ/mol)	ΔS (J/mol/K)	ΔG (kJ/mol)	-TΔS (kJ/mol)	K _a (M ⁻¹)	ΔH (kJ/mol)	ΔS (J/mol/K)	ΔG (kJ/mol)	-TΔS (kJ/mol)
ACN	0.1	3180	-1.38	62.44	-19.99	-18.62	1087	-4.36	43.50	-17.33	-12.97
AC2	0.1	1056	-7.42	33.01	-17.26	-9.84	752	-8.13	27.79	-16.42	-8.29
AC3	0.1	375	-11.96	9.16	-14.69	-2.73	932	-8.20	29.33	-16.95	-8.75
AC6	0.1	1166	-7.05	35.05	-17.51	-10.45	275	-15.19	-4.24	-13.92	1.27
BCN	0.1	179	-14.20	-4.50	-12.86	1.34	251	-12.34	4.57	-13.70	-1.36
BC2	0.1	395	-11.00	12.81	-14.82	-3.82	191	-16.19	-10.64	-13.02	3.17
BC3	0.1	208	-22.17	-29.98	-13.23	8.94	119	-33.72	-73.35	-11.85	21.87
BC6	0.1	1690	-6.25	40.85	-18.43	-12.18	212	-22.01	-29.28	-13.28	8.73
KCRN	0.1	2848	-7.46	41.11	-19.72	-12.26	451	-18.39	-15.29	-15.15	3.24
KCR2	0.1	693	-22.09	-19.71	-16.22	5.87	717	-18.52	-7.45	-16.30	2.22
KCR3	0.1	840	-32.74	-53.81	-16.69	16.05	444	-26.48	-38.12	-15.11	11.37
KCR6	0.1	951	-46.09	-97.56	-17.00	29.09	1334	-12.61	17.53	-17.84	-5.23
KCON	0.1	2273	-8.49	35.80	-19.16	-10.68	526	-12.75	9.33	-15.53	-2.78
KCO2	0.1	895	-19.41	-8.59	-16.85	2.56	1589	-4.07	47.60	-18.27	-14.21
KCO3	0.1	1188	-28.99	-38.37	-17.55	11.44	562	-22.73	-23.61	-15.69	7.04
KCO6	0.1	2180	-0.82	61.18	-19.06	-18.24	1527	-6.62	38.73	-18.17	-11.55
<i>Pooled SD</i>	-	256	1.1	2.1	0.3	0.6	104	0.8	2.1	0.2	0.6

Average of duplicates for each. $\overline{DP}n$: number-average degree of polymerization of procyanidins, K_a: affinity level, n: stoichiometry, ΔH: enthalpy, ΔG: free enthalpy, ΔS: entropy. AC: apple cell wall, BC: beet cell wall, KC: kiwifruit cell wall, pH values-: 2: pH 2.0, 3: pH 3.5, 6: pH 6.0. Maturity-: R: -Ripe, O: -Overripe.

4.1.4 Discussion

4.1.4.1 Comparison of spectroscopy, calorimetry and binding isotherm methods

Using ATR-FTIR, isothermal titration calorimetry and binding isotherm, cell walls with different levels of porosity, pectin linearity (homogalacturonan chains), side-chain abundance, and degree of esterification were shown to interact with procyanidins (DP12 and DP39). The spectra of procyanidins DP12 and DP39 were close, as well as for other procyanidin fractions, e.g., pear procyanidins (Brahem et al., 2019). Therefore, the following characteristic spectra can be used to distinguish between initial cell walls and cell wall-procyanidin complexes. Bands at 1604, 1519 and 1440 cm^{-1} can be attributed to C=C and C-C stretching bond vibrations in typical aromatic rings (Alfaro-Viquez, Esquivel-Alvarado, Madrigal-Carballo, Krueger, & Reed, 2020; Edelmann, Diewok, Schuster, & Lendl, 2001). Bands at 1284 and 1196 cm^{-1} can be assigned to phenolic OH and C-O group deformation vibrations and bending vibrations (Velasco et al., 2014).

Binding isotherms of cell wall-procyanidin interactions were well described by previous research as type I isotherms (the so-called Langmuir isotherms), e.g., apple, pear and grape cell walls (Bindon et al., 2012; Brahem et al., 2019; Le Bourvellec, Guyot, et al., 2004; Le Bourvellec & Renard, 2005; Renard et al., 2001c). However, this fit is an empirical description and is not equivalent to the same mechanism described by Langmuir (Langmuir, 1918) for the adsorption of gases on solid surfaces. This method can provide some adsorption parameters and behaviors. The amount of procyanidins (DP12 and 39) bound to each cell wall ranged from 61 mg/g cell wall to 148 mg/g cell wall, with an apparent affinity constant range of 0.11 to 0.60 L/g. Their interactions detected by ITC seem to be exothermic, and driven by both entropy and enthalpy contributions, which are caused by hydrophobic interactions (or changes in solvation and conformation) and hydrogen bonds, respectively (Leavitt & Freire, 2001; X. Liu et al., 2020; Poncet-Legrand, Gautier, Cheynier, & Imberty, 2007). The order of magnitudes of their affinity constant (K_a) ranged from 10^2 to 10^3 M^{-1} . These three

methods are complementary: (i) rapid and sensitive to detect the presence of procyanidins in complexes (ATR-FTIR); (ii) allowing determination of the binding parameters, e.g., bound amount, K_L and N_{max} (binding isotherms); (iii) enabling access to thermodynamic (enthalpy/enthalpy) changes, i.e., mechanism, and K_a /affinity (ITC).

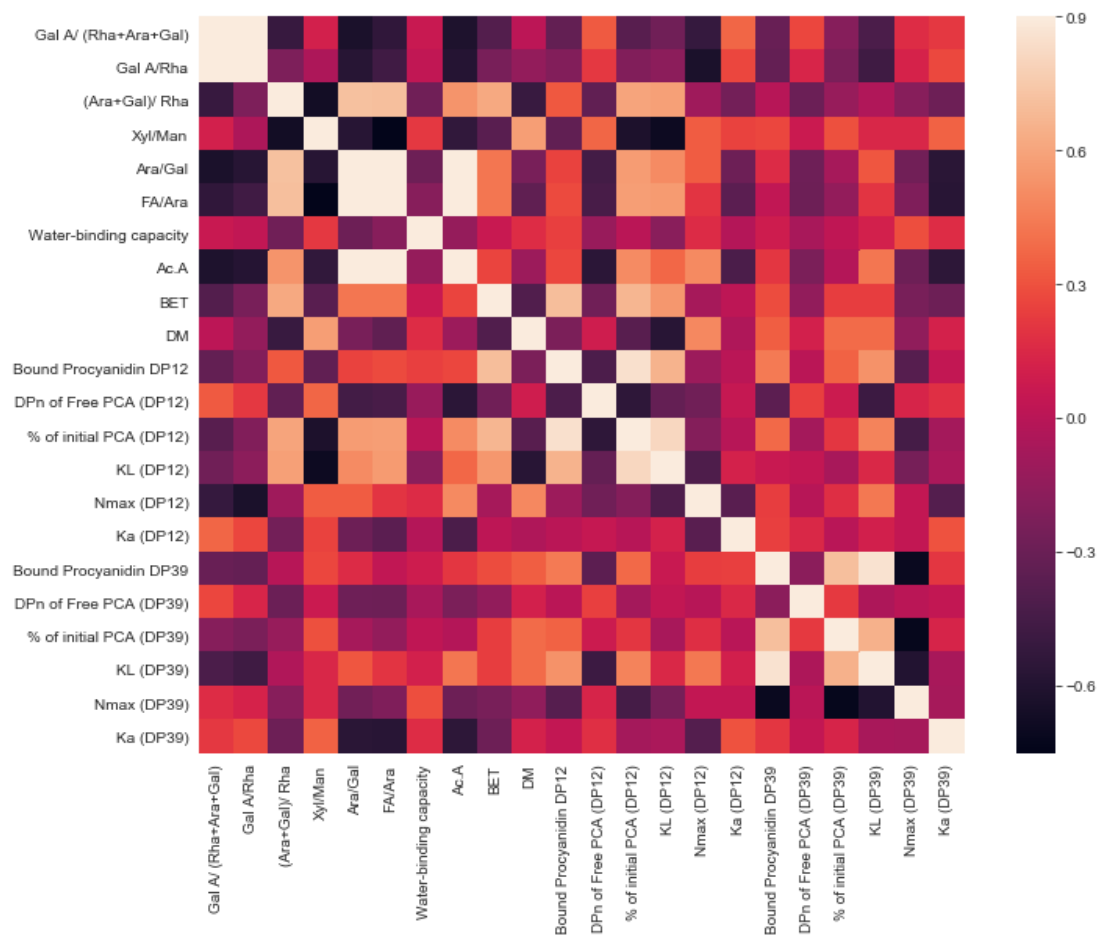


Figure 4.3 Correlation matrix heatmap between carbohydrate compositions and structural characteristics of cell walls and binding properties after interaction with procyanidins. Ratios Gal A/(Rha+Ara+Gal) is characteristic for linearity of pectin. Gal A/Rha for contribution of homogalacturonans to pectin. (Ara+Gal)/Rha for branching of RG-I. Ara/Gal for the proportion of arabinans/galactans. Xyl/Man for contribution of mannans to hemicelluloses. DM: degree of methylation. FA and Ac.A: ferulic acid and acetic acid content, respectively. BET and WBC are characteristic for specific surface area and water-binding capacity, respectively.

The above indicators are the main evaluation parameters indicating the strength of the interactions. The effect of different cell wall composition/structure on the interactions was assessed by PCA and correlation analysis. The PCA results are presented in [Supplementary Fig. 4.1](#). PC1 and PC2 explained 52% of the total variance

of cell wall characteristics and their interaction with procyanidin DP12 and DP39. According to [Supplementary Fig. 4.1](#), some interaction parameters were distributed separately for different procyanidins, implying that the mechanisms of interaction may be different. This was also reflected in the correlation analysis ([Fig. 4.3](#)). To be specific, the linearity of pectin was correlated with K_a (by ITC) for procyanidin DP12 and 39. This suggested a significant contribution of homogalacturonan content to the affinity. In addition, porosity/surface area (by BET) showed correlation with bound procyanidin DP12 and their K_L (DP12, binding isotherms) and moderate correlation with bound procyanidin DP39 and their K_L (DP39, binding isotherms). This inferred that low polymerized procyanidins are more readily bound by porous cell walls, whereas high polymerized procyanidins may be restricted. Although side-chain abundance and ferulic acid content showed some correlation with K_L , these factors are detrimental to the interactions. This implied that porosity was probably antagonistic to side-chain abundance and ferulic acid content, but that porosity played a dominant role in cell wall-procyanidin interactions.

4.1.4.2 Pectin content and linearity in cell walls

Firstly, during heat treatment at different pH, cell walls are modified so that a portion of the soluble polysaccharides are extracted giving extractable pectins. The second point to note is that irrespective of the pectin content of the cell wall starting material, the main goal of our study was to determine the effect of the chemical composition and physical structure of the cell wall on their binding properties for procyanidins. This is because the changes in cell wall adsorption of procyanidins resulting from pectin extraction are already reflected in cell wall modifications. That is, not only the composition changes, but also the porosity of the cell wall increases (i.e., enables more internal cavities) or decreases (i.e., cell wall collapse or shrinkage) with the difference in the original structure or the treatment conditions.

The higher affinities for procyanidins DP12/39 were obtained for mostly unmodified cell walls, with both higher K_a and more bound procyanidins. In contrary,

lower affinities were observed for most modified cell walls. This confirms the findings of Ruiz-Garcia et al. (2014) who suggested that the removal of pectin significantly reduces the adsorption of proanthocyanidins by cell wall residues, however, despite pectin elimination the cell wall still have an affinity for procyanidins (Le Bourvellec et al., 2012a). Native cell walls (A/B/KC/KOCN) exhibited the highest extractable pectin contents, while the modified cell walls, to varying degrees, lost extractable pectins (loss ratio pH 6.0 > 3.5 > 2.0). Extractable pectins have a high binding capacity and affinity for procyanidins (Le Bourvellec et al., 2005, 2012a; X. Liu et al., 2020; Ruiz-Garcia et al., 2014). Pectin content and linearity did not make a significant difference to the binding capacity, i.e., K_L obtained using binding isotherms, of different cell walls with procyanidins, as other factors are also involved in the regulation of their interactions. The affinity K_a (obtained using ITC) of beet cell walls was relatively lower than that of apple and kiwifruit cell walls. This may be due to their complex arabinan side-chain structures and the presence of ferulic acid covalently linked to arabinans that limit interactions (P. A. R. Fernandes et al., 2020; X. Liu, Renard, Rolland-Sabaté, & Le Bourvellec, 2021; Watrelot et al., 2014). Binding isotherms appear to be more sensitive than ITC to factors influencing interactions, as they could take into account the physical aspects of the binding.

Different conditions of processing or treatments can also significantly influence interactions. For example, pH 2.0 modification caused removal of most of the neutral sugar side-chains while degrees of methylation remained high, thus increasing the linearity of pectin and homogalacturonan content with high DM in the A/B/KC/KOC2 cell walls. This structure probably caused AC2 and BC2 to bind more procyanidins by stacking than after the other pH treatments, obtained by binding isotherms. However, this trend was not evident for the affinity K_a results obtained by ITC. For kiwifruit cell walls, no relevant pattern was found, probably due to the fact that pH modification did not drastically affect the linearity of pectins insofar as the initial kiwifruit pectins are already linear with low side-chain content, and the other physical factors (e.g., porosity) could also combine to influence this result (X. Liu et al., 2020).

4.1.4.3 Surface area/porosity

BC6, with the lowest pectin linearity and DM, and the highest side-chains and branching ratios, could be expected to have the lowest binding capacity and affinity to procyanidins. This was not the case, however, as it had a relatively high binding capacity and affinity for the procyanidin DP12. This may be attributed to the fact that BC6 had the highest specific surface area (16.7 m²/g), i.e., the highest porosity, of all cell walls. Solvent exchange drying increased the porosity of the cell walls, which could allow encapsulation of the procyanidins in a more open conformation (Le Bourvellec et al., 2012a). The remodeling and loosening of the grape cell wall due to ripening also increased the porosity of cell walls, leading to an increase in the adsorption of proanthocyanidins (Bindon et al., 2012). The porosity of cell walls of different tissues also varies considerably, for example, the stone cells of pears are secondary cell walls with a dense structure and less porosity, and therefore have a lower affinity for procyanidins (Brahem et al., 2019).

Despite the high porosity of BC6, its binding capacity and affinity for procyanidin DP39 was not better than that for DP12. This could be attributed not only to its high branching ratio preventing the entry of larger molecules of procyanidin DP39, but also to the size and type of pore. In general, the limiting pore size of the cell wall is about 5 nm (equivalent to the size of DP34) (Carpita et al., 1979), while the pores may have slits, interstices, spherical, cylindrical, and conical forms (X. Liu et al., 2020). These two factors may conjointly modulate the interaction between cell walls with different porosity and procyanidins with different sizes. The water-binding capacity of the cell walls, regulated by porosity levels and cell wall components (Klaassen & Trindade, 2020; Paudel, Boom, van Haaren, Siccama, & van der Sman, 2016), may influence their capacity to adsorb procyanidins, but no causal link can be established between the two at this point. Notedly, the specific surface areas given here are measured as dry matter and may differ in aqueous media, thus the next important work should be to focus on the wet porosity.

4.1.4.4 Substitution of the galacturonic acids

Highly methylated pectin has already been demonstrated to have a high affinity with highly polymerized procyanidins (X. Liu et al., 2020; Watrelot et al., 2013). However, this result may be counterbalanced by other factors in the cell wall. The cell walls modified at pH 6.0, i.e., AC/BC/KCR/KCO6, had the lowest pectin DM in each species due to β -elimination. The binding capacity and affinity of these cell walls for procyanidins were not always the least (Tables 4.2 and 4.3). Other cell wall components, e.g., cellulose and hemicelluloses, as well as their physical characteristic like porosity, may combine to influence the final interactions.

Beet cell walls had the highest acetic acid content, but it appears not to be a positive factor for interactions. This may be related to a reduction in potential binding sites. Likewise, anthocyanins bind more to low-esterified beet and citrus pectins than to highly esterified pectins (A. Fernandes et al., 2020; Larsen et al., 2019). The reduction in acetic acid increased the number of hydroxyl groups available on the surface, while alleviating the hindrance of groups at adjacent positions on the binding surface, therefore potentially facilitating the accumulation of procyanidins on the cell wall surface.

4.1.4.5 Degree of polymerization of procyanidins

Generally, the higher the degree of polymerization of procyanidins, the stronger the interaction with cell walls. For example, the cell walls have higher binding capacities and affinities for the procyanidin DP39 than for DP12 (Table 4.2). This may be due to the higher number of hydroxyl groups and aryl rings, allowing a higher number of hydrogen bonds and hydrophobic interaction sites. However, there were two trends in the affinity of cell walls for procyanidin DP39. AC3, BCN, KCR2/6 and KCO2 had a higher affinity for DP39 than DP12 by ITC, but ACN/2/6, BC2/3/6, KCRN/3 and KCON/3/6 had a lower affinity for DP39 than DP12 by ITC. It is likely that both porosity and chemical composition were responsible for this result. As discussed in the previous section on porosity, cell walls such as KCR/ON (ca. 1 m²/g)

had a very low porosity and larger procyanidins might not easily enter inside their internal pores. On the other hand, BC2/3/6 had high neutral sugar side-chain branching ratio, together with high ferulic acid content (Table 4.1). Therefore, this structure might cross-link the side-chains and hindered the available binding sites limiting their interaction with procyanidin DP39. Moreover, the change in entropy/enthalpy also explains this result, as only hydrogen bonding drives the interaction with procyanidin DP39, while both hydrophobic interactions and hydrogen bonds for DP12.

Notably, the natural cell wall architecture and organization are also a very important factor, i.e., cell wall matrix interactions (Varner & Lin, 1989). For example, natural pectins can also strongly interact with other cell wall components, such as cellulose, which may limit their potential for interactions with other biomolecules (Broxterman & Schols, 2018). Similarly, the presence of many other covalent or non-covalent interactions such as interactions between cellulose, xyloglucan/xylan and RG-I side-chains, may also limit the exposure of binding sites (Ralet et al., 2016; Zykwiniska et al., 2005). However, the extent to which these interactions may vary in different plant cell walls may also be an important factor in their interaction with polyphenols. Therefore, future work will require a more precise identification of the architecture and conformation of the cell wall.

4.1.5 Conclusions

Cell walls from apple, beet and kiwifruit have different levels of binding selectivity depending on their chemical composition and physical structure. For extractable polysaccharides (soluble state), e.g., pectins, the linearity and degree of methylation were important, but for native and modified cell walls (insoluble state), porosity appears to be a major factor. Binding isotherms play an essential role in the study of physical adsorption. The ranking of factors affecting cell wall selectivity were, for those which favor interactions, high porosity (including the size and type) and pectin linearity and homogalacturonan content (as synergists), while high xylose, ferulic acid and acetic acid contents, and pectin branching were detrimental (as antagonists). Further work is

needed to confirm the role of wet porosity (i.e., in suspension) of cell walls.

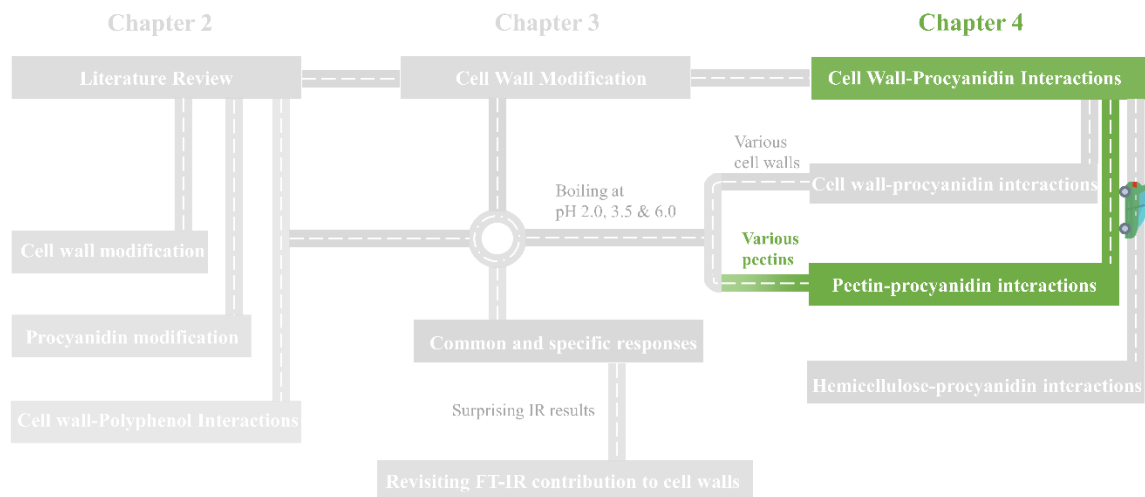
The cell wall structure is generally altered during food processing and digestion. Each cell wall has its own unique chemical composition, molecular architecture and physical structure, and has common and specific responses to processing and digestion. All these factors interact with each other to impact the interactions. Understanding the relations between the chemical and physical factors remains a huge challenge, and more work is needed to clarify the mechanisms involved and internal relationships. Systematic studies of interactions between biomacromolecules allows to better establish a bridge between food processing and the binding/retention of bioactive substances in food industry.

Highlights

- Porosity, sugar ratio, and pectin contents of cell walls influence procyanidin adsorption.
- Highly porous cell walls interact strongly with oligomeric procyanidins.
- High DP might hinder procyanidins' binding specifically to beet cell walls.
- Branching of pectins, xylose, ferulic and acetic acids limit interactions.

Section 4.2

Exploring interactions between pectins and procyanidins: Structure-function relationships



A version of this section has been published as:

Liu, X., Renard, M. G. C. C., Rolland-Sabaté, A., & Le Bourvellec, C. (2021). Exploring interactions between pectins and procyanidins: Structure-function relationships. *Food Hydrocolloids*, 113, 106498.

In this study, the effect of native pectin's structural features (both composition and spatial conformation) on their interactions with procyanidins were systematically investigated. These pectins with different HG / RG ratios, side-chains and esterification were prepared by extraction from apple, beet and kiwifruit (at two maturities) cell walls at pH 2.0, 3.5, and 6.0.

This allowed to answer the following questions:

- ※ How naturally extracted pectins of different structures interact with procyanidins?
- ※ Which structures of pectin are conducive to their interactions with procyanidins?
- ※ Which structures of pectins limit their interaction with procyanidins?

During fruit and vegetable processing, procyanidins interact with cell walls and form complexes, which further impact their potential health effects. Among cell wall polysaccharides, pectins have the highest affinity for procyanidins. Binding of two procyanidin fractions with twelve pectins of different linearity and size was investigated by ITC, UV-Visible spectrophotometry and HPSEC-MALLS. Pectins interacted preferentially with highly polymerized procyanidins except beet pectins probably because of steric hindrance due to abundant feruloylated arabinans. Linear pectins had higher affinity for procyanidins: this was verified both for comparison between botanical origins (kiwifruit > apple > beet pectins) and between extraction conditions. Debranched pectins, extracted at pH 2.0, had higher affinity and aggregation capacities with procyanidins than those extracted at other pHs. However, the factors affecting pectins of different origins seemed to be different. High molar mass, intrinsic viscosity and hydrodynamic radius contributed more to increased adsorption of procyanidins by apple and beet pectins. Highly linear kiwifruit pectins, with high homogalacturonan content and lower branching ratio bound preferentially to procyanidins. The enthalpy/entropy proportion of the interaction between kiwifruit pectins and procyanidins was higher than that of apple and beet pectins, which suggested more hydrogen bonding. Predominance of homogalacturonan regions and high degree of methylation thus appeared key structural features of pectins for high affinity for procyanidins, while high degree of branching was detrimental. These findings provide the structural foundation for selectivity of interactions in molecular-level.

4.2 Exploring interactions between pectins and procyanidins: Structure-function relationships

4.2.1 Introduction

In plant-based food systems (such as fruits, vegetables, and grains), secondary metabolites (e.g., polyphenols) and macromolecules (e.g., proteins and polysaccharides) coexist in strictly compartmented parts of the plant cells and commonly come in contact with each other during processing, mastication and digestion (Le Bourvellec et al., 2019; Le Bourvellec & Renard, 2012). Structure-function relationships of the main non-digestible biologically active components in plant-based functional foods, polysaccharides and polyphenols, may be regulated by their interactions (Dobson et al., 2019; Kardum & Glibetic, 2018). Dietary polysaccharide-polyphenol interactions might affect the physical properties of polysaccharides, e.g., texture and stability, in food systems (Jin et al., 2020; X. Li et al., 2019; X. Liu et al., 2020; Tudorache & Bordenave, 2019; Tudorache et al., 2020) as well as their biological activity (Le Bourvellec et al., 2019). In addition, the bioaccessibility, bioavailability and bioefficacy of polyphenols depends on their interaction with other food ingredients, e.g., dietary fiber in particular (Ribas-Agustí et al., 2018). Such dietary fibers, e.g., apple matrix, apple cell wall (Le Bourvellec et al., 2019; Monfoulet et al., 2020) and pure cellulose (Phan et al., 2020), can be used as a carrier for polyphenols to transport these antioxidants to the human gut microbiota and further produce beneficial physiological effects after their fermentation in small phenolic compounds (Loo et al., 2020; Saura-Calixto, 2011).

Plant polyphenols have at least one aromatic ring and one or more hydroxyl groups (phenol group), ranging from simple phenolic acids to complex flavonoids. Procyanidins, also known as condensed tannins, are a type of proanthocyanidins and in particular they have a high affinity for polysaccharides. They are polymers and oligomers of catechin/epicatechin (flavan-3-ol units) and most commonly connected by B-type bonds, namely C4-C8 or C4-C6 interflavanic linkages with a number average

degree of polymerization (\overline{DPn}) varying between 2 and more than 100 (Guyot, Marnet, & Drilleau, 2001). The interactions between macromolecules and procyanidins are dependent on their structural characteristics, i.e. molar mass, interflavanic bonds, the presence of galloyl groups and conformation (Le Bourvellec & Renard, 2019; X. Liu et al., 2020). In general, their affinity for polysaccharides increases with their \overline{DPn} and molar mass (Le Bourvellec, Guyot, et al., 2004; Le Bourvellec & Renard, 2005, 2012b; Mamet et al., 2018; Renard et al., 2001c). For example, procyanidins have been demonstrated to bind strongly to pectins, a major constituent of most fruit and vegetable plant cell walls (Le Bourvellec & Renard, 2005; X. Liu et al., 2020; Renard et al., 2001c). Increasing the level of galloylation of procyanidins also enhances their affinity with pectins due to the increased number of hydroxyl groups and aromatic rings (Le Bourvellec, Guyot, et al., 2004; McManus et al., 1985; Tang et al., 2003). (+)-Catechin and polymers composed mainly of (+)-catechin units bind more to polysaccharides than (-)-epicatechin and polymer composed mainly of (-)-epicatechin due to the stereochemistry of flavan-3-ols pyran rings (Le Bourvellec, Guyot, et al., 2004).

Pectins are complex polysaccharides widely found in primary plant cell walls, and are acid hetero-polysaccharides. The pectic polysaccharides contain three main structural units as follows. Homogalacturonan (HG) is a long and smooth chains of linear α -1,4-linked D-galacturonic acid, in which most of the C-6 carboxyl groups are methyl-esterified and some of the secondary alcohols at the O-2 and/or the O-3 positions may be acetyl-esterified (Caffall & Mohnen, 2009; Mohnen, 2008; Ridley, O'Neill, & Mohnen, 2001a). Rhamnogalacturonan-I (RG-I) is composed of a backbone of repeating units of galacturonic acid and rhamnose linked by α -1,2 and α -1,4 glycosidic bonds: $[\rightarrow 4)\text{-}\alpha\text{-D-GalpA-(1}\rightarrow 2)\text{-}\alpha\text{-L-Rhap-(1}\rightarrow]$ and may be substituted at the O-2 and/or the O-3 positions of α -L-rhamnose residues (Mohnen, 2008; Voragen, Coenen, Verhoef, & Schols, 2009). Rhamnogalacturonan II (RG-II), making up $\sim 10\%$ of pectins, is the most structurally complex and branched polysaccharide in this family of pectic polysaccharides (Caffall & Mohnen, 2009; Ridley et al., 2001a). The highly complex polymer structure of RG-II is composed of an HG backbone of seven to nine

(and most probably more) 1,4-linked α -D-Gal-A residues including four side chains clearly consisting of 12 different kinds of monosaccharides through more than 20 different linkages (Pérez, Rodríguez-Carvajal, & Doco, 2003). Pectins with high degree of methylation (DM) display the strongest affinity for procyanidins due to hydrophobic interactions, while highly branched pectins have more limited interactions with procyanidins, probably due to steric hindrance (Watrelet et al., 2013, 2014). Pectins, especially HG, are susceptible to various enzymatic and non-enzymatic conversion reactions during processing of plant-based products, modifying their structure and, hence, their physicochemical properties (Dongowski, 2001; Fraeye et al., 2007; Renard & Thibault, 1996), which in turn may affect their interaction with procyanidins (Le Bourvellec et al., 2012).

Interactions of procyanidins has been studied with pectins of different commercial origins (apple or citrus) or with pectin structural units. Higher affinities were recorded for citrus pectins or for highly methylated homogalacturonans (Watrelet et al., 2013), while type I rhamnogalacturonans with different side-chains (Watrelet et al., 2014) or arabinans (P. A. R. Fernandes et al., 2020) had lower affinities. Also, different pectin components will interact in a complex manner determining the fine structure of the biopolymer (e.g., hydrogen, hydrophobic, or ionic bonding) and its spatial conformation (Janaswamy & Chandrasekaran, 2005; Pérez, Mazeau, & Hervé du Penhoat, 2000) that will further affect their interaction with procyanidins (Watrelet et al., 2014). However, there is little systematic information on the effect of native pectin's structural features (both composition and spatial conformation) on their interaction with procyanidins, particularly involving combinations of light scattering and spectroscopy techniques, and together with thermodynamics. Therefore, the determination of the impact of conformational properties and composition of pectins is crucial. To do this, pectins differing for their main structural features, i.e., molar mass, size, proportion of branching, length and content of HG, HG / RG ratio and degrees of methylation and acetylation, were used to gain in-depth understanding of the structure/function relationships that govern their interactions with procyanidins. For this, a series of

twelve pectins with different HG / RG ratios, side-chains and esterification was prepared by extraction from apple, beet and kiwifruit (two maturities for kiwifruit) cell walls at pH 2.0, 3.5, and 6.0. These twelve different pectins were incubated with procyanidins solutions of intermediate and high \overline{DP}_n , DP9 and DP79, respectively. Interactions were characterized by aggregates formation using UV-visible spectroscopy and by isothermal titration calorimetry. The pectin macromolecular characteristics before and after interactions were determined by size-exclusion chromatography coupled with multi-angle laser light scattering and viscometric detections to better understand the selectivity of their interactions with procyanidins. A deep understanding of the molecular mechanisms that drive the interaction between pectins and procyanidins can enable us to better bridge the gap between food processing and the bioavailability of commensal microbiota fermentation products of pectin and procyanidins. Further, this promotes the design of more rational processing conditions and healthier and more nutritious foods.

4.2.2 Materials and methods

4.2.2.1 Standards and Chemicals

Ethanol and acetone were provided from Fisher Scientific (Strasbourg, France). Acetonitrile, methanol of HPLC grade were obtained from VWR International (Radnor, USA). Hexane was from Merck (Darmstadt, Germany). Sugar standards (arabinose, fucose, galactose, xylose, mannose and rhamnose) were from Fluka (Buchs, Switzerland). Methanol- d_3 was from Acros Organics (Geel, Belgium). Formic acid, chlorogenic acid, benzyl mercaptan, sodium carbonate, sodium hydroxide, $NaBH_4$, N-methylimidazole, acetic anhydride, toluene- α -thiol, (+)-catechin and (-)-epicatechin were from Sigma-Aldrich (Saint Quentin Fallavier, France). 4-Coumaric acid was obtained from Extrasynthese (Lyon, France). Phloridzin was obtained from Fluka (Buchs, Switzerland).

4.2.2.2 Extraction, purification and characterization of procyanidins

4.2.2.2.1 Plant material

Apple fruits (*Malus × domestica* Borkh.) from the ‘Marie Menard’ and ‘Avrolles’ cider cultivars were harvested at maturity (after starch regression) in the experimental orchard of the Institut Français des Productions Cidricoles (Sées, Orne, France). Fruits were mechanically cored and a formic acid solution (10 mL/L) was sprayed on the fresh material to avoid phenolic oxidation. Cortex tissues were then frozen, freeze-dried, and stored at -20 °C until used.

4.2.2.2.2 Procyanidin extraction and purification

Apple polyphenols were extracted from the freeze-dried apple powder (150 g) sequentially by hexane, methanol and aqueous acetone according to a procedure described by (Guyot, Marnet, & Drilleau, 2001). Hexane and methanol extracts were discarded as they did not contain the required procyanidin fractions and to eliminate lipids, sugars, organic acids and phenolic compounds of low molar mass. Aqueous acetone extracts containing procyanidins were pooled and concentrated on a rotary evaporator prior to freeze-drying. The freeze-dried aqueous acetone extracts were dissolved (100 g/L) in water acidified with formic acid (99.9:0.1, v/v), centrifuged (16 800 x g, 15 min) and then filtered. They were injected on a 20×5 cm column of LiChrospher 100 RP-18 (12 µm, Merck, Darmstadt, Germany) and purified as described by Brahem, Renard, Bureau, Watrelot, & Le Bourvellec (2019). Procyanidin fractions were concentrated on a rotary evaporator then freeze-dried and stored under vacuum at -80 °C until used. The purified procyanidin fractions are designated as DP9 (from ‘Marie Ménéard’) and DP79 (from ‘Avrolles’).

4.2.2.2.3 Procyanidin characterizations

Procyanidins were analyzed by high-performance liquid chromatography (HPLC) with diode array detection (DAD) with or without thioacidolysis as described by Guyot et al. (2001). Analysis was performed using the ultra-fast liquid chromatography and

controlled by LC Solution software (Shimadzu Prominence system, Kyoto, Japan). The system was operated by two LC-20AD pumps Prominence LC UFLC, a DGU-20A5 Prominence degasser, a SIL-20AHT Prominence autosampler, a CTO-20AC Prominence column oven, an SPD-M20A Prominence diode array detector and a CBM-20A Prominence communication bus module. Separations were achieved as described in Le Bourvellec et al. (2011). The average degree of polymerization of procyanidins (\overline{DP}_n) was calculated as the molar ratio of all flavan-3-ol units (thioether adduct plus terminal units minus (+)-catechin and (-)-epicatechin naturally present in the samples and determined by analysis of the samples without thiolysis) to (+)-catechin and (-)-epicatechin corresponding to the terminal units minus (+)-catechin and (-)-epicatechin naturally present in the samples and determined by analysis of the samples without thiolysis.

4.2.2.3 Preparation of pectin fractions

Pectins from apple (A-), beet (B-) and kiwifruits (K-) (ripe R- and overripe O-) were prepared as described by (X. Liu, Renard, Rolland-Sabaté, Bureau, & Le Bourvellec, 2021a). Cell walls were isolated from the parenchyma of the different edible plant materials as alcohol insoluble solids. Subsequently, pectins were extracted from each cell wall material by boiling for 20 min in a citrate-phosphate solution (0.1 M) at three pH values: 2.0, 3.5 and 6.0. Thus, twelve pectin fractions were obtained. That is, apple, beet, kiwifruit (ripe) and kiwifruit (overripe) pectins extracted at pH 2.0/3.5/6.0 were designated AP2/3/6, BP2/3/6, KPR2/3/6 and KPO2/3/6, respectively. The purpose of this step is to obtain pectins of different compositions and structures.

4.2.2.4 Initial and free pectin macromolecular characteristics

The pectins (2.5 g/L) were analyzed by High Performance Size-Exclusion Chromatography coupled with Multi-Angle Laser Light Scattering (HPSEC-MALLS) after being filtered as described by Liu et al. (2021). Samples (100 μ L) were injected and the mobile phase was 0.1 M citrate/phosphate buffer with pH 3.8, and eluted at 0.6 mL/min. The system comprised three HPSEC columns (PolySep-GFC-P3000, P5000

and P6000, 300 × 7.8 mm) and a guard column from Phenomenex (Le Pecq, France) maintained at 40 °C, a MALLS detector (DAWN HELEOS 8+ fitted with a K5 flow cell and a GaAs laser ($\lambda = 660$ nm), a Viscostar III viscometer, both from Wyatt Technology Corporation (Santa Barbara, CA, USA), a diode array detector (SPD-M20A) and a fluorescence detector (RF-20A) set at 360 nm (280 nm excitation) and a refractive index detector (RID-10A) from Shimadzu (Shimadzu Prominence system, Kyoto, Japan).

M_i and R_{Gi} , the molar mass and the radius of gyration at each slice of the chromatogram, was determined using the concentration (calculated from the refractometric signal) and the light scattering signal from 5 angles (from 20.4° to 90°) and data extrapolation to zero angle using the Zimm formalism with a one order polynomial fit (A. Rolland-Sabaté et al., 2004) using ASTRA® software from Wyatt Technology Corporation (version 7.1.4 for PC). R_{hi} , the viscometric hydrodynamic radius at each slice of the chromatogram for the equivalent sphere, was calculated by combining viscosity and molar mass measurements using the following equation derived from the Einstein and Simha relation (Einstein, 1906, 1911; Simha, 1940):

$$[\eta]_i M_i = \gamma N_A V_{hi} = \frac{10\pi}{3} N_A R_{hi}^3 \quad (1)$$

where $[\eta]_i$ and V_{hi} are the intrinsic viscosity and the hydrodynamic volume at each slice of the chromatogram, $\gamma = 2.5$ for spheres and N_A the Avogadro number.

The z-average intrinsic viscosity ($[\overline{\eta}]_z$), z-average and weight average viscometric hydrodynamic radii (\overline{R}_{Hz} and \overline{R}_{Hw}) and weight-average molar mass (\overline{M}_w) were established using the averaging described in Rolland-Sabaté *et al.* (A. Rolland-Sabaté et al., 2004; A. Rolland-Sabaté, Mendez-Montealvo, Colonna, & Planchot, 2008) on the whole peaks. A value of 0.146 mL/g was used as the refractive index increment (dn/dc) for glycans and the normalization of photodiodes was achieved using a low molar mass pullulan standard (P20) from Showa Denko K.K. (Tokyo, Japan). The average apparent molecular density (\overline{d}_{Happ}) was calculated using the following equation:

$$\bar{d}_{Happ} = \overline{M_w} / (4\pi/3) * \bar{R}_{Hw}^3 \quad (2)$$

The log-log plot of hydrodynamic radius versus the molar mass and the Mark-Houwink-Sakurada plot were established for each sample by using the data taken at each slice of the chromatogram. The power law exponent (α) can be calculated according to the following equations:

$$[\eta]_i = K_a M_i^\alpha \quad (3)$$

where K_a is a constant and α is the hydrodynamic coefficient which depends on the polymer shape in the solvent.

4.2.2.5 Phase Diagram

The formation of aggregates was analyzed by spectrophotometry during the pectin-procyanidin interactions as described by Watrelot et al. (2013). All measurements were done in duplicates. The turbidity measurements were carried out with a SAFAS flx-Xenius XM spectrofluorimeter (SAFAS, Monaco) at 650 nm on a 96-well microplate at 25 °C. A serial procyanidin solutions (0, 0.03, 0.06, 0.12, 0.24, 0.47, 0.94, 1.875, 3.75, 7.5, 15 and 30 mM (-)-epicatechin equivalent for ‘Avrolles’; 0, 0.06, 0.12, 0.24, 0.46, 0.94, 1.875, 3.75, 7.5, 15, 30 and 60 mM (-)-epicatechin equivalent for ‘Marie Ménard’) and pectins (0, 0.015, 0.03, 0.06, 0.24, 0.94, 3.75 and 15 mM galacturonic acid equivalent for ‘Avrolles’; 0, 0.03, 0.06, 0.24, 0.94, 3.75, 15 and 30 mM galacturonic acid equivalent for ‘Marie Ménard’) were prepared along the lines and columns, respectively. Solutions were prepared in citrate/phosphate buffer at pH 3.8, 0.1 M ionic strength. Equal amounts (50 μ L) of pectins and procyanidins solutions were mixed and stirred for 20 s before each measurement. Controls were a line or column containing only procyanidins or pectins in buffer. After spectra were collected, microplates were centrifuged 10 min at 2100 x g. Supernatants of control wells (pectins at 15/30 mM in buffer, named S1A) and (procyanidins at a concentration of 30/60 mM, named S1B) and supernatants of wells containing procyanidins at a concentration of 30/60 mM with pectin at a concentration of 15/30 mM (named S2) were analyzed using High-Performance Liquid Chromatography with Diode Array Detection (HPLC-DAD)

and High Performance Size-exclusion Chromatography coupled with Multi-Angle Laser Light Scattering (HPSEC-MALLS). ($\Delta M_w = S2-S1A$) and ($\Delta DP_n = S2-S1B$) were used to define qualitative changes in weight-average molar mass of pectins and in number average degree of polymerization of procyanidins, respectively.

4.2.2.6 Isothermal Titration Calorimetry (ITC)

The entropy and enthalpy changes caused by the interactions between procyanidins and pectins were determined by ITC, using TAM III microcalorimeter (TA instruments, New Castle, USA). Purified procyanidins (60 mM in (-)-epicatechin equivalent) and pectins (7.5 mM galacturonic acid equivalent) were dissolved in the same citrate/phosphate buffer pH 3.8, 0.1 M ionic strength. The reference cell was filled by water. All solutions were degassed prior to measurements. The pectin solution was placed in the 850 mL sample cell of the calorimeter and the procyanidin solution was loaded into the injection syringe and titrated into the sample cell by 50 injections of 5 μ L. Each injection lasted 5 s, with separating delay of 20 min. The content of the sample cell was stirred throughout the experiment at 90 rev/min. The raw ITC data as a plot of heat flow (microjoules per second) against time (minutes) were then integrated peak-by peak and normalized to obtain a plot of observed enthalpy change per mole of injectant (ΔH , kJ/mol) against the molar ratio (epicatechin/galacturonic acid). Peak integration was performed and the experimental data were fitted to a theoretical titration curve using the instrument software (NanoAnalyze 3.10.0). Control experiments include the titration of procyanidin fractions into buffer and are subtracted from titration experiments. The thermodynamic parameters including binding stoichiometry (n), binding constant (K_a), enthalpy (ΔH) and entropy (ΔS), the 'S' shape curve as adjustable parameters. Experiments were carried out in duplicates.

4.2.2.7 Statistical analysis

Results were expressed as mean values, and their reproducibility was presented as the pooled standard deviation (Pooled SD). For each series of repeated samples, the pooled SDs were calculated using the sum of their respective variances multiplied by

their respective degrees of freedom (Box et al., 1978b). Principal Component Analysis (PCA) was realized using the functions of the library FactoMineR and Factoextra in R statistical software (R Core Team., 2014). Correlation matrix map was performed with Python 3.5 software using the Seaborn package (Waskom, 2014).

4.2.3 Results

4.2.3.1 Structure and composition of fractions

4.2.3.1.1 Procyanidins

The two apple varieties ‘Marie M nard’ and ‘Avrolles’ were chosen to obtain two purified fractions of intermediate and high degree of polymerization, respectively (Le Bourvellec et al., 2009). The composition of isolated apple phenolic fractions is shown in [Table 4.4](#). The purified extracts from ‘Marie M nard’ and ‘Avrolles’ contained ca. 700 mg/g of polyphenols, mainly procyanidins plus traces of flavan-3-ol monomer i.e. (-)-epicatechin, hydroxycinnamic acids, i.e., 5'-caffeoylquinic acid and *p*-coumaroylquinic acid, dihydrochalcones, i.e., phloretin xyloglucoside and phloridzine, and a mix of flavonols. ‘Marie M nard’ and ‘Avrolles’ procyanidins were characterized by $\overline{DP}_n = 9$ and 79, respectively. Both were constituted by more than 98 % (-)-epicatechin units and contained a homologous structure differing by their degree of polymerization. All the results were consistent with Le Bourvellec et al. (2004) and (2012).

4.2.3.1.2 Pectins

Detailed compositions of the pectins are available in X. Liu et al. (2021) and the sugar ratios based on the sugar content and macromolecular characteristic for pectins are calculated in [Table 4.4](#). HPSEC chromatograms and molar mass distributions of the pectins are presented in [Fig. 4.4](#). Structural diversity was obtained on two major parameters, namely (i) the nature and composition of side-chains and (ii) macromolecular characteristics, which varied independently in this series of pectins (as described by principal component analysis loading and sample plots in [Supplementary](#)

Fig. 4.2). Concerning the neutral sugar side chain abundance and composition, apple pectins were characterized by high xylose, signaling presence of xylogalacturonans (Schols, Bakx, Schipper, & Voragen, 1995). Only beet pectins contained detectable ferulic acid, and they had the highest content of neutral sugars, notably arabinose, and highest degree of acetylation. Kiwifruit pectins appeared to be the richest in homogalacturonans, with the lowest arabinose content and arabinose to galactose ratio. All these characteristics were further modulated by the pH used for pectin solubilization, with pectins solubilized at pH 2.0 displaying the most extreme characteristics for their respective origins. Unsaturated double bonds resulting from β -elimination have been detected in AP6, BP6, KPR6 and KPO6 (X. Liu, Renard, Rolland-Sabaté, Bureau, et al., 2021b), leading to reduction of the HG chain length and its potential binding sites after pH 6.0 treatment.

Further information on pectin conformations in solution, calculated by plotting the molar mass versus the intrinsic viscosity obtained with HPSEC-MALLS, is given in Table 4.5. Two regions were used to determine the Mark-Houwink-Sakurada conformation parameters at different peaks. In the main peak, the exponent α varied between 0.96 and 1.32 indicating an organization close to stiff coils in a good solvent (Flory, 1953), with various chain flexibility in agreement with literature data (Fishman, Chau, Kolpak, & Brady, 2001), excepted for AP2 ($\alpha = 0.55$) which exhibited a value corresponding to random coil conformation in a θ solvent. Most pectins (except AP2) also presented a less important fraction (generally shoulder in the chromatogram from 20 – 23 mL, Fig. 4.4) exhibiting a spheroidal or denser conformation (Table 4.5) (α between 0 and 0.41) that could correspond to branched aggregates or more folded conformation (Alba, Bingham, Gunning, Wilde, & Kontogiorgos, 2018; Lopez-Torrez, Nigen, Williams, Doco, & Sanchez, 2015). This minor fraction represented a higher proportion in AP6 and KPRs (Fig. 4.4) and seemed to correspond to the main peak in AP2. The lower values of the exponent α (0.55) thus obtained for the main peak in AP2 could be due to a more folded molecule, and this intermediate value (between the sphere and the rod) was most probably caused by the presence of two populations under the

Pectin-procyanidin interactions

Table 4.4 Chemical characteristics of the procyanidins and pectins. A) Composition (mg/g dry matter) of purified acetonetic fraction from ‘Marie Ménéard’ and ‘Avrolles’ apple. B) Composition ratios and pectin region % based on the mol % quantifiable neutral sugars, galacturonic acid and pectin macromolecular characteristics.

A											
	PCA	\overline{DP}_n	Purified PCA constitutive units (%)			EC	DHC	CQA	PCQ	FLV	Total phenolics
			CAT _t	EC _t	EC _{ext}						
Marie Ménéard	680	9	1.5	9.1	89.4	19.4	8.6	34.8	0.5	7.5	751
Avrolles	723	79	0.1	1.2	98.7	0	2.2	6.1	1.3	0	733
<i>Pooled SD</i>	<i>7.9</i>	<i>0.3</i>	<i>0.004</i>	<i>0.3</i>	<i>0.3</i>	<i>0.3</i>	<i>0.6</i>	<i>0.1</i>	<i>0.02</i>	<i>0.05</i>	<i>8.6</i>

B											
	Gal A/Rha	(Ara+Gal)/Rha	Ara/Gal	Xyl* (mg/g)	FA* (mg/g)	DM* (%)	DAC* (%)	\overline{M}_w^* ($\times 10^3$ g/mol)	$[\eta]_z$ (mL/g)	\overline{R}_{Hz} (nm)	\overline{d}_{Happ} (g/mol/nm ³)
AP2	28.8	11.2	2.0	19.3	-	86	17	431	1018	50.4	3.1
AP3	34.6	10.5	2.0	20.6	-	77	15	149	635	31.9	6.2
AP6	27.0	6.6	2.0	11.9	-	95	16	217	265	34.6	21.7
BP2	43.5	37.0	8.4	1.4	8.1	83	67	147	462	28.5	6.7
BP3	55.1	20.4	6.1	1.1	4.3	90	73	117	470	23.9	5.3
BP6	45.3	8.6	3.5	1.1	2.2	81	67	65	198	18.4	18.7
KPR2	56.5	11.6	0.2	7.8	-	73	5	287	426	37.4	9.1
KPR3	66.7	10.2	0.3	4.5	-	75	3	285	500	43.8	8.8
KPR6	35.4	8.1	0.3	4.3	-	79	6	161	195	27.6	23.1
KPO2	91.0	7.3	0.5	9.1	-	82	2	80	258	21.8	20.7
KPO3	68.8	5.8	0.5	8.8	-	82	7	137	378	37.2	22.4
KPO6	42.5	3.9	0.5	6.5	-	81	4	79	289	36.7	56.0
<i>Pooled SD</i>	<i>2.5</i>	<i>0.7</i>	<i>0.1</i>	<i>1.1</i>	<i>0.1</i>	<i>3.3</i>	<i>1.3</i>	<i>11.3</i>	<i>15</i>	<i>1.1</i>	<i>0.5</i>

PCA: procyanidins, \overline{DP}_n : number-average degree of polymerization of procyanidins, CAT_t: terminal (+)-catechin units, EC_t: terminal (-)-epicatechin units, EC_{ext}: extension

(-)-epicatechin units, EC: (-)-epicatechin as flavan-3-ol monomer, DHC: dihydrochalcones, CQA: 5'-caffeoylquinic acid, PCQ, p-coumaroylquinic acid, FLV: flavonols. Ratios are calculated using the yields of neutral sugar expressed in mol%. The ratio between different sugars can contribute to understand information on polymer levels. The ratios of Gal A / Rha, (Ara+Gal) / Rha and Ara / Gal are characteristic for pectin backbone homogalacturonan / rhamnogalacturonan contribution, the branching of RG and the proportion of arabinans / galactans, respectively. Xyl and FA are indicators for the presence of xylogalacturonans and ferulic acids, respectively. DM and DAc are the degree of methylation and acetylation, respectively. \bar{M}_w , weight-average molar mass. $[\eta]_z$, z-average intrinsic viscosity. \bar{R}_{Hz} , z-average hydrodynamic radius. $\bar{d}_{Happ} = \bar{M}_w / (4\pi/3) * \bar{R}_{Hw}^3$, average apparent molecular density. AP: pectins from apple cell wall, BP: pectins from beet cell wall, KP: pectins from kiwifruit cell wall, Gal A: galacturonic acid, Rha: rhamnose, Ara: arabinose, Gal: galactose, pH values-: 2: pH 2.0, 3: pH 3.5, 6: pH 6.0. Maturity-: R: -Ripe, O: -Overripe. * data adapted from (X. Liu, Renard, Rolland-Sabaté, Bureau, et al., 2021b). Pooled SD: pooled standard deviation.

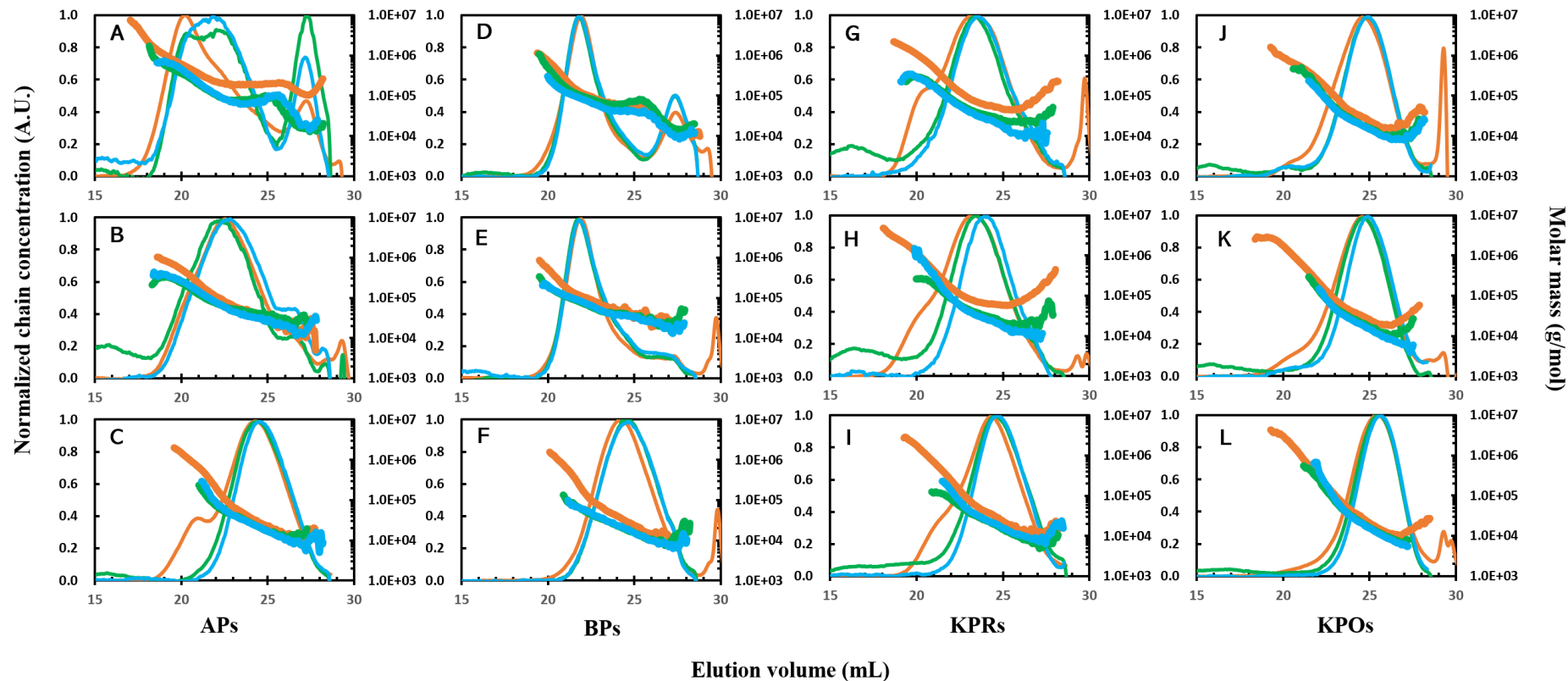


Figure 4.4 HPSEC-MALLS chromatograms and molar mass vs elution volume of the pectin samples. A, B and C: AP2, AP3 and AP6, respectively; D, E and F: BP2, BP3 and BP6, respectively; G, H and I: KPR2, KPR3 and KPR6, respectively; J, K and L: KPO2, KPO3 and KPO6, respectively. Thin orange solid line —: normalized chain concentration of pectins before interaction; Thin green solid line —: normalized chain concentration of free pectins after interaction with DP9; Thin blue solid line —: normalized chain concentration of free pectins after interaction with DP79. Orange thick solid line —: molar mass of pectins before interaction; Green thick solid line —: molar mass of free pectins after interaction with DP9; Blue thick solid line —: molar mass of free pectins after interaction with DP79.

Table 4.5 Relationships between molar masses and intrinsic viscosity.

Samples	Main peak		HMM region	
	M_i range (g/mol)	α	M_i range (g/mol)	α
AP2	2×10^5 - 2×10^6	0.55	NA	NA
AP3	2×10^4 - 2×10^5	1.17	2×10^5 - 2×10^6	0.34
AP6	2×10^4 - 2×10^5	1.07	5×10^5 - 5×10^6	0
BP2	5×10^4 - 2×10^5	1.04	2×10^5 - 2×10^6	0.12
BP3	5×10^4 - 2×10^5	1.16	10^5 - 10^6	0.41
BP6	10^4 - 10^5	0.96	10^5 - 10^6	0.17
KPR2	10^4 - 2×10^5	NA	2×10^5 - 2×10^6	0
KPR3	10^4 - 2×10^5	NA	2×10^5 - 2×10^6	0
KPR6	2×10^4 - 8×10^4	1.16	10^5 - 2×10^6	0
KPO2	10^4 - 7×10^4	1.02	10^5 - 10^6	0.41
KPO3	2×10^4 - 7×10^4	1.32	10^5 - 10^6	0.21
KPO6	10^4 - 6×10^4	0.94	6×10^4 - 10^6	0.17

HMM: high molar mass component. α : hydrodynamic coefficient for a given polymer calculated from the Mark-Houwink -Sakurada equation ($[\eta]_i = K_a M_i^\alpha$) for pectin samples in citrate/phosphate buffer at pH 3.8, 0.1 M ionic strength. $\alpha = 0$: Spheres, 0.5-0.8: Random coils, 1.0: Stiff coils, 2.0: Rods. NA: Not applicable.

main peak, which produced artificially one lower exponent instead of two exponents. Meanwhile, the population of these peaks will undergo some modifications after interaction with procyanidins. Detailed information will be given in the interaction section.

Good diversities and variabilities were obtained in this sample set for pectin linearity, length of side chains, arabinans / galactans ratio, degree of acetylation, molar mass and conformation. No pectins with a low degree of methylation ($DM < 30$) were present. This should not affect the investigation of the subsequent interactions as it has been proved that the affinity of low methylated pectins to procyanidins is very low (Watrelet et al., 2013).

4.2.3.2 Interactions with procyanidins of DP9

4.2.3.2.1 Isothermal titration calorimetry

Thermodynamic parameters from ITC titration of pectins by procyanidins DP9 are shown in [Table 4.6A](#). Typical thermograms were obtained for AP2/3, BP2, KPR2/3/6 and KPO2 (7.5 mM galacturonic acid equivalent) titrated by procyanidin DP9 (60 mM

Pectin-procyanidin interactions

(-)-epicatechin equivalent) with strong exothermic peaks (data not shown). In contrast,

Table 4.6 Thermodynamic parameters of interactions between pectins (7.5 mM galacturonic acid equivalent) and procyanidins DP9 (A) and DP79 (60 mM (-)-epicatechin equivalent) (B) measured by Isothermal Titration Microcalorimetry (ITC).

A								
DP9	n	K _a (M ⁻¹)	ΔH (kJ/mol)	ΔS (J/mol/K)	ΔG (kJ/mol)	-TΔS (kJ/mol)	Enthalpy (%)	Entropy (%)
AP2	0.081	4801	-5.18	53	-21	-16	25	75
AP3	0.108	2035	-1.32	59	-19	-18	7	93
AP6	-	-	-	-	-	-	-	-
BP2	0.088	2177	-1.88	58	-19	-17	10	90
BP3	-	-	-	-	-	-	-	-
BP6	-	-	-	-	-	-	-	-
KPR2	0.137	8160	-6.64	53	-22	-16	30	70
KPR3	0.071	4506	-3.34	59	-21	-18	16	84
KPR6	0.065	4554	-6.64	47	-21	-14	32	68
KPO2	0.111	12060	-6.20	57	-23	-17	27	73
KPO3	-	-	-	-	-	-	-	-
KPO6	-	-	-	-	-	-	-	-
<i>Pooled</i>	<i>0.02</i>	<i>242</i>	<i>0.55</i>	<i>4.5</i>	<i>0.7</i>	<i>0.6</i>	-	-
<i>SD</i>								
B								
DP79	n	K _a (M ⁻¹)	ΔH (kJ/mol)	ΔS (J/mol/K)	ΔG (kJ/mol)	-TΔS (kJ/mol)	Enthalpy (%)	Entropy (%)
AP2	0.442	5588	-2.248	64	-21	-19	11	89
AP3	0.106	3582	-1.422	63	-20	-19	7	93
AP6	0.273	3183	-0.582	65	-20	-19	3	97
BP2	0.356	339	-1.861	42	-14	-13	13	87
BP3	0.614	351	-1.351	44	-15	-13	9	91
BP6	0.161	351	-2.278	39	-15	-12	15	85
KPR2	0.196	10649	-5.944	56	-23	-17	26	74
KPR3	0.100	2125	-2.187	56	-19	-18	12	88
KPR6	0.069	2715	-4.182	51	-19	-15	22	78
KPO2	0.210	12214	-8.019	51	-23	-15	35	65
KPO3	0.145	7090	-1.044	70	-22	-21	5	95
KPO6	0.093	7527	-3.893	61	-22	-18	18	82
<i>Pooled</i>	<i>0.04</i>	<i>443</i>	<i>0.35</i>	<i>6.3</i>	<i>0.5</i>	<i>0.4</i>	-	-
<i>SD</i>								

Average of duplicates for each. n: stoichiometry, K_a: affinity level, ΔH: enthalpy, ΔS: entropy, ΔG: free enthalpy, T: temperature. Enthalpy (%) = ΔH / (ΔH - TΔS) × 100%; Entropy (%) = - TΔS / (ΔH - TΔS) × 100%. Pooled SD: pooled standard deviation.

no titration could be observed for AP6, BP3/6 and KPO3/6 by procyanidin DP9.

Stoichiometry (defined as ratio of (-)-epicatechin/galacturonic acid) was ca. 0.1 for AP2/3, BP2 and KPO2 (1 molecule of (-)-epicatechin bound 10 units of galacturonic acid) and ca. 0.14 for KPR2 (1 molecule of (-)-epicatechin bound 7 units of galacturonic acid) using a one-site model.

4.2.3.2.2 Phase diagram

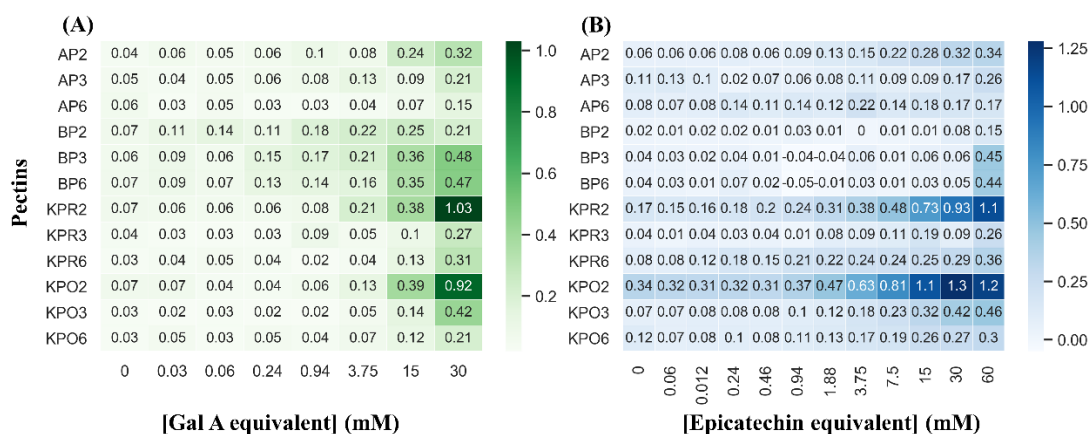


Figure 4.5 Heat map of the turbidity characteristics of pectin-procyanidin DP9 interactions. Absorbance at 650 nm after interactions in 0.1 M citrate/phosphate buffer pH 3.8 (in triplicates). (A) Variation of absorbance of pectins at different concentrations (galacturonic acid equivalent) with procyanidins DP9 (60 mM (-)-epicatechin equivalent). (B) Variation of absorbance of procyanidins DP9 ((-)-epicatechin equivalent) at different concentrations with pectins (30 mM galacturonic acid).

The association constant ranged between $2.0 \times 10^3 \text{ M}^{-1}$ and $1.2 \times 10^4 \text{ M}^{-1}$ and increased in the following order: AP3 \approx BP2 < KPR3 \approx KPR6 \approx AP2 \ll KPR2 \llll KPO2 (Table 4.6A). KPO2 with the highest Gal A/Rha ratio (91) had the highest affinity for procyanidin DP9, showing a strong positive impact of pectin linearity on their ability to interact with procyanidins. Analysis of the thermodynamic contributions ($\Delta G = \Delta H - T\Delta S$) related to the exothermic reactions indicated a strong entropy contribution ($-T\Delta S$ from -18 to -14 kJ/mol) showing that the interactions were mostly driven by entropy, i.e., by hydrophobic interactions and the release of water molecules (Le Bourvellec & Renard, 2012b; Poncet-Legrand et al., 2007; Watrelot et al., 2013, 2014). The enthalpy contributions were very limited for AP3, AP2 and KPR3 (ΔH from -1 to -4 kJ/mol) and higher for AP2, KPR2/6 and KPO2 (ΔH from -6 to -5 kJ/mol) indicating that interactions also involved hydrogen bonds. The proportion of enthalpy for KPR/Os was significantly higher than that of AP3 and BP2 (Table 4.6A) due to hydrogen bonds which increased their affinity for procyanidin DP9.

Fig. 4.5A, B present the heat-map of turbidity at 650 nm. Turbidity of all pectin mixtures with procyanidins DP9 rose with increasing pectin concentrations (Fig. 4.5A). This increase was more marked at 30 mM galacturonic acid equivalent for KPR2 and KPO2, with absorbance values of 1.03 and 0.92, respectively, than for other pectins (absorbance from 0.21 to 0.48) at the same concentration. These results were consistent with the results of ITC. The interactions between highly linear pectins and procyanidin DP9 led to formation of aggregates with marked turbidity. For APs, BP3/6, KPR2/3 and KPO2/3, the absorbances at 650 nm increased slightly at a concentration of 30 mM galacturonic acid equivalent. After 3.75 mM pectin concentration, the absorbance of BP2 stabilized around at 0.2. However, AP6, BP3/6 and KPO3/6 also showed increased turbidity while no interactions had been detected by ITC. This result may indicate that the resulting released or absorbed heat during the interaction stayed below the limit of detection of the nanocalorimetric method. Absorbance of all pectins at 30 mM (-)-galacturonic acids equivalent rose with increased procyanidins DP9 concentrations (Fig. 4.5B), which was consistent with the trend of Fig. 4.5A.

4.2.3.2.3 Characterization of unbound pectin and procyanidins

The free pectins and procyanidins remaining in the wells after interactions with 30 mM galacturonic acid and 60 mM (-)-epicatechin equivalents were investigated to further understand the impact of the interactions on their macromolecular structure (Fig. 4.4, Table 4.7). Fig. 4.4 showed the chromatograms obtained by HPSEC-MALLS of the initial pectic compounds in buffer (S1A) and the free pectin compounds (at 30 mM in galacturonic acid equivalent) after binding with procyanidins (S2, i.e., pectic compounds that had not formed aggregates). Table 4.7 showed the corresponding pectin macromolecular characteristics.

After interaction, only 2% -5% of pectins remained in the supernatant. More pectin remained free for AP6, BP6 and KPO/R6 than for AP2/3, BP2/3 and KPO/R2/3, respectively (Table 4.7). On the one hand, the \bar{M}_w of free pectins after binding with procyanidins was lower than the \bar{M}_w of initial pectin sample (Table 4.7). Procyanidin

DP9 may have strong selectivity for the bigger molecules of pectin fractions, especially AP2 (ΔM_w : -266), KPR2 (ΔM_w : -216) and KPR3 (ΔM_w : -223). On the other hand, the \overline{DP}_n of free procyanidins after interaction with pectins was lower than the \overline{DP}_n of initial procyanidin sample, whatever pHs and species (Table 4.7), confirming that pectins preferentially interacted with highly polymerized procyanidins.

In comparison with the initial pectin solutions, the main peaks of free APs, BPs, KPRs and KPOs in the solutions slightly shifted to higher elution volumes indicating a decrease in hydrodynamic volume (Fig. 4.4). Moreover, the shoulder at a lower elution time (corresponding to the high molar mass fraction) in the main peak of AP6 and KPR/Os decreased after interaction due to complexation with procyanidins. The molecules that remained in supernatants after pectin-procyanidin interactions were smaller procyanidins DP9 and smaller pectins. The large-sized pectins and the larger procyanidins were co-aggregated, or the aggregates contained procyanidins of higher \overline{DP}_n and pectins with larger hydrodynamic volume. Nevertheless, it was challenging to use the α value obtained from Mark-Houwink-Sakurada equation to determine which pectin conformation was more conducive to interaction as this value did not show clear trend probably because it only provided some general structural information on these pectins (Table 4.5).

4.2.3.3 Interactions with procyanidins of DP79

4.2.3.3.1 Isothermal titration calorimetry

Titration of all pectins by procyanidins DP79 showed complex curves characterized by strong exothermic peaks. Thermodynamic parameters are shown in Table 4.6B. Stoichiometry (n) results, suggested that approximately 1 (-)-epicatechin constitutive unit bound to 5 units of galacturonic acid for high linearity KPO2. For AP3, KPR3/6 and KPO3/6 with medium linearity, approximately 1 (-)-epicatechin constitutive unit bound to 10 units of galacturonic acid. While, the stoichiometry for AP2 with high molar mass and size, and BP2/3 with high arabinans side chains were ca. 0.5.

Pectin-procyanidin interactions

Table 4.7 Changes in the molecular mass and concentrations of pectins and the degree of polymerization of procyanidins before and after interactions between pectic fractions and procyanidins DP9/79 (30/60 mM (-)-epicatechin equivalent).

Sample	Initial pectins	Unbound pectins	Unbound pectins	Unbound PCA	Unbound pectins	Unbound pectins	Unbound PCA DP79
	\bar{M}_w *	with PCA DP9	with PCA DP9	DP9 with pectins	with PCA DP79	with PCA DP79	with pectins
	($\times 10^3$ g·mol ⁻¹)	Concentration (g/l)	\bar{M}_w ($\times 10^3$ g·mol ⁻¹)	\overline{DP}_n of free PCA	Concentration (g/l)	\bar{M}_w ($\times 10^3$ g·mol ⁻¹)	\overline{DP}_n of free PCA
AP2	431	0.27 (2% ^a)	165 (-266 ^b)	6 (-3 ^c)	0.44 (7% ^a)	139 (-292 ^b)	39 (-40 ^c)
AP3	149	0.36 (3%)	104 (-45)	7 (-2)	0.39 (6%)	78 (-71)	39 (-40)
AP6	217	0.65 (5%)	37 (-180)	6 (-3)	0.60 (9%)	24 (-193)	41 (-38)
BP2	147	0.58 (3%)	99 (-48)	6 (-3)	0.58 (6%)	63 (-84)	33 (-46)
BP3	117	0.45 (3%)	75 (-42)	7 (-2)	0.52 (7%)	72 (-45)	39 (-40)
BP6	65	0.58 (5%)	22 (-43)	7 (-2)	0.50 (8%)	21 (-44)	27 (-52)
KPR2	287	0.51 (4%)	71 (-216)	7 (-2)	0.45 (7%)	49 (-238)	23 (-56)
KPR3	285	0.34 (4%)	62 (-223)	6 (-3)	0.20 (4%)	53 (-232)	26 (-53)
KPR6	161	0.62 (5%)	29 (-132)	7 (-2)	0.55 (9%)	29 (-132)	33 (-46)
KPO2	80	0.37 (3%)	32 (-48)	7 (-2)	0.51 (8%)	31 (-49)	31 (-48)
KPO3	137	0.57 (6%)	49 (-88)	5 (-4)	0.44 (9%)	36 (-101)	41 (-38)
KPO6	79	0.72 (6%)	35 (-44)	7 (-2)	0.69 (11%)	22 (-57)	40 (-39)
<i>Pooled SD</i>	<i>11.3</i>	<i>0.06</i>	<i>3.6</i>	<i>0.6</i>	<i>0.09</i>	<i>11.5</i>	<i>1.8</i>

*data adapted from (X. Liu, Renard, Rolland-Sabaté, Bureau, et al., 2021a). Average of duplicates for each. \bar{M}_w : weight-average molar mass. \overline{DP}_n : number-average degree of polymerization. ^a Pectin retention (%) = Unbound pectin concentration / Initial pectin concentration; ^b ΔM_w : difference of weight-average molar mass between pectic fractions unbound to procyanidin solutions after interaction with procyanidins and initial pectic fractions in buffer; ^c ΔDP_n : difference of degree of polymerization between procyanidins unbound to pectic fractions after interaction with pectins and initial procyanidins in buffer.

The association constant K_a between pectins and procyanidins DP79 ranged from $0.3 \times 10^2 \text{ M}^{-1}$ to $1.2 \times 10^4 \text{ M}^{-1}$ in the order $\text{BP2} \approx \text{BP3} \approx \text{BP6} \ll \text{KPR3} < \text{KPR6} < \text{AP6} < \text{AP3} \ll \text{AP2} < \text{KPO3} < \text{KPO6} \ll \text{KPR2} < \text{KPO2}$. In particular, the BP2, AP2, KPR2 and KPO2 pectins were the most different from our sample set (Supplementary Fig. 4.2) and cover a wide range of affinity. Regarding the interactions between all pectins and procyanidins DP79, contribution of entropy ($-\Delta S$ from -12 to -19 kJ/mol) related to the exothermic reactions, indicated that the interactions were mostly driven by entropy indicating hydrophobic interactions and water released. Moreover, an enthalpy contribution especially for KPR2 ($\Delta H = -6.0$ kJ/mol) and KPO2 ($\Delta H = -8.0$ kJ/mol) was also observed indicating that hydrogen bonds were also involved.

4.2.3.3.2 Phase diagram

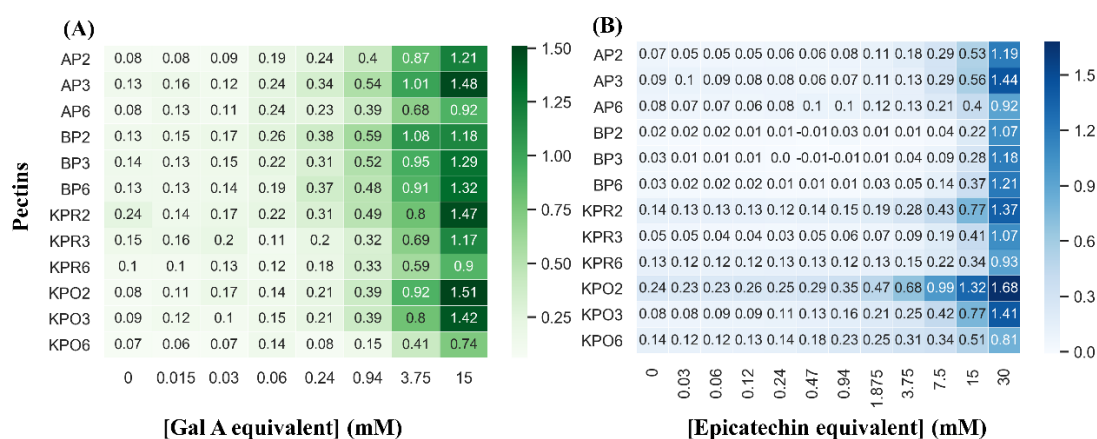


Figure 4.6 Heat map of the turbidity characteristics of pectin-procyanidin DP79 interactions. Absorbance at 650 nm after interactions in 0.1 M citrate/phosphate buffer pH 3.8 (in triplicates). (A) Variation of absorbance of pectins at different concentrations (galacturonic acid equivalent) with procyanidins DP79 (30 mM (-)-epicatechin equivalent). (B) Variation of absorbance of procyanidins DP79 ((-)-epicatechin equivalent) at different concentrations with pectins (15 mM galacturonic acid).

More precipitation was obtained with procyanidins of DP79 (Fig 4.6 A, B) than of DP 9, regardless of pectin type. Turbidity increased dramatically with the increase of concentration of galacturonic acid and procyanidins for AP2, BP2, KPR2 and KPO2, indicating strong interactions, which confirmed the result of ITC. The turbidity for AP2, BP2, KPR2 and KPO2 with procyanidins DP79 at 15 mM galacturonic acid equivalent or 30 mM (-)-epicatechin equivalent increased in the following the order: $\text{KPO6} < \text{KPR6} < \text{AP6} < \text{KPR3} \approx \text{BP2} < \text{AP2} < \text{BP3} < \text{BP6} < \text{KPO3} < \text{KPR2} < \text{AP3} < \text{KPO2}$.

4.2.3.3.3 Characterization of unbound pectin and procyanidins

After interactions between pectins (30 mM galacturonic acid equivalent) and procyanidin DP79 (60 mM epicatechin equivalent), 4% - 11% of the pectins remained in the supernatants (Table 4.7). Similarly, more pectins remained in solution for AP6, BP6 and KPO/R6 than for AP2/3, BP2/3 and KPO/R2/3, respectively. \bar{M}_w of all pectins and \overline{DP}_n of procyanidin DP79 obviously decreased after interactions (Table 4.7). The ΔM_w obtained between APs, BPs, KPR/Os and procyanidins DP79 were higher than the ones obtained with procyanidin DP9, especially for AP2. Procyanidin DP79 gave a higher ΔDP_n for all pectins ranging from - 56 to - 38. This high decrease of the degree of polymerization and molar mass indicated that highly polymerized procyanidins of fraction DP79 associated selectively with pectins of higher molar mass. HPSEC-MALLS chromatograms of the pectins also support this conclusion. Like with procyanidin DP9, the main population of free APs, BPs, KPRs and KPOs was slightly shifted to lower sizes after complexation/aggregation and the largest population disappeared (Fig. 4.6). This suggested that the large-sized pectin aggregates from the largest population preferentially interact with large-sized procyanidins DP79 and produce precipitates (Alba et al., 2018; Carn et al., 2012). However, this specificity can not be distinguished in different conformations of pectins, because α values of large populations are all in the range of 0 - 0.41 representing large-sized folded structures or branched aggregates did not show clear trend (Table 4.5).

4.2.4 Discussion

4.2.4.1 Comparison of calorimetry and turbidity methods

Using both isothermal titration calorimetry and turbidity, pectins with different linearity (or side-chain abundance) and macromolecular characteristics were shown to interact with procyanidins (DP9 and DP79). These interactions were mainly driven by entropy, which may be caused by hydrophobic interactions, or changes in solvation and conformation (Leavitt & Freire, 2001; Poncet-Legrand et al., 2007). Enthalpy contributions were also observed indicating that interactions also involved some

hydrogen bonds. Haze formation was observed for all pectins with procyanidins DP9, while for some pectin fractions, AP6, BP3/6, and KPO3/6, the interactions were below the detection limit for nano calorimetry. The reason may be that the ITC signal generated by these pectin-procyanidin interactions (exothermic) is masked by the concurrent endothermic signal from chain-chain interaction during pectin aggregation. In addition, the pectins for which no titration could be detected were generally characterized by higher arabinose contents: although procyanidins do interact with arabinans (P. A. R. Fernandes et al., 2020), this polymer appeared to lead to less intense binding. This was not observed with procyanidins DP79, which had higher energies of interactions and generally higher affinities than DP9. Turbidity appeared to be more sensitive than ITC for detection of interactions. Haze formation is a complex process which involves the modification of intra-molecular and molecule-solvent interactions. A limit to measuring turbidity however is that it must be observed under static conditions, and the lack of stirring during the complete measurement may result in uneven cloudiness / aggregate formation (WatreLOT, Renard, & Le Bourvellec, 2015). Moreover, procyanidins, and notably the larger procyanidins, can auto-aggregate (Carn et al., 2012) and their sedimentation increased with $\overline{DP}n$. The turbidity measurement provided information on the formation of insoluble complexes, but it cannot provide information on the mechanism and binding sites. These two methods are complementary, allowing higher sensitivity for detection of the interactions (haze formation) on the one hand and access to stoichiometric ratio and binding enthalpy (ITC) on the other hand.

4.2.4.2 Pectin linearity

The highest affinities for procyanidins DP9/79 were obtained for kiwifruit pectins KPO2 and KPR2, with both the highest K_a and the most marked aggregate formation, and the lowest affinities were observed for beet pectins. KPR/Os exhibited the highest linearity, HG and galactans contents, and lower RG-I content (Table 4.4 and Supplementary Fig. 4.2). Ripening involves a decrease in arabinose and a loss of pectic side chains (X. Liu, Renard, Rolland-Sabaté, Bureau, et al., 2021a) resulting in even

higher linearity and higher HG ratio in KPO2, which strengthen the binding to procyanidins. Brahem et al. (2019) also reported that cell walls from pear at an overripe stage have a higher affinity for procyanidins than those from the ripe stage, due to removal of arabinan and galactan pectin side chains during ripening, allowing better access to galacturonic acid-rich molecules. Moreover, the adsorption of anthocyanins on blueberry linear chelator-soluble pectins is four times higher than on the highly branched water-soluble pectin (Koh et al., 2020). On the other hand, Watrelot et al. (2014) described that the affinity of procyanidin DP30 to pectic compounds increases in the following order: arabinans < arabinans + galactans II < galactan I. This may be due to the length and the flexibility of galactan side chains, while arabino-galactan side chains are short, more branched and stiff (M'sakni et al., 2006). Highly branched arabinans have more globular structures which limit their interactions with polyphenols (P. A. R. Fernandes et al., 2020). KPR/Os contained more galactan side chains, while BPs contained more arabinans, followed by APs. Therefore, structure of the side-chains may also have contributed to the higher affinity of KPR/Os for procyanidins DP79. Interactions between BPs and procyanidin DP79 showed association constants of the order of 10^2 M^{-1} . The differences in affinity constants between the different pH fractions were very limited, ranging between $0.3 \times 10^2 \text{ M}^{-1}$ (BP2) and $0.4 \times 10^2 \text{ M}^{-1}$ (BP3/6). The low affinity performance of BPs may be not only due to their complex arabinan side chain structures, but also to the presence of ferulic acid covalently linked to arabinans, and to their acetylation. Ferulic acid cross-linking, by further rigidifying the arabinan side-chains, might lower interactions with procyanidins due to steric hindrance. This is consistent with Fernandes et al. (2020) who reported that the branched arabinan side chains in pectin limit their interactions with polyphenols.

4.2.4.3 Impact of pectins molar mass on interactions

AP2, with higher molar mass, intrinsic viscosity, hydrodynamic radius and lower density, had higher affinity for procyanidin DP9/79 than AP3 and AP6; this was also true when comparing KPR2 or KPO2 to KPR3/6 and KPO3/6. This was the same relation as with corn silk polysaccharides, for which the binding capacity to flavonoids

increases with molar mass (Guo et al., 2018). However, this relationship only appeared true within a series with otherwise similar structural features, as KPR2 and KPO2 had lower molar masses but higher affinities than AP2. This suggests that increasing the molar mass of pectins alone may not increase their adsorption capacity. The linear structure of pectins was more important than their molar mass for binding to procyanidins.

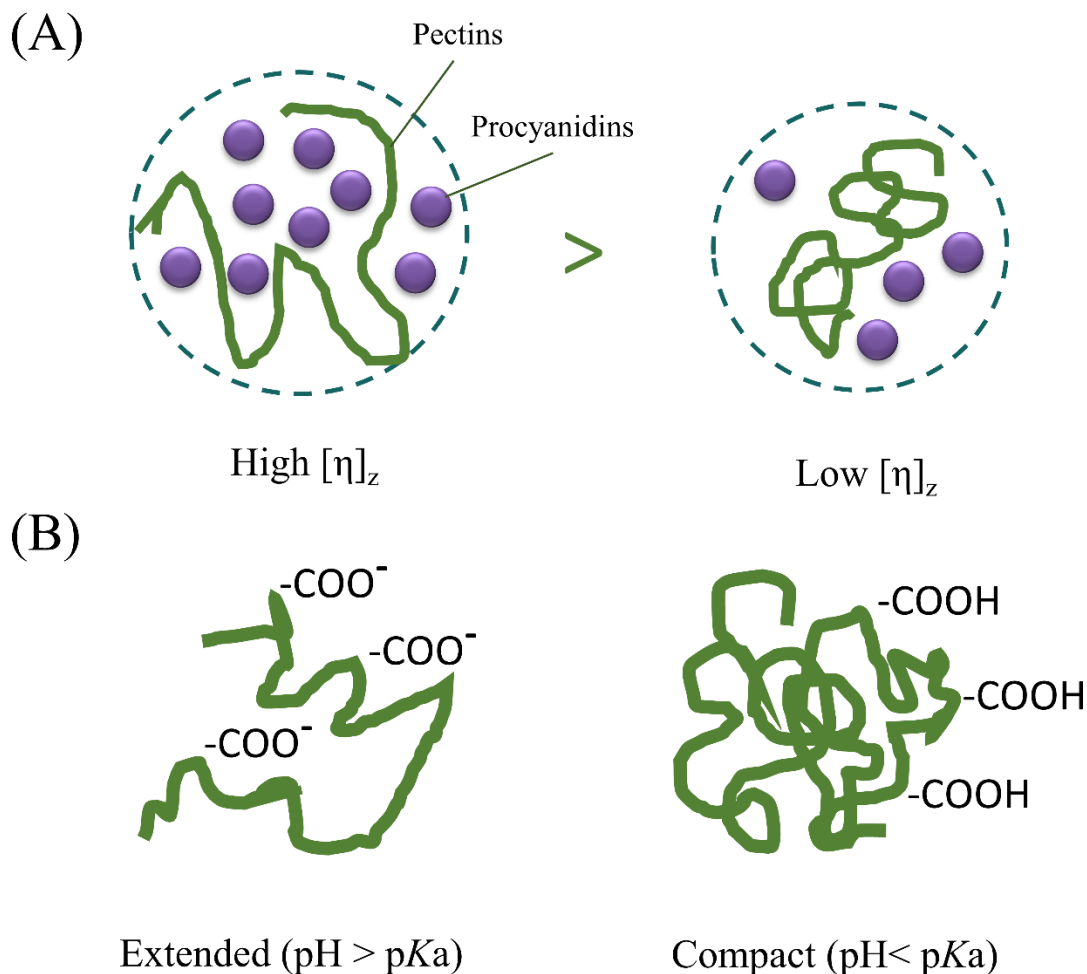


Figure 4.7 (A) High and low intrinsic viscosity pectin chains, (B) Conformations of pectin chain extended (pH > pKa) and compact (pH < pKa).

Higher molar mass pectins have more glycosidic bonds, therefore more potential binding sites, which contribute to the adsorption of polyphenols. Moreover, a larger hydrodynamic radius and lower density may also mean that there was more space for procyanidins to interact with the polysaccharide molecule. Meanwhile, a larger space for bending and turning, a larger effective volume, a larger flow resistance, and a higher frequency of collisions between segments produce high intrinsic viscosity (BeMiller &

Whistler, 1996). Pectins with higher intrinsic viscosity, that is existing as expanded chains in solution, might better interact with procyanidins (Fig. 4.74A). In addition, most carboxyl groups in pectins are ionized when the pH is higher than their pKa, which was the case in the experiments (pH 3.8 > pKa 3.5). This ionization leads to coulomb repulsion between the consecutive free carboxyls on a pectin molecule, increasing its stiffness (Stoddart, Spiers, & Tipton, 1969), and preventing spatial proximity between segments of two pectin molecules (Fig. 4.7B). This causes the chain to stretch, which may result in more space to adsorption.

4.2.4.4 Substitution of the galacturonic acids

The DM of pectin has already been demonstrated to be a very important factor for interactions. However, all the pectins used here had high degrees of methylation (> 70), allowing strong interactions with procyanidins (Watrelet et al. (2013). Although KPR/Os were less methylated than APs and BPs, they still had a high DM (> 73), which did not limit their high affinity for procyanidins. Moreover, the intensity of the interaction seems to decrease with increasing acetylation. KPR/Os have the lowest degree of acetylation with a high affinity for procyanidins, while BPs have the highest degree of acetylation with the lowest affinity. However, a simple comparison may be misleading as there are confounding factors which should be considered, e.g., pectin linearity.

We noted that the overall enthalpy of interactions with KPR/Os were significantly higher than with APs and BPs, especially KPR/O2 (Table 4.6), suggesting more hydrogen bonds. Most previous studies focused on commercial pectin (usually not acetylated and sometimes demethylated), purified HG or RG. Watrelet et al. (2013) reported that interactions between commercial apple and citrus pectins and procyanidins is also mostly driven by entropy. However, the interactions between rhamnogalacturonans and hairy regions of pectins and procyanidins could be driven by either enthalpy or entropy or both (Watrelet et al., 2014). Similarly, the interactions between apple pectins extracted at pH 3.8 (from 'Ariane' cultivar) and procyanidins (DP9) are entropy-driven (Le Bourvellec et al., 2012a). Most pectin-procyanidin

interactions are driven by both entropy and enthalpy, but their proportions may be regulated by the degree of esterification of pectins.

4.2.4.5 Degree of polymerization of procyanidins

As expected, the interactions were higher with the procyanidins of the highest degree of polymerization. With procyanidins DP79, marked aggregation appeared for all pectin fractions (absorbance > 0.9) at the maximum concentration of both, while with procyanidins DP9 formation of cloud or aggregate were relatively lower. However, two trends were observed for ITC results. APs, BP3/6, KPR2 and KPRs had a higher affinity with DP79 than DP9 by ITC, but BP2 and KPR3/6 had a lower affinity with DP79 than DP9, especially BP2, the affinity of which was lower by one order of magnitude. This may be due to the conformational constraints of the two molecules that limit their interactions with each other. BP2 had low pectin linearity and HG content, together with the highest neutral sugar side-chains content of the twelve pectins, especially arabinans, and high ferulic acid content. On the one hand, these structures might cross-link the chains and limit the available binding sites for complexation with procyanidins. On the other hand, procyanidins DP79 may exhibit longer length and larger size, and are less uniform than procyanidins DP30 and DP9. Using the Fisher-Burford model to fit the SAXS spectrum, Vernhet, Carrillo, & Poncet-Legrand (2014) reported that the apple proanthocyanidins of DP69 and DP80 have a more dense shape with branches. Zanchi et al. (2009) described polymeric proanthocyanidins containing about 6% ramifications. Therefore, high DP procyanidins may induce intramolecular hydrophobic interactions and hydrogen bonds resulting in more aggregated and less extended structure. Watrelot et al. (2013, 2014) showed that pectins interact preferentially with highly polymerized procyanidins DP30, and that structure and size of procyanidins DP30 facilitates aggregates formation. Using larger procyanidins facilitated detection of the selectivity of various pectins, DP79 being less favorable with some specific structures due to its conformation.

Each polysaccharide has its own unique chemical composition, structure, molecular architecture or conformation, and these factors interact with each other to

influence their adsorption to procyanidins. The interaction between these factors remains complex, and more work will be needed to clarify their internal relationship.

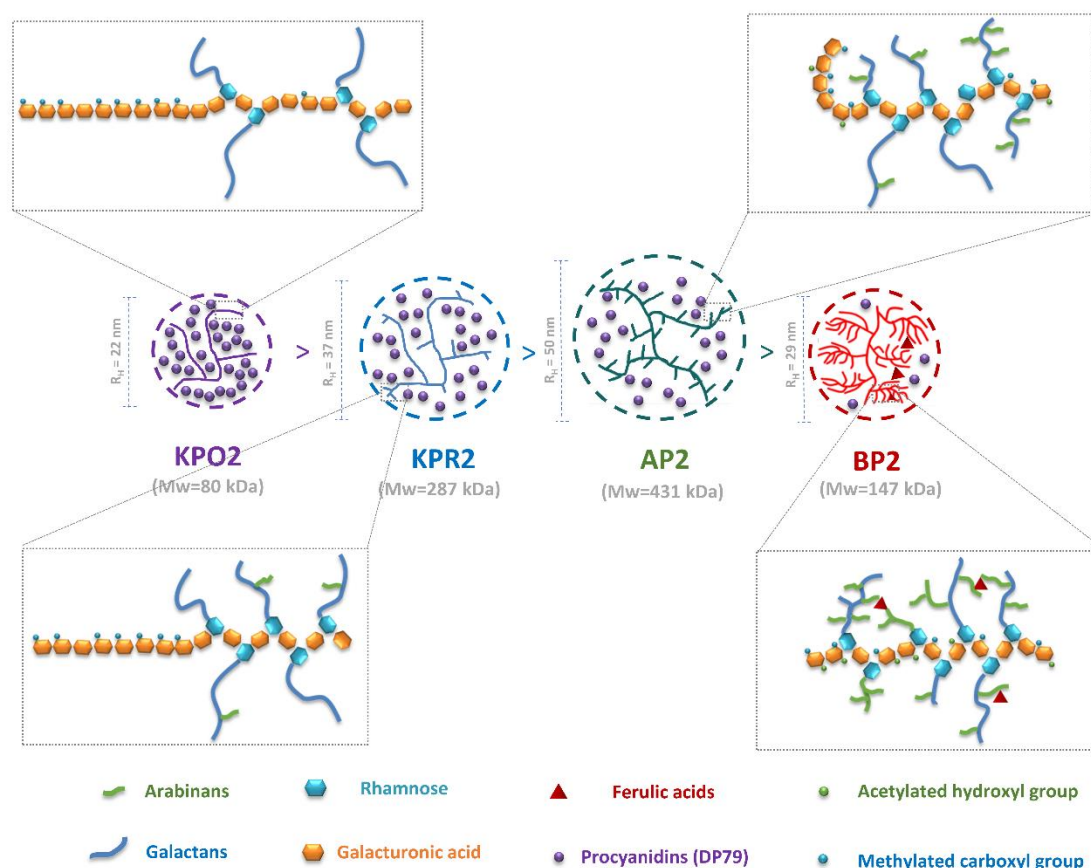


Figure 4.8 Schematic representation of four populations of pectins adsorption of procyanidins DP79 and the corresponding local details based on chemical composition and macromolecular characteristic data (molar mass and hydrodynamic radius). Representation of KPO2 a linear polymer chain and less branched polymer structures with KPR2 less long-chain branches, AP2 moderate RG content with long/short-chain mixture branches, and BP2 both much RG region with short-chain and long-chain branches, and some covalently bound ferulic acid.

4.2.5 Conclusions

Procyanidins showed different binding selectivity to apple, beet and kiwifruit pectins depending on the compositions and macromolecular features of the pectins and degree of polymerization of procyanidins. High molar mass and low density contributed to procyanidin adsorption. Pectins with high linearity and HG content, and low arabinan branching had highest interaction with procyanidins. On the contrary, high RG-I branching and ferulic acid content limited the affinity to procyanidins. Higher number average DP of procyanidins might hinder the adsorption of pectins with high side chain

branching. The importance of factors affecting pectin selectivity were linearity (proportion of side-chains) > molar mass > density \approx hydrodynamic radius, with high branching and density being detrimental to interaction while high molar mass was favorable. Combining different factors, capacity of association between procyanidin DP79 and pectins could be ranked: KPO2 > KPR2 > AP2 > BP2 (Fig. 4.8).

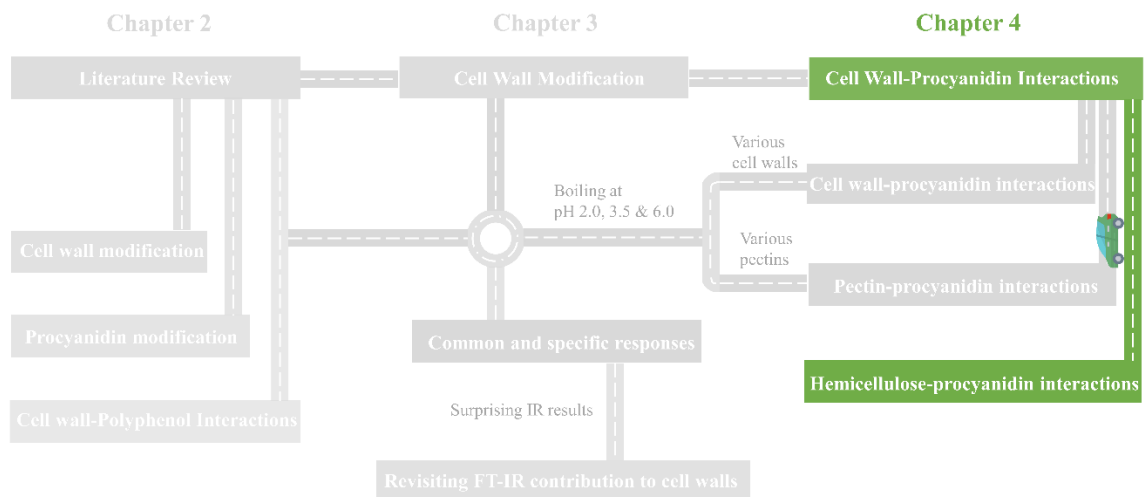
Consequently, a deep understanding of various processing-structures-binding capacity of pectins to procyanidins aids food workers customize the functional characteristics of plant-derived products and provide effective guidance for processing. Systematic variation of pectin structural features thus allows to better understand polyphenol affinity and may pave the way to anticipate the variability of retention of polyphenols in different fruits and vegetables.

Highlights

- Pectin linearity, molar mass and size influenced procyanidin adsorption.
- Highly branched beet pectins had the lowest interactions with procyanidins.
- Highest interactions were found with kiwifruit pectins, richest in homogalacturonans.
- High degree of polymerization of procyanidins might hinder their binding to beet pectins.

Section 4.3

Experimental and theoretical investigation on interactions between xylose-containing hemicelluloses and procyanidins



A version of this section has been written as:

Liu, X., Li, J., Renard, M. G. C. C., Rolland-Sabaté, A., Perez, S., & Le Bourvellec, C. (2021). Experimental and theoretical investigation on interactions between xylose-containing hemicelluloses and procyanidins.

In this study, the interactions between xylose-containing hemicelluloses and procyanidins were investigated by using a combination of multi- techniques including isothermal titration calorimetry (ITC), UV-Vis spectroscopy, high performance size-exclusion chromatography coupled with multi-angle laser light scattering (HPSEC-MALLS), and computational simulation.

This allowed to answer the following questions:

- ※ Which hemicelluloses had the strongest affinity for procyanidins?
- ※ Do the results of the computational simulations agree with the experimental results?
- ※ How does the structure of hemicelluloses influence their interactions with procyanidins?

During the processing of plant-based foods, cell wall polysaccharides and polyphenols, such as procyanidins, interact extensively, thereby affecting either their physicochemical properties along with their potential health effects. Although hemicelluloses are second only to pectins in affinity for procyanidins in cell walls, a detailed study of their interactions lacks. We investigated the interactions between representative xylose-containing water-soluble hemicelluloses and macromolecular procyanidins. Turbidity, ITC and DLS were used to determine their kind of interactions, and interaction mechanisms and theoretical calculations further ascertained the interactions. Xyloglucan and xylan exhibited respectively the strongest and weakest interactions with procyanidins. The different types of arabinoxylans interacted with procyanidins in a similar strength, intermediate between xyloglucans and xylans. Therefore, the strength of the interaction depended on the structure itself rather than on some incidental properties, e.g., viscosity and molar mass. The arabinose side-chain of arabinoxylan did not inhibit interactions. The computational investigation corroborated the experimental results in that the region of interaction between xyloglucan and procyanidins was significantly stronger than that of other hemicelluloses. Understanding hemicellulose-procyanidin interactions is crucial for the optimization of process conditions and the formulation of food products.

4.3 Experimental and theoretical investigation on interactions between xylose-containing hemicelluloses and procyanidins

4.3.1. Introduction

The polyphenols in fruits and vegetables display many potential biological activities, and their dietary intake is related to a reduced risk of suffering from a variety of chronic diseases (Koch, 2019). In addition to some endogenous factors, such as microbiota and related digestive enzymes, food substrates (e.g., dietary fiber) can also significantly regulate their bioavailability and further metabolism (Seal, Courtin, Venema, & de Vries, 2021). In general, most of the ingested polyphenols, especially the macromolecular polyphenols (e.g., procyanidins) are non-bioavailable in the stomach and small intestine. These unabsorbed polyphenols can be transported to the colon by dietary fiber, where bacteria may metabolize them as bioavailable simple phenolic acids (J. Cui et al., 2019). This process may mediate the potential beneficial effects of dietary fiber-polyphenol complexes, as they or their catabolites may be absorbed and utilized by the human body (Jakobek & Matić, 2019; Le Bourvellec et al., 2019). Therefore, the interactions between dietary fibers and polyphenols may affect the bioavailability of polyphenols.

Among the dietary fibres, hemicelluloses have not benefited from significant attention. They are heteropolysaccharides, such as xylan, arabinoxylan and xyloglucan, including various sugar monomers. They have a moderate affinity with polyphenols in cell walls. Hence, the affinity of procyanidins is greatest for pectins followed by xyloglucan, and lowest for cellulose (Le Bourvellec et al., 2005). In addition, by a step-wise removal of pectins and hemicelluloses in the grape cell wall or apple cell wall, the binding capacity of proanthocyanidins to the remaining cell walls is significantly reduced (Le Bourvellec et al., 2012a; Ruiz-Garcia et al., 2014), but cell walls still have an affinity for proanthocyanidins. However, Phan, Flanagan, D'Arcy, & Gidley (2017) compared the selection of different cellulose-based composite materials (cellulose, cellulose-xyloglucan, cellulose-arabinoxylan, cellulose-pectin) for the adsorption

capacity of polyphenols. They found that cellulose is the main binder, whereas hemicelluloses (e.g., xyloglucan and arabinoxylan) do not contribute to the adsorption of catechins (Phan et al., 2017). Therefore, the adsorption capacity of specific polysaccharides to specific polyphenols differs. The knowledge of the nature of the interaction occurring between different hemicelluloses and polyphenols is still missing.

Polyphenols constitute a large group of plant compounds, mainly divided into phenolic acids, flavonoids, stilbenes, and lignans. Procyanidins are the most abundant macromolecular antioxidants in food and diet (Saura-Calixto & Pérez-Jiménez, 2018). They are primarily composed of (-)-epicatechin units. Their number average degree of polymerization (\overline{DP}_n) varies significantly between species and cultivars. Generally, the ability of polysaccharides to interact with procyanidins is directly proportional to their molecular weight, that is, \overline{DP}_n (X. Liu et al., 2020; Renard et al., 2017).

The interactions between pectins and procyanidins has been thoroughly studied (X. Liu et al., 2020; X. Liu, Renard, Rolland-Sabaté, & Le Bourvellec, 2021; Watrelot et al., 2014). The corresponding knowledge for hemicelluloses, which are the other main non-cellulosic component in the cell walls, is limited. Moreover, the relative binding capacity of procyanidins to various hemicellulose components, along with affinity and binding mechanism, remains to be resolved. Therefore, the present study aims to explore the interaction mechanism occurring between hemicelluloses and procyanidins using a combination of techniques including isothermal titration calorimetry (ITC), UV-Vis spectroscopy, high performance size-exclusion chromatography coupled with multi-angle laser light scattering (HPSEC-MALLS) and dynamic light scattering (DLS). In complement, the reactive sites of procyanidins and different hemicelluloses were explored using at the density functional theory (DFT) level, through electrostatic potential (ESP) and frontier molecular orbital (FMO) analysis. Further conformational analysis of intra and intermolecular interactions provided detailed insights about the nature and the strength of the mechanism underlying the interactions between procyanidins and hemicelluloses. The present study contributes to the understanding of the effects of structure, molar mass, viscosity and side chains on interactions through

probing the binding of selected procyanidins to different types of hemicellulose components: xylan, xyloglucan and five arabinoxylans. This set of results provides a reference for further study on the effect of the whole plant cell wall system on the bioavailability of procyanidins to better understand the underlying implications of both human nutrition and health interactions.

4.3.2 Materials and methods

4.3.2.1 Standards and Chemicals

The standards of arabinose, mannose, glucose, fucose, xylose, rhamnose, and galactose) were obtained from Fluka (Buchs, Switzerland). Arabinoxylan with low /medium/high viscosity, arabinoxylan with 30% and 22% arabinose content xyloglucan, and xylan were purchased from Megazyme (Bray, Ireland).

4.3.2.2 Procyanidins preparation

Procyanidins (DP9 and DP39) were prepared from two apple varieties ('Marie Menard' and 'Avrolles'), respectively, as described in Liu, Renard, Rolland-Sabaté, & Le Bourvellec (2021). Briefly, aqueous acetone fractions were collected after washing by hexane and methanol, and then purified using a LiChrospher 100 RP-18 (12 μm , Merck, Darmstadt, Germany) column and further characterized following the principles described by Guyot, Marnet, Sanoner, & Drilleau, (2001). The procyanidins contained about 800 mg/g of phenolic compounds, primarily procyanidins plus traces of (-)-epicatechin, 5'-caffeoylquinic acid, *p*-coumaroylquinic acid, phloridzine, and flavonols (Supplementary Table 4.2).

4.3.2.3 Macromolecular characteristics of hemicelluloses

Macromolecular features of initial (2.5 g/L) and free hemicelluloses were detected by HPSEC-MALLS as described by Liu, Renard, Rolland-Sabaté, Bureau, & Le Bourvellec (2021). Briefly, samples (100 μL) after being filtered were injected into the instrument composed of a Shimadzu series LC system including a diode array detector (DAD) and a refractive index detector (RID) (Shimadzu, Kyoto, Japan), and a MALLS

(DAWN HELEOS 8+, equipped with a K5 flow cell and a GaAs laser at $\lambda = 660$ nm) from Wyatt Technology Co. (Santa Barbara, CA, USA). Hemicelluloses were separated on PolySep-GFC-P3000, P5000 and P6000 300×7.8 mm columns (40 °C) equipped with a guard column from Phenomenex (Le Pecq, France) eluted by citrate/phosphate buffer (0.1 M, pH 3.8) at 0.6 mL/min. Zimm fitting method with a one order polynomial fit was used to calculate the weight-average molar mass (\bar{M}_w) (A. Rolland-Sabaté et al., 2004). A refractive index increment (dn/dc) value of 0.146 mL/g was used to calculate the concentration of hemicelluloses. Astra software® (version 7.1.4, Wyatt Technology Co.) was used to calculate and analyze the results. Injections were carried out in duplicates.

4.3.2.4 Isothermal titration calorimetry

The entropy and enthalpy changes of procyanidins binding to hemicelluloses were measured in a citrate/phosphate buffer (0.1 M, pH 3.8) at 25 °C with stirring at 90 rev/min, using a TAM III isothermal microcalorimeter (TA instruments, New Castle, USA) as described by Liu, Renard, Rolland-Sabaté, & Le Bourvellec (2021). The hemicellulose samples (15 mM xylose equivalent, a similar concentration for xyloglucan, ca. 3.75 g/L) were injected into an 850 μ L sample cell of stainless steel and equilibrated until the baseline was stable. Over 20 min time intervals, 50 injections of 5 μ L procyanidins (30 mmol/L in (-)-epicatechin equivalent) were titrated into the sample cell. The raw ITC data, measured as the heating power input against time, were collected continuously and peak integration was fitted by TAM assistant software (NanoAnalyze 3.10.0). The experiments were carried out in duplicates.

4.3.2.5 Phase diagram

A spectrophotometric method was used to study hemicellulose-procyanidin interactions as described by Liu, Renard, Rolland-Sabaté, & Le Bourvellec (2021). The absorbance values were collected using a SAFAS flx-Xenius XM spectrofluorimeter (SAFAS, Monaco) at 650 nm on a 96-well microplate. Each experiment was performed in triplicate, and the data were recorded at 25 °C, in a citrate/phosphate buffer (0.1 M,

pH 3.8). A serial procyanidin solutions (0, 0.06, 0.12, 0.24, 0.46, 0.94, 1.875, 3.75, 7.5, 15, 30 and 60 mM (-)-epicatechin equivalent) and hemicellulose solutions (0, 0.03, 0.06, 0.117, 0.47, 1.875, 7.5 and 30 mM xylose equivalent, a similar concentration for xyloglucan) were prepared along the lines and columns, respectively. Each procyanidin/hemicellulose mixture was prepared by mixing a constant volume of procyanidin and hemicellulose solutions (50 μ L). The mixture was stirred for 20 s before each measurement. After the test, microplates were centrifuged 10 min at 2100 \times g. Free procyanidins and hemicelluloses were collected in the supernatant and then analyzed by HPLC-DAD with thioacidolysis and HPSEC-MALLS, respectively.

4.3.2.6 Theoretical calculation method

The initial structures of monosaccharides (rhamnose, arabinose, xylose, mannose, glucose) and procyanidin B2 were download from PubChem Compound database (<https://pubchem.ncbi.nlm.nih.gov/>). Five structure of hemicelluloses (AXHB: arabinoxylan (38% Ara), AXMB: arabinoxylan (30% Ara), AXLB: Arabinoxylan (22% Ara), Xyloglucan, Xylan were built using Polys-Glycan Builder (Pérez & Rivet, 2021) and displayed using SweetUnitMol software (Pérez, Tubiana, Imberty, & Baaden, 2015). Structural optimizations were obtained at the B3LYP-D3/6-31+G** level. Single-point energy calculations were performed on the optimized structures using a larger basis set standard Pople style, 6-311+G(d,p) basis sets and SMD solvation model correction. As for the five different hemicelluloses, PM7 method was applied to optimize these initial geometries in a rough level, and Gaussian 16 (Frisch et al., 2016) software was adopted to obtain the precise geometries at a level of B3LYP-D3 /6-31+G**.

Since conformational space increases rapidly with degrees of freedom in small molecules, we conducted modeling studies of samples based on an efficient conformer search algorithm developed by the Grimme group, which can provide adequate sampling of the conformational space. Possible initial geometries were generated using xtb software (Grimme, Bannwarth, & Shushkov, 2017). All the lowest-energy

conformations were obtained with the conformer rotamer ensemble sampling tool (CREST) (Pracht, Bohle, & Grimme, 2020) and Molclus program, (See details in the Supporting Information). Then, non-covalent interaction (NCI) analysis was carried out (additional notes in the Supporting Information). Frontier Molecular Orbital (FMO) analysis (Q. Huang et al., 2020) and Electrostatic potential (ESP) analysis were finally performed by Multiwfn 3.7 software package (Lu & Chen, 2012).

4.3.2.7 Statistical analysis

All chemical analyses were expressed as mean values of analytical duplicates and triplicates, and the reproducibility of the results was presented as pooled standard deviations (Pooled SD) (Box, Hunter, & Hunter, 1978). Heatmap analyses were performed using Python software (version 3.6) with Seaborn package (Waskom, 2014).

4.3.3 Results and discussion

4.3.3.1 Characterization of hemicelluloses

Table 4.8 lists the compositions and structures of the hemicelluloses, whereas Fig. 4.9 displays their molar mass and size distributions. Arabinoxylan (low viscosity) (AXLV), arabinoxylan (medium viscosity) (AXMV) and arabinoxylan (high viscosity) (AXHV) have similar sugar compositions, e.g., arabinose content (35 %), and their molar mass increase with their viscosity (from 2.2 to 3.9 x 10⁵ g/mol). Moreover, to compare the influence of the arabinose substitution on their interaction with procyanidins, arabinoxylans with different arabinose contents were introduced, i.e., with 30% arabinose substituents (AXMB) and with 22% (AXLB): AXMB exhibited a molar mass similar to AXMV whereas AXLV showed a ten times lower molar mass. The addition of xyloglucan (XYLO) and xylan (XYLA) allowed the comparison of the effect of xylose-containing hemicelluloses on procyanidin interactions. XYLO exhibited the highest molar mass, while AXLB showed the lowest (Table 4.8). The molar mass of xylan was not applicable due to possible interaction with the column.

4.3.3.2 Phase diagram

Turbidity analysis is an effective method for the direct detection of interactions; the increase in turbidity is proportional to the number and size of the complexes (Watrelet et al., 2013, 2014). The turbidity of the xyloglucan mixture containing procyanidin DP9 increased significantly with increasing xyloglucan concentration (Fig. 4.10A). However, there was minimal change for the hemicelluloses with a xylan backbone, with an increase only at 30 mM xylose equivalents. Similarly, the absorbance of xyloglucan at the highest concentration increased with increasing procyanidin DP9 concentration (Figure 4.10B), while the hemicelluloses with a xylan backbone remained constant, which was consistent with the trend in Fig. 4.10A. The overall aggregation capacity of hemicelluloses (AXHV, AXMV, AXLV, AXMB, AXLB and xylan) with procyanidin DP9 was lower than that of pectins, but the aggregation capacity of xyloglucan with procyanidin DP9 was the same as that of kiwifruit pectins (X. Liu, Renard, Rolland-Sabaté, & Le Bourvellec, 2021).

Interaction between hemicelluloses and procyanidin DP39 produced significantly more aggregates than with DP9 (Fig. 4.10 C and D), the turbidity increased significantly with increasing concentrations of either hemicellulose or procyanidin for all the hemicelluloses tested, indicating a strong interaction with procyanidin DP39. The addition of procyanidin DP39 also resulted in a significant increase in the particle diameter of complexes determined by DLS (Supplementary Table 4.3). Procyanidin DP39, rich in ortho phenolic groups and aryl rings, leads to a more extensive aggregation of colloidal particles. The turbidity for hemicelluloses with procyanidins DP39 at 30 mM xylose equivalent (a similar concentration for xyloglucan: 7.5 g/L) or 60 mM (-)-epicatechin equivalent increased in the following order: Xylan < AXLB \approx AXMV \approx AXHV \approx AXLV < AXMB < Xyloglucan. Therefore, xyloglucan had the strongest aggregation capacity with procyanidins, followed by arabinoxylan and xylan had the weakest aggregation capacity. The different types of arabinoxylans had similar capacities. This result was consistent with the results of DLS (Supplementary Table 4.3): the size of xylan increased the least, while xyloglucan cannot be measured, because it

directly produced obvious flocculent precipitation with procyanidins. The viscosity and molar mass of hemicellulose were not the main determinants (medium impact) of the strength of the interactions, a result that was consistent with pectins (X. Liu, Renard, Rolland-Sabaté, & Le Bourvellec, 2021). However, the arabinose side-chain of arabinoxylan did not inhibit the interactions. This observation contrasted with the inhibition of interaction with procyanidins observed for the pectin side-chains. The length of arabinoxylan side-chain composed of only one monosaccharide may be not sufficient to cause spatial site blocking, while it does contribute to decrease rigidity of the backbone.

4.3.3.3 Characterization of unbound hemicelluloses and procyanidins

The changes in free hemicelluloses and procyanidins after interaction were explored using supernatants collected after turbidity measurements. After mixing of the two participants (60 mM epicatechin equivalent for procyanidins and 30 mM xylose equivalent for hemicelluloses, a similar concentration for xyloglucan: 7.5 g/L), most of the hemicellulose-procyanidin complexes precipitated, and only a small amount remained in the supernatant. \overline{M}_w values of free hemicelluloses and \overline{DP}_n of free procyanidins exhibited a drastic decrease after interactions (Table 4.9). This indicated that procyanidin DP9/39 were highly selective for the high molar mass fractions of hemicellulose, especially for xyloglucan. Similarly, hemicelluloses were highly selective for higher \overline{DP}_n of procyanidins, that is, DP39. Moreover, xyloglucan was barely detectable in the supernatant of the DP39-xyloglucan complex solution.

Fig. 4.9 shows the HPSEC-MALLS chromatograms of hemicelluloses that did not form aggregates with procyanidins after interaction. The main peaks of unbounded AXLB and AXMB after interaction with procyanidin DP9 were not significantly different from originals, while after interaction with procyanidin DP39, these main peaks were slightly shifted to higher elution volumes indicating a lower molecular size. The main peaks of unbounded AXLV, AXMV and AXHV similarly shifted to higher elution volumes after interaction with procyanidin DP9 and DP39. Whatever the

Table 4.8 Neutral sugar compositions (mg/g dry weight) and weight-average molar mass ($\times 10^3$ g/mol) of hemicelluloses.

Samples	Rha	Fuc	Ara	Xyl	Man	Gal	Glc	Total	\bar{M}_w
AXLV	1	0	331	608	3	8	5	955	222
AXMV	1	0	335	636	2	6	3	984	261
AXHV	1	0	343	641	0	2	3	990	391
AXMB	1	0	288	693	0	7	5	995	257
AXLB	1	0	209	733	0	6	5	954	24
XYLO	1	0	12	282	140	0	399	834	774
XYLA	12	0	6	716	10	0	8	753	NA
<i>Pooled SD</i>	<i>0.7</i>	<i>0</i>	<i>3.3</i>	<i>17.2</i>	<i>1.1</i>	<i>0.4</i>	<i>5.3</i>	<i>23.1</i>	<i>19.6</i>

Rha: rhamnose, Fuc: fucose, Ara: arabinose, Xyl: xylose, Man: mannose, Gal: galactose, Glc: glucose. \bar{M}_w , weight-average molar mass. AXLV: Arabinoxylan (low viscosity); AXMV: Arabinoxylan (medium viscosity); AXHV: Arabinoxylan (high viscosity); AXMB: Arabinoxylan (30% Ara); AXLB: Arabinoxylan (22% Ara); XYLO: Xyloglucan; XYLA: Xylan. Pooled SD: pooled standard deviation. NA: Not applicable.

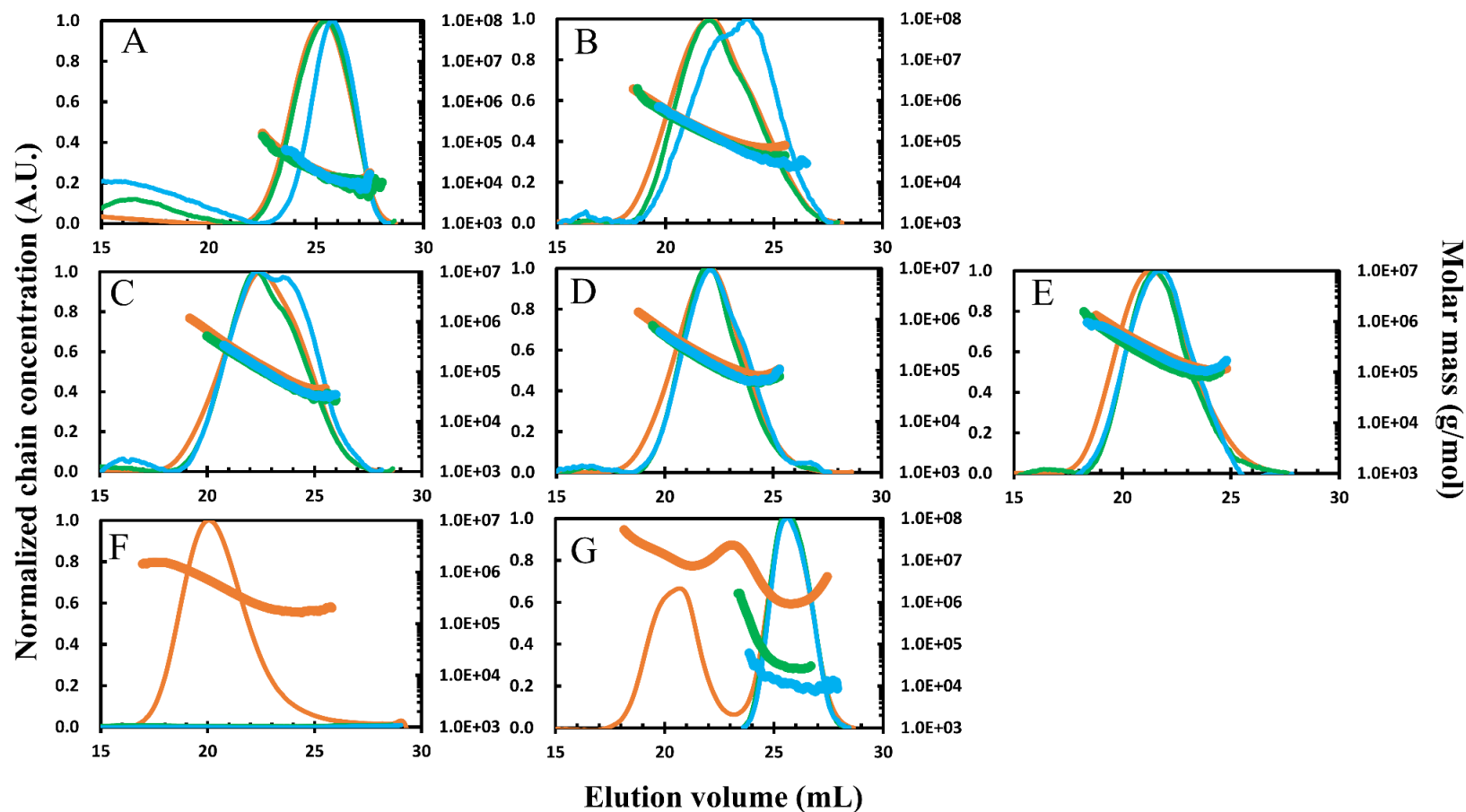


Figure 4.9 HPSEC-MALLS chromatograms and molar mass vs elution volume for the hemicellulose samples. A, B, C, D, E, F and G: AXLB, AXMB, AXLV, AXMV, AXHV, XYLO and XYLA, respectively. —, — and —: normalized chain concentration of hemicelluloses before interaction, after interaction with DP9 and DP 39, respectively; —, — and —: molar mass of hemicelluloses before interaction, after interaction with DP9 and DP 39. AXLB: Arabinoxylan (22% Ara); AXMB: Arabinoxylan (30% Ara); AXLV: Arabinoxylan (low viscosity); AXMV: Arabinoxylan (medium viscosity); AXHV: Arabinoxylan (high viscosity); XYLO: Xyloglucan; XYLA: Xylan.

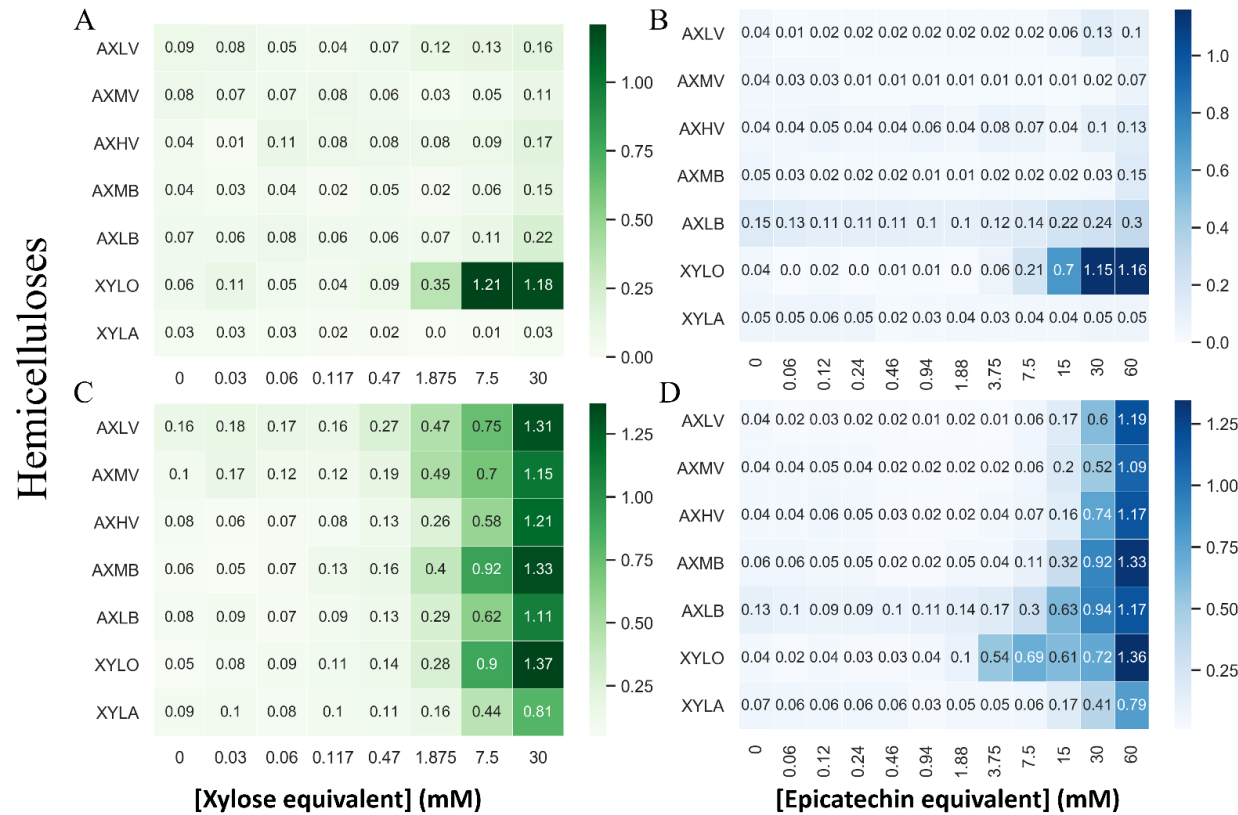


Figure 4.10 Heat map of the turbidity characteristics of interactions between hemicelluloses and procyanidins DP9/39. Absorbance at 650 nm, 25 °C, pH 3.8, 0.1 M, citrate/phosphate buffer. (A) and (C): Variation of absorbance of hemicelluloses at different concentrations (xylose equivalent, a similar concentration for xyloglucan) with procyanidins DP9/39 (60 mM epicatechin equivalent). (B) and (D): Variation of absorbance of procyanidins DP9/39 (epicatechin equivalent) at different concentrations with hemicelluloses (30 mM xylose equivalent, a similar concentration for xyloglucan: 7.5 g/L). AXLB: Arabinoxylan (22% Ara); AXMB: Arabinoxylan (30% Ara); AXLV: Arabinoxylan (low viscosity); AXMV: Arabinoxylan (medium viscosity); AXHV: Arabinoxylan (high viscosity); XYLO: Xyloglucan; XYLA: Xylan. The experiments were done in triplicates.

procyanidins' DP, xyloglucan was barely detectable in the supernatant after interaction, which indicated that procyanidins interacted strongly with it.

While xylan lose its first main peak after interaction indicating that procyanidins associated selectively with higher size fraction of xylan (Fig. 4.9G). Therefore, large-sized hemicelluloses and highly polymerized procyanidins were preferentially aggregated.

4.3.3.4 Isothermal Titration Calorimetry (ITC)

ITC provides access to stoichiometric ratios and thermodynamic parameters, e.g., entropy and enthalpy changes, free energy and binding constants during the interactions (Callies & Hernández Daranas, 2016; X. Liu et al., 2020). This method provides detailed information which complements those derived from turbidity in the detection of interactions. The titration of different hemicelluloses (7.5 and/or 15 mM xylose equivalent, a similar concentration for xyloglucan, ca. 3.75/7.5 g/L) by procyanidin DP9 (30 mM) led to endothermic peaks, but no curve and no titration could be observed (data not shown). Therefore, no interaction could be measured for the procyanidin DP9 using ITC.

Typical thermograms of titration of AXLV, AXMV, AXHV, AXMB, AXLB and xylan (15 mM xylose equivalent, a similar concentration for xyloglucan, ca. 3.75 g/L) titrated by procyanidin DP39 (30 mM (-)-epicatechin equivalent) showed strong exothermic peaks. Blank experiments (procyanidin DP39 injection in buffer) produced only small endothermic peaks, which were subtracted before integration (Supplementary Fig. 4.3). These ITC titration curves are consistent with previous studies on pectins (P. A. R. Fernandes et al., 2020; X. Liu, Renard, Rolland-Sabaté, & Le Bourvellec, 2021; Watrelot et al., 2014). However, xyloglucan behaved very differently from arabinoxylan and xylan upon mixing with procyanidin DP39 solution (Fig. 4.11). The curve was similar to the typical curve of protein-ligand interactions (Poncet-Legrand et al., 2007), with a relatively sharply reduced exothermic peak upon addition of procyanidins. As the concentration of procyanidin increased, the number of

available binding sites on xyloglucan decreased until saturation, and the addition of more procyanidin led to a plateau. The mechanism of their interaction may consist of three consecutive stages corresponding to (i) the presence of very few particles, (ii) the formation of xyloglucan-procyanidin aggregates of relatively small size, and (iii) the formation of precipitation upon further addition of procyanidins.

Stoichiometry (defined as ratio of (-)-epicatechin/xylose) was c.a. 0.1 for AXLV, AXHV, AXMB and xylan (1 molecule of (-)-epicatechin bound 10 molecules of xylose) and c.a. 0.6 for xyloglucan (1 molecule of (-)-epicatechin bound 2 molecules of xylose) using a one-site model. The association constant ranged between 424 M^{-1} and 7949 M^{-1} and increased in the sequence below: $\text{AXLB} < \text{Xylan} < \text{AXHV} \approx \text{AXMB} \approx \text{AXMV} \approx \text{AXLV} < \text{Xyloglucan}$ (Table 4.10). The affinity range of hemicelluloses binding to procyanidins is between that of whole cell walls ($10^2/10^3 \text{ M}^{-1}$) and pectins ($10^3/10^4 \text{ M}^{-1}$) (Brahem et al., 2019; P. A. R. Fernandes et al., 2020; X. Liu et al., 2020; X. Liu, Renard, Rolland-Sabaté, & Le Bourvellec, 2021). The association constants for strong affinity are generally larger than 10^4 M^{-1} (Turnbull & Daranas, 2003). Xyloglucan with a glucose backbone and xylose side-chains structure, and the highest molar mass had the highest affinity for procyanidin DP39, indicating that glucose backbone facilitated the interaction with procyanidins. AXLB and xylan with the least arabinose and lower molar mass had lowest affinity for procyanidin DP39. For the other arabinoxylans, although they had different sugar ratios, molar mass and viscosities, their affinities with procyanidins were very close. The strong entropy contribution ($-\Delta S$ from -21 to -17 kJ/mol) showed that the interactions between hemicelluloses (except for AXLB) and procyanidins were mostly driven by entropy, i.e., by hydrophobic interactions and the release of water molecules (X. Liu, Renard, Rolland-Sabaté, & Le Bourvellec, 2021; Poncet-Legrand et al., 2007). The enthalpy contributions were higher for AXLB (ΔH : -14 kJ/mol) indicating that interactions mostly involved hydrogen bonds. Therefore, of xylose-containing hemicelluloses, xyloglucan have highest affinity for procyanidins.

Hemicellulose-procyanidin interactions

Table 4.9 Changes in molar mass of hemicelluloses and in the degree of polymerization of procyanidins before and after interactions between xylose-containing hemicelluloses and procyanidins DP9/39.

Sample	Initial hemicelluloses \bar{M}_w * ($\times 10^3$ g/mol)	Unbound	Unbound PCA DP9	Unbound	Unbound PCA DP39 with
		hemicelluloses with PCA DP9	with hemicelluloses	hemicelluloses with PCA DP39	hemicelluloses
		\bar{M}_w ($\times 10^3$ g·mol ⁻¹)	\overline{DP}_n of free PCA	\bar{M}_w ($\times 10^3$ g·mol ⁻¹)	\overline{DP}_n of free PCA
AXLV	222	130 (-92 ^a)	8 (-1 ^b)	125 (-97 ^a)	25 (-11 ^b)
AXMV	261	175 (-86)	7 (-2)	162 (-99)	20 (-19)
AXHV	391	244 (-147)	7 (-2)	238 (-159)	18 (-21)
AXMB	257	182 (-75)	6 (-3)	118 (-139)	17 (-22)
AXLB	24	20 (-4)	7 (-2)	16 (-8)	19 (-20)
XYLO	774	NA	6 (-3)	NA	16 (-23)
XYLA	NA	NA	8 (-1)	NA	19 (-20)
<i>Pooled SD</i>	<i>19.6</i>	<i>5.3</i>	<i>0.5</i>	<i>3.4</i>	<i>1.2</i>

*data adapted from Table 1. Average of duplicates for each. \bar{M}_w : weight-average molar mass. \overline{DP}_n : number-average degree of polymerization. NA: Not applicable.

^a $\Delta\bar{M}_w$: difference of molar mass between hemicellulose unbound to procyanidin solutions after interaction with procyanidins and initial hemicelluloses in buffer. ^b $\Delta\overline{DP}_n$: difference of degree of polymerization between procyanidins unbound to hemicelluloses after interaction with hemicelluloses and initial procyanidins in buffer.

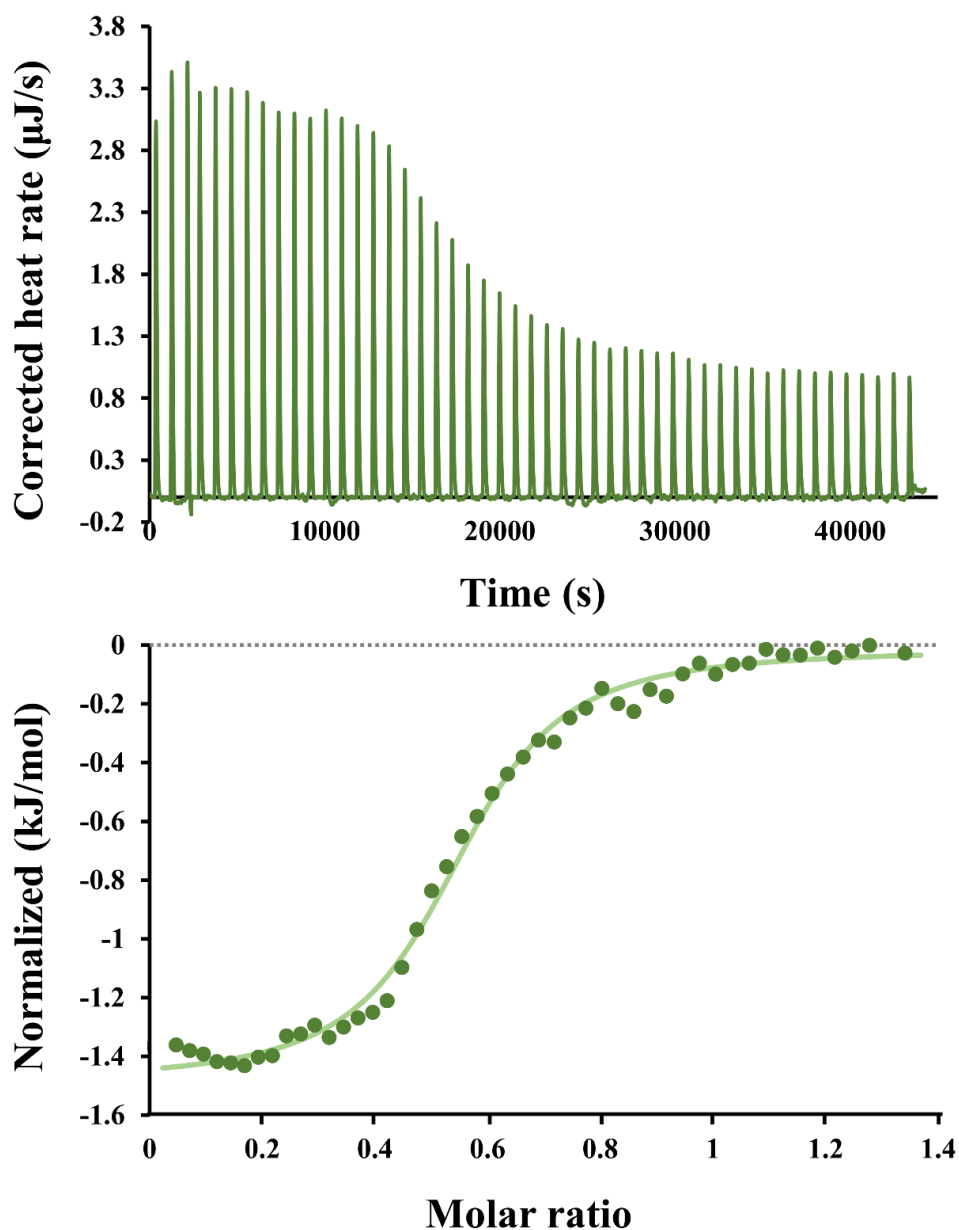


Figure 4.11 Thermogram of titration of xyloglucan with procyanidins DP39. The measurement of heat release at the top, while the molar enthalpy changes against (-)-epicatechin/xylose equivalent ratio after peak integration at the bottom.

All other affinities were lower for hemicelluloses with a xylan backbone, especially when the ramification by arabinose was limited. This observation confirmed the results derived from the turbidity experiment. However, Phan et al. (2017) found that small polyphenol molecules (e.g., catechins and ferulic acid) selectively bind to the relatively hydrophobic and rigid cellulose, rather than to the more hydrophilic and flexible arabinoxylan or xyloglucan. This highlighted the role of polyphenol structure, that is,

hemicelluloses may preferentially bind macromolecular procyanidins, because procyanidins can provide more hydroxyl groups and hydrophobic sites (X. Liu et al., 2020; X. Liu, Renard, Rolland-Sabaté, & Le Bourvellec, 2021).

Table 4.10 Thermodynamic parameters of interactions measured by ITC: hemicelluloses (15 mM xylose equivalent, 7.5 mM for xyloglucan) and procyanidins DP39 (30 mM (-)-epicatechin equivalent).

DP39	n	K _a (M ⁻¹)	ΔH (kJ/mol)	ΔS (J/mol/K)	ΔG (kJ/mol)	-TΔS (kJ/mol)	Enthalpy (%)	Entropy (%)
AXLV	0.094	5849	-0.31	71.09	-21.50	-21.20	1%	99%
AXMV	0.010	5472	-2.26	63.99	-21.34	-19.08	11%	89%
AXHV	0.089	4509	-0.34	68.81	-20.86	-20.52	2%	98%
AXMB	0.108	4600	-0.22	69.39	-20.90	-20.69	1%	99%
AXLB	0.010	424	-13.65	4.52	-14.99	-1.35	91%	9%
XYLO	0.554	7949	-1.47	69.73	-22.26	-20.79	7%	93%
XYLA	0.107	1452	-0.69	58.19	-18.04	-17.35	4%	96%
<i>Pooled</i>	<i>0.002</i>	<i>144</i>	<i>0.54</i>	<i>0.85</i>	<i>0.77</i>	<i>0.86</i>	-	-
<i>SD</i>								

Pooled SD: pooled standard deviation. n: stoichiometry, K_a: affinity level, ΔH, ΔS and ΔG: enthalpy, entropy and free enthalpy, respectively. T: temperature. AXLV: Arabinoxylan (low viscosity); AXMV: Arabinoxylan (medium viscosity); AXHV: Arabinoxylan (high viscosity); AXMB: Arabinoxylan (30% Ara); AXLB: Arabinoxylan (22% Ara); XYLO: Xyloglucan; XYLA: Xylan. Enthalpy (%) = ΔH / (ΔH - TΔS) × 100%; Entropy (%) = - TΔS / (ΔH - TΔS) × 100%. Average of duplicates for each.

4.3.3.5 Theoretical calculation of the interactions

4.3.3.5.1 Reactivity of monosaccharides

Theoretical calculations revealed a mechanism that goes beyond the widely accepted frontier molecular orbital (FMO) theory, which stated that the frontier orbitals, that is, the highest occupied molecular orbital (HOMO) and the lowest unoccupied molecular orbital (LUMO), were mainly responsible for chemical reactivity (Q. Huang et al., 2020). The smaller HOMO-LUMO gap defined the high chemical reactivity and polarizability of compounds. Among the different monosaccharide structural units, glucose and mannose had the relatively lower HOMO-LUMO gap of 8.10 eV and 8.28 eV, respectively (Supplementary Fig. 4.4). Compared with a higher HOMO-LUMO gap of 8.52 eV and 8.53 eV in xylose and rhamnose, respectively, glucose and mannose units had the higher chemical reactivity and could more easily interact with other molecules. Xyloglucan contains the highest proportion of glucose. However, the

content of xylose in xylan was the highest, and the chemical properties of xylose and rhamnose are relatively inactive, making it difficult for xylan to combine with other molecules to form a complex. For AXLB, AXMB, and AXHB, the structure had a certain regularity: the content of arabinose side-chains gradually increased, while the content of xylose (backbone) gradually decreased. The higher content of xylose, which has less polarizability than the other sugar monomers, explains the lower reactivity of AXLB. However, the reactivity of the atoms on the monosaccharide structure is only one among other factor, and the appropriate relative conformation of hemicelluloses and procyanidins remains the dominant factor that drive the interactions. The backbone of xyloglucan and xylan/arabinoxylan are the glucose and xylose backbone, respectively. In addition, xylans are highly ordered, while arabinoxylans are less ordered and their arabinose substituents influence the degree of rigidity of the structure (Selig, Thygesen, Felby, & Master, 2015; Shrestha et al., 2019).

4.3.3.5.2 Structured hemicelluloses

Considering the large number of unit structures and the excessive number of atoms in polymerized procyanidins, it is not possible at current stage for computers to modelize these structures. Therefore, procyanidin B2 was used to model the local interaction between hemicelluloses and procyanidins. The simulation of local interactions is an important guide to subsequent global simulations. The molecular electrostatic potential (ESP) on the molecular van der Waals (vdW) surfaces was calculated and mapped for the five different xylose-containing hemicelluloses and procyanidin B2, in order to gain further understanding of the molecular recognition behavior (Fig. 4.12). The ESP on the van der Waals surface is appropriate to gather information about the reaction site, molecular property, which is critical for studying and predicting intermolecular interaction (Murray & Politzer, 2011). The pyran ring skeleton (PRS) and CH₂OH group outside the ring presented quite different electrostatic potential characters for different types of hemicellulose. The ESP value over the PRS carbons was moderately negative, reflecting the rich π -cloud features. As for non-PRS part, that is, CH₂OH group, lone pair of each oxygen atom leads to one or more ESP

minima on the vdW surface. Each surface maximum in the non-PRS part corresponds to a hydrogen atom. In addition, the structural optimization of xyloglucan yields the formation of clusters, while hemicelluloses with a xylan backbone still maintain long-chain extension.

Lowest-energy conformer after conformation search were kept for further calculations. The optimized binding geometry was meaningful since molecules interact in a complementary manner of the electrostatic potential ESP to form intermolecular interaction. The overall interaction energies in aqueous solution were estimated to be -480, -319, -315, -306 and -246 kJ/mol and -274, -201, -193, -187 and -160 kJ/mol before and after the counterpoise correction, in the cases of procyanidin B2-Xyloglucan, procyanidin B2-AXLB, procyanidin B2-AXMB, procyanidin B2-AXHB and procyanidin B2-Xylan, respectively.

Independent gradient model (IGM) analysis revealed the existence of extensive non-covalent interaction occurring between the procyanidin B2 and hemicelluloses. The interactions occur through weak hydrogen bonds (light-blue area in isosurfaces) and van der Waals interactions (green area in isosurfaces). It indicated the vital role of non-covalent contacts that facilitating the effective accommodation of target hemicelluloses (Fig. 4.13). A π -stacking interaction complements the interactions occurring between the aromatic ring of procyanidin B2 and hemicellulose. The main contributions to these complexations occur between procyanidin B2 and hemicelluloses (as schematically enlighten by the colouring of the atoms according to their contribution to the complexation - see Fig. 4.12). The relative importance of various atoms in inter-fragmentary interaction was demonstrated by using colors, with the atoms in brighter red contributing more strongly to the interactions. In Fig. 4.12, the volume of the interacting regions could be taken as an indication of the extent of interaction. As a result, procyanidin B2 formed more and less extensive interaction with xyloglucan and xylan residues, respectively, while other hemicelluloses were in the middle. This observation was consistent with the results of the experimental study conducted above.

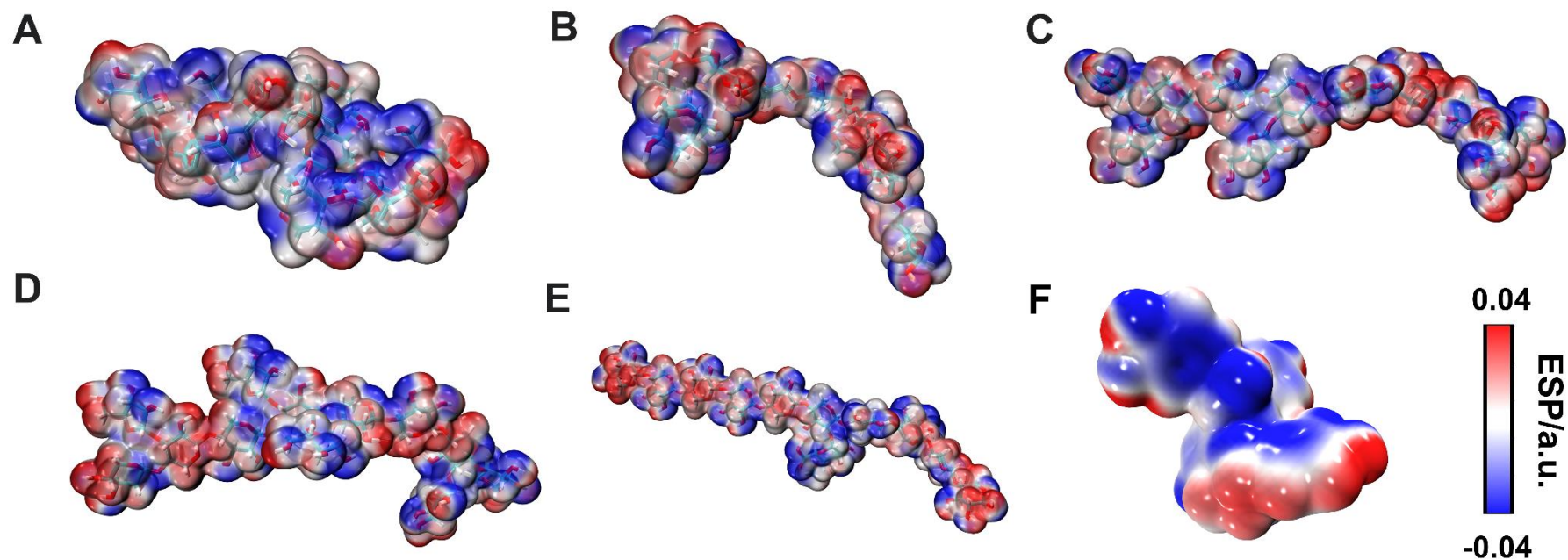


Figure 4.12 Molecular electrostatic potential maps. The optimized geometry of the five different hemicellulose compounds at the B3LYP-D3/6-31G(d,p)/SMD (water) level of theory and the molecular electrostatic potential (ESP) analysis results on 0.001 a.u. contours of the electronic density. (A): Xyloglucan, (B): AXLB (22% Ara), (C): AXMB (30% Ara), (D): AXHB (38% Ara), (E): Xylan, (F): Procyanidin B2, respectively. (Blue: negative regions; Red: positive regions). The color scale is also given in a.u.. AXLB: Arabinoxylan (22% Ara); AXMB: Arabinoxylan (30% Ara); AXHB: Arabinoxylan (38% Ara).

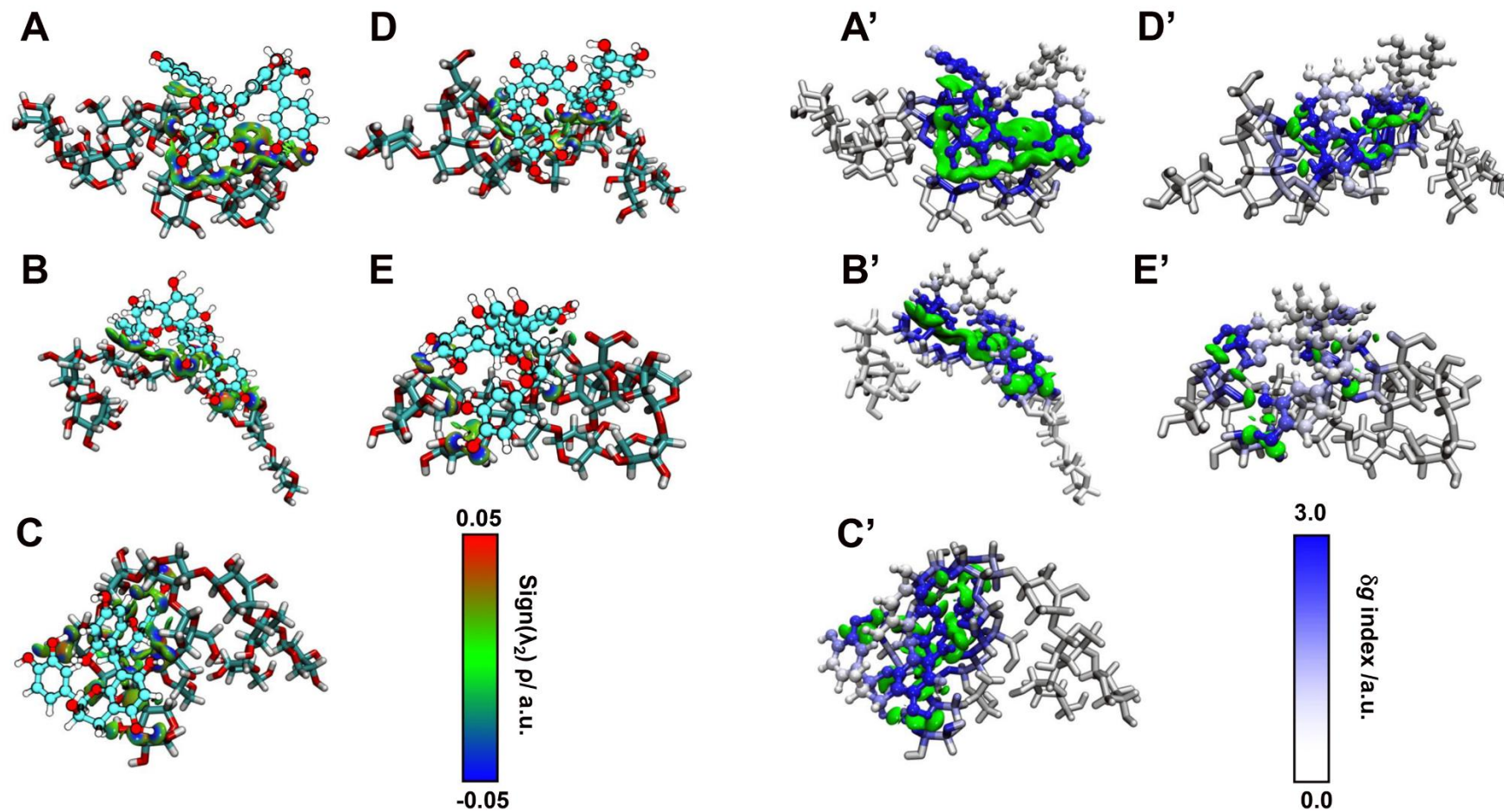


Figure 4.13 Intermolecular interactions (isosurfaces: 0.05 a.u.) using Independent Gradient Model (IGM) analysis. The non-covalent interaction existed in procyanidin B2 and different hemicellulose compounds. Procyanidin B2-Xyloglucan (A), procyanidin B2-AXLB (B), procyanidin B2-AXMB (C), procyanidin B2-AXHB (D) and procyanidin B2-

xylan (E). Blue color represented hydrogen bonding interaction, and green represented van der Waals interaction. All isosurfaces are colored according to a BGR (blue-green-red) scheme over the electron density range $-0.05 < \text{sign}(\lambda^2) \rho < 0.05$ a.u. Molecular structures were also colored based on atom g indices using IGM analysis for procyanidin B2-Xyloglucan (A'), procyanidin B2-AXLB (B'), procyanidin B2-AXMB (C'), procyanidin B2-AXHB (D') and procyanidin B2-xylan (E') colored according to their contributions to the binding. The relative importance of various atoms in inter-fragment interactions is demonstrated by color intensity. White indicates no contribution to the complexation, and atoms in brighter blue contribute more strongly to the interactions. The green ovals indicate the presence of interactions. AXLB: Arabinoxylan (22% Ara); AXMB: Arabinoxylan (30% Ara); AXHB: Arabinoxylan (38% Ara).

The simulations by Shrestha et al. (2019) showed that the intermolecular interaction with cellulose was not influenced by arabinose side-chain in arabinoxylan.

4.3.4 Conclusions

The present study evaluated the nature of the interactions between xylose-containing hemicelluloses, having either a xylan or a glucan backbone, and procyanidins by experimental and theoretical methods. Across all methods used, a consistent ranking of the capacity of association with procyanidins emerges as xyloglucan > arabinoxylans > xylan. Hemicelluloses preferentially associate with the high polymerized procyanidin DP39. The various processing-structure-interaction of hemicelluloses and procyanidins could tailor the functional properties of plant-derived products and provide a practical guide to the retention and changes in polyphenols during processing.

Hightlights

- Experimental and computational methods gave congruent and complementary results on hemicellulose-procyanidin interactions.
- The highest interaction with procyanidins were found for xyloglucan.
- Neither viscosity, molar mass nor side-chains influenced strongly arabinoxylan-procyanidin interactions.
- Stronger interactions with hemicelluloses were found for highly polymerized procyanidins.

Conclusions & Perspectives

Conclusions

This thesis aimed to clarify the impact of raw material/processing relationships on the composition and structure of apple, beet and kiwifruit cell wall polysaccharides and to systematically investigate the mechanisms of their interactions with procyanidins. The knowledge of such specificities in different natural sources can improve the quality of plant-derived products and the understanding of precision processing, and point out important differences concerning the behavior of individual F&Veg species. Moreover, systematic variation of cell wall polysaccharides' structural features allows to better understand polyphenol affinity and may pave the way to anticipate the variability of retention of polyphenols in different F&Vegs.

Previous studies mainly describe texture loss of plant tissues after enzyme inactivation or thermal processing, but each concerns a single plant material at its natural pH (from 3.0 – 6.5). Moreover, although the interactions between the cell wall polysaccharides and procyanidins have been the focus of previous research, to date, there does not appear to be systematic interaction studies which investigate the impact of botanical origins, maturity and processing modifications and evolutions of cell walls in the establishment of cell wall polysaccharide-procyanidin associations. Therefore, this study first examines the specific responses of cell walls from different plant origins processed at different pH under heating conditions and the different levels of common or specific responses. Second, we examined the capacity of sixteen cell walls and twelve pectins from apple, beet and kiwifruit at two maturity stages (ripe and overripe), and seven hemicelluloses differing for their main structural features to interact with procyanidins. They are summarized in the following:

i) Common and specific responses

Cell wall modifications after heating and polysaccharide solubilization occurring in commonly used fruits (apple and kiwifruit) and vegetable (beet) revealed some common features but also some striking differences for the same pH. For all cell walls, all the treatments led to a marked loss of arabinose and galacturonic acid, and by balance a relative increase in xylose, mannose and cellulose. The least pronounced

pectin depolymerization was observed at pH 3.5, that is, β -elimination reaction and acid hydrolysis occur simultaneously at this pH, but both had a low intensity. At pH 2.0, arabinans were lost in apple and beet cell walls due to acid hydrolysis, while galacturonic acids were mostly retained. With regard to treatment at pH 6.0, the galacturonic acid contents decreased significantly after treatment in all cell walls, especially the kiwifruit cell walls, due to β -elimination. Acid hydrolysis and β -elimination appeared to be common mechanisms that cause loss of neutral sugars, often from pectin side-chains, and galacturonic acid, respectively, but their effects were of different intensities. This study improved the understanding of structure/processing relationships and pointed out important differences concerning the behavior of individual species.

When using ATR-FTIR to characterize the changes in the cell walls, we found that: relevant wavenumbers can be easily used to determine the following cell wall polysaccharides, e.g., 1035 cm^{-1} was attributed to xylose-containing hemicelluloses, 1065 and 807 cm^{-1} to mannose-containing hemicelluloses, 988 cm^{-1} to cellulose, 1740 and 1600 cm^{-1} to homogalacturonans according to their degree of methylation. However, some challenges exist due to absence of specific ATR-FTIR response of some cell wall polysaccharides. For example, some difficulties remain to identify intact cell wall components and in particular to discriminate cell walls of apple and beet in relation to the bands of arabinans and galactans.

ii) Cell wall polysaccharide-procyanidin interactions

Cell walls from apple, beet and kiwifruit have different levels of binding selectivity depending on their chemical composition and physical structure. The cell walls interacted more with highly polymerized procyanidins. For extractable polysaccharides (soluble state), e.g., pectins, the linearity and degree of methylation were important, but for native and modified cell walls (insoluble state), porosity appears to be a major factor. The ranking of factors affecting cell wall selectivity were, for those which favor interactions, high porosity (including the size and type) and pectin linearity and homogalacturonan content (as synergists). By contrast, high xylose, ferulic and acetic

acid contents, and pectin branching were detrimental to procyanidin binding (as antagonists).

We further investigated the interactions between pectins and procyanidins using a structure-function relationships approach. Procyanidins showed different binding selectivity to apple, beet and kiwifruit pectins depending on the compositions and macromolecular features and also as function of their degree of polymerization. In general, high affinities were observed between highly methylated pectins and highly polymerized procyanidins, further substantiating the knowledge acquired previously on pectin subunits. High molar mass and low density also contributed to procyanidin adsorption. Pectins with high linearity and HG content, and low arabinan branching had highest interactions with procyanidins. On the contrary, high RG-I branching and ferulic acid content limited the interaction with procyanidins. The importance of factors affecting pectin selectivity were linearity (proportion of side-chains) > molar mass > density \approx hydrodynamic radius, with high branching and density being detrimental to interaction while high molar mass was favorable. For example, highly linear kiwifruit pectins, with high homogalacturonan content and lower branching ratio bound preferentially to procyanidins. A deep understanding of various processing structures-binding capacity of pectins to procyanidins aids food workers to customize the functional characteristics of plant-derived products and provide effective guidance for processing.

Hemicelluloses are second only to pectins in affinity for procyanidins in cell walls. A consistent ranking of the capacity of association with procyanidins emerges as xyloglucan > arabinoxylans > xylan. The different types of arabinoxylans interacted with procyanidins at a similar strength. The arabinose side-chain of arabinoxylan did not inhibit interactions like pectin side-chains. Meanwhile, the computational simulations confirmed the experimental results. Understanding hemicellulose-procyanidin interactions is crucial for the optimization of process conditions and the formulation of food products.

The main results can be summarized as follows:

- Pectin depolymerization was the least pronounced at pH 3.5.
- The main skeleton of pectins was significantly degraded after treatments at pH 6.0 by β -elimination reaction, while the acid treatment at pH 2.0 removed the arabinan side-chains, and their effects were of different intensities for various cell walls.
- The cellulose, hemicelluloses and pectin homogalacturonans can be distinguished by ATR-FTIR, while galactans and arabinans can not.
- Of all cell walls, pectins have the highest affinity for procyanidins.
- Pectins with high linearity and HG content, and low arabinan branching had highest interaction with procyanidins.
- Xyloglucan and xylan exhibited respectively the strongest and weakest interactions with procyanidins in hemicelluloses.

Perspectives

These results still leave some questions. Some of them were considered in this thesis but could not be approached in detail.

Further questions concerning cell walls.

The porosity of the cell wall is a very important factor for the adsorption of polyphenols. Further work is needed to confirm the role of wet porosity (i.e., in suspension) of cell walls. Although high methylated pectin has a high interaction capacity, its level and distribution in HG is also a significant important influencing factor. In addition, the different types of xyloglucans in hemicellulose have not been fully studied.

Both botanical origins and processing were shown to alter cell wall compositions and structure. However, in this study, the focus on cell wall modifications by thermal processing. Questions remain on non-thermal processing and how it affects cell wall microstructure and how this will in turn affect final plant-based products. Moreover, to increase the understanding of the impact cell wall microstructure on structural factors of the processed products, the analyses could be extended to more extensive fruit and vegetables.

Further questions concerning polyphenols.

A limitation of the current study is that only native procyanidins were used, while greater structural flexibility of polyphenols is known to facilitate their binding to cell walls. More work is still needed to understand how interactions are modified by conformational changes of native polyphenols, e.g., interflavanic bond and chiral type, and also oxidation, cleavage and polymerization, which occur during processing. In fact, the proportion and concentration of various polyphenols vary widely in various foodstuffs during the interactions. Further investigations should be carried out in actual food systems to reinforce the implications of this study.

Most polyphenols are sensitive to high temperature; thus, it is important to explore the effects of non-thermal processing, e.g., ultra-high-pressure processing, pulsed electric fields, nonthermal plasma, UV and infrared light, on the interactions between polyphenols and polysaccharides. Moreover, the understanding and quantification of the impact of the proanthocyanidin-cell-wall interactions in food processing, notably in juice extraction, as a function of the state of cell-walls and processing options, should be improved. Alternatively, other flavan-3-ol rich matrices such as tea or cocoa could be studied.

Further questions on food structure and nutrition.

The past has seen the relationship between diet, nutrition, and human health largely focused on the role of individual macronutrients, i.e., proteins, lipids, and carbohydrates; as well as micronutrients, e.g., vitamins and minerals. Such practice of linking an individual nutrient, instead of a whole food, to a defined physiological outcome has resulted in great differences between the predicted and actual health effects of foods. This inconsistency generally stems from the implicit, though often overlooked, role that the structure of a food plays on nutrient absorption, availability, and stability. Whole food structure is the hierarchical organization of food molecules that assemble into defined structural elements, e.g., starch granules, cell walls, oil bodies, polyphenols or protein fibrils that then assemble into larger domains responsible for a food's functional, nutritive, and sensory attributes. Naturally occurring structures are inherently present

in raw food materials, whereas processed structures are created through deconstructing and restructuring processes during food preparation, processing, and consumption. Ultimately, composition, processing, and structure define how a food interacts with the gastrointestinal tract.

The deconstructing (e.g., degradation, depolymerization or cleavage) and restructuring (i.e., interactions) processes of foods influence each other, and ultimately, along with composition, dictate nutrient assimilation in the body. Therefore, most importantly, the native and modified phenolics and dietary fiber, and their interactions, play a potential role in the prevention and management of chronic diseases mediated by the gut microbiota. For example, growing evidence indicates that the biological effects of proanthocyanidins should be attributed to their colonic metabolites rather than to the native proanthocyanidins present in foods. Therefore, more attention should be paid to the nutritional consequences of dietary fiber–polyphenol complexes in the colon, that is, the different fermentation modes of the complexes, as well as the enzymes and bacteria involved. More studies on the interrelationships between polyphenols, polyphenol- dietary fiber and microbial phenolic metabolites in the gut microbiota and a better molecular understanding of their activity in the gut microbiota, as well as a wider range of bacterial species tested, would allow for more accurately determine the potential health benefits consistent with realistic dietary intake and maximize the applications of these health-promoting dietary components.

References

A

- Ahmed, M., & Eun, J. B. (2018). Flavonoids in fruits and vegetables after thermal and nonthermal processing: A review. *Critical Reviews in Food Science and Nutrition*, 58(18), 3159–3188. <https://doi.org/10.1080/10408398.2017.1353480>
- Alba, K., Bingham, R. J., Gunning, P. A., Wilde, P. J., & Kontogiorgos, V. (2018). Pectin Conformation in Solution. *Journal of Physical Chemistry B*, 122(29), 7286–7294. <https://doi.org/10.1021/acs.jpcc.8b04790>
- Albersheim, P., Neukom, H., & Deuel, H. (1960). Splitting of pectin chain molecules in neutral solutions. *Archives of Biochemistry and Biophysics*, 90(1), 46–51. [https://doi.org/10.1016/0003-9861\(60\)90609-3](https://doi.org/10.1016/0003-9861(60)90609-3)
- Aleixandre-Tudo, J. L., & du Toit, W. (2018). Cold maceration application in red wine production and its effects on phenolic compounds: A review. *LWT - Food Science and Technology*, 95, 200–208. <https://doi.org/10.1016/j.lwt.2018.04.096>
- Alejo-Armijo, A., Salido, S., & Altarejos, J. (2020). Synthesis of A-Type Proanthocyanidins and Their Analogues: A Comprehensive Review. *Journal of Agricultural and Food Chemistry*, 68(31), 8104–8118. <https://doi.org/10.1021/acs.jafc.0c03380>
- Alfaro-Viquez, E., Esquivel-Alvarado, D., Madrigal-Carballo, S., Krueger, C. G., & Reed, J. D. (2020). Antimicrobial proanthocyanidin-chitosan composite nanoparticles loaded with gentamicin. *International Journal of Biological Macromolecules*, 162, 1500–1508. <https://doi.org/10.1016/j.ijbiomac.2020.07.213>
- Ali, H., & Guthrie, J. T. (1981). *The Chemistry and Technology of Cellulosic Copolymers*. (A. Hebeish & T. J. Guthrie, Eds.), *Journal of Chemical Information and Modeling* (Vol. 53). Springer, Berlin, Heidelberg. <https://doi.org/10.1007/978-3-642-67707-6>
- Allothman, M., Bhat, R., & Karim, A. A. (2009). Effects of radiation processing on phytochemicals and antioxidants in plant produce. *Trends in Food Science and Technology*, 20(5), 201–212. <https://doi.org/10.1016/j.tifs.2009.02.003>
- Amoako, D. B., & Awika, J. M. (2019). Resistant starch formation through intrahelical V-complexes between polymeric proanthocyanidins and amylose. *Food Chemistry*, 285, 326–333. <https://doi.org/10.1016/j.foodchem.2019.01.173>
- Ananingsih, V. K., Sharma, A., & Zhou, W. (2013). Green tea catechins during food processing and storage: A review on stability and detection. *Food Research International*, 50(2), 469–479. <https://doi.org/10.1016/j.foodres.2011.03.004>
- Anderson, C. T., & Kieber, J. J. (2020). Dynamic Construction, Perception, and Remodeling of Plant Cell Walls. *Annual Review of Plant Biology*, 71(1), 39–69. <https://doi.org/10.1146/annurev-arplant-081519-035846>
- Ando, Y., Hagiwara, S., & Nabetani, H. (2017). Thermal inactivation kinetics of pectin methylesterase and the impact of thermal treatment on the texture, electrical impedance characteristics and cell wall structure of Japanese radish (*Raphanus sativus* L.). *Journal of Food Engineering*, 199, 9–18. <https://doi.org/10.1016/j.jfoodeng.2016.12.001>

- Appeldoorn, M. M., Vincken, J. P., Gruppen, H., & Hollman, P. C. H. (2009). Procyanidin dimers A1, A2, and B2 are absorbed without conjugation or methylation from the small intestine of rats. *Journal of Nutrition*, *139*(8), 1469–1473. <https://doi.org/10.3945/jn.109.106765>
- Aprotosoiaie, A. C., Luca, S. V., & Miron, A. (2016). Flavor chemistry of cocoa and cocoa products-An overview. *Comprehensive Reviews in Food Science and Food Safety*, *15*(1), 73–91. <https://doi.org/10.1111/1541-4337.12180>
- Aron, P. M., & Kennedy, J. A. (2008). Flavan-3-ols: Nature, occurrence and biological activity. *Molecular Nutrition and Food Research*, *52*(1), 79–104. <https://doi.org/10.1002/mnfr.200700137>
- Arshad, R. N., Abdul-Malek, Z., Roobab, U., Munir, M. A., Naderipour, A., Qureshi, M. I., ... Aadil, R. M. (2021). Pulsed electric field: A potential alternative towards a sustainable food processing. *Trends in Food Science and Technology*, *111*, 43–54. <https://doi.org/10.1016/j.tifs.2021.02.041>
- Asano, K., Ohtsu, K., Shinagawa, K., & Hashimoto, N. (1984). Affinity of proanthocyanidins and their oxidation products for haze-forming proteins of beer and the formation of chill haze'. *Agricultural and Biological Chemistry*, *48*(5), 1139–1146. <https://doi.org/10.1271/bbb1961.48.1139>
- Aura, A. M., Mattila, I., Hyötyläinen, T., Gopalacharyulu, P., Cheynier, V., Souquet, J. M., ... Orešič, M. (2013). Characterization of microbial metabolism of Syrah grape products in an in vitro colon model using targeted and non-targeted analytical approaches. *European Journal of Nutrition*, *52*(2), 833–846. <https://doi.org/10.1007/s00394-012-0391-8>

B

- Barba, F. J., Mariutti, L. R. B., Bragagnolo, N., Mercadante, A. Z., Barbosa-Cánovas, G. V., & Orlien, V. (2017). Bioaccessibility of bioactive compounds from fruits and vegetables after thermal and nonthermal processing. *Trends in Food Science and Technology*, *67*, 195–206. <https://doi.org/10.1016/j.tifs.2017.07.006>
- Baron, A., Dénes, J. M., & Durier, C. (2006). High-pressure treatment of cloudy apple juice. *LWT - Food Science and Technology*, *39*(9), 1005–1013. <https://doi.org/10.1016/j.lwt.2006.02.016>
- Barrett, A., Ndou, T., Hughey, C. A., Straut, C., Howell, A., Dai, Z., & Kaletunc, G. (2013). Inhibition of α -amylase and glucoamylase by tannins extracted from cocoa, pomegranates, cranberries, and grapes. *Journal of Agricultural and Food Chemistry*, *61*(7), 1477–1486. <https://doi.org/10.1021/jf304876g>
- Barros, F., Awika, J. M., & Rooney, L. W. (2012). Interaction of tannins and other sorghum phenolic compounds with starch and effects on in vitro starch digestibility. *Journal of Agricultural and Food Chemistry*, *60*(46), 11609–11617. <https://doi.org/10.1021/jf3034539>
- BeMiller, J. N., & Whistler, R. L. (1996). Carbohydrates. In O. R. Fennema. (Ed.), *Food Chemistry* (pp. 157–225). New York: Marcel Dekker.
- Bermúdez-Aguirre, D., & Barbosa-Cánovas, G. V. (2011). An Update on High

- Hydrostatic Pressure, from the Laboratory to Industrial Applications. *Food Engineering Reviews*, 3(1), 44–61. <https://doi.org/10.1007/s12393-010-9030-4>
- Bermúdez-Oria, A., Rodríguez-Gutiérrez, G., Fernández-Prior, Á., Knicker, H., & Fernández-Bolaños, J. (2020). Confirmation by solid-state NMR spectroscopy of a strong complex phenol-dietary fiber with retention of antioxidant activity in vitro. *Food Hydrocolloids*, 102, 105–584. <https://doi.org/10.1016/j.foodhyd.2019.105584>
- Bermúdez-Oria, A., Rodríguez-Gutiérrez, G., Fernández-Prior, Á., Vioque, B., & Fernández-Bolaños, J. (2019). Strawberry dietary fiber functionalized with phenolic antioxidants from olives. Interactions between polysaccharides and phenolic compounds. *Food Chemistry*, 280, 310–320. <https://doi.org/10.1016/j.foodchem.2018.12.057>
- Bernillon, S., Guyot, S., & Renard, C. M. G. C. (2004). Detection of phenolic oxidation products in cider apple juice by high-performance liquid chromatography electrospray ionisation ion trap mass spectrometry. *Rapid Communications in Mass Spectrometry*, 18(9), 939–943. <https://doi.org/10.1002/rcm.1430>
- Betts, M. J., Brown, B. R., Brown, P. E., & Pike, W. T. (1967). Degradation of condensed tannins: Structure of the tannin from common heather. *Chemical Communications (London)*, (21), 1110–1112. <https://doi.org/10.1039/C19670001110>
- Bevilacqua, A., Petruzzi, L., Perricone, M., Speranza, B., Campaniello, D., Sinigaglia, M., & Corbo, M. R. (2018). Nonthermal technologies for fruit and vegetable juices and beverages: Overview and advances. *Comprehensive Reviews in Food Science and Food Safety*, 17(1), 2–62. <https://doi.org/10.1111/1541-4337.12299>
- Bhargava, N., Mor, R. S., Kumar, K., & Sharanagat, V. S. (2021). Advances in application of ultrasound in food processing: A review. *Ultrasonics Sonochemistry*, 70, 105293. <https://doi.org/10.1016/j.ultsonch.2020.105293>
- Billerach, G., Roumeás, L., Dubreucq, E., & Fulcrand, H. (2020). Furanolysis with menthofuran: A new depolymerization method for analyzing condensed tannins. *Journal of Agricultural and Food Chemistry*, 68(10), 2917–2926. <https://doi.org/10.1021/acs.jafc.9b00497>
- Bindon, K. A., Bacic, A., & Kennedy, J. A. (2012). Tissue-specific and developmental modifications of grape cell walls influence the adsorption of proanthocyanidins. *Journal of Agricultural and Food Chemistry*, 60(36), 9249–9260. <https://doi.org/10.1021/jf301552t>
- Bindon, K. A., & Kennedy, J. A. (2011). Ripening-induced changes in grape skin proanthocyanidins modify their interaction with cell walls. *Journal of Agricultural and Food Chemistry*, 59(6), 2696–2707. <https://doi.org/10.1021/jf1047207>
- Bindon, K. A., Li, S., Kassara, S., & Smith, P. A. (2016). Retention of proanthocyanidin in wine-like solution is conferred by a dynamic interaction between soluble and insoluble grape cell wall components. *Journal of Agricultural and Food Chemistry*, 64(44), 8406–8419. <https://doi.org/10.1021/acs.jafc.6b02900>
- Bindon, K. A., & Smith, P. A. (2013). Comparison of the affinity and selectivity of insoluble fibres and commercial proteins for wine proanthocyanidins. *Food*

- Chemistry*, 136(2), 917–928. <https://doi.org/10.1016/j.foodchem.2012.08.016>
- Bindon, K. A., Smith, P. A., Holt, H., & Kennedy, J. A. (2010). Interaction between grape-derived proanthocyanidins and cell wall material. 2. implications for vinification. *Journal of Agricultural and Food Chemistry*, 58(19), 10736–10746. <https://doi.org/10.1021/jf1022274>
- Bindon, K. A., Smith, P. A., & Kennedy, J. A. (2010). Interaction between grape-derived proanthocyanidins and cell wall material. 1. effect on proanthocyanidin composition and molecular mass. *Journal of Agricultural and Food Chemistry*, 58(4), 2520–2528. <https://doi.org/10.1021/jf9037453>
- Birtic, S., Régis, S., Le Bourvellec, C., & Renard, C. M. G. C. (2019). Impact of air-drying on polyphenol extractability from apple pomace. *Food Chemistry*, 296, 142–149. <https://doi.org/10.1016/j.foodchem.2019.05.131>
- Blumenkrantz, N., & Asboe-Hansen, G. (1973). New method for quantitative determination of uronic acids. *Analytical Biochemistry*, 54(2), 484–489. [https://doi.org/10.1016/0003-2697\(73\)90377-1](https://doi.org/10.1016/0003-2697(73)90377-1)
- Boléa, G., Ginies, C., Vallier, M. J., & Dufour, C. (2019). Lipid protection by polyphenol-rich apple matrices is modulated by pH and pepsin in in vitro gastric digestion. *Food and Function*, 10(7), 3942–3954. <https://doi.org/10.1039/c9fo00705a>
- Bordenave, N., Hamaker, B. R., & Ferruzzi, M. G. (2014). Nature and consequences of non-covalent interactions between flavonoids and macronutrients in foods. *Food and Function*, 5(1), 18–34. <https://doi.org/10.1039/c3fo60263j>
- Box, G. E., Hunter, W. G., & Hunter, J. S. (1978). *An introduction to design, data analysis, and model building*. John Wiley & Sons New York, NY.
- Brahem, M., Eder, S., Renard, C. M. G. C., Loonis, M., & Le Bourvellec, C. (2017). Effect of maturity on the phenolic compositions of pear juice and cell wall effects on procyanidins transfer. *LWT - Food Science and Technology*, 85, 380–384. <https://doi.org/10.1016/j.lwt.2016.09.009>
- Brahem, M., Renard, C. M. G. C., Bureau, S., Watrelot, A. A., & Le Bourvellec, C. (2019). Pear ripeness and tissue type impact procyanidin-cell wall interactions. *Food Chemistry*, 275, 754–762. <https://doi.org/10.1016/j.foodchem.2018.09.156>
- Brahem, M., Renard, C. M. G. C., Gouble, B., Bureau, S., & Le Bourvellec, C. (2017). Characterization of tissue specific differences in cell wall polysaccharides of ripe and overripe pear fruit. *Carbohydrate Polymers*, 156, 152–164. <https://doi.org/10.1016/j.carbpol.2016.09.019>
- Brandão, E., Fernandes, A., Guerreiro, C., Coimbra, M. A., Mateus, N., de Freitas, V., & Soares, S. (2020). The effect of pectic polysaccharides from grape skins on salivary protein – procyanidin interactions. *Carbohydrate Polymers*, 236, 116044. <https://doi.org/10.1016/j.carbpol.2020.116044>
- Brianceau, S., Turk, M., Vitrac, X., & Vorobiev, E. (2015). Combined densification and pulsed electric field treatment for selective polyphenols recovery from fermented grape pomace. *Innovative Food Science and Emerging Technologies*, 29, 2–8. <https://doi.org/10.1016/j.ifset.2014.07.010>
- Brownmiller, C., Howard, L. R., & Prior, R. L. (2009). Processing and storage effects

- on procyanidin composition and concentration of processed lueberry products. *Journal of Agricultural and Food Chemistry*, 57(5), 1896–1902.
<https://doi.org/10.1021/jf803015s>
- Broxterman, S. E., Picouet, P., & Schols, H. A. (2017). Acetylated pectins in raw and heat processed carrots. *Carbohydrate Polymers*, 177, 58–66.
<https://doi.org/10.1016/j.carbpol.2017.08.118>
- Broxterman, S. E., & Schols, H. A. (2018). Interactions between pectin and cellulose in primary plant cell walls. *Carbohydrate Polymers*, 192, 263–272.
<https://doi.org/10.1016/j.carbpol.2018.03.070>
- Brummell, D. A. (2006). Cell wall disassembly in ripening fruit. *Functional Plant Biology*, 33(2), 103–119. <https://doi.org/10.1071/FP05234>
- Brummell, D. A., & Harpster, M. H. (2001). Cell wall metabolism in fruit softening and quality and its manipulation in transgenic plants. *Plant Molecular Biology*, 47(1–2), 311–339. <https://doi.org/10.1023/A:1010656104304>
- Brunauer, S., Emmett, P. H., & Teller, E. (1938). Adsorption of Gases in Multimolecular Layers. *Journal of the American Chemical Society*, 60(2), 309–319. <https://doi.org/10.1021/ja01269a023>
- Bruylants, G., Wouters, J., & Michaux, C. (2005). Differential scanning calorimetry in life science: thermodynamics, stability, molecular recognition and application in drug design. *Current Medicinal Chemistry*, 12(17), 2011–2020.
<https://doi.org/10.2174/0929867054546564>
- Buchweitz, M., Speth, M., Kammerer, D. R., & Carle, R. (2013a). Impact of pectin type on the storage stability of black currant (*Ribes nigrum* L.) anthocyanins in pectic model solutions. *Food Chemistry*, 139(1–4), 1168–1178.
<https://doi.org/10.1016/j.foodchem.2013.02.005>
- Buchweitz, M., Speth, M., Kammerer, D. R., & Carle, R. (2013b). Stabilisation of strawberry (*Fragaria x ananassa* Duch.) anthocyanins by different pectins. *Food Chemistry*, 141(3), 2998–3006. <https://doi.org/10.1016/j.foodchem.2013.04.117>
- Bujor, O. C., Ginies, C., Popa, V. I., & Dufour, C. (2018). Phenolic compounds and antioxidant activity of lingonberry (*Vaccinium vitis-idaea* L.) leaf, stem and fruit at different harvest periods. *Food Chemistry*, 252, 356–365.
<https://doi.org/10.1016/j.foodchem.2018.01.052>
- Bureau, S., Ścibisz, I., Le Bourvellec, C., & Renard, C. M. G. C. (2012). Effect of sample preparation on the measurement of sugars, organic acids, and polyphenols in apple fruit by mid-infrared spectroscopy. *Journal of Agricultural and Food Chemistry*, 60(14), 3551–3563. <https://doi.org/10.1021/jf204785w>
- Burger, J. F. W., Kolodziej, H., Hemingway, R. W., Steynberg, J. P., Young, D. A., & Ferreira, D. (1990). Oligomeric flavanoids. Part W. base-catalyzed pyran rearrangements of procyanidin B-2, and evidence for the oxidative transformation of B- to A-type procyanidins. *Tetrahedron*, 46(16), 5733–5740.
[https://doi.org/10.1016/S0040-4020\(01\)87771-1](https://doi.org/10.1016/S0040-4020(01)87771-1)
- Burton, R. A., Gidley, M. J., & Fincher, G. B. (2010). Heterogeneity in the chemistry, structure and function of plant cell walls. *Nature Chemical Biology*, 6(10), 724–732. <https://doi.org/10.1038/nchembio.439>

C

- Caffall, K. H., & Mohnen, D. (2009). The structure, function, and biosynthesis of plant cell wall pectic polysaccharides. *Carbohydrate Research*, *344*(14), 1879–1900. <https://doi.org/10.1016/j.carres.2009.05.021>
- Cai, Y., Gaffney, S. H., Lilley, T. H., Magnolato, D., Martin, R., Spencer, C. M., & Haslam, E. (1990). Polyphenol interactions. Part 4. Model studies with caffeine and cyclodextrins. *Journal of the Chemical Society, Perkin Transactions 2*, (12), 2197–2209. <https://doi.org/10.1039/P29900002197>
- Callies, O., & Hernández Daranas, A. (2016). Application of isothermal titration calorimetry as a tool to study natural product interactions. *Natural Product Reports*, *33*(7), 881–904. <https://doi.org/10.1039/c5np00094g>
- Campos, E. M., Jakobs, L., & Simon, M.-C. (2020). Antidiabetic effects of flavan-3-ols and their microbial metabolites. *Nutrients*, *12*(6), 1592. <https://doi.org/10.3390/nu12061592>
- Candrawinata, V. I., Golding, J. B., Roach, P. D., & Stathopoulos, C. E. (2013). From Apple to Juice-The Fate of Polyphenolic Compounds. *Food Reviews International*, *29*(3), 276–293. <https://doi.org/10.1080/87559129.2013.790049>
- Canteri, M. H. G., Renard, C. M. G. C., Le Bourvellec, C., & Bureau, S. (2019). ATR-FTIR spectroscopy to determine cell wall composition: Application on a large diversity of fruits and vegetables. *Carbohydrate Polymers*, *212*, 186–196. <https://doi.org/10.1016/j.carbpol.2019.02.021>
- Carn, F., Guyot, S., Baron, A., Pérez, J., Buhler, E., & Zanchi, D. (2012). Structural properties of colloidal complexes between condensed tannins and polysaccharide hyaluronan. *Biomacromolecules*, *13*(3), 751–759. <https://doi.org/10.1021/bm201674n>
- Carpita, N., & Gibeaut, D. M. (1993). Structural models of primary cell walls in flowering plants: Consistency of molecular structure with the physical properties of the walls during growth. *Plant Journal*, *3*(1), 1–30. <https://doi.org/10.1111/j.1365-313X.1993.tb00007.x>
- Carpita, N., Sabularse, D., Montezinos, D., & Delmer, D. P. (1979). Determination of the pore size of cell walls of living plant cells. *Science*, *205*(4411), 1144–1147. <https://doi.org/10.1126/science.205.4411.1144>
- Castro-López, L. D. R., Gómez-Plaza, E., Ortega-Regules, A., Lozada, D., & Bautista-Ortín, A. B. (2016). Role of cell wall deconstructing enzymes in the proanthocyanidin-cell wall adsorption-desorption phenomena. *Food Chemistry*, *196*, 526–532. <https://doi.org/10.1016/j.foodchem.2015.09.080>
- Cebrián-Tarancón, C., Sánchez-Gómez, R., Gómez-Alonso, S., Hermosín-Gutierrez, I., Mena-Morales, A., García-Romero, E., ... Zalacain, A. (2018). Vine-shoot tannins: Effect of post-pruning storage and toasting treatment. *Journal of Agricultural and Food Chemistry*, *66*(22), 5556–5562. <https://doi.org/10.1021/acs.jafc.8b01540>
- Çelik, E. E., & Gökmen, V. (2021). Interactions between free and bound antioxidants under different conditions in food systems. *Critical Reviews in Food Science and Nutrition*, 1–17. <https://doi.org/10.1080/10408398.2021.1892584>

- Chamorro, S., Goñi, I., Hervert-Hernández, D., Viveros, A., & Brenes, A. (2012). Changes in polyphenolic content and antioxidant activity after thermal treatments of grape seed extract and grape pomace. *European Food Research and Technology*, 234(1), 147–155. <https://doi.org/10.1007/s00217-011-1621-7>
- Chen, D., Melton, L. D., McGillivray, D. J., Ryan, T. M., & Harris, P. J. (2019). Changes in the orientations of cellulose microfibrils during the development of collenchyma cell walls of celery (*Apium graveolens* L .). *Planta*, 250(6), 1819–1832. <https://doi.org/10.1007/s00425-019-03262-8>
- Chen, G., Huang, K., Miao, M., Feng, B., & Campanella, O. H. (2019). Molecular Dynamics Simulation for Mechanism Elucidation of Food Processing and Safety: State of the Art. *Comprehensive Reviews in Food Science and Food Safety*, 18(1), 243–263. <https://doi.org/10.1111/1541-4337.12406>
- Chen, J., Liu, W., Liu, C. M., Li, T., Liang, R. H., & Luo, S. J. (2015). Pectin Modifications: A Review. *Critical Reviews in Food Science and Nutrition*, 55(12), 1684–1698. <https://doi.org/10.1080/10408398.2012.718722>
- Chen, L., Yuan, P., Chen, K., Jia, Q., & Li, Y. (2014). Oxidative conversion of B- to A-type procyanidin trimer: Evidence for quinone methide mechanism. *Food Chemistry*, 154, 315–322. <https://doi.org/10.1016/j.foodchem.2014.01.018>
- Chen, S., Shen, X., Tao, W., Mao, G., Wu, W., Zhou, S., ... Pan, H. (2020). Preparation of a novel emulsifier by self-assembling of proanthocyanidins from Chinese bayberry (*Myrica rubra* Sieb. et Zucc.) leaves with gelatin. *Food Chemistry*, 319, 126570. <https://doi.org/10.1016/j.foodchem.2020.126570>
- Chen, T. T., Zhang, Z. H., Wang, Z. W., Chen, Z. L., Ma, H., & Yan, J. K. (2021). Effects of ultrasound modification at different frequency modes on physicochemical, structural, functional, and biological properties of citrus pectin. *Food Hydrocolloids*, 113, 106484. <https://doi.org/10.1016/j.foodhyd.2020.106484>
- Chen, Z., Zhu, Q., Tsang, D., & Huang, Y. (2001). Degradation of green tea catechins in tea drinks. *Journal of Agricultural and Food Chemistry*, 49(1), 477–482. <https://doi.org/10.1021/jf000877h>
- Chesson, A., Gardner, P. T., & Wood, T. J. (1997). Cell wall porosity and available surface area of wheat straw and wheat gram fractions. *Journal of the Science of Food and Agriculture*, 75(3), 289–295. [https://doi.org/10.1002/\(SICI\)1097-0010\(199711\)75:3<289::AID-JSFA879>3.0.CO;2-R](https://doi.org/10.1002/(SICI)1097-0010(199711)75:3<289::AID-JSFA879>3.0.CO;2-R)
- Cheynier, V. (2012). Phenolic compounds: From plants to foods. *Phytochemistry Reviews*, 11(2–3), 153–177. <https://doi.org/10.1007/s11101-012-9242-8>
- Cheynier, V., & da Silva, J. M. R. (1991). Oxidation of grape procyanidins in model solutions containing trans-caffeoyltartaric acid and polyphenol oxidase. *Journal of Agricultural and Food Chemistry*, 39(6), 1047–1049. <https://doi.org/10.1021/jf00006a008>
- Chirug, L., Okun, Z., Ramon, O., & Shpigelman, A. (2018). Iron ions as mediators in pectin-flavonols interactions. *Food Hydrocolloids*, 84, 441–449. <https://doi.org/10.1016/j.foodhyd.2018.06.039>
- Christiaens, S., Van Buggenhout, S., Houben, K., Jamsazzadeh Kermani, Z., Moelants,

- K. R. N., Ngouémazong, E. D., ... Hendrickx, M. (2016a). Process–Structure–Function Relations of Pectin in Food. *Critical Reviews in Food Science and Nutrition*, 56(6), 1021–1042. <https://doi.org/10.1080/10408398.2012.753029>
- Christofi, S., Malliaris, D., Katsaros, G., Panagou, E., & Kallithraka, S. (2020). Limit SO₂ content of wines by applying high hydrostatic pressure. *Innovative Food Science and Emerging Technologies*, 62, 102342. <https://doi.org/10.1016/j.ifset.2020.102342>
- Chylinska, M., Szymanska-Chargot, M., & Zdunek, A. (2016). FT-IR and FT-Raman characterization of non-cellulosic polysaccharides fractions isolated from plant cell wall. *Carbohydrate Polymers*, 154, 48–54. <https://doi.org/10.1016/j.carbpol.2016.07.121>
- Coimbra, M. A., Barros, A., Barros, M., Rutledge, D., & Delgadillo, I. (1998). Multivariate analysis of uronic acid and neutral sugars in whole pectic samples by FT-IR spectroscopy. *Carbohydrate Polymers*, 37, 241–248. [https://doi.org/10.1016/S0144-8617\(98\)00066-6](https://doi.org/10.1016/S0144-8617(98)00066-6)
- Coimbra, M. A., Barros, A., Rutledge, D. N., & Delgadillo, I. (1999). FTIR spectroscopy as a tool for the analysis of olive pulp cell-wall polysaccharide extracts. *Carbohydrate Research*, 317(1–4), 145–154. [https://doi.org/10.1016/S0008-6215\(99\)00071-3](https://doi.org/10.1016/S0008-6215(99)00071-3)
- Connors, K. A. (1997). The stability of cyclodextrin complexes in solution. *Chemical Reviews*, 97(5), 1325–1357. <https://doi.org/10.1021/cr960371r>
- Cordella, C. B. Y., & Bertrand, D. (2014). SAISIR: A new general chemometric toolbox. *TrAC - Trends in Analytical Chemistry*, 54, 75–82. <https://doi.org/10.1016/j.trac.2013.10.009>
- Costa, T. dos S., Rogez, H., & Pena, R. da S. (2015). Adsorption capacity of phenolic compounds onto cellulose and xylan. *Food Science and Technology (Campinas)*, 35(2), 314–320. <https://doi.org/10.1590/1678-457x.6568>
- Cui, J., Lian, Y., Zhao, C., Du, H., Han, Y., Gao, W., ... Zheng, J. (2019). Dietary Fibers from Fruits and Vegetables and Their Health Benefits via Modulation of Gut Microbiota. *Comprehensive Reviews in Food Science and Food Safety*, 18(5), 1514–1532. <https://doi.org/10.1111/1541-4337.12489>
- Cui, J., Zhao, C., Feng, L., Han, Y., Du, H., Xiao, H., & Zheng, J. (2021). Pectins from fruits: Relationships between extraction methods, structural characteristics, and functional properties. *Trends in Food Science and Technology*, 110, 39–54. <https://doi.org/10.1016/j.tifs.2021.01.077>
- Cui, R., & Zhu, F. (2021). Ultrasound modified polysaccharides: A review of structure, physicochemical properties, biological activities and food applications. *Trends in Food Science and Technology*, 107, 491–508. <https://doi.org/10.1016/j.tifs.2020.11.018>
- Daas, P. J. H., Meyer-Hansen, K., Schols, H. A., De Ruiter, G. A., & Voragen, A. G. J. (1999). Investigation of the non-esterified galacturonic acid distribution in pectin with endopolygalacturonase. *Carbohydrate Research*, 318(1–4), 135–145. [https://doi.org/10.1016/S0008-6215\(99\)00093-2](https://doi.org/10.1016/S0008-6215(99)00093-2)
- Dai, T., Chen, J., McClements, D. J., Hu, P., Ye, X., Liu, C., & Li, T. (2019). Protein-

- polyphenol interactions enhance the antioxidant capacity of phenolics: Analysis of rice glutelin-procyanidin dimer interactions. *Food and Function*, *10*(2), 765–774. <https://doi.org/10.1039/c8fo02246a>
- Davidov-Pardo, G., Arozarena, I., & Marín-Arroyo, M. R. (2011). Kinetics of thermal modifications in a grape seed extract. *Journal of Agricultural and Food Chemistry*, *59*(13), 7211–7217. <https://doi.org/10.1021/jf200833a>
- De Bruyne, T., Pieters, L., Deelstra, H., & Vlietinck, A. (1999). Condensed vegetable tannins: Biodiversity in structure and biological activities. *Biochemical Systematics and Ecology*, *27*(4), 445–459. [https://doi.org/10.1016/S0305-1978\(98\)00101-X](https://doi.org/10.1016/S0305-1978(98)00101-X)
- De Freitas, V., & Mateus, N. (2001a). Structural features of procyanidin interactions with salivary proteins. *Journal of Agricultural and Food Chemistry*, *49*(2), 940–945. <https://doi.org/10.1021/jf000981z>
- De Mejia, E. G., Zhang, Q., Penta, K., Eroglu, A., & Lila, M. A. (2020). The Colors of Health: Chemistry, Bioactivity, and Market Demand for Colorful Foods and Natural Food Sources of Colorants. *Annual Review of Food Science and Technology*, *11*, 145–182. <https://doi.org/10.1146/annurev-food-032519-051729>
- De Roeck, A., Duvetter, T., Fraeye, I., Plancken, I. Van der, Sila, D. N., Loey, A. Van, & Hendrickx, M. (2009). Effect of high-pressure/high-temperature processing on chemical pectin conversions in relation to fruit and vegetable texture. *Food Chemistry*, *115*(1), 207–213. <https://doi.org/10.1016/j.foodchem.2008.12.016>
- De Roeck, A., Sila, D. N., Duvetter, T., Van Loey, A., & Hendrickx, M. (2008). Effect of high pressure/high temperature processing on cell wall pectic substances in relation to firmness of carrot tissue. *Food Chemistry*, *107*(3), 1225–1235. <https://doi.org/10.1016/j.foodchem.2007.09.076>
- De Taeye, C., Bodart, M., Caultet, G., & Collin, S. (2017). Roasting conditions for preserving cocoa flavan-3-ol monomers and oligomers: interesting behaviour of Criollo clones. *Journal of the Science of Food and Agriculture*, *97*(12), 4001–4008. <https://doi.org/10.1002/jsfa.8265>
- De Taeye, C., Caultet, G., Eyamo Evina, V. J., & Collin, S. (2017). Procyanidin A2 and its degradation products in raw, fermented, and roasted cocoa. *Journal of Agricultural and Food Chemistry*, *65*(8), 1715–1723. <https://doi.org/10.1021/acs.jafc.6b05262>
- De Taeye, C., Kankolongo Cibaka, M. L., Jerkovic, V., & Collin, S. (2014). Degradation of (-)-epicatechin and procyanidin b2 in aqueous and lipidic model systems. First evidence of “chemical” flavan-3-ol oligomers in processed cocoa. *Journal of Agricultural and Food Chemistry*, *62*(36), 9002–9016. <https://doi.org/10.1021/jf502016z>
- Debelo, H., Li, M., & Ferruzzi, M. G. (2020). Processing influences on food polyphenol profiles and biological activity. *Current Opinion in Food Science*, *32*, 90–102. <https://doi.org/10.1016/j.cofs.2020.03.001>
- Del Fresno, J. M., Morata, A., Ricardo-da-Silva, J. M., Escott, C., Loira, I., & Lepe, J. A. S. (2019). Modification of the polyphenolic and aromatic fractions of red wines aged on lees assisted with ultrasound. *International Journal of Food Science and*

- Technology*, 54(9), 2690–2699. <https://doi.org/10.1111/ijfs.14179>
- Del Pino-García, R., González-SanJosé, M. L., Rivero-Pérez, M. D., García-Lomillo, J., & Muñiz, P. (2017). The effects of heat treatment on the phenolic composition and antioxidant capacity of red wine pomace seasonings. *Food Chemistry*, 221, 1723–1732. <https://doi.org/10.1016/j.foodchem.2016.10.113>
- Déprez, S., Brezillon, C., Rabot, S., Philippe, C., Mila, I., Lapierre, C., & Scalbert, A. (2000). Polymeric proanthocyanidins are catabolized by human colonic microflora into low-molecular-weight phenolic acids. *Journal of Nutrition*, 130(11), 2733–2738. <https://doi.org/10.1093/jn/130.11.2733>
- Devic, E., Guyot, S., Daudin, J. D., & Bonazzi, C. (2010). Effect of temperature and cultivar on polyphenol retention and mass transfer during osmotic dehydration of apples. *Journal of Agricultural and Food Chemistry*, 58(1), 606–614. <https://doi.org/10.1021/jf903006g>
- Dhital, S., Brennan, C., & Gidley, M. J. (2019). Location and interactions of starches in planta: Effects on food and nutritional functionality. *Trends in Food Science and Technology*, 93, 158–166. <https://doi.org/10.1016/j.tifs.2019.09.011>
- Diaz, J. V., Anthon, G. E., & Barrett, D. M. (2007). Nonenzymatic degradation of citrus pectin and pectate during prolonged heating: Effects of pH, temperature, and degree of methyl esterification. *Journal of Agricultural and Food Chemistry*, 55(13), 5131–5136. <https://doi.org/10.1021/jf0701483>
- Diwani, N., Fakhfakh, J., Athmouni, K., Belhaj, D., El Feki, A., Allouche, N., ... Bouaziz-Ketata, H. (2020). Optimization, extraction, structure analysis and antioxidant properties of flavan-3-ol polymers: Proanthocyanidins isolated from *Periploca angustifolia* using surface response methodology. *Industrial Crops and Products*, 144, 112040. <https://doi.org/10.1016/j.indcrop.2019.112040>
- Dobson, C. C., Mottawea, W., Rodrigue, A., Buzati Pereira, B. L., Hammami, R., Power, K. A., & Bordenave, N. (2019a). Impact of molecular interactions with phenolic compounds on food polysaccharides functionality. In L. B. Isabel C.F.R. Ferreira (Ed.), *Advances in Food and Nutrition Research* (Vol. 90, pp. 135–181). Elsevier Inc. <https://doi.org/10.1016/bs.afnr.2019.02.010>
- Dongowski, G. (2001). Enzymatic degradation studies of pectin and cellulose from red beets. *Nahrung - Food*, 45(5), 324–331. [https://doi.org/10.1002/1521-3803\(20011001\)45:5<324::AID-FOOD324>3.0.CO;2-C](https://doi.org/10.1002/1521-3803(20011001)45:5<324::AID-FOOD324>3.0.CO;2-C)
- Donlao, N., & Ogawa, Y. (2019). The influence of processing conditions on catechin, caffeine and chlorophyll contents of green tea (*Camelia sinensis*) leaves and infusions. *LWT - Food Science and Technology*, 116, 108567. <https://doi.org/10.1016/j.lwt.2019.108567>
- Donovan, J. L., Lee, A., Manach, C., Rios, L., Morand, C., Scalbert, A., & Rémésy, C. (2002). Procyanidins are not bioavailable in rats fed a single meal containing a grapeseed extract or the procyanidin dimer B 3. *British Journal of Nutrition*, 87(4), 299–306. <https://doi.org/10.1079/bjn2001517>
- Dorenkott, M. R., Griffin, L. E., Goodrich, K. M., Thompson-Witrick, K. A., Fundaro, G., Ye, L., ... Neilson, A. P. (2014). Oligomeric cocoa procyanidins possess enhanced bioactivity compared to monomeric and polymeric cocoa procyanidins

- for preventing the development of obesity, insulin resistance, and impaired glucose tolerance during high-fat feeding. *Journal of Agricultural and Food Chemistry*, 62(10), 2216–2227. <https://doi.org/10.1021/jf500333y>
- Dörnenburg, H., & Knorr, D. (1993). Cellular permeabilization of cultured plant tissues by high electric field pulses or ultra high pressure for the recovery of secondary metabolites. *Food Biotechnology*, 7(1), 35–48.
- E**
- Edelmann, A., Diewok, J., Schuster, K. C., & Lendl, B. (2001). Rapid method for the discrimination of red wine cultivars based on mid-infrared spectroscopy of phenolic wine extracts. *Journal of Agricultural and Food Chemistry*, 49(3), 1139–1145. <https://doi.org/10.1021/jf001196p>
- Edwards, S. L. (1976). *An Investigation of the Vibrational Spectra of the Pentose Sugars*. Lawrence University.
- Einstein, A. (1906). Eine neue Bestimmung der Moleküldimensionen. *Annalen der Physik*, 324(2), 289–306.
- Einstein, A. (1911). Berichtigung zu meiner Arbeit: Eine neue Bestimmung der Moleküldimensionen. *Annalen der Physik*, 339(3), 591–592.
- El-Seedi, H. R., El-Said, A. M. A., Khalifa, S. A. M., Göransson, U., Bohlin, L., Borg-Karlson, A. K., & Verpoorte, R. (2012). Biosynthesis, natural sources, dietary intake, pharmacokinetic properties, and biological activities of hydroxycinnamic acids. *Journal of Agricultural and Food Chemistry*, 60(44), 10877–10895. <https://doi.org/10.1021/jf301807g>
- El Darra, N., Turk, M. F., Ducasse, M. A., Grimi, N., Maroun, R. G., Louka, N., & Vorobiev, E. (2016). Changes in polyphenol profiles and color composition of freshly fermented model wine due to pulsed electric field, enzymes and thermovinification pretreatments. *Food Chemistry*, 194(2016), 944–950. <https://doi.org/10.1016/j.foodchem.2015.08.059>
- Ella Missang, C., Maingonnat, J. F., Renard, C. M. G. C., & Audergon, J. M. (2012). Apricot cell wall composition: Relation with the intra-fruit texture heterogeneity and impact of cooking. *Food Chemistry*, 133(1), 45–54. <https://doi.org/10.1016/j.foodchem.2011.12.059>
- Ellinger, S., Reusch, A., Henckes, L., Ritter, C., Zimmermann, B. F., Ellinger, J., ... Helfrich, H.-P. (2020). Low plasma appearance of (+)-catechin and (–)-catechin compared with epicatechin after consumption of beverages prepared from nonalkalized or alkalized cocoa—A randomized, double-Blind trial. *Nutrients*, 12(1), 231. <https://doi.org/10.3390/nu12010231>
- Engelhardt, U. H. (2020). Tea chemistry – What do and what don't we know? – A micro review. *Food Research International*, 132, 109120. <https://doi.org/10.1016/j.foodres.2020.109120>
- Englyst, H., Wiggins, H. S., & Cummings, J. H. (1982). Determination of the non-starch polysaccharides in plant foods by gas-liquid chromatography of constituent sugars as alditol acetates. *The Analyst*, 107(1272), 307–318.

- <https://doi.org/10.1039/an9820700307>
- Eran Nagar, E., Okun, Z., & Shpigelman, A. (2020). Digestive fate of polyphenols: updated view of the influence of chemical structure and the presence of cell wall material. *Current Opinion in Food Science*, 31, 38–46.
<https://doi.org/10.1016/j.cofs.2019.10.009>
- Esatbeyoglu, T., & Winterhalter, P. (2010). Preparation of dimeric procyanidins B1, B2, B5, and B7 from a polymeric procyanidin fraction of black chokeberry (*Aronia melanocarpa*). *Journal of Agricultural and Food Chemistry*, 58(8), 5147–5153. <https://doi.org/10.1021/jf904354n>
- Esatbeyoglu, T., Wray, V., & Winterhalter, P. (2010). Dimeric procyanidins: screening for B1 to B8 and semisynthetic preparation of B3, B4, B6, And B8 from a polymeric procyanidin fraction of white willow bark (*Salix alba*). *Journal of Agricultural and Food Chemistry*, 58(13), 7820–7830.
<https://doi.org/10.1021/jf101023e>
- Esparza, I., Jiménez-Moreno, N., Bimbela, F., Ancín-Azpilicueta, C., & Gandía, L. M. (2020). Fruit and vegetable waste management: Conventional and emerging approaches. *Journal of Environmental Management*, 265, 110510.
<https://doi.org/10.1016/j.jenvman.2020.110510>

F

- Fan, F. Y., Shi, M., Nie, Y., Zhao, Y., Ye, J. H., & Liang, Y. R. (2016). Differential behaviors of tea catechins under thermal processing: Formation of non-enzymatic oligomers. *Food Chemistry*, 196, 347–354.
<https://doi.org/10.1016/j.foodchem.2015.09.056>
- FAO. (2021). *Fruit and vegetables – your dietary essentials. The International Year of Fruits and Vegetables, 2021, background paper*. Rome, Italy: FAO.
<https://doi.org/10.4060/cb2395en>
- Feliciano, R. P., Shea, M. P., Shanmuganayagam, D., Krueger, C. G., Howell, A. B., & Reed, J. D. (2012). Comparison of isolated cranberry (*Vaccinium macrocarpon* Ait.) proanthocyanidins to catechin and procyanidins A2 and B2 for use as standards in the 4-(dimethylamino)cinnamaldehyde assay. *Journal of Agricultural and Food Chemistry*, 60(18), 4578–4585. <https://doi.org/10.1021/jf3007213>
- Fernandes, A., Brás, N. F., Mateus, N., & De Freitas, V. (2014). Understanding the molecular mechanism of anthocyanin binding to pectin. *Langmuir*, 30(28), 8516–8527. <https://doi.org/10.1021/la501879w>
- Fernandes, A., Brás, N. F., Oliveira, J., Mateus, N., & De Freitas, V. (2016). Impact of a pectic polysaccharide on oenin copigmentation mechanism. *Food Chemistry*, 209, 17–26. <https://doi.org/10.1016/j.foodchem.2016.04.018>
- Fernandes, A., Oliveira, J., Fonseca, F., Ferreira-da-silva, F., Vincken, J., & Freitas, V. De. (2020). Molecular binding between anthocyanins and pectic polysaccharides – Unveiling the role of pectic polysaccharides structure. *Food Hydrocolloids*, 105–625. <https://doi.org/10.1016/j.foodhyd.2019.105625>
- Fernandes, P. A. R., Le Bourvellec, C., Renard, C. M. G. C., Nunes, F. M., Bastos, R.,

- Coelho, E., ... Cardoso, S. M. (2019). Revisiting the chemistry of apple pomace polyphenols. *Food Chemistry*, 294, 9–18.
<https://doi.org/10.1016/j.foodchem.2019.05.006>
- Fernandes, P. A. R., Le Bourvellec, C., Renard, C. M. G. C., Wessel, D. F., Cardoso, S. M., & Coimbra, M. A. (2020). Interactions of arabinan-rich pectic polysaccharides with polyphenols. *Carbohydrate Polymers*, 230, 115–644.
<https://doi.org/10.1016/j.carbpol.2019.115644>
- Fernández-Romero, E., Chavez-Quintana, S. G., Siche, R., Castro-Alayo, E. M., & Cardenas-Toro, F. P. (2020). The kinetics of total phenolic content and monomeric Flavan-3-ols during the roasting process of Criollo Cocoa. *Antioxidants*, 9(2), 7–10. <https://doi.org/10.3390/antiox9020146>
- Ferreira, D., Barros, A., Coimbra, M. A., & Delgadillo, I. (2001). Use of FT-IR spectroscopy to follow the effect of processing in cell wall polysaccharide extracts of a sun-dried pear. *Carbohydrate Polymers*, 45(2), 175–182.
[https://doi.org/10.1016/S0144-8617\(00\)00320-9](https://doi.org/10.1016/S0144-8617(00)00320-9)
- Ferreira, D., Guyot, S., Marnet, N., Delgadillo, I., Renard, C. M. G. C., & Coimbra, M. A. (2002). Composition of phenolic compounds in a Portuguese pear (*Pyrus communis* L. var. S. Bartolomeu) and changes after sun-drying. *Journal of Agricultural and Food Chemistry*, 50(16), 4537–4544.
<https://doi.org/10.1021/jf020251m>
- Filippov, M. P., & Kohn, R. (1975). Determination of the esterification degree of carboxyl groups of pectin with methanol by means of infrared spectroscopy. *Chemical Papers*, 29(1), 88–91. Retrieved from
<https://www.chempap.org/?id=7&paper=5409>
- Fischer, M., Wegryzn, T. F., Hallett, I. C., & Redgwell, R. J. (1996). Chemical and structural features of kiwifruit cell walls: Comparison of fruit and suspension-cultured cells. *Carbohydrate Research*, 295, 195–208.
[https://doi.org/10.1016/S0008-6215\(96\)00234-0](https://doi.org/10.1016/S0008-6215(96)00234-0)
- Fishman, M. L., Chau, H. K., Kolpak, F., & Brady, J. (2001). Solvent effects on the molecular properties of pectins. *Journal of Agricultural and Food Chemistry*, 49(9), 4494–4501. <https://doi.org/10.1021/jf0013171>
- Fletcher, A. C., Porter, L. J., & Haslam, E. (1976). Hindered rotation and helical structures in natural procyanidins. *Journal of the Chemical Society, Chemical Communications*, (16), 627–629. <https://doi.org/10.1039/C39760000627>
- Flory, P. J. (1953). Molecular configuration of polyelectrolytes. *The Journal of Chemical Physics*, 21(1), 162–163.
- Fraeye, I., De Roeck, A., Duvetter, T., Verlent, I., Hendrickx, M., & Van Loey, A. (2007). Influence of pectin properties and processing conditions on thermal pectin degradation. *Food Chemistry*, 105(2), 555–563.
<https://doi.org/10.1016/j.foodchem.2007.04.009>
- Frisch, M. J., Trucks, G. W., Schlegel, H. B., Scuseria, G. E., Robb, M. A., Cheeseman, J. R., ... others. (2016). Gaussian 16, Revision A. 03, Gaussian, Inc., Wallingford CT. *City*.
- Fry, S. C. (1983). Feruloylated pectins from the primary cell wall: their structure and

- possible functions. *Planta*, 157(2), 111–123. <https://doi.org/10.1007/BF00393644>
- Fry, S. C. (1988). The growing plant cell wall: chemical and metabolic analysis. *John Wiley and Sons, New York*, 203, 333. <https://doi.org/10.1111/j.1469-8137.2003.00980.x>
- Fulcrand, H., Dueñas, M., Salas, E., & Cheynier, V. (2006). Phenolic reactions during winemaking and aging. *American Journal of Enology and Viticulture*, 57(3), 289–297.
- Fuleki, T., & Ricardo-Da-Silva, J. M. (2003). Effects of cultivar and processing method on the contents of catechins and procyanidins in grape juice. *Journal of Agricultural and Food Chemistry*, 51(3), 640–646. <https://doi.org/10.1021/jf020689m>
- Fumi, M. D., Galli, R., Lambri, M., Donadini, G., & De Faveri, D. M. (2011). Effect of full-scale brewing process on polyphenols in Italian all-malt and maize adjunct lager beers. *Journal of Food Composition and Analysis*, 24(4–5), 568–573. <https://doi.org/10.1016/j.jfca.2010.12.006>

G

- Gacon, K., Peleg, H., & C.Noble, A. (1999). II-29. Bitterness and astringency of flavan-3-OL monomers, dimers and trimers. *Food Quality and Preference*, 7, 1123–1128. [https://doi.org/10.1016/S0950-3293\(96\)90245-1](https://doi.org/10.1016/S0950-3293(96)90245-1)
- Galvez-Lopez, D., Laurens, F., Quémener, B., & Lahaye, M. (2011). Variability of cell wall polysaccharides composition and hemicellulose enzymatic profile in an apple progeny. *International Journal of Biological Macromolecules*, 49(5), 1104–1109. <https://doi.org/10.1016/j.ijbiomac.2011.09.007>
- Gao, C., Cunningham, D. G., Liu, H., Khoo, C., & Gu, L. (2018). Development of a thiolysis HPLC method for the analysis of procyanidins in cranberry products. *Journal of Agricultural and Food Chemistry*, 66(9), 2159–2167. <https://doi.org/10.1021/acs.jafc.7b04625>
- Gaulton, A., Hersey, A., Nowotka, M. L., Patricia Bento, A., Chambers, J., Mendez, D., ... Leach, A. R. (2017). The ChEMBL database in 2017. *Nucleic Acids Research*, 45(D1), D945–D954. <https://doi.org/10.1093/nar/gkw1074>
- Genova, G., Tosetti, R., & Tonutti, P. (2016). Berry ripening, pre-processing and thermal treatments affect the phenolic composition and antioxidant capacity of grape (*Vitis vinifera* L.) juice. *Journal of the Science of Food and Agriculture*, 96(2), 664–671. <https://doi.org/10.1002/jsfa.7138>
- Gibis, M., Thellmann, K., Thongkaew, C., & Weiss, J. (2014). Interaction of polyphenols and multilayered liposomal-encapsulated grape seed extract with native and heat-treated proteins. *Food Hydrocolloids*, 41, 119–131. <https://doi.org/10.1016/j.foodhyd.2014.03.024>
- Gidley, M. J., & Yakubov, G. E. (2019). Functional categorisation of dietary fibre in foods: Beyond 'soluble' vs 'insoluble.' *Trends in Food Science and Technology*, 86, 563–568. <https://doi.org/10.1016/j.tifs.2018.12.006>
- Gill, S. K., Rossi, M., Bajka, B., & Whelan, K. (2020). Dietary fibre in gastrointestinal

- health and disease. *Nature Reviews Gastroenterology and Hepatology*.
<https://doi.org/10.1038/s41575-020-00375-4>
- Gille, S., & Pauly, M. (2012). O-acetylation of plant cell wall polysaccharides. *Frontiers in Plant Science*, 3, 12. <https://doi.org/10.3389/fpls.2012.00012>
- Girard, A. L., & Awika, J. M. (2021). Impact of condensed tannin interactions with grain proteins and non-starch polysaccharides on batter system properties. *Food Chemistry*, 359, 129969. <https://doi.org/10.1016/j.foodchem.2021.129969>
- Giteru, S. G., Oey, I., & Ali, M. A. (2018). Feasibility of using pulsed electric fields to modify biomacromolecules: A review. *Trends in Food Science and Technology*, 72, 91–113. <https://doi.org/10.1016/j.tifs.2017.12.009>
- Gnanasambandam, R., Proctor, A. (2000). Determination of pectin degree of esterification by diffuse reflectance, 68, 327–332.
- Gobert, M., Rémond, D., Loonis, M., Buffière, C., Santé-Lhoutellier, V., & Dufour, C. (2014). Fruits, vegetables and their polyphenols protect dietary lipids from oxidation during gastric digestion. *Food and Function*, 5(9), 2166–2174. <https://doi.org/10.1039/c4fo00269e>
- Goldstein, J. I., Newbury, D. E., Michael, J. R., Ritchie, N. W. M., Scott, J. H. J., & Joy, D. C. (2017). *Scanning electron microscopy and X-ray microanalysis*. Springer. <https://doi.org/10.1007/978-1-4939-6676-9>
- Gómez-Maqueo, A., Welti-Chanes, J., & Cano, M. P. (2020). Release mechanisms of bioactive compounds in fruits submitted to high hydrostatic pressure: A dynamic microstructural analysis based on prickly pear cells. *Food Research International*, 130, 108909. <https://doi.org/10.1016/j.foodres.2019.108909>
- Gómez-Mascaraque, L. G., Dhital, S., López-Rubio, A., & Gidley, M. J. (2017). Dietary polyphenols bind to potato cells and cellular components. *Journal of Functional Foods*, 37, 283–292. <https://doi.org/10.1016/j.jff.2017.07.062>
- Gong, L., Li, T., Chen, F., Duan, X., Yuan, Y., Zhang, D., & Jiang, Y. (2016). An inclusion complex of eugenol into β -cyclodextrin: Preparation, and physicochemical and antifungal characterization. *Food Chemistry*, 196, 324–330. <https://doi.org/10.1016/j.foodchem.2015.09.052>
- González-Aguilar, G. A., Blancas-Benítez, F. J., & Sáyago-Ayerdi, S. G. (2017). Polyphenols associated with dietary fibers in plant foods: molecular interactions and bioaccessibility. *Current Opinion in Food Science*, 13, 84–88. <https://doi.org/10.1016/j.cofs.2017.03.004>
- Gordillo, B., Rodríguez-Pulido, F. J., González-Miret, M. L., Quijada-Morín, N., Rivas-Gonzalo, J. C., García-Estévez, I., ... Escribano-Bailón, M. T. (2015). Application of differential colorimetry to evaluate anthocyanin-flavonol-flavanol ternary copigmentation interactions in model solutions. *Journal of Agricultural and Food Chemistry*, 63(35), 7645–7653. <https://doi.org/10.1021/acs.jafc.5b00181>
- Grabber, J. H., Hatfield, R. D., Ralph, J., Zon, J., & Amrhein, N. (1995). Ferulate cross-linking in cell walls isolated from maize cell suspensions. *Phytochemistry*, 40(4), 1077–1082. [https://doi.org/10.1016/0031-9422\(95\)00413-2](https://doi.org/10.1016/0031-9422(95)00413-2)
- Grabber, J. H., & Zeller, W. E. (2020). Direct versus sequential analysis of procyanidin-

- and prodelphinidin-based condensed tannins by the HCl-Butanol-Acetone-Iron assay. *Journal of Agricultural and Food Chemistry*, *68*(10), 2906–2916. <https://doi.org/10.1021/acs.jafc.9b01307>
- Grabber, J. H., Zeller, W. E., & Mueller-Harvey, I. (2013). Acetone enhances the direct analysis of procyanidin- and prodelphinidin-based condensed tannins in lotus species by the butanol-HCl-iron assay. *Journal of Agricultural and Food Chemistry*, *61*(11), 2669–2678. <https://doi.org/10.1021/jf304158m>
- Granato, D., Santos, J. S., Escher, G. B., Ferreira, B. L., & Maggio, R. M. (2018). Use of principal component analysis (PCA) and hierarchical cluster analysis (HCA) for multivariate association between bioactive compounds and functional properties in foods: A critical perspective. *Trends in Food Science and Technology*, *72*, 83–90. <https://doi.org/10.1016/j.tifs.2017.12.006>
- Grant, L. J., Mikkelsen, D., Phan, A. D. T., Kang, S., Ouwerkerk, D., Klieve, A. V., ... Williams, B. A. (2020). Purified plant cell walls with adsorbed polyphenols alter porcine faecal bacterial communities during in vitro fermentation. *Food and Function*, *11*(1), 834–845. <https://doi.org/10.1039/c9fo02428j>
- Grimme, S.; Bannwarth, C.; Shushkov, P. (2017) A Robust and Accurate Tight-Binding Quantum Chemical Method for Structures, Vibrational Frequencies, and Noncovalent Interactions of Large Molecular Systems Parametrized for All spd-Block Elements (Z=1-86). *Journal of Chemical Theory and Computation*, *13* (5), 1989-2009. <https://doi.org/10.1021/acs.jctc.7b00118>
- Gu, L., Kelm, M. A., Hammerstone, J. F., Beecher, G., Holden, J., Haytowitz, D., ... Prior, R. L. (2004). Concentrations of Proanthocyanidins in Common Foods and Estimations of Normal Consumption. *The Journal of Nutrition*, *134*(3), 613–617. <https://doi.org/10.1093/jn/134.3.613>
- Gu, L., Kelm, M., Hammerstone, J. F., Beecher, G., Cunningham, D., Vannozzi, S., & Prior, R. L. (2002). Fractionation of polymeric procyanidins from lowbush blueberry and quantification of procyanidins in selected foods with an optimized normal-phase HPLC-MS fluorescent detection method. *Journal of Agricultural and Food Chemistry*, *50*(17), 4852–4860. <https://doi.org/10.1021/jf020214v>
- Guerreiro, C., Jesus, M., Brandão, E., Mateus, N., De Freitas, V., & Soares, S. (2020). Interaction of a procyanidin mixture with human saliva and the variations of salivary protein profiles over a 1-year period. *Journal of Agricultural and Food Chemistry*, *68*(47), 13824–13832. <https://doi.org/10.1021/acs.jafc.0c05722>
- Guo, Q., Ma, Q., Xue, Z., Gao, X., & Chen, H. (2018). Studies on the binding characteristics of three polysaccharides with different molecular weight and flavonoids from corn silk (Maydis stigma). *Carbohydrate Polymers*, *198*, 581–588. <https://doi.org/10.1016/j.carbpol.2018.06.120>
- Gupta, R. K., & Haslam, E. (1978). Plant proanthocyanidins. Part 5. Sorghum polyphenols. *Journal of the Chemical Society, Perkin Transactions 1*, (892), 892–896. <https://doi.org/10.1039/P19780000892>
- Gupta, S., Padole, R., Variyar, P. S., & Sharma, A. (2015). Influence of radiation processing of grapes on wine quality. *Radiation Physics and Chemistry*, *111*, 46–56. <https://doi.org/10.1016/j.radphyschem.2015.02.019>

- Guyot, S., Marnet, N., & Drilleau, J. F. (2001). Thiolytic - HPLC characterization of apple procyanidins covering a large range of polymerization states. *Journal of Agricultural and Food Chemistry*, *49*(1), 14–20.
<https://doi.org/10.1021/jf000814z>
- Guyot, S., Marnet, N., Laraba, D., Sanoner, P., & Drilleau, J. F. (1998). Reversed-phase HPLC following thiolytic for quantitative estimation and characterization of the four main classes of phenolic compounds in different tissue zones of a french cider apple variety (*Malus domestica* Var. Kermerrien). *Journal of Agricultural and Food Chemistry*, *46*(5), 1698–1705. <https://doi.org/10.1021/jf970832p>
- Guyot, S., Marnet, N., Sanoner, P., & Drilleau, J.-F. (2001). Direct thiolytic on crude apple materials for high-performance liquid chromatography characterization and quantification of polyphenols in cider apple tissues and juices. In L. Packer (Ed.), *Methods in Enzymology* (pp. 57–70). Elsevier Inc. [https://doi.org/10.1016/S0076-6879\(01\)35231-X](https://doi.org/10.1016/S0076-6879(01)35231-X)
- Guyot, S., Marnet, N., Sanoner, P., & Drilleau, J. F. (2003). Variability of the polyphenolic composition of cider apple (*Malus domestica*) fruits and juices. *Journal of Agricultural and Food Chemistry*, *51*(21), 6240–6247.
<https://doi.org/10.1021/jf0301798>
- Guyot, S., Vercauteren, J., & Cheynier, V. (1996). Colourless and yellow dimers resulting from (+)-catechin oxidative coupling catalysed by grape polyphenoloxidase. *Phytochemistry*, *42*(5), 1279–1288.
[https://doi.org/10.1016/0031-9422\(96\)00127-6](https://doi.org/10.1016/0031-9422(96)00127-6)
- ## H
- Han, J., Britten, M., St-Gelais, D., Champagne, C. P., Fustier, P., Salmieri, S., & Lacroix, M. (2011). Effect of polyphenolic ingredients on physical characteristics of cheese. *Food Research International*, *44*(1), 494–497.
<https://doi.org/10.1016/j.foodres.2010.10.026>
- Haslam, E. (1989). *Plant polyphenols: vegetable tannins revisited*. Cambridge University Press. ISBN 0 521 32189 1
- Haslam, E., & Lilley, T. H. (1988). Natural astringency in foodstuffs — a molecular interpretation. *Critical Reviews in Food Science and Nutrition*, *27*(1), 1–40.
<https://doi.org/10.1080/10408398809527476>
- He, H. (2017). Research progress on theaflavins: Efficacy, formation, and preparation. *Food and Nutrition Research*, *61*(1), 1344521.
<https://doi.org/10.1080/16546628.2017.1344521>
- He, X., Lu, W., Sun, C., Khalesi, H., Mata, A., Andaleeb, R., & Fang, Y. (2021). Cellulose and cellulose derivatives: Different colloidal states and food-related applications. *Carbohydrate Polymers*, *255*, 117334.
<https://doi.org/10.1016/j.carbpol.2020.117334>
- He, Y., Wang, S., Li, J., Liang, H., Wei, X., Peng, D., ... Li, B. (2019). Interaction between konjac glucomannan and tannic acid: Effect of molecular weight, pH and temperature. *Food Hydrocolloids*, *94*, 451–458.

- <https://doi.org/10.1016/j.foodhyd.2019.03.044>
- Hemingway, R. W., & Karchesy, J. J. (1989). *Chemistry and significance of condensed tannins*. Springer Science & Business Media. <https://doi.org/10.1007/978-1-4684-7511-1>
- Höhne, G., Hemminger, W. F., & Flammersheim, H.-J. (2013). *Differential scanning calorimetry*. Springer Science & Business Media. <https://doi.org/10.1007/978-3-662-06710-9>
- Holland, C., Ryden, P., Edwards, C. H., & Grundy, M. M. L. (2020). Plant cell walls: Impact on nutrient bioaccessibility and digestibility. *Foods*, 9(2), 1–16. <https://doi.org/10.3390/foods9020201>
- Hollander, J. M., & Jolly, W. L. (1970). X-Ray Photoelectron Spectroscopy. *Accounts of Chemical Research*, 3(6), 193–200. <https://doi.org/10.1021/ar50030a003>
- Houben, K., Jolie, R. P., Fraeye, I., Van Loey, A. M., & Hendrickx, M. E. (2011). Comparative study of the cell wall composition of broccoli, carrot, and tomato: Structural characterization of the extractable pectins and hemicelluloses. *Carbohydrate Research*, 346(9), 1105–1111. <https://doi.org/10.1016/j.carres.2011.04.014>
- Huang, Q., Li, J., Shi, T., Liang, J., Wang, Z., Bai, L., ... Zhao, Y. L. (2020). Defense Mechanism of Phosphorothioated DNA under Peroxynitrite-Mediated Oxidative Stress. *ACS Chemical Biology*, 15(9), 2558–2567. <https://doi.org/10.1021/acscchembio.0c00591>
- Huang, S., Liu, X., Chang, C., & Wang, Y. (2020). Recent developments and prospective food-related applications of cellulose nanocrystals: a review. *Cellulose*, 27(6), 2991–3011. <https://doi.org/10.1007/s10570-020-02984-3>
- Huber, D. J. (1984). Strawberry fruit softening: the potential roles of polyuronides and hemicelluloses. *Journal of Food Science*, 49(5), 1310–1315. <https://doi.org/10.1111/j.1365-2621.1984.tb14976.x>
- Huck, C. W. (2015). Advances of infrared spectroscopy in natural product research. *Phytochemistry Letters*, 11, 384–393. <https://doi.org/10.1016/j.phytol.2014.10.026>
- Hümmer, W., & Schreier, P. (2008). Analysis of proanthocyanidins. *Molecular Nutrition and Food Research*, 52(12), 1381–1398. <https://doi.org/10.1002/mnfr.200700463>
- Hurst, W. J., Krake, S. H., Bergmeier, S. C., Payne, M. J., Miller, K. B., & Stuart, D. A. (2011). Impact of fermentation, drying, roasting and Dutch processing on flavan-3-ol stereochemistry in cacao beans and cocoa ingredients. *Chemistry Central Journal*, 5(1), 1–10. <https://doi.org/10.1186/1752-153X-5-53>
- Hutzler, P., Fischbach, R., Heller, W., Jungblut, T. P., Reuber, S., Schmitz, R., ... Schnitzler, J. P. (1998). Tissue localization of phenolic compounds in plants by confocal laser scanning microscopy. *Journal of Experimental Botany*, 49(323), 953–965. <https://doi.org/10.1093/jxb/49.323.953>

Huvaere, K., Sinnaeve, B., Van Bocxlaer, J., & Skibsted, L. H. (2012). Flavonoid deactivation of excited state flavins: Reaction monitoring by mass spectrometry. *Journal of Agricultural and Food Chemistry*, *60*(36), 9261–9272. <https://doi.org/10.1021/jf301823h>

I

Iharco, L. M., Garcia, A. R., Lopes da Silva, J., & Vieira Ferreira, L. F. (1997). Infrared Approach to the Study of Adsorption on Cellulose: Influence of Cellulose Crystallinity on the Adsorption of Benzophenone. *Langmuir*, *13*(15), 4126–4132. <https://doi.org/10.1021/la962138u>

Ioannone, F., Di Mattia, C. D., De Gregorio, M., Sergi, M., Serafini, M., & Sacchetti, G. (2015). Flavanols, proanthocyanidins and antioxidant activity changes during cocoa (*Theobroma cacao* L.) roasting as affected by temperature and time of processing. *Food Chemistry*, *174*, 256–262. <https://doi.org/10.1016/j.foodchem.2014.11.019>

Ioannou, I., Hafsa, I., Hamdi, S., Charbonnel, C., & Ghoul, M. (2012). Review of the effects of food processing and formulation on flavonol and anthocyanin behaviour. *Journal of Food Engineering*, *111*(2), 208–217. <https://doi.org/10.1016/j.jfoodeng.2012.02.006>

Iqbal, A., Murtaza, A., Hu, W., Ahmad, I., Ahmed, A., & Xu, X. (2019). Activation and inactivation mechanisms of polyphenol oxidase during thermal and non-thermal methods of food processing. *Food and Bioprocess Processing*, *117*(1), 170–182. <https://doi.org/10.1016/j.fbp.2019.07.006>

Ishii, T. (1991). Isolation and characterization of a diferuloyl arabinoxylan hexasaccharide from bamboo shoot cell-walls. *Carbohydrate Research*, *219*, 15–22. [https://doi.org/10.1016/0008-6215\(91\)89039-I](https://doi.org/10.1016/0008-6215(91)89039-I)

Ishii, T. (1997). Structure and functions of feruloylated polysaccharides. *Plant Science*, *127*(2), 111–127. [https://doi.org/10.1016/S0168-9452\(97\)00130-1](https://doi.org/10.1016/S0168-9452(97)00130-1)

Ishizu, T., Kintsu, K., & Yamamoto, H. (1999). NMR Study of the Solution Structures of the Inclusion Complexes of β -Cyclodextrin with (+)-Catechin and (-)-Epicatechin. *Journal of Physical Chemistry B*, *103*(42), 8992–8997. <https://doi.org/10.1021/jp991178e>

Islam, M. N., Zhang, M., & Adhikari, B. (2014). The Inactivation of Enzymes by Ultrasound-A Review of Potential Mechanisms. *Food Reviews International*, *30*(1), 1–21. <https://doi.org/10.1080/87559129.2013.853772>

Islam, M. S., Patras, A., Pokharel, B., Wu, Y., Vergne, M. J., Shade, L., ... Sasges, M. (2016). UV-C irradiation as an alternative disinfection technique: Study of its effect on polyphenols and antioxidant activity of apple juice. *Innovative Food Science and Emerging Technologies*, *34*, 344–351. <https://doi.org/10.1016/j.ifset.2016.02.009>

Israelachvili, J. (2011). *Intermolecular and Surface Forces*. *Intermolecular and Surface Forces*. Elsevier Inc. <https://doi.org/10.1016/C2009-0-21560-1>

J

- Jahed, V., Zarrabi, A., Bordbar, A. K., & Hafezi, M. S. (2014). NMR (1H, ROESY) spectroscopic and molecular modelling investigations of supramolecular complex of β -cyclodextrin and curcumin. *Food Chemistry*, *165*, 241–246. <https://doi.org/10.1016/j.foodchem.2014.05.094>
- Jakobek, L. (2015). Interactions of polyphenols with carbohydrates, lipids and proteins. *Food Chemistry*, *175*, 556–567. <https://doi.org/10.1016/j.foodchem.2014.12.013>
- Jakobek, L., & Matic, P. (2019). Non-covalent dietary fiber - Polyphenol interactions and their influence on polyphenol bioaccessibility. *Trends in Food Science and Technology*, *83*, 235–247. <https://doi.org/10.1016/j.tifs.2018.11.024>
- Janaswamy, S., & Chandrasekaran, R. (2005). Polysaccharide structures from powder diffraction data: Molecular models of arabinan. *Carbohydrate Research*, *340*(5), 835–839. <https://doi.org/10.1016/j.carres.2004.12.035>
- Janeiro, P., & Oliveira Brett, A. M. (2004). Catechin electrochemical oxidation mechanisms. *Analytica Chimica Acta*, *518*(1–2), 109–115. <https://doi.org/10.1016/j.aca.2004.05.038>
- Jin, W., Xiang, L., Peng, D., Liu, G., He, J., Cheng, S., ... Huang, Q. (2020). Study on the coupling progress of thermo-induced anthocyanins degradation and polysaccharides gelation. *Food Hydrocolloids*, *105*, 105822. <https://doi.org/10.1016/j.foodhyd.2020.105822>
- Jöbstl, E., O'Connell, J., Fairclough, J. P. A., & Williamson, M. P. (2004). Molecular model for astringency produced by polyphenol/protein interactions. *Biomacromolecules*, *5*(3), 942–949. <https://doi.org/10.1021/bm0345110>
- Jockusch, R. A., Kroemer, R. T., Talbot, F. O., Snoek, L. C., Çarçabal, P., Simons, J. P., ... Von Helden, G. (2004). Probing the Glycosidic Linkage: UV and IR Ion-Dip Spectroscopy of a Lactoside. *Journal of the American Chemical Society*, *126*(18), 5709–5714. <https://doi.org/10.1021/ja031679k>
- Jolie, R. P., Christiaens, S., De Roeck, A., Fraeye, I., Houben, K., Van Buggenhout, S., ... Hendrickx, M. E. (2012). Pectin conversions under high pressure: Implications for the structure-related quality characteristics of plant-based foods. *Trends in Food Science and Technology*, *24*(2), 103–118. <https://doi.org/10.1016/j.tifs.2011.11.003>

K

- Kacurakova, M., Capek, P., Sasinkova, V., Wellner, N., & Ebringerova, A. (2000). FT-IR study of plant cell wall model compounds: pectic polysaccharides and hemicelluloses. *Carbohydrate Polymers*, *43*(2), 195–203. [https://doi.org/10.1016/S0144-8617\(00\)00151-X](https://doi.org/10.1016/S0144-8617(00)00151-X)
- Kačuráková, M., & Mathlouthi, M. (1996). FTIR and laser-Raman spectra of oligosaccharides in water: Characterization of the glycosidic bond. *Carbohydrate Research*, *284*(2), 145–157. [https://doi.org/10.1016/0008-6215\(95\)00412-2](https://doi.org/10.1016/0008-6215(95)00412-2)
- Kačuráková, M., Wellner, N., Ebringerová, A., Hromádková, Z., Wilson, R. H., & Belton, P. S. (1999). Characterisation of xylan-type polysaccharides and

- associated cell wall components by FT-IR and FT-Raman spectroscopies. *Food Hydrocolloids*, 13(1), 35–41. [https://doi.org/10.1016/S0268-005X\(98\)00067-8](https://doi.org/10.1016/S0268-005X(98)00067-8)
- Kang, X., Kirui, A., Dickwella Widanage, M. C., Mentink-Vigier, F., Cosgrove, D. J., & Wang, T. (2019). Lignin-polysaccharide interactions in plant secondary cell walls revealed by solid-state NMR. *Nature Communications*, 10(1), 1–9. <https://doi.org/10.1038/s41467-018-08252-0>
- Kanou, M., Nakanishi, K., Hashimoto, A., & Kameokaj, T. (2005). Influences of monosaccharides and its glycosidic linkage on infrared spectral characteristics of disaccharides in aqueous solutions. *Applied Spectroscopy*, 59(7), 885–892. <https://doi.org/10.1366/0003702054411760>
- Kardum, N., & Glibetic, M. (2018). Polyphenols and their interactions with other dietary compounds: implications for human health. In F. Toldrá (Ed.), *Advances in Food and Nutrition Research* (Vol. 84, pp. 103–144). Elsevier Inc. <https://doi.org/10.1016/bs.afnr.2017.12.001>
- Kebe, M., Renard, C. M. G. C., El Maâtaoui, M., Amani, G. N. G., & Maingonnat, J. F. (2015). Leaching of polyphenols from apple parenchyma tissue as influenced by thermal treatments. *Journal of Food Engineering*, 166, 237–246. <https://doi.org/10.1016/j.jfoodeng.2015.05.037>
- Keijbets, M. J. H., & Pilnik, W. (1974). β -Elimination of pectin in the presence of anions and cations. *Carbohydrate Research*, 33(2), 359–362. [https://doi.org/10.1016/S0008-6215\(00\)82815-3](https://doi.org/10.1016/S0008-6215(00)82815-3)
- Kennedy, J. A., & Jones, G. P. (2001). Analysis of proanthocyanidin cleavage products following acid-catalysis in the presence of excess phloroglucinol. *Journal of Agricultural and Food Chemistry*, 49(4), 1740–1746. <https://doi.org/10.1021/jf001030o>
- Khan, M. K., Ahmad, K., Hassan, S., Imran, M., Ahmad, N., & Xu, C. (2018). Effect of novel technologies on polyphenols during food processing. *Innovative Food Science and Emerging Technologies*, 45, 361–381. <https://doi.org/10.1016/j.ifset.2017.12.006>
- Kiatgrajai, P., Wellons, J. D., Gollob, L., & White, J. D. (1982). Kinetics of epimerization of (+)-catechin and its rearrangement to catechinic acid. *Journal of Organic Chemistry*, 47(15), 2910–2912. <https://doi.org/10.1021/jo00136a021>
- Kim, E. S., Liang, Y. R., Jin, J., Sun, Q. F., Lu, J. L., Du, Y. Y., & Lin, C. (2007). Impact of heating on chemical compositions of green tea liquor. *Food Chemistry*, 103(4), 1263–1267. <https://doi.org/10.1016/j.foodchem.2006.10.031>
- Kim, S., Chen, J., Cheng, T., Gindulyte, A., He, J., He, S., ... Bolton, E. E. (2019). PubChem 2019 update: Improved access to chemical data. *Nucleic Acids Research*, 47(D1), D1102–D1109. <https://doi.org/10.1093/nar/gky1033>
- Kimura, H., Ogawa, S., Akihiro, T., & Yokota, K. (2011). Structural analysis of A-type or B-type highly polymeric proanthocyanidins by thiolytic degradation and the implication in their inhibitory effects on pancreatic lipase. *Journal of Chromatography A*, 1218(42), 7704–7712. <https://doi.org/10.1016/j.chroma.2011.07.024>
- Klaassen, M. T., & Trindade, L. M. (2020). RG-I galactan side-chains are involved in

- the regulation of the water-binding capacity of potato cell walls. *Carbohydrate Polymers*, 227, 115353. <https://doi.org/10.1016/j.carbpol.2019.115353>
- Klemm, D., Heublein, B., Fink, H. P., & Bohn, A. (2005). Cellulose: Fascinating biopolymer and sustainable raw material. *Angewandte Chemie - International Edition*, 44(22), 3358–3393. <https://doi.org/10.1002/anie.200460587>
- Knaze, V., Zamora-Ros, R., Luján-Barroso, L., Romieu, I., Scalbert, A., Slimani, N., ... González, C. A. (2012). Intake estimation of total and individual flavan-3-ols, proanthocyanidins and theaflavins, their food sources and determinants in the European Prospective Investigation into Cancer and Nutrition (EPIC) study. *British Journal of Nutrition*, 108(6), 1095–1108. <https://doi.org/10.1017/S0007114511006386>
- Knorr, D., & Augustin, M. A. (2021). Food processing needs, advantages and misconceptions. *Trends in Food Science and Technology*, 108, 103–110. <https://doi.org/10.1016/j.tifs.2020.11.026>
- Koch, W. (2019). Dietary polyphenols-important non-nutrients in the prevention of chronic noncommunicable diseases. A systematic review. *Nutrients*, 11(5), 1–35. <https://doi.org/10.3390/nu11051039>
- Koh, J., Xu, Z., & Wicker, L. (2020). Binding kinetics of blueberry pectin-anthocyanins and stabilization by non-covalent interactions. *Food Hydrocolloids*, 99, 105–354. <https://doi.org/10.1016/j.foodhyd.2019.105354>
- Kondo, K., Kurihara, M., Fukuhara, K., Tanaka, T., Suzuki, T., Miyata, N., & Toyoda, M. (2000). Conversion of procyanidin B-type (catechin dimer) to A-type: Evidence for abstraction of C-2 hydrogen in catechin during radical oxidation. *Tetrahedron Letters*, 41(4), 485–488. [https://doi.org/10.1016/S0040-4039\(99\)02097-3](https://doi.org/10.1016/S0040-4039(99)02097-3)
- Koshani, R., Jafari, S. M., & van de Ven, T. G. M. (2020). Going deep inside bioactive-loaded nanocarriers through Nuclear Magnetic Resonance (NMR) spectroscopy. *Trends in Food Science and Technology*, 101, 198–212. <https://doi.org/10.1016/j.tifs.2020.05.010>
- Kothe, L., Zimmermann, B. F., & Galensa, R. (2013). Temperature influences epimerization and composition of flavanol monomers, dimers and trimers during cocoa bean roasting. *Food Chemistry*, 141(4), 3656–3663. <https://doi.org/10.1016/j.foodchem.2013.06.049>
- Koyama, K., Ikeda, H., Poudel, P. R., & Goto-Yamamoto, N. (2012). Light quality affects flavonoid biosynthesis in young berries of Cabernet Sauvignon grape. *Phytochemistry*, 78, 54–64. <https://doi.org/10.1016/j.phytochem.2012.02.026>
- Krall, S. M., & McFeeters, R. F. (1998). Pectin Hydrolysis: Effect of Temperature, Degree of Methylation, pH, and Calcium on Hydrolysis Rates. *Journal of Agricultural and Food Chemistry*, 46(4), 1311–1315. <https://doi.org/10.1021/jf970473y>
- Kroon-Batenburg, L. M. J., & Kroon, J. (1997). The crystal and molecular structures of cellulose I and II. *Glycoconjugate Journal*, 14(5), 677–690. <https://doi.org/10.1023/A:1018509231331>

- Krupkova, O., Ferguson, S. J., & Wuertz-Kozak, K. (2016). Stability of (-)-epigallocatechin gallate and its activity in liquid formulations and delivery systems. *Journal of Nutritional Biochemistry*, *37*, 1–12. <https://doi.org/10.1016/j.jnutbio.2016.01.002>
- Kyomugasho, C., Christiaens, S., Shpigelman, A., Van Loey, A. M., & Hendrickx, M. E. (2015). FT-IR spectroscopy, a reliable method for routine analysis of the degree of methylesterification of pectin in different fruit- and vegetable-based matrices. *Food Chemistry*, *176*, 82–90. <https://doi.org/10.1016/j.foodchem.2014.12.033>

L

- Lachowicz, S., Michalska, A., Lech, K., Majerska, J., Oszmiański, J., & Figiel, A. (2019). Comparison of the effect of four drying methods on polyphenols in saskatoon berry. *LWT - Food Science and Technology*, *111*(2018), 727–736. <https://doi.org/10.1016/j.lwt.2019.05.054>
- Ladbury, J. E., & Doyle, M. L. (2004). *BioCalorimetry 2: applications of calorimetry in the biological sciences*. John Wiley & Sons. <https://doi.org/10.1002/0470011122>
- Lagunas-Solar, M. C. (1995). Radiation processing of foods: An overview of scientific principles and current status. *Journal of Food Protection*, *58*(2), 186–192. <https://doi.org/10.4315/0362-028X-58.2.186>
- Lan, W., Renard, C. M. G. C., Jaillais, B., Leca, A., & Bureau, S. (2020). Fresh, freeze-dried or cell wall samples: Which is the most appropriate to determine chemical, structural and rheological variations during apple processing using ATR-FTIR spectroscopy? *Food Chemistry*, *330*, 127357. <https://doi.org/10.1016/j.foodchem.2020.127357>
- Langmuir, I. (1918). The adsorption of gases on plane surfaces of glass, mica and platinum. *Journal of the American Chemical Society*, *40*(9), 1361–1403. <https://doi.org/10.1021/ja02242a004>
- Larsen, L. R., Buerschaper, J., Schieber, A., & Weber, F. (2019). Interactions of anthocyanins with pectin and pectin fragments in model solutions. *Journal of Agricultural and Food Chemistry*, *67*, 9344–9353. <https://doi.org/10.1021/acs.jafc.9b03108>
- Latorre, M. E., de Escalada Plá, M. F., Rojas, A. M., & Gerschenson, L. N. (2013). Blanching of red beet (*Beta vulgaris* L. var. *conditiva*) root. Effect of hot water or microwave radiation on cell wall characteristics. *LWT - Food Science and Technology*, *50*(1), 193–203. <https://doi.org/10.1016/j.lwt.2012.06.004>
- Le Bourvellec, C., Boas, P. B. V., Lepercq, P., Comtet-Marre, S., Auffret, P., Ruiz, P., ... Mosoni, P. (2019). Procyanidin—cell wall interactions within apple matrices decrease the metabolization of procyanidins by the human gut microbiota and the anti-inflammatory effect of the resulting microbial metabolome in vitro. *Nutrients*, *11*(3), 664. <https://doi.org/10.3390/nu11030664>
- Le Bourvellec, C., Bouchet, B., & Renard, C. M. G. C. (2005). Non-covalent interaction between procyanidins and apple cell wall material. Part III: Study on model

- polysaccharides. *Biochimica et Biophysica Acta - General Subjects*, 1725(1), 10–18. <https://doi.org/10.1016/j.bbagen.2005.06.004>
- Le Bourvellec, C., Bouzerzour, K., Ginies, C., Regis, S., Plé, Y., & Renard, C. M. G. C. (2011). Phenolic and polysaccharidic composition of applesauce is close to that of apple flesh. *Journal of Food Composition and Analysis*, 24, 537–547. <https://doi.org/10.1016/j.jfca.2010.12.012>
- Le Bourvellec, C., Gouble, B., Bureau, S., Loonis, M., Plé, Y., & Renard, C. M. G. C. (2013). Pink discoloration of canned pears: Role of procyanidin chemical depolymerization and procyanidin/cell wall interactions. *Journal of Agricultural and Food Chemistry*, 61(27), 6679–6692. <https://doi.org/10.1021/jf4005548>
- Le Bourvellec, C., Gouble, B., Bureau, S., Reling, P., Bott, R., Ribas-Agusti, A., ... Renard, C. M. G. C. (2018). Impact of canning and storage on apricot carotenoids and polyphenols. *Food Chemistry*, 240, 615–625. <https://doi.org/10.1016/j.foodchem.2017.07.147>
- Le Bourvellec, C., Guyot, S., & Renard, C. M. G. C. (2004). Non-covalent interaction between procyanidins and apple cell wall material: Part I. Effect of some environmental parameters. *Biochimica et Biophysica Acta - General Subjects*, 1672(3), 192–202. <https://doi.org/10.1016/j.bbagen.2004.04.001>
- Le Bourvellec, C., Guyot, S., & Renard, C. M. G. C. (2009). Interactions between apple (*Malus x domestica* Borkh.) polyphenols and cell walls modulate the extractability of polysaccharides. *Carbohydrate Polymers*, 75(2), 251–261. <https://doi.org/10.1016/j.carbpol.2008.07.010>
- Le Bourvellec, C., Le Quere, J. M., & Renard, C. M. G. C. (2007). Impact of noncovalent interactions between apple condensed tannins and cell walls on their transfer from fruit to juice: Studies in model suspensions and application. *Journal of Agricultural and Food Chemistry*, 55(19), 7896–7904. <https://doi.org/10.1021/jf071515d>
- Le Bourvellec, C., Le Quéré, J. M., Sanoner, P., Drilleau, J. F., & Guyot, S. (2004). Inhibition of apple polyphenol oxidase activity by procyanidins and polyphenol oxidation products. *Journal of Agricultural and Food Chemistry*, 52(1), 122–130. <https://doi.org/10.1021/jf034461q>
- Le Bourvellec, C., Picot, M., & Renard, C. M. G. C. (2006). Size-exclusion chromatography of procyanidins: Comparison between apple and grape procyanidins and application to the characterization of fractions of high degrees of polymerization. *Analytica Chimica Acta*, 563(1-2 SPEC. ISS.), 33–43. <https://doi.org/10.1016/j.aca.2005.06.040>
- Le Bourvellec, C., & Renard, C. M. G. C. (2005). Non-covalent interaction between procyanidins and apple cell wall material. Part II: Quantification and impact of cell wall drying. *Biochimica et Biophysica Acta - General Subjects*, 1725(1), 1–9. <https://doi.org/10.1016/j.bbagen.2005.06.003>
- Le Bourvellec, C., & Renard, C. M. G. C. (2012). Interactions between polyphenols and macromolecules: Quantification methods and mechanisms. *Critical Reviews in Food Science and Nutrition*, 52(3), 213–248. <https://doi.org/10.1080/10408398.2010.499808>

- Le Bourvellec, C., & Renard, C. M. G. C. (2019). Interactions between polyphenols and macromolecules: Effect of tannin structure. In L. Melton, F. Shahidi, & P. Varelis (Eds.), *Encyclopedia of Food Chemistry* (pp. 515–521). Elsevier. <https://doi.org/10.1016/B978-0-08-100596-5.21486-8>
- Le Bourvellec, C., Watrelot, A. A., Ginies, C., Imbert, A., & Renard, C. M. G. C. (2012). Impact of processing on the noncovalent interactions between procyanidin and apple cell wall. *Journal of Agricultural and Food Chemistry*, *60*(37), 9484–9494. <https://doi.org/10.1021/jf3015975>
- Lea, A. G. H., & Arnold, G. M. (1978). The phenolics of ciders: Bitterness and astringency. *Journal of the Science of Food and Agriculture*, *29*(5), 478–483. <https://doi.org/10.1002/jsfa.2740290512>
- Leavitt, S., & Freire, E. (2001). Direct measurement of protein binding energetics by isothermal titration calorimetry. *Current Opinion in Structural Biology*, *11*(5), 560–566. [https://doi.org/10.1016/S0959-440X\(00\)00248-7](https://doi.org/10.1016/S0959-440X(00)00248-7)
- Lee, H., Ha, M. J., Shahbaz, H. M., Kim, J. U., Jang, H., & Park, J. (2018). High hydrostatic pressure treatment for manufacturing of red bean powder: A comparison with the thermal treatment. *Journal of Food Engineering*, *238*(March), 141–147. <https://doi.org/10.1016/j.jfoodeng.2018.06.016>
- Lee, S. Y., Yim, D. G., Lee, D. Y., Kim, O. Y., Kang, H. J., Kim, H. S., ... Hur, S. J. (2020). Overview of the effect of natural products on reduction of potential carcinogenic substances in meat products. *Trends in Food Science and Technology*, *99*, 568–579. <https://doi.org/10.1016/j.tifs.2020.03.034>
- Lei, X., Zhu, Y., Wang, X., Zhao, P., Liu, P., Zhang, Q., ... Guo, Y. (2019). Wine polysaccharides modulating astringency through the interference on interaction of flavan-3-ols and BSA in model wine. *International Journal of Biological Macromolecules*, *139*, 896–903. <https://doi.org/10.1016/j.ijbiomac.2019.08.050>
- Li, F., Chen, G., Zhang, B., & Fu, X. (2017). Current applications and new opportunities for the thermal and non-thermal processing technologies to generate berry product or extracts with high nutraceutical contents. *Food Research International*, *100*, 19–30. <https://doi.org/10.1016/j.foodres.2017.08.035>
- Li, M., Ho, K. K. H. Y., Hayes, M., & Ferruzzi, M. G. (2019). The Roles of Food Processing in Translation of Dietary Guidance for Whole Grains, Fruits, and Vegetables. *Annual Review of Food Science and Technology*, *10*(1), 569–596. <https://doi.org/10.1146/annurev-food-032818-121330>
- Li, N., Taylor, L. S., Ferruzzi, M. G., & Mauer, L. J. (2012). Kinetic study of catechin stability: Effects of pH, concentration, and temperature. *Journal of Agricultural and Food Chemistry*, *60*(51), 12531–12539. <https://doi.org/10.1021/jf304116s>
- Li, N., Taylor, L. S., Ferruzzi, M. G., & Mauer, L. J. (2013). Color and chemical stability of tea polyphenol (-)-epigallocatechin-3-gallate in solution and solid states. *Food Research International*, *53*(2), 909–921. <https://doi.org/10.1016/j.foodres.2012.11.019>
- Li, S., Wilkinson, K. L., Mierczynska-Vasilev, A., & Bindon, K. A. (2019). Applying nanoparticle tracking analysis to characterize the polydispersity of aggregates resulting from tannin–polysaccharide interactions in wine-like media. *Molecules*,

- 24(11), 2100. <https://doi.org/10.3390/molecules24112100>
- Li, S., & Duan, C. (2019). Astringency, bitterness and color changes in dry red wines before and during oak barrel aging: An updated phenolic perspective review. *Critical Reviews in Food Science and Nutrition*, 59(12), 1840–1867. <https://doi.org/10.1080/10408398.2018.1431762>
- Li, X., Liu, G., Tu, Y., Li, J., & Yan, S. (2019). Ferulic acid pretreatment alleviates the decrease in hardness of cooked Chinese radish (*Raphanus sativus* L. var. *longipinnatus* Bailey). *Food Chemistry*, 278, 502–508. <https://doi.org/10.1016/j.foodchem.2018.10.086>
- Liang, X. quan, Fan, S. lin, Zhang, J. xing, & Song, X. rong. (2019). Polyphenol Removal from Sugarcane Juice by Using Magnetic Chitosan Composite Microparticles. *Sugar Tech*, 21(1), 104–112. <https://doi.org/10.1007/s12355-018-0625-z>
- Lin, Z., Fischer, J., & Wicker, L. (2016). Intermolecular binding of blueberry pectin-rich fractions and anthocyanin. *Food Chemistry*, 194, 986–993. <https://doi.org/10.1016/j.foodchem.2015.08.113>
- Liu, D., Lopez-Sanchez, P., & Gidley, M. J. (2019). Cellular barriers in apple tissue regulate polyphenol release under different food processing and in vitro digestion conditions. *Food and Function*, 10(5), 3008–3017. <https://doi.org/10.1039/c8fo02528b>
- Liu, D., Lopez-Sanchez, P., Martinez-Sanz, M., Gilbert, E. P., & Gidley, M. J. (2019). Adsorption isotherm studies on the interaction between polyphenols and apple cell walls: Effects of variety, heating and drying. *Food Chemistry*, 282, 58–66. <https://doi.org/10.1016/j.foodchem.2018.12.098>
- Liu, D., Martinez-Sanz, M., Lopez-Sanchez, P., Gilbert, E. P., & Gidley, M. J. (2017). Adsorption behaviour of polyphenols on cellulose is affected by processing history. *Food Hydrocolloids*, 63, 496–507. <https://doi.org/10.1016/j.foodhyd.2016.09.012>
- Liu, J., Bi, J., McClements, D. J., Liu, X., Yi, J., Lyu, J., ... Liu, D. (2020). Impacts of thermal and non-thermal processing on structure and functionality of pectin in fruit- and vegetable- based products: A review. *Carbohydrate Polymers*, 250(2), 116890. <https://doi.org/10.1016/j.carbpol.2020.116890>
- Liu, L., Zeng, Q., Zhang, R., Wei, Z., Deng, Y., Zhang, Y., ... Zhang, M. (2015). Comparative study on phenolic profiles and antioxidant activity of litchi juice treated by high pressure carbon dioxide and thermal processing. *Food Science and Technology Research*, 21(1), 41–49. <https://doi.org/10.3136/fstr.21.41>
- Liu, R., Xu, C., Cong, X., Wu, T., Song, Y., & Zhang, M. (2017). Effects of oligomeric procyanidins on the retrogradation properties of maize starch with different amylose/amylopectin ratios. *Food Chemistry*, 221, 2010–2017. <https://doi.org/10.1016/j.foodchem.2016.10.131>
- Liu, X., Le Bourvellec, C., Guyot, S., & Renard, C. M. G. C. (2021). Reactivity of flavanols: Their fate in physical food processing and recent advances in their analysis by depolymerization. *Comprehensive Reviews in Food Science and Food Safety*. 20(5), 4841–4880. <https://doi.org/10.1111/1541-4337.12797>

- Liu, X., Le Bourvellec, C., & Renard, C. M. G. C. (2020). Interactions between cell wall polysaccharides and polyphenols: Effect of molecular internal structure. *Comprehensive Reviews in Food Science and Food Safety*, *19*(6), 3574–3617. <https://doi.org/10.1111/1541-4337.12632>
- Liu, X., Renard, C. M. G. C., Bureau, S., & Le Bourvellec, C. (2021a). Interactions between heterogeneous cell walls and two procyanidins: Insights from the effects of chemical composition and physical structure. *Food Hydrocolloids*, *121*, 107018. <https://doi.org/10.1016/j.foodhyd.2021.107018>
- Liu, X., Renard, C. M. G. C., Bureau, S., & Le Bourvellec, C. (2021b). Revisiting the contribution of ATR-FTIR spectroscopy to characterize plant cell wall polysaccharides. *Carbohydrate Polymers*, *117935*. <https://doi.org/10.1016/j.carbpol.2021.117935>
- Liu, X., Renard, C. M. G. C., Rolland-Sabaté, A., Bureau, S., & Le Bourvellec, C. (2021). Modification of apple, beet and kiwifruit cell walls by boiling in acid conditions: common and specific responses. *Food Hydrocolloids*, *112*, 106266. <https://doi.org/10.1016/j.foodhyd.2020.106266>
- Liu, X., Renard, C. M. G. C., Rolland-Sabaté, A., & Le Bourvellec, C. (2021). Exploring interactions between pectins and procyanidins: Structure-function relationships. *Food Hydrocolloids*, *113*, 106498. <https://doi.org/10.1016/j.foodhyd.2020.106498>
- Liu, Y., Ying, D., Sanguansri, L., & Augustin, M. A. (2019). Comparison of the adsorption behaviour of catechin onto cellulose and pectin. *Food Chemistry*, *271*, 733–738. <https://doi.org/10.1016/j.foodchem.2018.08.005>
- Liu, Y., Ying, D., Sanguansri, L., Cai, Y., & Le, X. (2018). Adsorption of catechin onto cellulose and its mechanism study: Kinetic models, characterization and molecular simulation. *Food Research International*, *112*, 225–232. <https://doi.org/10.1016/j.foodres.2018.06.044>
- Liu, Z., & Yang, L. (2018). Antisolvent precipitation for the preparation of high polymeric procyanidin nanoparticles under ultrasonication and evaluation of their antioxidant activity in vitro. *Ultrasonics Sonochemistry*, *43*(June 2017), 208–218. <https://doi.org/10.1016/j.ultsonch.2018.01.019>
- Loo, Y. T., Howell, K., Chan, M., Zhang, P., & Ng, K. (2020). Modulation of the human gut microbiota by phenolics and phenolic fiber-rich foods. *Comprehensive Reviews in Food Science and Food Safety*, *19*(4), 1268–1298. <https://doi.org/10.1111/1541-4337.12563>
- López-Giral, N., González-Arenzana, L., González-Ferrero, C., López, R., Santamaría, P., López-Alfaro, I., & Garde-Cerdán, T. (2015). Pulsed electric field treatment to improve the phenolic compound extraction from Graciano, Tempranillo and Grenache grape varieties during two vintages. *Innovative Food Science and Emerging Technologies*, *28*, 31–39. <https://doi.org/10.1016/j.ifset.2015.01.003>
- Lopez-Torrez, L., Nigen, M., Williams, P., Doco, T., & Sanchez, C. (2015). Acacia senegal vs. Acacia seyal gums - Part 1: Composition and structure of hyperbranched plant exudates. *Food Hydrocolloids*, *51*, 41–53. <https://doi.org/10.1016/j.foodhyd.2015.04.019>

Lu, T., & Chen, F. (2012). Multiwfn: A multifunctional wavefunction analyzer. *Journal of Computational Chemistry*, 33(5), 580–592. <https://doi.org/10.1002/jcc.22885>

M

M'sakni, N. H., Majdoub, H., Roudesli, S., Picton, L., Le Cerf, D., Rihouey, C., & Morvan, C. (2006). Composition, structure and solution properties of polysaccharides extracted from leaves of *Mesembryanthemum crystallinum*. *European Polymer Journal*, 42(4), 786–795.

<https://doi.org/10.1016/j.eurpolymj.2005.09.014>

Madrau, M. A., Piscopo, A., Sanguinetti, A. M., Del Caro, A., Poiana, M., Romeo, F. V., & Piga, A. (2009). Effect of drying temperature on polyphenolic content and antioxidant activity of apricots. *European Food Research and Technology*, 228(3), 441–448. <https://doi.org/10.1007/s00217-008-0951-6>

Makkar, H. P. S., Gamble, G., & Becker, K. (1999). Limitation of the butanol-hydrochloric acid-iron assay for bound condensed tannins. *Food Chemistry*, 66(1), 129–133. [https://doi.org/10.1016/S0308-8146\(99\)00043-6](https://doi.org/10.1016/S0308-8146(99)00043-6)

Mamet, T., Ge, Z. zhen, Zhang, Y., & Li, C. mei. (2018). Interactions between highly galloylated persimmon tannins and pectins. *International Journal of Biological Macromolecules*, 106, 410–417. <https://doi.org/10.1016/j.ijbiomac.2017.08.039>

Manach, C., Scalbert, A., Morand, C., Rémésy, C., & Jiménez, L. (2004). Polyphenols: Food sources and bioavailability. *American Journal of Clinical Nutrition*, 79(5), 727–747. <https://doi.org/10.1093/ajcn/79.5.727>

Marka, S. C., Mullen, W., Borges, G., & Crozier, A. (2009). Absorption, metabolism, and excretion of cider dihydrochalcones in healthy humans and subjects with an ileostomy. *Journal of Agricultural and Food Chemistry*, 57(5), 2009–2015. <https://doi.org/10.1021/jf802757x>

Martin, A. H., Douglas Goff, H., Smith, A., & Dalgleish, D. G. (2006). Immobilization of casein micelles for probing their structure and interactions with polysaccharides using scanning electron microscopy (SEM). *Food Hydrocolloids*, 20(6), 817–824. <https://doi.org/10.1016/j.foodhyd.2005.08.004>

Matsui, T. (2015). Condensed catechins and their potential health-benefits. *European Journal of Pharmacology*, 765, 495–502.

<https://doi.org/10.1016/j.ejphar.2015.09.017>

Matsumoto, S., Obara, T., & Luh, B. S. (1983). Changes in Chemical Constituents of Kiwifruit During Post-Harvest Ripening. *Journal of Food Science*, 48(2), 607–611. <https://doi.org/10.1111/j.1365-2621.1983.tb10800.x>

Matsuo, T., Tamaru, K., & Itoo, S. (1984). Chemical degradation of condensed tannin with phloroglucinol in acidic solvents. *Agricultural and Biological Chemistry*, 48(5), 1199–1204. <https://doi.org/10.1080/00021369.1984.10866303>

Matthews, S., Mila, I., Scalbert, A., Pollet, B., Lapierre, C., Hervé Du Penhoat, C. L. M., ... Donnelly, D. M. X. (1997). Method for estimation of proanthocyanidins based on their acid depolymerization in the presence of nucleophiles. *Journal of Agricultural and Food Chemistry*, 45(4), 1195–1201.

- <https://doi.org/10.1021/jf9607573>
- Maza, M. A., Martínez, J. M., Cebrián, G., Sánchez-Gimeno, A. C., Camargo, A., Álvarez, I., & Raso, J. (2020). Evolution of polyphenolic compounds and sensory properties of wines obtained from grenache grapes treated by pulsed electric fields during aging in bottles and in oak barrels. *Foods*, *9*(5), 542. <https://doi.org/10.3390/foods9050542>
- Maza, M. A., Martínez, J. M., Hernández-Orte, P., Cebrián, G., Sánchez-Gimeno, A. C., Álvarez, I., & Raso, J. (2019). Influence of pulsed electric fields on aroma and polyphenolic compounds of Garnacha wine. *Food and Bioproducts Processing*, *116*, 249–257. <https://doi.org/10.1016/j.fbp.2019.06.005>
- Mazor Jolić, S., Radojčić Redovnikovic, I., Marković, K., Ivanec Šipušić, D., & Delonga, K. (2011). Changes of phenolic compounds and antioxidant capacity in cocoa beans processing. *International Journal of Food Science and Technology*, *46*(9), 1793–1800. <https://doi.org/10.1111/j.1365-2621.2011.02670.x>
- McCann, M. C., Wells, B., & Roberts, K. (1990). Direct visualization of cross-links in the primary plant cell wall. *Journal of Cell Science*, *96*(2), 323–334.
- McCann, M. C., Hammouri, M., Wilson, R., Belton, P., & Roberts, K. (1992). Fourier transform infrared microspectroscopy is a new way to look at plant cell walls. *Plant Physiology*, *100*(4), 1940–1947. <https://doi.org/10.1104/pp.100.4.1940>
- McManus, J. P., Davis, K. G., Beart, J. E., Gaffney, S. H., Lilley, T. H., & Haslam, E. (1985). Polyphenol interactions. Part 1. Introduction; some observations on the reversible complexation of polyphenols with proteins and polysaccharides. *Journal of the Chemical Society, Perkin Transactions 2*, *28*(9), 1429. <https://doi.org/10.1039/p29850001429>
- McNeil, M., Darvill, A. G., Fry, S. C., & Albersheim, P. (1984). Structure and function of the primary cell walls of plants. *Annual Review of Biochemistry*, *53*, 625–663. <https://doi.org/10.1146/annurev.bi.53.070184.003205>
- McRae, J. M., Falconer, R. J., & Kennedy, J. A. (2010). Thermodynamics of grape and wine tannin interaction with polyproline: Implications for red wine astringency. *Journal of Agricultural and Food Chemistry*, *58*(23), 12510–12518. <https://doi.org/10.1021/jf1030967>
- McSweeney, M., & Seetharaman, K. (2015). State of polyphenols in the drying process of fruits and vegetables. *Critical Reviews in Food Science and Nutrition*, *55*(5), 660–669. <https://doi.org/10.1080/10408398.2012.670673>
- Medved', I., & Černý, R. (2011). Surface diffusion in porous media: A critical review. *Microporous and Mesoporous Materials*, *142*(2–3), 405–422. <https://doi.org/10.1016/j.micromeso.2011.01.015>
- Mehta, P. P., & Whalley, W. B. (1963). The stereochemistry of some catechin derivatives. *Journal of the Chemical Society*, 5327–5332.
- Metaxas, D. J., Syros, T. D., Yupsanis, T., & Economou, A. S. (2004). Peroxidases during adventitious rooting in cuttings of *Arbutus unedo* and *Taxus baccata* as affected by plant genotype and growth regulator treatment. *Plant Growth Regulation*, *44*(3), 257–266. <https://doi.org/10.1007/s10725-004-5931-7>

- Micard, V., Renard, C. M. G. C., & Thibault, J. F. (1994). Studies on enzymic release of ferulic acid from sugar-beet pulp. *LWT - Food Science and Technology*, 27(1), 59–66. <https://doi.org/10.1006/FSTL.1994.1013>
- Michalska, A., Wojdyło, A., Honke, J., Ciska, E., & Andlauer, W. (2018). Drying-induced physico-chemical changes in cranberry products. *Food Chemistry*, 240, 448–455. <https://doi.org/10.1016/j.foodchem.2017.07.050>
- Mieszczakowska-Fraç, M., Dyki, B., & Konopacka, D. (2016). Effects of ultrasound on polyphenol retention in apples after the application of predrying treatments in liquid medium. *Food and Bioprocess Technology*, 9, 543–552. <https://doi.org/10.1007/s11947-015-1648-z>
- Moens, L. G., De Laet, E., Van Wambeke, J., Van Loey, A. M., & Hendrickx, M. E. G. (2020). Pulsed electric field and mild thermal processing affect the cooking behaviour of carrot tissues (*Daucus carota*) and the degree of methylesterification of carrot pectin. *Innovative Food Science and Emerging Technologies*, 66, 102483. <https://doi.org/10.1016/j.ifset.2020.102483>
- Moens, L. G., Huang, W., Van Loey, A. M., & Hendrickx, M. E. G. (2021). Effect of pulsed electric field and mild thermal processing on texture-related pectin properties to better understand carrot (*Daucus carota*) texture changes during subsequent cooking. *Innovative Food Science and Emerging Technologies*, 70, 102700. <https://doi.org/10.1016/j.ifset.2021.102700>
- Mohanta, V., Madras, G., & Patil, S. (2014). Layer-by-layer assembled thin films and microcapsules of nanocrystalline cellulose for hydrophobic drug delivery. *ACS Applied Materials and Interfaces*, 6(22), 20093–20101. <https://doi.org/10.1021/am505681e>
- Mohnen, D. (2008). Pectin structure and biosynthesis. *Current Opinion in Plant Biology*, 11(3), 266–277. <https://doi.org/10.1016/j.pbi.2008.03.006>
- Monfoulet, L.-E., Buffière, C., Istas, G., Dufour, C., Le Bourvellec, C., Mercier, S., ... Morand, C. (2020). Effects of the apple matrix on the postprandial bioavailability of flavan-3-ols and nutrigenomic response of apple polyphenols in minipigs challenged with a high fat meal. *Food and Function*, 6(11), 5077–5090. <https://doi.org/10.1039/d0fo00346h>
- Monsoor, M. A., Kalapathy, U., & Proctor, A. (2001). Determination of polygalacturonic acid content in pectin extracts by diffuse reflectance Fourier transform infrared spectroscopy. *Food Chemistry*, 74(2), 233–238. [https://doi.org/10.1016/S0308-8146\(01\)00100-5](https://doi.org/10.1016/S0308-8146(01)00100-5)
- Morikawa, H., Okuda, K., Kunihiro, Y., Inada, A., Miyagi, C., Matsuo, Y., ... Tanaka, T. (2019). Oligomerization mechanism of tea catechins during tea roasting. *Food Chemistry*, 285, 252–259. <https://doi.org/10.1016/j.foodchem.2019.01.163>
- Morris, G. A., & Ralet, M. C. (2012). A copolymer analysis approach to estimate the neutral sugar distribution of sugar beet pectin using size exclusion chromatography. *Carbohydrate Polymers*, 87(2), 1139–1143. <https://doi.org/10.1016/j.carbpol.2011.08.077>
- Mota, T. R., Oliveira, D. M. de, Marchiosi, R., Ferrarese-Filho, O., & Santos, W. D. dos. (2018). Plant cell wall composition and enzymatic deconstruction. *AIMS*

- Bioengineering*, 5(1), 63–77. <https://doi.org/10.3934/bioeng.2018.1.63>
- Mouls, L., & Fulcrand, H. (2012). UPLC-ESI-MS study of the oxidation markers released from tannin depolymerization: Toward a better characterization of the tannin evolution over food and beverage processing. *Journal of Mass Spectrometry*, 47(11), 1450–1457. <https://doi.org/10.1002/jms.3098>
- Mouls, L., & Fulcrand, H. (2015). Identification of new oxidation markers of grape-condensed tannins by UPLC-MS analysis after chemical depolymerization. *Tetrahedron*, 71(20), 3012–3019. <https://doi.org/10.1016/j.tet.2015.01.038>
- Mouls, L., Hugouvieux, V., Mazauric, J. P., Sommerer, N., Mazerolles, G., & Fulcrand, H. (2014). How to gain insight into the polydispersity of tannins: A combined MS and LC study. *Food Chemistry*, 165, 348–353. <https://doi.org/10.1016/j.foodchem.2014.05.121>
- Mu, R., Hong, X., Ni, Y., Li, Y., Pang, J., Wang, Q., ... Zheng, Y. (2019). Recent trends and applications of cellulose nanocrystals in food industry. *Trends in Food Science and Technology*, 93, 136–144. <https://doi.org/10.1016/j.tifs.2019.09.013>
- Muroga, Y., Yamada, Y., Noda, I., & Nagasawa, M. (1987). Local conformation of polysaccharides in solution investigated by small-angle X-ray scattering. *Macromolecules*, 20(12), 3003–3006. <https://doi.org/10.1021/ma00178a009>
- Murray, J. S., & Politzer, P. (2011). The electrostatic potential: An overview. *Wiley Interdisciplinary Reviews: Computational Molecular Science*, 1(2), 153–163. <https://doi.org/10.1002/wcms.19>

N

- Neilson, A. P., O’Keefe, S. F., & Bolling, B. W. (2016). High-molecular-weight proanthocyanidins in foods: Overcoming analytical challenges in pursuit of novel dietary bioactive components. *Annual Review of Food Science and Technology*, 7, 43–64. <https://doi.org/10.1146/annurev-food-022814-015604>
- Neto, R. T., Santos, S. A. O., Oliveira, J., & Silvestre, A. J. D. (2020). Biorefinery of high polymerization degree proanthocyanidins in the context of circular economy. *Industrial Crops and Products*, 151, 112450. <https://doi.org/10.1016/j.indcrop.2020.112450>
- Ngure, F. M., Wanyoko, J. K., Mahungu, S. M., & Shitandi, A. A. (2009). Catechins depletion patterns in relation to theaflavin and thearubigins formation. *Food Chemistry*, 115(1), 8–14. <https://doi.org/10.1016/j.foodchem.2008.10.006>
- Nikonenko, N. A., Buslov, D. K., Sushko, N. I., & Zhbankov, R. G. (2000). Investigation of stretching vibrations of glycosidic linkages in disaccharides and polysaccharides with use of IR spectra deconvolution. *Biopolymers (Biospectroscopy)*, 57(4), 257–262. [https://doi.org/10.1002/1097-0282\(2000\)57:4<257::AID-BIP7>3.0.CO;2-3](https://doi.org/10.1002/1097-0282(2000)57:4<257::AID-BIP7>3.0.CO;2-3)

O

- Olivati, C., de Oliveira Nishiyama, Y. P., de Souza, R. T., Janzantti, N. S., Mauro, M.

- A., Gomes, E., ... Lago-Vanzela, E. S. (2019). Effect of the pre-treatment and the drying process on the phenolic composition of raisins produced with a seedless Brazilian grape cultivar. *Food Research International*, *116*, 190–199. <https://doi.org/10.1016/j.foodres.2018.08.012>
- Oliveira, D. M., Finger-Teixeira, A., Rodrigues Mota, T., Salvador, V. H., Moreira-Vilar, F. C., Correa Molinari, H. B., ... Dantas dos Santos, W. (2015). Ferulic acid: A key component in grass lignocellulose recalcitrance to hydrolysis. *Plant Biotechnology Journal*, *13*(9), 1224–1232. <https://doi.org/10.1111/pbi.12292>
- Oracz, J., Nebesny, E., & Żyżelewicz, D. (2015). Changes in the flavan-3-ols, anthocyanins, and flavanols composition of cocoa beans of different *Theobroma cacao* L. groups affected by roasting conditions. *European Food Research and Technology*, *241*(5), 663–681. <https://doi.org/10.1007/s00217-015-2494-y>
- Osman, A. M., & Wong, K. K. Y. (2007). Laccase (EC 1.10.3.2) catalyses the conversion of procyanidin B-2 (epicatechin dimer) to type A-2. *Tetrahedron Letters*, *48*(7), 1163–1167. <https://doi.org/10.1016/j.tetlet.2006.12.075>
- Ottaviani, J. I., Heiss, C., Spencer, J. P. E., Kelm, M., & Schroeter, H. (2018). Recommending flavanols and procyanidins for cardiovascular health: Revisited. *Molecular Aspects of Medicine*, *61*, 63–75. <https://doi.org/10.1016/j.mam.2018.02.001>
- Ottaviani, J. I., Momma, T. Y., Heiss, C., Kwik-Urbe, C., Schroeter, H., & Keen, C. L. (2011). The stereochemical configuration of flavanols influences the level and metabolism of flavanols in humans and their biological activity in vivo. *Free Radical Biology and Medicine*, *50*(2), 237–244. <https://doi.org/10.1016/j.freeradbiomed.2010.11.005>

P

- Padayachee, A., Day, L., Howell, K., & Gidley, M. J. (2017). Complexity and health functionality of plant cell wall fibers from fruits and vegetables. *Critical Reviews in Food Science and Nutrition*, *57*(1), 59–81. <https://doi.org/10.1080/10408398.2013.850652>
- Padayachee, A., Netzel, G., Netzel, M., Day, L., Mikkelsen, D., & Gidley, M. J. (2013). Lack of release of bound anthocyanins and phenolic acids from carrot plant cell walls and model composites during simulated gastric and small intestinal digestion. *Food and Function*, *4*(6), 906–916. <https://doi.org/10.1039/c3fo60091b>
- Padayachee, A., Netzel, G., Netzel, M., Day, L., Zabaras, D., Mikkelsen, D., & Gidley, M. J. (2012a). Binding of polyphenols to plant cell wall analogues - Part 1: Anthocyanins. *Food Chemistry*, *134*(1), 155–161. <https://doi.org/10.1016/j.foodchem.2012.02.082>
- Padayachee, A., Netzel, G., Netzel, M., Day, L., Zabaras, D., Mikkelsen, D., & Gidley, M. J. (2012b). Binding of polyphenols to plant cell wall analogues - Part 2: Phenolic acids. *Food Chemistry*, *135*(4), 2287–2292. <https://doi.org/10.1016/j.foodchem.2012.07.004>
- Palafox-Carlos, H., Ayala-Zavala, J. F., & González-Aguilar, G. A. (2011). The Role

- of Dietary Fiber in the Bioaccessibility and Bioavailability of Fruit and Vegetable Antioxidants. *Journal of Food Science*, 76(1). <https://doi.org/10.1111/j.1750-3841.2010.01957.x>
- Pascal, C., Poncet-Legrand, C., Imbert, A., Gautier, C., Sarni-Manchado, P., Cheynier, V., & Vernhet, A. (2007). Interactions between a non glycosylated human proline-rich protein and flavan-3-ols are affected by protein concentration and polyphenol/protein ratio. *Journal of Agricultural and Food Chemistry*, 55(12), 4895–4901. <https://doi.org/10.1021/jf0704108>
- Patel, A. R., Seijen Ten-Hoorn, J., Hazekamp, J., Blijdenstein, T. B. J., & Velikov, K. P. (2013). Colloidal complexation of a macromolecule with a small molecular weight natural polyphenol: Implications in modulating polymer functionalities. *Soft Matter*, 9(5), 1428–1436. <https://doi.org/10.1039/c2sm27200h>
- Patel, A. R., Seijen Ten-Hoorn, J., & Velikov, K. P. (2011). Colloidal complexes from associated water soluble cellulose derivative (methylcellulose) and green tea polyphenol (Epigallocatechin gallate). *Journal of Colloid and Interface Science*, 364(2), 317–323. <https://doi.org/10.1016/j.jcis.2011.08.054>
- Paudel, E., Boom, R. M., van Haaren, E., Siccama, J., & van der Sman, R. G. M. (2016). Effects of cellular structure and cell wall components on water holding capacity of mushrooms. *Journal of Food Engineering*, 187, 106–113. <https://doi.org/10.1016/j.jfoodeng.2016.04.009>
- Pauly, M., & Keegstra, K. (2016). Biosynthesis of the plant cell wall matrix polysaccharide xyloglucan. *Annual Review of Plant Biology*, 67, 235–259. <https://doi.org/10.1146/annurev-arplant-043015-112222>
- Payne, M. J., Hurst, W. J., Miller, K. B., Rank, C., & Stuart, D. A. (2010). Impact of fermentation, drying, roasting, and dutch processing on epicatechin and catechin content of cacao beans and cocoa ingredients. *Journal of Agricultural and Food Chemistry*, 58(19), 10518–10527. <https://doi.org/10.1021/jf102391q>
- Payne, M. J., Hurst, W. J., Stuart, D. A., Ou, B., Fan, E., Ji, H., & Kou, Y. (2010). Determination of total procyanidins in selected chocolate and confectionery products using DMAC. *Journal of AOAC International*, 93(1), 89–96. <https://doi.org/10.1093/jaoac/93.1.89>
- Pedroza, M. A., Carmona, M., Pardo, F., Salinas, M. R., & Zalacain, A. (2012). Waste grape skins thermal dehydration: Potential release of colour, phenolic and aroma compounds into wine. *CYTA - Journal of Food*, 10(3), 225–234. <https://doi.org/10.1080/19476337.2011.633243>
- Peng, J., Song, Y., Zhang, X., Pan, L., & Tu, K. (2019). Calcium absorption in asparagus during thermal processing: Different forms of calcium ion and cell integrity in relation to texture. *LWT - Food Science and Technology*, 111, 889–895. <https://doi.org/10.1016/j.lwt.2019.05.095>
- Percy, A. E., Melton, L. D., & Jameson, P. E. (1997). Xyloglucan and hemicelluloses in the cell wall during apple fruit development and ripening. *Plant Science*, 125(1), 31–39. [https://doi.org/10.1016/S0168-9452\(97\)04618-9](https://doi.org/10.1016/S0168-9452(97)04618-9)
- Pérez-Jiménez, J., Díaz-Rubio, M. E., & Saura-Calixto, F. (2013). Non-extractable polyphenols, a major dietary antioxidant: Occurrence, metabolic fate and health

- effects. *Nutrition Research Reviews*, 26(2), 118–129.
<https://doi.org/10.1017/S0954422413000097>
- Pérez-Jiménez, J., & Saura-Calixto, F. (2015). Macromolecular antioxidants or non-extractable polyphenols in fruit and vegetables: Intake in four European countries. *Food Research International*, 74, 315–323.
<https://doi.org/10.1016/j.foodres.2015.05.007>
- Pérez, S., Mazeau, K., & Hervé du Penhoat, C. (2000). The three-dimensional structures of the pectic polysaccharides. *Plant Physiology and Biochemistry*, 38(1–2), 37–55.
[https://doi.org/10.1016/S0981-9428\(00\)00169-8](https://doi.org/10.1016/S0981-9428(00)00169-8)
- Pérez, S., & Rivet, A. (2021). Polys Glycan Builder: An online application for intuitive construction of 3D structures of complex carbohydrates, in methods in molecular biology. In T. Lutteke (Ed.), *Glycoinformatics: Methods and protocols* (Second Edi).
- Pérez, S., Rodríguez-Carvajal, M. A., & Doco, T. (2003). A complex plant cell wall polysaccharide: Rhamnogalacturonan II. A structure in quest of a function. *Biochimie*, 85(1–2), 109–121. [https://doi.org/10.1016/S0300-9084\(03\)00053-1](https://doi.org/10.1016/S0300-9084(03)00053-1)
- Pérez, S., Sarkar, A., Rivet, A., Breton, C., & Imberty, A. (2015). Glyco3D: a portal for structural glycosciences. In *Glycoinformatics* (pp. 241–258). Springer.
https://doi.org/10.1007/978-1-4939-2343-4_18
- Pérez, S., Tubiana, T., Imberty, A., & Baaden, M. (2015). Three-dimensional representations of complex carbohydrates and polysaccharides - SweetUnityMol: A video game-based computer graphic software. *Glycobiology*, 25(5), 483–491.
<https://doi.org/10.1093/glycob/cwu133>
- Phan, A. D. T., D’Arcy, B. R., & Gidley, M. J. (2016). Polyphenol-cellulose interactions: effects of pH, temperature and salt. *International Journal of Food Science & Technology*, 51(1), 203–211. <https://doi.org/10.1111/ijfs.13009>
- Phan, A. D. T., Flanagan, B. M., D’Arcy, B. R., & Gidley, M. J. (2017). Binding selectivity of dietary polyphenols to different plant cell wall components: Quantification and mechanism. *Food Chemistry*, 233, 216–227.
<https://doi.org/10.1016/j.foodchem.2017.04.115>
- Phan, A. D. T., Netzel, G., Wang, D., Flanagan, B. M., D’Arcy, B. R., & Gidley, M. J. (2015). Binding of dietary polyphenols to cellulose: Structural and nutritional aspects. *Food Chemistry*, 171, 388–396.
<https://doi.org/10.1016/j.foodchem.2014.08.118>
- Phan, A. D. T., Williams, B. A., Netzel, G., Mikkelsen, D., D’Arcy, B. R., & Gidley, M. J. (2020). Independent fermentation and metabolism of dietary polyphenols associated with a plant cell wall model. *Food and Function*, 11(3), 2218–2230.
<https://doi.org/10.1039/c9fo02987g>
- Pianet, I., André, Y., Ducasse, M. A., Tarascou, I., Lartigue, J. C., Pinaud, N., ... Laguerre, M. (2008). Modeling procyanidin self-association processes and understanding their micellar organization: A study by diffusion NMR and molecular mechanics. *Langmuir*, 24(19), 11027–11035.
<https://doi.org/10.1021/la8015904>
- Pieczywek, P. M., Kozioł, A., Konopacka, D., Cybulska, J., & Zdunek, A. (2017).

- Changes in cell wall stiffness and microstructure in ultrasonically treated apple. *Journal of Food Engineering*, 197, 1–8.
<https://doi.org/10.1016/j.jfoodeng.2016.10.028>
- Pieczywek, P. M., Koziół, A., Płaziński, W., Cybulska, J., & Zdunek, A. (2020). Resolving the nanostructure of sodium carbonate extracted pectins (DASP) from apple cell walls with atomic force microscopy and molecular dynamics. *Food Hydrocolloids*, 104, 105726. <https://doi.org/10.1016/j.foodhyd.2020.105726>
- Pietta, P. G. (2000). Flavonoids as antioxidants. *Journal of Natural Products*, 63(7), 1035–1042. <https://doi.org/10.1021/np9904509>
- Pimenta Inada, K. O., Nunes, S., Martínez-Blázquez, J. A., Tomás-Barberán, F. A., Perrone, D., & Monteiro, M. (2020). Effect of high hydrostatic pressure and drying methods on phenolic compounds profile of jaboticaba (*Myrciaria jaboticaba*) peel and seed. *Food Chemistry*, 309, 125794.
<https://doi.org/10.1016/j.foodchem.2019.125794>
- Pingret, D., Fabiano-Tixier, A. S., & Chemat, F. (2013). Degradation during application of ultrasound in food processing: A review. *Food Control*, 31(2), 593–606.
<https://doi.org/10.1016/j.foodcont.2012.11.039>
- Poncet-Legrand, C., Cabane, B., Bautista-Ortín, A. B., Carrillo, S., Fulcrand, H., Pérez, J., & Vernhet, A. (2010). Tannin oxidation: Intra-versus intermolecular reactions. *Biomacromolecules*, 11(9), 2376–2386. <https://doi.org/10.1021/bm100515e>
- Poncet-Legrand, C., Gautier, C., Cheynier, V., & Imberty, A. (2007). Interactions between flavan-3-ols and poly(L-proline) studied by isothermal titration calorimetry: Effect of the tannin structure. *Journal of Agricultural and Food Chemistry*, 55(22), 9235–9240. <https://doi.org/10.1021/jf071297o>
- Porter, L. J., Hrstich, L. N., & Chana, B. G. (1985). The conversion of procyanidins and prodelphinidins to cyanidin and delphinidin. *Phytochemistry*, 25(1), 223–230.
[https://doi.org/10.1016/S0031-9422\(00\)94533-3](https://doi.org/10.1016/S0031-9422(00)94533-3)
- Posé, S., Paniagua, C., Matas, A. J., Gunning, A. P., Morris, V. J., Quesada, M. A., & Mercado, J. A. (2019). A nanostructural view of the cell wall disassembly process during fruit ripening and postharvest storage by atomic force microscopy. *Trends in Food Science and Technology*, 87, 47–58.
<https://doi.org/10.1016/j.tifs.2018.02.011>
- Poupard, P., Guyot, S., Bernillon, S., & Renard, C. M. G. C. (2008). Characterisation by liquid chromatography coupled to electrospray ionisation ion trap mass spectrometry of phloroglucinol and 4-methylcatechol oxidation products to study the reactivity of epicatechin in an apple juice model system. *Journal of Chromatography A*, 1179(2), 168–181.
<https://doi.org/10.1016/j.chroma.2007.11.083>
- Poupard, P., Sanoner, P., Baron, A., Renard, C. M. G. C., & Guyot, S. (2011). Characterization of procyanidin B2 oxidation products in an apple juice model solution and confirmation of their presence in apple juice by high-performance liquid chromatography coupled to electrospray ion trap mass spectrometry. *Journal of Mass Spectrometry*, 46(11), 1186–1197.
<https://doi.org/10.1002/jms.2007>

- Pracht, P.; Bohle, F.; Grimme, S. (2020). Automated exploration of the low-energy chemical space with fast quantum chemical methods. *Physical Chemistry Chemical Physics*, 22, 7169–7192. <https://doi.org/10.1039/c9cp06869d>
- Prieur, C., Rigaud, J., Cheynier, V., & Moutounet, M. (1994). Oligomeric and polymeric procyanidins from grape seeds. *Phytochemistry*, 36(3), 781–784. [https://doi.org/10.1016/S0031-9422\(00\)89817-9](https://doi.org/10.1016/S0031-9422(00)89817-9)
- Prior, R. L., Fan, E., Ji, H., Howell, A., Nio, C., Paynef, M. J., & Reed, J. (2010). Multi-laboratory validation of a standard method for quantifying proanthocyanidins in cranberry powders. *Journal of the Science of Food and Agriculture*, 90(9), 1473–1478. <https://doi.org/10.1002/jsfa.3966>

Q

- Qiu, W. Y., Cai, W. D., Wang, M., & Yan, J. K. (2019). Effect of ultrasonic intensity on the conformational changes in citrus pectin under ultrasonic processing. *Food Chemistry*, 297, 125021. <https://doi.org/10.1016/j.foodchem.2019.125021>
- Quideau, S., Deffieux, D., Douat-Casassus, C., & Pouységu, L. (2011). Plant polyphenols: Chemical properties, biological activities, and synthesis. *Angewandte Chemie International Edition*, 50(3), 586–621. <https://doi.org/10.1002/anie.201000044>
- Quiroz-Reyes, C. N., & Fogliano, V. (2018). Design cocoa processing towards healthy cocoa products: The role of phenolics and melanoidins. *Journal of Functional Foods*, 45, 480–490. <https://doi.org/10.1016/j.jff.2018.04.031>

R

- R Core Team. (2014). A Language and Environment for Statistical Computing. *R Foundation for Statistical Computing*, 2. Retrieved from <http://www.r-project.org>
- Ralet, M. C., Crépeau, M. J., Vigouroux, J., Tran, J., Berger, A., Sallé, C., ... North, H. M. (2016). Xylans provide the structural driving force for mucilage adhesion to the Arabidopsis seed coat. *Plant Physiology*, 171(1), 165–178. <https://doi.org/10.1104/pp.16.00211>
- Ralet, M. C., Williams, M. A. K., Tanhatan-Nasseri, A., Ropartz, D., Quémener, B., & Bonnin, E. (2012). Innovative enzymatic approach to resolve homogalacturonans based on their methylesterification pattern. *Biomacromolecules*, 13(5), 1615–1624. <https://doi.org/10.1021/bm300329r10.1021/bm300329r>
- Ramos-Pineda, A. M., Carpenter, G. H., Garcíá-Estévez, I., & Escribano-Bailón, M. T. (2020). Influence of chemical species on polyphenol-protein interactions related to wine astringency. *Journal of Agricultural and Food Chemistry*, 68(10), 2948–2954. <https://doi.org/10.1021/acs.jafc.9b00527>
- Ranganathan, K., Subramanian, V., & Shanmugam, N. (2016). Effect of Thermal and Nonthermal Processing on Textural Quality of Plant Tissues. *Critical Reviews in Food Science and Nutrition*, 56(16), 2665–2694. <https://doi.org/10.1080/10408398.2014.908348>

- Rauf, A., Imran, M., Abu-Izneid, T., Iahtisham-Ul-Haq, Patel, S., Pan, X., ... Rasul Suleria, H. A. (2019). Proanthocyanidins: A comprehensive review. *Biomedicine and Pharmacotherapy*, *116*, 108999. <https://doi.org/10.1016/j.biopha.2019.108999>
- Rawson, A., Patras, A., Tiwari, B. K., Noci, F., Koutchma, T., & Brunton, N. (2011). Effect of thermal and non thermal processing technologies on the bioactive content of exotic fruits and their products: Review of recent advances. *Food Research International*, *44*(7), 1875–1887. <https://doi.org/10.1016/j.foodres.2011.02.053>
- Redgwell, R. J., Fischer, M., Kendal, E., & MacRae, E. A. (1997). Galactose loss and fruit ripening: High-molecular-weight arabinogalactans in the pectic polysaccharides of fruit cell walls. *Planta*, *203*(2), 174–181. <https://doi.org/10.1007/s004250050179>
- Redgwell, R. J., MacRae, E., Hallett, I., Fischer, M., Perry, J., & Harker, R. (1997). In vivo and in vitro swelling of cell walls during fruit ripening. *Planta*, *203*(2), 162–173. <https://doi.org/10.1007/s004250050178>
- Redgwell, R. J., Melton, L. D., & Brasch, D. J. (1988). Cell-wall polysaccharides of kiwifruit (*Actinidia deliciosa*): Chemical features in different tissue zones of the fruit at harvest. *Carbohydrate Research*, *182*(2), 241–258. [https://doi.org/10.1016/0008-6215\(88\)84006-0](https://doi.org/10.1016/0008-6215(88)84006-0)
- Redgwell, R. J., Melton, L. D., & Brasch, D. J. (1991). Cell-wall polysaccharides of kiwifruit (*Actinidia deliciosa*): effect of ripening on the structural features of cell-wall materials. *Carbohydrate Research*, *209*(C), 191–202. [https://doi.org/10.1016/0008-6215\(91\)80156-H](https://doi.org/10.1016/0008-6215(91)80156-H)
- Reimer, L. (2013). *Transmission electron microscopy: physics of image formation and microanalysis* (Vol. 36). Springer. <https://doi.org/10.1007/978-3-662-13553-2>
- Reintjes, M., Musco, D. D., & Joseph, G. H. (1962). Infrared Spectra of Some Pectic Substances. *Journal of Food Science*, *27*(5), 441–445. <https://doi.org/10.1111/j.1365-2621.1962.tb00124.x>
- Renard, C.M.G.C. (2005a). Effects of conventional boiling on the polyphenols and cell walls of pears. *Journal of the Science of Food and Agriculture*, *85*(2), 310–318. <https://doi.org/10.1002/jsfa.1987>
- Renard, C.M.G.C. (2005b). Variability in cell wall preparations: Quantification and comparison of common methods. *Carbohydrate Polymers*, *60*(4), 515–522. <https://doi.org/10.1016/j.carbpol.2005.03.002>
- Renard, C.M.G.C., Crépeau, M. J., & Thibault, J. F. (1995). Structure of the repeating units in the rhamnogalacturonic backbone of apple, beet and citrus pectins. *Carbohydrate Research*, *275*(1), 155–165. [https://doi.org/10.1016/0008-6215\(95\)00140-O](https://doi.org/10.1016/0008-6215(95)00140-O)
- Renard, C.M.G.C., & Ginies, C. (2009). Comparison of the cell wall composition for flesh and skin from five different plums. *Food Chemistry*, *114*(3), 1042–1049. <https://doi.org/10.1016/j.foodchem.2008.10.073>
- Renard, C.M.G.C., & Jarvis, M. C. (1999). A Cross-Polarization, Magic-Angle-Spinning, ¹³C-Nuclear-Magnetic-Resonance Study of Polysaccharides in Sugar Beet Cell Walls. *Plant Physiology*, *119*(4), 1315–1322.

- <https://doi.org/10.1104/pp.119.4.1315>
- Renard, C.M.G.C., & Thibault, J. F. (1993). Structure and properties of apple and sugar-beet pectins extracted by chelating agents. *Carbohydrate Research*, *244*(1), 99–114. [https://doi.org/10.1016/0008-6215\(93\)80007-2](https://doi.org/10.1016/0008-6215(93)80007-2)
- Renard, C.M.G.C. (2005). Effects of conventional boiling on the polyphenols and cell walls of pears. *Journal of the Science of Food and Agriculture*, *85*(2), 310–318. <https://doi.org/10.1002/jsfa.1987>
- Renard, C.M.G.C., Baron, A., Guyot, S., & Drilleau, J. F. (2001). Interactions between apple cell walls and native palle polyphenols/quantification and some consequences. *International Journal of Biology Macromolecules*, *29*, 115–125. [https://doi.org/10.1016/S0141-8130\(01\)00155-6](https://doi.org/10.1016/S0141-8130(01)00155-6)
- Renard, C.M.G.C., Le Quéré, J. M., Bauduin, R., Symoneaux, R., Le Bourvellec, C., & Baron, A. (2011a). Modulating polyphenolic composition and organoleptic properties of apple juices by manipulating the pressing conditions. *Food Chemistry*, *124*(1), 117–125. <https://doi.org/10.1016/j.foodchem.2010.05.113>
- Renard, C.M.G.C., & Thibault, J. F. (1996). Pectins in mild alkaline conditions: β -elimination and kinetics of demethylation. A.G.J. Voragen, J. Visser (Eds.), *Progress in Biotechnology: 14 Pectins and Pectinases*, Elsevier, Amsterdam, *14*(C), 603–608. [https://doi.org/10.1016/S0921-0423\(96\)80292-9](https://doi.org/10.1016/S0921-0423(96)80292-9)
- Renard, C.M.G.C., Voragen, A. G. J., Thibault, J. F., & Pilnik, W. (1990). Studies on apple protopectin: I. Extraction of insoluble pectin by chemical means. *Carbohydrate Polymers*, *12*(1), 9–25. [https://doi.org/10.1016/0144-8617\(90\)90101-W](https://doi.org/10.1016/0144-8617(90)90101-W)
- Renard, C.M.G.C., Voragen, A. G. J., Thibault, J. F., & Pilnik, W. (1991). Studies on apple protopectin. IV: Apple xyloglucans and influence of pectin extraction treatments on their solubility. *Carbohydrate Polymers*, *15*(4), 387–403. [https://doi.org/10.1016/0144-8617\(91\)90089-U](https://doi.org/10.1016/0144-8617(91)90089-U)
- Renard, C.M.G.C., Watrelot, A. A., & Le Bourvellec, C. (2017). Interactions between polyphenols and polysaccharides: Mechanisms and consequences in food processing and digestion. *Trends in Food Science and Technology*, *60*, 43–51. <https://doi.org/10.1016/j.tifs.2016.10.022>
- Ribas-Agustí, A., Martín-Belloso, O., Soliva-Fortuny, R., & Elez-Martínez, P. (2018). Food processing strategies to enhance phenolic compounds bioaccessibility and bioavailability in plant-based foods. *Critical Reviews in Food Science and Nutrition*, *58*(15), 2531–2548. <https://doi.org/10.1080/10408398.2017.1331200>
- Ribas-Agustí, A., Martín-Belloso, O., Soliva-Fortuny, R., & Elez-Martínez, P. (2019). Enhancing hydroxycinnamic acids and flavan-3-ol contents by pulsed electric fields without affecting quality attributes of apple. *Food Research International*, *121*(November 2018), 433–440. <https://doi.org/10.1016/j.foodres.2018.11.057>
- Ridley, B. L., O'Neill, M. A., & Mohnen, D. (2001a). Pectins: Structure, biosynthesis, and oligogalacturonide-related signaling. *Phytochemistry*, *57*(6), 929–967. [https://doi.org/10.1016/S0031-9422\(01\)00113-3](https://doi.org/10.1016/S0031-9422(01)00113-3)
- Rodriguez-Mateos, A., Vauzour, D., Krueger, C. G., Shanmuganayagam, D., Reed, J.,

- Calani, L., ... Crozier, A. (2014). Bioavailability, bioactivity and impact on health of dietary flavonoids and related compounds: an update. *Archives of Toxicology*, 88(10), 1803–1853. <https://doi.org/10.1007/s00204-014-1330-7>
- Rodríguez-Pérez, C., Quirantes-Piné, R., Contreras, M. D. M., Uberos, J., Fernández-Gutiérrez, A., & Segura-Carretero, A. (2015). Assessment of the stability of proanthocyanidins and other phenolic compounds in cranberry syrup after gamma-irradiation treatment and during storage. *Food Chemistry*, 174, 392–399. <https://doi.org/10.1016/j.foodchem.2014.11.061>
- Rolland-Sabaté, A., Colonna, P., Potocki-Véronèse, G., Monsan, P., & Planchot, V. (2004). Elongation and insolubilisation of α -glucans by the action of *Neisseria polysaccharea* amylosucrase. *Journal of Cereal Science*, 40(1), 17–30. <https://doi.org/10.1016/j.jcs.2004.04.001>
- Rolland-Sabaté, A., Mendez-Montevalvo, M. G., Colonna, P., & Planchot, V. (2008). Online determination of structural properties and observation of deviations from power law behavior. *Biomacromolecules*, 9(7), 1719–1730. <https://doi.org/10.1021/bm7013119>
- Rolland-Sabaté, A. (2017). High-Performance Size-Exclusion Chromatography coupled with on-line Multi-angle Laser Light Scattering (HPSEC-MALLS). In M. Masuelli & D. Renard (Eds.), *Advances in Physicochemical Properties of Biopolymers (Part 1)* (pp. 92–136). <https://doi.org/10.2174/97816810845341170101>
- Rombouts, F. M., & Thibault, J. F. (1986). Feruloylated pectic substances from sugar-beet pulp. *Carbohydrate Research*, 154(1), 177–187. [https://doi.org/10.1016/S0008-6215\(00\)90031-4](https://doi.org/10.1016/S0008-6215(00)90031-4)
- Roy, D., Semsarilar, M., Guthrie, J. T., & Perrier, S. (2009). Cellulose modification by polymer grafting: A review. *Chemical Society Reviews*, 38(7), 2046–2064. <https://doi.org/10.1039/b808639g>
- Rue, E. A., Rush, M. D., & van Breemen, R. B. (2018). Procyanidins: a comprehensive review encompassing structure elucidation via mass spectrometry. *Phytochemistry Reviews*, 17(1), 1–16. <https://doi.org/10.1007/s11101-017-9507-3>
- Ruiz-Garcia, Y., Smith, P. A., & Bindon, K. A. (2014). Selective extraction of polysaccharide affects the adsorption of proanthocyanidin by grape cell walls. *Carbohydrate Polymers*, 114, 102–114. <https://doi.org/10.1016/j.carbpol.2014.07.024>
- Ruosi, M. R., Cordero, C., Cagliero, C., Rubiolo, P., Bicchi, C., Sgorbini, B., & Liberto, E. (2012). A further tool to monitor the coffee roasting process: Aroma composition and chemical indices. *Journal of Agricultural and Food Chemistry*, 60(45), 11283–11291. <https://doi.org/10.1021/jf3031716>

S

- Saeman, J. F., Moore, W. E., Mitchell, R. L., & Millett, M. A. (1954). Techniques for the determination of pulp constituents by quantitative paper chromatography. *Tappi Journal*, 37(8), 336–343.

- Sakakibara, H., Honda, Y., Nakagawa, S., Ashida, H., & Kanazawa, K. (2003). Simultaneous determination of all polyphenols in vegetables, fruits, and teas. *Journal of Agricultural and Food Chemistry*, *51*(3), 571–581. <https://doi.org/10.1021/jf020926l>
- San Martín, M. F., Barbosa-Cánovas, G. V., & Swanson, B. G. (2002). Food processing by high hydrostatic pressure. *Critical Reviews in Food Science and Nutrition*, *42*(6), 627–645. <https://doi.org/10.1080/20024091054274>
- Sang, S., Lee, M. J., Hou, Z., Ho, C. T., & Yang, C. S. (2005). Stability of tea polyphenol (-)-epigallocatechin-3-gallate and formation of dimers and epimers under common experimental conditions. *Journal of Agricultural and Food Chemistry*, *53*(24), 9478–9484. <https://doi.org/10.1021/jf0519055>
- Sanoner, P., Guyot, S., Marnet, N., Molle, D., & Drilleau, J. F. (1999). Polyphenol profiles of French cider apple varieties (*Malus domestica* sp.). *Journal of Agricultural and Food Chemistry*, *47*(12), 4847–4853. <https://doi.org/10.1021/jf990563y>
- Santhakumar, A. B., Battino, M., & Alvarez-Suarez, J. M. (2018). Dietary polyphenols: Structures, bioavailability and protective effects against atherosclerosis. *Food and Chemical Toxicology*, *113*, 49–65. <https://doi.org/10.1016/j.fct.2018.01.022>
- Santos, M. C., Nunes, C., Ferreira, A. S., Jourdes, M., Teissedre, P. L., Rodrigues, A., ... Coimbra, M. A. (2019). Comparison of high pressure treatment with conventional red wine aging processes: impact on phenolic composition. *Food Research International*, *116*, 223–231. <https://doi.org/10.1016/j.foodres.2018.08.018>
- Santos, M. C., Nunes, C., Jourdes, M., Teissedre, P. L., Rodrigues, A., Amado, O., ... Coimbra, M. A. (2016). Evaluation of the potential of high pressure technology as an enological practice for red wines. *Innovative Food Science and Emerging Technologies*, *33*, 76–83. <https://doi.org/10.1016/j.ifset.2015.11.018>
- Saura-Calixto, F. (2011). Dietary fiber as a carrier of dietary antioxidants: An essential physiological function. *Journal of Agricultural and Food Chemistry*, *59*(1), 43–49. <https://doi.org/10.1021/jf1036596>
- Saura-Calixto, F. (2012). Concept and health-related properties of nonextractable polyphenols: The missing dietary polyphenols. *Journal of Agricultural and Food Chemistry*, *60*(45), 11195–11200. <https://doi.org/10.1021/jf303758j>
- Saura-Calixto, F., & Pérez-Jiménez, J. (2018). *Non-extractable Polyphenols and Carotenoids*. (F. Saura-Calixto & J. Pérez-Jiménez, Eds.) (Vol. 5). Royal Society of Chemistry. <https://doi.org/doi.org/10.1039/9781788013208>
- Saura-Calixto, F., Pérez-Jiménez, J., Touriño, S., Serrano, J., Fuguet, E., Torres, J. L., & Goñi, I. (2010). Proanthocyanidin metabolites associated with dietary fibre from in vitro colonic fermentation and proanthocyanidin metabolites in human plasma. *Molecular Nutrition and Food Research*, *54*(7), 939–946. <https://doi.org/10.1002/mnfr.200900276>
- Sauvageau, J., Hinkley, S. F., Carnachan, S. M., & Sims, I. M. (2010). Characterisation of polysaccharides from gold kiwifruit (*Actinidia chinensis* Planch. 'Hort16A'). *Carbohydrate Polymers*, *82*(4), 1110–1115.

- <https://doi.org/10.1016/j.carbpol.2010.06.039>
- Schofield, P., Mbugua, D. M., & Pell, A. N. (2001). Analysis of condensed tannins: A review. *Animal Feed Science and Technology*, *91*(1–2), 21–40. [https://doi.org/10.1016/S0377-8401\(01\)00228-0](https://doi.org/10.1016/S0377-8401(01)00228-0)
- Schols, H. A., Bakx, E. J., Schipper, D., & Voragen, A. G. J. (1995). A xylogalacturonan subunit present in the modified hairy regions of apple pectin. *Carbohydrate Research*, *279*, 265–279. [https://doi.org/10.1016/0008-6215\(95\)00287-1](https://doi.org/10.1016/0008-6215(95)00287-1)
- Schultz, S., Wagner, G., Urban, K., & Ulrich, J. (2004). High-pressure homogenization as a process for emulsion formation. *Chemical Engineering and Technology*, *27*(4), 361–368. <https://doi.org/10.1002/ceat.200406111>
- Seal, C. J., Courtin, C. M., Venema, K., & de Vries, J. (2021). Health benefits of whole grain: effects on dietary carbohydrate quality, the gut microbiome, and consequences of processing. *Comprehensive Reviews in Food Science and Food Safety*. <https://doi.org/10.1111/1541-4337.12728>
- Sedaghat Doost, A., Akbari, M., Stevens, C. V., Setiowati, A. D., & Van der Meeren, P. (2019). A review on nuclear overhauser enhancement (NOE) and rotating-frame overhauser effect (ROE) NMR techniques in food science: Basic principles and applications. *Trends in Food Science and Technology*, *86*, 16–24. <https://doi.org/10.1016/j.tifs.2019.02.001>
- Selig, M. J., Thygesen, L. G., Felby, C., & Master, E. R. (2015). Debranching of soluble wheat arabinoxylan dramatically enhances recalcitrant binding to cellulose. *Biotechnology Letters*, *37*(3), 633–641. <https://doi.org/10.1007/s10529-014-1705-0>
- Serra, A., MacI, A., Romero, M. P., Valls, J., Bladé, C., Arola, L., & Motilva, M. J. (2010). Bioavailability of procyanidin dimers and trimers and matrix food effects in in vitro and in vivo models. *British Journal of Nutrition*, *103*(7), 944–952. <https://doi.org/10.1017/S0007114509992741>
- Seto, R., Nakamura, H., Nanjo, F., & Hara, Y. (1997). Preparation of epimers of tea catechins by heat treatment. *Bioscience, Biotechnology, and Biochemistry*, *61*, 1434–1439. Retrieved from <http://www.mendeley.com/research/geology-volcanic-history-eruptive-style-yakedake-volcano-group-central-japan/>
- Shi, C., Tang, H., Xiao, J., Cui, F., Yang, K., Li, J., ... Li, Y. (2017). Small-angle X-ray scattering study of protein complexes with tea polyphenols. *Journal of Agricultural and Food Chemistry*, *65*(3), 656–665. <https://doi.org/10.1021/acs.jafc.6b04630>
- Shi, M., Nie, Y., Zheng, X. Q., Lu, J. L., Liang, Y. R., & Ye, J. H. (2016). Ultraviolet B (UVB) photosensitivities of tea catechins and the relevant chemical conversions. *Molecules*, *21*(10), 1345. <https://doi.org/10.3390/molecules21101345>
- Shi, M., Ying, D., Hlaing, M. M., Ye, J. H., Sanguansri, L., & Augustin, M. A. (2019). Development of broccoli by-products as carriers for delivering EGCG. *Food Chemistry*, *301*, 125–301. <https://doi.org/10.1016/j.foodchem.2019.125301>
- Shkolnikov, H., Belochvostov, V., Okun, Z., & Shpigelman, A. (2020). The effect of pressure on the kinetics of polyphenolics degradation – Implications to hyperbaric

- storage using Epigallocatechin-gallate as a model. *Innovative Food Science and Emerging Technologies*, 59, 102273. <https://doi.org/10.1016/j.ifset.2019.102273>
- Shrestha, U. R., Smith, S., Pingali, S. V., Yang, H., Zahran, M., Breunig, L., ... Petridis, L. (2019). Arabinose substitution effect on xylan rigidity and self-aggregation. *Cellulose*, 26(4), 2267–2278. <https://doi.org/10.1007/s10570-018-2202-8>
- Siebert, K. J., Troukhanova, N. V., & Lynn, P. Y. (1996). Nature of polyphenol-protein interactions. *Journal of Agricultural and Food Chemistry*, 44(1), 80–85. <https://doi.org/10.1021/jf9502459>
- Sieniawska, E., Ortan, A., Fierascu, I., & Fierascu, R. C. (2020). Procyanidins in Food. In J. Xiao, S. D. Sarker, & Y. Asakawa (Eds.), *Handbook of Dietary Phytochemicals* (pp. 1–40). https://doi.org/10.1007/978-981-13-1745-3_43-1
- Sila, D. N., Van Buggenhout, S., Duvetter, T., Fraeye, I., De Roeck, A., Van Loey, A., & Hendrickx, M. (2009). Pectins in processed fruits and vegetables: Part II - Structure-function relationships. *Comprehensive Reviews in Food Science and Food Safety*, 8(2), 86–104. <https://doi.org/10.1111/j.1541-4337.2009.00071.x>
- Silva, G. G., Dutra, M. da C. P., de Oliveira, J. B., Rybka, A. C. P., Pereira, G. E., & dos Santos Lima, M. (2019). Processing methods with heat increases bioactive phenolic compounds and antioxidant activity in grape juices. *Journal of Food Biochemistry*, 43(3), 1–10. <https://doi.org/10.1111/jfbc.12732>
- Simha, R. (1940). The Influence of brownian movement on the viscosity of solutions. *The Journal of Physical Chemistry*, 44(1), 25–34.
- Simonović, J., Stevanic, J., Djikanović, D., Salmén, L., & Radotić, K. (2011). Anisotropy of cell wall polymers in branches of hardwood and softwood: A polarized FTIR study. *Cellulose*, 18(6), 1433–1440. <https://doi.org/10.1007/s10570-011-9584-1>
- Singh, B., Suri, K., Shevkani, K., Kaur, A., Kaur, A., & Singh, N. (2018). Enzymatic browning of fruit and vegetables: A review. In K. Mohammed (Ed.), *Enzymes in Food Technology: Improvements and Innovations* (pp. 63–78). Springer, Singapore. https://doi.org/10.1007/978-981-13-1933-4_4
- Smeriglio, A., Barreca, D., Bellocco, E., & Trombetta, D. (2017). Proanthocyanidins and hydrolysable tannins: occurrence, dietary intake and pharmacological effects. *British Journal of Pharmacology*, 174(11), 1244–1262. <https://doi.org/10.1111/bph.13630>
- Smidsrød, O., Haug, A., Larsen, B., von Hofsten, B., Williams, D. H., Bunnberg, E., ... Records, R. (1966). The influence of pH on the rate of hydrolysis of acidic polysaccharides. *Acta Chemica Scandinavica*, 20, 1026–1034. <https://doi.org/10.3891/acta.chem.scand.20-1026>
- Soares, S., Brandão, E., Guerreiro, C., Soares, S., Mateus, N., & De Freitas, V. (2020). Tannins in food: Insights into the molecular perception of astringency and bitter taste. *Molecules*, 25(11), 1–26. <https://doi.org/10.3390/molecules25112590>
- Soares, S., Gonçalves, R. M., Fernandes, I. V. A., Mateus, N., & De Freitas, V. (2009). Mechanistic approach by which polysaccharides inhibit α -amylase/ procyanidin aggregation. *Journal of Agricultural and Food Chemistry*, 57(10), 4352–4358. <https://doi.org/10.1021/jf900302r>

- Stanley, T. H., Van Buiten, C. B., Baker, S. A., Elias, R. J., Anantheswaran, R. C., & Lambert, J. D. (2018). Impact of roasting on the flavan-3-ol composition, sensory-related chemistry, and in vitro pancreatic lipase inhibitory activity of cocoa beans. *Food Chemistry*, 255, 414–420. <https://doi.org/10.1016/j.foodchem.2018.02.036>
- Sterling, T., & Irwin, J. J. (2015). ZINC 15 - Ligand Discovery for Everyone. *Journal of Chemical Information and Modeling*, 55(11), 2324–2337. <https://doi.org/10.1021/acs.jcim.5b00559>
- Stoddart, R. W., Spires, I. P., & Tipton, K. F. (1969). Solution properties of polygalacturonic acid. *The Biochemical Journal*, 114(4), 863–870. <https://doi.org/10.1042/bj1140863>
- Sun, B., Ricardo-da-Silva, J. M., & Spranger, I. (1998). Critical factors of vanillin assay for catechins and proanthocyanidins. *Journal of Agricultural and Food Chemistry*, 46(10), 4267–4274. <https://doi.org/10.1021/jf980366j>
- Suo, H., Tian, R., Xu, W., Li, L., Cui, Y., Zhang, S., & Sun, B. (2019). Novel catechin-tiopronin conjugates derived from grape seed proanthocyanidin degradation: Process optimization, high-speed counter-current chromatography preparation, as well as antibacterial activity. *Journal of Agricultural and Food Chemistry*, 67(41), 11508–11517. <https://doi.org/10.1021/acs.jafc.9b04571>
- Suzuki, M., Sano, M., Yoshida, R., Degawa, M., Miyase, T., & Maeda-Yamamoto, M. (2003). Epimerization of tea catechins and O-methylated derivatives of (-)-Epigallocatechin-3-O-gallate: Relationship between epimerization and chemical structure. *Journal of Agricultural and Food Chemistry*, 51(2), 510–514. <https://doi.org/10.1021/jf0210627>
- Symoneaux, R., Baron, A., Marnet, N., Bauduin, R., & Chollet, S. (2014). Impact of apple procyanidins on sensory perception in model cider (part 1): Polymerisation degree and concentration. *LWT - Food Science and Technology*, 57(1), 22–27. <https://doi.org/10.1016/j.lwt.2013.11.016>
- Szychowski, P. J., Lech, K., Sendra-Nadal, E., Hernández, F., Figiel, A., Wojdyło, A., & Carbonell-Barrachina, Á. A. (2018). Kinetics, biocompounds, antioxidant activity, and sensory attributes of quinces as affected by drying method. *Food Chemistry*, 255, 157–164. <https://doi.org/10.1016/j.foodchem.2018.02.075>
- Szymanska-Chargot, M., Chylinska, M., Kruk, B., & Zdunek, A. (2015). Combining FT-IR spectroscopy and multivariate analysis for qualitative and quantitative analysis of the cell wall composition changes during apples development. *Carbohydrate Polymers*, 115, 93–103. <https://doi.org/10.1016/j.carbpol.2014.08.039>
- Szymanska-Chargot, M., & Zdunek, A. (2013). Use of FT-IR Spectra and PCA to the Bulk Characterization of Cell Wall Residues of Fruits and Vegetables Along a Fraction Process. *Food Biophysics*, 8(1), 29–42. <https://doi.org/10.1007/s11483-012-9279-7>

T

- Tanaka, T., Matsuo, Y., & Kouno, I. (2005). A novel black tea pigment and two new oxidation products of epigallocatechin-3-O-gallate. *Journal of Agricultural and Food Chemistry*, *53*(19), 7571–7578. <https://doi.org/10.1021/jf0512656>
- Tang, H. R., Covington, A. D., & Hancock, R. A. (2003). Structure-Activity Relationships in the Hydrophobic Interactions of Polyphenols with Cellulose and Collagen. *Biopolymers*, *70*(3), 403–413. <https://doi.org/10.1002/bip.10499>
- Tao, W., Zhang, Y., Shen, X., Cao, Y., Shi, J., Ye, X., & Chen, S. (2019). Rethinking the mechanism of the health benefits of proanthocyanidins: Absorption, metabolism, and interaction with gut microbiota. *Comprehensive Reviews in Food Science and Food Safety*, *18*, 971–985. <https://doi.org/10.1111/1541-4337.12444>
- Tao, Y., Wu, Y., Han, Y., Chemat, F., Li, D., & Show, P. L. (2020). Insight into mass transfer during ultrasound-enhanced adsorption/desorption of blueberry anthocyanins on macroporous resins by numerical simulation considering ultrasonic influence on resin properties. *Chemical Engineering Journal*, *380*, 122530. <https://doi.org/10.1016/j.cej.2019.122530>
- Tarascou, I., Mazauric, J. P., Meudec, E., Souquet, J. M., Cunningham, D., Nojeim, S., ... Fulcrand, H. (2011). Characterisation of genuine and derived cranberry proanthocyanidins by LC-ESI-MS. *Food Chemistry*, *128*(3), 802–810. <https://doi.org/10.1016/j.foodchem.2011.03.062>
- Tarko, T., & Duda-Chodak, A. (2020). Influence of food matrix on the bioaccessibility of fruit polyphenolic compounds. *Journal of Agricultural and Food Chemistry*, *68*(5), 1315–1325. <https://doi.org/10.1021/acs.jafc.9b07680>
- Thommes, M., Kaneko, K., Neimark, A. V., Olivier, J. P., Rodriguez-Reinoso, F., Rouquerol, J., & Sing, K. S. W. (2015). Physisorption of gases, with special reference to the evaluation of surface area and pore size distribution (IUPAC Technical Report). *Pure and Applied Chemistry*, *87*(9–10), 1051–1069. <https://doi.org/10.1515/pac-2014-1117>
- Thompson, R. S., Jacques, D., Haslam, E., & Tanner, R. J. N. (1972). Plant proanthocyanidins. Part I. Introduction; the isolation, structure, and distribution in nature of plant procyanidins. *Journal of the Chemical Society, Perkin Transactions 1*, 1387–1399. <https://doi.org/10.1039/P19720001387>
- Thongkaew, C., Gibis, M., Hinrichs, J., & Weiss, J. (2014). Polyphenol interactions with whey protein isolate and whey protein isolate-pectin coacervates. *Food Hydrocolloids*, *41*, 103–112. <https://doi.org/10.1016/j.foodhyd.2014.02.006>
- Thorngate, J. H., & Noble, A. C. (1995). Sensory evaluation of bitterness and astringency of 3R(-)-epicatechin and 3S(+)-catechin. *Journal of the Science of Food and Agriculture*, *67*(4), 531–535. <https://doi.org/10.1002/jsfa.2740670416>
- Tinello, F., & Lante, A. (2018). Recent advances in controlling polyphenol oxidase activity of fruit and vegetable products. *Innovative Food Science and Emerging Technologies*, *50*, 73–83. <https://doi.org/10.1016/j.ifset.2018.10.008>
- Treutter, D. (2001). Biosynthesis of phenolic compounds and its regulation in apple. *Plant Growth Regulation*, *34*(1), 71–89.

- <https://doi.org/10.1023/A:1013378702940>
- Tu, X., Wang, M., Liu, Y., Zhao, W., Ren, X., Li, Y., ... Luo, L. (2019). Pretreatment of grape seed proanthocyanidin extract exerts neuroprotective effect in murine model of neonatal hypoxic-ischemic brain injury by its antiapoptotic property. *Cellular and Molecular Neurobiology*, *39*(7), 953–961. <https://doi.org/10.1007/s10571-019-00691-7>
- Tudorache, M., & Bordenave, N. (2019). Phenolic compounds mediate aggregation of water-soluble polysaccharides and change their rheological properties: Effect of different phenolic compounds. *Food Hydrocolloids*, *97*, 1–6. <https://doi.org/10.1016/j.foodhyd.2019.105193>
- Tudorache, M., McDonald, J.-L., & Bordenave, N. (2020). Gallic acid reduces the viscosity and water binding capacity of soluble dietary fibers. *Food and Function*, *11*, 5866–5874. <https://doi.org/10.1039/d0fo01200a>
- Tuohy, K., & Del Rio, D. (2014). *Diet-microbe interactions in the gut: Effects on human health and disease*. Elsevier Inc. <https://doi.org/10.1016/C2012-0-01316-6>
- Turk, M. F., Baron, A., & Vorobiev, E. (2010). Effect of pulsed electric fields treatment and mash size on extraction and composition of apple juices. *Journal of Agricultural and Food Chemistry*, *58*(17), 9611–9616. <https://doi.org/10.1021/jf1016972>
- Turk, M. F., Billaud, C., Vorobiev, E., & Baron, A. (2012). Continuous pulsed electric field treatment of French cider apple and juice expression on the pilot scale belt press. *Innovative Food Science and Emerging Technologies*, *14*, 61–69. <https://doi.org/10.1016/j.ifset.2012.02.001>
- Turk, M. F., Vorobiev, E., & Baron, A. (2012). Improving apple juice expression and quality by pulsed electric field on an industrial scale. *LWT - Food Science and Technology*, *49*(2), 245–250. <https://doi.org/10.1016/j.lwt.2012.07.024>
- Turnbull, W. B., & Daranas, A. H. (2003). On the value of c: Can low affinity systems be studied by isothermal titration calorimetry? *Journal of the American Chemical Society*, *125*(48), 14859–14866. <https://doi.org/10.1021/ja036166s>
- Tuyet Lam, T. B., Iiyama, K., & Stone, B. A. (1992). Cinnamic acid bridges between cell wall polymers in wheat and phalaris internodes. *Phytochemistry*, *31*(4), 1179–1183. [https://doi.org/10.1016/0031-9422\(92\)80256-E](https://doi.org/10.1016/0031-9422(92)80256-E)

U

- Unusan, N. (2020). Proanthocyanidins in grape seeds: An updated review of their health benefits and potential uses in the food industry. *Journal of Functional Foods*, *67*, 103861. <https://doi.org/10.1016/j.jff.2020.103861>

V

- van Boekel, M., Fogliano, V., Pellegrini, N., Stanton, C., Scholz, G., Lalljie, S., ... Eisenbrand, G. (2010). A review on the beneficial aspects of food processing.

- Molecular Nutrition and Food Research*, 54(9), 1215–1247.
<https://doi.org/10.1002/mnfr.200900608>
- Van Buggenhout, S., Sila, D. N., Duvetter, T., Van Loey, A., & Hendrickx, M. (2009). Pectins in processed fruits and vegetables: Part III - Texture engineering. *Comprehensive Reviews in Food Science and Food Safety*, 8(2), 105–117.
<https://doi.org/10.1111/j.1541-4337.2009.00072.x>
- Varner, J. E., & Lin, L. S. (1989). Plant cell wall architecture. *Cell*, 56(2), 231–239.
[https://doi.org/10.1016/0092-8674\(89\)90896-9](https://doi.org/10.1016/0092-8674(89)90896-9)
- Velasco, F. G., Luzardo, F. H. M., Guzman, F., Rodriguez, O., Coto Hernandez, I., Barroso, S., & Diaz Rizo, O. (2014). Gamma radiation effects on molecular characteristic of vegetable tannins. *Journal of Radioanalytical and Nuclear Chemistry*, 299(3), 1787–1792. <https://doi.org/10.1007/s10967-014-2921-8>
- Vergne, M. J., Patras, A., Bhullar, M. S., Shade, L. M., Sages, M., Rakariyatham, K., ... Xiao, H. (2018). UV-C irradiation on the quality of green tea: Effect on catechins, antioxidant activity, and cytotoxicity. *Journal of Food Science*, 83(5), 1258–1264. <https://doi.org/10.1111/1750-3841.14131>
- Vernhet, A., Carrillo, S., & Poncet-Legrand, C. (2014). Condensed tannin changes induced by autoxidation: Effect of the initial degree of polymerization and concentration. *Journal of Agricultural and Food Chemistry*, 62(31), 7833–7842. <https://doi.org/10.1021/jf501441j>
- Vernhet, A., Dubascoux, S., Cabane, B., Fulcrand, H., Dubreucq, E., & Poncet-Legrand, C. (2011). Characterization of oxidized tannins: Comparison of depolymerization methods, asymmetric flow field-flow fractionation and small-angle X-ray scattering. *Analytical and Bioanalytical Chemistry*, 401(5), 1563–1573. <https://doi.org/10.1007/s00216-011-5076-2>
- Vidal, S., Francis, L., Guyot, S., Marnet, N., Kwiatkowski, M., Gawel, R., ... Waters, E. J. (2003). The mouth-feel properties of grape and apple proanthocyanidins in a wine-like medium. *Journal of the Science of Food and Agriculture*, 83(6), 564–573. <https://doi.org/10.1002/jsfa.1394>
- Vogel, J. (2008). Unique aspects of the grass cell wall. *Current Opinion in Plant Biology*, 11(3), 301–307. <https://doi.org/10.1016/j.pbi.2008.03.002>
- Voragen, A. G. J., Coenen, G. J., Verhoef, R. P., & Schols, H. A. (2009). Pectin, a versatile polysaccharide present in plant cell walls. *Structural Chemistry*, 20(2), 263–275. <https://doi.org/10.1007/s11224-009-9442-z>
- Vorwerk, S., Somerville, S., & Somerville, C. (2004). The role of plant cell wall polysaccharide composition in disease resistance. *Trends in Plant Science*, 9(4), 203–209. <https://doi.org/10.1016/j.tplants.2004.02.005>

W

- Waldron, K. W., Ng, A., Parker, M. L., & Parr, A. J. (1997). Ferulic acid dehydrodimers in the cell walls of *Beta vulgaris* and their possible role in texture. *Journal of the Science of Food and Agriculture*, 74(2), 221–228.
[https://doi.org/10.1002/\(SICI\)1097-0010\(199706\)74:2<221::AID-](https://doi.org/10.1002/(SICI)1097-0010(199706)74:2<221::AID-)

- JSFA792>3.0.CO;2-Q
- Waldron, K. W., Smith, A. C., Parr, A. J., Ng, A., & Parker, M. L. (1997). New approaches to understanding and controlling cell separation in relation to fruit and vegetable texture. *Trends in Food Science and Technology*, 8(7), 213–221. [https://doi.org/10.1016/S0924-2244\(97\)01052-2](https://doi.org/10.1016/S0924-2244(97)01052-2)
- Wallace, T. C., Bailey, R. L., Blumberg, J. B., Burton-Freeman, B., Chen, C. y. O., Crowe-White, K. M., ... Wang, D. D. (2020). Fruits, vegetables, and health: A comprehensive narrative, umbrella review of the science and recommendations for enhanced public policy to improve intake. *Critical Reviews in Food Science and Nutrition*, 60(13), 2174–2211. <https://doi.org/10.1080/10408398.2019.1632258>
- Wang, D., Yeats, T. H., Uluisik, S., Rose, J. K. C., & Seymour, G. B. (2018). Fruit Softening: Revisiting the Role of Pectin. *Trends in Plant Science*, 23(4), 302–310. <https://doi.org/10.1016/j.tplants.2018.01.006>
- Wang, Huaifu, & Helliwell, K. (2000). Epimerisation of catechins in green tea infusions. *Food Chemistry*, 70(3), 337–344. [https://doi.org/10.1016/S0308-8146\(00\)00099-6](https://doi.org/10.1016/S0308-8146(00)00099-6)
- Wang, Hui, Wang, J., Mujumdar, A. S., Jin, X., Liu, Z.-L., Zhang, Y., & Xiao, H.-W. (2021). Effects of postharvest ripening on physicochemical properties, microstructure, cell wall polysaccharides contents (pectin, hemicellulose, cellulose) and nanostructure of kiwifruit (*Actinidia deliciosa*). *Food Hydrocolloids*, 118, 106808. <https://doi.org/10.1016/j.foodhyd.2021.106808>
- Wang, J., & Nie, S. (2019). Application of atomic force microscopy in microscopic analysis of polysaccharide. *Trends in Food Science and Technology*, 87, 35–46. <https://doi.org/10.1016/j.tifs.2018.02.005>
- Wang, R., Zhou, W., & Jiang, X. (2008). Reaction kinetics of degradation and epimerization of epigallocatechin gallate (EGCG) in aqueous system over a wide temperature range. *Journal of Agricultural and Food Chemistry*, 56(8), 2694–2701. <https://doi.org/10.1021/jf0730338>
- Wang, W., Chen, W., Zou, M., Lv, R., Wang, D., Hou, F., ... Liu, D. (2018). Applications of power ultrasound in oriented modification and degradation of pectin: A review. *Journal of Food Engineering*, 234, 98–107. <https://doi.org/10.1016/j.jfoodeng.2018.04.016>
- Wang, Yifei, Singh, A. P., Hurst, W. J., Glinski, J. A., Koo, H., & Vorsa, N. (2016). Influence of degree-of-polymerization and linkage on the quantification of proanthocyanidins using 4-dimethylaminocinnamaldehyde (DMAC) assay. *Journal of Agricultural and Food Chemistry*, 64(11), 2190–2199. <https://doi.org/10.1021/acs.jafc.5b05408>
- Wang, Yu, & Ho, C. T. (2009). Polyphenols chemistry of tea and coffee: A century of progress. *Journal of Agricultural and Food Chemistry*, 57(18), 8109–8114. <https://doi.org/10.1021/jf804025c>
- Wang, Yuxue, Liu, J., Chen, F., & Zhao, G. (2013). Effects of molecular structure of polyphenols on their noncovalent interactions with oat β -glucan. *Journal of Agricultural and Food Chemistry*, 61(19), 4533–4538. <https://doi.org/10.1021/jf400471u>

- Wani, S. M., Masoodi, F. A., Haq, E., Ahmad, M., & Ganai, S. A. (2020). Influence of processing methods and storage on phenolic compounds and carotenoids of apricots. *LWT - Food Science and Technology*, *132*, 109846. <https://doi.org/10.1016/j.lwt.2020.109846>
- Wannenmacher, J., Gastl, M., & Becker, T. (2018). Phenolic substances in beer: structural diversity, reactive potential and relevance for brewing process and beer quality. *Comprehensive Reviews in Food Science and Food Safety*, *17*(4), 953–988. <https://doi.org/10.1111/1541-4337.12352>
- Waskom, M. (2014). Seaborn: Statistical Data Visualization. Retrieved from <http://stanford.edu/~mwaskom/software/seaborn/>
- WatreLOT, A. A., Heymann, H., & Waterhouse, A. L. (2020). Red wine dryness perception related to physicochemistry. *Journal of Agricultural and Food Chemistry*, *68*(10), 2964–2972. <https://doi.org/10.1021/acs.jafc.9b01480>
- WatreLOT, A. A., Le Bourvellec, C., Imbert, A., & Renard, C. M. G. C. (2013). Interactions between pectic compounds and procyanidins are influenced by methylation degree and chain length. *Biomacromolecules*, *14*(3), 709–718. <https://doi.org/10.1021/bm301796y>
- WatreLOT, A. A., Le Bourvellec, C., Imbert, A., & Renard, C. M. G. C. (2014). Neutral sugar side chains of pectins limit interactions with procyanidins. *Carbohydrate Polymers*, *99*, 527–536. <https://doi.org/10.1016/j.carbpol.2013.08.094>
- WatreLOT, A. A., & Norton, E. L. (2020). Chemistry and reactivity of tannins in vitis spp.: A review. *Molecules*, *25*(9), 1–24. <https://doi.org/10.3390/molecules25092110>
- WatreLOT, A. A., Renard, C. M. G. C., & Le Bourvellec, C. (2015). Comparison of microcalorimetry and haze formation to quantify the association of B-type procyanidins to poly-l-proline and bovine serum albumin. *LWT - Food Science and Technology*, *63*(1), 376–382. <https://doi.org/10.1016/j.lwt.2015.03.064>
- Wefers, D., Gmeiner, B. M., Tyl, C. E., & Bunzel, M. (2015). Characterization of diferuloylated pectic polysaccharides from quinoa (*Chenopodium quinoa* Willd.). *Phytochemistry*, *116*(1), 320–328. <https://doi.org/10.1016/j.phytochem.2015.04.009>
- Wei, X., Li, J., & Li, B. (2019). Multiple steps and critical behaviors of the binding of tannic acid to wheat starch: Effect of the concentration of wheat starch and the mass ratio of tannic acid to wheat starch. *Food Hydrocolloids*, *94*(1), 174–182. <https://doi.org/10.1016/j.foodhyd.2019.03.019>
- Wen, K. S., Ruan, X., Wang, J., Yang, L., Wei, F., Zhao, Y. X., & Wang, Q. (2019). Optimizing nucleophilic depolymerization of proanthocyanidins in grape seeds to dimeric proanthocyanidin B1 or B2. *Journal of Agricultural and Food Chemistry*, *67*(21), 5978–5988. <https://doi.org/10.1021/acs.jafc.9b01188>
- Wiercigroch, E., Szafraniec, E., Czamara, K., Pacia, M. Z., Majzner, K., Kochan, K., ... Malek, K. (2017). Raman and infrared spectroscopy of carbohydrates: A review. *Spectrochimica Acta - Part A: Molecular and Biomolecular Spectroscopy*, *185*, 317–335. <https://doi.org/10.1016/j.saa.2017.05.045>
- Willats, W. G. T., Knox, J. P., & Mikkelsen, J. D. (2006). Pectin: New insights into an

- old polymer are starting to gel. *Trends in Food Science and Technology*, 17(3), 97–104. <https://doi.org/10.1016/j.tifs.2005.10.008>
- Williamson, G., Kay, C. D., & Crozier, A. (2018). The bioavailability, transport, and bioactivity of dietary flavonoids: A review from a historical perspective. *Comprehensive Reviews in Food Science and Food Safety*, 17(5), 1054–1112. <https://doi.org/10.1111/1541-4337.12351>
- Wojdyło, A., Figiel, A., Lech, K., Nowicka, P., & Oszmiański, J. (2014). Effect of convective and vacuum-microwave drying on the bioactive compounds, color, and antioxidant capacity of sour cherries. *Food and Bioprocess Technology*. <https://doi.org/10.1007/s11947-013-1130-8>
- Wojdyło, A., Figiel, A., Legua, P., Lech, K., Carbonell-Barrachina, Á. A., & Hernández, F. (2016). Chemical composition, antioxidant capacity, and sensory quality of dried jujube fruits as affected by cultivar and drying method. *Food Chemistry*, 207, 170–179. <https://doi.org/10.1016/j.foodchem.2016.03.099>
- Wojdyło, A., Figiel, A., & Oszmiański, J. (2009). Effect of drying methods with the application of vacuum microwaves on the bioactive compounds, color, and antioxidant activity of strawberry fruits. *Journal of Agricultural and Food Chemistry*, 57(4), 1337–1343. <https://doi.org/10.1021/jf802507j>
- Wong-Paz, J. E., Guyot, S., Aguilar-Zárate, P., Muñiz-Márquez, D. B., Contreras-Esquivel, J. C., & Aguilar, C. N. (2021). Structural characterization of native and oxidized procyanidins (condensed tannins) from coffee pulp (*Coffea arabica*) using phloroglucinolysis and thioglycolysis-HPLC-ESI-MS. *Food Chemistry*, 340, 127830. <https://doi.org/10.1016/j.foodchem.2020.127830>
- Wu, L. Y., Guo, Y. L., Cao, L. L., Jin, S., Lin, H. Z., Wu, M. Y., ... Ye, J. H. (2016). Application of NaOH-HCl-Modified Apple Pomace to Binding Epigallocatechin Gallate. *Food and Bioprocess Technology*, 9(6), 917–923. <https://doi.org/10.1007/s11947-016-1683-4>
- Wu, L. Y., Melton, L. D., Sanguansri, L., & Augustin, M. A. (2014). The batch adsorption of the epigallocatechin gallate onto apple pomace. *Food Chemistry*, 160, 260–265. <https://doi.org/10.1016/j.foodchem.2014.03.098>
- Wu, L. Y., Sanguansri, L., & Augustin, M. A. (2014). Protection of epigallocatechin gallate against degradation during in vitro digestion using apple pomace as a carrier. *Journal of Agricultural and Food Chemistry*, 62(50), 12265–12270. <https://doi.org/10.1021/jf504659n>
- Wu, L. Y., Sanguansri, L., & Augustin, M. A. (2015). Processing treatments enhance the adsorption characteristics of epigallocatechin-3-gallate onto apple pomace. *Journal of Food Engineering*, 150, 75–81. <https://doi.org/10.1016/j.jfoodeng.2014.10.027>
- Wu, Q., Liang, Y., Ma, S., Li, H., & Gao, W. (2019). Stability and stabilization of (–)-gallocatechin gallate under various experimental conditions and analyses of its epimerization, auto-oxidation, and degradation by LC-MS. *Journal of the Science of Food and Agriculture*, 99(13), 5984–5993. <https://doi.org/10.1002/jsfa.9873>
- Wu, X., Li, M., Xiao, Z., Daglia, M., Dragan, S., Delmas, D., ... Xiao, J. (2020). Dietary polyphenols for managing cancers : What have we ignored ? *Trends in Food*

- Science & Technology*, 101, 150–164. <https://doi.org/10.1016/j.tifs.2020.05.017>
- Wu, Z., Li, H., Ming, J., & Zhao, G. (2011). Optimization of adsorption of tea polyphenols into oat β -glucan using response surface methodology. *Journal of Agricultural and Food Chemistry*, 59(1), 378–385. <https://doi.org/10.1021/jf103003q>

X

- Xu, Y. Q., Yu, P., & Zhou, W. (2019). Combined effect of pH and temperature on the stability and antioxidant capacity of epigallocatechin gallate (EGCG) in aqueous system. *Journal of Food Engineering*, 250, 46–54. <https://doi.org/10.1016/j.jfoodeng.2019.01.016>

Y

- Yan, X., Zhang, X., McClements, D. J., Zou, L., Liu, X., & Liu, F. (2019). Co-encapsulation of epigallocatechin gallate (EGCG) and curcumin by two proteins-based nanoparticles: role of EGCG. *Journal of Agricultural and Food Chemistry*, 67(48), 13228–13236. <https://doi.org/10.1021/acs.jafc.9b04415>
- Yang, W., Ma, X., Laaksonen, O., He, W., Kallio, H., & Yang, B. (2019). Effects of latitude and weather conditions on proanthocyanidins in blackcurrant (*Ribes nigrum*) of finnish commercial cultivars. *Journal of Agricultural and Food Chemistry*, 67(51), 14038–14047. <https://doi.org/10.1021/acs.jafc.9b06031>
- Yapo, B. M. (2011). Rhamnogalacturonan-I: A structurally puzzling and functionally versatile polysaccharide from plant cell walls and mucilages. *Polymer Reviews*, 51(4), 391–413. <https://doi.org/10.1080/15583724.2011.615962>
- Ye, J. H., Jin, J., Liang, H. L., Lu, J. L., Du, Y. Y., Zheng, X. Q., & Liang, Y. R. (2009). Using tea stalk lignocellulose as an adsorbent for separating decaffeinated tea catechins. *Bioresource Technology*, 100(2), 622–628. <https://doi.org/10.1016/j.biortech.2008.07.003>

Z

- Zainol, M. K. M., Abdul-Hamid, A., Bakar, F. A., & Dek, S. P. (2009). Effect of different drying methods on the degradation of selected flavonoids in *Centella asiatica*. *International Food Research Journal*, 16(4), 531–537.
- Zamora-Ros, R., Knaze, V., Rothwell, J. A., Hémon, B., Moskal, A., Overvad, K., ... Scalbert, A. (2016). Dietary polyphenol intake in europe: The european prospective investigation into cancer and nutrition (EPIC) study. *European Journal of Nutrition*, 55(4), 1359–1375. <https://doi.org/10.1007/s00394-015-0950-x>
- Zanchi, D., Konarev, P. V., Tribet, C., Baron, A., Svergun, D. I., & Guyot, S. (2009). Rigidity, conformation, and solvation of native and oxidized tannin macromolecules in water-ethanol solution. *Journal of Chemical Physics*, 130(24).

- <https://doi.org/10.1063/1.3156020>
- Zdunek, A., Pieczywek, P. M., & Cybulska, J. (2020). The primary, secondary, and structures of higher levels of pectin polysaccharides. *Comprehensive Reviews in Food Science and Food Safety*, 20(1), 1101–1117. <https://doi.org/10.1111/1541-4337.12689>
- Zeller, W. E. (2019). Activity, purification, and analysis of condensed tannins: Current state of affairs and future endeavors. *Crop Science*, 59(3), 886–904. <https://doi.org/10.2135/cropsci2018.05.0323>
- Zeller, W. E., Reinhardt, L. A., Robe, J. T., Sullivan, M. L., & Panke-Buisse, K. (2020). Comparison of protein precipitation ability of structurally diverse procyanidin-rich condensed tannins in two buffer systems. *Journal of Agricultural and Food Chemistry*, 68(7), 2016–2023. <https://doi.org/10.1021/acs.jafc.9b06173>
- Zeng, J., Xu, H., Cai, Y., Xuan, Y., Liu, J., Gao, Y., & Luan, Q. (2018). The effect of ultrasound, oxygen and sunlight on the stability of (–)-epigallocatechin gallate. *Molecules*, 23(9), 1–13. <https://doi.org/10.3390/molecules23092394>
- Zhang, H., Chen, L., Lu, M., Li, J., & Han, L. (2016). A novel film-pore-surface diffusion model to explain the enhanced enzyme adsorption of corn stover pretreated by ultrafine grinding. *Biotechnology for Biofuels*, 9(1), 1–12. <https://doi.org/10.1186/s13068-016-0602-2>
- Zhang, L., Cao, Q. Q., Granato, D., Xu, Y. Q., & Ho, C. T. (2020). Association between chemistry and taste of tea: A review. *Trends in Food Science and Technology*, 101, 139–149. <https://doi.org/10.1016/j.tifs.2020.05.015>
- Zhang, L., Ho, C. T., Zhou, J., Santos, J. S., Armstrong, L., & Granato, D. (2019). Chemistry and biological activities of processed camellia sinensis teas: A comprehensive review. *Comprehensive Reviews in Food Science and Food Safety*, 18(5), 1474–1495. <https://doi.org/10.1111/1541-4337.12479>
- Zhang, M., Vervoort, L., Moalin, M., Mommers, A., Douny, C., den Hartog, G. J. M., & Haenen, G. R. M. M. (2018). The chemical reactivity of (–)-epicatechin quinone mainly resides in its B-ring. *Free Radical Biology and Medicine*, 124, 31–39. <https://doi.org/10.1016/j.freeradbiomed.2018.05.087>
- Zhao, W., Shehzad, H., Yan, S., Li, J., & Wang, Q. (2017). Acetic acid pretreatment improves the hardness of cooked potato slices. *Food Chemistry*, 228, 204–210. <https://doi.org/10.1016/j.foodchem.2017.01.156>
- Zhao, Y., Man, Y., Wen, J., Guo, Y., & Lin, J. (2019). Advances in Imaging Plant Cell Walls. *Trends in Plant Science*, 24(9), 867–878. <https://doi.org/10.1016/j.tplants.2019.05.009>
- Zhou, J., Wu, Y., Long, P., Ho, C. T., Wang, Y., Kan, Z., ... Wan, X. (2019). LC-MS-based metabolomics reveals the chemical changes of polyphenols during high-temperature roasting of large-leaf yellow tea. *Journal of Agricultural and Food Chemistry*, 67(19), 5405–5412. <https://doi.org/10.1021/acs.jafc.8b05062>
- Zhu, F. (2015). Interactions between starch and phenolic compound. *Trends in Food Science and Technology*, 43(2), 129–143. <https://doi.org/10.1016/j.tifs.2015.02.003>
- Zhu, F. (2017). Interactions between cell wall polysaccharides and polyphenols.

- Critical Reviews in Food Science and Nutrition*, 58(11), 1808–1831. <https://doi.org/10.1080/10408398.2017.1287659>
- Zhu, J., Zhang, D., Tang, H., & Zhao, G. (2018). Structure relationship of non-covalent interactions between phenolic acids and arabinan-rich pectic polysaccharides from rapeseed meal. *International Journal of Biological Macromolecules*, 120, 2597–2603. <https://doi.org/10.1016/j.ijbiomac.2018.09.036>
- Zhu, K., Ouyang, J., Huang, J., & Liu, Z. (2020). Research progress of black tea thearubigins: a review. *Critical Reviews in Food Science and Nutrition*, 1–11. <https://doi.org/10.1080/10408398.2020.1762161>
- Zhu, Y., Sun, J., Xu, D., Wang, S., Yuan, Y., & Cao, Y. (2018). Investigation of (+)-catechin stability under ultrasonic treatment and its degradation kinetic modeling. *Journal of Food Process Engineering*, 41(8), 1–7. <https://doi.org/10.1111/jfpe.12904>
- Zhu, Y., Zhang, J., Chen, F., Hu, X., Xu, D., & Cao, Y. (2020). Epimerisation and hydrolysis of catechins under ultrasonic treatment. *International Journal of Food Science and Technology*, 1–9. <https://doi.org/10.1111/ijfs.14633>
- Zuleta-Correa, A., Chinn, M. S., Alfaro-Córdoba, M., Truong, V. Den, Yencho, G. C., & Bruno-Bárcena, J. M. (2020). Use of unconventional mixed acetone-butanol-ethanol solvents for anthocyanin extraction from purple-fleshed sweetpotatoes. *Food Chemistry*, 314, 125959. <https://doi.org/10.1016/j.foodchem.2019.125959>
- Zykwinska, A. W., Ralet, M.-C. J., Garnier, C. D., & Thibault, J.-F. J. (2005). Evidence for In Vitro Binding of Pectin Side Chains to Cellulose. *Plant Physiology*, 139(1), 397–407. <https://doi.org/10.1104/pp.105.065912>

Acronyms

A

Ac. A	Aceric Acid
AG I	Arabinogalactan I
AG II	Arabinogalactan II
AIS	Alcohol Insoluble Solid
ANOVA	Analysis of Variance
ANR	Agence Nationale de la Recherche (English: French National Agency)
Ara	Arabinose

C

C	Catechin
CG	Catechin gallate
CNRS	Centre National de la Recherche Scientifique (English: French National Centre for Scientific Research)
CWP	Cell wall polysaccharide
CSP	Calcium Chelator Soluble Pectin

D

DAc	Degree of Acetylation
DAD	Diode Array Detector
DLS	Dynamic Light Scattering
DB	Degree of Blockiness
DM	Degree of Methylation
DP	Degree of polymerization
\overline{DP}_n	Number-average degree of polymerization of procyanidins
DW	Dry Weight
DASP	Sodium Carbonate Soluble Pectin

E

EDTA	Ethylenediaminetetraacetic Acid
EGCG	Epigallocatechin gallate
ECG	Epicatechin gallate
EGC	Epigallocatechin
EC	Epicatechin

F

FAO	Food and Agriculture Organization of the United Nations
FID	Flame Ionization Detector
Frc	Fructose
FTIR	Fourier Transform Infrared

Acronyms

Fuc	Fucose
FW	Fresh Weight
G	
Gal	Galactose
GalA	Galacturonic Acid
GC	Gas Chromatography
Glc	Glucose
GCG	Gallocatechin gallate
GC	Gallocatechin
H	
HCl	Hydrochloric Acid
HG	Homogalacturonan
HCA	Hierarchical Cluster Analysis
HPLC	High Pressure Liquid Chromatography
HPSEC	High Performance Size Exclusion Chromatography
I	
INRAE	Institut National de Recherche pour l'Agriculture, l'Alimentation et l'Environnement (English: National Research Institute for Agriculture, Food and Environment)
ITC	Isothermal Titration Calorimetry
IGM	Independent Gradient Model
K	
KOH	Potassium hydroxide
M	
MALLS	Multi-Angle Laser Light Scattering
Man	Mannose
MeOH	Methanol
MS	Mass Spectrometry
N	
NaCl	Sodium Chloride
NaN ₃	Sodium Azide
NaOH	Sodium Hydroxide
NMR	Nuclear Magnetic Resonance
NR	Not Refined

Acronyms

P

PAE	Pectin acetylerase
PAL	Pectate Lyase
PCA	Principal Component Analysis
PG	Polygalacturonase
PL	Pectin Lyase
PME	Pectin Methylesterase

R

RG I	Rhamnogalacturonan I
RG II	Rhamnogalacturonan II
Rha	Rhamnose
RID	Refractive Index Detector

S

SEM	Scanning Electron Microscopy
SQPOV	Sécurité et Qualité des Produits d'Origine Végétale (English: Safety and Quality of Processed Fruit and Vegetables)

T

TEM	Transmission Electron Microscopy
-----	----------------------------------

V

VMD	Visual Molecular Dynamics
-----	---------------------------

W

WHO	World Health Organization
WIS	Water Insoluble Soldis
WBC	Water Binding Capacity
WSP	Water Soluble Pectin

X

XGA	Xylogalacturonan
Xyl	Xylose

Supplementary data

Supplementary data

Supplementary Table 4.1 Composition (mg/g dry matter) of purified acetonic fractions from ‘Marie Ménard’ and ‘Avrolles’ apple.

	PCA	$\overline{DP}n$	Purified PCA constitutive units (%)			EC	DHC	CQA	PCQ	FLV	Total phenolics
			CAT _t	EC _t	EC _{ext}						
Marie Ménard	667	12	0.7	7.7	91.6	40.5	4.6	88.2	0.9	2.4	804
Avrolles	821	39	0.4	2.2	97.4	0	17.4	13.3	2.9	3.8	859
<i>Pooled SD</i>	<i>21</i>	<i>0.2</i>	<i>0.02</i>	<i>0.09</i>	<i>0.11</i>	<i>0.4</i>	<i>0.5</i>	<i>0.6</i>	<i>0.2</i>	<i>0.02</i>	<i>22</i>

PCA: procyanidins, $\overline{DP}n$: number-average degree of polymerization of procyanidins, CAT_t: terminal (+)-catechin units, EC_t: terminal (-)-epicatechin units, EC_{ext}: extension (-)-epicatechin units, EC: (-)-epicatechin as flavan-3-ol monomer, DHC: dihydrochalcones, CQA: 5'-caffeoylquinic acid, PCQ, *p*-coumaroylquinic acid, FLV: flavonols, Pooled SD: pooled standard deviation.

Supplementary Table 4.2 Composition (mg/g dry matter) of purified acetonic fraction from ‘Marie Ménard’ and ‘Avrolles’ apple.

	PCA	$\overline{DP}n$	Purified PCA constitutive units (%)			EC	DHC	CQA	PCQ	FLV	Total phenolics
			CAT _t	EC _t	EC _{ext}						
Marie Ménard	680	9	1.5	9.1	89.4	19.4	8.6	34.8	0.5	7.5	751
Avrolles	821	39	0.4	2.1	97.5	0	17.4	13.3	2.9	3.8	858
<i>Pooled SD</i>	<i>17.9</i>	<i>0.2</i>	<i>0.02</i>	<i>0.1</i>	<i>0.9</i>	<i>0.4</i>	<i>0.6</i>	<i>0.6</i>	<i>0.2</i>	<i>0.03</i>	<i>22</i>

PCA: procyanidins, $\overline{DP}n$: number-average degree of polymerization of procyanidins, CAT_t: terminal (+)-catechin units, EC_t: terminal (-)-epicatechin units, EC_{ext}: extension (-)-epicatechin units, EC: (-)-epicatechin as flavan-3-ol monomer, DHC: dihydrochalcones, CQA: 5'-caffeoylquinic acid, PCQ, *p*-coumaroylquinic acid, FLV: flavonols, Pooled SD: pooled standard deviation.

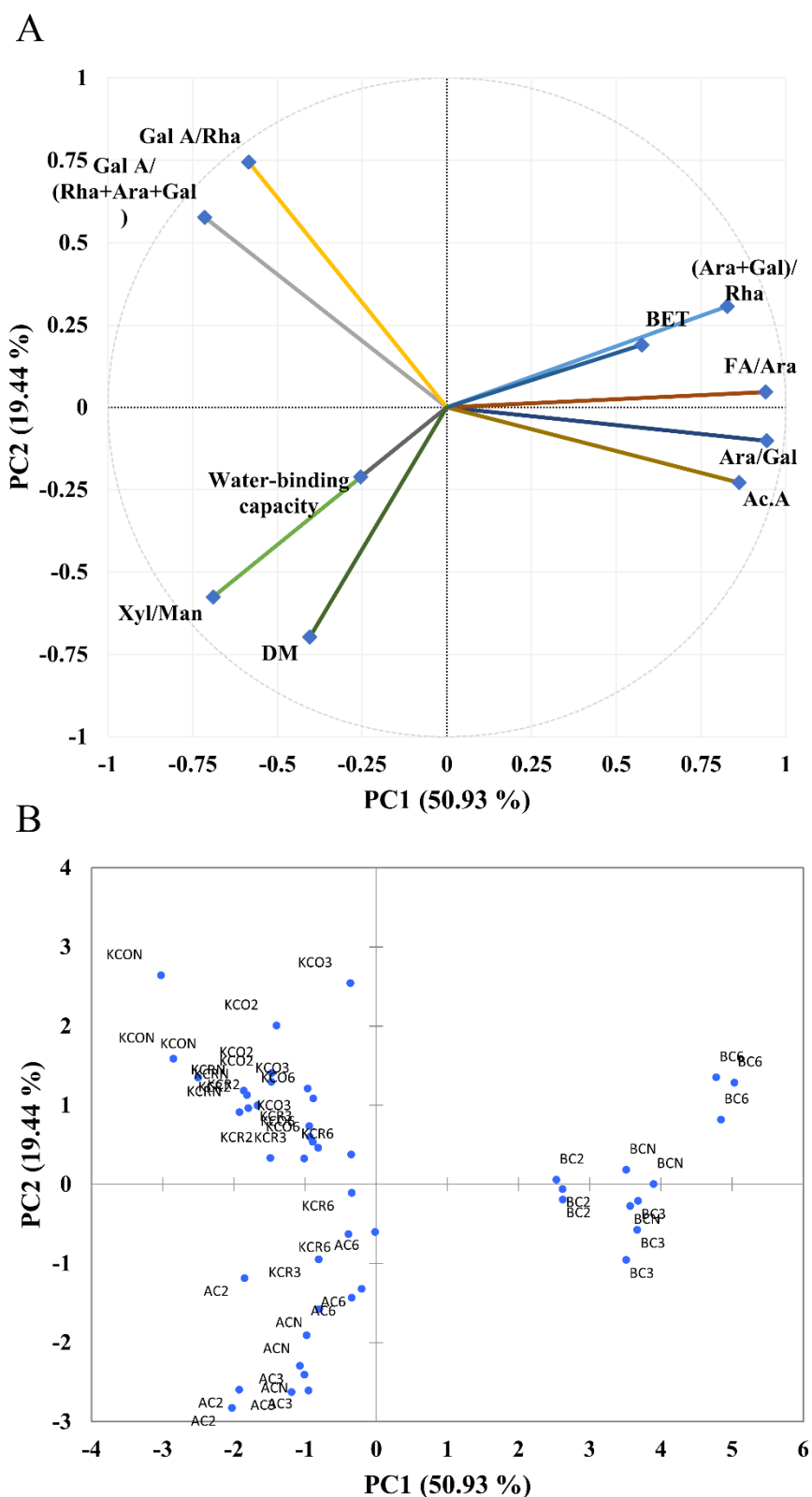
Dynamic Light Scattering (DLS)

Z-average particle diameter was measured at 25 °C in a citrate-phosphate solution (0.1 M, pH 3.8) DLS at 135° using a laser diode at 657 nm on a VASCO particle size analyzer (Cordouan Technologies, Pessac, France). The samples were filtered through a 0.45 µm hydrophilic PTFE syringe filter (Macherey-Nagel, Düren, Germany) before measurement. Samples with complexes were not filtrated. The nanoQ software (Version 2.6.4.x) was used in the multi-acquisition mode with each correlogram acquisition processed by the Padé-Laplace inversion algorithm for polydisperse samples. Solutions of hemicelluloses (5 g/L) alone were used as references compared to the same solutions containing: 10 mM (epicatechin equivalent) procyanidin DP9 or DP39.

Supplementary Table 4.3 Average particle diameter (nm) obtained by DLS for hemicelluloses and hemicellulose-procyanidin solutions.

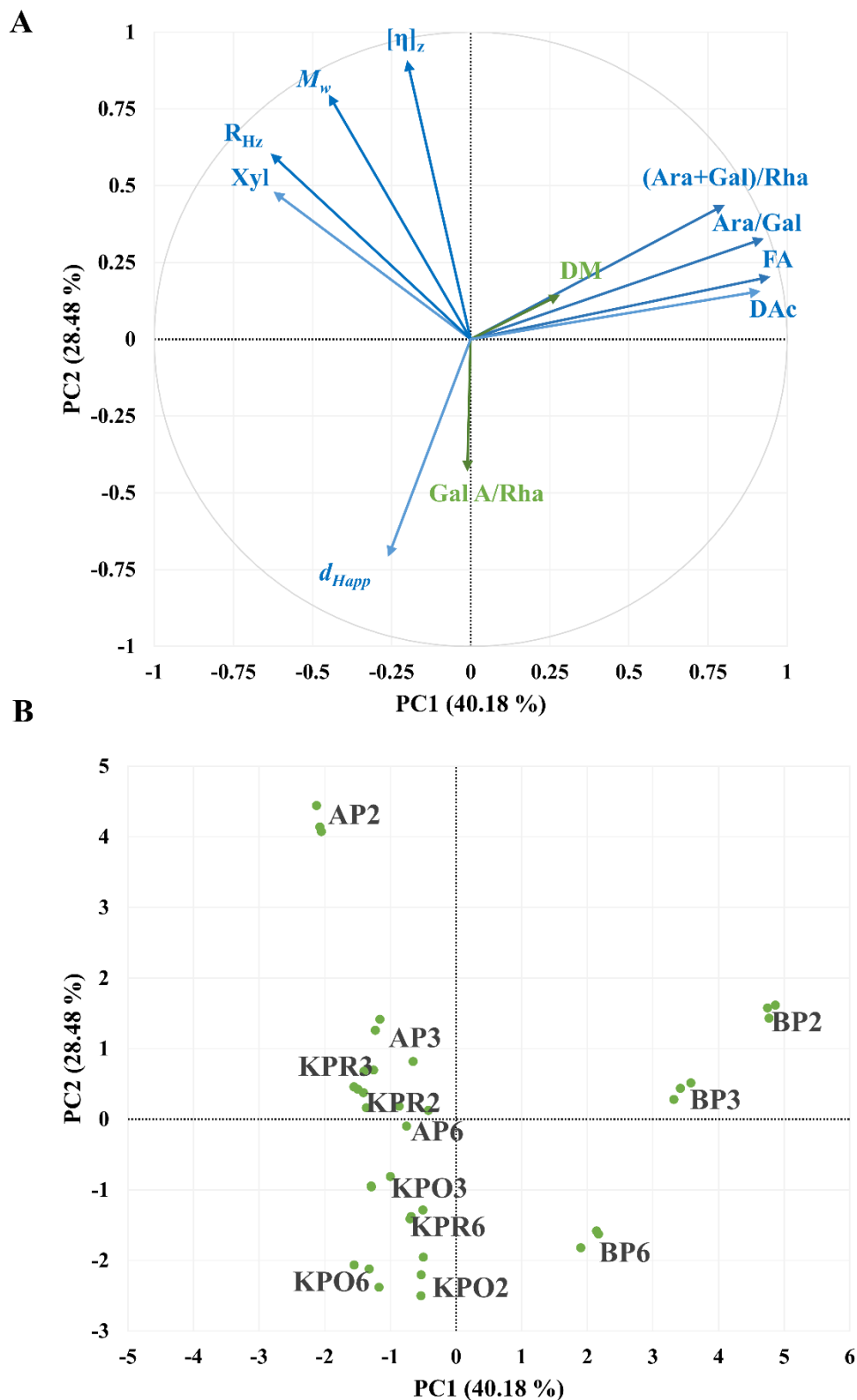
	Hemicellulose solutions (Intensity)		Solutions with DP9 (Intensity)		Solutions with DP39 (Intensity)	
	Small particle	Large particle	Small particle	Large particle	Small particle	Large particle
AXLV	128 (0.10)	1806 (0.85)	273 (0.21)	2186 (0.76)	440 (0.59)	2440 (0.37)
AXMV	81 (0.07)	2283 (0.91)	248 (0.11)	1324 (0.78)	367 (0.35)	1784 (0.61)
AXHV	90 (0.08)	3131 (0.88)	264 (0.17)	2905 (0.77)	1035 (0.52)	4238 (0.42)
AXMB	193 (0.11)	3684 (0.84)	225 (0.14)	3297 (0.78)	456 (0.50)	3634 (0.46)
AXLB	NA	2661 (0.86)	NA	3195 (0.98)	NA	3875 (0.92)
XYLO	98 (0.25)	3914 (0.69)	NA	NA	NA	NA
XYLA	86 (0.39)	453 (0.56)	124 (0.31)	693 (0.65)	125 (0.39)	781 (0.55)
<i>Pooled SD</i>	<i>11 (0.02)</i>	<i>179 (0.02)</i>	<i>20 (0.02)</i>	<i>110 (0.02)</i>	<i>49 (0.03)</i>	<i>331 (0.04)</i>

Pooled SD: pooled standard deviation. AXLV: Arabinoxylan (low viscosity); AXMV: Arabinoxylan (medium viscosity); AXHV: Arabinoxylan (high viscosity); AXMB: Arabinoxylan (30% Ara); AXLB: Arabinoxylan (22% Ara); XYLO: Xyloglucan; XYLA: Xylan. NA: Not applicable.



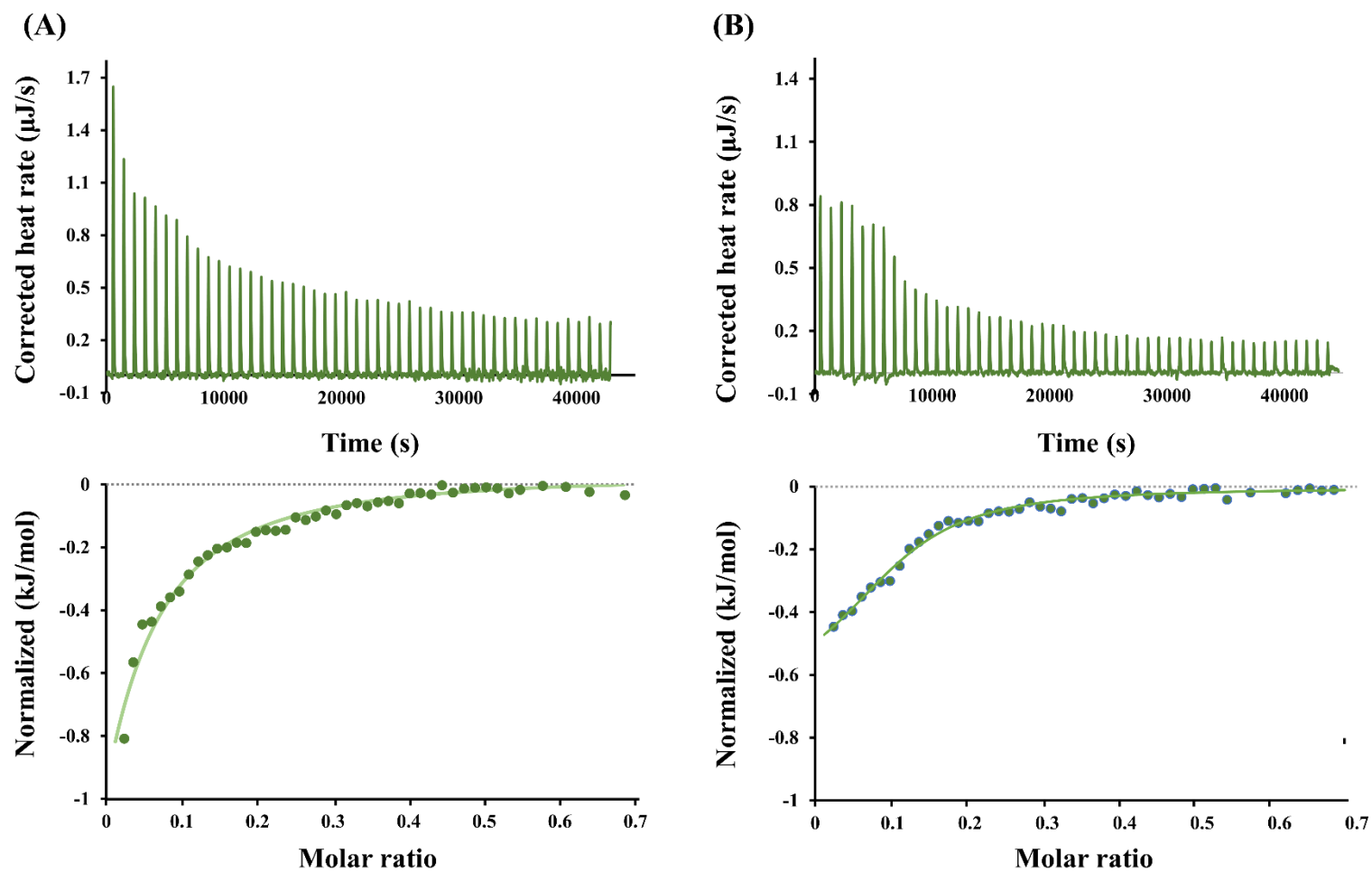
Supplementary Figure 4.1 Principal component analysis on the carbohydrate compositions of apple, beet and kiwifruit cell walls boiling at different pHs. Correlation circle on variable loading on PC1 and PC2 associated with sample map of scores on PC1 and PC2. AC: apple cell wall, BC: beet cell wall, KC: kiwifruit cell wall, pH values-: 2: pH 2.0, 3: pH 3.5, 6: pH 6.0. Maturity-: R: –Ripe, O: –Overripe.

The first two principal components (PC1 and PC2) explained more than 70% of the total variance (Supplementary Fig. 4.1). The correlation map indicated that the composition and structure of the cell walls varied independently in this series of cell walls. The first PC-score (PC1) was highly correlated with the neutral sugar side-chain abundance and branching of RG-I, the proportion of arabinans/galactans, FA and Ac.A, and negatively correlated to homogalacturonan content and linearity of pectin, Xyl / Man and DM. The second PC-score PC2 was positively correlated to Gal A / Rha and Gal A / (Rha+Ara+Gal) and negatively correlated to Xyl / Man, DM and water-binding capacity. The sample map highlighted the structural diversity of the cell walls with different sample groups. KCON, AC2/3 and BC6 formed an approximately equilateral triangle on the Supplementary Fig. 4.1B. KCON at the top left exhibited highest homogalacturonan content and linearity of pectin. At the bottom, AC2/3 showed the highest Xyl / Man ratio and DM indicating the highest Xyl and the degree of methylation. On the right of the map, BC6 was rich in arabinan side-chains and ferulic acids and had highest specific surface area.

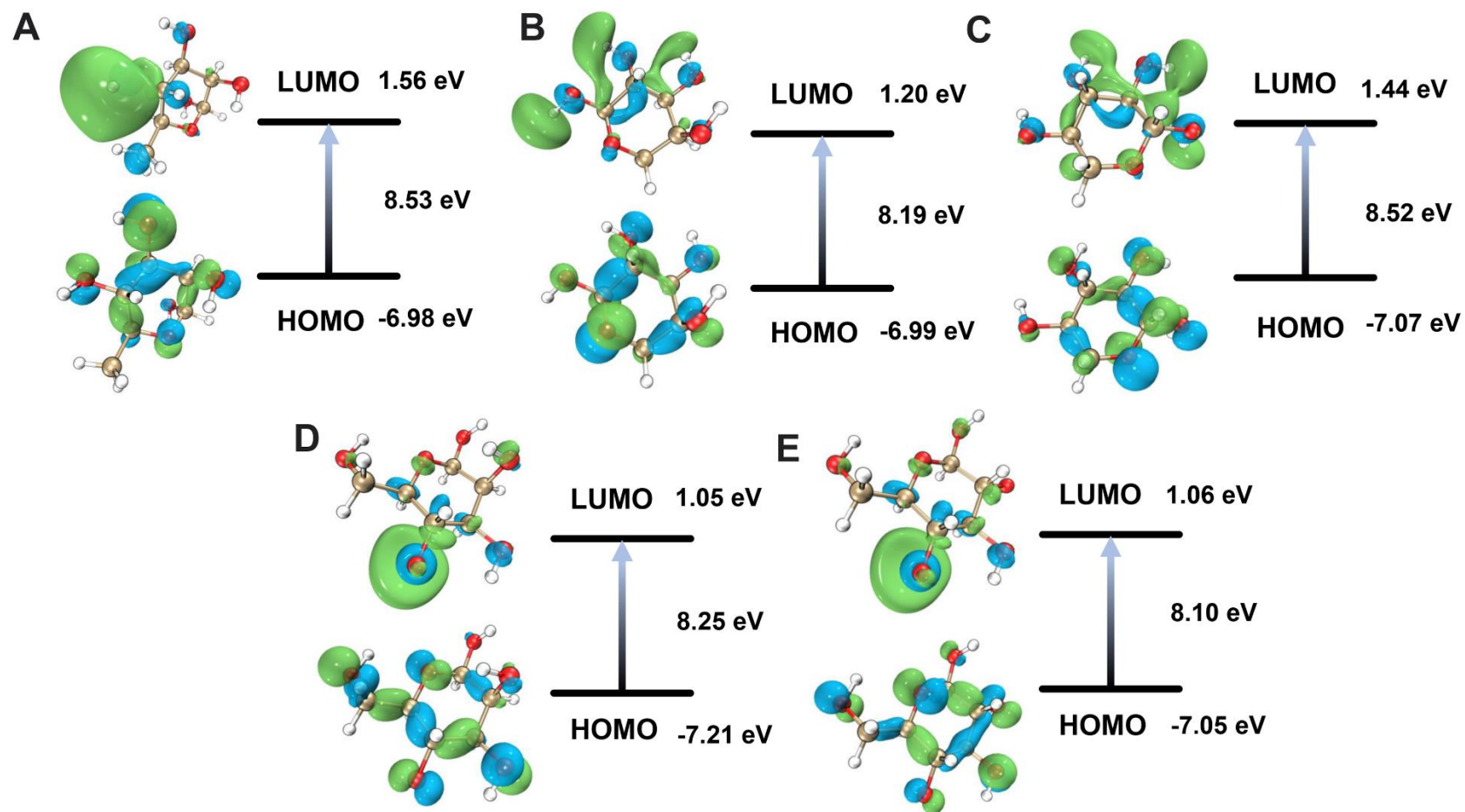


Supplementary Figure 4.2 Principal component analysis (PCA) on the carbohydrate compositions of apple, beet and kiwifruit pectins extracted at different pHs. Correlation circle on variable loading on PC1 and PC2 associated with sample map of scores on PC1 and PC2. AP: pectins from apple cell wall, BP: pectins from beet cell wall, KP: pectins from kiwifruit cell wall, pH values-: 2: pH 2.0, 3: pH 3.5, 6: pH 6.0. Maturity-: R: -Ripe, O: -Overripe.

The two first principal components (PC1 and PC2) explained more than 69% of the total variance (Supplementary Fig. 4.2). The correlation map indicated that the side-chains and macromolecular characteristics of the pectins varied independently in this series of pectins. The first PC-score (PC1) was highly correlated with the neutral sugar side chain abundance and composition ((Ara + Gal) / Rha and Ara / Gal), FA and DAc, and negatively correlated to Xyl, \bar{R}_{Hz} and \bar{M}_w . The second PC-score PC2 was positively correlated to $[\eta]_z$, \bar{R}_{Hz} and \bar{M}_w and negatively correlated to Gal A / Rha and \bar{d}_{Happ} . The sample map highlighted the structural diversity of the extracted pectins with different sample groups. AP2, BP2 and KPO2 formed an approximately equilateral triangle on the supplementary Fig. 4.2B. AP2 at the top left exhibited relatively higher Xyl, \bar{M}_w , $[\eta]_z$ and \bar{R}_{Hz} , which suggested a larger size and the presence of xylogalacturonans. At the bottom, KPO2 showed the highest Gal A/Rha ratio indicating the highest pectin linearity and the predominance of HG in the backbone. On the right of the map, BP2 was rich in arabinan side chains and ferulic acids, which progressively decreased in BP3 then BP6. In the third quadrant, KPO6 had the highest density. The samples including AP3, AP6, KPR3, KPR2 and KPO3 were intermediate and close to the center. Among these samples, KPR2 displayed the lowest Ara/Gal ratio and the second-highest molar mass.



Supplementary Figure 4.3 Representative thermograms of titration of A) Arabinoxylan (22% Ara) and B) Xylan with procyanidins DP39. The measurement of heat release at the top, while the molar enthalpy changes against (-)-epicatechin/ xylose equivalent ratio after peak integration at the bottom.



Supplementary Figure 4.4 Prediction of the active sites by frontier molecular orbitals (FMO). Isosurface of the LUMO and HOMO of (A): rhamnose, (B): arabinose, (C): xylose, (D): mannose (E): glucose, respectively. Green and blue isosurfaces represent positive and negative parts, respectively.

Computational Details

Quantum Mechanical Calculations

Conformational search was performed using xTB program developed by the Grimme group. Conformation was determined through the following procedure. First, more than 2000 possible initial geometries were generated using xtb software version 6.3. Due to the conformational flexibility, we performed extensive conformational searches using Grimme's program named conformer rotamer ensemble sampling tool (CREST) We also using Molclus3 to screened out the low-energy conformers. The geometry optimization and frequency analysis of these structures were performed using the extended tight-binding semiempirical program package (xTB); the geometries and energies were obtained with GFN2-xTB (Bannwarth, Ehlert, & Grimme, 2019; Grimme, Bannwarth, & Shushkov, 2017). These initial geometries in a rough level conformation with relatively low energy and different geometry were screened out by Molclus. The parameter settings used the default values in the program, i.e., the energy threshold for distinguishing clusters, 0.5 kcal/mol, and the geometric threshold for distinguishing clusters, 0.25 Å. The structure of each species was submitted for precise geometry optimization at B3LYP-D3(BJ)/6-31+G(d) level (Grimmea, Antony, Ehrlich, & Krieg, 2010) with SMD solvation model for aqueous solution using Gaussian 16 software, followed by frequency calculation at the same theoretical level. The final configurations of the complexes were selected utilizing Boltzmann distribution law based on Gibbs free energies. All of the calculations were conducted without any symmetry constraint using Gaussian 16 program. The interaction energy (ΔE_{int}) is calculated as the

difference between the total energy of a complex and the sum of the total energies of its components. The BSSE correction was incorporated in each case using the counterpoise correction method (Simon & Duran, 1996).

Non-covalent interaction (NCI) analysis

In order to analyze the non-covalent interaction of interface residues in complex, an independent gradient model (IGM) (Lefebvre et al., 2017) analysis was carried out with the Multiwfn 3.7 program in the study. Molecular plots were visualized by the VMD 1.9.3 program (Humphrey, Dalke, & Schulten, 1996). The IGM analysis depends on the topological characteristics of the electron density, ρ . The IGM descriptor δg^{inter} is given by the difference between the first derivatives of the charge densities for the total system and the fragments:

$$\delta g(\mathbf{r})^{\text{inter}} = |\nabla \rho^{\text{IGM,inter}}| - |\nabla \rho|$$

$\delta g^{\text{inter}} > 0$ indicates the presence of weak interactions, and the magnitude of the descriptor at a point in space indicates the strength of the interaction.

Résumé

Le sujet de cette thèse est de développer une nouvelle vision des interactions entre les polysaccharides de la paroi cellulaire et les procyanidines au cours de la transformation des fruits et des légumes. Ainsi des parois isolées de fruits ou légumes connus comme ayant des comportements différents (pomme, betterave et kiwi) ont été soumises à une ébullition (20 min) à pH de 2.0, 3.5 et 6.0. Pour toutes les parois, tous les traitements conduisent à une perte en pectines. La paroi de pomme est la plus sensible à la dégradation, que ce soit en milieu acide ou neutre, et la betterave en milieu acide. Par contre, la paroi de kiwi, pauvre en pectines, est la moins sensible à la dégradation quel que soit le pH. La dépolymérisation des pectines est moins prononcée à pH 3.5 pour toutes les parois. Le squelette principal des pectines est dégradé après traitement à pH 6.0 (milieu neutre) par β -élimination, conduisant à une extraction de petites molécules, notamment dans le kiwi. Le traitement à pH 2.0 provoque l'hydrolyse des chaînes latérales de pectines mais les polysaccharides solubilisés ont un volume hydrodynamique plus élevé, notamment dans la pomme. La cellulose, les hémicelluloses et les homogalacturonanes peuvent être distingués par ATR-FTIR contrairement aux chaînes latérales d'arabinanes et de galactanes. Les parois cellulaires qui interagissent le plus avec les procyanidines sont caractérisées par leur porosité élevée ainsi que par leur teneur élevée en pectines linéaires. Par ailleurs, la prédominance de régions homogalacturoniques et le degré de méthylation élevé (par exemple, les pectines de kiwi) sont des caractéristiques structurelles clés des pectines favorisant leur affinité vis-à-vis des procyanidines, tandis qu'un degré de ramification et des teneurs en acide férulique élevés (par exemple, les pectines de betterave) sont préjudiciables. Les pectines interagissent préférentiellement avec les procyanidines hautement polymérisées sauf dans le cas des pectines de betterave. Les hémicelluloses sont en deuxième position après les pectines en termes d'affinité pour les procyanidines. Parmi elles, la plus forte interaction avec les procyanidines a été observée avec les xyloglucanes. En revanche, les xylanes présentent l'affinité la plus faible vis-à-vis des procyanidines. Ce résultat a permis de mieux comprendre les mécanismes moléculaires qui régissent les interactions entre les parois cellulaires et les polyphénols.

Malus x domestica Borkh; *Beta vulgaris* L.; *Actinidia deliciosa*; transformation; pectine; hémicellulose; masse molaire; liaison non covalente, porosité, solubilité

Abstract

The subject of this thesis is to develop new insight of interactions between cell wall polysaccharides and procyanidins during processing. Cell walls isolated from apple, beet and kiwifruit are subjected to boiling (20 min) at pH 2.0, 3.5 and 6.0, allowing the abundant cell wall polysaccharides obtained above used to model their interactions with procyanidins. The least disruptive condition is pH 3.5. Acid hydrolysis and β -elimination appeared to be common mechanisms that cause loss of neutral sugars, often from pectin side-chains, and galacturonic acid, respectively, but their effects are of different intensities as function of the plant origin. The cellulose, hemicelluloses and pectin homogalacturonans can be distinguished by ATR-FTIR, contrary to arabinans and galactans. The differently structured cell wall polysaccharides further interacted with procyanidins. Highly porous cell walls interact strongly with oligomeric procyanidins. The cell walls that interact more with procyanidins are characterized by their high pectin content, high linearity, and high porosity. Moreover, predominance of homogalacturonan regions and high degree of methylation (e.g., kiwifruit pectins) thus appeared key structural features of pectins for high affinity for procyanidins, while high degree of branching and ferulic acid (e.g., beet pectins) is detrimental. Pectins interacted preferentially with highly polymerized procyanidins except in the case of beet pectins. Hemicelluloses are second only to pectins in affinity for procyanidins. Among them, the highest interaction with procyanidins was found for xyloglucan, and xylan exhibited the weakest. This result improved understanding of the molecular mechanisms that drive interactions between cell walls and polyphenols.

Malus x domestica Borkh; *Beta vulgaris* L.; *Actinidia deliciosa*; processing; pectin; hemicellulose; molar mass; noncovalent binding, porosity, solubility